ASDF

Proceeding of the International Conference on Systems, Science, Control, Communication, Engineering and Technology 2015

ICSSCCET 2015

10-11 Aug 2015

Karpagam Institute of Technology, Coimbatore

Editors

Ramachandran T
Kokula Krishna Hari K, Thiruvengadam B, Daniel James

ISBN 13 : 978-81-929866-1-6
ISBN 10 : 81-929866-1-6

$499

International Conference on Systems, Science, Control, Communication, Engineering and Technology 2015

ICSSCCET 2015

International Conference on Systems, Science, Control, Communication, Engineering and Technology 2015

Volume 1

By

ASDF, India

Financially Sponsored By

Association of Scientists, Developers and Faculties, India

Multiple Areas

10-11, August 2015

Karpagam Institute of Technology,

Coimbatore, India

Editor-in-Chief

Ramachandran T

Editors:

Kokula Krishna Hari K, Daniel James, Thiruvengadam B

Published by

Association of Scientists, Developers and Faculties
Address: RMZ Millennia Business Park, Campus 4B, Phase II, 6th Floor, No. 143, Dr. MGR Salai, Kandanchavady, Perungudi, Chennai – 600 096, India.
Email: admin@asdf.org.in || www.asdf.org.in

International Conference on Systems, Science, Control, Communication, Engineering and Technology (ICSSCCET 2015)

VOLUME 1

Editor-in-Chief: **Ramachandran T**
Editors: **Kokula Krishna Hari K, Daniel James, Thiruvengadam B**

Disclaimer:

No responsibility is assumed by the ICSSCCET 2015 Organizers/Publisher for any injury and/ or damage to persons or property as a matter of products liability, negligence or otherwise, or from any use or operation of any methods, products or ideas contained in the material herein. Contents, used in the papers and how it is submitted and approved by the contributors after changes in the formatting. Whilst every attempt made to ensure that all aspects of the paper are uniform in style, the ICSSCCET 2015 Organizers, Publisher or the Editor(s) will not be responsible whatsoever for the accuracy, correctness or representation of any statements or documents presented in the papers.

ISBN-13: 978-81-929866-1-6
ISBN-10: 81-929866-1-6

TECHNICAL REVIEWERS

- A Amsavalli, Paavai Engineering College, Namakkal, India
- A Ayyasamy, Annamalai University, Chidambaram, India
- A C Shagar, Sethu Institute of Technology, India
- A Kavitha, Chettinad College of Engineering & Technology, Karur, India
- A Padma, Madurai Institute of Engineering and Technology, Madurai, India
- A S N Chakravarthy, JNTU Kakinada, India
- A Tamilarasi, Kongu Engineering College, Perundurai, India
- Abdelbasset Brahim, University of Granada, Spain
- Abdelnaser Omran, Universiti Utara Malaysia, Malaysia
- Abdul Aziz Hussin, Universiti Sains Malaysia, Malaysia
- Abdul Nawfar Bin Sadagatullah, Universiti Sains Malaysia, Malaysia
- Abhishek Shukla, U.P.T.U. Lucknow, India
- Aede Hatib Musta'amal, Universiti Teknologi Malaysia, Malaysia
- Ahmed Mohammed Kamaruddeen, Universiti Utara Malaysia, Malaysia
- Ahmed Salem, Old Dominion University, United States of America
- Ali Berkol, Baskent University & Space and Defence Technologies (SDT), Turkey
- Alphin M S, SSN College of Engineering, Chennai, India
- Alwardoss Velayutham Raviprakash, Pondicherry Engineering College, Pondicherry, India
- Anand Nayyar, KCL Institute of Management and Technology, Punjab
- Anbuchezhiyan M, Valliammai Engineering College, Chennai, India
- Ang Miin Huey, Universiti Sains Malaysia, Malaysia
- Anirban Mitra, VITAM Berhampur, Odisha, India
- Ariffin Abdul Mutalib, Universiti Utara Malaysia, Malaysia
- Arniza Ghazali, Universiti Sains Malaysia, Malaysia
- Arumugam Raman, Universiti Utara Malaysia, Malaysia
- Asha Ambhaikar, Rungta College of Engineering & Technology, Bhilai, India
- Asrulnizam Bin Abd Manaf, Universiti Sains Malaysia, Malaysia
- Assem Abdel Hamied Mousa, EgyptAir, Cairo, Egypt
- Aziah Daud, Universiti Sains Malaysia, Malaysia
- B Paramasivan, National College of Engineering, Tirunelveli, India
- Badruddin A. Rahman, Universiti Utara Malaysia, Malaysia

- Balachandran Ruthramurthy, Multimedia University, Malaysia
- Balasubramanie Palanisamy, Professor & Head, Kongu Engineering College, India
- Brahim Abdelbasset, University of Granada, Spain
- C Poongodi, Bannari Amman Institute of Technology, Sathyamangalam, India
- Chandrasekaran Subramaniam, Professor & Dean, Anna University, India
- Choo Ling Suan, Universiti Utara Malaysia, Malaysia
- Cristian-Gyozo Haba, Technical University of Iasi, Romania
- D Deepa, Bannari Amman Institute of Technology, Sathyamangalam, India
- D Gracia Nirmala Rani, Thiagarajar College of Engineering, Madurai, Tamil Nadu
- D Sheela, Tagore Engineering College, Chennai, India
- Daniel James, Senior Researcher, United Kingdom
- David Rathnaraj Jebamani, Sri Ramakrishna Engineering College, India
- Deepali Sawai, Director - MCA, University of Pune (Savitribai Phule Pune University), India
- Dewi Nasien, Universiti Teknologi Malaysia, Malaysia
- Doug Witten, Oakland University, Rochester, United States of America
- Dzati Athiar Ramli, Universiti Sains Malaysia, Malaysia
- G A Sathish Kumar, Sri Venkateswara College of Engineering, India
- G Ganesan, Adikavi Nannaya University, India
- Ganesan Kanagaraj, Thiagarajar College of Engineering, Madurai, Tamil Nadu
- Geetha G, Jerusalem College of Engineering, Chennai, India
- Geetha V, Pondicherry Engineering College, Pondicherry, India
- Guobiao Yang, Tongji University, China
- Hanumantha Reddy T, RYM Engineering College, Bellary, India
- Hareesh N Ramanathan, Toc H Institute of Science and Technology, India
- Hari Mohan Pandey, Amity University, Noida, India
- Hidayani Binti Jaafar, Universiti Malaysia Kelantan, Malaysia
- Itebeddine GHORBEL, INSERM, France
- J Baskaran, Adhiparasakthi Engineering College, Melmaruvathur, India
- J Karthikeyan, Anna University, Chennai, India
- J Sadhik Basha, International Maritime College, Oman
- Jebaraj S, Universiti Teknologi PETRONAS (UTP), Malaysia
- Jia Uddin, International Islamic University Chittagong, Bangladesh
- Jinnah Sheik Mohamed M, National College of Engineering, Tirunelveli, India

- Julie Juliewatty Mohamed, Universiti Sains Malaysia, Malaysia
- K Latha, Anna University, Chennai, India
- K Mohamed Bak , GKM College of Engineering and Technology, India
- K Nirmalkumar, Kongu Engineering College, Perundurai, India
- K P Kannan, Bannari Amman Institute of Technology, Sathyamangalam, India
- K Parmasivam, K S R College of Engineering, Thiruchengode, India
- K Senthilkumar, Erode Sengunthar Engineering College, Erode, India
- K Suriyan, Bharathiyar University, India
- K Thamizhmaran, Annamalai University, Chidambaram, India
- K Vijayaraja, PB College of Engineering, Chennai, India
- Kamal Imran Mohd Sharif, Universiti Utara Malaysia, Malaysia
- Kannan G R, PSNA College of Engineering and Technology, Dindigul, India
- Kathiravan S, Kalaignar Karunanidhi Institute of Technology, Coimbatore, India
- Khairul Anuar Mohammad Shah, Universiti Sains Malaysia, Malaysia
- Kokula Krishna Hari Kunasekaran, Chief Scientist, Techno Forum Research and Development Center, India
- Krishnan J, Annamalai University, Chidambaram, India
- Kumaratharan N, Sri Venkateswara College of Engineering, India
- L Ashok Kumar, PSG College of Technology, Coimbatore, India
- Laila Khedher, University of Granada, Spain
- Lakshmanan Thangavelu, SA College of Engineering, Chennai, India
- M Ayaz Ahmad, University of Tabuk, Saudi Arabia
- M Chandrasekaran, Government College of Engineering, Bargur, India
- M K Kavitha Devi, Thiagarajar College of Engineering, Madurai, Tamil Nadu
- M Karthikeyan, Knowledge Institute of Technology, India
- M Shanmugapriya, SSN College of Engineering, Chennai, India
- M Thangamani, Kongu Engineering College, India
- M Venkatachalam, RVS Technical Campus - Coimbatore, India
- M Vimalan, Thirumalai Engineering College, Kanchipuram, India
- Malathi R, Annamalai University, Chidambaram, India
- Mansoor Zoveidavianpoor, Universiti Teknologi Malaysia, Malaysia
- Manvender Kaur Chahal, Universiti Utara Malaysia, Malaysia
- Mariem Mahfoudh, MIPS, France
- Marinah Binti Othman, Universiti Sains Islam Malaysia, Malaysia

- Mathivannan Jaganathan, Universiti Utara Malaysia, Malaysia
- Mehdi Asadi, IAU (Islamic Azad University), Iran
- Mohammad Ayaz Ahmad, University of Tabuk, Saudi Arabia
- Mohd Hanim Osman, Universiti Teknologi Malaysia, Malaysia
- Mohd Hashim Siti Z, Universiti Teknologi Malaysia, Malaysia
- Mohd Murtadha Mohamad, Universiti Teknologi Malaysia, Malaysia
- Mohd Zulkifli Bin Mohd Yunus, Universiti Teknologi Malaysia, Malaysia
- Moniruzzaman Bhuiyan, University of Northumbria, United Kingdom
- Mora Veera Madhava Rao, Osmania University, India
- Muhammad Iqbal Ahmad, Universiti Malaysia Kelantan, Malaysia
- Muhammad Javed, Wayne State University, United States of America
- N Rajesh Jesudoss Hynes, Mepco Schlenk Engineering College, Sivakasi, Tamilnadu, India
- N Karthikeyan, SNS College of Engineering, Coimbatore, India
- N Malmurugan, Vidhya Mandhir Institute of Technology, India
- N Senthilnathan, Kongu Engineering College, Perundurai, India
- N Shanthi, Nandha Engineering College, Erode, India
- N Suthanthira Vanitha, Knowledge Institute of Technology, India
- Nasrul Humaimi Mahmood, Universiti Teknologi Malaysia, Malaysia
- Nida Iqbal, Universiti Teknologi Malaysia, Malaysia
- Nithya Kalyani S, K S R College of Engineering, Thiruchengode, India
- Nor Muzlifah Mahyuddin, Universiti Sains Malaysia, Malaysia
- Norma Binti Alias, Universiti Teknologi Malaysia, Malaysia
- P Dhanasekaran, Erode Sengunthar Engineering College, Erode, India
- P Ganesh Kumar, K. L. N. College of Information Technology, Madurai, India
- P Kumar, K S R College of Engineering, Thiruchengode, India
- P Ramasamy, Sri Balaji Chockalingam Engineering College, India
- P Raviraj, Kalaignar Karunanidhi Institute of Technology, Coimbatore, India
- P Sengottuvelan, Bannari Amman Institute of Technology, Sathyamangalam, India
- P Shunmuga Perumal, Anna University, Chennai, India
- P Tamizhselvan, Bharathiyar University, India
- P Thamilarasu, Paavai Engineering College, Namakkal, India
- Pasupuleti Visweswara Rao, Universiti Malaysia Kelantan, Malaysia
- Pethuru Raj, IBM Research, India

- Qais Faryadi, USIM: Universiti Sains Islam Malaysia, Malaysia
- R Ashokan, Kongunadu College of Engineering and Technology, India
- R Dhanasekaran, Syed Ammal Engineering College, Ramanathapuram, India
- R Muthukumar, Shree Venkateshwara Hi-Tech Engineering College, India
- R Nallusamy, Principal, Nandha college of Technology, Erode, India
- R Ragupathy, Kongu Engineering College, Perundurai, India
- R Sudhakar, Dr. Mahalingam College of Engineering and Technology, India
- R Suguna, SKR Engineering College, Chennai, India
- R Sundareswaran, SSN College of Engineering, Chennai, India
- Radzi Ismail, Universiti Sains Malaysia, Malaysia
- Rajesh Deshmukh, Shri Shankaracharya Institute of Professional Management and Technology, Raipur
- Rathika P, V V College of Engineering, Tirunelveli, India
- Rathinam Maheswaran, Mepco Schlenk Engineering College, Sivakasi, Tamilnadu, India
- Razauden Mohamed Zulkifli, Universiti Teknologi Malaysia, Malaysia
- Reza Gharoie Ahangar, Islamic Azad University, Iran
- Roesnita Ismail, USIM: Universiti Sains Islam Malaysia, Malaysia
- Rohaizah Saad, Universiti Utara Malaysia, Malaysia
- Roselina Binti Salleh, Universiti Teknologi Malaysia, Malaysia
- Ruba Soundar K, P. S. R. Engineering College, Sivakasi, India
- S Albert Alexander, Kongu Engineering College, Perundurai, India
- S Anand, V V College of Engineering, Tirunelveli, India
- S Appavu @ Balamurugan, K. L. N. College of Information Technology, Madurai, India
- S Balaji, Jain University, India
- S Balamuralitharan, SRM University, Chennai, India
- S Balamurugan, Kalaignar Karunanidhi Institute of Technology, Coimbatore, India
- S Geetha, VIT University, Chennai, India
- S Jaganathan, Dr. N. G. P. Institute of Technology, Coimbatore, India
- S Natarajan, United Institute of Technology, Coimbatore, India
- S Poorani, Erode Sengunthar Engineering College, Erode, India
- S Prakash, Nehru Colleges, Coimbatore, India
- S Rajkumar, University College of Engineering Ariyalur, India
- S Ramesh, Vel Tech High Tech Dr.Rangarajan Dr.Sakunthala Engineering College, India
- S Selvaperumal, Syed Ammal Engineering College, Ramanathapuram, India

- S Selvi, Institute of Road and Transport Technology, India
- S Senthamarai Kannan, Kalasalingam University, India
- S Senthilkumar, Sri Shakthi Institute of Engineering and Technology, Coimbatore, India
- S Vengataasalam, Kongu Engineering College, Perundurai, India
- Samuel Charles, Dhanalakshmi Srinivasan College of Engineering, Coimbatore, India
- Sangeetha R G, VIT University, Chennai, India
- Sanjay Singhal, Founder, 3nayan Consulting, India
- Saratha Sathasivam, Universiti Sains Malaysia, Malaysia
- Sarina Sulaiman, Universiti Teknologi Malaysia, Malaysia
- Sathish Kumar Nagarajan, Sri Ramakrishna Engineering College, Coimbatore, India
- Sathishbabu S, Annamalai University, Chidambaram, India
- Seddik Hassene, ENSIT, Tunisia
- Selvakumar Manickam, Universiti Sains Malaysia, Malaysia
- Shamshuritawati Sharif, Universiti Utara Malaysia, Malaysia
- Shankar S, Kongu Engineering College, Perundurai, India
- Shazida Jan Mohd Khan, Universiti Utara Malaysia, Malaysia
- Sheikh Abdul Rezan, Universiti Sains Malaysia, Malaysia
- Shilpa Bhalerao, Acropolis Institute of Technology and Research, Indore, India
- Singaravel G, K. S. R. College of Engineering, India
- Sivakumar Ramakrishnan, Universiti Sains Malaysia, Malaysia
- Somasundaram Sankaralingam, Coimbatore Institute of Technology, India
- Subash Chandra Bose Jeganathan, Professional Group of Institutions, India
- Subramaniam Ganesan, Oakland University, Rochester, United States of America
- Suganthi Appalasamy, Universiti Malaysia Kelantan, Malaysia
- Sunil Chowdhary, Amity University, Noida, India
- Suresh Sagadevan, Indian Institute of Science, Bangalore, India
- Syed Sahal Nazli Alhady, Universiti Sains Malaysia, Malaysia
- T Krishnakumar, Tagore Engineering College, Chennai, India
- T Ramayah, Universiti Sains Malaysia, Malaysia
- T Subbulakshmi, VIT University, Chennai, India
- T V P Sundararajan, Bannari Amman Institute of Technology, Sathyamangalam, India
- Tom Kolan, IBM Research, Israel
- Uma N Dulhare, Muffkham Jah College of Engineering & Technology, Hyderabad, India
- Uvaraja V C, Bannari Amman Institute of Technology, Sathyamangalam, India

Table of Content

Volume	01	ISBN	978-81-929866-1-6
Month	August	Year	2015

International Conference on Systems, Science, Control, Communication, Engineering and Technology 2015

PREFACE

It is a great honour to welcome for the International Conference on Systems, Science, Control, Communication, Engineering and Technology - ICSSCCET 2015 at Karpagam Institute of Technology, Coimbatore, Tamilnadu, India, Asia on 10 – 11 August, 2015.

ICSSCCET 2015 aims to provide a chance for academic and industry professionals to share ideas on progress in the field of technology and to bring together the researchers and practitioners to discuss the problems and find solutions for the multifaceted aspects of Interdisciplinary Research Theory and Technology.

This conference provides an opportunity for various departments in the field of Engineering and Technology. It also focuses on the important aspects of advances in Systems, Science, Management, Medical Sciences, Communication, Engineering, Technology and Interdisciplinary Research Theory and Technology. This conference highlights the new concepts and the improvements related to the research and technology.

It provides a chance for academic and industry professionals to discuss recent progress in the area of Interdisciplinary Research Theory and Technology. The proceeding of the conference consists of the information of various advancements in the field of Research and Developments globally and would act as a primary source for researchers to gain knowledge on the latest developments.

With the constant support and encouragement from the ASDF Global President Dr. S. Prithiv Rajan, ASDF International President Dr. P. Anbuoli and ASDF International Secretary Dr. K. Kokula Krishna Hari, this conference will stay in our hearts. Without them, this proceeding could not have been completed within the shortest span.

Heartfelt Gratitude are due to the team members of Association of Scientists, Developers and Faculties – International, Our Management, Friends and Colleagues for their cooperation and commitment for making this conference a successful one.

Dr. T. Ramachandran,
Chief Editor cum Convener,
Principal, Karpagam Institute of Technology, Coimbatore, TN, India.

International Conference on Systems, Science, Control, Communication, Engineering and Technology 2015 [ICSSCCET 2015]

ISBN	978-81-929866-1-6	**VOL**	01
Website	icssccet.org	**eMail**	icssccet@asdf.res.in
Received	10 - July - 2015	**Accepted**	31- July - 2015
Article ID	ICSSCCET001	**eAID**	ICSSCCET.2015.001

OVERVIEW AND SIGNIFICANCE OF VISCOSE YARN QUALITY CHARACTERISTICS AND SUGGESTIVE PROCESS TO IMPROVE IT

Dr. T. Ramachandran[1], A. Thirunarayanan[2]
[1]Principal, Karpagam Institute of Technology, Coimbatore, India.
[2]Department of Textile Technology, Karpagam University, Coimbatore, India

Abstract: *Viscose ring spun yarn has more hairiness than cotton &polyester of same linear density and poses problem in the subsequent processes due to protruding of hairs. It is also quite peculiar that despite Viscose being man made and comes in precise 'cut length' with zero short fibres, it behaves differently than other fibres like polyester or cotton as far as hairiness is concerned. This article gives an insight as to why Viscose fibre-yarn characteristics are different than cotton and polyester. Despite all these limitations, still Viscose is the most preferred fibres for blending with either cotton or other synthetic fibres for better usage in textile applications.*

Keywords*:* Viscose, hairiness, linear density, blending, synthetic fibres, textile applications

Introduction

It is proven fact that Viscose Ring spun yarn is more hairy than cotton and polyester of the same linear density. It is quite peculiar that despite viscose fibre being man made and supplied in fixed cut length with no trace of short fibres like cotton, yet the hairiness is relatively higher. In general, synthetic fibres like polyester is less hairy due to advantage of zero short fibres and fixed cut length unlike viscose. Viscose although being more hairy still has several good characteristics than polyester and hence viscose is generally blended with polyester & cotton for better use in apparel applications and textile applications in general. This paper gives answer as to why viscose yarn behaves differently and its impact on quality characteristics.

Manufacture of Viscose

Wood pulp is dissolved in caustic soda and after steeping it for a specific period of time it is shredded and allowed to age. Ageing contributes to viscosity of viscose. Longer the ageing time, lesser the viscosity value. The aged pulp is then treated with carbon disulphide to form a yellow colour cellulose Xanthate, which is dissolved in lower concentrated caustic soda again. This is starting stage of viscose formation. An acetate dope is added to alkali cellulose for yarn lustre.

Cite this article as: Dr. T. Ramachandran, A. Thirunarayanan. "OVERVIEW AND SIGNIFICANCE OF VISCOSE YARN QUALITY CHARACTERISTICS AND SUGGESTIVE PROCESS TO IMPROVE IT." *International Conference on Systems, Science, Control, Communication, Engineering and Technology (2015)*: 01-04.

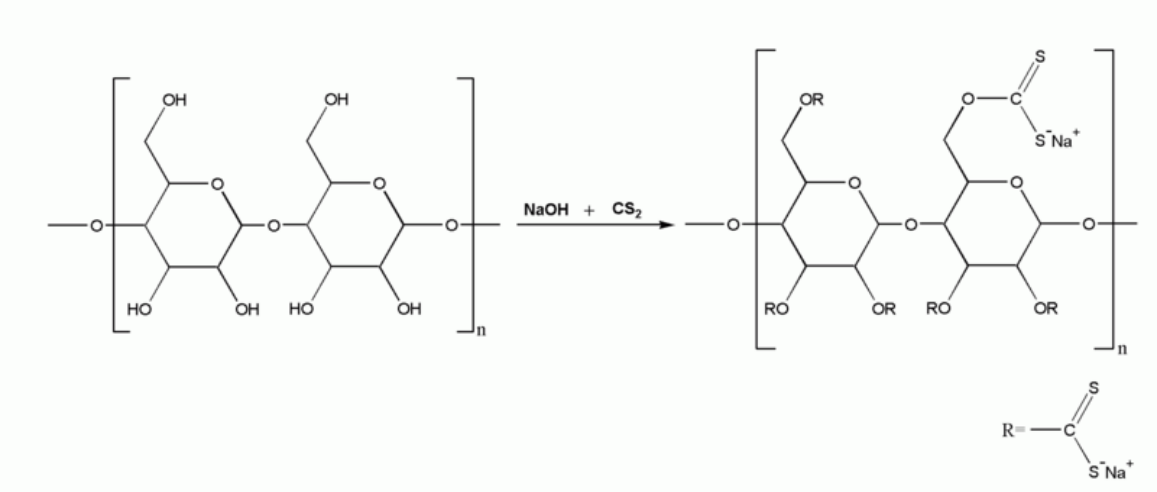

Fig 1: Cellulose is treated with alkali and carbon disulphide to yield viscose (Source: Wikipedia)

Viscose Fibre Morphology

Viscose is a fine regular filament or staple fibre. The staple fibre is manufactured in a crimped configuration to enhance the inter fibre friction for better fibre cohesion for easy further processing. Crimped viscose staple fibre spins into yarn with sufficient irregularity to make the crimped fibre yarn aesthetically more desirable.

Viscose Polymer structure

Viscose polymer is a linear cellulose polymer, which is similar to cotton but without spiral configuration like cotton polymer. Unlike cotton, Viscose polymer is 60-65% amorphous and shorter polymers. On the contrary, Cotton has 65-70% crystalline region and 30-35% amorphous region. Polymer thickness of all viscose and cotton is similar, which is 0.8nm. Degree of polymerization of viscose is very low as 175 than cotton, which has high degree of polymerization of 5000. Due to this, polymer length of viscose is just 180 causing low strength than cotton, which has polymer length of as high as 5000.

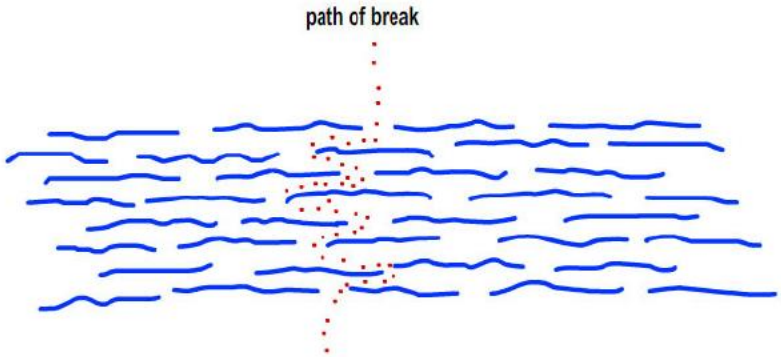

Fig 2: Weak fibre as it has short 'path of break' (source: www.nptel.ac.in)

Effect of polymer structure on quality characteristics of viscose yarn

The very high amorphous region, shorter and poor alignment of viscose polymers gives rise to fewer hydrogen bonds. Very amorphous nature of its polymer system permits the entry of water molecules , which pushes the polymer molecules apart, breaking a significant number of hydrogen bonds, resulting the weaker fibre when wet.

When the fibre is put under strain, its amorphous region and fewer hydrogen bonds give away easily causing permanent de-shape. Hence viscose material will become distorted, stretched, wrinkled or creased.

Due to very high amorphous region (60-65%) of viscose fibre, it has following properties by virtue of it:

- More absorbent
- Weak
- Less durable
- More easily degradable by chemical
- More easily dyed
- More pliable and softer handling
- Plastic and more easily distorted

The table below shows the comparative rating of Cotton, Viscose and Polyester

Cite this article as: Dr. T. Ramachandran, A. Thirunarayanan. "OVERVIEW AND SIGNIFICANCE OF VISCOSE YARN QUALITY CHARACTERISTICS AND SUGGESTIVE PROCESS TO IMPROVE IT." *International Conference on Systems, Science, Control, Communication, Engineering and Technology (2015)*: 01-04.

Sl No	Parameter	Comparative Rating		
		Cotton	Viscose	Polyester
I	**Comfort**			
1	Moisture Regain	Good	Very Good	Poor
2	Thermal Protection	Good	Very Good	Poor
3	Air Permeability	Very Good	Good	Poor
4	Softness	Good	Very Good	Poor
5	Smoothness	Poor	Good	Very Good
6	Static dissipation	Good	Very good	Poor
II	**Aesthetic**			
1	Drape	Good	Very Good	Poor
2	Lustre	Poor	Very Good	Very Good
3	Crease recovery	Poor	Poor	Very Good
4	Colour Uniformity	Poor	Very Good	Good
III	**Utility Performance**			
1	Anti-Pilling	Good	Very Good	Poor
2	Wash & Wear	Good	Poor	Very Good
3	Durability	Fair	Fair	Very Good

Table 1: Comparative rating of Cotton, Viscose & Polyester (Source: www.Swicofil.com/viscose)

From the above table it is evident that viscose has several good characteristics than other synthetic fibres and hence when blended properly with other synthetic fibres, it exhibits extraordinary quality characteristics for the blended yarn-fabric.
Viscose fibre when processed to form a yarn, particularly in Ring spinning route, passes through several mechanical actions at different processes from fibre stage to yarn stage and also up to winding. Due to peculiar viscose polymer structure as explained above, these mechanical processes give rise to more strain to the fibres causing lesser inter fibre cohesion and leading to fibre migration and more hairiness than cotton or other synthetic fibres like polyester.

Yarn Hairiness

Yarn hairiness is either being a desirable or undesirable property; hence it assumes importance in measurement and controlling. Hairiness keeps important role for producing quality yarn. High hairiness causes pilling on fabric. Hairiness imparts fuzzy appearance to the yarn and reduces lustre of yarn. It also hampers sizing process and causes more breaks during weaving.
As per study conducted by Pinar celik & Huseyin Kadoglu[2], Viscose yarn has the least liveliness factor, Kr (Kringel factor) than cotton & polyester for the same twist factor values. This proves that due to mechanical action of viscose during various processes, the internal polymer structure causes permanent damage to the structure and behaves like plastic. Hence more the mechanical action is involved to viscose fibre, more hairiness is generated. This causes even the compact spinning of viscose is not as successful as for cotton although

Cite this article as: Dr. T. Ramachandran, A. Thirunarayanan. "OVERVIEW AND SIGNIFICANCE OF VISCOSE YARN QUALITY CHARACTERISTICS AND SUGGESTIVE PROCESS TO IMPROVE IT." *International Conference on Systems, Science, Control, Communication, Engineering and Technology (2015)*: 01-04.

efforts are on to bring in more successes. Therefore, the best way to remove hairiness is by singeing process, where the removal of hairs is permanent and less chance for pilling at later processes and usage. By singeing process the hairiness on viscose yarn surface can be controlled very effectively than other processes like compact spinning.
Recently vortex method of spinning is quite popular and proven to produce less hairy viscose yarns and the hairiness on vortex viscose yarn surface is much lower than the ring spun viscose yarn of same linear density, but at the cost of compromise on fabric feel with vortex yarn. Vortex viscose yarn is relatively rougher than ring spun viscose yarn of same count. So ring spun viscose yarn with singeing process can yield better hairiness results without compromise on yarn and fabric feel.

Conclusion

Viscose fibre polymer has high amorphous region of 60-65% and crystalline region of only 35%-40%. The high amorphous region together with shorter polymer chain and less degree of polymerization (175) than cotton (5000) causes viscose yarn more weak. The above is responsible for viscose to behave like plastic causing permanent damage to the yarn structure. However, by virtue of presence of high amorphous region, viscose has certain good properties, which makes the fibre best suitable for blends for achieving ultimate fabric properties for textile applications. The fabrics made out of viscose blends are widely popular due to its user friendly quality characteristics.

References

1. X Wang and L Chang: An Experimental Study on Effect of Test Speed on Yarn Hairiness, Textile Research Journal 1999 69: 25.
2. Pinar celik & Huseyin Kadoglu: A Research on Yarn Liveliness tendency of Staple yarns, Tekstil ve Konfeksiyon 3/2009: 189
3. K.P.R. Pillay, A study of the hairiness of cotton yarns, Textile Research Journal, 1964 34: 663.
4. Bhupender S. Gupta, Dame S. Hamby, Fibre migration in staple yarns, Textile Research Journal, 1969 39: 55.
5. J. W. S. Hearle, B.C. Goswami, Migration of fibres in yarns, Textile Research Journal, 1968 38: 780.
6. Hassan M. El-Behery, Study of theories of fibre migration, Textile Research Journal, 1968 38: 321.
7. J.P.Rust, S. Peykamian, Yarn hairiness and the process of winding, Textile Research Journal, 1992 62: 685.
8. D.R.Morey, The relation of orientation to physical properties of Cotton and Rayons, Textile Research Journal, 1935 5: 483.
9. Nazan Erdumlu et al, Investigation of Vortex Spun Yarn Properties in Comparison with Conventional Ring and Open-end rotor spun yarns, Textile Research Journal 2009 79:585
10. Huseyin Gazi Ortlek, Levent Onal, Comparative study on the characteristics of knitted fabrics made of Vortex-spun viscose yarns, fibers and polymers 2008, Vol 9, No.2, 194-199
11. www.ssm.ch
12. http://www.nptel.ac.in/courses/116102026/classifications
13. http://www.nptel.ac.in/courses/116102026/cotton
14. http://www.nptel.ac.in/courses/116102026/esstential properties

Cite this article as: Dr. T. Ramachandran, A. Thirunarayanan. "OVERVIEW AND SIGNIFICANCE OF VISCOSE YARN QUALITY CHARACTERISTICS AND SUGGESTIVE PROCESS TO IMPROVE IT." *International Conference on Systems, Science, Control, Communication, Engineering and Technology (2015)*: 01-04.

International Conference on Systems, Science, Control, Communication, Engineering and Technology 2015 [ICSSCCET 2015]

ISBN	978-81-929866-1-6	**VOL**	01
Website	icssccet.org	**eMail**	icssccet@asdf.res.in
Received	10 - July - 2015	**Accepted**	31- July - 2015
Article ID	ICSSCCET002	**eAID**	ICSSCCET.2015.002

INFLUENCE OF PLASMA TREATMENT ON FASTNESS PROPERTIES OF NATURAL DYES APPLIED ON HANDLOOM COTTON FABRICS

S.R. Kalimuthu[1], Dr. T. Ramachandran[2]
[1]Department of Textile Technology, Karpagam University, Coimbatore, India.
[2]Principal, Karpagam Institute of Technology, Coimbatore, India.

Abstract: *Many unconventional methods and techniques are tried in wet processing of textile material to have better environmental pollution free and eco-friendly process. The plasma is the one of techniques which enable to modify the surface structure of textile materials. In this work, plasma technique is adopted to develop surface modified handloom cotton fabric. The treated cotton fabric is subjected to dye using natural materials like Camellia sinensis (Tea leaves powder), Vulgaris Conditiva (Beet root) and Curcuma longa (Turmeric). There is a significant improvement in colour fastness both washing and rubbing of plasma treated fabric when compared to untreated fabric. This study has very good scope for the value addition of handloom fabrics which inturn enhance the livelihood condition of the handloom society.*

Keywords: Natural dyes , Plasma, Mordant and Handloom Fabric

1. Introduction

The plasma is the one of techniques which enable to modify the surface structure of textile materials. Since the plasma treated fabric having better absorbancy characteristic, it saves water, chemicals and energy during wet processing. The natural dyes are widely being accepted due to its biodegradability and low toxicity when compare to synthetic dyes. Plasma treatment and natural dyeing are having very good scope due to eco-friendly, less allergic to skin, biodegradability and low toxicity.
So the plasma technique was experimented in this study, to modify the surface property of the handloom cotton fabrics which inturn improves the absorbency characteristic of the fabric. This enhances dyeability and fastness properties of the handloom cotton fabrics at affortable cost. Due to this attempt, the value addtion of handloom cotton fabrics tends to enhance the socioeconomic conditions of handloom cotton weavers.

2. Materials and Methods

2.1 Materials

The handloom cotton fabric of plain weave was selected for this study. The warp count is $2/40^{S,}$ weft count is $14^{S,}$ with 54 Ends per inch and 42 Picks per inch. The Natural dyes such as *Camellia sinensis* (Tea Leaves Powder) , *Vulgaris* Conditiva (Beet Root), and *Curcuma longa* (Turmeric) have been used for this study.

Cite this article as: S.R. Kalimuthu, Dr. T. Ramachandran. "INFLUENCE OF PLASMA TREATMENT ON FASTNESS PROPERTIES OF NATURAL DYES APPLIED ON HANDLOOM COTTON FABRICS." *International Conference on Systems, Science, Control, Communication, Engineering and Technology (2015)*: 05-08. Print.

Most of the vegetable ingredients do not colour the cellulosic materials directly. It requires a metallic or vegetable mordant to retain the colour on the material. Commonly used mordents are Alum and Myrobolan. Myrobolan is a universal vegetable mordant containing tannic acid which act as a mordant to combine with metallic salt to anchor the natural dyes.

2.2 Methods

The Plasma System with frequency of 60KHZ and an Aluminum & Electrode with Gap of 7.5 cm with the high voltage of 300 volts X 50m.amp have been used. The Oxygen and Organ gases with a Pressure of 5 X 10^{-2}m.bar are used. Then the handloom cotton samples were dyed using the above mentioned natural dyes. The assessment of colour fastness has been carried out as per ISO namely ISO 105-C10: 2006 for washing fastness and ISO 105- X12: 2001 for rubbing fastness.

3. Result & Discussion

The test results of handloom cotton fabrics of plasma treated and untreated samples dyed with natural dyes such as *Camellia sinensis* (Tea Leaves Powder) , *Vulgaris* Conditiva (Beet Root), and *Curcuma longa* (Turmeric) with Myrobolan and Alum as mordants have been shown.

Table 1 Colour fastness test results of treated and untreated plasma handloom cotton fabric

Sl No	Sample	Details		Washing Fastness		Rubbing Fastness	
				Change in color	Staining	Staining	
						Dry	Wet
1	Sample 1 *Camellia sinensis* (Tea leaves Powder) with Myrobolan	Untreated Fabric	-	1	1	1	1
		Treated Fabric	Oxygen	2	2	2	1
			Organ	2	2	2	1
2	Sample 2 *Camellia sinensis* (Tea leaves Powder) with Alum	Untreated Fabric	-	1	1	1	1
		Treated Fabric	Oxygen	2	2	2	1
			Organ	2	2	2	1
3	Sample 3 *Vulgaris* Conditiva (Beet Root) with Myrobolan	Untreated Fabric	-	1	1	1	1
		Treated Fabric	Oxygen	2	2	2	1
			Organ	2	2	2	1
4	Sample 4 *Vulgaris* Conditiva (Beet Root) with Alum	Untreated Fabric	-	1	1	1	1
		Treated Fabric	Oxygen	2	2	2	1
			Organ	2	2	2	1
5	Sample 5 *Curcuma longa* (Turmeric) with Myrobolan	Untreated Fabric	-	1-2	2	1-2	1
		Treated Fabric	Oxygen	2-3	2-3	2-3	2-3
			Organ	2-3	2-3	2-3	2-3
6	Sample 6 *Curcuma longa* (Turmeric) with Alum	Untreated Fabric	-	1-2	2	1-2	1
		Treated Fabric	Oxygen	3	3	3	3
			Organ	3	3	3	3
7	Sample 7 *Curcuma longa* (Turmeric) with Myrobolan & Alum	Untreated Fabric	-	2-3	2-3	2-3	2-3
		Treated Fabric	Oxygen	4-5	4	4-5	4
			Organ	4	4	4	4

From the table 1, *Camellia sinensis* (Tea leaves Powder) and *Vulgaris* Conditiva (Beet Root) natural dyes with Alum and Myropolan mordants have poor fastness property. *Curcuma longa* (Turmeric) natural dye with Alum mordant with oxygen gas plasma show good fastness property (sample 6). *Curcuma longa* (Turmeric) natural dye with Alum and Myrobolan double mordants with oxygen gas plasma shows better fastness property (sample 7) than *Curcuma longa* (Turmeric) natural dye with alum single mordant (sample 6).

Cite this article as: S.R. Kalimuthu, Dr. T. Ramachandran. "INFLUENCE OF PLASMA TREATMENT ON FASTNESS PROPERTIES OF NATURAL DYES APPLIED ON HANDLOOM COTTON FABRICS." *International Conference on Systems, Science, Control, Communication, Engineering and Technology (2015)*: 05-08. Print.

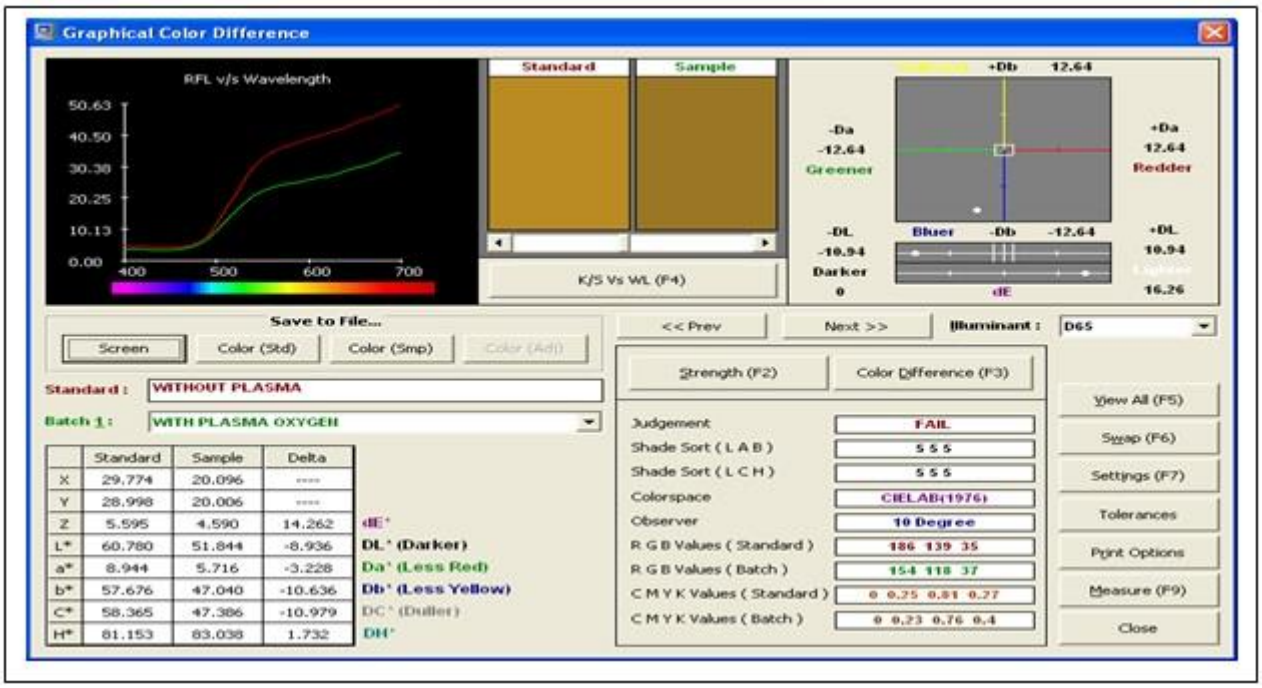

Figure 1 Computer colour matching results of treated and untreated plasma with oxygen gas on handloom cotton Fabric.

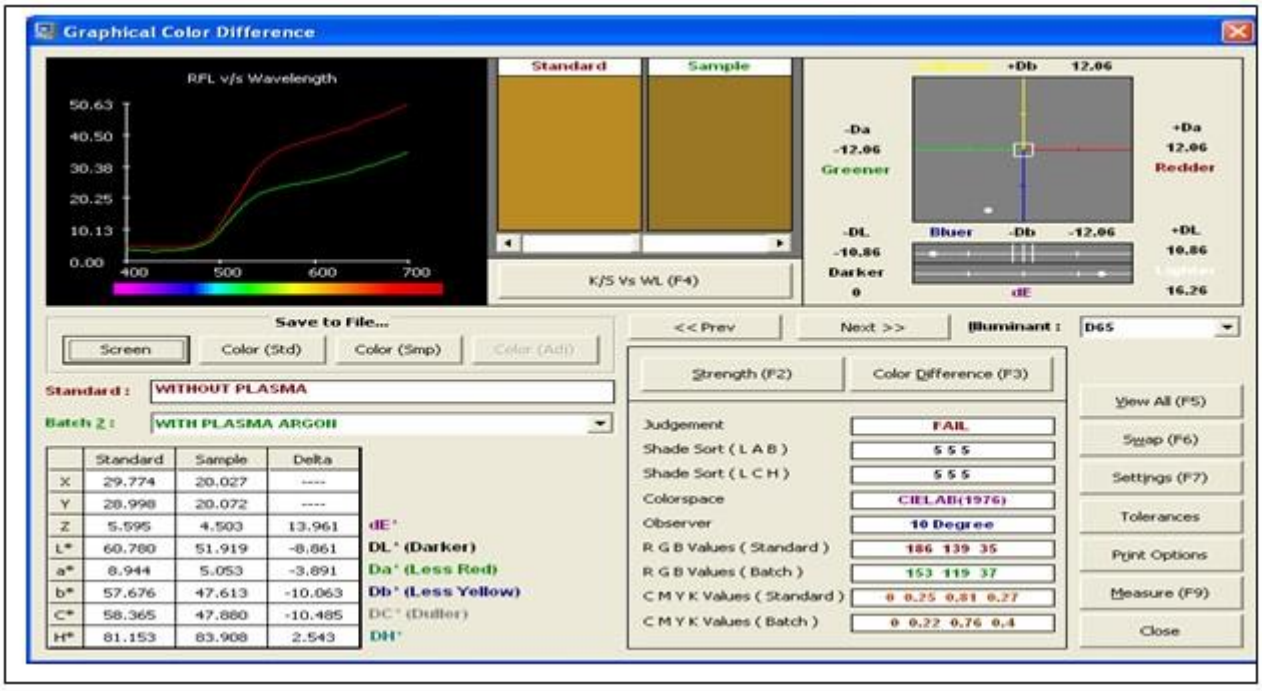

Figure 2 Computer colour matching results of treated and untreated plasma with argon gas on handloom cotton fabric

From figure 1 and 2 dE colour value for oxygen gas plasma treated with *Curcuma longa* (Turmeric) natural dyed handloom cotton fabric has better value of 14.262 than that of organ gas plasma treated *Curcuma longa* (Turmeric) natural dyed handloom cotton fabric has better dE value 13.961.

4. Conclusion

The Myrobolan and Alum double mordants natural dye *Curcuma longa* (Turmeric) on handloom cotton fabric treated with oxygen gas plasma has better washing and rubbing colour fastness than Myrobolan or Alum single mordant. Simillarly the computer colour

Cite this article as: S.R. Kalimuthu, Dr. T. Ramachandran. "INFLUENCE OF PLASMA TREATMENT ON FASTNESS PROPERTIES OF NATURAL DYES APPLIED ON HANDLOOM COTTON FABRICS." *International Conference on Systems, Science, Control, Communication, Engineering and Technology (2015)*: 05-08. Print.

matching results also shows that the Myrobolan and Alum combined mordants with natural dye *Curcuma longa* (Turmeric) on handloom cotton fabric treated with oxygen gas has better dE value of 14.262 than that of organ gas plasma treated dE value of 13.961. Hence for the value addition of handloom cotton fabric can be done by using natural dye namely *Curcuma longa* (Turmeric) on plasma treated handloom cotton fabrics.

5. References

1) Natural dyes for textiles and their eco friendly applications by Niyathi Battachayya
2) Chemistry of dyes and principles of dyeing by V A Shenai
3) Novel trends in Textile Wet Processing by Dr.T.Ramachandran, Vol 89,IE (I)Journal of Textiles
4) Application of Plasma in Textile Industry by O.L.Shanmugasundram,Textile Asia Vol5 2006
5) Effect of Plasma on Fabrics by M N Subulakshmi,Indian Textile journal, vol 10,1998
6) Plasma Textile Technology by P B Jhala , NID Publications 2006
7) A review of Plasma treatment for application on textile substrate by Aasim Ahmed 2007
8) Plasma treatment advantages for textiles by Amelia Sparavigna
9) Natural dyes in Textile Application By G W Taylor Vol 16,1986
10) Dyeing Of Textiles With Natural Dyes - An Eco-Friendly Approach by R.Kanchana and Reshma Mohan, International Journal of Chem Tech Research 2013
11) Application natural dyes on Textiles by Ashis Kumar Smatha, Indian Journal of Fibres & Textile Research Sep 2009.

Cite this article as: S.R. Kalimuthu, Dr. T. Ramachandran. "INFLUENCE OF PLASMA TREATMENT ON FASTNESS PROPERTIES OF NATURAL DYES APPLIED ON HANDLOOM COTTON FABRICS." *International Conference on Systems, Science, Control, Communication, Engineering and Technology (2015)*: 05-08. Print.

International Conference on Systems, Science, Control, Communication, Engineering and Technology 2015 [ICSSCCET 2015]

ISBN	978-81-929866-1-6
Website	icssccet.org
Received	10 - July - 2015
Article ID	ICSSCCET003

VOL	01
eMail	icssccet@asdf.res.in
Accepted	31- July - 2015
eAID	ICSSCCET.2015.003

INFLUENCE OF CHITOSAN NANOPARTICLES ON REACTIVE DYEING OF COTTON FABRICS

K. Karthikeyan[1], Dr.T. Ramachandran[2]
[1]Department of Textile Technology, Karpagam University, Coimbatore
[2]Principal, Karpagam Institute of Technology, Coimbatore

ABSTRACT: Cotton textiles are dyed mostly with reactive dyes because they produce a wide range of bright colors with excellent colour fastness to washing. However, the reactive dyeing requires considerable quantities of inorganic salt and alkali for efficient utilization and application of dyes. These inorganic salts when drained to effluent generate huge amounts of total dissolved solids leading to serious environmental pollution. Considerable remedies are being measured within the textile processing industry to reduce the effluent pollution and to fulfill the environmental regulations. This work is a part of such efforts and presents results where cotton fabrics pretreated with chitosan nanoparticles and reactive dyeing carried out without salt. In this work, chitosan nanoparticle was used for developing salt free eco-friendly reactive dyeing. The effect of chitosan nanoparticles in color strength (K/S value), color difference, color fastness to crocking and washing of the cotton fabric was investigated. The cotton fabric treated with 0.5 (w/v) chitosan nanoparticles had higher K/S values.

Keywords: Cotton, chitosan nanoparticles, colour strength, fastness, reactive dye

INTRODUCTION

Eco-friendly textile wet processing techniques have been increasing in recent years due to the increased awareness of environmental issues throughout the world. Now-a-days consumers in developed countries are demanding bio-degradable and eco-friendly textiles. In dyeing of textiles, ecological restrictions are strictly followed from raw material selection, processing and water management to the final product. Cotton fibers are widely applied in textile industry due to its excellent properties of moisture regain, permeability of air, bio-degradability, no static electricity, etc.

The dyeing of these fibers is generally done with reactive dyes due to its variety of hue, high fastness, convenient usage and range of applicability. These reactive dyes contain a reactive group i.e. vinyl sulphone or triazine , that, when applied to a fiber in an alkaline dye bath, forms a chemical bond with hydroxyl (OH) group on the cellulosic fiber.

In recent years, reactive dyes maintain the largest annual consumption in the world among the dyes used for which establishes its important status in the dye manufacture industry. But important problems, such as low dye substantivity to cotton require large amount of electrolyte used and high volume of wastewater discharged, always exist in the application of reactive dyes. The dyeing of cotton with reactive dyes demands from 70 to 150 liter water, 0.6-0.8 Kg NaC1 and from 30 to 60 g dyestuffs. Due to these important problems, reactive dyes is the most unfavorable one from the ecological point of view, these effluents produced high values of Total Dissolved Solids and increases salinity of the rivers affects the delicate of aquatic life. Tons of reactive dyes are produced and

Cite this article as: K. Karthikeyan, Dr. T. Ramachandran. "INFLUENCE OF CHITOSAN NANOPARTICLES ON REACTIVE DYEING OF COTTON FABRICS." *International Conference on Systems, Science, Control, Communication, Engineering and Technology (2015)*: 09-12. Print.

consumed each year, making it possible to intensify the total amount of pollution caused by their use. Therefore, the better approach would be required to improve the textile processing in the discharge of pollution. The unique characters of nanoparticles for their small size and quantum size effect supposedly promised chitosan nanoparticles to exhibit superior dye ability improvement. The main objective of this research is to study influence of chitosan nanoparticles on cotton reactive dyeing and possibilities to reduce the colorants and chemical auxiliaries in the dyeing effluents.

2. MATERIALS AND METHODS

The grey cotton fabric for dyeing having the specification of 140 g/ m^2, warp 34 threads/cm, Yarn count 40/1, weft 33 threads/cm was used. Reactive dyes namely C.I. Reactive Red 6 was purchased. Chitosan was provided by Indian sea food industry, Cochin. (Degree of deacetylation (DD) = 92.5%, Molecular Weight=1000kD. All other reagents are commonly used laboratory reagent grade.

2.1 Preparation of chitosan nanoparticles

Chitosan was dissolved in a dilute aqueous acetic acid solution of 0.5 % (w/v) using microwave. Aqueous ammonia was then dropped into the chitosan solution to precipitate the chitosan. The obtained gel-like swollen chitosan was washed to neutral with DI water, and was then transferred into a 25 mL volumetric flask. The total volume of liquid was added to 25 mL with DI water. An ultrasound processor with a probe of 6 mm diameter was used. The ultrasound probe was put into the volumetric flask and was kept at 1 cm below the water level. Ultrasound treatment was conducted under an ice-water bath. Finally, a milky emulsion was obtained.

2.2 Pre-treatment of cotton with nano chitosan

Pre-washed cotton fabrics were soaked for 15 minutes in the emulsions with different concentrations separately: 0.01%, 0.05%, 0.1%, 0.3% and 0.5% (w/v). The padding processes were then completed with pick up weight of around 80%. Finally, the cotton fabrics were dried at 80 °C for 3 min and cured at 150 °C for 3 min and finally rinsed with warm water (40 °C) for 1 min. Finally fabric rinsed with running cold water and dried again.

2.3 Reactive Dyeing

In a dye bath containing 3% of CI Reactive Red 6 with liquor ratio 1:30, cotton fabric was added at 35 °C and the temperature is raised to 80 °C over 20 min. Liquor ratio 1:30 is used due to maximum depth of shade on fabric. After which time the dyeing is continued for 30 min. Then 5 g/l soda ash added portion wise and the dyeing is maintained for further 45 min. For comparison, conventional dyeing carried out in untreated cotton fabrics. Dyed samples were thoroughly washed in hot water at 60°C, then washing with a solution containing 4g/l nonionic detergent and 1g/l sodium carbonate at 30°C for 15 min. and finally rinsing with cold water then air dried.

2.4 Evaluation of the dyed cotton fabrics

The color strength (K/S) of the treated sample using the untreated samples as blank was determined using X-rite spectrophotometer, Model colour- i5 equipped with integrated sphere according to Kubelka- Munk equation.

$$K/S = (1-R)^2 / 2R \quad (1)$$

R: Decimal fraction of the reflectance of dyed samples,
K: Absorption coefficient,
S: scattering coefficient

3. RESULTS AND DISCUSSION

3.1 Colour Strength

K/S value of a dyed material has a close relationship to the amount of dye absorbed by the yarn. K/S values of pretreated with nano chitosan cotton dyed samples with Reactive Red 6 are shown in *Table 1*. It can be concluded that the K/S values of 0.5% chitosan treated dyed fabrics are higher than that of untreated dyed samples. As the chitosan concentration increases, the dye uptake also increases.

Cite this article as: K. Karthikeyan, Dr. T. Ramachandran. "INFLUENCE OF CHITOSAN NANOPARTICLES ON REACTIVE DYEING OF COTTON FABRICS." *International Conference on Systems, Science, Control, Communication, Engineering and Technology (2015)*: 09-12. Print.

Table 1 K/S Values of dyed fabrics

Dyes	Chitosan concentration (%)	ΔE	K/S
Reactive Red 6	0	-	8.246
	0.01	1.546	7.254
	0.05	1.454	7.374
	0.1	1.310	7.523
	0.3	1.012	7.975
	0.5	0.654	8.256

The enhanced dyeability of the modified fabric is likely resulted from the reduction of the coulombic repulsion between the fabric surface and the anionic dye molecules in the presence of the positively charged chitosan on the surface. The cationic charged amino groups may be involved in the adsorption of anionic chromospheres of reactive dyes. The improved dye ability is due to the presence of amine groups available from the chitosan which also tends to improve the reactivity of cellulosic substrate.

.

3.2 Fastness Properties

The attachment of the dye molecules onto the partially-modified cellulosic substrate is by covalent bonding since no dyes strips out from the dyed sample. This is indicative through the fastness properties. Table 2 shows the fastness values of all such dyed samples are quite satisfactory and comparable with those of conventional dyed samples.

Table 2 Colour Fastness Properties

Dyes	Chitosan concentration (%)	Wash Fastness		Crock Fastness		Light Fastness
		Colour change	Staining on cotton	Dry	Wet	
Reactive Red 6	0	4	4-5	4-5	3-4	4
	0.01	4	4-5	4-5	3-4	4
	0.05	4	4-5	4-5	3-4	4
	0.1	4	4-5	4-5	3-4	4
	0.3	4	4-5	4-5	3-4	4
	0.5	4	4-5	4-5	3-4	4

3.3 Physical Properties

It is inferred from the Table 3 that there is a change in air permeability of the nano-chitosan treated cotton fabric as compared to the untreated one. It is perhaps due to the attachment of chitosan to all over the whole structure of the fabric. The slight losses of air permeability in the pretreated fabrics have not affected intact breathability of the cotton fabrics. There is no apparent change in tensile strength of dyed fabrics.

Cite this article as: K. Karthikeyan, Dr. T. Ramachandran. "INFLUENCE OF CHITOSAN NANOPARTICLES ON REACTIVE DYEING OF COTTON FABRICS." *International Conference on Systems, Science, Control, Communication, Engineering and Technology (2015)*: 09-12. Print.

Table 3 Physical Properties of dyed fabrics

Dyes	Chitosan concentration (%)	Tensile Strength – Warp (N)	Air Permeability ($l/m^2/s$)
Reactive Red 6	0	351.5	480.5
	0.01	347.4	465.5
	0.05	345.6	463.7
	0.1	344.2	461.2
	0.3	343.9	458.4
	0.5	343.5	456.7

3.4 Dyeing Effluent Analysis

Table 4 shows that new method of eco friendly dyeing (0.5% chitosan treated) provided around 72% Total Dissolved Solids reduction in the effluent of CI Reactive Red 6.

Table 4 TDS of dyeing effluents

Dye	Effluent samples (Dyebath recipes diluted 100 times)	TDS (mg/l)
Reactive Red 6	Untreated Sample	1360
	Chitosan Treated Sample	380

4. CONCLUSION

The cotton fabrics were treated with different amounts of chitosan nanoparticles and reactive dyeing carried out without salt. It was found that reactive dye by increasing in chitosan concentration, there was a significant improvement in color strength (K/S). Pretreatment of cotton with chitosan nanoparticles enhances the possibility of dyeing cotton with reactive dyes without addition of salt. Reactive dyes can be much more efficiently exhausted onto cellulosic fabrics under neutral conditions in the absence of salt due to change of electrokinetic potential of chitosan treated samples. Moreover, the fastness values of all such dyed samples are quite satisfactory and comparable with those of conventional dyed samples. Dyeing effluent showed enormous reduction of Total Dissolved Solid content (TDS), which is essential requirement for textile industry.

5. REFERENCE

1. Allegre, C. **2006**, Treatment and reuse of reactive dyeing effluents, Journal of Membrane Science 269: 15 –34
2. Anderson, C. B. **1994**, Dyeing reactive dyes using less salt, *American Dyestuff Reporter,* 83: 103-105
3. Cakara, D., Fras Zemljic, L., Bracic, M., Stana-Kleinschek, K**. 2009**. Protonation behavior of cotton fabric with irreversibly adsorbed chitosan: A potentiometric titration study. *Carbohydrate polymers.*78, 1: 36-40
4. Myllyte, P., Salmi, J., Laine j**. 2009**. The influence of pH on the adsorption and interaction of chitosan with cellulose. *Bio Resources*, 4, 4: 1674
5. Lili Wang, Wei Ma. **2009**, Preparation of cationic cotton with two-bath pad-bake process and its application in salt-free dyeing, Carbohydrate Polymers 78: 602–608
6. Kunal Singha, Subh Maity, Mri Singha.**2012**, The Salt-Free Dyeing on Cotton, Jou.of Textile science 6:69-77

Cite this article as: K. Karthikeyan, Dr. T. Ramachandran. "INFLUENCE OF CHITOSAN NANOPARTICLES ON REACTIVE DYEING OF COTTON FABRICS." *International Conference on Systems, Science, Control, Communication, Engineering and Technology (2015)*: 09-12. Print.

International Conference on Systems, Science, Control, Communication, Engineering and Technology 2015 [ICSSCCET 2015]

ISBN	978-81-929866-1-6	**VOL**	01
Website	icssccet.org	**eMail**	icssccet@asdf.res.in
Received	10 - July - 2015	**Accepted**	31- July - 2015
Article ID	ICSSCCET004	**eAID**	ICSSCCET.2015.004

EFFECT OF SURFACE MODIFICATION ON COMFORT PROPERTIES OF INNER LAYER LYOCELL FABRIC IN MULTILAYERED TECHNICAL TEXTILES

Dr. T. Ramachandran[1], L.Hari Gopalakrishnan[2]
[1]Principal, Karpagam Institute of Technology, Coimbatore, India.
[2] Department of Textile Technology, Karpagam University, Coimbatore, India

ABSTRACT: *Lyocell microfibre fabrics were produced using rapier weaving machine, which is to be used as inner layer while developing the Multilayered Technical Tecxtiles. The lyocell microfibre fabric has been treated with plasma using low pressure Oxygen. Then the plasma treated and untreated fabrics were dyed using reactive dyes. The dyed lyocell fabrics of plasma treated and untreated were tested for the comfort properties such as Wickablity, Air Permeablilty and Water Vapour Permeablilty. The results of the study confirmed that there is a significant improvments in Wickablilty and Air permeablilty of plasma treated fabrics which are essential characteristics for inner layer of the Multilayered Technical Textiles. The significant improvements due to new porus in the treated fabrics allow more air to penterate and also to increase the Wickablilty. Where as the Water Vapour Permeablilty characteristics of the untreated fabric have better results than plasma treated fabrics due to new etching on the surface of the treated fabrics which retain more vapour than untreated fabrics. The Plasma treated lyocell fabric can be used as inner layer for the development of Multilayered Technical Textiles.*

Keywords: Microfibre, Lyocell, Plasma, Reactive, Water Vapour, Wicking, Multilayered Fabrics.

1. INTRODUCTION

The plasma is an ionized gas and at a high temperatur the molecules in the ionized gas gain energy. The energy is used to modify the surface of the textile materials to produced new pours and etching effects.This resulting in improvements in certain characteristics of textiles material such as absorbency,wickablilty and air permeablilty when compare to conventional fabrics. From an ecological point of view plasma technology has many advantages such as ecofriendly and less pollution when compared to conventional methods of chemical wet processing.

Recently, plasma treatments have been investigated for producing hygroscopicity in fibers, making them more comfort which suit for sports and active wear. Plasma treatment of polymers results in etching and changes in a microstructure on the surface by occurrence of new functional groups and cross linking of macromolecular chains.

Cite this article as: Dr. T. Ramachandran, L. Hari Gopalakrishnan. "EFFECT OF SURFACE MODIFICATION ON COMFORT PROPERTIES OF INNER LAYER LYOCELL FABRIC IN MULTILAYERED TECHNICAL TEXTILES." *International Conference on Systems, Science, Control, Communication, Engineering and Technology (2015)*: 13-16. Print.

Plasma processes have been utilized to improve the surface properties of fibres in many applications. The fibres that can be modified by plasma include almost all kinds of fibres, likes metallic fibres, glass fibres, carbon fibres and organic fibres. Microfibers are very fine fiber compared to conventional fibers that define its unique and desirable properties. Microfibers are synthetic fibres that are finer than any other natural fibres. Microfibers are usually produced in polyester, polyamide, acrylic, modal, Lyocell and viscose in the range of 0.5-1.2 dtex. In this work Lyocell Microfibre is identify to develop inner layer fabrics.

Lyocell is a biodegradable material made from wood pulp cellulose and it is recyclable. Lyocell is an improved fibre, in terms of performance & properties and also friendly to the environment. This work aims at plasma treatment for lyocell microfiber fabrics for improvement in comfort properties and dyeability.The plasma treated fabrics has significantly suitable as inner layer which is kin to skin towards the comfort characteristics.

2. MATERIALS AND METHODS

In this work the inner layer Lyocell fabrics is made out of both warp and weft in Ne 60 ^{s} by using 0.7dtex denier fibre in the yarn.The fabric has palin weave with 80grams per squre meter weight .The light weight fabric more suitable for the inner layer of multilayered fabric which enhace the better comfort charcteristics. In plasma treatment the Oxygen is used and Hydropneo Vac Technologies apparatus was employed for the treatment of low temperature plasma on the Lyocell fabric. In the treatment, oxygen gas was used as plasma throughout this study. The gas flow rate and plasma temperature were kept at 10 Pa, 4 cc/min and 33°C respectively. The output power used was kept at 300 V and the experiment was carried out for 10 minutes.

The plasma treated and untreated fabrics were subjected to test the comfort properties like Wickablity (AATCC 197 /198), Air Permeability (ISO 9237) and Water Vapour Permeability (ASTM E96) by using standard testing procedures.

3. RESULTS AND DISCUSSION

The surface modified lyocell inner layer fabric and untreated fabric have been tested to assess the characteristics of wickablity; air permeablity and water vapour permeablity. The test report have been critically analysed and details are given below

3.1 WICKING

The table 1 shows wicking time in seconds for untreated and plasma treated lyocell fabric in both warp and weft direction at different wicking heights.The wicking time to reach a height of 5cm is 34.34 seconds in warp and 30.20 Seconds in weft direction. The wickability of lyocell fabric treated with oxygen plasma increased from 28% to 40 %.

Table 1. Wicking tests for untreated and plasma treated tencel fabric samples.

Sl No	Sample Particulars	Untreated fabric		Plasma treated fabric	
	Wicking Height in CMS	Warp wicking Time in Sec	Weft wicking time in Sec	Warp Wicking Time in sec	Weft Wicking Time in sec
1	1 CM	02.99	00.55	02.00	00.57
2	2 CM	08.43	03.42	04.70	02.54
3	3 CM	18.27	10.32	08.99	05.60
4	4 CM	49.55	24.41	19.58	16.21
5	5 CM	56.95	41.89	34.34	30.20

The fig 1 indicates the wicking behaviour of plasma treated and untreated samples and it is absorbed from that the plasma treated lyocell fabrics in both warp and weft directions show a significant reduction in wicking time (sec) indicating a faster rate of absorption.

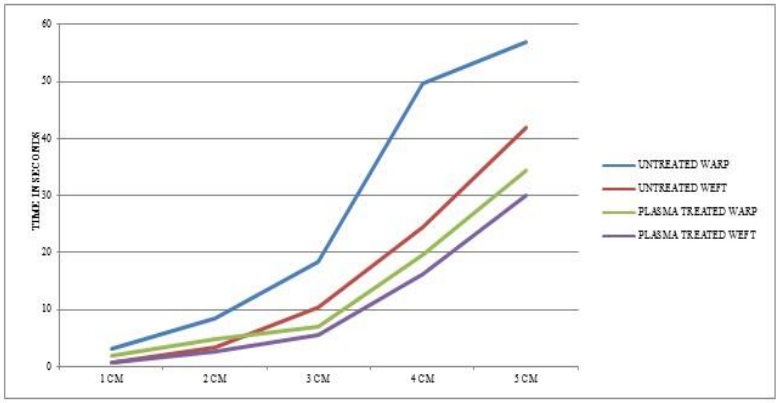

Fig 1. Wickablilty Curve for untreated and plasma treated samples in warp and weft direction.

Cite this article as: Dr. T. Ramachandran, L. Hari Gopalakrishnan. "EFFECT OF SURFACE MODIFICATION ON COMFORT PROPERTIES OF INNER LAYER LYOCELL FABRIC IN MULTILAYERED TECHNICAL TEXTILES." *International Conference on Systems, Science, Control, Communication, Engineering and Technology (2015)*: 13-16. Print.

The improvements in the wickability of plasma treated samples are due to the enhancement in the surface roughness property. It is because of the introduction of polar groups which are generated during the oxygen plasma treatements. The wickablity of warp is 39.5% and weft is 27.90%.

3.2 AIR PERMEABILITY

In Air permeablility test the plasma treated and untreated samples have been assessing by using ISO 9237 standard methods. The Air permeablility in of plasma treated sample is 74.16* (cm3 cm^2 sec) and untreated samples is 56.66*(cm3 cm^2 sec). The plasma treated samples have 30% more air permeability due to the formation of new pores on the surface of the fabric. The untreated sample has lower value than plasma treated fabric.
*indicates that the samples were statistically significant.

3.3 *WATER VAPOUR PERMEABILITY*

In water vapour permeability test, the plasma treated and untreated samples were weighing in grams before and after water vapour treatment. The difference in mass is converted into water vapour permeablility values which are given in Table 2

Table 2 Wwater Vapour Permeability for untreated and plasma treated fabric samples

S No	Sample Name	Weight in Grams [Before test] M1 In grams	Weight in Grams [After test] M2 In grams	Loss of Mass in grams M [M1-M2] in grams	Water Vapour Permeability [g/m^2/day]
1	Plasma treated Sample	140.23	132.80	2.43	2155.49*
2	Untreated Sample	139.24	136.55	2.69	2386.12*

*indicates that the samples were statistically significant.

In table 2 indicate that the moisture vapour permeability of the plasma treated sample is lowered than the untreated samples. This may be due to the surface etching that occurs due to the plasma treatment. Surface etching opens the fibres on the surface of fabric which in turn hinders the flow of water vapour through the fabric.

4. CONCLUSION

In the development of multilayered fabrics, the inner layer fabric sholud have better wickability and airpermeabliltiy properties in view of comfort characteristics. In this work, the effect of surface modification on comfort properties of inner layer lyocell fabric has been studyed. The air permeablility of plasma treated fabric has been increased to 30 % when compare with untrearted fabric, it is due to new porus has been developed on the surface during plasma treatment which allows more air to pentrate. Smillarlly the wickablity characteristics of plasma treated fabrics has been increased in the range of 28 to 40 %. This is due to its etching nature on the surface while doing plasma treatement. Where as the water vapour permeablilty of untreated sample has more as compared to plasma treated sample, it may be due to the pours imparts during the plasma treatements accumulates more water vapour than untreared fabrcis.

5. REFERENCE

1. Shishoo.R, *plasma technology for textiles*, **2007**, Woodhead publishing.
2. Keiko Gotoh and Akemi Yasukawa., "Atmospheric pressure plasma modification of polyester fabric for improvement of textile-specific properties", *Textile Research Journal*, **2010**, 81: 368.
3. MoriM and Inagaki N., "Relationship between anti-felting properties and physicochemical properties of wool fibres treated with Air-plasma", *Textile Research Journal,* **2006**, 79: 687-694.
4. Canal C, Erra P, Molina R and Bertran E., "Regulation of surface hydrophilicity of plasma treated wool fabrics", *Textile Research Journal*, **2007**, 77: 559-564.
5. Moravej M, Yang X, Hicks RF, Penelon J and Babayan SE., "A radio-frequency nonequilibrium atmospheric pressure plasma operation with argon and oxygen", *Journal of Applied Physics*, **2006**, 99: 093305. 6. S. Mukhopadhyay. S & Ramakrishnan .G., Microfibres, *Textile Progress,* **2008**, 40:1, 1-86.
6. Marija Gorjanc, Vili Bukošek and Marija Gorenšek, "The Influence of Water Vapor Plasma Treatment on Specific Properties of Bleached and Mercerized Cotton Fabric", *Textile Research Journal,* **2010**, 80: 557.
7. Muryam Naebe, Peter G. Cookson, John Rippon, Rex Peter Brady, Xungai Wang, Narelle Brack and Grant van Riessen., "Effects of Plasma Treatment of Wool on the Uptake of Sulfonated Dyes with Different Hydrophobic",*Textile Research Journal*, **2010**, 80 (7). 611-622.
8. C.M.Mak, C.W.M Yuen, S. K. A.Ku & C.W. Kan, "Low-temperature plasma treatment of Tencel", *Journal Of Textile Institute*, **2006,** vol 97(6), pg 533-540.
9. B. P. Saville., *Physical Testing of Textiles*, Jan **1999**, Woodhead Publishing Limited.

Cite this article as: Dr. T. Ramachandran, L. Hari Gopalakrishnan. "EFFECT OF SURFACE MODIFICATION ON COMFORT PROPERTIES OF INNER LAYER LYOCELL FABRIC IN MULTILAYERED TECHNICAL TEXTILES." *International Conference on Systems, Science, Control, Communication, Engineering and Technology (2015)*: 13-16. Print.

10. Zeynep Ömerogullari and Dilek Kut, "Application of low-frequency oxygen plasma treatment to polyester fabric to reduce the amount of flame retardant agent", *Textile Research Journal,* **2012**, 82: 613
11. Karahan H.A, Ozdogan E, Demir A, Ayhan H and Seventekin N, "Effects of atmospheric pressure plasma treatments on certain properties of cotton fabrics" *Fibers Text East Eur*, **2009**, vol 73, pg 19-22.
12. Ozdogan E, Demir A, Karahan AA, Ayhan H and Seventekin N. "Effects of atmospheric plasma on the printability of wool fabrics", *Tekstil ve Konfeksiyon* ,**2009,** vol 19, pg 123-127.

Cite this article as: Dr. T. Ramachandran, L. Hari Gopalakrishnan. "EFFECT OF SURFACE MODIFICATION ON COMFORT PROPERTIES OF INNER LAYER LYOCELL FABRIC IN MULTILAYERED TECHNICAL TEXTILES." *International Conference on Systems, Science, Control, Communication, Engineering and Technology (2015)*: 13-16. Print.

International Conference on Systems, Science, Control, Communication, Engineering and Technology 2015 [ICSSCCET 2015]

ISBN	978-81-929866-1-6	**VOL**	01
Website	icssccet.org	**eMail**	icssccet@asdf.res.in
Received	10 - July - 2015	**Accepted**	31- July - 2015
Article ID	ICSSCCET005	**eAID**	ICSSCCET.2015.005

Wind Tunnel Testing of NACA 0021 Aerofoil with Co- Flow Jet

Emilon Zeon Rajan[1], T S Gowthaman[2], C Ganesan[3], K Balaji[4], K M Kiran Babu[5]
[1, 2, 3, 4, 5] Department of Aeronautical Engineering
Karpagam Institute of Technology, Coimbatore, Tamilnadu, India

Abstract: *The performance augmentation of an aircraft is possible by delaying the flow separation which causes stall. This research paper discusses the flow control method to increase the performance of the aircraft by inducing the circulation. The flow characteristic over an airfoil to control the flow separation using co-flow jet (CFJ) is investigated using analytical and experimental methods. The concept of CFJ airfoil is to open an injection slot near leading edge and suction slot near trailing edge which induces circulation control to the flow field over the aerofoil. The results obtained upon performing the experiments indicate that co-flow jet airfoil with injection and suction slot has better performance characteristics.*

I. INTRODUCTION

The projected substantial increase of air traffic in next 20 years, the air transportation system which needs to reducing emission and noise, airport capacity, and reliability of operation to minimize flight interruption due to severe weather conditions. High aerodynamic efficiency with reduced emission is needed for the next generation airplane, which is provided by blended wing body or flying wing configurations still mostly rely on optimizing geometry shapes without flow control. The conventional heavy high lift system used only for take-off and landing still needs to be carried for the whole flight mission, which is very inefficient. Lift is provided by modifying the wing surfaces configuration either with slat, mid-wing or flap. The control of flow is achieved by both passive and active means.
The Active flow control technique co-flow jet (CFJ) is considered for improving the effectiveness of the aerofoil. The co-flow jet aerofoil has an injection slot near leading edge and a suction slot near trailing edge. Enhancement of lift, reduces drag and increases stall margin is done by providing the co-flow jet. The CFJ airfoil recirculates the air mass flow and hence can significantly reduce the penalty to propulsion system by reducing the drag. The schematic representation of Co-flow jet (CFJ) aerofoil is shown in the figure 1.

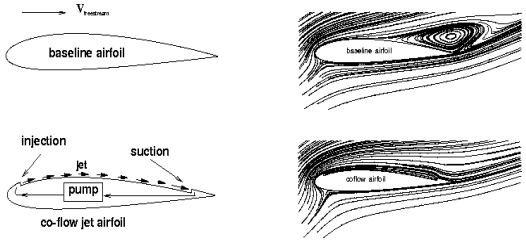

Figure 1. Schematic Representation of Co-Flow Jet Aerofoil and Its Effect on Flow Field

Cite this article as: Emilon Zeon Rajan, T S Gowthaman, C Ganesan, K Balaji, K M Kiran Babu. "Wind Tunnel Testing of NACA 0021 Aerofoil with Co- Flow Jet." *International Conference on Systems, Science, Control, Communication, Engineering and Technology (2015)*: 17-21. Print.

II. LITERATURE REVIEW

Xi Xia et. al. experimentally investigated the synthetic jets in a co flow wake. A round synthetic jet issuing into a co flow wake is investigated experimentally in this research. The flow field of the jet is measured using hot-wire anemometry. The spreading and decaying of the synthetic jet is studied after taking into account the effect of the wake velocities. The stream wise variation of centreline velocity show good agreement with the semi empirical integral model. By verifying the theoretical model, it can be concluded that the jet decay is not affected by the presence of ambient co flow. [1]

Dano et. al. investigated the study of CFJ airfoil using discrete jets. Aerodynamic forces measured and DPIV measurements show that the Discrete CFJ airfoil can achieve up to a 250% increase of maximum lift, and simultaneously generates a tremendous thrust. Nearly 80% of the injection momentum is converted to drag reduction, which indicates that CFJ airfoils are highly energy efficient. The stall angle of attack is also significantly increased. [2]

Riajun Noor et. al. numerically investigated the flow characteristics over an airfoil to control the flow separation by Co-Flow Jet technique. CFD study over NACA 2415 airfoil is carried on the basis of 2-D compressible Navier-Stokes equations with 2-equation standard k-ε turbulent model and standard wall function. The grid used for the study is shown in the figure 2. From the simulation result it is observed that that the CFJ airfoil delay flow separation over the airfoil and allows the aircraft to cruise with very high aerodynamic efficiency and also enhance the performance of taking off and landing within short distance. [3]

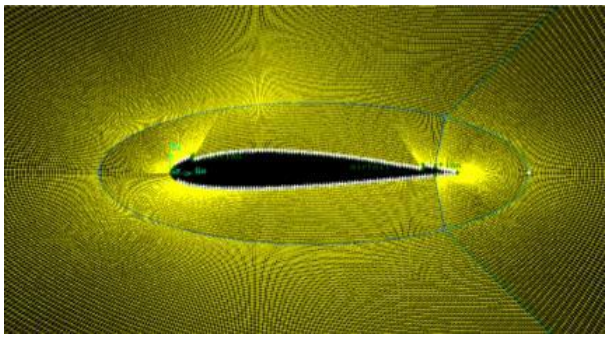

Figure 2. Mesh around the co flow jet airfoil [3]

Amzad Hossain et. al. carried out the wind tunnel testing of baseline airfoil NACA 0015 and CFJ0015-065-065 with the primary goal to investigate and compare the airfoil aerodynamic characteristics over a wide range of Angle of Attack (AOA) and with a wind tunnel free stream velocity of 12m/s , Re = 1.89×105, Cμ = 0.07 at M = 0.030 kg/s. The CFJ increases C_{Lmax} by 82.5% and decreases Drag by 16.5% at Stall AOA when compared to the baseline airfoil. [4]

Abdul khalid sherief et. al. described Co-Flow Jet as an alternative for civil aircraft high lift configuration. The major aim of this research was to present an alternative for the existing high lift devices in the conventional passenger aircraft. The objective was to use a flow control method, which would be incorporated in the wing to attain the same required value of LIFT, thus there by relieving off the additional penalty in terms of movable control surfaces. [5]

Ge-Cheng Zha et. al. investigated the CFJ aerofoil with the bleed air from the power plant and CFJ aerofoil with the suction from the aerofoil flow field. The computational fluid dynamics solutions based on the Reynolds-averaged Navier–Stokes model are used to provide the breakdowns of lift and drag contributions from the airfoil surface force integral and jet duct's reactionary forces. The results are compared with experiment for validation. The study indicates that the suction occurring on the airfoil suction surface of the co flow jet airfoil is more beneficial than the suction occurring through the engine inlet such as the airfoil with injection only. The co-flow jet airfoil with both injection and suction yields stronger mixing, larger circulation, more filled wake, higher stall angle of attack, less drag, and lower energy expenditure. [6]

Y. Cui et. al. investigated numerically and experimentally the implementation of Co-Flow Jet on aerofoil with low Reynolds Number**.** The experimental study has shown that it does not always give better performance in comparison with that of suction or jet injection only. To use CFJ concept effectively, the momentum coefficient is found to be in the range of 5% to 13%. When the momentum coefficient is less than 5%, the use of suction alone is recommended, while for the momentum coefficient is higher than 13%, the implementation of jet injection alone is a better option. [7]

A. Abdullah et. al. studied the Lift/Drag ratio enhancement using continuous normal suction by the wind tunnel testing. The wing model with NACA-0015 has been made to achieve normal suction from the wing upper surface by means of four slot channels. The satisfaction of the suction is done by using vacuum pump. The tests are to be done for incompressible flow over wing with and without a continuous normal suction for three different angle of attack 8^0,12^0 and 16^0 and for three different Reynolds numbers 13.6×104, 20.4×104 and 24.5×104. The results showed continuous normal that the suction can significantly increase the lift to drag force ratio, and this ratio is increasing more as the strength of the suction increases. [8]

The objective of this research paper is to the aerodynamic characteristic with co flow jet aerofoil and baseline aero foil. First fixing the baseline aerofoil in the wind tunnel and find out pressure coefficient values similarly co flow jet aerofoil is also tested along the test

Cite this article as: Emilon Zeon Rajan, T S Gowthaman, C Ganesan, K Balaji, K M Kiran Babu. "Wind Tunnel Testing of NACA 0021 Aerofoil with Co- Flow Jet." *International Conference on Systems, Science, Control, Communication, Engineering and Technology (2015)*: 17-21. Print.

section. The aerofoil's are analyzed at various angle of attack to measure the values of pressure coefficient with the help of fourteen column manometer.

III. EXPERIMENTAL SETUP

The wind tunnel of suction type with an axial flow fan driven by 28880rpm, 15HP, 440V, 50 cycles, 3 phase AC motors as shown in the figure 3 is used for the study. It consists of an entrance section with a fuel mouth inlet containing flow straightness and screens. This section is followed by it contraction, test section and a diffuser. The duct contains butterfly value for controlling air velocity inside the duct along with rough calibration of wind velocity mark on the duct and containing zframes the complete wind tunnel expect that the test section is made of mild steel and plexy glass wind for visual observation of flow phenomenon the electrical control panel.

Figure 3.Wind Tunnel used for the study

The CFJ airfoils used for testing at the Karpagam institute of technology was a modified NACA 0021. The NACA 0021 airfoil was chosen for its ease of manufacturing and relative thickness and also it was used for the baseline study. The thickness made it easier to fit all instrumentation and duct work into the airfoil given the size constraints imposed by the 30cm × 30cm wind tunnel test section. However the CFJ concept can be implemented on any airfoil geometry. The modified NACA 0021 airfoil used in testing had a span of 22cm and a chord length of 25.5cm. As shown in figure 4, the airfoil was modified by recessing the suction surface (upper surface). This recession opened up a slot towards the leading edge of the airfoil (injection slot) and another slot towards the trailing edge (suction slot). The slot towards the leading edge was used to inject air tangentially over the suction surface, while the slot towards the trailing edge was used to remove air tangentially from the suction surface. One airfoil was manufactured with this modification. The airfoil had a 1.5cm or 1.67% chord length injection slot height. The airfoils are named by their injection and suction slot sizes according to the convention CFJ4digit-INJ-SUC. So the airfoil with the 1.5cm injection slot was named CFJ0021-167-167. The reason the suction slot size was larger than the injection slot is because the density of the air being removed by the suction slot is less than the density of the air being injected. Therefore, to balance the mass flow rates, the suction area has to be larger or the velocity greater. But the velocity is limited because the flow will eventually become choked. The location of the injection slot and suction slot are respectively, 7.11% and 83.18% of the chord length from the leading edge. The slots are positioned perpendicular to the suction surface making them parallel to the flow direction. The Factor driving the geometry of the injection and suction cavities are the aerodynamic characterises of the internal structure. It was important to have negligible losses, if any from the flow entering the inside of the aerofoil to the jet exiting the injection slot. This would allow for the most accurate mass flow, pressure and temperature reading across the slot. Fourteen pressure taping have been used along the aerofoil. The seven taps located upper surface of the aerofoil and similarly seven taps located lower surface of the aerofoil. Sheet metal has been used for the fabrication of CFJ aerofoil with injection and suction slots. A nylon tube has been used for the connecting the blower with injection and suction slots.

IV. RESULTS AND DISCUSSION

This research is successfully find out by the experimental set up of subsonic wind tunnel test taken for the coefficient of pressure measurement. the CFJ aerofoil was tested in many angle of attack . These will be described by the curve of graph.

Cite this article as: Emilon Zeon Rajan, T S Gowthaman, C Ganesan, K Balaji, K M Kiran Babu. "Wind Tunnel Testing of NACA 0021 Aerofoil with Co- Flow Jet." *International Conference on Systems, Science, Control, Communication, Engineering and Technology (2015)*: 17-21. Print.

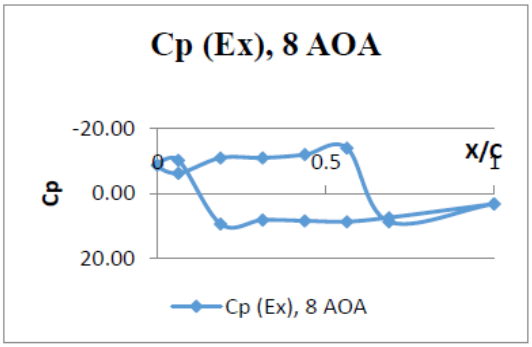

Figure 4. C_p Plot of CFJ Aerofoil

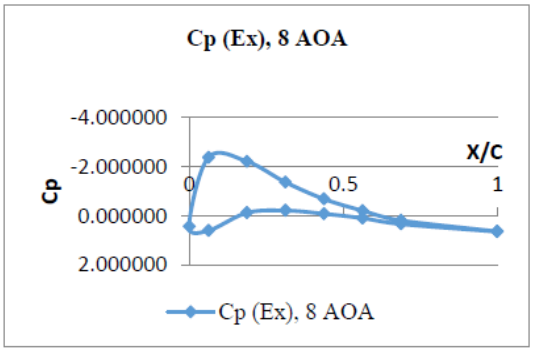

Figure 5. C_p plot of Baseline Aerofoil

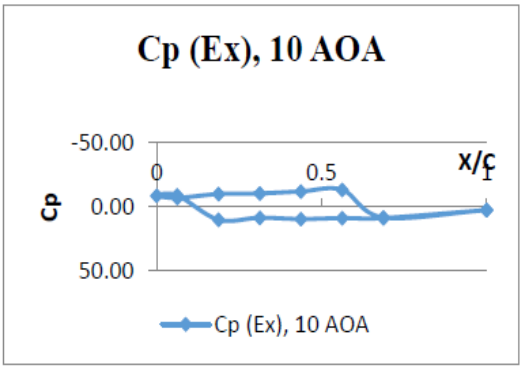

Figure 6. C_p plot of CFJ Aerofoil

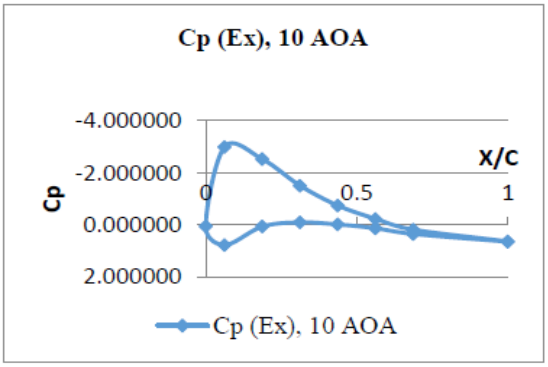

Figure 7. C_p plot of Baseline Aerofoil

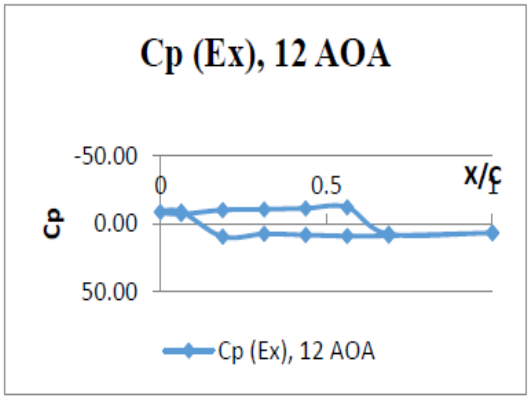

Figure 8. C_p plot of CFJ Aerofoil

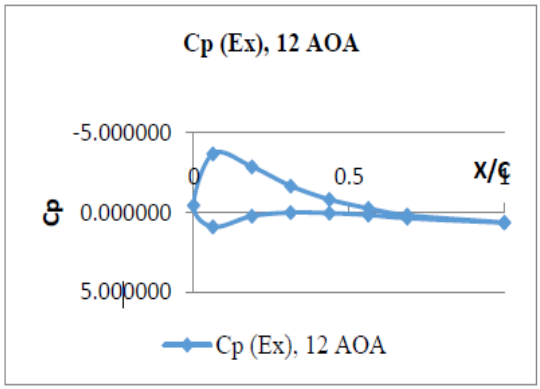

Figure 9. C_p plot of Baseline Aerofoil

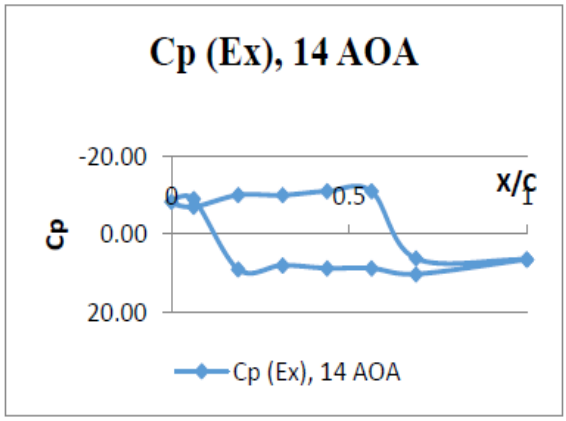

Figure 10. C_p plot of CFJ Aerofoil

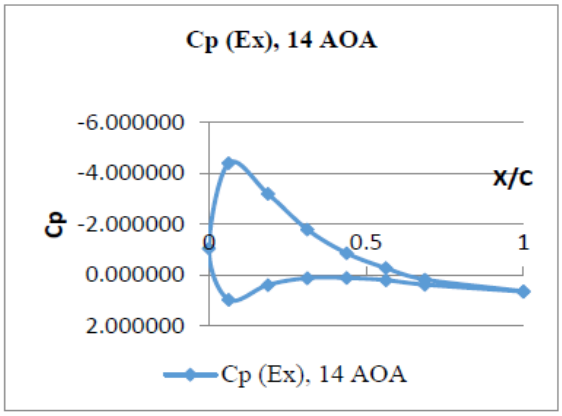

Figure 11. C_p plot of Baseline Aerofoil

Cite this article as: Emilon Zeon Rajan, T S Gowthaman, C Ganesan, K Balaji, K M Kiran Babu. "Wind Tunnel Testing of NACA 0021 Aerofoil with Co- Flow Jet." *International Conference on Systems, Science, Control, Communication, Engineering and Technology (2015)*: 17-21. Print.

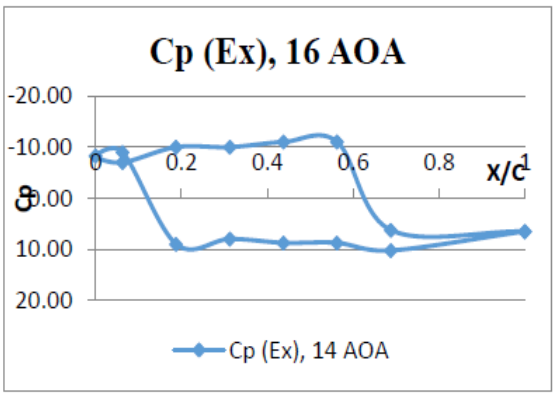

Figure 12. C_p plot of CFJ Aerofoil

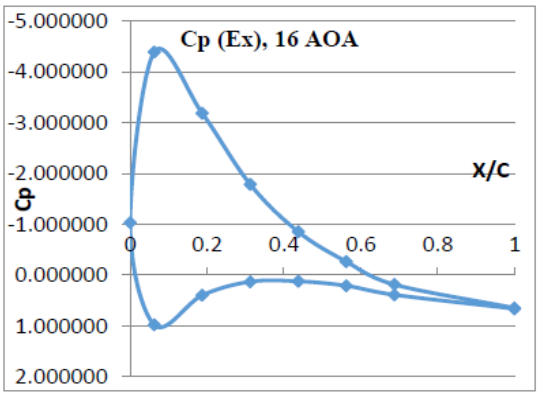

Figure 13. C_p plot of Baseline Aerofoil

Various angles of attacks the pressure values are plotted in above graphs for CFJ and base aerofoil. The coefficient of pressure value will changes from base aerofoil. The percentage of coefficient of pressure value for CFJ is greater when compared with base aerofoil

V. CONCLUSION

The research described in this paper successfully demonstrates how the CFJ airfoil is design and tested in the wind tunnel testing. The research proved the high performance capabilities of the CFJ airfoil. It was shown the CFJ airfoil performed better than the baseline airfoil with respect to maximum lift and stall margin. It was also declare that the lift for a given angle of attack and drag reduction

ACKNOWLEDGMENT

With great pleasure and deep gratitude, The authors wish and express their sincere gratitude to beloved Principal **Dr. T. Ramachandran** for providing an opportunity and necessary facilities in carrying out this work and express their sincere thanks to Head of department, all the staff members of Aeronautical Engineering whose assistance played a big role in this work and have been of immeasurable value.

REFERENCES

[1] Xi Xia, Gopi Krishnan and Kamran Mohseni, "An Experimental Investigation of Synthetic Jets in A Coow Wake," 40th Fluid Dynamics Conference and Exhibit, 28 June - 1 July 2010, Chicago, Illinois, AIAA 2010-4594.

[2] Bertrand P. E. Dano, Gecheng Zha and Michael Castillo, "Experimental Study of Co-Flow Jet Airfoil Performance Enhancement Using Discrete Jets," 49th AIAA Aerospace Sciences Meeting including the New Horizons Forum and Aerospace Exposition, 4 - 7 January 2011, Orlando, Florida, AIAA 2011-941

[3] Md. Riajun Noor, Md. Assad-Uz-Zaman, and Mashud "Effect of Co-Flow Jet over an Airfoil: Numerical Approach," Contemporary Engineering Sciences, Vol. 7, No. 17, pp. 845 -851, 2014.

[4] Md. Amzad Hossain Md. Nizam Uddin, Md. RasedulIslam and Mohammad Mashud "Enhancement of Aerodynamic Properties of an Airfoil by Co Flow Jet (CFJ) Flow," American Journal of Engineering Research , Volume-4, Issue-1, pp-103-112,2015.

[5] Abdul khalid sherief, Ajithkumar,K.P, Karlmarx,Ashish jayandar, and Manikandan "Co-flow jet control as an alternative for civil aircraft high lift configuration," International Journal of Mechanical And Production Engineering, ISSN: 2320-2092, Volume- 2, Issue- 4,pp. 99-103, April-2014.

[6] Ge-Cheng Zha, Wei Gao, and Craig D. Paxton "Jet Effects on Co flow Jet Airfoil Performance," AIAA JOURNAL.Vol.45,No.6,June 2007.

[7] H. Mitsudharmadi and Y. Cui, "Implementation of Co-Flow Jet Concept on Low Reynolds Number Airfoil," 40th Fluid Dynamics Conference and Exhibit 28 June - 1 July 2010, Chicago, Illinois, AIAA 2010-4717.

[8] A. Abdullah, Laith M. Jasim, Amir S. Dawood "Excremental Study of Lift/Drag Ratio Enhancement Using Continuous Norma Suction" Al-Rafadain Engineering Journal;2012, Vol. 20 Issue 1, pp. 76, February 2012.

Cite this article as: Emilon Zeon Rajan, T S Gowthaman, C Ganesan, K Balaji, K M Kiran Babu. "Wind Tunnel Testing of NACA 0021 Aerofoil with Co- Flow Jet." *International Conference on Systems, Science, Control, Communication, Engineering and Technology (2015)*: 17-21. Print.

International Conference on Systems, Science, Control, Communication, Engineering and Technology 2015 [ICSSCCET 2015]

ISBN	978-81-929866-1-6	**VOL**	01
Website	icssccet.org	**eMail**	icssccet@asdf.res.in
Received	10 - July - 2015	**Accepted**	31- July - 2015
Article ID	ICSSCCET006	**eAID**	ICSSCCET.2015.006

GAS LEAKAGE DEDUCTION WITH AUTO SHUT-OFF

[1]Dr. K. KEERTHIVASAN, [2]SARAVANA MANIKANDAN.B, [3]DEVASRRI.P, [4]ANURADHA.R
[1]Professor and head of ece department, Karpagam Institute of Technology
[2]Assistant Professor, Department of electronics and communication engineering, Karpagam Institute of Technology
[3, 4]III BE ECE, Department of electronics and communication, Karpagam Institute of Technology, Coimbatore

ABSTRACT: *Latest surveys have provided us an atrocious information that, these days, deaths due to domestic fire accidents have taken a giant leap, especially in India. Among the causes of such mishaps, LPG leakage accidents top the list. Though this issue is becoming more crucial with passing days, no exact remedial systems have been designed. The systems available in present day markets are capable of just alerting people in case of a gas leakage. But, so far, no systems have been designed to obstruct the main cause of the accident – the leakage. Now, when man has already set his foot on the other planets, and is planning to start a life there, the technology he uses must also escalate. This gave us an idea to develop a system to control the leakage at its onset. Like the existing systems, this system provides LCD, buzzer and SMS alerts. But the innovation of our proposed system lies in its ability to shut off the gas cylinder's regulator automatically. Thus the system takes the entire responsibility of providing the safety measures, while the user can just luxuriate. The prime motive of this system is to save lives. After all, LPG cylinders in households are to eliminate rawness, not lives.*

INTRODUCTION

An unexpected increase in accidental domestic fire deaths revealed by the latest statistics suggests that a review of home fire safety is needed. One of the most common reasons of domestic fire is leakage of LPG gas. And we still do not have any proper solution for the same. Safety equipments after fire catches are available but nothing is there to avoid the fire itself. Now when technology has reached up to the moon, conquering the universe, there has to be something to prevent fire due to LPG gas leak at houses. This encouraged us to give the society a technology that can prevent such fire. Like the previous systems, this system also provides LCD, buzzer and SMS alerts. But the innovation in our proposed system lies in its ability to shut off the gas cylinder's regulator automatically. This prevents the occurrence of any accidents, by its own, without human assistance. Implementing this application can be useful for companies, houses, etc., which can save lives of people.

REPUTATION BASED SYSTEM

Our proposed system requires only a supply from a DC battery. It monitors continuously for the LPG gas leak in the house. In case, the gas level exceeds the normal, it provides an LCD display of the gas level along with a buzzer alarm which continues till the gas level

Cite this article as: Dr. K. KEERTHIVASAN, SARAVANA MANIKANDAN.B, DEVASRRI.P, ANURADHA.R. "GAS LEAKAGE DEDUCTION WITH AUTO SHUT-OFF." *International Conference on Systems, Science, Control, Communication, Engineering and Technology (2015)*: 22-23. Print.

comes back to normal. It also sends the message "GAS LEAKAGE", to a pre-defined number. In addition to this, it turns on the exhaust fan to expel the leaked gas. But the main emphasis of this novel system lies in its ability to stop the leakage. It turns off the regulator automatically. All these operations take place simultaneously, such that, the hazards due to gas leakage are prevented, and also, the gas is conserved rather than being wasted.

The proposed system consists of following steps,

The gas leakage is detected using a gas sensor MQ5.once when the gas lekage is detected the information is passed to the microcontroller PIC16F877A.when the particular threshold level is reached. The microcontroller begins its process. It provides an LCD display along with the buzzer alarm which continues till the gas level comes back to normal. It also sends the message "GAS LEAKAGE", to a pre-defined number using a GSM module. In addition to this, it turns on the exhaust fan to expel the leaked gas the main emphasis of this novel system lies in its ability to stop the leakage. It turns off the regulator automatically. All these process takes place simultaneously.

Final outlook of the project

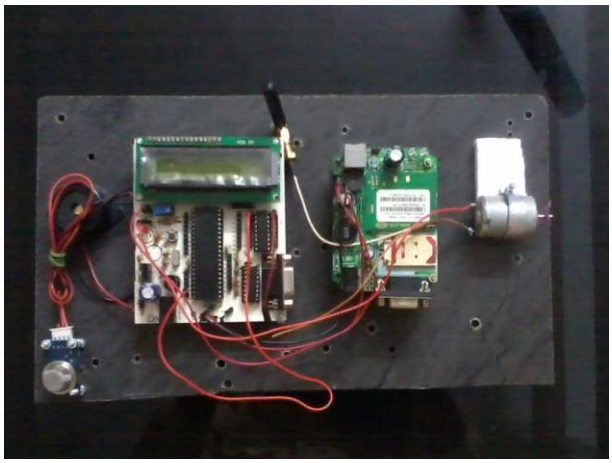

RESULT

The leakage detection system available in the market works on AC power supply.It is efficient in detecting gas leakage. It gives LCD alert accompanied by a continuous buzzer alarm. It also sends SMS alerts. But the system does not have the facility of auto shut-off. the present system does not have the capability to prevent further leakage (i.e.) it cannot turn off the regulator automatically. Our proposed system requires only a supply from a DC battery and it provides the LCD display along with a buzzer.It also has a auto suht-off system.All these process takes places simultaneously All these operations take place simultaneously, such that, the hazards due to gas leakage are prevented, and also, the gas is conserved rather than being wasted.

CONCLUSION

By the realization of the above proposed system one can learn many aspects of a digital electronics circuit. This will give the complete knowledge of designing microcontroller based system and developing embedded software.From the consumers' point of view, this system not only helps in averting accidents caused by gas leakage, but, it also paves the way for conservation of gas by preventing undesired leakage.

REFERENCE

Embedded Books& Websites:

[1]Davies J H, Microcontroller Basics, Elsevier, 2011.
[2]Muhammad Ali Mazidi, Rolin McKinlay, Danny Causey, PIC Microcontroller and Embedded Systems: Using assembly and C, Pearson, 2008.
[3]Han-Way Huang, PIC Microcontroller: An Introduction to Software and Hardware Interfacing, Course Technology.

[4]R.P. Jain, Digital Electronics, Tata McGraw-Hill]
[5]www.discovercircuits.com
[6]www.electronicsforu.com

Cite this article as: Dr. K. KEERTHIVASAN, SARAVANA MANIKANDAN.B, DEVASRRI.P, ANURADHA.R. "GAS LEAKAGE DEDUCTION WITH AUTO SHUT-OFF." *International Conference on Systems, Science, Control, Communication, Engineering and Technology (2015)*: 22-23. Print.

International Conference on Systems, Science, Control, Communication, Engineering and Technology 2015 [ICSSCCET 2015]

ISBN	978-81-929866-1-6	**VOL**	01
Website	icssccet.org	**eMail**	icssccet@asdf.res.in
Received	10 - July - 2015	**Accepted**	31- July - 2015
Article ID	ICSSCCET007	**eAID**	ICSSCCET.2015.007

OPTIMIZED MULTICAST ROUTING AND TRAFFIC DISCOVERY IN MANET

M. S. Gowtham[1], S. Sureshkumar[2]
[1, 2] Department of ECE, Rathinam Technical Campus, Coimbatore

ABSTRACT: *Mobile ad hoc networks in emergency communications where network needs to be constructed at that moment and faster.Since the nodes move in random manner, routing protocols must be highly effective and reliable to guarantee successful packet delivery and traffic discovery. In this paper, we propose an Enhanced STARS for MANETs. STARS are basically an attackers, which only needs to capture the raw traffic from the PHY/MAC layer without looking into the contents of the intercepted packets.*

***KEYWORDS*:** Anonymous communication, mobile ad hoc networks, statistical traffic analysis.

I. INTRODUCTION

A **mobile ad hoc network** (**MANET**) is a continuously self-configuring, infrastructure-less network of mobile devices connected without wires. Ad hoc is Latin and means "for this purpose". Each device in a MANET is free to move independently in any direction, and will therefore change its links to other devices frequently. Each must forward traffic unrelated to its own use, and therefore be a router. The primary challenge in building a MANET is equipping each device to continuously maintain the information required to properly route traffic. Such networks may operate by themselves or may be connected to the larger Internet. They may contain one or multiple and different transceivers between nodes. This results in a highly dynamic, autonomous topology. MANETs are a kind of Wireless ad hoc network that usually has a routable networking environment on top of a Link Layer ad hoc network. MANETs consist of a peer-to-peer, self-forming, self-healing network in contrast to a mesh network has a central controller (to determine, optimize, and distribute the routing table). MANETs circa 2000-2015 typically communicate at radio frequencies (30 MHz - 5 GHz). Multi-hop relays date back to at least 500BC. The growth of laptops and 802.11/Wi-Fi wireless networking have made MANETs a popular research topic since the mid-1990s. Many academic papers evaluate protocols and their abilities, assuming varying degrees of mobility within a bounded space, usually with all nodes within a few hops of each other. Different protocols are then evaluated based on measures such as the packet drop rate, the overhead introduced by the routing protocol, end-to-end packet delays, network throughput, ability to scale, etc.

II. OUR PROPOSAL

In the proposed system, we enhance our protocol called E-STARS. We include Channel Aware technique in our protocol for secure and lost less communication between sources to destinations. Channel - aware scheduling is a technique that adapts the transmission start time of a packet to the channel condition. Sending packets over a channel in a bad state is avoided. There are four modules: Node formation, Channel prediction, Applying E-STARS, Packet transmission.

Cite this article as: M. S. Gowtham, S. Sureshkumar. "OPTIMIZED MULTICAST ROUTING AND TRAFFIC DISCOVERY IN MANET." *International Conference on Systems, Science, Control, Communication, Engineering and Technology (2015)*: 24-26. Print.

ARCHITECTURE DIAGRAM:

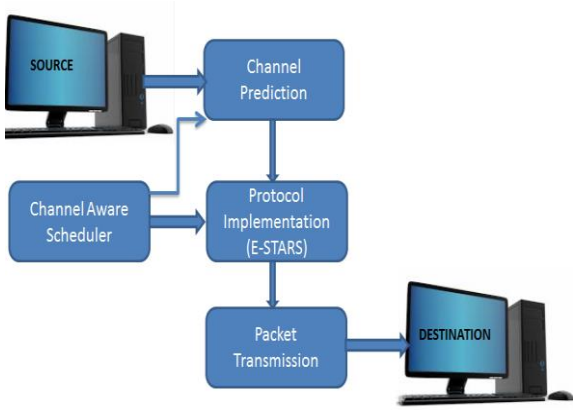

MODULE DESCRIPTION:

Node Formation:

- In a network, a node is a connection point, either a redistribution point or an end point for data transmissions. In general, a node has programmed or engineered capability to recognize and process or forward transmissions to other nodes. In this module we format all the nodes and group in to one network.
- **Technique:** Star Topology

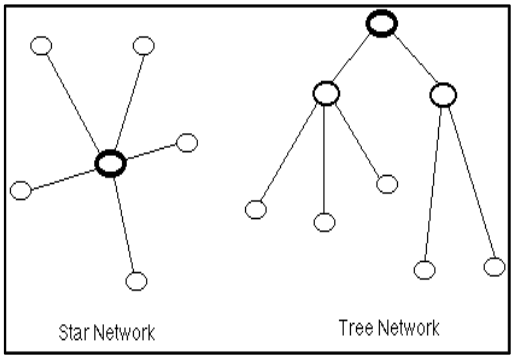

Channel Prediction:

- The random movement of nodes in multi-channel MANETs has significant impact upon the stability of network topology due to connection loss and co-channel interference. To solve this problem, a channel aware scheduler algorithm is proposed, which adjusts nodes' power levels and transmission channels according to the link state predicted by a probabilistic network, so as to maintain the stability of links and network topology.

Applying E-STARS:

- In this module used for applying E- STARS for MANETs. E-STARS are basically an attacking system, which only needs to capture the raw traffic from the PHY/MAC layer without looking into the contents of the intercepted packets. From the captured packets, STARS constructs a sequence of point-to-point traffic matrices to derive the end-to-end traffic matrix, and then uses a heuristic data processing model to reveal the hidden traffic patterns from the end-to end matrix and also it contains channel aware technique for overcome a connection lost in channel reconfiguring.

Packet Transmission:

- The emerging need for wireless mesh networks and secured data transmission phase is of crucial importance depending upon the environments like military. In this paper, a new way to improve the reliability of message transmission is presented. In the open collaborative networking environment, any node can maliciously or selfishly disrupt and deny communication of other nodes.

III. SOFTWARE USED

NETWORK SIMULATOR – NS-2: is an open-source event-driven simulator designed specifically for research in computer communication networks. Since its inception in 1989, NS2 has continuously gained tremendous interest from industry, academia, and government. Having been under constant investigation and enhancement for years, NS2 now contains modules for numerous network components such as routing, transport layer protocol, application, etc. To investigate network performance, researchers can simply

Cite this article as: M. S. Gowtham, S. Sureshkumar. "OPTIMIZED MULTICAST ROUTING AND TRAFFIC DISCOVERY IN MANET." *International Conference on Systems, Science, Control, Communication, Engineering and Technology (2015)*: 24-26. Print.

use an easy-to-use scripting language to configure a network, and observe results generated by NS2. Undoubtedly, NS2 has become the most widely used open source network simulator, and one of the most widely used network simulators. Unfortunately, most research needs simulation modules which are beyond the scope of the built-in NS2 modules. Incorporating these modules into NS2 requires profound understanding of NS2 architecture. Currently, most NS2 beginners rely on online tutorials. Most of the available information mainly explains how to configure a network and collect results, but does not include sufficient information for building additional modules in NS2. Despite its details about NS2 modules, the formal documentation of NS2 is mainly written as a reference book, and does not provide much information for beginners. The lack of guidelines for extending NS2 is perhaps the greatest obstacle, which discourages numerous researchers from using NS2.

IV. CONCLUSION

In this system we propose we enhance our protocol called E-STARS. We include Channel Aware technique in our protocol for secure and lost less communication between sources to destination.Channel - aware scheduling is a technique that adapts the transmission start time of a packetsto a channel condition.sending packets over a channel in a bad state and communication loss is avoided.

REFERENCES:

1. J. Kong, X. Hong, and M. Gerla, "An Identity-Free and On- Demand Routing Scheme against Anonymity Threats in Mobile Ad Hoc Networks," IEEE Trans. Mobile Computing, vol. 6, no. 8, pp. 888-902, Aug. 2007.
2. Y. Zhang, W. Liu, W. Lou, and Y. Fang, "MASK: Anonymous On- Demand Routing in Mobile Ad Hoc Networks," IEEE Trans. Wireless Comm., vol. 5, no. 9, pp. 2376-2385, Sept. 2006.
3. Y. Qin and D. Huang, "OLAR: On-Demand Lightweight Anonymous Routing in MANETs," Proc. Fourth Int'l Conf. Mobile Computing and Ubiquitous Networking (ICMU '08), pp. 72-79, 2008.
4. M. Blaze, J. Ioannidis, A. Keromytis, T. Malkin, and A. Rubin, "WAR: Wireless Anonymous Routing," Proc. Int'l Conf. Security Protocols, pp. 218-232, 2005.
5. A. Boukerche, K. El-Khatib, L. Xu, and L. Korba, "SDAR: A Secure Distributed Anonymous Routing Protocol for Wireless and Mobile Ad Hoc Networks," Proc. IEEE 29th Ann. Int'l Conf. Local Computer Networks (LCN '04), pp. 618-624, 2004.
6. S. Seys and B. Preneel, "ARM: Anonymous Routing Protocol for Mobile Ad Hoc Networks," Proc. IEEE 20th Int'l Conf. Advanced Information Networking and Applications Workshops (AINA Work- shops '06), pp. 133-137, 2006.
7. R. Shokri, M. Yabandeh, and N. Yazdani, "Anonymous Routing in MANET Using Random Identifiers," Proc. Sixth Int'l Conf. Networking (ICN '07), p. 2, 2007.
8. R. Song, L. Korba, and G. Yee, "AnonDSR: Efficient Anonymous Dynamic Source Routing for Mobile Ad-Hoc Networks," Proc. Third ACM Workshop Security of Ad Hoc and Sensor Networks (SASN '05), pp. 33-42, 2005.
9. M. Reed, P. Syverson, and D. Goldschlag, "Anonymous Connec- tions and Onion Routing," IEEE J. Selected Areas in Comm., vol. 16, no. 4, pp. 482-494, May 2002.
10. D. Chaum, "Untraceable Electronic Mail, Return Addresses, and Digital Pseudonyms," Comm. ACM, vol. 24, no. 2, pp. 84-88, 1981.
11. J. Raymond, "Traffic Analysis: Protocols, Attacks, Design Issues, and Open Problems," Proc. Int'l Workshop Designing Privacy Enhancing Technologies: Design Issues in Anonymity and Unobserva- bility, pp. 10-29, 2001.
12. W. Dai, "Two Attacks against a PipeNet-Like Protocol Once Used by the Freedom Service," http://weidai.com/freedom-attacks.txt, 2013.
13. X. Wang, S. Chen, and S. Jajodia, "Network Flow Watermarking Attack on Low-Latency Anonymous Communication Systems," Proc. IEEE Symp.Security and Privacy, pp. 116-130, 2007.
14. M. Reiter and A. Rubin, "Crowds: Anonymity for Web Transac- tions," ACM Trans. Information and System Security, vol. 1, no. 1, pp. 66-92, 1998.
15. M. Wright, M. Adler, B. Levine, and C. Shields, "The Predecessor Attack: An Analysis of a Threat to Anonymous Communications Systems," ACM Trans. Information and System Security, vol. 7, no. 4, pp. 489-522, 2004.

Cite this article as: M. S. Gowtham, S. Sureshkumar. "OPTIMIZED MULTICAST ROUTING AND TRAFFIC DISCOVERY IN MANET." *International Conference on Systems, Science, Control, Communication, Engineering and Technology (2015)*: 24-26. Print.

International Conference on Systems, Science, Control, Communication, Engineering and Technology 2015 [ICSSCCET 2015]

ISBN	978-81-929866-1-6	**VOL**	01
Website	icssccet.org	**eMail**	icssccet@asdf.res.in
Received	10 - July - 2015	**Accepted**	31- July - 2015
Article ID	ICSSCCET008	**eAID**	ICSSCCET.2015.008

An enhanced Rough Set Based Technique for Elucidating Learning styles in E-Learning System

K.S.Bhuvaneshwari[1], Dr.D. Bhanu[2], Dr. S. Sophia[3]
[1]Assistant Professor, Department of CSE, Karpagam College of Engineering, India
[2]Professor, Department of Computer Science and Engineering, Karpagam Institute of Technology, Coimbatore, India
[3]Professor, Department of ECE, Sri Krishna College Of Engineering and Technology, Coimbatore, India

Abstract: *Rough set theory is considered as the most essential strategy significantly suitable for illustrating distinctive sorts of learning styles controlled by the learners during e-learning process through feature information selection. The Rough set hypothesis is likewise utilized for effectively finding relations with conflicting or fragmented information which is incomplete in nature. Be that as it may, when harsh set hypothesis is consolidated, they are not sufficiently effective to evaluate ideal subsets. Hence, this paper provides a comparison of various rough set based techniques for adapting learning styles. The paper provides the analysis of rough set based clustering methods in terms of two parameters cohesion and coupling. In addition, the paper also proposes an enhanced methodology based on normalized score value for finding the deviation between data's through the equivalence property of rough set theory. The experimental results show that the proposed algorithm maximizes the stated metrics.*

Keywords: Rough set theory, e-learning, Learning styles, Normalization, Standard deviation.

1 Introduction

E-learning is one of the emerging technologies incorporated by the worldwide educational organization for the purpose of enabling services like i) providing virtual learning facilities, ii) creating content for various domains for learners, iii) creating the virtual class environment by means of online admission, online attendance and online conduction of classes[1]. In order to give successful online administrative services in an e-learning system, the information about the learners and their interested domains of learning must be known. This type of learners' information assumes a vital role for the effective usage of e-learning framework [2]. However, the problem associated with this implementation methodology is growth of learners' information exponentially towards the time factor [3]. Then, the analysis of learning factors in a large amount of learners' information becomes a challenging issue. Hence, there is a need arises to incorporate a set of adaptable rules to analyze the learners' information for designing an effective and efficient e-learning system.

This paper contributes a rough set theory based data analysis model for mining relevant and significant information from the large amount of learners' data of the e-learning system. This model incorporates the principle of reducts in rough set theory for extracting knowledge from the learners' information [4].

The learning style of an individual is one of the imperative data to be derived from the learners' information. Since, the nature of the

training and the adequacy of the information about the specific domain not just rely on the substance given in the e-learning framework

Cite this article as: K.S.Bhuvaneshwari, Dr. D. Bhanu, Dr. S. Sophia. "An enhanced Rough Set Based Technique for Elucidating Learning styles in E-Learning System." *International Conference on Systems, Science, Control, Communication, Engineering and Technology (2015)*: 27-32. Print.

additionally the presentation that has more effects on the learners [5]. For an effective e-learning system we need to analyze the learning style of an individual in the collected learners' information. Hence, in this paper, we incorporate rough set theory based data analytics model for mining rules and analyzing about the learners' learning styles in order to facilitate efficient learning. The main advantage of using rough set theory for this data analytics model due its potential towards extraction of relevant information, ii) decision friendly and iii) high user understandability.

The remaining part of the paper is organized as follows. Section 2 depicts the related work that portrays the role of rough set theory in elucidating relations for estimating the various learning styles in e-learning process. Section 3 presents the Minimum Normalized Dissimilarity between Objects (MNDBO) techniques with the associated algorithm. Section 4 presents the experimental comparison carried out with MNDBO with the considered benchmark systems. Finally, Section 5 concludes with the conclusion.

2 Related Work

In the recent past, a number of rough set theory based clustering mechanisms have been contributed by the researchers. Some of the existing rough set theory based approaches are enumerated below.

Initially in 1980, the rough theory was proposed by Zdzislaw Pawlak [6], to analyze the information present in the data tables for deriving relationships among the given data. Further, this theory is also used to reduce the size of the data, deriving hidden patterns of the data and extraction of rules from the data [7]. It can also be well applicable for refining improper or incomplete information given. Researcher of the past decade have proved that rough set theory can be implemented for wide range of problems such as i) correlated and uncorrelated analysis, ii) rule extractions for expert systems iii) learning from examples and switching circuits design.

Analyzing learning style of a learner plays a key role in designing an e-learning system. Each and every learner has different style of learning. Studying and analyzing learning styles based on various classification methods have been proposed by the researchers in the past decade [8]. Many of them were focused on learning style scales, some of them focused on learning style inventory [9] [10]. Few researchers have given a survey on learning style analysis, learner preference checklists, preferable questionnaire to assess the learning style and ability of the learners [11] [12] [13]. Hence, this review concludes that, there is lack of mathematical model for determining the learning style of an individual in order to design an effective e-learning system.

In addition, the first benchmark system is the min-min-roughness (MMR) technique proposed in [14] that utilizes the minimum of mean roughness by considering only a single attribute into account for cluster analysis. The maximum value of mean roughness is considered for estimating the partitioning attribute. Further, Tripathy and Gosh [15] presented an algorithm that clusters categorical data together based on the property of standard deviation based score for calculating estimated roughness (SDR).The technique incorporates a characteristic attribute with minimum SDR value for choosing the partitioning attribute. Finally, Prabha Dhadayudhan and Ilango [16] proposed the Minimum Average Dissimilarity between Objects (MADO) that utilizes the elements of rough set theory for clustering data through the estimation of dissimilarity between objects.

From the literature review carried out with the various clustering techniques [17-19] that involves rough set theory, it is found to have following limitations,

- A rough theory based normalized score technique that incorporates an equivalence property in clustering has not been explored to the best of our knowledge.
- A rough set theory based clustering mechanism that could identify different learning styles of e-learning has not been much explored.

Hence, a Minimum Normalized Dissimilarity between Objects (MNDBO) techniques that maximizes cohesion and minimizes coupling has been proposed.

3 The Minimum Normalized Dissimilarity between Objects (MNDBO)

In an e-learning environment, the manipulation of dependencies and roughness between the attributes that determine the learning capability of students depends on factors like interest, psychology, graphics content and audio content. But, it is highly difficult due to dynamic learning capabilities of target audience. However, Minimum Normalized Dissimilarity between Objects (MNDBO) techniques overcomes this limitation by incorporating a significant property of rough set theory called equivalence property. The clustering attribute is determined based on the deviation of scores estimated between the objects of each equivalent class.

Let "S_1" and "S_2" be the sets that contain the attributes in the data and the data's whose value is equal for a specific attribute. In each and every manipulation, the set "S_2"elucidates the data's of each and very equivalence class. The deviation score (Dev_{Score}) estimated between data's within the set "S2"., is determined through equation (1) as

$$Dev_{Score} = \frac{\sigma_{(x_a,x_b)}}{M_{(x_a,x_b)}} \times 100 \qquad (1)$$

Where, the standard deviation and expected mean of the datum of the attributes are derived through equation (2) and (3) as,

$$\sigma_{(x_a,x_b)} = \sqrt{\frac{\sum_{i=1}^{n}(x-\overline{x_i})^2}{n}} \qquad (2)$$

$$M_{(x_a,x_b)} = \frac{\sum_{i=1}^{n} x_i}{n} \qquad (3)$$

Cite this article as: K.S.Bhuvaneshwari, Dr. D. Bhanu, Dr. S. Sophia. "An enhanced Rough Set Based Technique for Elucidating Learning styles in E-Learning System." *International Conference on Systems, Science, Control, Communication, Engineering and Technology (2015)*: 27-32. Print.

From the deviation score manipulated from equation (1), the normalized_score that depicts the actual deviation between data of each attribute from each of the sets of data is given by equation (4) as

$$Normalized\_score = \frac{Dev\_score(i) - Dev\_Min\ Score(i)}{Dev\_Max\ score(i) - Dev\_Min\ Score(i)} \quad (4)$$

This normalized_score is calculated based on the ratio of difference of deviation between individual cluster score and the minimum individual cluster score to the difference of deviation between maximum individual cluster score and the minimum individual cluster score. This normalized_score factor is considered as the significant factor utilized for optimal identification of clusters in order to extract knowledge from the datasets to interpret the learning styles of students during the e-learning process.

In the next section, the proposed Minimum Normalized Dissimilarity between Objects (MNDBO) algorithm is presented, the MNDBO algorithm initially considers the set S_1 as a single cluster, then based on the deviation_score and normalized_score, the equivalent classes are derived from S_1 .The equivalent classes enumerated from the S_1, is considered as S_2 that contains collection of sets of data based on the number of clusters 'k' considered for cluster analysis. The number of elements of each set grouped from set S_2 depends on the number of elements that are present in each of the individual cluster. Further, the partitioning element utilized for each clustering process depends upon the minimum normalized_score, which determines the point of datum that is considered as the estimation point of knowledge used for cluster analysis through rough set theory.

The MNDBO clustering algorithm is given below:

Algorithm MNDBA_Cluster(Data_Set DS, Cluster Required C)

//*Input:* Data Set for Clustering, Number of Clusters needed

Begin
Initialize the number of clusters IC = 1;
Set C as the number of clusters;
S_2- set of equivalent classes derived from S1 based on Normalized_Score
Intialize the parent node to Data Set DS
do
for each attribute a_i from Data Set DS (i varies from 1 to n, where 'n' denotes the number of attributes in each data set DS
for j varies from 1 to m, where 'm' is the possible different values of each attribute a_i
in parent node(DS), determine the group of equivalence classes for a_i with attribute value 'j' denoted through set S2
manipulate Dev_{score}(S2) based on $\sigma_{(x_a,x_b)}$ and $M_{(x_a,x_b)}$.
next
next
set Normalized_Score = Min(Normlized_Score(S2)) for every set with constraints $|S2| \geq 1$
estimate the partitioning attribute ai based on minimum Normalized_Score
increment the number of cluster to 1 (ie)IC=IC+1
set Parent_Node (DS) = New_ Parent_Node (IC)
while (INC < k)
End
Algorithm New_Parent_Node(IC)
Begin
for(i varies from 1 to IC)
size of cluster (i) = number of cluster (i)
next
estimate Maximum(Size of cluster(i))
return (Number of elements(i) equals to Maximum(Size of Cluster(i))
end

Furthermore, the proposed algorithm is compared with existing benchmark techniques like MADO, SDR and MMR through parameters like cohesion and coupling for estimating the superior performance of the proposed algorithm.

4 EXPERIMENTAL RESULTS

In the experimental analysis, real data sets are elucidated from the feedback form of three e-learning tutorial institutions are collected for segmentation and cluster analysis. The feedback form was collected for a period of three years. The data-set1 contains 5642 records, data set2 contains 4539 and data set3 contains 3403 records. From the feedback form, four attributes of e-learning viz., accessibility, and cost effectiveness, understanding and, time-saving were used to define the values of A, C, U and T values. Where,

Cite this article as: K.S.Bhuvaneshwari, Dr. D. Bhanu, Dr. S. Sophia. "An enhanced Rough Set Based Technique for Elucidating Learning styles in E-Learning System." *International Conference on Systems, Science, Control, Communication, Engineering and Technology (2015)*: 27-32. Print.

'A' represents the e-content accessibility index, 'C' represents the cost incurred in accessing the e-content, 'U' represents the understanding quotient that differs from each and every student and 'T' represents the amount of time saved through e-learning rather than the traditional method. Hence, all the three datasets contains only four attributes viz., A, C, U and T for each of the student. The values of A, C, U and T are normalized as follows:

1) Arrange the data set in ascending of A, C, U and T.
2) Partition the data set into five equal parts with 20% of the available records in each part.
3) Assign classification index to each of the divided part into highly significant, significant, moderate, tolerable, least significant

Initially, the MNDBO algorithm is applied into the normalized dataset for segmenting the learning styles of the students into various categories. Then, the benchmark techniques considered for study like MADO, SDR and MMR are applied to the same three normalized dataset for studying the superior performance of the proposed MNDBO algorithm. Further, performance metrics like cohesion and coupling are considered for measuring the consistent quality of the cluster, in which cohesion defines the mean similarity among each elements of the cluster while coupling denotes the degree of similarity between each pair of elements of the cluster. Furthermore, in a dataset, the degree of cohesion must be greater than the degree of coupling.

4.1 Aggregate cohesion value for dataset-1

AGGREGATE COHESION	CLUSTER GROUPS			
	4	5	6	7
MNDBO	1.24121	1.6323	2.1253	2.8121
MADO	1.23111	1.6010	2.0945	2.7122
SDR	1.22498	1.5813	2.0345	2.6012
MMR	1.22323	1.5345	2.0407	2.5119

From Table 1, it is evident that the dataset 1 clusters produced by MNDBO algorithm perform better than MADO by 11%, 14% than SDR and 16% than MMR in terms of maximizing cohesion. Further, on an average the proposed MNDBO algorithm enhances the degree of cohesion by 15%. Since, the proposed clustering technique utilizes a normalized score for estimating the degree of deviation between the each data of the equivalence class.

4.2 Aggregate coupling value for dataset-1

AGGREGATE COUPLING	CLUSTER GROUPS			
	4	5	6	7
MNDBO	0.38111	0.50121	0.71223	0.92151
MADO	0.41211	0.52212	0.72343	0.93121
SDR	0.42228	0.53223	0.73257	0.93862
MMR	0.43212	0.53455	0.74253	0.94819

From Table 2, it is evident that the dataset 1 clusters produced by MNDBO algorithm perform better than MADO by 13%, 18% than SDR and 20% than MMR in minimizing coupling. Further, on an average the proposed MNDBO algorithm minimizes the degree of coupling by 18%. Since, the proposed clustering technique estimates a normalized score based on standard deviation and mean that represents the central tendency of each equivalent class for estimating the degree of coupling between the each data of the equivalence class.

4.3 Aggregate Cohesion value for dataset-2

AGGREGATE COHESION	CLUSTER GROUPS			
	4	5	6	7
MNDBO	1.1771	1.8121	2.4151	2.9121
MADO	1.1621	1.8019	2.3232	2.9101
SDR	1.1611	1.8010	2.2112	2.8151
MMR	1.1522	1.7919	2.2001	2.8101

From Table 3, it is evident that the dataset 1 clusters produced by MNDBO algorithm perform better than MADO by 11%, 14% than SDR and 16% than MMR in terms of maximizing cohesion. Further, on an average the proposed MNDBO algorithm enhances the

Cite this article as: K.S.Bhuvaneshwari, Dr. D. Bhanu, Dr. S. Sophia. "An enhanced Rough Set Based Technique for Elucidating Learning styles in E-Learning System." *International Conference on Systems, Science, Control, Communication, Engineering and Technology (2015)*: 27-32. Print.

degree of cohesion by 15%. Since, the proposed clustering technique utilizes a normalized score for estimating the degree of deviation between the each data of the equivalence class.

4.4 Aggregate Coupling value for dataset-2

AGGREGATE COUPLING	CLUSTER GROUPS			
	4	5	6	7
MNDBO	0.54127	0.70121	0.90121	1.09122
MADO	0.55111	0.71131	0.92212	1.100120
SDR	0.55221	0.71291	0.93343	1.102241
MMR	0.55411	0.72483	0.93996	1.103112

From Table 4, it is evident that the dataset 1 clusters produced by MNDBO algorithm perform better than MADO by 13%, 18% than SDR and 20% than MMR in minimizing coupling. Further, on an average the proposed MNDBO algorithm minimizes the degree of coupling by 18%. Since, the proposed clustering technique estimates a normalized score based on standard deviation and mean that represents the central tendency of each equivalent class for estimating the degree of coupling between the each data of the equivalence class.

Aggregate Cohesion value for dataset-3

AGGREGATE COHESION	CLUSTER GROUPS			
	4	5	6	7
MNDBO	1.1771	1.8121	2.4151	2.9121
MADO	1.1621	1.8019	2.3232	2.9101
SDR	1.1611	1.8010	2.2112	2.8151
MMR	1.1522	1.7919	2.2001	2.8101

From Table 5, it is evident that the dataset 1 clusters produced by MNDBO algorithm perform better than MADO by 11%, 14% than SDR and 16% than MMR in terms of maximizing cohesion. Further, on an average the proposed MNDBO algorithm enhances the degree of cohesion by 15%. Since, the proposed clustering technique utilizes a normalized score for estimating the degree of deviation between the each data of the equivalence class.

Aggregate Coupling value for dataset-3

AGGREGATE COUPLING	CLUSTER GROUPS			
	4	5	6	7
MNDBO	0.54127	0.70121	0.90121	1.09122
MADO	0.55111	0.71131	0.92212	1.100120
SDR	0.55221	0.71291	0.93343	1.102241
MMR	0.55411	0.72483	0.93996	1.103112

From Table 6, it is evident that the dataset 1 clusters produced by MNDBO algorithm perform better than MADO by 13%, 18% than SDR and 20% than MMR in minimizing coupling. Further, on an average the proposed MNDBO algorithm minimizes the degree of coupling by 18%. Since, the proposed clustering technique estimates a normalized score based on standard deviation and mean that represents the central tendency of each equivalent class for estimating the degree of coupling between the each data of the equivalence class.

5 Conclusion

In this paper, a Minimum Normalized Dissimilarity between Objects (MNDBO) algorithms is presented. This MNDBO algorithm estimates the degree of deviation between data's of the same equivalence class. This algorithm also estimates the quality of cluster for the three real data pertaining to student's learning styles during e-learning process. The experimental results also infers that the MNDBO algorithm generates clusters with high degree of cohesion and low degree of coupling when the cluster size is varied from 4 to 7 in increments of 1.The suitability of MNDBO algorithm is proved through the process of testing with synthetic data sets that contains high dimension. Finally, the results also infers that the MNDBO algorithm is highly successful than the benchmark clustering algorithms like MADO, SDR and MMR considered for investigation.

References

Cite this article as: K.S.Bhuvaneshwari, Dr. D. Bhanu, Dr. S. Sophia. "An enhanced Rough Set Based Technique for Elucidating Learning styles in E-Learning System." *International Conference on Systems, Science, Control, Communication, Engineering and Technology (2015)*: 27-32. Print.

[1] C. Bean, and C. Kambhampati, "Autonomous clustering using rough set theory," International Journal of Automation and Computing, 5(1), pp. 90-102, 2008.
[2] F.Cao, J. Liang, Li, D., L. Bai, and C. Dang, "A dissimilarity measure for the k-Modes clustering algorithm," Knowledge Based Systems, 26, pp. 120-127, 2011.
[3] H. Chen, K. Chuang, and M.Chen, "On data labeling for clustering categorical data," IEEE Transactions on Knowledge and Data Engineering, 20(11), pp. 1458-1471, 2008.
[4] C.Cheng, and Y.Chen, 2009, "Classifying the segmentation of customer value via RFM model and RS theory," Expert Systems with Applications, 36(3), pp. 4176-4184, 2009.
[5] V.Ganti, J.Gehrke, and R.Ramakrishnan, "CACTUS-Clustering categorical data using summaries," Proceedings of 5th ACM SIGKDD International conference on Knowledge Discovery and Data Mining, San Diego, CA, USA, pp. 73-83, 1999.
[6] Z. Pawlak, "Rough sets: Theoretical aspects of reasoning about data," Norwell, MA, USA: Kluwer Academic Publishers, 1992.
[7] Z. Pawlak, and A. Skowron, "Rudiments of rough sets. Information Sciences," 177(1), pp.3 – 27, 2007.
[8] S. Guha, R. Rastogi, and K.Shim, "ROCK: A robust clustering algorithm for categorical attributes," Information Systems, 25(5), pp. 345-366, 2000
[9] T. Herawan, M.M. Deris, and J.H. Abawajy, "A rough set approach for selecting clustering attribute," Knowledge Based Systems, 23(3), pp. 220-231, 2010.
[10] T. Herawan, R. Ghazali, I.T.R. Yanto, and M.M. Deris, "Rough set approach for categorical data clustering," International Journal of Database Theory and Application, 3(1), pp. 33-52, 2010.
[11] P. Kumar, and B.K.Tripathy., "MMeR: an algorithm for clustering heterogeneous data using rough set theory," International Journal of Rapid Manufacturing, 1(2), pp. 189-207, 2009.
[12] T. Kunz, and J.P. Black, "Using automatic process clustering for design recovery and distributed debugging," IEEE Transactions on Software Engineering, 21(6), pp. 515 -527, 1995.
[13] R. Ling, and D.C. Yen, "Customer relationship management: An analysis framework and implementation strategies," Journal of Computer Information Systems, 41(3), pp. 82-97, 2001.
[14] B.K.Tripathy, and A. Ghosh, "SDR: An algorithm for clustering categorical data using rough set theory," Proceedings of IEEE conference on Recent Advances in Intelligent Computational Systems, Trivandrum, India, pp. 867-872, 2011.
[15] B.K. Tripathy, and A. Ghosh, "SSDR: An algorithm for clustering categorical data using rough set theory," Advances in Applied Science Research, 2(3), pp. 314-326, 2011.
[16] Prabha dhandayudhan and Ilango Krishnamurthi, MADO: an algorithm for clustering categorical data using rough set theory," Data and Knowledge Engineering, 63(3), pp. 879-893, 2014.
[17] Z. Pawlak, "Rough set," International Journal of Computer and Information Sciences, 11(5), pp. 341-356, 1982.
[18] Z. Pawlak, "Rough sets: Theoretical aspects of reasoning about data," Norwell, MA, USA: Kluwer Academic Publishers, 1992.
[19] J.Y. Shyng, F.K. Wang, G.H.Tzeng, and Wu, K.S., "Rough set theory in analyzing the attributes of combination values for the insurance market," Expert Systems with Applications, 32(1), pp. 56-64, 2007.

Cite this article as: K.S.Bhuvaneshwari, Dr. D. Bhanu, Dr. S. Sophia. "An enhanced Rough Set Based Technique for Elucidating Learning styles in E-Learning System." *International Conference on Systems, Science, Control, Communication, Engineering and Technology (2015)*: 27-32. Print.

International Conference on Systems, Science, Control, Communication, Engineering and Technology 2015 [ICSSCCET 2015]

ISBN	978-81-929866-1-6	**VOL**	01
Website	icssccet.org	**eMail**	icssccet@asdf.res.in
Received	10 - July - 2015	**Accepted**	31- July - 2015
Article ID	ICSSCCET009	**eAID**	ICSSCCET.2015.009

Mechanical Behaviour Of Natural Fiber Reinforced Polymer Matrix Composites

S.Karthik, S.N.Vijayan
Assistant Professor, Department of Mechanical Engineering,
Karpagam Institute of Technology, Coimbatore, India

Abstract: *Fiber-reinforced polymer composites have played a dominant role for a long time in a variety of applications for their high specific strength and modulus. The fiber which serves as a reinforcement in reinforced polymer is in the form of natural fibers. In this connection, an investigation has been carried out to make use of coconut fiber which is available abundantly in India. Natural fibers are not only strong and lightweight but also relatively very cheap. The present work describes the development and characterization of a new set of research was carried out by reinforcing the matrix (Epoxy resin) with natural material (Coconut fiber). The newly developed composites are characterized with respect to their mechanical characteristics. The natural fibers were exposure to chemical treatment (NaOH) before manufacturing of laminates. Samples of coconut-Epoxy laminate were manufactured using compression moulding method were the stacking of fibers takes place. Specimens were cut from the fabricated laminate according to the ASTM standards for different experiments. For Tensile test, flexural test and Impact test samples were cut in the desired shape. Tensile Strength, Flexural Strength and Impact Strength were observed and compared to each other. Tensile test showed maximum ultimate tensile strength for untreated 80 mm length fiber compared to others. Flexural test showed maximum ultimate flexural strength for untreated 80 mm length fiber compared to others. Impact test showed higher impact energy for treated 40 mm length fiber compared to others.*

Keywords: CoconutInflorescence, NaOH, Epoxy Resin;Compression moulding, Tensile test, Flexural test, Impact test.

I. INTRODUCTION TO COMPOSITE MATERIAL

A composite is a material made by combining two or more dissimilar materials in such a way that the resultant material is endowed with properties superior to any of its parental ones. Fiber-reinforced composites, owing to their superior properties, are usually applied in different fields like defense, aerospace, engineering applications, sports goods, etc. Nowadays, natural fiber composites have gained increasing interest due to their eco-friendly properties. A lot of work has been done by researchers based on these natural fibers. Natural fibers such as jute, sisal, silk and coir are inexpensive, abundant and renewable, lightweight, with low density, high toughness, and biodegradable. Natural fibres such as jute have the potential to be used as a replacement for traditional reinforcement materials in composites for applications which requires high strength to weight ratio and further weight reduction. Bagasse fiber has lowest density so able to reduce the weight of the composite upto very less. So by using these fibers (jute, bagasse, and lantana camara) the composite developed is cost effective and perfect utilization of waste product. Natural fiber reinforced polymer composites have raised great attentions and interests among materials scientists and engineers in recent years due to the considerations of developing an

Cite this article as: S.Karthik, S.N.Vijayan. "Mechanical Behaviour Of Natural Fiber Reinforced Polymer Matrix Composites." *International Conference on Systems, Science, Control, Communication, Engineering and Technology (2015)*: 33-37. Print.

environmental friendly material and partly replacing currently used glass or carbon fibers in fiber reinforced composites. They are high specific strength and modulus materials, low prices, recyclable, easy available in some countries, etc.

II. MATERIALS AND METHODS

1. Materials Used

i. Natural fiber
Coconut inflorescence
ii. Epoxy resin –LY 556
iii. Hardener –HY 951

2. Coconut Inflorescence

An Inflorescence is a group or cluster of flowers arranged on a stem that is composed of a main branch or a complicated arrangement of branches. Morphologically, it is the part of the shoot of seed plants where flowers are formed and which is accordingly modified. The modifications can involve the length and the nature of the Internodes and the phyllotaxis, as well as variations in the proportions, compressions, swellings, adnations, connations and reduction of main and secondary axes. Inflorescence can also be defined as the reproductive portion of a plant that bears a cluster of flowers in a specific pattern. The stem holding the whole inflorescence is called a peduncle and the main stem holding the flowers or more branches within the inflorescence is called the rachis. The stalk of each single flower is called a pedicel. The fruiting stage of an inflorescence is known as an infructescence. A flower that is not part of an inflorescence is called a solitary flower and its stalk is also referred to as a peduncle. Any flower in an inflorescence may be referred to as a floret, especially when the individual flowers are particularly small and borne in a tight cluster, such as in a pseudanthium. Fig.1 shows the clear picture of coconut inflorescence.

Figure 1. Coconut Inflorescence

3.Fiber Preparation

The various steps in preparation of fiber are fiber extraction, pre-treatment, and chopping according to requirement.

4. Fiber Extraction

The coconut inflorescence contains fiber which is surrounded by thick flesh material. In order to obtain the fiber the inflorescence is placed in water for about 10 days. Then the coconut inflorescence is hammered such that fiber comes out of the flesh. Then the fiber which is obtained is placed in a room without contact with sunlight such that the fiber gets separated individually. Then the fiber can be prepared for chemical treatment.

5.Fiber Treatment

The extracted fibers are to be chemically treated with NaOH for making the surface of the fiber rougher such that bonding will be better during composite fabrication. In this work the fibers were treated with 5% of NaOH. The chemical treatment erodes the material from the fiber. The chemical treatment erodes the cellulose, lignin and wax contents is shown in fig.2.

Figure 2. Chemical Treatment of Coconut Inflorescence

Cite this article as: S.Karthik, S.N.Vijayan. "Mechanical Behaviour Of Natural Fiber Reinforced Polymer Matrix Composites." *International Conference on Systems, Science, Control, Communication, Engineering and Technology (2015)*: 33-37. Print.

6.Fiber Chopping

Treated fibers were chopped uniformly for different length of 40mm & 80mm.

7.Fabrication Of Composite

The composite specimen is fabricated by compression moulding technique.

8.Sizing Of Fiber

The fiber treated with 5% of NaOH solution, and non treated fiber, both the materials are cutted into a specific sizes that are 40mm & 80 mm. Composite specimens of coconut fiber consist of four type of fiber material that are.

1. Treated 40mm size fiber with NaOH
2. Treated 80mm size fiber with NaOH
3. Non treated 40mm fiber
4. Non treated 80mm fiber

9.Fabrication Of Fiber Plates

Fiber plates are made by using compression moulding process. Required dimension of fiber plates are 270mm square and thickness of 3mm. fabricated image of fiber plate is shown in fig.3.

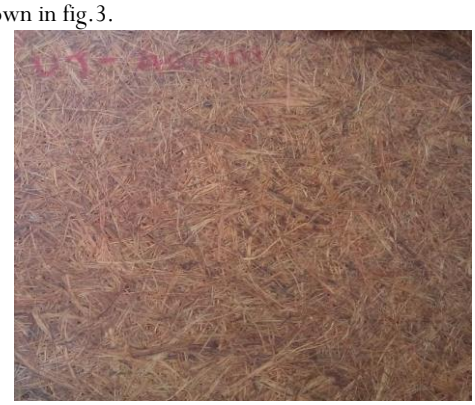

Figure 3. Fabrication of Fiber Plates.

Dies are selected with accurate dimensions of required plate size, addition of clearance 20mm because of compression force elongate the fiber and it may increase the size. Poly vinyl alcohol is pouring on the surface of female die as well as the male die to remove the fiber plate safely. Fiber plate should contain Epoxy Resin of 30% to increasing the strength. Compression pressures play a leading role in fiber plate fabrications. Applied Pressure to the male die is 1500 psi and the temperature maintained at 70-80 C. Dies are keep in the position and hold it for 2 hours . The four type of fiber plates are fabricated by using compression moulding process.

10.Sample Dimensions Analyse

Three type of tests are involved in this process to measure the strength of a specimen. Before testing we made cut samples. Various test need a various dimensions that are given below, Tensile test needs dimensions with the ASTM D638 standard: 19 mm width, 165 mm length and 3 mm thickness and 10 mm min-1 crosshead speed. Flexural tests, a load were applied on the specimen at 2.8 mm min-1 crosshead motion rate. It needs dimensions with the ASTM D 790 standard: 25 mm width,76 mm length and 3mm thickness. Impact tests needs dimensions with the ASTM D 6110 standard: 12 mm with, 63.5 mm length and 3mm thickness to evaluate its impact strength.

11.Mechanical Testings

Experimental investigation on the mechanical properties of natural fiber.

1. Tensile strength
2. Flexural strength
3. Impact strength

III. RESULT AND DISCUSSION

1.Results of Tensile Test

The UTS vs Length of fiber reinforcement is shown in fig.4 The strength of 80mm untreated fiber reinforcement reach the maximum content, compared to other. That is 18.179 N/mm^2.

Cite this article as: S.Karthik, S.N.Vijayan. "Mechanical Behaviour Of Natural Fiber Reinforced Polymer Matrix Composites." *International Conference on Systems, Science, Control, Communication, Engineering and Technology (2015)*: 33-37. Print.

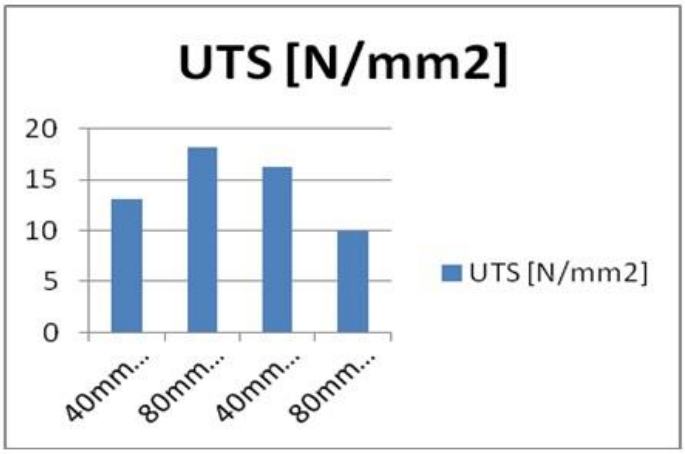

Figure 4. UTS VS Length of Fiber Reinforcement

2.Results of Flexural Test

The flexural properties of the fibers/PR composites with different proportions were tested and the results are shown in fig.5. The volume fraction of fibers and resin was used is 70:30.And 80mm untreated fiber reinforcement reach the maximum content, compare to other. Thatis52.049Mpa.

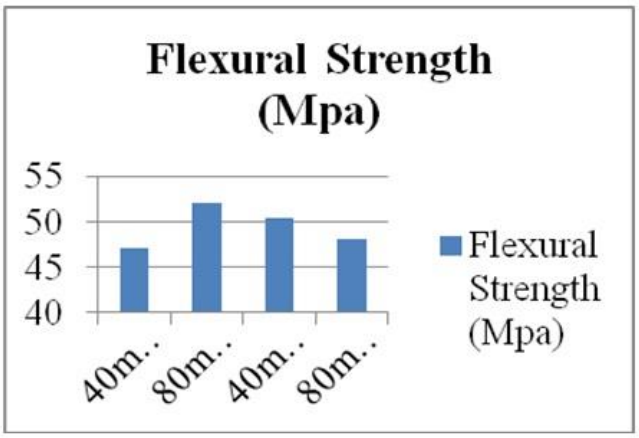

Figure 5. Flexural Strength VS Length of Fiber Reinforcement

3.Results of Impact Test

Izod impact tests were conducted based on ASTM D256 standard is shown in fig.6. Four samples for each reinforcement were tested and among them 40 mm treated fiber reinforcement has high impact strength of about 0.616 joules.

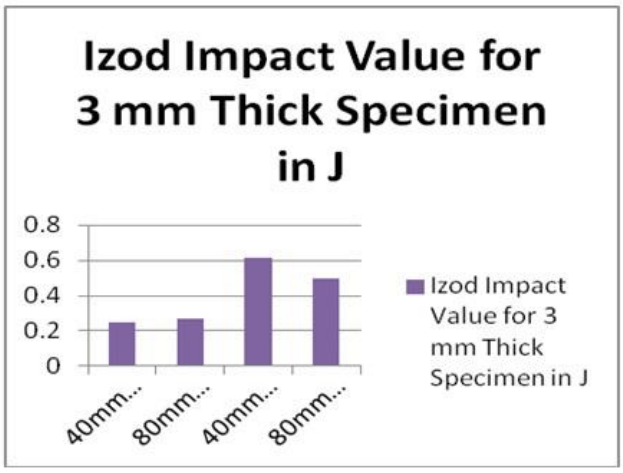

Figure 6. Impact Strength

Cite this article as: S.Karthik, S.N.Vijayan. "Mechanical Behaviour Of Natural Fiber Reinforced Polymer Matrix Composites." *International Conference on Systems, Science, Control, Communication, Engineering and Technology (2015)*: 33-37. Print.

IV. CONCLUSION

The experimental investigation on the mechanical properties of coconut fiber reinforced polymer matrix composites leads to the following conclusions:

- ✓ Mercerization of coconut inflorescence fiber leads to thinner fiber with higher elongation.
- ✓ It is possible to make use of coconut inflorescence fiber as an alternate for synthetic fibers in the reinforcement of polymer matrix composites.
- ✓ Composites have been fabricated according to different length of fiber.
- ✓ According to the ASTM standards, the mechanical properties that have been founded are tensile, flexural, &impact test.
- ✓ Tensile test showed maximum ultimate tensile strength of 18.179 N/mm^2 for untreated 80 mm length fiber compared to others.
- ✓ Flexural test showed maximum ultimate flexural strength of 52.049 N/mm^2 for untreated 80 mm length fiber compared to others.
- ✓ Impact test showed higher impact energy of about 0.616 joules for treated 40 mm length fiber compared to others.

Reference

[1] Sudhir.A, Madhukiran.J, Dr.S.Srinivasa Rao, Dr.S.Madhusudan (2014), "Tensile and Flexural Properties of Sisal/Jute Hybrid Natural Fiber Composites",ISSN:2249-6645.

[2] D.Chandramohan, Dr.K.Marimuthu (2011),"Tensile and Hardness Tests on Natural Fiber Reinforced Polymer Composite Material", ISSN:2230-7818.

[3] Girisha.C, Sanjeevamurthy,Gunti Ranga srinivas (2012),"Sisal/Coconut Coir Natural Fibers-Epoxy Composites: Water Absorption and Mechanical Properties", ISSN:2277-3754.

[4] Subramanian Raman, Chattopadhyay Subhanjan Salil Kumar , Sharan Chandran M (2014),"Fabrication, Testing and Analysis of Braided and Short fibre reinforced Jute Epoxy Bio-composite", pp.1721-1724.

[5] Alok Singh, Savita Singh, Aditya Kumar (2013),"Study of mechanical properties and absorption behaviour of coconut shell powder-epoxy composites", pp.157-161.

[6] P. Hari Sankar , H.Raghavendra Rao (2011),"Chemical Resistance and Tensile Properties of Bamboo and Glass Fibers Reinforced Epoxy Hybrid Composites", ISSN 2277-7164.

[7] Abdul Hakim Abdullah,Siti Khadijiah Alias,Norhisyam Jenal, Khalina Abdan,Aidy Ali (2012),"Fatigue behavior of kenaf fibre reinforced epoxy composites", ISSN 0125-8281.

[8] Kishore Debnath, Vikas Dhawan, Inderdeep Singh, Akshay Dvivedi (2014),"Adhesive Wear and Frictional Behavior of Rice Husk Filled Glass/Epoxy Composites", pp.247-667.

[9] Dr. Shajan Kuriakose, Dr. Deviprasad Varma, Vaisakh V.G (2012),"Mechanical Behaviour of Coir reinforced Polyster Composites–An Experimental Investigation", ISSN 2250-2459.

[10] Dheeraj Kumar (2014),"Mechanical Characterization of Treated Bamboo Natural Fiber Composite", pp. 551-556.

[11] E. F. Cerqueira, C. A. R. P. Baptista, D. R. Mulinari (2011)"Mechanical behaviour of polypropylene reinforced sugarcane bagasse fibers composites",pp. 2046–2051.

[12] Goulart.S.A.S, Oliveira.T.A, Teixeira.A, Mileo.P.C, Mulinari.D.R. (2011),"Mechanical Behaviour of Polypropylene Reinforced Palm Fibers Composites", pp. 2034–2039.

[13] P. S. Souza, E. F. Rodrigues, J. M. C Preta, S. A. S. Goulart, D. R. Mulinari (2011),"Mechanical properties of HDPE/textile fibers composites", pp. 2040–2045.

Cite this article as: S.Karthik, S.N.Vijayan. "Mechanical Behaviour Of Natural Fiber Reinforced Polymer Matrix Composites." *International Conference on Systems, Science, Control, Communication, Engineering and Technology (2015)*: 33-37. Print.

International Conference on Systems, Science, Control, Communication, Engineering and Technology 2015 [ICSSCCET 2015]

ISBN	978-81-929866-1-6	**VOL**	01
Website	icssccet.org	**eMail**	icssccet@asdf.res.in
Received	10 - July - 2015	**Accepted**	31- July - 2015
Article ID	ICSSCCET010	**eAID**	ICSSCCET.2015.010

MULTIPATH BROADCAST AND GOSSIP BASED APPROACH FOR VIDEO CIRCULATION

S.Ganapathi Ammal[1], T.Yawanikha[2], S.Thavasi Anand[3]
[1]Assistant Professor, Department of IT, Karpagam Institute of Technology, Coimbatore, India
[2]Assistant Professor, Department of IT, Karpagam Institute of Technology, Coimbatore, India
[3]Department of ECE, Karpagam Institute of Technology, Coimbatore, India

Abstract: *LIVE media streaming applications have become more and more popular. IP multicast is the most efficient mechanism but Due to the practical issues of routers, IP multicast has not been widely deployed in the wide-area network infrastructure. The application-level solution build a peer-to-peer (P2P) overlay network out of unicast tunnels across cooperative participating users. P2P media streaming has become a promising approach to broadcast non interactive live media from one source to a large number of receivers. Design of a live P2P streaming system faces many challenges. Therefore, no single application-level multicast stream can meet the requirements of everyone. The proposed architecture aims to provide higher streaming quality and to provide robustness. In the Proposed System the Parallel efforts have been exerted in the media streaming field and networking field to avoid the problem of distributing LIVE video. The tree-based approaches are vulnerable for dynamic group variation but the gossip based mesh-like topology for overlay network systems allow peers to form multiple neighbors, so multilayered video contents are distributed among mesh-like network. Due to this multisource transmission scheme, packets can be exchanged among clients efficiently. In Proposed, The system can achieve improved performance on video delivery quality, bandwidth utilization, and service reliability when using the peer-assisted multipath transmission.*

I INTRODUCTION

Multicasting is a natural paradigm for streaming live multimedia to multiple end receivers. Since IP multicast is not widely deployed, many application-layer multicast protocols have been proposed. However, all of these schemes focus on the construction of multicast trees, where a relatively small number of links carry the multicast streaming load, while the capacity of most of the other links in the overlay network remain unused. Recently, there are many research interests in providing efficient and scalable multimedia distribution service. However, stringent quality-of-service (QoS) requirements for media distribution, as well as dynamically changing and heterogeneous network capacity in today's best effort Internet, bring many challenges. A novel framework for multimedia distribution service based on peer-to-peer (P2P) networks is introduced. A topology-aware overlay is proposed in which hosts self-organize into groups. End hosts within the same group have similar network conditions and can easily collaborate with each other to achieve QoS awareness. In order to improve media delivery quality and provide high service availability, there are two distributed heuristic replication strategies, intergroup replication and intragroup replication, based on this topology-aware overlay. Specifically, intergroup replication is aimed to improve the efficiency of media content delivery between the group where a request is issued and the group where the content is stored. Also, intragroup replication is targeted at improving the availability of the content. The requirement of global knowledge impairs their applicability to very large-scale groups. Gossip-based protocols for group communication provide attractive scalability and reliability properties.

Cite this article as: S. Ganapathi Ammal, T. Yawanikha, S. Thavasi Anand. "MULTIPATH BROADCAST AND GOSSIP BASED APPROACH FOR VIDEO CIRCULATION." *International Conference on Systems, Science, Control, Communication, Engineering and Technology (2015)*: 38-42. Print.

II RELATED WORKS

Although there have been significant research efforts in peer-to-peer systems during the past five years, one category of peer-to-peer systems has so far received less attention: the peer-to-peer media streaming system. The major difference between a general peer-to-peer system and a peer-to-peer media streaming system [4] lies in the data sharing mode among peers: the former uses the 'open-after-downloading' mode, while the latter uses the 'play-while-downloading' mode. More specifically, in a peer-to-peer media streaming system, a subset of peers own a certain media file, and they stream the media file to requesting peers. On the other hand, the requesting peers playback and store the media data during the streaming session, and they become supplying peers of the media file after the streaming session.

Multimedia distribution services basically fall into three categories:

1) centralized multimedia distribution;
2) CDN-based multimedia distribution; and
3) P2P networks. In the centralized multimedia distribution approach, a centralized multimedia server is deployed to support clients to access multimedia content across the Internet.

In order to enhance the storage and capacity of the centralized server and to improve the service availability, server clustering or mirroring are proposed. Although those techniques are widely deployed in traditional distribution service, the performance of the centralized architecture is very limited, as this architecture does not work well when there is a bottleneck in the network. To overcome the limitation in centralized distribution architecture, CDN-based multimedia distribution service [3], e.g.,Akamai, deploys a large number of servers at the edge of the network. The objective is to efficiently redirect user requests to appropriate servers so that request latency is reduced and load among servers are balanced. The infrastructure, including servers and network links, is engineered to provide a high level of performance guarantee. However, there are some limitations for the CDN-based architecture to provide efficient distribution service.

III PROBLEM STATEMENT

In the Internet architecture, the internetworking layer, or IP, implements a minimal functionality — a best-effort unicast datagram service, and end systems implement all other important functionality such as error, congestion, and flow control. Such a minimalist approach is one of the most important technical reasons for the Internet's growth from a small research network into a global, commercial infrastructure with heterogeneous technologies, applications, and administrative authorities. The growth of this network has in turn unleashed the development of new applications, which require richer network functionality.

IPMulticast is the first significant feature that has been added to the IPlayer since its original design and most routers today implement IPMulticast. Despite this, IPMulticast [1] has several drawbacks that have so far prevented the service from being widely deployed. First, IPMulticast requires routers to maintain per group state, which not only violates the "stateless" architectural principle of the original design, but also introduceshigh complexity and serious scaling constraints at the IPla yer. Second, IPMulticast is a best effort service, and attempts toconform to the traditional separation of routing and transport that has worked well in the unicast context. However, providing higher level features such as reliability, congestion control, flow control, and security has been shown to be more difficult than in the unicast case. Finally, IPMulticast calls for changes at the infrastructural level, and this slows down the pace of deployment. In this paper, the issue of whether multicast related functionality should be implemented at the IPlayer [6] or at the end systems. In particular, a model in which multicast related features, such as group membership, multicast routing and packet duplication, are implemented at end systems, assuming only unicast IPservice [1].

Tree-based protocols and extensions

Many overlay streaming systems employ a tree structure, stemmed from IP multicast. Constructing and maintaining an efficient disuibution tree among the overlay nodes is a key issue to these systems. In CoopNet [8], the video source, as the root of the tree, collects the information of all the nodes for tree construction and maintenance. Such a centralized algorithm can be very efficient. but relies on a powerful and dedicated root node. To the contrary, drstributed algorithms, such as SpreadIt, NICE [15], and ZIGZAG [9], perform the constructing and routing functions across a series of nodes. For a large-scale network, these algorithms adopt hierarchical clustering to achieve minimized transmission delay (in terms of tree height) as well as bounded node workload (in terms of fanout[17] degree). Still, an internal node in a tree has a higher load and its Ieave or crash often causes buffer underflow in a large population of descendants.

Gossip-based protocols

Gossip (or epidemic) algorithms have recently became popular solutions to multicast message dissemination in peer-to-peer systems. In a typical gossip algorithm, a node sends a newly generated message to a set of randomly selected nodes; these nodes do similarly in the next round, and so do other nodes until the message is spread to all. The random choice of gossip targets achieves resilience to

Cite this article as: S. Ganapathi Ammal, T. Yawanikha, S. Thavasi Anand. "MULTIPATH BROADCAST AND GOSSIP BASED APPROACH FOR VIDEO CIRCULATION." *International Conference on Systems, Science, Control, Communication, Engineering and Technology (2015)*: 38-42. Print.

random failures and enables decentralized operations. The data delivery method in UONet [12] is also partially motivated by the gossip concept. Nevertheless, the use of gossip for streaming is not straightforward because its random push may cause significant redundancy. which is particularly severe for high-bandwidth streaming applications.

IV PEER-TO-PEER NETWORK

The P2P network that facilitates the Peer Streaming system is for a particular streaming session, let the server be a node that originates the streaming media. Let the client be a node that currently requests the streaming media. Let the serving peer be a node that serves the client with a complete or partial copy of the streaming media. In the Peer Streaming system, the server, the client and the serving peers are all end-user nodes connected to the Internet. Because the server is always capable of serving the streaming media, the server node is always a serving peer.

Intra-overlay optimization

With the improvement of network bandwidth, multimedia services based on streaming live media, such as IPTV have gained much attention recently. Significant progress has been made on the efficient distribution of live streams in a real-time manner over a large population of spectators with good QoS.

Due to the practical issues of routers, IP multicast has not been widely deployed. Therefore, researchers have expended a lot of effort building an efficient streaming overlay multicast scheme based on P2P networks in which spectators behave as routers for other users. Efficient and scalable live-streaming overlay construction has become a best approach.

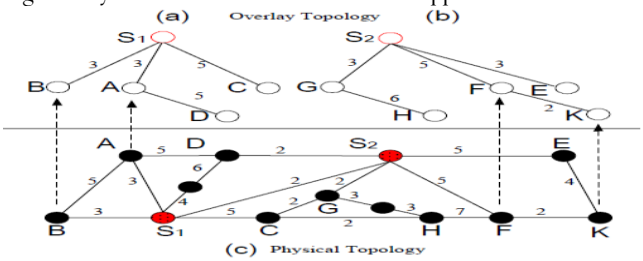

Fig 2: Intra-overlay optimization:(a) optimal multicast tree rooted at S1:(b) optimal multicast tree rooted at S2; (c) physical topology

Fig 2 shows an example of intra-overlay optimization with two logical streaming overlays. Peers A, B, C and D join the stream originating at S1 and peers E, F, G, H and K join the stream originating at S2. The number on each edge represents the cost of the link between two nodes.

B. P2P-based multimedia distribution service architecture

P2P based multimedia distribution service framework that will be QoS-aware, scalable, and cost-effective. The clients join the P2P network and contribute resources such as storage to the system. The multimedia contents are stored in peers storage, and each peer distributes the contents or streaming service to other peers. In order to provide QoS-aware multimedia distribution service, a topology-aware network is necessary. This architecture is proposed to build a topology-aware overlay network. In such a network, nearby hosts or peers are clustered into application groups. Since peers within one group are very close to each other, the QoS requirements for content delivery, such as latency, can be easily satisfied. Generally speaking, hosts that go through the same gateway to the Internet or within a subnetwork can naturally belong to one group.

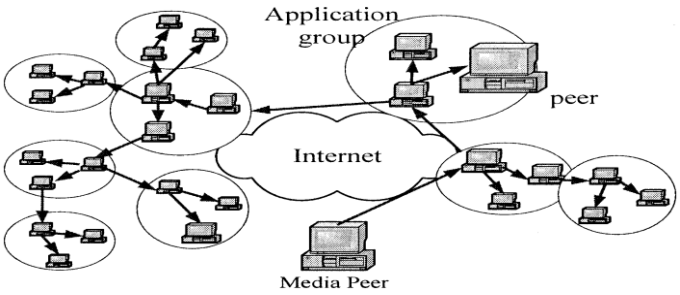

Fig 3: Peer-to-peer based multimedia distribution service.

The constructed overlay network can significantly decrease the communication cost between end-hosts by ensuring that a message reaches its destination with small overhead and highly efficient forwarding. Resource management is one of most important

Cite this article as: S. Ganapathi Ammal, T. Yawanikha, S. Thavasi Anand. "MULTIPATH BROADCAST AND GOSSIP BASED APPROACH FOR VIDEO CIRCULATION." *International Conference on Systems, Science, Control, Communication, Engineering and Technology (2015)*: 38-42. Print.

components in our P2P-based multimedia distribution service. In order to improve system delivery performance and provide high service availability, efficient replication strategies are key elements of the resource management. The purpose of replication strategies is to determine how many replicas of multimedia contents are needed and where to place those replicas. Replication among groups is helpful for accelerating the dissemination of multimedia content. Replication within one group improves the robustness of media distribution service.

Node join and membership management

Each DONet node has a unique identifier, such as its IP address. and maintains a membership cache (mCache) containing a partial list of the identifiers for the active nodes in the DONet. In a basic node joining algorithm a newly joined node first contacts the origin node, which randomly selects a deputy node from its mCache and redirects the new node to the deputy.

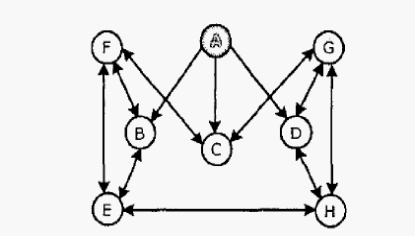

Fig 4: Illustration of partnership in DONet.

The new node can then obtain a list of partner candidates from the deputy, and contacts these candidates to establish its partners in the overlay.

V PEERSTREAMING OPERATIONS

Locating serving peers

The first task that the PeerStreaming client performs is to obtain the IP addresses and the listening ports of a list of neighbor serving peers that hold a complete or partial copy of the serving media. This list is also updated during the media streaming session.

There are in general these approaches that this list can be obtained:
1) from the media server.
2) from one known serving peer.
3) using a distributed hash table (DHT) approach.

Network link: the tcp connection

Most media streaming clients, such as the windows media player or RealPlayer, use the real time transport protocol (RTP), which is carried on top of UDP. The UDP/RTP protocol is chosen for media streaming applications because:

1) The UDP protocol supports IP multicast, which can be efficient in sending media to a set of nodes on an IP multicast enabled network.
2) The UDP protocol does not have any re-transmission or data-rate management functionality. The streaming server and client may implement advanced packet delivery functionality, e.g., forward error correction (FEC), to ensure the timely delivery of media packets.

Peerstreaming requests and replies

The client generates the request and sends it through the outbound TCP connection to a certain serving peer. In network delivery, TCP may bundle the request with prior requests issued to the same peer. If a prior request is lost in transmission, TCP handles the retransmission of the request as well. After the request packet is delivered, it is stored in the TCP receiving buffer of the serving peer. The peer processes the request one at a time. For each request, it reads the requested erasure coded blocks from its disk storage, and sends the requested content back to the client. In case the TCP socket from the serving peer to the client is blocked, i.e., no more bandwidth is available, the serving peer will block until the TCP connection opens up.

VI CONCLUSION

The proposed peerstreaming framework for multimedia distribution service is based on P2P network. The application-level solution build a peer-to-peer (P2P) overlay network out of unicast tunnels across cooperative participating users. P2P media streaming has become a promising approach to broadcast non interactive live media from one source to a large number of receivers. A peer-to-peer

Cite this article as: S. Ganapathi Ammal, T. Yawanikha, S. Thavasi Anand. "MULTIPATH BROADCAST AND GOSSIP BASED APPROACH FOR VIDEO CIRCULATION." *International Conference on Systems, Science, Control, Communication, Engineering and Technology (2015)*: 38-42. Print.

media streaming system is self growing, server less. Peers are heterogeneous in their out-bound bandwidth contribution to the system. This heterogeneity may be caused either by different access networks connecting the peers, or by different willingness of the peers to contribute.

Proxy caching is an efficient technology for handling network bottlenecks in multimedia distribution systems by caching popular content from origin server to proxy servers located at the edge of Internet. Here the peer can able to share data with a group of other peers and searches for the desired data to neighbors or to directory server. Once the desired data are located, the peer downloads the data directly from the other peer's computer. As the data are selectively replicated among peers, this structure allows sharing of data by a large community at low cost. as dedicated servers are not needed, When a new host arrives it uses a locating method to join a nearest group or form its own group according to the group criterion.

REFERENCES

1. Hui Guo, Kwok-Tung Lo, Yi Qian "Peer-to-Peer Live Video Distribution under Heterogeneous Bandwidth Constraints" IEEE TRANSACTIONS ON PARALLEL AND DISTRIBUTED SYSTEMS, VOL. 20, NO. 2, FEBRUARY 2009.
2. S.E. Deering, "Multicast Routing In A Datagram Internetwork," Phd Dissertation, Dept. Of Electrical Eng., Stanford Univ., Dec. 1991.
3. D. Xu, M. Hefeeda, S. Hambrusch, And B. Bhargava, "On Peer-To-Peer Media Streaming," Proc. IEEE Int'l Conf. Distributed Computing Systems (ICDCS '02), July 2002.
4. Z. Xiang, Q. Zhang, W. Zhu, Z. Zhang, And Y.-Q. Zhang, "Peer-To-Peer Based Multimedia Distribution Service," IEEE Trans. Multimedia, Vol. 6, No. 2, Pp. 343-355, Apr. 2004.
5. Y. Chu, S.G. Rao, And H. Zhang, "A Case For End System Multicast," Proc. ACM SIGMETRICS '00, June 2000.
6. S. Banerjee, B. Bhattacharjee, And C. Kommareddy, "Scalable Application Layer Multicast," Proc. ACM SIGCOMM '02, Aug. 2002.
7. D. Tran, K. Hua, And T. Do, "ZIGZAG: An Efficient Peer-To-Peer Scheme For Media Streaming," Proc. IEEE INFOCOM '03, Apr. 2003.
8. N. Magharei And R. Rejaie, "Understanding Mesh-Based Peer-To-Peer Streaming," Proc. 16th NOSSDAV '06, May 2006.
9. X. Zhang, J. Liu, B. Li, And T.-S.P. Yum, "Coolstreaming/Donet: A Data-Driven Overlay Network For Live Media Streaming," Proc. IEEE INFOCOM '05, Mar. 2005.
10. Y. Cui, B. Li, And K. Nahrstedt, "Ostream: Asynchronous Streaming Multicast In Application-Layer Overlay Networks," IEEE J. Selected Areas In Comm., Vol. 22, No. 1, Pp. 91-106, Jan. 2004.
11. M. Castro, P. Druschel, And A.-M. Kermarrec, "Splitstream: High-Bandwidth Content Distribution In A Cooperative Environment," Proc. Second Int'l Workshop Peer-To-Peer Systems (IPTPS '03), Feb. 2003.
12. R. Rejaie And S. Stafford, "A Framework For Architecting Peer-To-Peer Receiver-Driven Overlays," Proc. 14th ACM NOSSDAV '04, June 2004.
13. S. Banerjee, S. Lee, And B. Bhattacharjee, "Resilient Multicast Using Overlays," Proc. ACM SIGMETRICS '04, June 2004.
14. V. Venkatraman, K. Yoshida, And P. Francis, "Chunkyspread: Heterogeneous Unstructured End System Multicast," Proc. 14th IEEE Int'l Conf. Network Protocols (ICNP '06), Nov. 2006.
15. P.T. Eugster Et Al., "Lightweight Probabilistic Broadcast," ACM Trans. Computer Systems, Vol. 21, No. 4, Pp. 341-374, Nov. 2003.
16. M. Sasabe Et Al., "Scalable And Continuous Media Streaming On Peer-To-Peer Networks," Proc. Third IEEE Int'l Conf. Peer-To-Peer Computing (P2P '03), Sept. 2003.
17. V.N. Padmanabhan, H.J. Wang, And P.A. Chou, "Resilient Peer-To- Peer Streaming," Proc. 11th IEEE Int'l Conf. Network Protocols (ICNP '03), Nov. 2003.
18. M. Zhang Et Al., "A Peer-To-Peer Network For Live Media Streaming—Using A Push-Pull Approach," Proc. ACM Multimedia '05, Nov. 2005.
19. X. Liao Et Al., "Anysee: Peer-To-Peer Live Streaming," Proc. IEEE INFOCOM '06, Apr. 2006.
20. J. Guo, Y. Zhu, And B.C. Li, "Codedstream: Live Media Streaming With Overlay Coded Multicast," Proc. SPIE/ACM Conf. Multimedia Computing And Networking (MMCN '04), Jan. 2004.

Cite this article as: S. Ganapathi Ammal, T. Yawanikha, S. Thavasi Anand. "MULTIPATH BROADCAST AND GOSSIP BASED APPROACH FOR VIDEO CIRCULATION." *International Conference on Systems, Science, Control, Communication, Engineering and Technology (2015)*: 38-42. Print.

International Conference on Systems, Science, Control, Communication, Engineering and Technology 2015 [ICSSCCET 2015]

ISBN	978-81-929866-1-6
Website	icssccet.org
Received	10 - July - 2015
Article ID	ICSSCCET011

VOL	01
eMail	icssccet@asdf.res.in
Accepted	31- July - 2015
eAID	ICSSCCET.2015.011

A Review on Springback Effect in Sheet metal Forming Process

P. Chandrasekaran[1], Dr. K. Manonmani[2]
[1]Research Scholar, Department of Mechanical Engineering,
Karpagam Institute of Technology, Coimbatore - 641 105.
[2]Associate Professor, Department of Mechanical Engineering,
Government college of Technology, Coimbatore - 641 013.

Abstract: *To study the significant effect of spring back on bending and other sheet metal forming process. Elastic recovery of formed part in unloading known as springback causes shape error in final product of sheet metal forming processes. The springback occurs at the last step of process and the final geometry of work piece can be obtained at the end of direct process modeling. Having the product geometry at the end of loading, geometry of die parts can be designed for production of target shape. The ultimate goal of the metal forming industry is to form components made of a specific material into a required shape without experiencing springback. The factors affecting the springback such as material properties, bend radius, sheet thickness etc.*

Keywords*:* spring back, sheet metal forming

1. Introduction

The sheet metal forming process involves a combination of elastic–plastic bending and stretch deformation of the workpiece. These deformations may lead to a large amount of springback of the formed part. It is desired to predict and reduce springback so that the final part dimensions can be controlled as much as possible.

One of the most common metal working operations is bending. This process is used not only to form parts such as flanges, seams etc. but also to impart stiffness to the part by increasing its moment of inertia. The terminology used in bending is shown in figure 1.

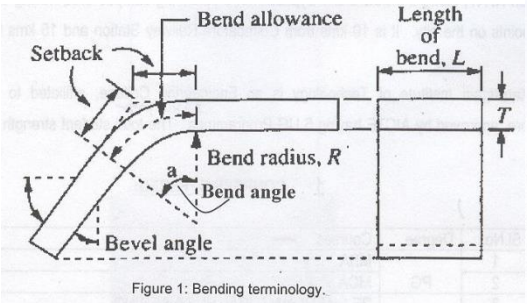

Figure 1: Bending terminology.

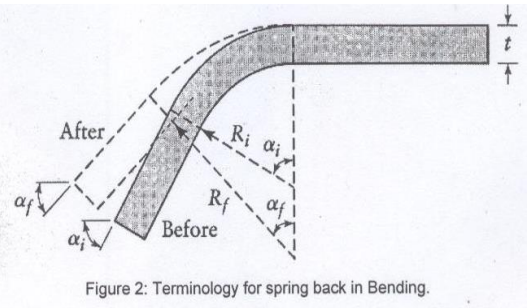

Figure 2: Terminology for spring back in Bending.

Cite this article as: P. Chandrasekaran, Dr. K. Manonmani. "A Review on Springback Effect in Sheet metal Forming Process." *International Conference on Systems, Science, Control, Communication, Engineering and Technology (2015)*: 43-49. Print.

The outer fibers of the material are in tension and the inner fibers are in compression. Theoretically, the strains at the outer and inner fibers are equal in magnitude and are given by the equation.

$$e_0 = e_i = \frac{1}{(2R/T)+1} \quad (1)$$

2. SpringBack

Because all materials have a finite modulus of elasticity, plastic deformation is follow' by elastic recovery upon removal of the load; in bending, this recovery is known as *springback.* As shown in Fig. 1, the final bend angle after spring back is smaller and the final bend radius is larger than before. This phenomenon can easily be observed by bending a piece of wire or a short strip metal. Spring back occurs not sheets or plate, but also in bending bars, rod, and wire of any cross-section. A quantity characterizing springback is the springback factor Ks, which is defined as follows. Because the bend allowance is the same before and after bending (see figure 1), the relationship obtained for pure bending is

$$\text{Bend allowances} = \left(R_i + \frac{t}{2}\right)\alpha_i = \left(R_f + \frac{t}{2}\right)\alpha_f \quad (2)$$

from this relationship, Spring factor, Ks is defined as:

$$K_s = \frac{\alpha_f}{\alpha_i} = \frac{(2R_i/t)+1}{(2R_f/t)+1} \quad (3)$$

where Ri and Rf are the initial and final bend radii, respictively. It can be noted Fromeqution 2 that Ks depends only on the R/t ratio.Where R is the minimum bend radius. A springback factor of Ks =1 indicates no springback, and Ks=0 indicates complete elastic recovery (see figure 3).

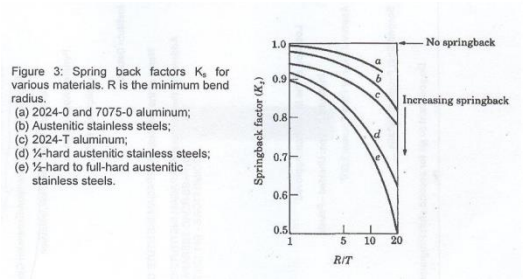

Figure.3

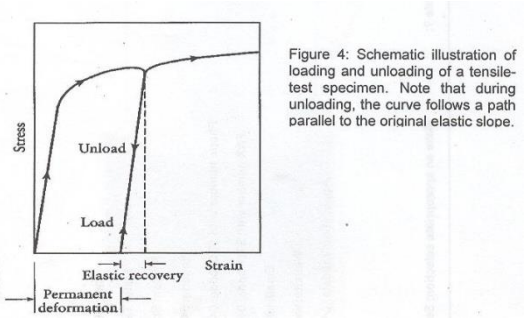

figure.4

The amount of elastic recovery - as shown in figure 4 - depends on the stress level and the modulus of elasticity, *E,* of the material; hence, elastic recovery increases with the stress level and with decreasing elastic modulus. Based on this observation, an approximate formula has been developed to estimate spring back:

$$\frac{R_i}{R_f} = 4\left(\frac{R_i Y}{Et}\right) - 3\left(\frac{R_i Y}{Et}\right) + 1 \quad (4)$$

In this equation, *Y* is the uniaxial yield stress of the material.

3. Negative springback

The spring back observed in Fig. 2 can be called positive spring back. However, undercertain conditions, negative spring back are also possible In other words, the bend angle in such cases become larger after the bend has been completed and the load is removed. This phenomenon is generally associated with V-die bending (Fig. 5)

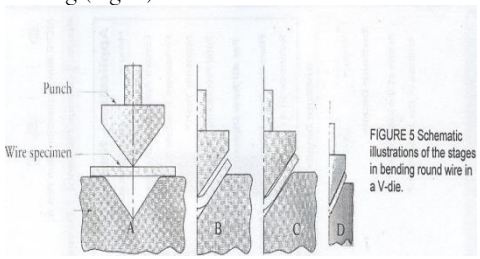

Figure.5

Cite this article as: P. Chandrasekaran, Dr. K. Manonmani. "A Review on Springback Effect in Sheet metal Forming Process." *International Conference on Systems, Science, Control, Communication, Engineering and Technology (2015)*: 43-49. Print.

The development of negative spring back can be explained by observing the sequence of deformation in Fig. 5. If we remove the bent piece at stage (b), it will undergo positive spring back. At stage (c), the ends of the piece are touching the male. Punch. Note that between stages (c) and (d), the part is actually being bent in the direction opposite to that between stages (a) and (b). Note also the lack of conformity of the punch radius and the inner radius of the part in both stage (b) and stage (c); in stage (d); however, the two radii are the same. Upon unloading, the part in stage (d) will spring back inwardly, because it is being *unbent* from stage (c), both at the tip of the punch and in the arms of the part. The amount of this inward (negative) spring back can be greater than the amount of positive spring back, because of the large strains that the material has undergone in the small bend area in stage (b), 1 net result is negative spring back.

4. Compensation for spring back

In practice, spring back is usually compensated for by using various techniques:

1. Over bending the part in the die (Figs. 6a and b) can compensate for spring back; over bending can also be achieved by the rotary bending technique_ in Fig. 6. The upper die has a cylindrical rocker (with an angle of $<90^0$ and is free to rotate; as it travels downward, the sheet is clamped and bent by rocker over the lowered die (die anvil). A relief angle in the lower die allows over bending of the sheet at the end of the stroke, thus compensating for spring back.

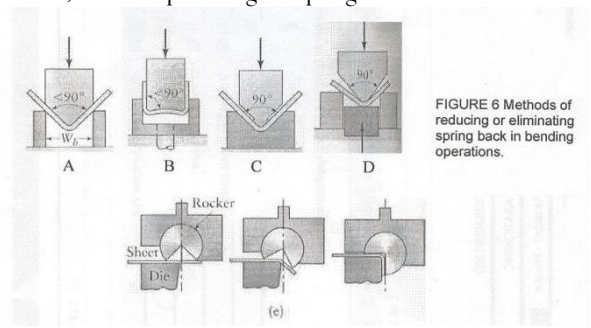

FIGURE 6 Methods of reducing or eliminating spring back in bending operations.

Figure.6

2. Coining the bend region by subjecting it to high-localized compressive stresses between the tip of the punch and the die surface (Figs. 6c and 6d), known as bottoming.
3. Stretch bending, in which the part is subjected to tension while being bent, may be applied. The bending moment required to make the sheet deform plastically will be reduced as the combined tension (due to bending of the outer fibers and the applied tension) in the sheet increases. Therefore, spring back, which is the result of no uniform stresses due to bending, will also decrease. This technique is used to limit spring back in stretch forming of shallow automotive bodies.
4. Because spring back decreases as yield stress decreases all other parameters being the same, bending may also be carried out at elevated temperatures to reduce springback.

Procedures:

1) Set the bending die on the pressing machine. 2) Set up the pressing machine for the test. 3) Select a sample test, and then measure its thickness (t). 4) Measure the die angle (αi) and die radius (Ri). 5) Perform the bending process by putting the flat sheet on the lower half of the bending die and then press the sheet to the required bending shape by the upper half of the bending die. 6) Measure the final sheet angle (αf) and radius (Rf). After bending. 7) Record all the measurements and observations. 8) Repeat the test for different sheet thick nesses and materials.

Example: 1

Sheet folding and elastic springback effect

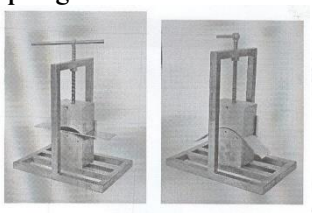

A simple device to apply circular bending

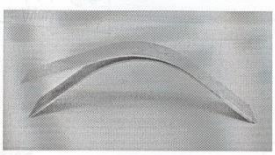

The final shape depends on material type (aluminium, steel) and on geometry

This sheet folding process, with very simple modelling conditions based on pure (circular) bending solutions. One objective is to make evidence of the importance of hardening laws, by using more realistic rules that include Bauschinger effects when predicting the final shape of the product after the elastic return produced by the unloading stage. The project is organized in two steps:

– one analytical approach, as a standard exercise, considering the perfectly plastic case,– extended conditions with various isotropic and kinematic hardening rules, with simple automatic simulations. The study is based on circular bending conditions, as shown on figure , on sheets of 1 or 2 mm thickness, in aluminium or steel, with a circular preform allowing to obtain under load a curvature radius of 70 mm. Values could be changed but, under these conditions, the problem meets the small strain assumption. Elastic limit is overpassed during the loading. When unloading, a residual stress field is established and the sheet does not recover its initial plane

Cite this article as: P. Chandrasekaran, Dr. K. Manonmani. "A Review on Springback Effect in Sheet metal Forming Process." *International Conference on Systems, Science, Control, Communication, Engineering and Technology (2015)*: 43-49. Print.

shape. However, it does not maintain its 70 mm curvature radius from loading condition, the final shape having a much larger radius. Final shapes are different for steel and aluminium. Figure illustrates this fact. The objective of the project is to predict the applied bending moment and the final shape of the sheet.

Yield Criteria

The yield criteria used in the finite element anaiysis of the stretch forming process, are described in this section. The selection of these critena is govemed by the behavior of thedifferent Numinium alloys examinai in the FE analysis.

Von Mises Yield Criterion

The von Mises yield critenon is employed in characterizing the isotropic materid behavior. This model can be employed in the stretch forming of some Aluminium alloys such as isotropic Al-Zn 7075-T6 Aluminium alloy. The von Mises yield critenon is represented by the following expression:

$$Y = \sigma_y^2 = \sigma_1^2 - \sigma_1\sigma_2 + \sigma_2^2$$

where Y yield locus function,

σ_y material yield stress, and

σ_1 and σ_2 major and minor principle stresses.

In view of its high fatigue resistance, resistance to corrosion and high specific strength, Aï-Zn 7075-T6 is currentiy being used in fonning of aircraft structures. Thus, N-Zn 7075-T6 was analyzed by using an isotropic material model. The chemicai composition of Ai-Zn 7075-T6 Aluminium alloy is given in Table A. 1 of Appendix A. The measured mechanical properties of this type of Aluminium are provided in Table. If the material under consideration exhibits an anisotropic behavior, other constitutive Iaws should be used. If the material under consideration exhibits an anisotropic behavior, other constitutive Iaws should be used.

E (GPa)	σ_{eff} (MPa)	σ_u (MPa)	K_{IC} (MPa$\sqrt{m}$)
72	552	598	28

Table Mechanical properties of Al-Zn 7075-T6 Aluminium alloy (After [3.4,3.5]).

Tool material

Tooling used in the finite element analysis consists of a punch and die system. Since the conducted analysis involves stretch forming of Aluminium alloy sheets. the material used in tooling should be tool steel. For this purpose, the punch and die used are specified to be rigid throughout *the* finite element modelling and analysis.

Hardening Rule

Material strain hardening is modelled by employing a bilinear elastoplastic hardening rule. Thus, in addition to specifying the material elastic rnodulus E, a tangentid modulus Er representing the de- of work hardening must be provided to the ANSYS finite element software.

Example: 2 Determining of springback in Stretch Forming

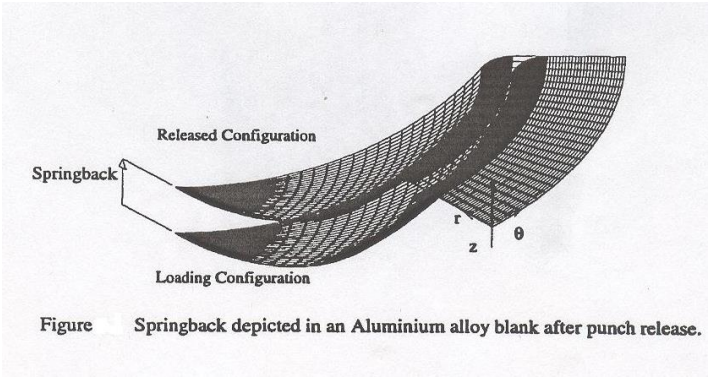

Figure Springback depicted in an Aluminium alloy blank after punch release.

Parameters Influencing Springback

The effec t of the geometric features and the tooling-blank interface fiction conditions upon the resulting blank springback are discussed in this section.

(i) Effect of blank thickness

In order to evaluate the effect of Al 3003-Hl4 Aluminium alloy blank thickness upon the resulting springback, three specimen thickness values of 1 mm, 1.5 mm, and 2 mm were chosen. The finite element solutions and experimental investigations were conducted using a punch radius r, = 17.5 mm. An unlubricated tooling-blank interface condition with a coefficient of friction p = 0.5 was assumed . The results obtained are given in Figures. From Figures, it is evident that the stretch forming force increases with the

Cite this article as: P. Chandrasekaran, Dr. K. Manonmani. "A Review on Springback Effect in Sheet metal Forming Process." *International Conference on Systems, Science, Control, Communication, Engineering and Technology (2015)*: 43-49. Print.

increased blank thickness. The punch loading force has increased by 29.7% due to an increase in the blank thickness from 1.5 to 2 mm. Springback results obtained by varying the blank thickness are given in Figure. It can be extracted from Figure that a maximum discrepancy of 10.3% exists between the springback experimental results and the FE maximum deviation prediction SPB 1. It also shows that the amount of springback, as given by the conducted experiments or numerically determined by the FE maximum deviation SPB 1, the average deviation SPB2 and the mean normal spacing SPB4,decreases by increasing the blank thickness. This finding can be attributed to the increased blank stiffness caused by increasing the blank thickness. Based on the mean normal spacing method, by increasing the blank thickness from 1.5 to 2 mm, a springback reduction of 18% is attained.

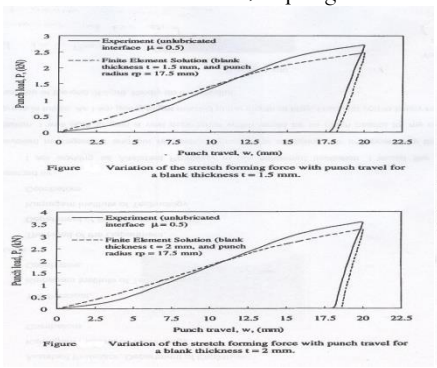

Figure Variation of the stretch forming force with punch travel for a blank thickness t = 1.5 mm.

Figure Variation of the stretch forming force with punch travel for a blank thickness t = 2 mm.

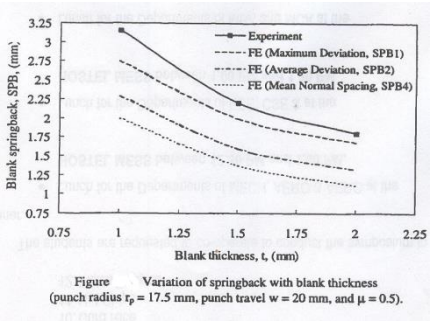

Figure Variation of springback with blank thickness (punch radius r_p = 17.5 mm, punch travel w = 20 mm, and μ = 0.5).

(ii) Effect of Punch Travel

In this subsection, we concentrate on the sensitivity of blank springback to the amount of plastic deformation caused by the prescribed punch travel. Blanlcs with 2 mm thickness were chosen for testing, since it was established in the previous subsection that they provided lower springback values than the thinner blanks. The punch travel w was varied from 10 mm to 20 mm in steps of 2.5 mm. A limiting value of w = 20 mm was used, since values of w *2* 25 mm resulted in inappropriate wrinkling and earning in the vicinity of the blank holder. Wrinkling of tested blanks at a punch travel w = 30 mm is shown in Figure .The analysis was carried out using the same punch, which under a tooling-blank unlubricated dry interface condition w = 30 mm. has a radius r, = 17.5 mm, and with a coefficient of friction p = 0.5 . The results obtained from the experiments and FE analysis for a punch travel w = 15 mm are presented in Figure . Springback findings, as defined by the maximum deviation SPB f and the average deviation SPB2, are also given in Figure . The findings extracted h m Figures illustrate that the blank springback decreases by reducing the prescribed punch travel . The springback was reduced by approximately 27.7% as a result of decreasing the punch travel w €rom 20 to 10 mm. This trend of the blank springback is due to the reduction in the elastic recovery energy at lower plastic deformations.

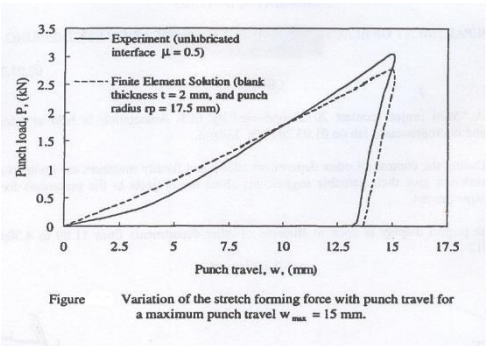

Figure Variation of the stretch forming force with punch travel for a maximum punch travel w_{max} = 15 mm.

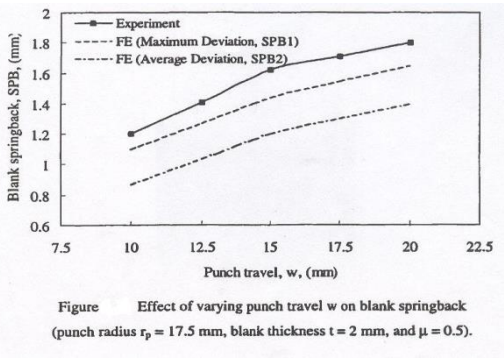

Figure Effect of varying punch travel w on blank springback (punch radius r_p = 17.5 mm, blank thickness t = 2 mm, and μ = 0.5).

(iii) Effect of Punch Radius

The analysis was further extended to examine the effect of varying the punch radius on springback. A smaller punch having a radius r, = 12.5 mm was utilized. Experiments were also carried out on blanks having a thickness of 2 mm and by assuming a coefficient of friction p = 0.5 for an unlubricated *dry* tooling-blank interface condition . The springback results obtained herein are given in Figure. Also presents the variation of the springback, as defined by the mean normal spacing SPB4, with the punch travel for two different punch radii. Figure indicates that smaller values of the punch radius r, for the same blank thickness and interface fiction condition result in smaller springback values in the deformed blanks. Springback reduction of 14.2% is evident at a punch travel w = 20 mm. as given by the mean normal spacing (SPB4) method.

Cite this article as: P. Chandrasekaran, Dr. K. Manonmani. "A Review on Springback Effect in Sheet metal Forming Process." *International Conference on Systems, Science, Control, Communication, Engineering and Technology (2015)*: 43-49. Print.

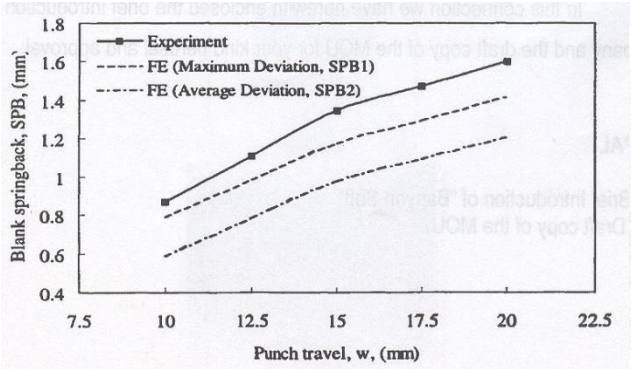

Figure Effect of varying punch travel w on blank springback (punch radius r_p = 12.5 mm, blank thickness t = 2 mm, and μ = 0.5).

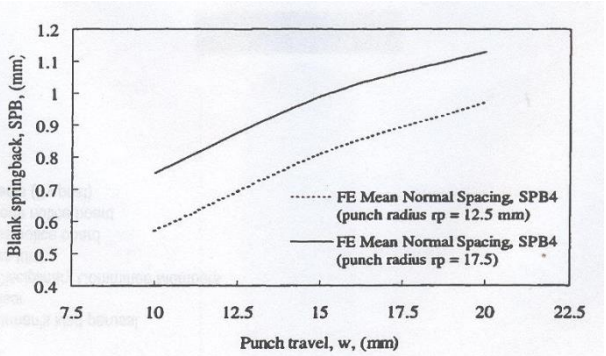

Figure Predicted dependence of springback on punch radius.

(iv) Effect of Tooling-Blank Interface Friction

The main emphasis of this subsection is to focus on the effect of friction and lubrication on the blank springback behavior. The stretch forming deformation process involves high loads and pressures at the tooling-blank contact surfaces. These forces and pressures were mitigated by using a fluid film to lubricate and cushion both the punch-blank and die blank contact interfaces. For this purpose. Grease NUiI Grade 2 was used in the conducted experiments. According to Bhushan and Szen , a coefficient of friction p = 0.05.The loading was carried out using a prescribed punch travel w = 20 mm through a punch with a radius r, = 17.5 mm. The blank thickness was 2 mm. The results obtained are depicted in Figure.

It is evident from Figure that the stretch forming force decreases with decrease interfacial friction at the tooling-blank contact surfaces. Compared to Figure , which indicated a maximum punch loading force P=3.35KN, at μ = 0.5, w = 20mm and for the same blank thickness and punch radius, results obtained from applying grease as a lubricant with p = *0.05* provided a maximum load = ,P 2.4 kN; a decrease of 32%. Grease provided a springback increase of 22.3% relative to the unlubricated dry interface condition (p = 0.5) at t = 2 mm, r, = 17.5 mm, and w = 20 mm. The above results show clearly that increasing the blank holder force as a result of friction decreases springback. This is due to the fact that in stretch forming, two deformation mechanisms operate: bending deformation and tensile deformation. Increasing the tensile deformation through friction decreases the bending component leading to an overall reduction in springback.

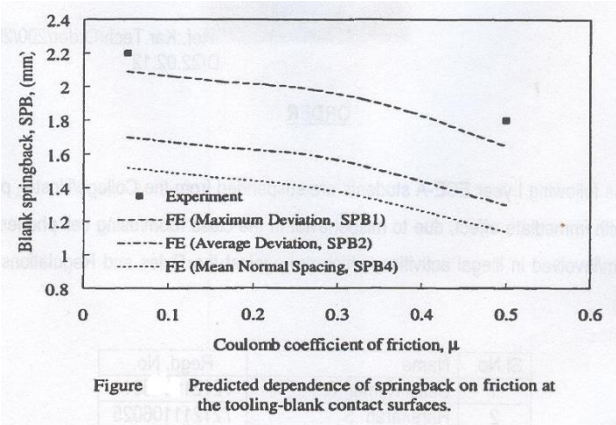

Figure Predicted dependence of springback on friction at the tooling-blank contact surfaces.

Conclusion

springback causes shape error in final product of sheet metal forming processes. The springback occurs at the last step of process and the final geometry of work piece .Parameters Influencing Springback such as blank thickness, Punch Travel, Punch Radius and Tooling-Blank Interface Friction. We can reduce this type of error for increasing blank thickness, varying bend radius, reducing the prescribed punch travel, reduce the friction between blank surfaces and die surfaces by lubricant, etc.

References

1.Finite element and experimental studies of Springback in sheet metal forming by Fahd Fathi Ahmed Abd El AII.Department of Mechanical eEngineering. University of Toronto.

2.Spring back in Bending of sheet metals and plates- Dr. Mohammad Al-tahat Department of Industrial Engineering. University of Jordan. Lab. Of Manufacturing Processes. Course No: 906412.

Cite this article as: P. Chandrasekaran, Dr. K. Manonmani. "A Review on Springback Effect in Sheet metal Forming Process." *International Conference on Systems, Science, Control, Communication, Engineering and Technology (2015)*: 43-49. Print.

3. Lee, J. K. etai. "Numerical Simulations of Sheet Metal Forming Processes, Verification of Simulations with Experiments." Numisheet 96 (1996).
4. Carleer, B. D., Hue tink.,Pijlman, H. H.and Vegter, H. "Application of the Vegter Criterion and a Physically Based Hardening Rule on Simulation of Sheet Metal Fonning." Simulation of Materials Processing: Theory, Methods and Applications, Numiform 98 (1998): pp. 763-768.
5. Batoz, I. L., Bouabdallah, S., Guo, Y. Q., Mercier, F. and Naceur, H. "On Some enhanced computational aspects of the inverse approach for sheet fonning analysis." Simulation of Materials Processing: Theory, Methods and Applications, Numiform 98 (1 998): pp. 807-8 12.

Cite this article as: P. Chandrasekaran, Dr. K. Manonmani. "A Review on Springback Effect in Sheet metal Forming Process." *International Conference on Systems, Science, Control, Communication, Engineering and Technology (2015)*: 43-49. Print.

International Conference on Systems, Science, Control, Communication, Engineering and Technology 2015 [ICSSCCET 2015]

ISBN	978-81-929866-1-6	**VOL**	01
Website	icssccet.org	**eMail**	icssccet@asdf.res.in
Received	10 - July - 2015	**Accepted**	31- July - 2015
Article ID	ICSSCCET012	**eAID**	ICSSCCET.2015.012

Load Balancing Algorithms in Cloud Environment

M. Aruna[1], Dr. D. Bhanu[2], Dr. S. Karthik[3]

[1]Assistant Professor, Department of Computer Science and Engineering, Sasurie Academy of Engineering,
[2]Professor and Head, Department of Information Technology, Karpagam Institute of Technology,
[3]Professor and Dean, Department of Computer Science and Engineering, SNS College of Technology, Coimbatore, India

Abstract: *Cloud Computing is a pool of resources that can be shared among the users. At present, Cloud Computing is an emerging technology since it provides services at the user level. There are several issues or challenges in the Cloud Computing environment such as availability, security and resource allocation, etc. The paper concentrates on availability of nodes in the cloud. Balancing load under the nodes will increase availability of nodes in Cloud. In order to enhance the performance of the entire cloud environment, efficient Load Balancing techniques are needed. Load Balancing (LB) algorithms distribute the load evenly across all the nodes in cloud. Load Balancing in Cloud Computing will also increase the reliability and user satisfaction.*

Keywords: Cloud Computing, Load Balancing, Virtualization

I. INTRODUCTION

Large business and small business companies are moving to cloud environment because of its scalability. The jobs arriving to the Cloud Environment are executed by the large data centers which have thousands of blade servers. It provides different types of services to the users. Users can get the services with no need to know their infrastructure i.e.,, users do not know where the service is originated and its infrastructure. Users need to pay only for what they used from cloud in the form of services, which is the simplicity of Cloud. The four different types of cloud environment are as follows,

- Public Cloud (Free of Cost, anyone can access)
- Private Cloud (Pay for what you used, only for single organization people)
- Hybrid Cloud (Combined both public & private Clouds)
- Community Cloud(For Communication purpose)

Users can access the cloud resources in the form of services. There are three basic services provided by the Cloud Environment. They are,

- Platform as a Service (PaaS)
- Software as a Service (SaaS)
- Infrastructure as a Service (IaaS)

A. Virtualization

Cloud Computing is based on the concept of Virtualization technology. Virtualization is the software implementation on the bare hardware so that the resources under the hardware can be utilized more effectively. Cloud Computing uses the virtualization technique

Cite this article as: M. Aruna, Dr. D. Bhanu, Dr. S. Karthik. "Load Balancing Algorithms in Cloud Environment." *International Conference on Systems, Science, Control, Communication, Engineering and Technology (2015)*: 50-54. Print.

to make use the cloud resources efficiently [3]. Two types of virtualization such as Full Virtualization and Para Virtualization can be used in cloud environment.

II. LOAD BALANCING

Load Balancing [1] is a technique to balance the load across cloud environment. It is the process of transferring load from heavily loaded nodes to low loaded nodes. As a result, no node should be heavily loaded which will increase the availability of nodes. If all the jobs are arrived to the single node, then its queue size is increased and it becomes overloaded. There is a need to balance the load across several nodes, so that every node is in running state but not in overloaded state. The goals of load balancing are as follows[2]:

- To increase the availability
- To increase the user satisfaction
- To improve the reource utilization ratio
- To minimize the waiting time of job in queue as well as to reduce job execution time
- To improve the overall performance of Cloud environment

Figure 1 shows the major works of Load Balancing Technique. The Load Balancer may be any software or hardware which receives jobs from different users in different locations. The received loads are distributed evenly across all the servers in Data Center. Table 1 shows the comparison of LB algorithms.

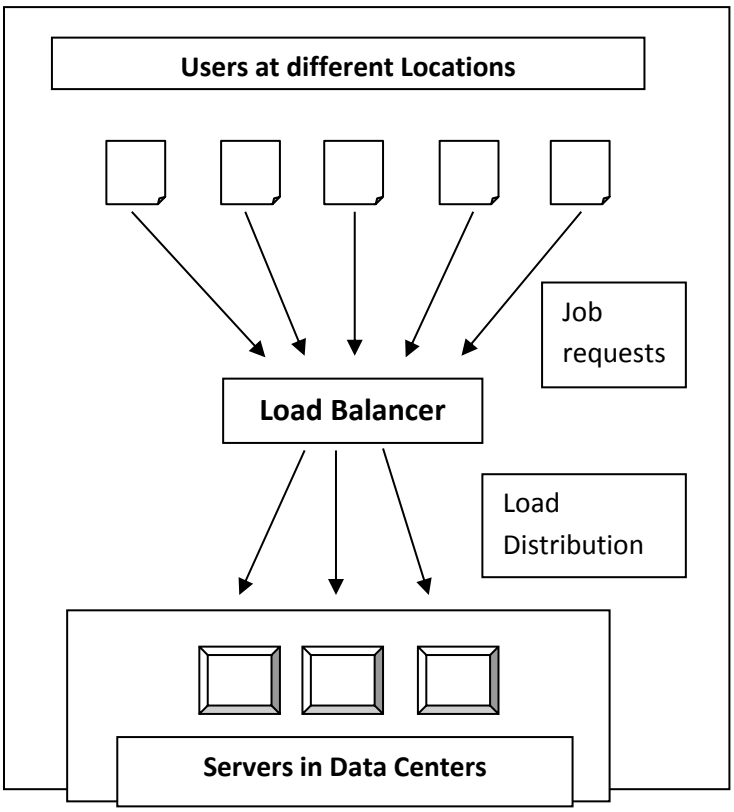

A. Basic Types of Load Balancing Algorithms

Depending on the initiator of the algorithm, Load Balancing algorithms can be categorized into three types [3]:

Sender Initiated - Sender identifies that the nodes are overwhelmed so that the sender initiates the execution of LB algorithm.

Receiver Initiated - The requirement of Load balancing situation can be identified by the receiver/server in cloud and that server initiates the execution of LB algorithm.

Symmetric -It is the combination of both the sender initiated and receiver initiated types. It takes advantages both types.

Based on the current state of the system, load balancing algorithms can be divided into two types:

Static Schemes - The current status of the node is not taken into account [6]. All the nodes and their properties are predefined. Since it does not use current system status information, it is less complex and it is easy to implement.

Dynamic Schemes - This type of algorithm is based on the current system information [6]. The algorithm works according to the changes in the state of nodes. Dynamic schemes are expensive one and are very complex to implement but it balances the load in effective manner.

Cite this article as: M. Aruna, Dr. D. Bhanu, Dr. S. Karthik. "Load Balancing Algorithms in Cloud Environment." *International Conference on Systems, Science, Control, Communication, Engineering and Technology (2015)*: 50-54. Print.

Status Table - Status table [1] is a data structure to maintain the current status of all the nodes in the cloud environment. This information can be used by some of the dynamic scheme algorithms to allocate jobs to the nodes that are not heavily loaded.

TABLE 1
COMPARISON OF LB ALGORITHMS

S.No.	Algorithm	Description	Advantages
1.	Dynamic round robin algorithm [7]	1. Uses two rules to save the power consumption 2. Works for consolidation of virtual machine	Reduce the power consumption
2.	Hybrid algorithm [1]	1. Combination of dynamic round robin and first-fit algorithm 2. Applied in non-rush hours and rush hours	1. Improved resource utilization 2. Reduced power consumption
3.	ESCE algorithm [8]	Estimate the size of job and look for availability of resources	Improved response time and processing time
4.	Central Load Balancing policy for VM	Balances the load evenly	Improves overall performance
5.	Enhanced Equally Distributed Load Balancing Algorithm [9]	Based on the counter variable, the job is allocated by Central Server	1. Computing Resource is distributed efficiently and fairly 2. Reduces request to response ratio
6.	Decentralized Content Aware Load Balancing Algorithm [9]	1. Uses Unique and Special Property (USP) of nodes 2. Uses content information to narrow down the search	1. Improves the searching performance hence increasing overall performance 2. Reduces idle time of nodes
7.	Join-Idle Queue Algorithm [10]	1. Assigns idle processors to dispatchers for the availability of idle processors 2. Then assigns jobs to processors to reduce average queue length	1. Reduces system load 2. Less communication overhead
8.	Honeybee Foraging Behavior [10]	Achieves global load balancing through local server actions	Improved scalability
9.	Min-Min Algorithm [7]	1. Estimates minimum execution time and minimum Completion time 2. Jobs having minimum completion time is executed first	Smaller tasks are executed quickly
10.	Max-Min Algorithm [11]	1. Same as Min-Min 2. Gives more priority to larger tasks than smaller one	Larger tasks are executed quickly and efficiently
11.	RASA Algorithm [11]	Combination of both Min-Min and Max-Min Algorithms	1. Efficient resource allocation 2. Minimum execution time
12.	Improved Max-Min Algorithm [12]	1. Improved version of Max-Min Algorithm 2. Assigns task with minimum execution time	Scheduling jobs effectively
13.	2-Phase Load Balancing Algorithm [7]	1. Uses OLB to keep each node busy 2. Uses LBMM to achieve minimum execution time of each job	1. Efficient utilization of resources 2. Enhances work efficiency
14.	PALB Algorithm [13]	1. Implemented in Cluster Controller 2. Use Job Scheduler to simulate requests from users for virtual machine instances	Physical Machines that are in idle state are move to power off state to conserve energy

II. PROPOSED WORK

Existing Load balancing algorithms have some drawbacks in improving overall performance of the cloud environment. Still there is a problem of overloading nodes in the Cloud environment. It is very difficult to manage entire cloud environment. Hence the proposed idea is to divide the entire cloud environment into several partitions based on its geographical locations [1]. Now the Load balancing algorithm can be applied only to the partitions, not to the entire cloud. Fig 2 shows the cloud environment after partitioning is done. The load balancing algorithm is applied to each partition in order to avoid overloading of nodes.

Cite this article as: M. Aruna, Dr. D. Bhanu, Dr. S. Karthik. "Load Balancing Algorithms in Cloud Environment." *International Conference on Systems, Science, Control, Communication, Engineering and Technology (2015)*: 50-54. Print.

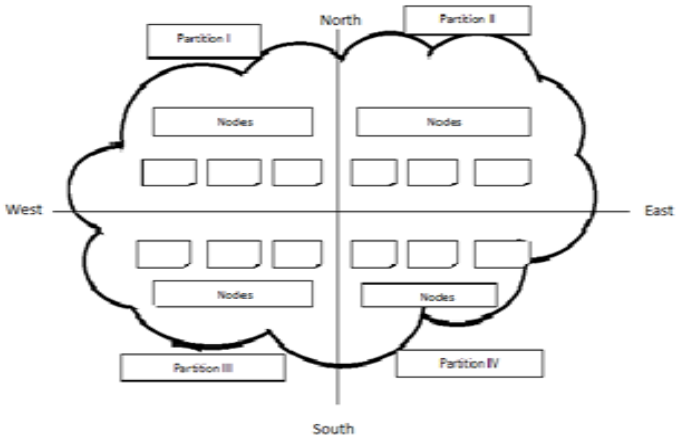

Figure 2. Partitioned Cloud Environment

For balancing load in cloud partition model [1] there are two important components needed:

- Load Balancer
- Main Controller

Load Balancer is associated with each partition whose work is to maintain the state information and is to be updated in periodic intervals. Whenever the controller receiving a job it has to communicate with each partition to collect state information. Then the job is allocated to the partition if it is in idle or normal state. After assigning job to the partition, the balancer has to update the status information of each node in that partition.

Main controller receives all the jobs that arrive from the cloud. Whenever the main controller receives the job it has to decide, which partition to receive the job. Each partition has the state information associated with it. It may be in idle state, normal state or heavily loaded state. The state of the node in particular partition is set by considering several parameters of that node and the parameters may be static or dynamic. Static parameters include number of CPUs, memory size and speed of the processor or CPU. Dynamic parameters include CPU utilization ratio and memory utilization ratio.
An algorithm will be designed for the nodes that are idle or normal and it has to update the status information of each node periodically. Load Balancer in each partition maintains the status table. The status table contains information about the load of all the nodes in that partition. This table is updated by a Load Balancer periodically. For better efficiency, balancer maintains the two status table and each of which are associated set by the "Flag".

IV. FUTURE WORK

The future work is to develop two algorithms, one for the partitions of Cloud environment that are in idle state and another one for the partitions that are in normal states. Switching mechanism is needed for applying these two alternative algorithms. If the partition is in idle state one simple algorithm is to be used and later the same partition can became normal state and alternative algorithm is to be used. The algorithm designed for normal state partitions should be more efficient so that it avoids the partition becoming overloaded.

V. CONCLUSION

Though there are several issues in cloud environment, it has been widely adopted by many organizations and industries. Researchers are doing many works to resolve those challenges and issues. For Load Balancing issue, the solution is to develop suitable algorithms that balance the load across the partitioned cloud environment. Both the algorithms should work accordingly as the partition status changes. It reduces the server overhead, increase throughput, increase performance, reduce server power consumption and also distribute the load across nodes.

REFERNECES

[1] Gaochao Xu, Junjie Pang and Xiaodong Fu, “A Load Balancing Model Based on Cloud Partitioning for the Public Load”, IEEE Transactions on Cloud Computing, 2013.
[2] Zenon Chaczko, Venkatesh Mahadevan, Shahrzad Aslanzadeh and Christopher Mcdermid, “Availability and Load Balancing in Cloud Computing”, International Conference on Computer and Software modeling IPCSI, 2011.
[3] Ratan Mishra and Anant Jaiswal, “Ant Colony Optimization: A solution of Load Balancing in Cloud”, International Journal of Web & Semantic Technology (IJWesT), April 2012.
[4] Liang Liu, Hao Wang, Xue Liu, Xing Jin, WenBo He, QingBo Wang, Ying Chen, "Green Cloud: A New Architecture for Green Data Center", ACM Journal, 2009.
[5] V.Srimathi, D.Hemalatha, R.Balachander, "Green Cloud Environmental Infrastructure", International Journal of Engineering and Computer Science, December 2012.

Cite this article as: M. Aruna, Dr. D. Bhanu, Dr. S. Karthik. “Load Balancing Algorithms in Cloud Environment.” *International Conference on Systems, Science, Control, Communication, Engineering and Technology (2015)*: 50-54. Print.

[6] Venubabu Kunamneni, "Dynamic Load Balancing for the cloud", International Journal of Computer Science and Electrical Engineering, 2012.
[7] Karanpreet Kaur, Ashima Narang, Kuldeep Kaur, "Load Balancing Techniques of Cloud Computing", International Journal of Mathematics and Computer Research, April 2013.
[8] Dr.Hemant S.Mahalle, Prof. Parag R. Kaveri, Dr. Vinay Chavan, "Load Balancing on Cloud Data Centers", International Journal of Advanced Research in Computer Science and Software Engineering, January 2013.
[9] Shreyas Mulay, Sanjay Jain, "Enhanced Equally Distributed Load Balancing Algorithm for Cloud Computing" International Journal of Research in Engineering and Technology, June 2013.
[10] Nidhi Jain Kansal, Inderveer Chana, "Cloud Load Balancing Techniques: A Step Towards Green Computing", International Journal of Computer Science, January 2012.
[11] S.Mohana Priya, B.Subramani, "A New Approach for Load Balancing in Cloud Computing", International Journal of Engineering and Computer Science, May 2013.
[12] O.M.Elzeki, M.Z.Reshad, M.A.Elsoud, "Improved Max-Min Algorithm in Cloud Computing", International Journal of Computer Applications, July 2012.
[13] Jeffrey M. Galloway, Karl L.Smith, Susan S. Vrbsky, "Power Aware Load Balancing for Cloud Computing", World Congress on Engineering and Computer Science, 2011.

Cite this article as: M. Aruna, Dr. D. Bhanu, Dr. S. Karthik. "Load Balancing Algorithms in Cloud Environment." *International Conference on Systems, Science, Control, Communication, Engineering and Technology (2015)*: 50-54. Print.

International Conference on Systems, Science, Control, Communication, Engineering and Technology 2015 [ICSSCCET 2015]

ISBN	978-81-929866-1-6
Website	icssccet.org
Received	10 - July - 2015
Article ID	ICSSCCET013

VOL	01
eMail	icssccet@asdf.res.in
Accepted	31- July - 2015
eAID	ICSSCCET.2015.013

On the Fabrication of Magnetorheological Brake with Optimum Design Factors

Thanikachalam.J[1], Nagaraj.P[2]
[1]Asst. Professor, Dept. of Mechanical Engg, Mepco Schlenk Engineering College, Sivakasi, India
[2]Professor & Head, Dept. of Mechanical Engg, Mepco Schlenk Engineering College, Sivakasi, India

Abstract: *In the recent trends, the automobile systems like transmission, suspension, brake, clutch are controlled through the wire systems called drive-by-wire concept, by replacing mechanical components, without affecting the functions. The advantages of the wire systems are the elimination of mechanical components and quick response when compared through conventional systems. In this work, we design and fabricate a Magnetorheological Brake (MRB) instead of a conventional brake like disk, grum and ABS brake which are currently used in automobile systems. The features of the MRB are no mechanical moving parts, less weight and quick response time. In this MRB, the Magnetorheological (MR) fluid is filled in the gap of outer casing unit and inner disk. The MR fluid has the change of rhological properties under magnetic fields. Commercially MR fluids are very costly. In this work we have prepare and charaterise the MR fluids. Next to the preparation, based on the fluid preparation, we optimize our design throught the COMSOL software. Based on the optimized design value we had design our MRB. Optimum design is found using Nelder Mead optomization technique combine with finite element simulations involving magnetostatic and heat transfer analysis finite element models are built to provide a means to analyze the performance of the MRB.*

Keywords: MR Brake, COMSOL Multiphysics®, Magnetorheological fluids, Optimization.

1. Introduction

MR fluids are smart fluids that change their rheological behavior when a magnetic field is applied. Typically and this change is manifested by the development of yield stress that increases with the applied field. When the magnetic field is absent, MR fluids behave like a Newtonian fluid. Jacob Rabinow at the US National Bureau of Standard discovers MR fluids in 1948 [1]. MR fluids consist of magnetically permeable micron-sized particles which are dispersed throughout the carrier medium. The carrier medium is either a polar or non-polar fluid, which influences the viscosity of the MR fluids. On the other hand, MR fluids are controllable fluids that exhibit dramatic reversible change in rheological properties (elasticity, plasticity or viscosity) either in solid-like state or free-flowing liquid state depending on the presence or absence of a magnetic field. When magnetic field is applied particles acquire dipole moment aligned with magnetic field to form linear chains parallel to field. The flow resistance (apparent viscosity) of the fluid is intensified by the particle chain. When the magnetic field is removed, the particles are returned to their original condition, which lowers the viscosity of the fluid [2].

Edward J. Park et al. (2006) developed an MRB in order to overcome the disadvantages of the Conventional Braking System. The proposed brake system consists of rotating disks immersed in MR fluid and is enclosed in an electromagnet. The yield stress of the fluid changes as a function of the applied magnetic field by the electromagnet. The controllable yield stress produces friction on the rotating

Cite this article as: Thanikachalam J, Nagaraj P. "On the Fabrication of Magnetorheological Brake with Optimum Design Factors." *International Conference on Systems, Science, Control, Communication, Engineering and Technology (2015)*: 55-63. Print.

disk surfaces and generates a retarding brake torque. The braking torque can be precisely controlled by changing the applied current to the electromagnet. An optimum MRB design with two rotating disks based on design optimization procedure using simulated annealing combined with FE simulations involving magneto static, fluid flow and heat transfer analysis are also carried out by them .The performance of the MRB in a vehicle is studied with the help of a quarter vehicle model. A sliding mode controller is also designed for an optimal wheel slip control. The simulation result shows the potential of their proposed MRB system to provide fast anti-lock braking [3]. J. Huang, J.Q. Zhang et al. (2002) investigated the geometric design method of the cylindrical MR fluid brake theoretically. The torque developed by the MRB under different magnetic field strength conditions has been analyzed. The equation for the torque transmitted by the MRB is derived to provide the theoretical foundation in the design of the MRB. Based on that equation, after analytical manipulation, the calculations of the thickness, volume and width of the annular MR fluid within the cylindrical MR fluids brake are yielded [4].

2. Design of the MRB

For MR brake, the analysis problem would simply consist of running the finite element models of a given brake configuration (i.e., with known dimensions and materials). Clearly, the solution to the design problem of finding the ideal configuration of the MR brake is not so direct. Without closed-form solutions of the equations describing its dynamics, no immediate approach exists. In such cases, the design problem generally consists of an iterative process involving a sequence of analysis problems. Based on the results of each analysis some changes are made to the design and the performance of the resulting configuration is compared with that of the previous one, continuing this process until no further improvements in the design are achieved. Hence, in order to design a suitable MR brake, two different tasks are necessary: a model capable of analyzing the performance of a given brake design and an optimization tool capable of using the results of such analyses to produce improved designs. Here the preliminary design, optimization, final design and analysis of the MRB are done in this paper.

In consideration of the dimensions of the various components of the MR brake, the first factor to take into account is the existence of physical limitations. For example, if the brake is to be placed within the wheel rim (where today's disk or drum brakes are located), the overall diameter must be such that it will fit within that area: it is recommended that a minimum clearance of 3 mm exists between the brake and wheel rim and spokes. The maximum acceptable diameter for the MR brake is then, for a 17" wheel, 16in x 25.4mm/in - 2 x 3mm = 425.8 mm i.e 42.58 cm, resulting in a maximum acceptable radius of 212.9 cm. Here we take the radius of the MR brake as 200 mm and set the disk radius to 17 cm and the width of the coil to 1 cm. In addition to these two quantities, the radius of the brake must also accommodate the fluid gap (0.1cm) adjacent to the edge of the disk, If the gap between disk and coil is chosen to have 4 mm, the maximum possible thickness for the end part of the casing is 20 - 18 - 0.1 - 1 - 0.4 = 1.5 cm. These are the values that had been used for the initial design. The 3D CAD model of the MRB was created using Unigraphics NX 8.0®. Fig.1 shows the 3D CAD model of the proposed MRB model and fig.2 shows the drawing view of the proposed model.

The major components of the MR Brake are Casing, Disc, MR fluid, Coil and Shaft. The material selection is a critical part of the MRB design process. Materials in the MRB have crucial influence on the magnetic circuit as well as the structural and thermal characteristics. Here, the material selection is discussed in terms of the (i) Magnetic properties and (ii) Structural and thermal properties.

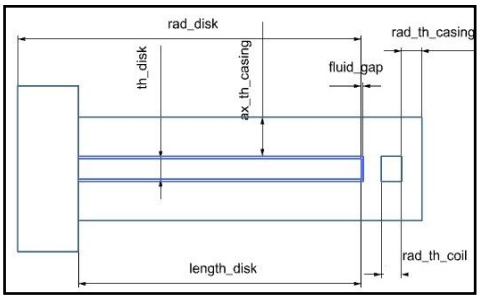

Figure 1. Drawing view of proposed MRB

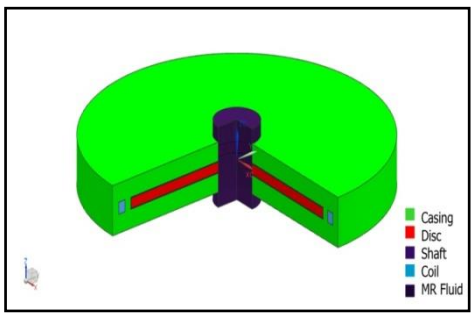

Figure 2. 3D CAD model of the proposed MRB

Cite this article as: Thanikachalam J, Nagaraj P. "On the Fabrication of Magnetorheological Brake with Optimum Design Factors." *International Conference on Systems, Science, Control, Communication, Engineering and Technology (2015)*: 55-63. Print.

Permeability (μ) is the property that defines a material's magnetic characteristics. It is the ratio between the applied magnetic field intensity (B) and magnetic flux density (H) due to B through the material .It is the ability of a material to transfer magnetic flux over itself. Relative permeability (μ_r) is the ratio between the material's permeability and vacuum's permeability (i.e. $\mu_o = 4\pi\times10^{-7}$H/m).

$$B = \mu H$$

$$B = \mu_r\mu_o H$$

In terms of structural considerations, there are two critical parts: the shaft and the shear disk. Thermal properties of the materials are another important factor. Since the permeability values of the ferromagnetic materials are temperature dependent and the MR fluid viscosity the heat generated in the brake should be quickly removed as soon as possible. In terms of material properties, in order to increase the heat flow from the brake, a material with high conductivity and high convection coefficient has to be selected as the material for the non-magnetic brake components. Aluminum is a good candidate material for the thermal considerations. AISI 1018, having a high yield stress is selected as the magnetic material in the magnetic circuit (i.e. the casing and disks) after considering the cost, permeability and availability. The B–H curve of steel 1018 with the saturation effect is shown in Fig.3.

Shaft should be non-ferromagnetic in order to keep, the flux far away from the seals that enclose the MR fluid, to avoid from MR fluid being solidified. 304 stainless steel is a suitable material for the shaft due to its high yield stress and availability. Thicker wires are capable of conducting greater currents but take more space and hence a smaller number of turns can be wound in the same area. The change in current carrying ability is inversely proportional to the number of turns per unit area. Magnetic flux produced by the coil is proportional to NI, the choice of a given wire dimension will not influence it. After referring American Wire Gauge (AWG) Cable / Conductor Sizes and Properties, AWG 21 is chosen The selection of MR fluid is important in the design of the MR brake. No-field viscosity of the MR fluid, operating temperature range and shear stress gradient are some of the key properties that have to be considered when making a selection. The density of the MR fluid chosen is 450 kg/m^3 and viscosity is 6 Ns/m^2. The flow curve and the BH curve for the selected MR fluid are shown in fig.4 and fig.5 respectively. The relationship between the magnetic field intensity and the generated shear stress of the MR fluid brake is shown in fig.6.

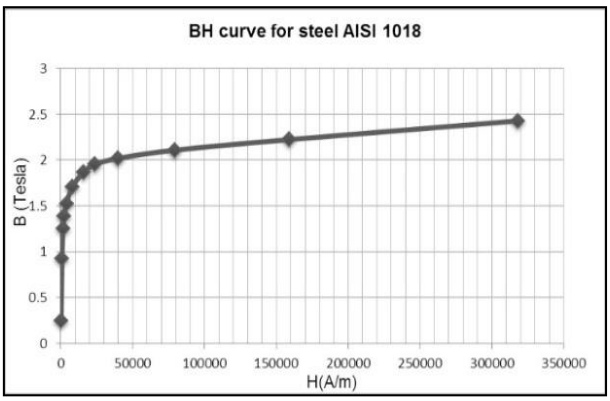

Figure 3. BH curve of steel AISI 1018

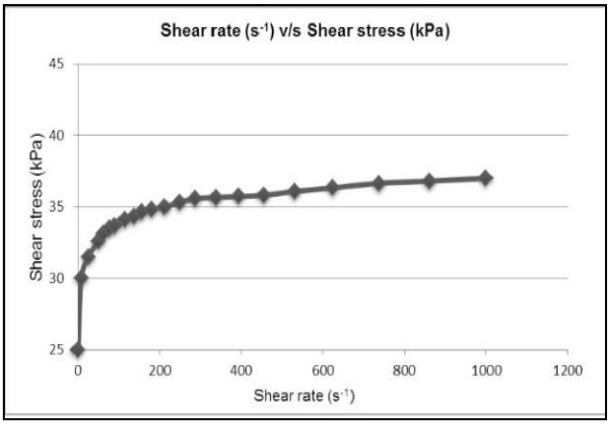

Figure 4. Flow curve of the MR fluid

Cite this article as: Thanikachalam J, Nagaraj P. "On the Fabrication of Magnetorheological Brake with Optimum Design Factors." *International Conference on Systems, Science, Control, Communication, Engineering and Technology (2015)*: 55-63. Print.

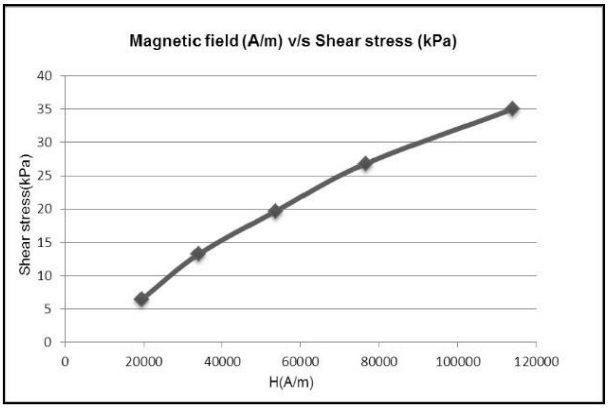

Figure 6. Magnetic field v/s shear stress curve

Figure 7. Viscosity v/s Time curve for MR fluid

3. Preparation of MR fluids

To prepare a low viscosity and high yield point MR fluids are prepared, which contains micron size of 1 – 2 µm iron particles, Silicone oil as career medium and additives as Triton X100.

These particles and oil are varied with a volume fraction method as per our requirements. As per the method, the required amount of iron powder, Silicone oil and additives are taken. First the Silicone oil and additives are mixed with a magnetic stirrer for more than 8 hrs for getting a homogeneous mixture. After obtaining the homogeneous mixture of oil and additives, the iron powder is poured and stirrered with mechanical stirrer. This procedure is followed to avoid sudden sedimentation ratio [5]. The viscosity of the above prepared fluid was then tested using the Brookfield Viscometer® and the results obtained is given in fig.7.

The volume fraction of iron particles is varied between 20% to 40% for improving the yield strength. For 20% volume fraction, the required volume of Silicone oil and iron powder is calculated as:-

Total volume of MR fluid = 100 cc

20% volume fraction of Iron powder = 0.35×100 = 20 cc

Mass density of Iron powder = 7.8 g/cc

Mass of Iron Powder = $7.8 \times 20 = 156$ g

80% volume fraction of Silicone oil = 0.8×100 = 80 cc

Table 1

MR Fluid Constituents for 20% Volume Fraction

Total Volume of MR fluid = 50 cc Density of Iron powder = 7.8 g/cc		
Vol. Fraction [%]	Mass of Iron powder [g]	Volume of Silicone oil [cc]
20	78	40

Table 2

Properties of MR Fluid Prepared

Carrier fluid	Silicone Oil
Solid particles	Carbonyl Iron
Volume fraction of Solid phase	20 %

Cite this article as: Thanikachalam J, Nagaraj P. "On the Fabrication of Magnetorheological Brake with Optimum Design Factors." *International Conference on Systems, Science, Control, Communication, Engineering and Technology (2015)*: 55-63. Print.

Mass density of Iron Powder	7.8 g/cc
Mass density of Silicone Oil	1.25 g/cc
Color	Dark grey

4. Analytical Modeling and FEA of MRB

We can describe devices and behaviors in many ways. Analytical modeling is the way of describing devices or behaviors using the language of mathematics. For the MRB, the braking torque produced by the MRB is to be derived in terms of applied magnetic field.

Braking force (F_b) is the tangential force acting between the disc and the stator Braking torque (T_b) is the moment of braking force about the center of rotation.

Braking torque,

$T_b = F_b r$ (1)

r = Effective radius

Shear stress, $\tau = \frac{F_b}{dA}$ (2) $F_b = \tau dA$

$T_b = \tau r dA$ (3)

Equation for τ can be derived from fitting the curve using the table values of the flow curve (τ v/s$\dot{Y}$) with and without magnetic field.

4.1 Without magnetic field

$\tau = \mu\dot{Y}$ (4)

μ = Viscosity of the fluid without magnetic field

$\dot{Y}$= Shear rate

4.2 With magnetic field

Experimental values of the flow curve (τ v/s $\dot{Y}$) is used to derive the relationship between τ and $\dot{Y}$. According to Bingham plastic model, the equation for shear stress of the MR fluid is given by

$\tau = \tau_y(H) + \mu\dot{Y}$ (5)

By applying the above equation in the torque equation we get

$T_b = (\tau_y(H) + \mu\dot{Y})\, rdA$ (6)

From the above curve a linear curve is fitted using the linear regression technique [6]. The equation for the above curve is found and is given as

$\tau = 32442 + 6.496\dot{Y}$ (7)

Correlating the above equation with Bingham plastic model

$\tau_y = 32442\ N/m^2$ & $\mu = 6.496\ Ns/m^2$

Considering an elemental section of disc the area of contact between disc and fluid

$A = \pi r^2 \rightarrow \frac{dA}{dr} = 2\pi r \rightarrow dA = 2\pi r dr$

$T_b = 2\pi r^2(\tau_y(H) + \mu\dot{Y})\, dr$ (8)

For single disk the contact is made on 2 opposite sides (n)

$T_b = 2n\pi r^2(\tau_y(H) + \mu\dot{Y})\, dr$ (9)

For entire cross section of the disc, integrating

$T_b = \int_{r1}^{r2} 2n\pi r^2(\tau_y(H) + \mu\dot{Y})dr$ (10)

Shear rate ($\dot{Y}$) is the rate of change of shear strain with respect to time along the gap. The curve between τ_y and B is drawn first and from the BH curve of the MR fluid the corresponding H values are found out and the curve between τ_y and H is drawn and is approximated to an exponential curve of the form y = ax + b. The relation between τ_y and H is found and is given by

$\tau_y = 0.2976H + 2505.504\ N/m^2$ (11)

Finally the relation for torque (T_b) in terms of H can be established as

$T_b = \left(\frac{2}{3}\right)n\pi(0.2976H + 2505.504)(r_2^3 - r_1^3) + \left(\frac{n\pi\omega}{2h}\right)(6.496)(r_2^4 - r_1^4)$ (12)

Where,

n = number of surfaces (2 for single disk)

H= Applied magnetic field (A/m)

r_1= Inner radius of disc (mm)

r_2= Outer radius of disc (mm)

h= MR fluid filling gap (mm)

ω= Angular speed of disc (rad/s)

The disciplines which are involved in the operation of a magneto-rheological brake are magneto statics, fluid flow, and heat transfer. Due to the multidiscipline and the presence of nonlinearities (magnetic saturation and non-Newtonian fluid behavior) and the absence of closed-form solutions, the analysis of MR brakes is to be carried out using finite element modeling. Hence, in order to

Cite this article as: Thanikachalam J, Nagaraj P. "On the Fabrication of Magnetorheological Brake with Optimum Design Factors." *International Conference on Systems, Science, Control, Communication, Engineering and Technology (2015)*: 55-63. Print.

obtain meaningful solutions with the weak formulation, it is necessary to divide the original problem domain (the system being analyzed) into many small domains (the elements), so that the "average" introduced by the weak formulation does not introduce significant errors in the solution. In this COMSOL Multiphysics® is used for the Finite Element Analysis. It is a flexible platform that allows users to model all relevant physical aspects of any type designs [7].

Since the MR fluid's viscosity is controlled by the magnetic field, the first step in the analysis of an MR brake system is a magnetostatics analysis that determines the magnetic field distribution. The electromagnetic analysis results in the magnetic field intensity distribution within the MRB design configuration is analyzed. The relationship between applied electric power and the braking torque can be determined using electromagnetic analysis. This is a non-linear problem and requires an iterative approach. In order to determine the magnetic field distribution, a 2D axisymmetric Finite Element Model of the brake is created using COMSOL Multiphysics®.

The response of a system depends not only on its geometry and the properties of the materials it is made of but also on the loads that are applied and on any constraints imposed (boundary conditions) on the problem. The load in the present problem is the current flowing through the coil, responsible for the magnetic flux. After meshing, the FEM was solved using a parametric nonlinear solver and the magnetic field distribution onto the MR fluid was obtained. Finally, the braking torque using eq.11 was calculated [8].

Once the magnetic field distribution is known, the shear stress can be obtained from the fluid's specifications and, together with the no-field viscosity, describes the behavior of the fluid flow. Thermal analysis can then be done to obtain the distribution of temperature within the brake. The temperature change is mainly due to the joule heating effect.

5. Optimization and fabrication of MRB

Optimum design for the MRB should be done to findout the significant geometric dimensions of MRB that maximizes the torque and minimizes the weight. The objectives for the Optimization problem are:-

1. Maximize the braking torque (T)
2. Minimize the weight (W)

Objective function is chosen using the utility function method (weighted sum method) as

$F = T - W$, after giving weightage factors of 0.8 and 0.2 for torque and weight respectively, the objective function is as follows

$F = 0.8T - 0.2W$

$F = 0.8(T/T_0) - 0.2(W/W_0)$

where,

T_0 =1010 Nm and W_0 = 65 kg, taken as reference values

Above is a maximization problem, which is solved by using Nelder Mead method (Simplex method) with the aid of the COMSOL Multiphysics®. The global objective is given as input in the optimization module and the optimization is carried out.

Nelder mead optimization has reduced number of function evaluations in each iteration. For N variables, (N+1) points are used in initial simplex. At each iteration, the worst point in the simplex is found first. The centroid of all but the worst point is determined. Worst point in the simplex is reflected about the centroid and new point X_r is found. If functional value at this point is better than the best point in the simplex, expansion along the direction from the centroid to the reflected point is performed. If the functional value is much worse than the worst point in the simplex.

Then contraction in the direction from the centroid to reflected point is made. The process continues until the termination criterion is satisfied [9]. The results obtained from the optimization process are given in table 3.

Table 3

Optimum Design Parameters

Parameter	Initial value	Optimum value
th_disk	0.01 m	0.0141 m
rad_disk	0.17 m	0.18 m
rad_th_coil	0.01 m	0.0134 m
rad_th_casing	0.015 m	0.01 m
ax_th_casing	0.019 m	0.015 m
length_disk	0.14 m	0.1382 m

After an optimum design is found by solving the defined optimization problem for the MRB then the MRB is slightly modified for ease of manufacturing and additional details such as bearings, seals and the surface finishes were defined. Silicone gel sealant is used for the sealing purposes. In addition, deep groove ball bearings, 6816ZZ, were used. The fabricated model is shown in the fig. 8 and the final specifications of the MRB is shown in table 4.

Cite this article as: Thanikachalam J, Nagaraj P. "On the Fabrication of Magnetorheological Brake with Optimum Design Factors." *International Conference on Systems, Science, Control, Communication, Engineering and Technology (2015)*: 55-63. Print.

Figure 8. Fabricated MRB

Table 4
Specifications of MRB

Weight	38.2 kg
Diameter	416.8 mm
Height	46.1 mm
Number of Disks	1
Amount of MR Fluid to be used	210.856 cm^3
Coil Wire Size	AWG 21
Number of Turns	60
Magnetic Materials Used	Steel AISI1018
Non-Magnetic Materials Used	SS 304
Sealant used	Anabond® 666 RTV Silicone sealant

6. Results and Discussions

For the optimum design, the magnetic field distribution plot obtained by giving input current as 1.5 A is shown in fig. 9. The results obtained from the magneto static analysis for the magnetic flux density within the MR brake for an input current of 1.5 A along the coil is given in the fig.10. The shear stress distribution and temperature distribution in the MRB when 1.5 A current is given to the coil is given in fig.11 and fig.12 respectively. Eventhough the simulation result shows that 383.532 Nm braking torque can be achieved by the present design, in practice this value may not be reached.

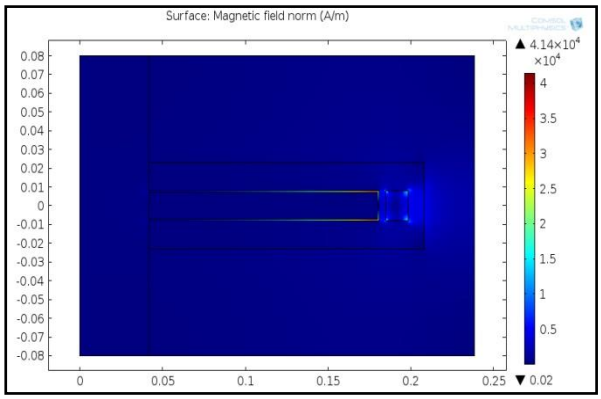

Figure 9. Magnetic field distribution along the MRB

Cite this article as: Thanikachalam J, Nagaraj P. "On the Fabrication of Magnetorheological Brake with Optimum Design Factors." *International Conference on Systems, Science, Control, Communication, Engineering and Technology (2015)*: 55-63. Print.

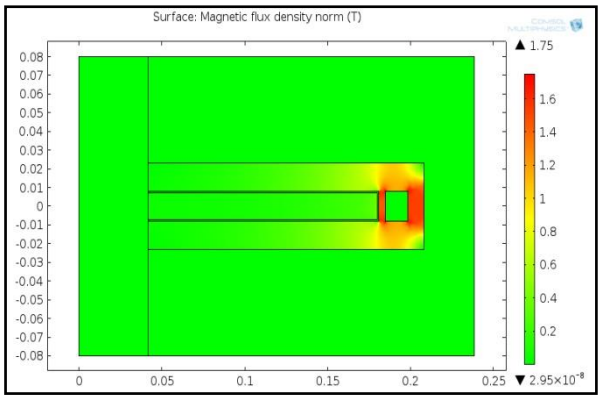

Figure 10. Magnetic flux density in MRB

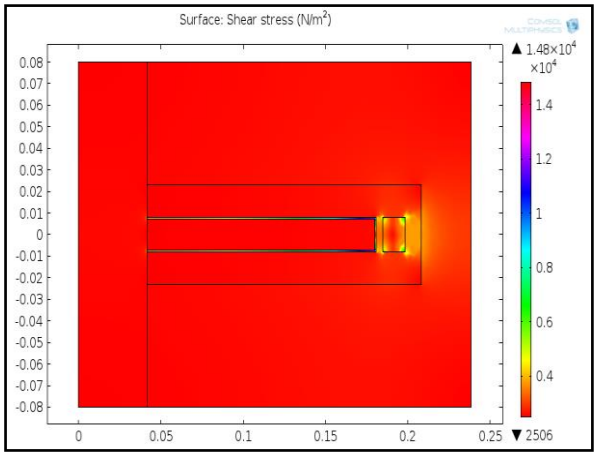

Figure 11. Shear stress distribution along the MRB

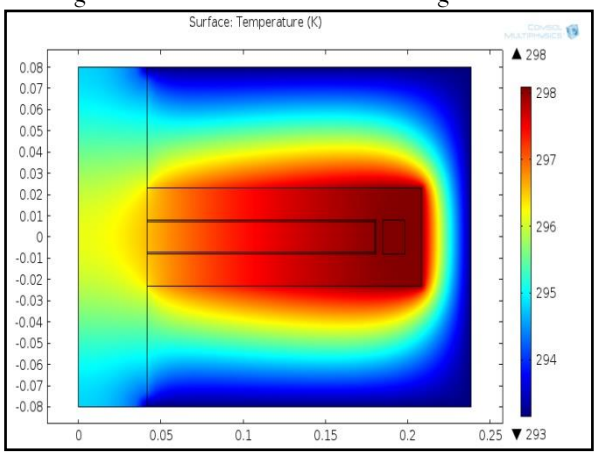

Figure 12. Temperature distribution along the MRB

7. Conclusion

In this paper, a magneto-rheological brake (MRB) with single disk design has been introduced as an alternative to the current conventional hydraulic brake (CHB) device. Analytical modeling results in the expression of torque for the MRB in terms of Magnetic field intensity. Optimization of design parameters to improve the torque and reduce weight was then carried out by Nelder Mead optimization technique using COMSOL and Finite element model for optimum design of MRB was created to simulate the steady-state magnetic flux flow within the MRB domain using COMSOL Electromagnetic module and solved for the magnetic field intensity distribution. In addition to the detailed electromagnetic analysis, a simple thermal analysis was also carried out to monitor the temperature distribution within the brake.

Cite this article as: Thanikachalam J, Nagaraj P. "On the Fabrication of Magnetorheological Brake with Optimum Design Factors." *International Conference on Systems, Science, Control, Communication, Engineering and Technology (2015)*: 55-63. Print.

The multiobjective optimization of the MRB was also carried out for minimizing the weight and maximizing the braking torque using the Nelder Mead optimization technique. For a vehicle travelling at a speed of 80 kmph, the shaft speed is found as 1040.88 rpm. When the brake is applied the torque generated is found to be 383.532 Nm with the help of the COMSOL Multiphysics®. The weight of the brake is found to be 39.158 kg. The MRB is also fabricated and the specifications are noted. Further testing procedure can be done to find the experimental results of braking torque for various speeds.

References

[1] J. Rabinow, The Magnetic Fluid Clutch, *Transactions of the AIEE, Vol. 67,* 1308-1315, (1948).

[2] Mark R. Jolly, Jonathan W. Bender, and J. David Carlson, Properties and Applications of Commercial Magnetorheological Fluids, *The Italian research on smart materials and MEMS*, 57-61 (2013).

[3] Edward J. Park, Dilian Stoikov, Luis Falcao da Luz, Afzal Suleman, A performance evaluation of an automotive magnetorheological brake design with a sliding mode controller, *Mechatronics 16,* 405–416 (2006).

[4] J. Huang, J.Q. Zhang, Y. Yang, Y.Q. Wei), Analysis and design of a cylindrical magneto-rheological fluid brake, *Journal of Materials Processing Technology 129*, 559–562 (2002)

[5] Chiranjit Sarkar, Harish Hirani, Synthesis and Characterization of Antifriction Magneto rheological Fluids for Brake, *Defence Science Journal*, Vol 63, NO 4

[6] line-of-best-fit.html [online], available: www.hotmath.com/ hotmath_help

[7] Introduction to COMSOL Multiphysics® [online], available: www.comsol.com

[8] M. Benetti, and E. Dragoni, Nonlinear Magnetic Analysis of Multi-plate Magnetorheological Brakes and Clutches, *Excerpt from the Proceedings of the COMSOL Users Conference 2006 Milano*

[9] Kalyanmoy Deb, Optimization for Engineering Design

Cite this article as: Thanikachalam J, Nagaraj P. "On the Fabrication of Magnetorheological Brake with Optimum Design Factors." *International Conference on Systems, Science, Control, Communication, Engineering and Technology (2015)*: 55-63. Print.

International Conference on Systems, Science, Control, Communication, Engineering and Technology 2015 [ICSSCCET 2015]

ISBN	978-81-929866-1-6	**VOL**	01
Website	icssccet.org	**eMail**	icssccet@asdf.res.in
Received	10 - July - 2015	**Accepted**	31- July - 2015
Article ID	ICSSCCET014	**eAID**	ICSSCCET.2015.014

DESIGN OF LOW POWER-DELAY PRODUCT CARRY LOOK AHEAD ADDER USING MANCHESTER CARRY CHAIN

M.KASISELVANATHAN[1], G.ARTHI[2], RAMABHARATHI.T.G[3]
[1]Assistant Professor, Department of ECE, Sri Ramakrishna Engineering College, Coimbatore.
[2]Department of ECE, Sri Ramakrishna Engineering College, Coimbatore.
[3]Department of ECE, Karpagam Institute of Technology, Coimbatore.

ABSTRACT: *An 8-bit Manchester carry chain (MCC) adder in multi output domino CMOS logic is designed using 180nm technology. The carries of this adder are computed in parallel by two independent 4-bit carry chains. Due to its limited carry chain length, the use of the proposed 8-bit adder module for the implementation of wider adders leads to significant operating speed improvement compared to the corresponding adders based on the standard 4-bit MCC adder module. The Power-Delay Product (PDP) of proposed adder also reduced compared to the conventional adders.*

Keywords: MCC Adders, Domino logic, PDP.

I. INTRODUCTION

Addition is a fundamental arithmetic operation that is widely used in many VLSI systems and architectures, such as application specific digital signal processing (DSP) architectures and microprocessors. As the need of higher performance, there is a continuing need to improve the performance of arithmetic logic units and to increase their performance. The combination of arithmetic units and higher performance processors are used in implementing High-speed adder architectures like carry look-ahead (CLA) adders, carry-skip adders, carry-select adders, conditional sum adders [2]-[5]. High-speed adders based on the CLA principle remain dominant, since the carry delay can be improved by calculating each stage in parallel. The CLA algorithm was first introduced in [6], and several parameters have developed.

Energy efficiency is one of the most required features for designing such adders for high performance applications. The Manchester carry chain is a variation of the CLA adder that uses shared logic to lower the transistor count. It is the most common dynamic (domino) CLA adder architecture with a regular, fast, and simple structure adequate for implementation in VLSI [7]. The recursive properties of the carries in MCC have enabled the development of multioutput domino gates, which produces area-speed improvements with respect to single-output gates. In this paper, a new 8-bit carry chain adder block in multioutput domino CMOS logic is designed proposed. The even and odd carries of this adder are computed in parallel by two independent 4-bit carry chains. Implementation of wider adders based on the use of the proposed 8-bit adder module shows significant operating speed improvement compared to their corresponding adders based on the standard 4-bit MCC adder module.

The design of MCC adder circuits using conventional logic are summarized in sections II. The section III explains the architecture of

Cite this article as: M.KASISELVANATHAN, G.ARTHI, RAMABHARATHI.T.G. "DESIGN OF LOW POWER-DELAY PRODUCT CARRY LOOK AHEAD ADDER USING MANCHESTER CARRY CHAIN." *International Conference on Systems, Science, Control, Communication, Engineering and Technology (2015)*: 64-68. Print.

double carry chain 8-bit MCC adders. The simulation results of MCC adder design using conventional logic styles and proposed logic style are compared in section IV and finally it is concluded in section V.

II. EXISTING LOGIC

Let us consider $A=a_{n-1}a_{n-2}\ldots a_1a_0$ and $B=b_{n-1}\ b_{n-2}\ldots\ B_1\ b_0$ represent two binary numbers to be added and $S=S_{n-1}S_{n-2}\ldots S_1S_0$ their sum. The symbols, +, $\oplus$, and − are used to denote the AND, Inclusive OR, Exclusive OR, and NOT logical operations, respectively. The addition of binary numbers, to compute the carry signals is based on the following recursive formula.

$$C_i=g_i+z_i.C_{i-1} \qquad (1)$$

Where, gi=ai.b_i and z_i are the carry generate and the carry propagate terms, respectively. In the case of Inclusive OR adders, is defined as $z_i=t_i=a_i+b_i$, while in the case of Exclusive OR adders, it is defined as $z_i=t_i=a_i\oplus b_i$. The implementation of the Domino generate and the Domino OR and XOR propagate signals are shown in figure.1.

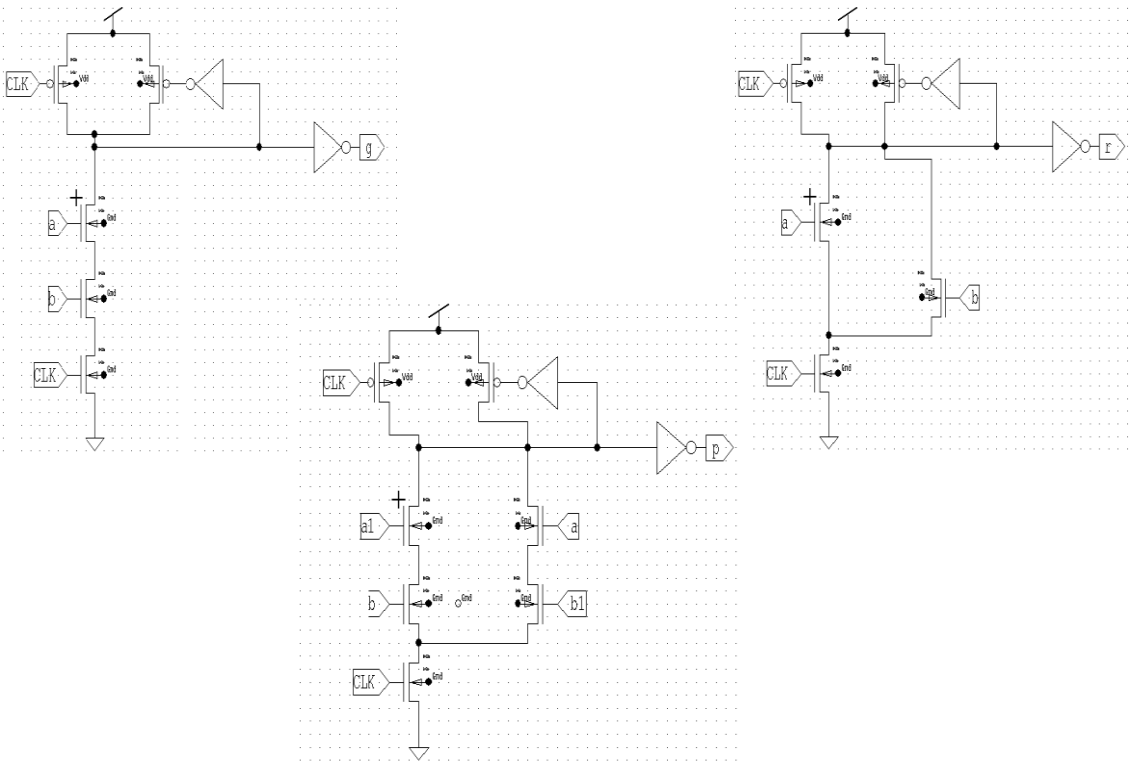

Figure 1. Domino implementation for the a) Generate b) Domino OR propagate c) Domino XOR propagate signals.

Equation (1) is expanded as follows.

$$C_i=g_i+z_i\ g_{i-1}+\ z_i\ z_{i-1}\ g_{i-2}+\ldots..\ z_i\ z_{i-1}\ldots\ z_1g_0+\ z_i\ z_{i-1}\ldots\ z_0C_{-1} \qquad (2)$$

The sum bits of the adder are defined as $Si=p_i\oplus C_{i-1}$, where C_{-1} is the input carry. The MCC generates all the carries computed according to relation (2) in parallel, using an iterative shared transistor structure. Practically, the CLA length is limited to four in order to cut down the number of series-connected transistors.

Cite this article as: M.KASISELVANATHAN, G.ARTHI, RAMABHARATHI.T.G. "DESIGN OF LOW POWER-DELAY PRODUCT CARRY LOOK AHEAD ADDER USING MANCHESTER CARRY CHAIN." *International Conference on Systems, Science, Control, Communication, Engineering and Technology (2015)*: 64-68. Print.

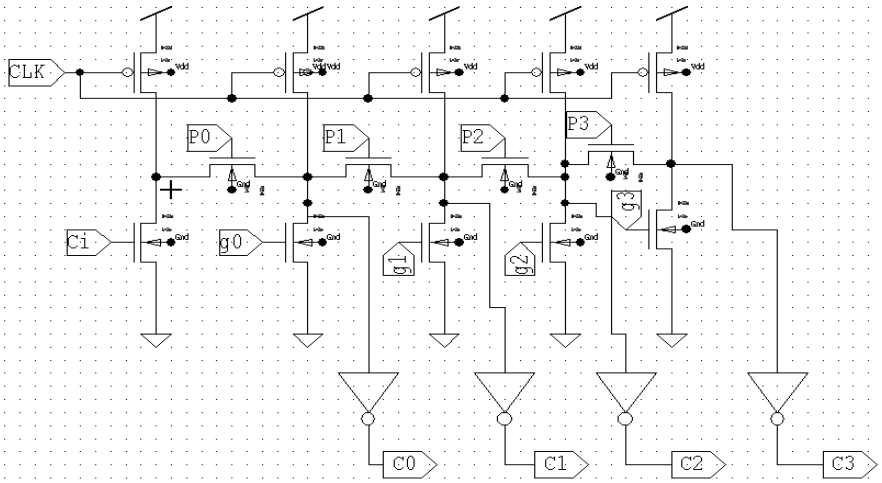

Figure.2 Conventional 4 bit Domino MCC

The implementation of the 4-bit carry chain using multioutput domino CMOS logic is shown in figure.2. The carry propagate signal is defined as $z_i=t_i=a_i+b_i$ to avoid false discharges reduced at the output nodes of the carry chain due to higher OR-AND forms of multioutput gates. To implement sum, the domino chain is terminated, and the sum bits of the MCC adder are the MCC is supported by the carry-skip capability to improve performance.

III. PROPOSED DOUBLE CARRY CHAIN ADDER

In an existing work, the length of their carry chains is limited to 4 bits due to the technological constraints. The Proposed design of an 8-bit MCC adder is implemented which is composed of two independent carry chains. These chains have the same length as the 4-bit MCC adders. The use of the proposed 8-bit adder as the basic block, instead of the 4-bit MCC adder, can lead to high-speed adder implementations. The implementation of the proposed double carry chain 8 bit MCC adder is shown in figure.4.

The derived here carry equations are similar to those for the Ling carries proposed in [11]–[13]. The derived carry equations allow the even carries to be computed separately of the odd ones. This separation allows the implementation of the carries by two independent 4-bit carry chains; one chain computes the even carries, while the other chain computes the odd carries. The design of the proposed 8-bit MCC adder is implemented in the following.

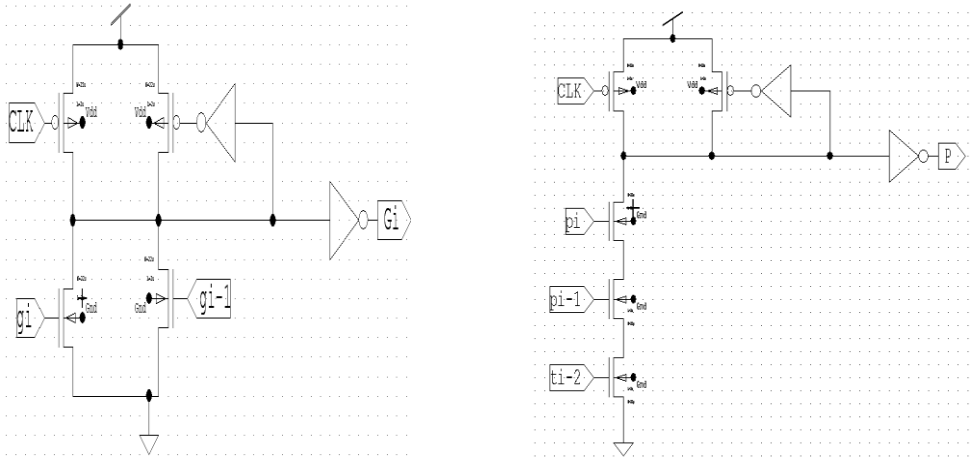

Figure.3 Proposed Domino a) Generate and b) Propagate signals.

(a) Computation of Even Carry:

For i=0 and $z_0=t_0$,

From the equation (1), then $c_0=g_0+t_0.c_{-1}$.

Since $g_i=g_i.t_i$, $c_0=t_0\ (g_0.c_{-1}) =t_0h_0$,

Where

$h_0= g_0+c_{-1}$ is the new carry.

From the equation (2),

Cite this article as: M.KASISELVANATHAN, G.ARTHI, RAMABHARATHI.T.G. "DESIGN OF LOW POWER-DELAY PRODUCT CARRY LOOK AHEAD ADDER USING MANCHESTER CARRY CHAIN." *International Conference on Systems, Science, Control, Communication, Engineering and Technology (2015)*: 64-68. Print.

For i=2 and $z_i=p_i$,

$c_2= C_2=g_2+p_2g_1+ p_2p_1g_0+p_2p_1p_0c_{-1}$

Since $g_i+p_i.g_{i-1}=g_i+t_ig_{i-1}$ and $p_i= p_it_i$,

$c_2= t_2 (g_2+g_1+ p_2 p_1 g_0+ p_2 p_1 p_0c_{-1})$

$= t_2 (g_2+g_1+ p_2 p_1 t_0 (g_0+c_{-1})) =t_2.h_2$

Where

$h_2= g_2+g_1+ p_2p_1t_0 (g0+c_{-1})$ is the new carry.

Similarly, h_4, h_6 values are computes as follows,

$h_4= g_4+g_3+ p_4p_1t_2 (g_2+g_1+ p_2p_1t_0 (g0+c_{-1}))$

$h_6= g_6+g_5+ p_6p_5p_4t_2 (g_4+g_3+ p_4p_1t_2 (g_2+g_1+ p_2p_1t_0 (g0+c_{-1})))$

(b) Computation of Odd Carry:

The odd carries for the values of i are computed according to the aforementioned methodology proposed for the even carries as follows.

$h_1= g_1+g_0+p_1p_0c_{-1}$

$h_3= g_3+g_2+p_3p_2t_1 (g_1+g_0+p_1p_0c_{-1})$

$h_5= g_5+g_4+ p_5p_4t_3 (g_3+g_2+p_3p_2t_1 (g_1+g_0+p_1p_0c_{-1}))$

$h_7= g_7+g_6+ p_7p_6t_4 (g_5+g_4+ p_5p_4t_3 (g_3+g_2+p_3p_2t_1 (g_1+g_0+p_1p_0c_{-1})))$

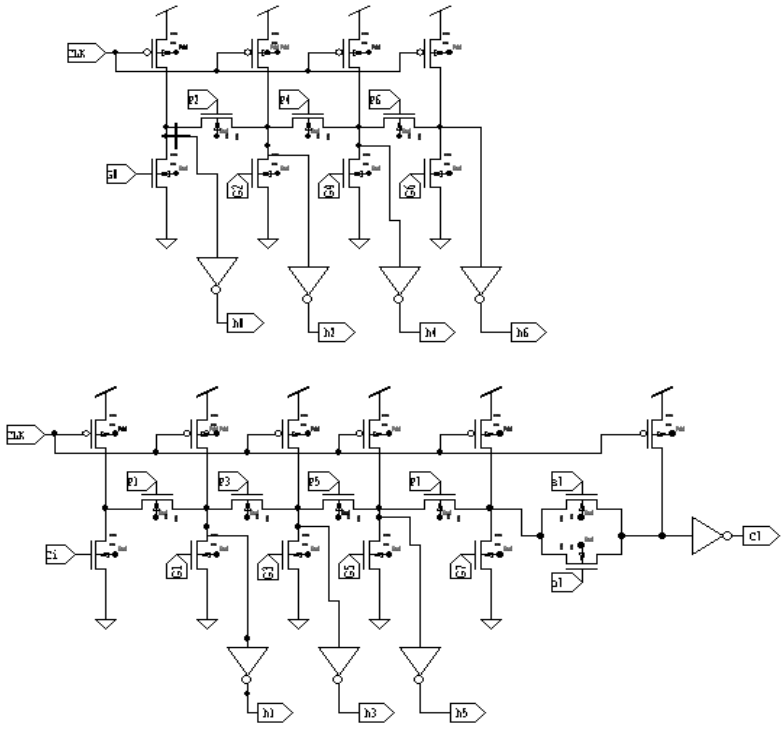

Figure.3 Proposed Double Carry Chain 8 bit MCC Adder

Let $G_i= g_i+g_{i-1}$ and $Pi= p_i+p_{i-1}$ be the new generate and propagate signals respectively, where, $g_{-i}=c_{-1}$ and $t_{-1}=1$. Then the equation is derived as follows.

For even values of i,

h2 =G2 + P2G0

h4 =G4 + P4G2 + P4P2G0

h6 =G6 + P6G4 + P6P4G2 + P6P4P2G0

While for odd values of I,

h1 =G1 + P1c−1

h3 =G3 + P3G1 + P3P1c−1

h5 =G5 + P5G3 + P5P3G1 + P5P3P1c−1

h7 =G7 + P7G5 + P7P5G3 + P7P5P3G1 + P7P5P3P1c−1.

Cite this article as: M.KASISELVANATHAN, G.ARTHI, RAMABHARATHI.T.G. "DESIGN OF LOW POWER-DELAY PRODUCT CARRY LOOK AHEAD ADDER USING MANCHESTER CARRY CHAIN." *International Conference on Systems, Science, Control, Communication, Engineering and Technology (2015)*: 64-68. Print.

IV. SIMULATION RESULTS AND DISCUSSION

The proposed 8 bit MCC adder and the conventional adder are designed in a 0.18-μm CMOS technology. The propagation delay, power consumption, and power-delay product are obtained at the supply voltage of 1.8 V. Due to the technological constraints, the length of the carry chains of conventional adder is limited to 4 bits. The proposed 8 bit double carry chain adder has a significantly reduced propagation delay compared to the conventional adder. The obtained simulation results for conventional and proposed adders are summarized in Table.1.

Table.1 Comparison Results of Conventional and Proposed Adders

Parameter	**Power Delay Product (Ws)**				
Logic	**8 bit MCC Adder**	**16 bit MCC Adder**	**32 bit MCC Adder**	**64 bit MCC Adder**	**128 bit MCC Adder**
Existing Method	$1.838\text{x}10^{-7}$	$3.662\text{x}10^{-7}$	$7.308\text{x}10^{-7}$	$1.458\text{x}10^{-6}$	$2.918\text{x}10^{-6}$
Proposed Method	$1.267\text{x}10^{-7}$	$2.524\text{x}10^{-7}$	$5.042\text{x}10^{-7}$	$1.008\text{x}10^{-6}$	$2.05\text{x}10^{-6}$

V. CONCLUSION

The proposed 8-bit MCC adder in multi output domino CMOS logic is designed using 180nm technology. The MCC is an efficient and widely accepted design approach to construct CLA adders. The proposed logic style is based on two independent 4-bit carry chains. Due to its limited carry chain length, the use of the proposed 8-bit MCC carry chain adder leads to significant operating speed improvement then compared to the corresponding adders based on the standard 4 bit adder module. module for the implementation of wider adders leads to significant operating speed improvement compared to the corresponding adders based on the standard 4-bit MCC adder module. The 8-, 16-, 32-, 64-, and 128-bit adders using both conventional and proposed logics are also implemented in 180nm technology. The simulated results show that the Power-Delay Product of the proposed design is less compared to the conventional design.

REFERENCES

[1]. Costas Efstathiou, Zaher Owda, and Yiorgos Tsiatouhas, "New High-Speed Multioutput Carry Look-Ahead Adders", IEEE Ttransactions on Circuits and Systems- Vol. 60, No. 10,Oct 2013.

[2]. K. Hwang, Computer Arithmetic: Principles, Architecture, and Design.New York, NY, USA: Wiley, 1979.

[3]. B. Parhami, Computer Arithmetic, Algorithms and Hardware. New York, NY, USA: Oxford Univ. Press, 2000.

[4]. I. Koren and A. K. Peters, Computer Arithmetic Algorithms, 2nd ed.Boca Raton, FL, USA: CRC Press, 2002.

[5]. M. D. Ercegovac and T. Lang, Digital Arithmetic. San Mateo, CA, USA:Morgan Kaufmann, 2004.

[6]. A. Weinberger and J. L. Smith, "A logic for high speed addition," Nat.Bureau Stand. Circulation, vol. 591, pp. 3-12, 1958.

[7]. J. P. Uyemura, CMOS Circuit Design. Boston, MA, USA: Kluwer, 2001.

[8]. N. Weste and D. Harris, CMOS VLSI Design, A Circuit and System Perspective. Reading, MA, USA: Addison-Wesley, 2004.

[9]. P. K. Chan and M. D. F. Schlag, "Analysis and design of CMOS Manchester adders with variable carry-skip," IEEE Trans. Comput., vol. 39, no. 8, pp. 983–992, Aug. 1990.

[10]. Z.Wang, G. Jullien,W.Miller, J.Wang, and S. Bizzan, "Fast adders using enhanced multiple-output domino logic," IEEE J. Solid State Circuits, vol. 32, no. 2, pp. 206–214, Feb. 1997.

[11]. H. Ling, "High-speed binary adder," IBM J. Res. Develop., vol. 25, pp. 156–166, Mar. 1981.

[12]. C. Efstathiou, H. T. Vergos, and D. Nikolos, "Ling adders in CMOS standard cell technologies," in Proc. 9th ICECS, Sep. 2002, vol. 2,pp. 485–489.

[13]. G. Dimitrakopoulos and D. Nikolos, "High-speed parallel-prefix VLSI Ling adders," IEEE Trans. Comput., vol. 54, no. 2, pp. 225–231, Feb. 2005.

Cite this article as: M.KASISELVANATHAN, G.ARTHI, RAMABHARATHI.T.G. "DESIGN OF LOW POWER-DELAY PRODUCT CARRY LOOK AHEAD ADDER USING MANCHESTER CARRY CHAIN." *International Conference on Systems, Science, Control, Communication, Engineering and Technology (2015)*: 64-68. Print.

International Conference on Systems, Science, Control, Communication, Engineering and Technology 2015 [ICSSCCET 2015]

ISBN	978-81-929866-1-6	**VOL**	01
Website	icssccet.org	**eMail**	icssccet@asdf.res.in
Received	10 - July - 2015	**Accepted**	31- July - 2015
Article ID	ICSSCCET015	**eAID**	ICSSCCET.2015.015

WEAKLY b-δ OPEN FUNCTIONS

S. Anuradha[1], S. Padmanaban[2], S. Sharmila banu[3]
[1]Prof & Head, P G & Research Dept. of Mathematics, Hindusthan College of Arts & Science
[2, 3]Assistant Professor, Department of Science & Humanities, Karpagam Institute of Technology

Abstract: *In this paper, we introduce and study new classes of functions called b-δ -open functions and weakly b-δ -open functions by using the notions of b-δ-open sets and b-δ-closed sets. Some of its basic properties of these functions are investigated.*

Keywords: b-open set, δ -open set, b- δ-open set, weakly b- δ -open function, weakly-b- δ -closed function.

1. INTRODUCTION

The notions of δ -open sets, δ -closed set where introduced by Velicko [11] for the purpose of studying the important class of H-closed spaces. 1996, Andrijević [3] introduced a new class of generalized open sets called b-open sets in a topological space. This class is a subset of the class of β-open sets [1]. Also the class of b-open sets is a superset of the class of semi- open sets [5] and the class of preopen sets [6]. The purpose of this paper is to introduce and investigate the notions of weakly b-δ-open functions and weakly b-δ-closed functions. We investigate some of the fundamental properties of this class of functions. We recall some basic definitions and known results. Throughout the paper, X and Y (or (X, τ) and (Y, σ)) stand for topological spaces with no separation axioms assumed unless otherwise stated. Let A be a subset of X. The closure of A and the interior of A will be denoted by cl(A) and int(A), respectively.

2. PRELIMINARY

Definition 2.1. A subset A of a space X is said to be b-open [3] if $A \subseteq cl(int(A)) \cup int(cl(A))$. The complement of a b-open set is said to be b-closed. The intersection of all b-closed sets containing $A \subseteq X$ is called the b-closure of A and shall be denoted by bcl(A). The union of all b-open sets of X contained in A is called the b-interior of A and is denoted by bint(A). A subset A is said to be b-regular if it is b-open and b-closed. The family of all b-open (resp. b-closed, b-regular) subsets of a space X is denoted by BO(X) (resp. BC (X), BR(X)) and the collection of all b-open subsets of X containing a fixed point x is denoted by BO(X, x). The sets BC(X, x) and BR(X, x) are defined analogously.

Definition 2.2. A point $x \in X$ is called a δ -cluster [11] point of A if $int(cl(U)) \cap A \neq \varphi$ for every open set U of X containing x.

The set of all δ -cluster points of A is called the δ - closure of A and is denoted by δ -cl (A)). A subset A is said to be δ -closed if δ -cl(A) = A. The complement of a δ -closed set is said to be δ-open. The δ -interior of A is defined by the union of all δ -open sets contained in A and is denoted by δ-int (A)).

Cite this article as: S. Anuradha, S. Padmanaban, S. Sharmila banu. "WEAKLY b-δ OPEN FUNCTIONS." *International Conference on Systems, Science, Control, Communication, Engineering and Technology (2015)*: 69-72. Print.

Definition 2.3. A point $x \in X$ is called a b-δ -cluster [8] point of A if $int(bcl(U)) \cap A \neq \varphi$ for every b-open set U of X containing x.The set of all b-δ -cluster points of A is called the b-δ - closure of A and is denoted by b-δ -cl (A)). A subset A is said to be b-δ -closed if b-δ-cl(A) = A. The complement of a b-δ -closed set is said to be b-δ-open. The b-δ -interior of A is defined by the union of all b-δ -open sets contained in A and is denoted by b-δ-int (A)). The family of all b-δ -open (resp. b-δ -closed) sets of a space X is denoted by $B\delta O(X, \tau)$ (resp. $B\delta C(X, \tau)$).

Definition 2.4. A subset A of a space X is said to be α-open [7] (resp. semi-open [5], preopen[6], β-open[1] or semi-preopen [2]) if $A \subseteq int(cl(int(A)))$ (resp. $A \subseteq d(int(A))$, $A \subseteq int(cl(A))$,$A \subseteq cl(int(cl(A)))$.

Definition 2.5. [4] $f : (X, \tau) \to (Y, \sigma)$ is said to be strongly continuous if for every subset A of (X, τ), $f(cl(A)) \subseteq f(A)$.

Definition 2.6. [6] $f : (X, \tau) \to (Y, \sigma)$ is said to be pre-continuous if $f^{-1}(V)$ is pre-open in (X, τ) for every open set V of (Y, σ).

Definition 2.7. [1] $f : (X, \tau) \to (Y, \sigma)$ is said to be β-open if the image of each open set U of (X, τ) is a β-open set.

Lemma 2.5. [3] For a subset A of a space X, the following properties hold:
(1) $bint(A) = sint(A) \cup pint(A)$;
(2) $bcl(A) = scl(A) \cap pcl(A)$;
(3) $bcl(X - A) = X - bint(A)$;
(4) $x \in bcl(A)$ if and only if $A \cap U = \varphi$ for every $U \in BO(X, x)$;
(5) $A \in BC(X)$ if and only if $A = bcl(A)$;
(6) $pint(bcl(A)) = bcl(pint(A))$.

Lemma 2.6. [2] For a subset A of a space X, the following properties are hold:
(1) $\alpha int(A) = A \cap int(cl(int(A)))$;
(2) $sint(A) = A \cap cl(int(A))$;
(3) $pint(A) = A \cap int(cl(A))$.

3. WEAKLY b-δ OPEN FUNCTIONS

Definition 3.1. A function $f : (X, \tau) \to (Y, \sigma)$ is said to be b-δ -open if for each open set U of (X, τ), f(U) is b-δ -open.

Definition 3.2. A function $f: (X, \tau) \to (Y, \sigma)$ is said to be weakly b-δ -open if $f(U) \subseteq$ b-δ-int(f(cl(U))) for each open set U of (X, τ).

Theorem 3.3. For a function $f: (X, \tau) \to (Y, \sigma)$, the following conditions are equivalent:
(1) f is weakly b-δ-open,
(2) $f(\delta\text{-int}(A)) \subseteq$ b-δ-int (f(A)) for every subset of A of (X, τ),
(3) $\delta\text{-int}(f^{-1}(B)) \subseteq f^{-1}(b\text{-}\delta\text{-int}(B))$ for every subset of B of (Y, σ),
(4) $f^{-1}(b\text{-}\delta\text{-cl}(B) \subseteq \delta\text{-cl}(f^{-1}(B))$ for every subset of B of (Y, σ).

Proof. (1)⇒(2): Let A be any subset of (X, τ) and $x \in \delta\text{-int}(A)$. Then there exists an open set U such that $x \in U \subseteq cl(U) \subseteq A$. Then, $f(x) \in f(U) \subseteq f(cl(U)) \subseteq f(A)$. Since f is weakly b-$\delta$ -open, $f(U) \subseteq$ b-δ-int $(f(cl(U))) \subseteq$ b-δ-int$(f(A))$.This implies that $f(x) \in$ b-δ-int $(f(A))$. This shows that $x \in f^{-1}$ (b-δ-int $(f(A)))$.Thus δ-int (A) $\subseteq f^{-1}$ (b-δ-int$(f(A)))$ and so $f(\delta\text{-int}(A)) \subseteq$ b-δ-int$(f(A))$.

(2)⇒(3): Let B be any subset of (Y, σ).Then by (2), $f(\delta\text{-int}(f^{-1}(B))) \subseteq$ b-δ-int$(f(f^{-1}(B)) \subseteq$ b-δ-int(B). Therefore $\delta\text{-int}(f^{-1}(B) \subseteq f^{-1}(b\text{-}\delta\text{-int}(B))$.

(3)⇒(4): Let B be any subset of (Y, σ).Using (3), we have $X - \delta\text{-cl}(f^{-1}(B)) = \delta\text{-int}(X - f^{-1}(B)) = \delta\text{-int}(f^{-1}(Y - B)) \subseteq f^{-1}(b\text{-}\delta\text{-int}(Y - B)) = f^{-1}(Y - b\text{-}\delta\text{-cl}(B)) = X - f^{-1}(b\text{-}\delta\text{-cl}(B))$.Therefore we obtain $f^{-1}(b\text{-}\delta\text{-cl}(B)) \subseteq \delta\text{-cl}(f^{-1}(B))$.

(4)⇒(1): Let V be any open set of (X, τ) and $B = Y - f(cl(V))$. By (4),

Cite this article as: S. Anuradha, S. Padmanaban, S. Sharmila banu. "WEAKLY b-δ OPEN FUNCTIONS." *International Conference on Systems, Science, Control, Communication, Engineering and Technology (2015)*: 69-72. Print.

$f^{-1}(\text{b-}\delta\text{-cl}(Y - f(\text{cl}(V)))) \subseteq \delta\text{-cl}(f^{-1}(Y - f(\text{cl}(V))))$.Therefore, we obtain $f^{-1}(Y - \text{b-}\delta\text{-int}(f(\text{cl}(V)))) \subseteq \delta\text{-cl}(X - f^{-1}(f(\text{cl}(V)))) \subseteq \delta\text{-cl}(X - \text{cl}(V))$.Hence $V \subseteq \delta\text{-int}(\text{cl}(V)) \subseteq f^{-1}(\text{b-}\delta\text{-int}(f(\text{cl}(V))))$ and $f(V) \subseteq \text{b-}\delta\text{-int}(f(\text{cl}(V)))$. This shows that f is weakly b-δ-open.

Theorem 3.4. For a function $f : (X, \tau) \to (Y, \sigma)$, the following conditions are equivalent:

(1) f is weakly b-δ-open;

(2) For each $x \in X$ and each open subset U of (X, τ) containing x, there exists a b-δ-open set V containing $f(x)$ such that $V \subseteq f(\text{cl}(U))$.

Proof. (1)⇒(2): Let $x \in X$ and U be an open set in (X, τ) with $x \in U$. Since f is weakly b-δ-open, $f(x) \in f(U) \subseteq$ b-δ-int(f(cl(U))). Let $V = \text{b-}\delta\text{-int}(f(\text{cl}(U)))$. Then V is b-δ-open and $f(x) \in V \subseteq f(\text{cl}(U))$.

(2)⇒(1): Let U be an open set in (X, τ) and let $y \in f(U)$. It follows from (2) that $V \subseteq f(\text{cl}(U))$ for some b-δ-open set V in (Y, σ) containing y. Hence, we have $y \in V \subseteq$ b-δ-int(f(cl(U))).This shows that f(U) ⊆ b-δ-int(f(cl(U))).Thus f is weakly b-δ-open.

Theorem 3.5. For a bijective function $f: (X, \tau) \to (Y, \sigma)$, the following conditions are equivalent:

(1) f is weakly b-δ-open,

(2) b-δ-cl(f(int(F))) ⊆ f(F) for each closed set F in (X, τ),

(3) b-δ-cl(f(U))) ⊆ f(cl(U)) for each open set U in (X, τ).

Proof. (1)⇒(2): Let F be a closed set in (X, τ). Then since f is weakly b-δ-open,
$f(X - F) = \subseteq \text{b-}\delta\text{-int}(f(\text{cl}(X - F))) = \text{b-}\delta\text{-int}(f(\text{cl}(X - F)))$ and so $Y - f(F) \subseteq Y - \text{b-}\delta\text{-cl}(f(\text{int}(F)))$. Hence b-δ-cl $(f(\text{int}(F))) \subseteq f(F)$.

(2)⇒(3): Let U be an open set in (X, τ). Since cl(U) is a closed set and $U \subseteq$ int(cl(U)), by (2), we have b-δ-cl(f(U)) ⊆ b-δ-cl(f(int(cl(U)))) ⊆ f(cl(U)).

(3)⇒(1): Let V be an open set of(X, τ).. Then we have Y - b-δ-int(f(cl(V))) = b-δ-cl(Y – f(cl(V))) = b-δ-cl(f(X – cl(V))) ⊆ f(cl(X – cl(V))) = f(X – int(cl(V))) ⊆f(X – V) = Y – f(V).Therefore, we have f(V) ⊆ b-δ-int(f(cl(V))) and hence f is weakly b-δ-open.

Theorem 3.6. For a function $f : (X, \tau) \to (Y, \sigma)$, the following conditions are equivalent:

(1) f is weakly b-δ open;

(2) f(U) ⊆ b-δ-int(f(cl(U))) for each preopen set U of (X, τ),

(3) f(U) ⊆ b-δ-int(f(cl(U))) for each α-open set U of (X, τ),

(4) f(int(cl(U))) ⊆ b-δ-int(f(cl(U))) for each open set U of (X, τ),

(5) f(int(F)) ⊆ b-δ-int(f(F)) for each closed set F of (X, τ).

Proof: Follows from definitions of open, pre-open, α-open sets.

Theorem 3.7. Let X be a regular space. A function $f: (X, \tau) \to (Y, \sigma)$ is weakly b-δ-open if and only if f is b-δ-open.

Proof. The sufficiency is clear.

For the necessity, let W be a nonempty open subset of (X, τ). For each x in W, let U_x be an open set such that $x \in U_x \subseteq \text{cl}(U_x) \subseteq W$. Hence we obtain that $W = \cup \{U_x : x \in W\} \subseteq \cup \{\text{cl}(U_x) : x \in W\}$ and $f(W) = \cup \{f(U_x) : x \in W\} \subseteq \cup \{\text{b-}\delta\text{-int}(f(\text{cl}(U_x))) : x \in W\} \subseteq \text{b-}\delta\text{-int}(f(\cup \{\text{cl}(U_x) : x \in W\})) = \text{b-}\delta\text{-int}(f(W))$. Thus f is b-δ-open.

Theorem 3.8. If $f: (X, \tau) \to (Y, \sigma)$ is weakly b-δ-open and strongly continuous, then f is b-δ-open.

Proof. Let U be an open subset of (X, τ). Since f is weakly b-δ-open, $f(U) \subseteq \text{b-}\delta\text{-int}(f(\text{cl}(U)))$.However, because f is strongly continuous, $f(U) \subseteq \text{b-}\delta\text{-int}(f(U))$. Therefore $f(U)$ is b-δ-open.

Theorem 2.22. If a function $f: (X, \tau) \to (Y, \sigma)$ is weakly b-δ-open and precontinuous , then f is β-open.

Proof. Let U be an open subset of X . Then by weak b-δ-openness of f, $f(U) \subseteq$ b-δ-int(f(cl(U))). Since f is precontinuous, f(cl(U)) ⊆ cl(f(U)).

Hence we obtain that

$$\begin{aligned} f(U) &\subseteq \text{b-}\delta\text{-int}(f(\text{cl}(U))) \\ &\subseteq \text{b-}\delta\text{-int}(\text{cl}(f(U))) \\ &= \text{bint}(\text{cl}(f(U))) \\ &= \text{sint}(\text{cl}(f(U))) \cup \text{pint}(\text{cl}(f(U))) \end{aligned}$$

Cite this article as: S. Anuradha, S. Padmanaban, S. Sharmila banu. "WEAKLY b-δ OPEN FUNCTIONS." *International Conference on Systems, Science, Control, Communication, Engineering and Technology (2015)*: 69-72. Print.

$$\subseteq \text{cl}(\text{int}(\text{cl}(\text{f}(\text{U})))) \cup \text{int}(\text{cl}(\text{f}(\text{U})))$$
$$\subseteq \text{cl}(\text{int}(\text{cl}(\text{f}(\text{U}))))$$

which shows that $\text{f}(\text{U})$ is a β-open set in Y. Thus f is a β-open function.

References

1. Abd El-Monsef M.E., El-Deeb S. N., Mahmoud R. A., β-open sets and β-continuous mappings, Bull. Fac. Sci. Assiut Univ. 12 (1983), 77–90.
2. Andrijević D., Semi-preopen sets, Mat. Vesnik 38 (1)(1986), 24–32.
3. Andrijević D., On b-open sets, Mat. Vesnik 48 (1996), 59–64.
4. Levine N., Strong continuity in topological spaces, Amer. Math. Monthly 67 (3) (1960), 269.
5. Levine N., Semi-open sets and semi-continuity in topological spaces, Amer. Math.Monthly 70 (1963), 36–41.
6. Mashhour A. S., Abd El-Monsef M. E., El-Deeb S. N., On precontinuous and weak precontinuous functions, Proc. Math. Phys. Soc. Egypt 53 (1982), 47–53.
7. Njåstad O., On some classes of nearly open sets, Pacific J. Math. 15 (1965), 961–970.
8. S.Padmanaban, On b- δ-open sets in topological spaces, Int Jr. of Mathematical Sciences & Applications,(3), 2013, 365-371.
9. Singal M.K ., Singal A. R., Almost continuous mappings, Yokohama Math. J. 16 (1968), 63–73.
10. Steen L. A., Seebach J.A, Jr., Counterexamples in Topology, Holt, Reinhart and Winston, Inc., New York, 1970.
11. Veličko N.V,, H -closed topological spaces, Amer. Math. Soc. Transl. Ser. 2 78 (1968),103–118.

Cite this article as: S. Anuradha, S. Padmanaban, S. Sharmila banu. "WEAKLY b-δ OPEN FUNCTIONS." *International Conference on Systems, Science, Control, Communication, Engineering and Technology (2015)*: 69-72. Print.

International Conference on Systems, Science, Control, Communication, Engineering and Technology 2015 [ICSSCCET 2015]

ISBN	978-81-929866-1-6	**VOL**	01
Website	icssccet.org	**eMail**	icssccet@asdf.res.in
Received	10 - July - 2015	**Accepted**	31- July - 2015
Article ID	ICSSCCET016	**eAID**	ICSSCCET.2015.016

TO STUDY THE WOVEN FABRIC OF BAMBOO&TENCEL FOR COMPFORT PROPERTIES

M. D. Jothilinkam[1], T. Ramachandran[2], G.Ramakrishnan[3]
[1]Karpagam University, Coimbatore, India
[2] Karpagam Institute of Technology, Coimbatore, India
[3]Department of Fashion Technology, Kumaraguru College of Technology, Coimbatore –641049 India,
(KCT-TIFAC CORE in Textile Technology & Machinery)

ABSTRACT: This research work aims at investigation of mechanical and moisture properties of fabrics made from bamboo and microtencel fibres. Woven fabrics made from these fibres were evaluated for mechanical properties such as tensile strength and elongation and moisture properties such as water vapour permeability, wicking. The. results indicated that 100% bamboo fabric showed very good water vapor permeability. Fabric wicking was similar in all samples. Tensile tests (warp way) conducted on all the 5 samples revealed that 100% bamboo fabric yielded the lowest strength and 30:70 bamboo: tencel blended fabric yielded the highest fabric strength. Tensile tests conducted in (weft way) for all the 5 samples revealed that 100% bamboo has lowest strength and 100% Tencel had the highest strength.

The material for research will include natural, regenerated and synthetics fibers such as cotton, viscose, modal, tencel, bamboo and polyester of both conventional and micro denier. This fiber will be made into yarn using ring and open end spinning method. The yarn will be converted into woven and knitted fabric using different woven and knitted structures suitable for use in apparel. The fabric will be treated with different types of plasma gases, dyed and finished. The fabric will be tested for thermal and moisture properties using of thermal and moisture testers and will be evaluated for thermal resistance and water vapor permeability in addition low stress mechanical properties for studying apparel comfort.

The result thus obtained will be very useful to textile/apparel manufacturing industry

1. INTRODUCTION

Bamboo fiber has particular and natural functions of anti-bacteria, bacteriostasis and deodorization. It is validated by Japan Textile Inspection Association that, even after fifty times of washing, bamboo fiber samples still possesses excellent function of anti-bacteria, bacteriostasis. Its test result shows over 70% death rate after bacteria being incubated on bamboo fiber samples. Bamboo fiber's natural anti-bacteria function differs greatly from that of chemical anti-microbial.More important, bamboo fiber is a unique biodegradable textile material.

As a natural cellulose fiber it can be 100% biodegraded in soil by micro organisms and sunshine. The decomposition process does not cause any pollution in the environment. "Bamboo fiber comes from nature and completely returns to nature in the end" Bamboo fiber is praised as "the natural, green and eco–friendly new type textile material of 21st century".Bamboo can thrive naturally without the use of pesticides as it is seldom eaten by pests or infected by pathogen. Scientists have found that bamboo contains a unique anti-bacteria and bacteriostasis bio-agent named "bamboo Kun". This substance

is maintained in the finished bamboo fabric as it is bound tightly to the bamboo cellulose molecule. Bacteria will propagate rapidly in

Cite this article as: M. D. Jothilinkam, T. Ramachandran, G.Ramakrishnan. "TO STUDY THE WOVEN FABRIC OF BAMBOO&TENCEL FOR COMPFORT PROPERTIES." *International Conference on Systems, Science, Control, Communication, Engineering and Technology (2015)*: 73-78. Print.

cotton and other fibers obtained from wood pulp, forming bad smell and even cause early degradation of the fiber in some cases. But it will be killed 75% after 24 hours later in bamboo fiber.

Tencel is the registered trade name for Lyocell, which a biodegradable fabric is made from wood pulp cellulose the fabric to be environmentally friendly and a good choice for people with sensitive skin. Yet this may not always be true. While Tencel is made from wood fibers and is biodegradable.

Tencel fabric is an amazing eco friendly fabric that represents a milestone in the development of environmentally sustainable textiles. Tencel is a natural, manmade fibre which is also referred to as Lyocell. Made with wood pulp from sustainable tree farms, tencel textiles are created though the use of nanotechnology in an award-winning closed-loop process that recovers or decomposes all solvents and emissions.

2. MATERIALS AND METHODS

The bamboo and tencel yarns were spun on a miniature ring frame with 22.57 twists per inch. Table 2.1 shows the properties of bamboo and tencel spun yarns. The fabrics were woven from 30s count warp and weft, bamboo and tencel yarns on a miniature weaving machine. The construction details of woven fabric were 30 ends per inch and 20 picks per inch for woven plain gauze fabric.

Table 2.1.Fiber Properties

SL.NO	FIBER	TEX	STAPLE LENGTH
1	Bamboo	1.33D tex	38mm
2	Tencel	0.8 D tex	38mm

The blending ratio of fibre both bamboo and tencel fibre staple length of 38mm with five different combination are mentioned below the table 2.2.

Table 2.2 Blending Ratio

Sl.no	FIBRES	BLENDING RATIO
1	Bamboo	100%
2	Tencel	100%
3	Bamboo/Tencel	50%/50%
4	Bamboo/Tencel	70%/30%
5	Bamboo/Tencel	30%/70%

The geometrical details of woven gauze fabric for medical textiles product using the functional fibers for wound dressing and bandages are shown in below Table 2.3.

Cite this article as: M. D. Jothilinkam, T. Ramachandran, G.Ramakrishnan. "TO STUDY THE WOVEN FABRIC OF BAMBOO&TENCEL FOR COMPFORT PROPERTIES." *International Conference on Systems, Science, Control, Communication, Engineering and Technology (2015)*: 73-78. Print.

Table 2.3 Geometrical Details

1	Warp	30Ne
2	Weft	30Ne
3	EPI	30
4	PPI	20
5	Cover factor	8.5
6	GSM	53 gms
7	Thickness	2.5 mm

3. RESULTS AND DISCUSSION

The testing method is shown below table 3.1 for the experimental work.

Table 3.1 Testing Method

SL NO	TEST PARAMETER	STANDARD
1	Tensile Properties	ASTM D 5035
2	Thickness	ASTM D 1777
3	Water vapor Permeability	ISO 11092 BS EN 31092:199
4	Fabric Wicking	INHOUSE METHOD

3.2 Wickability test

TESTING METHOD	Bamboo-100%	Tencel 100%	Bamboo/ Tencel 50%/50%	Bamboo/ Tencel 70%/30%	Bamboo/ Tencel 70%/30%
WICKABILITY IN MM AFTER 24 HRS	10	10	10	10	10

Discussion

It is observed from above table the Wickability is similar in all sample=10mm.

3.3 Tensile Strength

The tensile strength means the material under tensile stress in the largest deformation of homogeneous material stress. Material tensile strength is the maximum uniform plastic deformation of the stress. In the tensile test, the specimen until fracture suffered the biggest so far is the tensile strength of tensile stress.

Cite this article as: M. D. Jothilinkam, T. Ramachandran, G.Ramakrishnan. "TO STUDY THE WOVEN FABRIC OF BAMBOO&TENCEL FOR COMPFORT PROPERTIES." *International Conference on Systems, Science, Control, Communication, Engineering and Technology (2015)*: 73-78. Print.

Defaults Table	
Text Inputs: Specimen label	100% Bamboo - Warp
Number Inputs: Gauge Length (mm)	75.
Number Inputs: Speed (mm/min)	300.

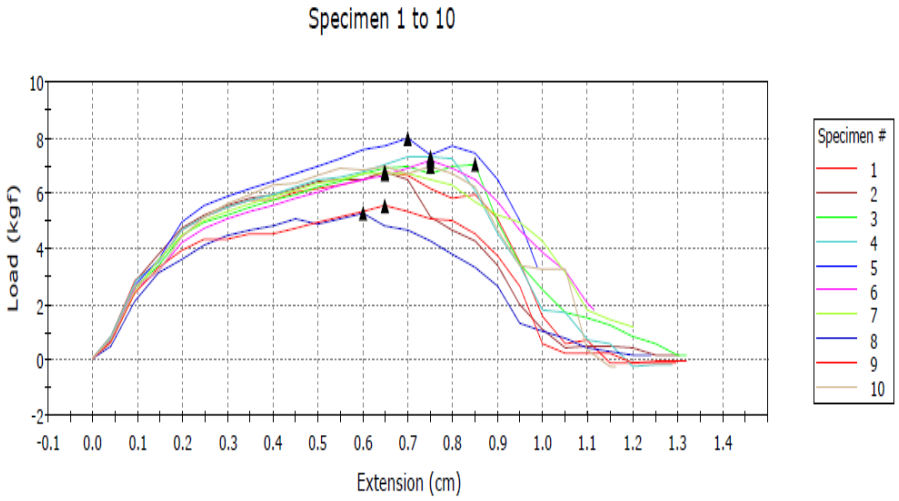

Figure1 Tensile Strength

Warp way
Discussion

It is observed from the table the Tensile Strength in warp way the following sample value are.

	Bamboo 100%		Tencel 100%		Bamboo/Tencel 50%/50%		Bamboo/Tencel 70%/30%		Bamboo/Tencel 30%/70%	
	Maximum Load (kgf)	Extension Load (cm)	Maximum Load (kgf)	Extension Load (cm)	Maximum Load (kgf)	Extension Load (cm)	Maximum Load (kgf)	Extension Load (cm)	Maximum Load (kgf)	Extension Load (cm)
maximum	8.00	0.85	11.84	0.65	11.13	0.65	9.26	0.90	12.48	0.65
minimum	5.26	0.60	6.59	0.55	7.10	0.40	6.64	0.65	8.69	0.45
mean	6.75	0.70	9.85	0.60	9.17	0.56	8.19	0.70	10.42	0.55

The warp way Maximum Load is bamboo/Tencel 30%/70% = 12.48 (kgf) is higher than other sample and lower value is bamboo100%= 8.00(kgf).
The warp way Extension Load is bamboo/Tencel 70%/30% = 0.90 (cm) is higher than other sample and lower value is bamboo 100% = 5.26(cm).

Weft Way
Discussion

It is observed from the table the Tensile Strength in weft way the following sample value are

Cite this article as: M. D. Jothilinkam, T. Ramachandran, G.Ramakrishnan. "TO STUDY THE WOVEN FABRIC OF BAMBOO&TENCEL FOR COMPFORT PROPERTIES." *International Conference on Systems, Science, Control, Communication, Engineering and Technology (2015)*: 73-78. Print.

	Bamboo 100%		Tencel 100%		Bamboo/Tencel 50%/50%		Bamboo/Tencel 70%/30%		Bamboo/Tencel 30%/70%	
	Maximum Load (kgf)	Extension Load (cm)	Maximum Load (kgf)	Extension Load (cm)	Maximum Load (kgf)	Extension Load (cm)	Maximum Load (kgf)	Extension Load (cm)	Maximum Load (kgf)	Extension Load (cm)
maximum	4.43	1.15	7.22	0.70	6.06	0.95	5.77	0.85	7.11	0.70
minimum	3.62	0.80	4.70	0.45	3.60	0.65	3.70	0.60	4.62	0.60
mean	4.11	0.90	6.44	0.62	5.03	0.81	4.85	0.73	5.27	0.66

Table 3.3.2 Weft way tensile strength

The weft way Maximum Load is Tencel 100% = 7.22(kgf) is higher than other sample and lower value is bamboo100%= 4.43(kgf).

The weft way Extension Load is Tencel 100% = 4.70(cm) is higher than other sample and lower value is bamboo /Tencel 50%/50% = 3.60(cm).

3.4 Water Vapor Permeability

The fabrics with hydrophilic components change their properties under different humidity conditions. The purpose of this study was to measure the water vapour permeability and evaporative resistance. The water vapour transmission rate (WVTR) was measured using the ASTM

Table3.4Water Vapor Permeability

Sample	Water Vapour permeability(gm/m²/day)
Bamboo-100%	4243
Tencel-100%	2894
Bamboo/tencel 50%/50%	3440
Bamboo/tencel 70%/30%	4208
Bamboo/tencel 30%/70%	3277

Discussion

It is observed from above table the water vapour permeability in bamboo 100% =4243 (gm/m²/day) is very high other samples. It has lowest value in Tencel 100% = 2894 (gm/m²/day).

4. CONCLUSION

- 100% bamboo fabric showed very good water vapor permeability.
- Fabric wicking was similar in all samples

Cite this article as: M. D. Jothilinkam, T. Ramachandran, G.Ramakrishnan. "TO STUDY THE WOVEN FABRIC OF BAMBOO&TENCEL FOR COMPFORT PROPERTIES." *International Conference on Systems, Science, Control, Communication, Engineering and Technology (2015)*: 73-78. Print.

- Tensile tests (warp way) conducted on all the 5 samples revealed that 100% bamboo fabric yielded the lowest strength and 30:70 bamboo: tencel blended fabric yielded the highest fabric strength.
- Tensile tests conducted in (weft way) for all the 5 samples revealed that 100% bamboo has lowest strength and 100% Tencel had the highest strength.

5. REFERERENCE

1. Textile-based smart wound dressings By: Bhuvanesh gupta Department of Textile Technology, Indian Institute of Technology, New Delhi Indian Journal of Fibre & Textile Research.
2. Bamboo fiber and its application in textiles - An Overview, By: K.Saravanan &C.Prakash, Sona College of technology, Salem, http://articles.fibre2fashion.com
3. Medical textiles by; chet ram meena, nitin ajmera, and pranaya kumarsabat http://articles.fibre2fashion.com
4. Tencel fibres, by:Lenzing Fibers Inc. http://www.lenzing.com
5. Handbook of medical textiles By: V. T. Bartels Woodhead Publishing Limited, 2011
6. Medical and health care textiles By: S. C. hand, J. F. Kennedy, M. Miraftab and S.Rajendran,Woodhead Publishing Limited, 2010
7. Green Story of Lyocell fiber, Ajay Sardana (Head – TRADC), Sanjay Vishwakarma (Head – QA, TRADC) the authors are M.Tech in Textile Engineering from IIT Delhi.
8. Physical, Chemical and mechanical properties of bamboo and its utilization potential for fiber board manufacturing By:Xiaobo Li, B.S. Beijing Forestry University, 1999M.S. Chinese Academy of Forestry, 2002
9. Ajay Sardana & Sanjay Vishwakarma "Green Story of Lyocell fiber" from IIT Delhi, 2009.
10. Dr.Jayalakshmi.I & Dinesh. B "Antimicrobial and MechanicalActivity of Eupatorium Dye on Tencel and Tencel-Viscose Fabrics"www.fibre2fashion.com

Cite this article as: M. D. Jothilinkam, T. Ramachandran, G.Ramakrishnan. "TO STUDY THE WOVEN FABRIC OF BAMBOO&TENCEL FOR COMPFORT PROPERTIES." *International Conference on Systems, Science, Control, Communication, Engineering and Technology (2015)*: 73-78. Print.

International Conference on Systems, Science, Control, Communication, Engineering and Technology 2015 [ICSSCCET 2015]

ISBN	978-81-929866-1-6
Website	icssccet.org
Received	10 - July - 2015
Article ID	ICSSCCET017

VOL	01
eMail	icssccet@asdf.res.in
Accepted	31- July - 2015
eAID	ICSSCCET.2015.017

Big Data - Reduced Task Scheduling

Kokula Krishna Hari K[1], Vignesh R[2], Long CAI[3], Rajkumar Sugumaran[4]
[1]Chief Scientist, Techno Forum Research and Development Center, Hong Kong
[2]Life Member, Association of Scientists, Developers and Faculties, India
[3]University of Hong Kong, HKSAR , Hong Kong
[4]Vice-President (HR), Techno Forum Research and Development Center, Bangkok

Abstract: Inspired by the success of Apache's Hadoop this paper suggests an innovative reduce task scheduler. Hadoop is an open source implementation of Google's MapReduce framework. Programs which are written in this functional style are automatically executed and parallelized on a large cluster of commodity machines. The details how to partition the input data, setting up the program's for execution across a set of machines, handling machine failures and managing the required inter-device communication is taken care by runtime system. In existing versions of Hadoop, the scheduling of map tasks is done with respect to the locality of their inputs in order to diminish network traffic and improve performance. On the other hand, scheduling of reduce tasks is done without considering data locality leading to degradation of performance at requesting nodes. In this paper, we exploit data locality that is inherent with reduce tasks. To accomplish the same, we schedule them on nodes that will result in minimum data- local traffic. Experimental results indicate an 11-80 percent reduction in the number of bytes shuffled in a Hadoop cluster.

Keyword: MapReduce, Hadoop, Reduce Task Scheduling, Data-Locality, Rack-Locality

I. INTRODUCTION

Every day, the Stock Exchange generates every day about one terabyte of new trade data [3]. Facebook generates 5 Billion terabytes of data every day. Any such data that cannot be placed into a database falls under the category of unstructured data. As an entity's data footprint grows, the amount of unstructured data to be handled becomes enormous. This is a major cause for several problems .First, where will all this Big Data, as it is being called today, be stored. Second, how do we access all this data, process and analyse the contents. Third, how do we ensure that this data is safe from disk failures, computer failures and so on. These problems are well-dealt by Hadoop; a reliable, scalable, distributed computing platform developed by Apache [5].It is an open source implementation of Google's MapReduce framework that allows for the distributed processing of huge data sets transversely clusters of computers using simple programming models. It is designed to level up from single datacenter to thousands of machines, each offering local computation and storage. At the application layer the library is designed to detect and handle failures, Instead of relying onhardware to deliver high-availability, so a highly-available service on top of a cluster of computers, can be delivered each of which may be prone to failures Page Layout. Hadoop has an underlying storage system called HDFS-Hadoop Distributed file system. To process the data in HDFS, Hadoop provides a MapReduce engine that runs on top of HDFS. This engine has master-slave architecture. The master node is called the JobTracker and the slaves are called TaskTrackers. MapReduce jobs are automatically parallelized across a large set of TaskTrackers. The JobTracker splits the job into several maps and reduce tasks. Hadoop divides the input to the job into fixed size pieces called input splits. The outputs of the map tasks are stored in the local disk. This intermediate output serves as input to the

Cite this article as:. Kokula Krishna Hari K, Vignesh R, Long CAI, Rajkumar Sugumaran . "Big Data - Reduced Task Scheduling." *International Conference on Systems, Science, Control, Communication, Engineering and Technology (2015)*: 79-84. Print.

reduce tasks. The consolidated output of the reduce task is the output of the MapReduce job and is stored in HDFS.

Recently, the non-profit organization Spamhaus, which publishes spam blacklists, faced one of the most powerful cyber-attacks seen. This led to cyberspace congestion which affected the Internet overall. The providers of Spamhaus as well as certain Tier 1 Internet Exchanges were the victims of the attack. Cloudflare dubbed it as the attack "that almost broke the Internet." These incidents do highlight the need to develop more efficient security measure to combat such attacks but it also indicates how uncontrolled network congestion can handicap the Internet as a whole. Measures must be taken to tackle any source of congestion within a network. With companies like Facebook, Amazon, AOL and The NY Times using the Hadoop framework which in turn is a cluster of computers connected via a LAN or MAN connection, there is a need to handle any areas that could result in network traffic and hence result in significant delay in providing services to the end user.

A typical Hadoop cluster is a set of computers connected via LAN connection. In case of companies like Facebook, Yahoo, Amazon these clusters consist of thousands of nodes. These Hadoop workers are located in different data centers that are present in geographically dispersed locations thereby avoiding the domino effect that is prevalent when all nodes are connected by a single LAN. A typical MapReduce job may use nodes across data centers .Each node has a local disk, it is efficient to move data processing operations to nodes where application data are located. If data are not available locally in a processing node, data have to be migrated via network interconnects to the node that performs the data processing operations. Migrating huge amount of data across data centers and in some cases within data centers may lead to excessive network congestion especially when petabytes of data have to be processed.

In Hadoop, scheduling reduce tasks results in severe congestion problems. The reason being Hadoop task scheduling is based on a 'pull strategy'. The JobTracker does not push map and reduce tasks to TaskTrackers but rather TaskTrackers pull them by making requests. Every TaskTrackers sends a periodic heart beat message requesting a map or reduce tasks. When the JobTracker schedules map tasks, it takes care to ensure that the task runs on a TaskTracker which contains the needed input split. As a result Hadoop MapReduce is said to be data local when scheduling map tasks. On the other hand Hadoop simply schedules any yet-to-run reduce task on any requesting TaskTracker regardless of the TaskTracker's network location [3].This has an adverse effect on network traffic .

This paper proposes scheduling data local reduce tasks. The method ensures that reduce tasks run on a suitable TaskTracker such that there is minimum bytes traveling across the network. Thus, there is a controlled use of the clusters network bandwidth. We have implemented our method on Hadoop 1.0.3.

The rest of this paper is organized as follows. A background on Hadoop MapReduce is given in Section 2. Our proposal and implementation is presented in Section 3, and a performance evaluation in Section 4.Lastly we indicate future works and conclude the paper in Section 5.

II. BACKGROUND :REDUCE TASK SCHEDULER

Hadoop assumes a tree-style network topology similar to the one shown in the figure. Nodes are distributed over different racks contained in one or many data centers. A salient point is that the bandwidth between two nodes is dependent on their relative locations in the network topology.

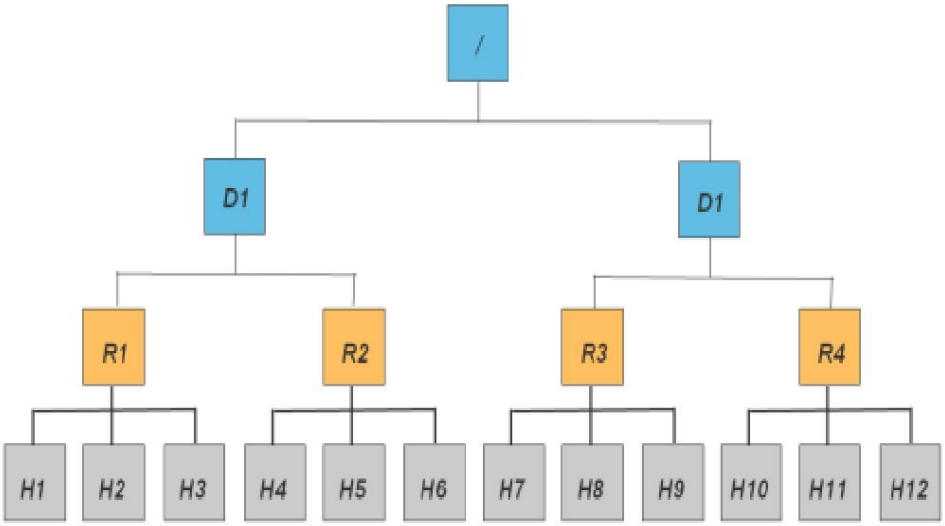

Fig1 : Network Topology in Hadoop (D= data center, R = rack, and H = node)

Cite this article as:. Kokula Krishna Hari K, Vignesh R, Long CAI, Rajkumar Sugumaran . "Big Data - Reduced Task Scheduling." *International Conference on Systems, Science, Control, Communication, Engineering and Technology (2015)*: 79-84. Print.

For example, nodes that are on the same rack will have higher bandwidth between them as opposed to nodes that are off-rack [19]. Previous attempts to make reduce tasks locality aware focused on rack-locality not data-locality .The tasks were scheduled in racks that held the largest intermediate output. However, this does not address the problem when using zero or one rack or the network traffic that is prevalent when scheduling reduce tasks within a single data center. There is need to penetrate deeper into the network hierarchy. In other words, optimization so far to make reduce tasks locality aware, addresses scenarios with many nodes connected via racks. The approach proposed in this paper further optimizes scheduling reduce tasks in small, medium and large clusters. Further, it works in the presence or absence of racks. It addresses the problem when there are two nodes and also when there are innumerable nodes.

III. THE DATA-LOCAL REDUCE TASK SCHEDULER

A. Motivation

Consider the scenario as shown in Fig.1. Node 1 holds 5 MB IO: R1 (intermediate output for reducer 1) and 10 MB IO: R2 (intermediate output for reducer 2). While Node 2 holds 2 MB IO: R1 and 26 MB IO: R2. Node 3 holds 15 MB IO: R1 and 1MB IO: R2 .Once the map tasks are scheduled, Node 2 requests the JobTracker for permission to run reducer 1. As a result 20 MB of intermediate output must be transferred over the network. On the other hand node 1 requests to run reducer 2.As a result 27 MB must be moved to node 1. Hence, a total of 47 MB utilizes the cluster bandwidth. If node 1 or node 2 is situated in different racks compared to other nodes more congestion in the network will be prevalent. If this scenario were modified, such that reducer 1 ran on node 3 and reducer 2 ran on node 2, then 7MB and 11MB of data would be shuffled. Clearly, this result in an improvement of 50 % reduction in the number of bytes shuffled. Hadoop's present reduce task scheduler is incapable of making such decisions.

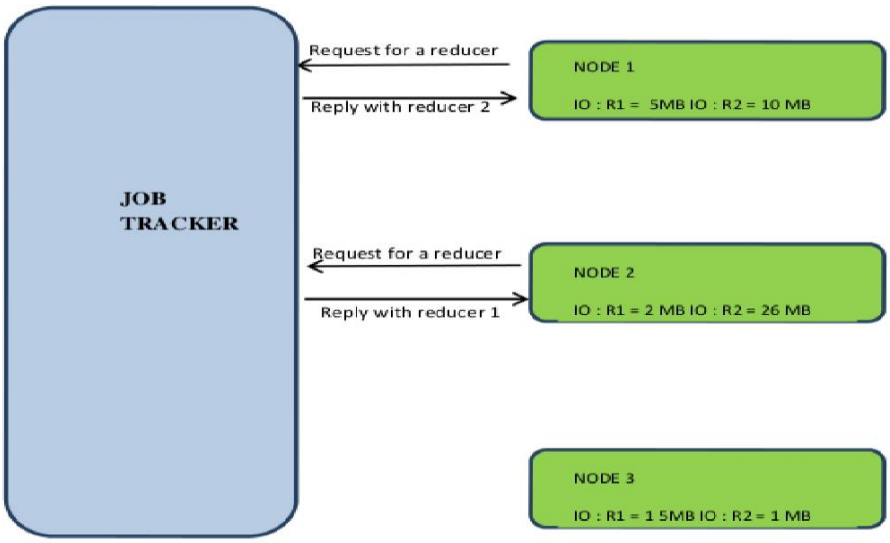

Fig 2 : Scheduling Reduce Tasks in native Hadoop

B. Implementation

We have implemented our method on Hadoop 1.0.3 as follows:

- Formulation of a data structure that keeps track of the size of intermediate output generated by a mapper for every reducer - There are two in-built features of Hadoop that are exploited to gather the input required by the reduce task scheduler: *Index File and Heartbeat protocol.* The size of the intermediate output generated by a map task is available in the current versions of Hadoop. However, the manner in which the intermediate output is intended to be divided among the reducers is necessary. This information is available in the index file and is stored in the local file system of every TaskTracker. Heartbeat is a mechanism for a TaskTracker to announce periodic availability to the JobTracker. Besides the heartbeat, the TaskTrackers send information regarding its states to the JobTracker. By making modifications in appropriate classes, the JobTracker

Cite this article as:. Kokula Krishna Hari K, Vignesh R, Long CAI, Rajkumar Sugumaran . "Big Data - Reduced Task Scheduling." *International Conference on Systems, Science, Control, Communication, Engineering and Technology (2015)*: 79-84. Print.

collects the index file information from the local file system of the TaskTracker via the information sent along with the heartbeat message.

- Controlling the scheduling of reduce tasks - Using the generated data structure, the TaskTracker that holds the largest intermediate output for a particular reduce task is determined. Upon which the reduce task scheduler takes the requesting TaskTracker as an input along with a set of unscheduled reduce tasks. For each reduce task that must be scheduled, the scheduler checks if the requesting TaskTracker is the one that contains the largest intermediate output. If so, the reduce task is scheduled on the requesting TaskTracker. Otherwise, another requesting TaskTracker is considered.

Algorithm 1 Reduce Task Scheduler

Input: RT: set of unscheduled reduce tasks
TT: the task tracker requesting a reduce task
STT: set of task trackers
Output: A reduce task R ∈ RT that can be scheduled at TT or -1

```
1.  for every reducer R ∈ RT do
2.   large = 0
3.   for every T ∈ STT do
4.      size = the size of the intermediate output on T
5.       if size > large then
6.       large = size
7.       LTT = T
8.       end if
9.   end for
10. end for
11. for the first reducer R ∈ RT do
12.  LTT =  the task tracker that holds the largest intermediate output
13.   if TT = LTT then
14.   return R
15.    else
16.   return -1(Request with another task tracker)
17. end for
```

C. Working Example

The JobTracker maintains a record that ensures that a reducer runs only on TaskTrackers that hold the largest intermediate output. The scenario mentioned previously is modified as shown in fig.3. In this case, to minimize data local traffic by a significant amount, the JobTracker analyzes and concludes that reducer 1 and reducer 2 must run on node 3 and node 2 respectively. The JobTracker initially is required to run reducer 1. The request from TaskTracker node 1 is rejected. Similarly, the request from TaskTracker node 2 is also overruled. Upon receiving a request from node 3, the JobTracker schedules the execution of reducer 1. Likewise, in the case of reducer 2, the requests of TaskTracker node 1 and node 3 are vetoed. The JobTracker schedules the execution of reducer 2 on node 2 upon receiving a request from the latter.

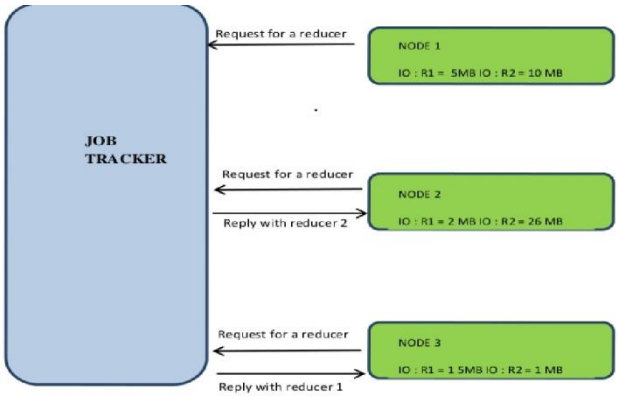

Cite this article as:. Kokula Krishna Hari K, Vignesh R, Long CAI, Rajkumar Sugumaran . "Big Data - Reduced Task Scheduling." *International Conference on Systems, Science, Control, Communication, Engineering and Technology (2015)*: 79-84. Print.

fig 3: Achieving Data-Local Reduce Tasks

IV. PERFORMANCE EVALUATION

All evaluations are performed on a four node cluster. Each node is a Intel® Core™2 Duo E8500 processor-based desktop. To run Hadoop, Ubuntu 12.10 and Sun/Oracle JDK 1.6, Update 20 has been installed on all computers.These nodes are connected by a 100Mbps Ethernet through a single switch. Three benchmarks are used for comparison with Native Hadoop .They are wordcount, pi estimator and muti-file wordcount. Besides, [10] reported that wordcount is one of the major benchmarks utilized for evaluating Hadoop at Yahoo. The wordcount is a CPU intensive job .It generates adequate amount of intermediate output .Multi-file count is another variation of word count that increases the workload and processes several files. Pi Estimator is suitable for testing the Hadoop scheduler when it deals with 1 KB data or lesser.It is a scenario with one reducer. This benchmark indicates that the modified Hadoop scheduler is capable of handling traffic prevalent within a single data center or a small cluster.

The native Hadoop scheduler is capable of making any reduce task scheduling decisions. As a result, large amount of network bandwidth and MapReduce execution time were lost trying to transfer huge amounts of data within and across networks. The difference in the number of bytes shuffled varies with the size of the intermediate output generated, the number of mappers and the number of reducers. Each benchmark is run three times as shown in Fig.4.

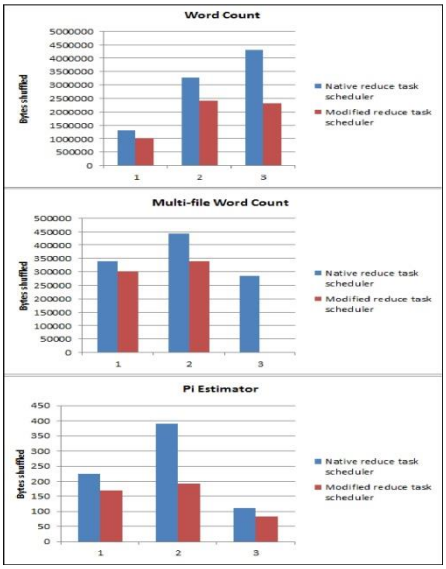

Fig 4: Variations in the number of bytes shuffled for three different benchmarks

In each case, the number of mappers and reducers are changed. The evaluation is performed on input size varying between120 bytes to 500 MB. The evaluation is performed when the number of mappers varies between 1 and 6. The number of reducers varies between 1 and 8. Further, as shown in Fig.5, the reduction in bytes shuffled grows with an increase in intermediate output and as a result with increase in the number of bytes input to the MapReduce program .The fluctuation is due to varying number of mappers and reducers. The modified Hadoop scheduler minimizes data-local traffic by 11-80 %.

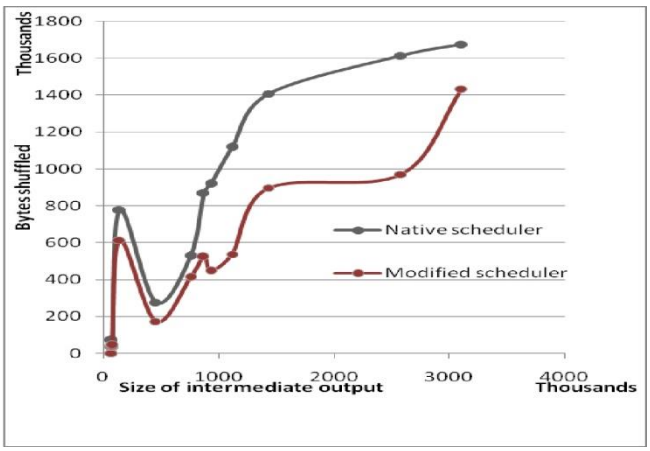

Cite this article as:. Kokula Krishna Hari K, Vignesh R, Long CAI, Rajkumar Sugumaran . "Big Data - Reduced Task Scheduling." *International Conference on Systems, Science, Control, Communication, Engineering and Technology (2015)*: 79-84. Print.

V. CONCLUSION AND FUTURE WORKS

Through this paper, we have proposed a reduce task scheduler that can be incorporated in future versions of Hadoop. Unlike previous attempts, this reduce task scheduler is not limited to achieving rack locality alone. Further, it ensures data local execution of reduce tasks in The most important business benefits of including the proposed reduce task scheduler in jobs. Furthermore Hadoop is fault-tolerant and network Hadoop is lesser failure rates. This results in faster completion of intelligent scenarios with less than four nodes besides cases with nodes geographically distributed across data centers. Although, in circumstances with few bytes of input data the reduce task scheduler may appear to increase the execution time of a MapReduce job. However, this trend does not continue on increasing the number of bytes Hadoop operates on. Test results indicate a reduction of 11-80% in data local traffic.

For companies using Hadoop, this could lead to saving several millions of dollars. As it eliminates the need to monitor traffic, and invest in more servers to achieve better load balancing.

After demonstrating, the prospects of the modified reduce task scheduler, we have set forth two future directions. Firstly, a proposal to introduce a rejection factor that imposes control to ensure uniform reduce task workload among all TaskTracker nodes. As a result, if a TaskTracker is rejected more than a predetermined number of times, the scheduler overrules data locality and ensures uniform workload distribution. Secondly, there may be situations where achieving rack locality is more essential than achieving data locality. Introduction of a locality factor that keeps track of the distance through which the information has to travel, the inherent congestion in the network lines chosen and if transporting more bytes can result in better MapReduce execution time. Based on the computed locality factor, the reduce task scheduler can make more intelligent decisions.

REFERENCES

[1] The New York Times archive article http://open.blogs.nytimes.com/2007/11/01/self-service-prorated super-computing-fun.
[2] Making of the New York Time archive called TimesMachine http://open.blogs.nytimes.com/2008/05/21/the- new-york-times-archives-amazon-web-services-timesmachine/
[3] Hadoop – The Definitive Guide by Tom White.
[4] Pro Hadoop by Jason Venner
[5] Official Hadoop Website - http://hadoop.apache.org/
[6] Distributed and Cloud Computing by K. Hwang, G. Fox and J. Dongarra
[7] Getting Started with Hadoop http://wiki.apache.org/hadoop/GettingStartedWithHadoop
[8] Getting Started with Maven - http://maven.apache.org/guides/getting-started/
[9] Hadoop operations by Eric Sammer
[10] S. Seo, I. Jang, K. Woo, I. Kim, J. Kim, S. Maeng, "HPMR: Prefetching and Pre-Shuffling in Shared MapReduce Computation Environment," *CLUSTER,* 2009.
[11] A Szalay, A. Bunn, J. Gray, I. Foster and I. Raicu, The Importance of DataLocality in Distributed Computing Applications," *NSF Workflow Workshop,* 2006.
[12] M. Zaharia, D. Borthakur, J. S. Sarma, K Elmeleegy, S Shenker, and I. Stoica,"Delay scheduling: a simple technique for achieving locality and fairness in cluster scheduling," *EuroSys 2012.*
[13] M. Zaharia, A. Konwinski, A. Joseph, R. Katz, I. Stoica, "Improving Mapreduce Performance in Heterogeneous Environments," *OSDI,* 2008.
[14] Amazon Elastic MapReduce, http://aws.amazon.com/elasticmapreduce/.
[15] P. C. Chen, Y. L. Su, J. B. Chang, and C. K. Shieh, "Variable- Sized Map and Locality-Aware Reduce on Public-Resource Grids," *GPC,* 2010.
[16] S. Chen and S. W. Schlosser, "MapReduce Meets Wider Varieties of Applications,"*IRP-TR-08-05, Intel Research,* 2008.
[17] J. Dean and S. Ghemawat, "Mapreduce: simplified data processing on large clusters," *OSDI,* 2004.
[18] http://download.oracle.com/javase/6/docs/.

Cite this article as:. Kokula Krishna Hari K, Vignesh R, Long CAI, Rajkumar Sugumaran . "Big Data - Reduced Task Scheduling." *International Conference on Systems, Science, Control, Communication, Engineering and Technology (2015)*: 79-84. Print.

International Conference on Systems, Science, Control, Communication, Engineering and Technology 2015 [ICSSCCET 2015]

ISBN	978-81-929866-1-6
Website	icssccet.org
Received	10 - July - 2015
Article ID	ICSSCCET018

VOL	01
eMail	icssccet@asdf.res.in
Accepted	31- July - 2015
eAID	ICSSCCET.2015.018

Innovation in Textiles: Integration of Nanoencapsulation of PCMs in Cotton fabric

Karthikeyan M[1], K.Visagavel[2], Ramachandran T[3], Ilangkumuran M[3], Kirubakaran M[4]
[1, 2] Department of Industrial Safety Engineering, Knowledge Institute of Technology, Salem
[3] Principal, Karpagam Institute of Technology, Coimbatore
[3, 4] Department of Mechatronics Engineerig, K.S.R College of Technology, Tiruchengode

Abstract: *Indian foundry industry stands the world's second largest producer of castings. At the same time, workers who work in uncomfortably hot environment without appropriate clothing for extreme conditions are most likely exposed to higher risks. Their prolonged exposure to high temperature causes thermal discomfort. It is largely concerned with the selection of improper clothing suitable for hot environment. This research is aimed to assess the effects of hot environment near the furnace area in foundry industry and to developing a thermal protection fabric using nanoencapsulated Phase Change Materials (PCMs) or nanocapsules. Polyethylene glycol (PEG) nanocapsules containing PEG as core material and urea-formaldehyde as shell material were successfully developed using in-situ polymerization method. Different characterization techniques were used to analyse the properties of the developed PEG nanocapsules. Scanning electron microscope (SEM) and Transmission Electron Microscope (TEM) study results indicated that the nanocapsules form a regular and spherical shape without agglomeration. The average diameter of the nanocapsules was found to be 161 nm. The size of the PEG nanocapsules was within the range of 100-300 nm. Energy Dispersive Spectroscopy (EDS) test results showed that the nanocapsules contains 38 wt.% carbon, 27 wt.%, oxygen and 35 wt.% nitrogen. Fourier transform infrared (FT-IR) spectroscopy confirmed that the PEG was successfully encapsulated within the urea-formaldehyde shell. Differential scanning calorimetry (DSC) results found that the latent heat energy storage capacity of the PEG nanocapsules was 81.1 J/g. The encapsulation ratio of the nanocapsules was 59.5%. The PEG nanocapsules showed good thermal stability, which makes the coated fabric appropriate for textile application.*

Introduction

According to the relationship between environment temperature and human thermal balance, living environments temperature above 35°C and working environments above 32°C can be considered as hot environments, and environments with relative humidity above 70% can be considered as humid (Zhao et al 2009). Textiles containing PCMs have different thermal properties from conventional textiles. Micro-or nano-capsules can be applied to a wide variety of textile substrates to improve thermo-regulation and insulation properties. Coating, lamination, finishing, melt spinning, bi-component synthetic fibre extrusion, injection moulding, foam techniques are some of the convenient processes for incorporation of PCMs into textile substrate.

Nanoencapsulation is defined as the process of enclosing nano-sized particles within solid or liquid particles. The products obtained by the process are called nanocapsules or nanoparticles. The term nanocapsule is used if the size of the particles is below 1 µm (Sari et al 2009; Ries et al 2006). Recently, nanocapsules have received considerable attention for TES systems because of their high surface area/volume ratio compared to microcapsules which results in a stronger driving force to increase thermodynamic processes. In the literature studied, some research has been carried out into the preparation of nanocapsules for TES. Zhang et al (2004) fabricated both

Cite this article as: Karthikeyan M, K.Visagavel, Ramachandran T, Ilangkumuran M, Kirubakaran M. "Innovation in Textiles: Integration of Nanoencapsulation of PCMs in Cotton fabric." *International Conference on Systems, Science, Control, Communication, Engineering and Technology (2015)*: 85-91. Print.

microcapsules and nanocapsules containing melamine-formaldehyde and n-octadecane as the shell material and core material using in-situ polymerization. The influence of stirring rate, emulsifier content and amount of cyclohexane on the diameters, morphology, phase change and thermal stability of the capsules were studied. The results indicated that the diameter of the microcapsule decreased to 0.8 μm, forming nanocapsules, with increased stirring rate, emulsifier content and cyclohexane content. According to the DSC results, the onset temperatures and phase change enthalpy remain unchanged with increased stirring rate and emulsifier content, but had little effect on cyclohexane. Wei et al (2007) synthesized micro-and nano-encapsulated PCMs with melamine-formaldehyde as the shell and n-octadecane as the core. The results showed that the core was well encapsulated with added sodium dodecyl sulphate as an emulsifier. The results also indicated that the average diameter of the microcapsules and nanocapsules was 65 μm and 850 nm, respectively. The encapsulation efficiency of the microcapsules and nanocapsules was 87% and 45%, respectively. Fan et al (2005) synthesized nanocapsule containing melamine-formaldehyde as the shell material and, n-octadecane (91.2%) and cyclohexane (8.8%) as the core material. The thermal effects of the nanocapsules after treatment at 120 °C, 140 °C, 160 °C and 180 °C for 30 min were studied. The results showed that pH value has some effect on the stability of emulsion and morphology of nanocapsules. The results also indicated that the size of the nanocapsules ranged between 0.4 and 1.0 μm. It was concluded that the heat treatment increased the thermal stability of nanocapsules initially, then decreased when the temperature exceeded 160 °C.
Li et al (2011) successfully prepared nanocapsules with urea-formaldehyde as the shell material and hexadecane as the core material using the two-step miniemulsion polymerization method. It was observed that the nanocapsules were spherical, and the particle size was 270 nm. It was further reported that the surfactant influenced the particle diameter, coefficient of variation, thickness of the shell and radius of the core. Therefore, this paper aimed to prepare nanocapsules and coated onto the cotton fabric, and to find the thermoprotection properties of cotton fabric.

3. Methodology

The research methodology adopted in this work comprises initially assessment of hot environment, synthesis of nanocapsules containing different core material such as PEG and paraffin wax using in-situ polymerization method.

4. Development of the PEG nanocapsules

PEG nanocapsules were prepared using in-situ polymerization method. This method involves two processes: preparation of emulsifier and pre-polymer. In preparation of emulsified PEG, 16 g of PEG, 2.9 g L^{-1} of SDS, and 100 mL water were emulsified mechanically at 80°C with a stirring rate of 2500 rpm for 45 min. Subsequently, 1.8 g L^{-1} of PVA was added to the mixture to stabilize the emulsion. In preparation of pre-polymer, 24 g of urea and 14.8% formaldehyde were added to water. The mixture was stirred and adjusted to pH 8.5- 9 with an aqueous solution of 10% sodium hydroxide. Then, the mixture was continuously stirred at 70-75° for 1 h to prepare pre-polymer solution. Finally, droplets of the pre-polymer solution were added to the emulsion where the emulsion mixture was stirred at a rate of 1000 rpm at 80°C. The pH was reduced to the range of 5 -5.5 by adding dilute hydrochloric acid into the mixture. Then, the mixture was agitated continuously at a stirring rate of 600 rpm for 1 h, and the temperature was slowly reduced to 35°C. The resultant nanocapsules were filtered, washed and dried in an oven at 70°C for 8 h to remove water.

5.1 Coating the nanocapsules onto the cotton fabric

For developing thermoprotected cotton fabric, the prepared PEG and paraffin wax nanocapsules using polyurethane binding agent were applied on-to cotton fabric using pad-dry-cure method. The details of coating composition for different ratios of nanocapsules to polyurethane binding agent are given in Table 1. The four different ratios related to PEG and polyurethane binding agent was prepared for this study. Correspondingly, two different ratios related to paraffin wax and polyurethane binding agent was selected.

Table 1 Details of the prepared coating compositions

S.No.	Sample code	Nanocapsules to binder ratio (in mass ratio)
1.	Untreated fabric	-
Polyethylene glycol		
1.	$PEGS_{131}$	3:1
2.	$PEGS_{132}$	3:2
3.	$PEGS_{133}$	3:3
4.	$PEGS_{141}$	4:1
Paraffin Wax		
1.	PWS_{115}	1:5
2.	PWS_{225}	2:5

Cite this article as: Karthikeyan M, K.Visagavel, Ramachandran T, Ilangkumuran M, Kirubakaran M. "Innovation in Textiles: Integration of Nanoencapsulation of PCMs in Cotton fabric." *International Conference on Systems, Science, Control, Communication, Engineering and Technology (2015)*: 85-91. Print.

5.2 Development of Thermoprotected cotton fabric containing PEG nanocapsules

Thermoprotected cotton fabric is prepared by embedding the prepared PEG nanocapsules on-to the cotton fabric based on the four compositions is given in Table 1. The surface morphologies of the PEG nanocapsules coated fabric were investigated to understand the performance of the nanocapsules and binding agent affinity towards the cotton fabric. The physical testing such as tensile strength of the treated fabrics was carried out to evaluate the related changes before and after coating. The durability of the PEG nanocapsules related to binding agent adhered to the cotton fabric was identified with respect to abrasion resistance. According to heat and water absorption management by the clothing during furnace operations in foundry division, water absorbency and latent heat absorption of the treated fabric are crucial, and so they are evaluated in this study.

5.2.1 Morphology of the PEG Nanocapsule Treated Fabrics

SEM analysis was performed to study the morphological changes after treatment with PEG nanocapsules. Figure 9 shows the morphology of the untreated cotton fabrics. Figure 1 (a) illustrates that there are some protruding fibres can be observed on the surface of the untreated cotton fabric. Figure 1 (b) shows the grooves, and fibrils can be observed on the surface of the untreated cotton fabric.

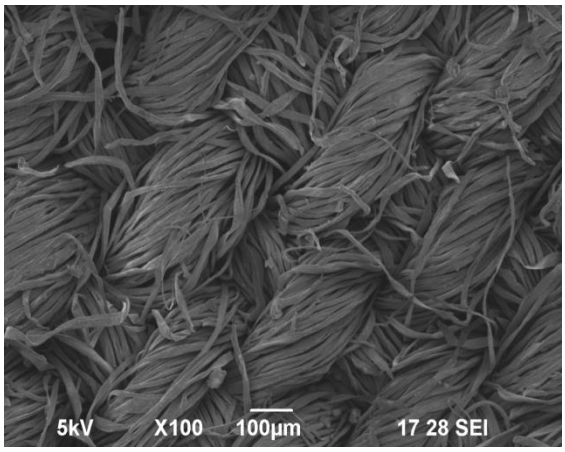

(a)

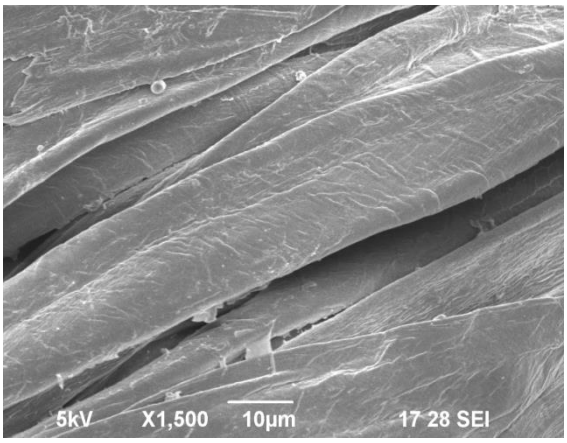

(b)

Figure 1 SEM Images of untreated fabric at different magnifications: (a) x100; (b) x1500 In Figure 2 (a), SEM image shows nanocapsules distributed over different locations on cotton fabric. The coated nanocapsules have a smooth and regular surface on the coated surface of the fabric, as observed in Figure 2 (b). It is also illustrated that the PEG nanocapsules are successfully coated on-to the cotton fabric without breaking or any deformation. Therefore, an even distribution of the PEG nanocapsules on the surface of the cotton fabric was achieved.

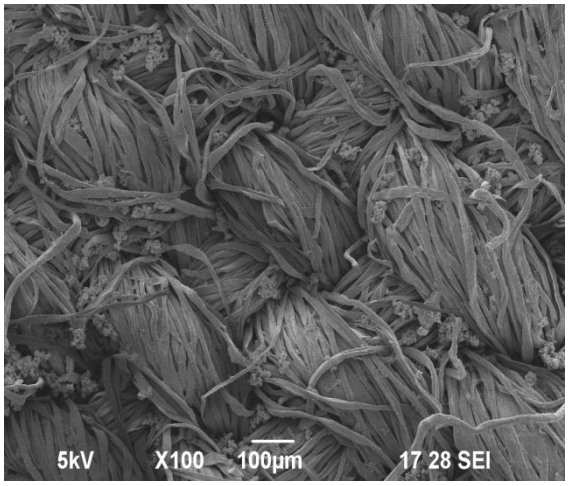

(a)

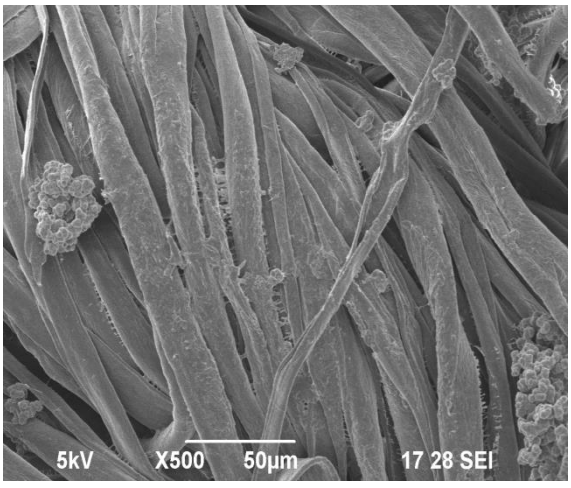

(b)

Figure 2 SEM images of PEG nanoc eated fabric at different magnifications (a) x100; (b) x500

5.2.2 Testing of Tensile Strength of PEG Nanocapsule Treated Fabrics

Cite this article as: Karthikeyan M, K.Visagavel, Ramachandran T, Ilangkumuran M, Kirubakaran M. "Innovation in Textiles: Integration of Nanoencapsulation of PCMs in Cotton fabric." *International Conference on Systems, Science, Control, Communication, Engineering and Technology (2015)*: 85-91. Print.

The tensile strength measurements of the PEG nanocapsules treated fabric and untreated fabric are given in Table 3. The fabrics were tested in both warp and weft directions. The maximum load and elongation of the fabric at break were observed and recorded, as also given in Table 3.

Table *2* Tensile strength of untreated and PEG nanocapsule treated fabrics

S.No.	Sample Code	Tensile strength (N)		Elongation at maximum load (mm)
		Warp	Weft	
1.	**Untreated fabric**	283.46±0.49	111.6±0.36	22.36±0.05
2.	**$PEGS_{131}$**	236.8±0.1	124.2±0.2	22.46±0.17
3.	**$PEGS_{132}$**	253.7±0.15	132.23±0.15	22.7±0.26
4.	**$PEGS_{133}$**	258.26±0.68	128.56±1.04	22.5±0.34
5.	**$PEGS_{141}$**	268.23±0.23	114.33±0.35	22.06±0.49

From Table 2, it is clear that the tensile strength of the PEG nanocapsules treated fabrics decreased compared to that of the untreated fabric. With the exception of treated fabric $PEGS_{141}$, the tensile strength of the treated fabrics ($PEGS_{131}$ to $PEGS_{133}$) increased with increasing binder agent. The treated fabric $PEGS_{141}$ had higher tensile strength on the warp side of the fabric compared to other treated fabrics due to the lower amount of binder agent in the chemical finish. In general, the addition of the chemical finishes to the cotton fabric results in deterioration of the tensile strength of the fabric. Similar to that, all of the treated fabrics were found to have a lower tensile strength in the warp direction. On the contrary, the tensile strength of the treated fabric on the weft side was higher compared to that of the untreated fabric. This result may be due to the binder accumulation on the surface of the weft side of the treated fabric. In addition, the tensile strength of treated fabric $PEGS_{141}$ in the weft direction was lower than that of the other treated fabrics. This finding may be due to the tendency of more chemical finish to accumulate on the weft side of the fabric. It was observed that the tensile strength of the treated fabrics ($PEGS_{131}$, $PEGS_{132}$ and $PEGS_{131}$) increased due to the increased content of the binder agent in both the warp and weft directions. The elongation at break did not show any considerable differences after treatment.

5.2.3 Testing of Water Absorbency of PEG Nanocapsule Treated Fabrics

The water absorbency measurements of the treated and untreated fabrics are shown in Figure 3. From the figure, it is evident that the untreated fabric took more time to absorb water because it had more protruding fibres on the surface of the fabric. The treated fabric $PEGS_{131}$ took the least amount of time for water absorption compared to all other treated fabrics due to coating materials and reduced number of protruding fibres during the drying and curing processes.

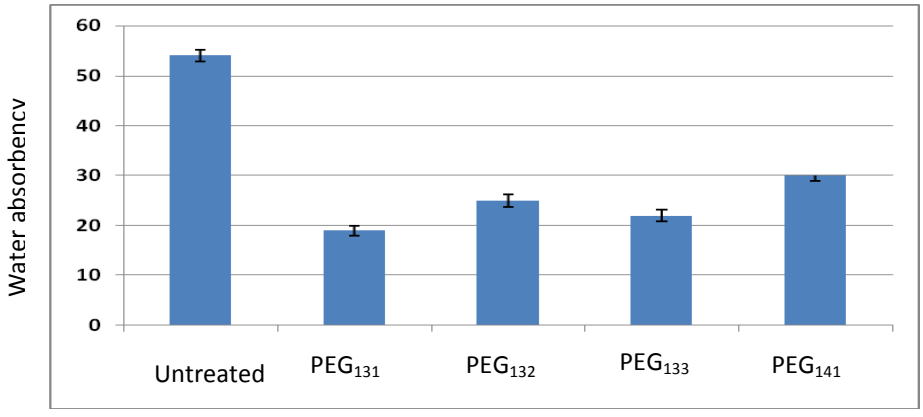

Figure 3 Water absorbency of untreated and PEG nanocapsule treated fabrics

The time taken for water absorption for treated fabric $PEGS_{132}$ was longer compared to that of the treated fabric $PEGS_{131}$. This result is due to higher amount of coating material added to the surface of the fabric, which reduces the number of pores on the surface of the fabric. In the case of treated fabric $PEGS_{133}$, larger amount of the coating materials on the surface of the fabric resulted in shorter time taken for water absorption is shorter compared to treated fabric $PEGS_{132}$ but longer than $PEGS_{131}$. This is due to the polar OH groups present in the cellulosic cotton that make the untreated fabric more hydrophilic than the fabrics treated with hydrophobic nanocapsules. For treated fabric $PEGS_{141}$, the fabric took longer time to absorb water than all other treated fabrics because of an insufficient amount of binder agent relative to the amount of nanocapsules. Hence, it is clearly indicates that the water absorbency rate is based on the deposition of amount of coating materials and treatment method.

Cite this article as: Karthikeyan M, K.Visagavel, Ramachandran T, Ilangkumuran M, Kirubakaran M. "Innovation in Textiles: Integration of Nanoencapsulation of PCMs in Cotton fabric." *International Conference on Systems, Science, Control, Communication, Engineering and Technology (2015)*: 85-91. Print.

5.2.4 Testing of Abrasion Resistance of PEG Nanocapsule Treated Fabrics

The abrasion resistance measurements of the tested samples are shown in Figure 4. The test was carried out until the fabric threads on the abraded surface broke down.

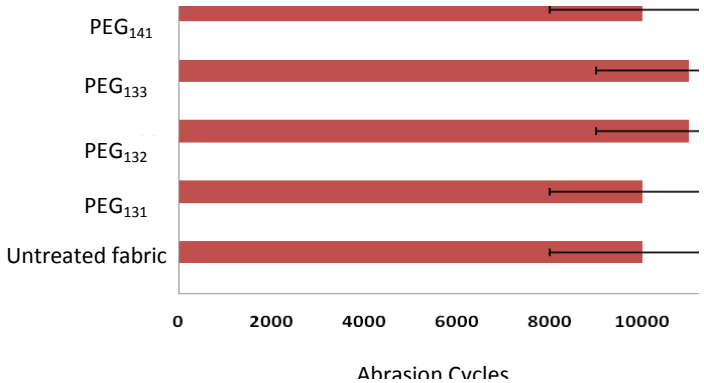

Figure 4 Abrasion resistance of untreated and PEG nanocapsule treated fabric

From the figure, it was found that the treated fabrics $PEGS_{131}$, $PEGS_{141}$ and the untreated fabric were abraded after 10,000 cycles, whereas the treated fabrics $PEGS_{132}$ and $PEGS_{133}$ were abraded after 11,000 cycles. The results of the reduced abrasion resistance of the treated fabrics may be due to the poor adhesion of the binding agent that added PEG nanocapsules on the surface of coated fabrics. Over-all, the treated fabrics $PEGS_{132}$ and $PEGS_{133}$ showed better durability, which was the result of the higher amount of binding agent added in the coating composition and increased the inter-molecular interactions between the PEG nanocapsules and textile surface.

5.2.5 Testing of Thermal Properties of the PEG Nanocapsule Treated Fabrics using DSC

The DSC curves of the PEG nanocapsule treated cotton fabrics are shown in Figure 5. Thermal properties of the treated fabrics, including melting temperature (Tm) and latent heat energy storage (ΔHm) are also illustrated in the figure. The figure also shows that the treated fabrics were capable of absorbing 1.98, 2.13, 3.19 and 2.03 J/g latent heat energy for the nanocapsules/binder agent ratio of 3:1, 3:2 3:3 and 4:1, respectively. Further, it is found that the melting temperature of the treated fabric $PEG_{132}$is higher than that of the other treated samples. This result shows that higher amount of PEG nanocapsules and binding agent may be present, according to the weight per unit area of the treated fabric PEG_{132} compared to the other treated fabrics.

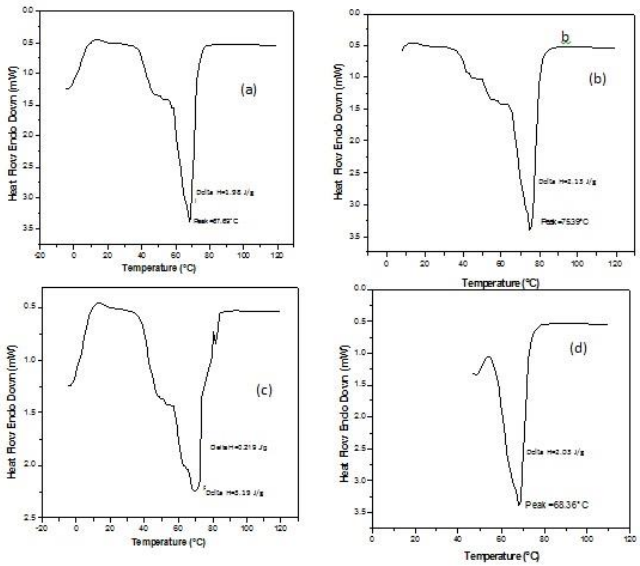

Figure 5 DSC analysis of PEG nanocapsule treated fabrics: (a) $PEGS_{131}$; (b) $PEGS_{132}$; (c) $PEGS_{133}$; (d) $PEGS_{141}$

5.2.6 Testing of Thermal Stability of the PEG Nanocapsule Treated Fabrics using TG Analyzer

Cite this article as: Karthikeyan M, K.Visagavel, Ramachandran T, Ilangkumuran M, Kirubakaran M. "Innovation in Textiles: Integration of Nanoencapsulation of PCMs in Cotton fabric." *International Conference on Systems, Science, Control, Communication, Engineering and Technology (2015)*: 85-91. Print.

A thermogravimetry analysis experiments was used to assess the thermal stability of the treated and untreated fabric samples. Figure 6 shows the TGA curves observed and demonstrate that the weight loss occurs between 20 to 900 °C. The thermal degradation interval data obtained from the TGA curves are given in Table 6. The table shows that all the PEG nanocapsule treated fabrics show two-step weight loss thermal degradation, but there is only single-step weight loss degradation for the untreated fabric. From Figure 6, it is observed that changes in the weight loss occurring at temperatures below 250 °C were due to the removal of physically adsorbed water in all cases. The untreated cotton fabric containing cellulose was found to lose 70% of its weight between the temperatures of 300 and 400 °C. At this stage, the rapid weight loss is due to the dehydration of cellulose. At temperatures above 476 °C, char formation occurs and produces CO_2, carbonyl and carboxyl products.

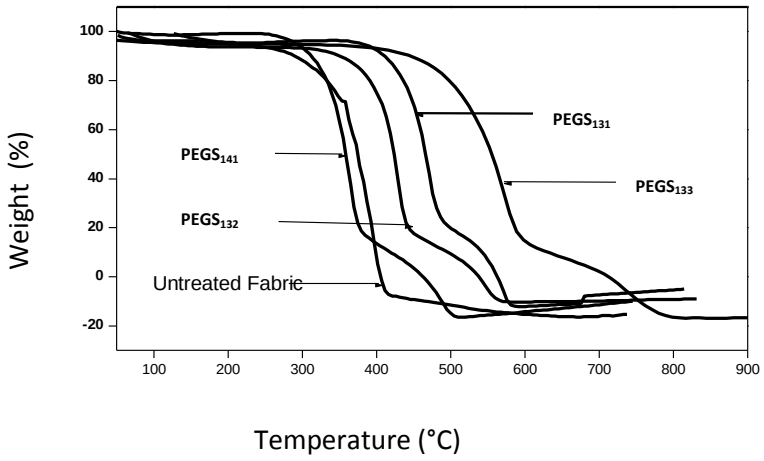

Figure 6 TGA of untreated fabric and PEG nanocapsule treated fabrics: $PEGS_{131}$; $PEGS_{132}$; $PEGS_{133}$; $PEGS_{141}$

The weight loss of the treated fabrics $PEGS_{132}$ and $PEGS_{141}$ between 300 and 400 °C was higher than that of the untreated fabric. The treated fabrics containing PEG nanocapsules/ binding agent ratio of 3:1 and 3:3 had a higher decomposition temperature in the first stage than the other treated fabrics. In the second stage, the decomposition temperature of treated fabric $PEGS_{133}$ (i.e. nanocapsules/binding agent ratio of 3:3) was higher than that of the other treated fabrics due to the cross-linking of the binding agent with cellulose in the cotton fabric. With the exception of treated fabric $PEGS_{141}$, the amount of final residue was lower in the treated samples than that of the untreated fabric. As a result, the treated fabric $PEGS_{133}$ containing PEG nanocapsules/binding agent with ratio of 3:3 reveals that the fabric has good thermal stability. Further, it is also confirmed by the DSC results, that the latent heat energy storage of the treated fabric $PEGS_{133}$ is 3.19 J/g, which is higher than that of the other treated fabrics.

6. Conclusion

The developed PEG and paraffin wax nanocapsules were successfully embedded onto cotton fabric using pad-dry-cure method. The morphology of the coated fabric was analysed using SEM. The results of the SEM illustrated that both PEG nanocapsules were successfully coated onto the cotton fabric without breaking or any deformation. The tensile strength test result showed that the treated fabrics with PEG nanocapsules exhibited decreased strength compared to the untreated fabric. The water absorbency test results demonstrated that the PEGS131 shows quick water absorbency rate than the other PEG nanocapsule treated fabrics. The result indicates that the least time taken due to the polar OH groups present in the cellulosic cotton makes the pure cotton fabric more hydrophilic than the fabrics treated with hydrophobic nanocapsules. The results also indicated that the water absorbency rate is based on the amount of coating materials deposited on the surface of the treated fabrics. According to DSC test results, the treated fabrics shows the latent heat energy storage in the order of PEGS133>PEGS132>PEGS141> PEGS131. The result is clearly indicates that the PEG nanocapsules with ratio 3:3 related to nanocapsules/binding agent shows superior latent heat energy storage than the other PEG nanocapsule treated fabrics. The result also indicates that the PEG nanocapsule plays a crucial role in the development of thermoprotected cotton fabric. This is due to the higher encapsulation ratio of PEG nanocapsules (59.5%). While considering the thermal stability of the treated fabrics analysed using TGA, the results indicated that the treated fabric PEGS133 exhibited good thermal stability than the other PEG nanocapsule treated fabrics. The results found that it is similar to the DSC results. This reason is due to the influence of larger amount of loaded nanocapsule binding with cellulose onto the cotton fabric using binding agent. Finally, it can be concluded that all the treated fabrics with PEG nanocapsules exhibited enhanced active thermal protection compared to passive thermal protection shown by cotton fabric. However, the treated fabric PEGS133 showed outstanding properties with regard to the thermal protection.

Cite this article as: Karthikeyan M, K.Visagavel, Ramachandran T, Ilangkumuran M, Kirubakaran M. "Innovation in Textiles: Integration of Nanoencapsulation of PCMs in Cotton fabric." *International Conference on Systems, Science, Control, Communication, Engineering and Technology (2015)*: 85-91. Print.

References

1. Zhao, Zhu, N & Lu, SL 2009, 'Productivity model in hot and humid environment based on heat tolerance time analysis', Building and Environments, vol. 44, pp. 2202-2207.
2. Sari, A, Alkan, C, Karaipekli, A & Uzun, O 2009, 'Microencapsulated n-octacosane as phase change material for thermal energy storage', Solar Energy, vol. 83, pp. 1757-1763.
3. Ries, CP, Neufeld, RJ, Ribeiro, AJ & Veiga, F 2006, 'Nanoencapsulation I. Methods for preparation of drug-loaded polymeric nanoparticles', Nanomedicine, vol. 2, pp. 8-21.
4. Zhang, XX, Fan, YF, Tao, XM & Yick, KL 2004, 'Fabrication and properties of microcapsule and nanocapsules containing n-octadecane', Materials Chemistry and Physics, vol. 88, pp. 300-307.
5. Wei, L, Zhang, XX, Wang, XC & Niu, JJ 2007, 'Preparation and characterization of microencapsulated phase change material with low remnant formaldehyde content', Materials Chemistry and Physics, vol. 106, pp. 437-442.
6. Fan, YS, Zhang, XX, Wan, XC, Niu, JJ & Cai, HL 2005, 'Miniemulsion polymerisation as a versatile tool for the synthesis of fuctionalized polymers', Poly. Mater. Sci. Eng., vol. 1, pp. 072.
7. Li, MG, Zhang, Y, Xu, YH & Zang, D 2011, 'Effect of different amounts of surfactants characteristics of nanoencapsulated phase-change materials', Polymer Bulletin,. vol. 67, pp. 541-552.

Cite this article as: Karthikeyan M, K.Visagavel, Ramachandran T, Ilangkumuran M, Kirubakaran M. "Innovation in Textiles: Integration of Nanoencapsulation of PCMs in Cotton fabric." *International Conference on Systems, Science, Control, Communication, Engineering and Technology (2015)*: 85-91. Print.

International Conference on Systems, Science, Control, Communication, Engineering and Technology 2015 [ICSSCCET 2015]

ISBN	978-81-929866-1-6
Website	icssccet.org
Received	10 - July - 2015
Article ID	ICSSCCET0019

VOL	01
eMail	icssccet@asdf.res.in
Accepted	31- July - 2015
eAID	ICSSCCET.2015.019

PERFORMANCE ENHANCEMENT OF REFRIGERATED AIR DRYER CANOPY BASE

Vijayan.S.N, Karthik.S, Maharaja.K
Assistant Professor, Department of Mechanical Engineering,
Karpagam Institute of Technology, Coimbatore ,Tamil Nadu, India.

Abstract: *Refrigerated air dryers are basically refrigeration system which is used to remove water vapor from compressed air. In this work the load carrying capacity of canopy base has been analyzed. Refrigerator, heat exchanging unit are to be placed in a canopy which has affected by static and dynamic stresses acting on it. Using alternative approaches the load carrying capacity of the canopy base has been analyzed. Finally adding circular disc and one rib on the back side of the base provide high load carrying capacity compare to other approaches.*

Keyword: Refrigeration, Stress, Deformation, Load.

I. INTRODUCTION

There are many applications where air from the atmosphere is compressed for use. When air is compressed, it leaves the compressor in saturated condition with moisture. Some of this moisture condenses in the air storage tank and is exhausted through a float. The air is still very close to saturated as it leaves the storage tank. This air may be dehydrated using refrigeration. Refrigerated air dryers are normally self contained refrigeration system that may be air cooled or water cooled. Refrigerated air dryers are basically refrigeration systems located in the air supply, after the storage tank. The air may be cooled in a heat exchanger, and then moved to the storage tank where much of the water will separate from the air. The air then passes through another heat exchange where the air temperature is reduced to below the dew point temperature.

Design of Canopy

Design and analysis of the canopy of air dryer for its existing dimensions have been modeled which is shown in the fig.1 Brain-storming sessions are used to generate ideas for alternatives in order to improve the various aspects of the product.

Figure 1. Assembled View Of Canopy

Cite this article as: Vijayan.S.N, Karthik.S, Maharaja.K. "PERFORMANCE ENHANCEMENT OF REFRIGERATED AIR DRYER CANOPY BASE." *International Conference on Systems, Science, Control, Communication, Engineering and Technology (2015)*: 92-97. Print.

The above figure shows the assembled view of the canopy. Canopy is the outer cover of the Refrigerated Air Dryer. It consists of base which is used to locate the components, pillars to provide support, and a roof. Since roof and pillars did not experienced any stress, analysis is carried out only for canopy base.

II. MATERIAL AND METHODS

The material used for the canopy is AISI 1020 Steel and the model type is linear elastic isotropic. The Table I shows the material specifications of canopy.

TABLE I
MATERIAL PROPERTIES OF CANOPY

Properties	Value	Unit
Poisson's ratio	0.29	NA
Mass density	7870	kg/m^3
Tensile strength	4.2e+008	N/m^2
Yield strength	3.5e+008	N/m^2

To overcome the Deformation and stress acting on the refrigerated air dryer canopy by using any one of the following approaches.

- Thickness improvement
- Providing ribs
- Providing circular disc

The above approaches are used to reduce the Deformation on the base due to acting of heavy load and it is reduces with increase in performance.

III. RESULTS AND DISCUSSION

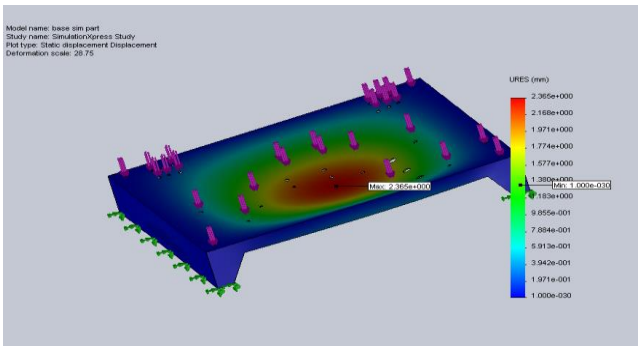

Figure 2. Static deformation of base

The fig. 2 shows the static Deformation of the canopy base. Static Deformation is used to denote how long the surface would deform under the application of load. Here the max. Deformation is 2.365mm.

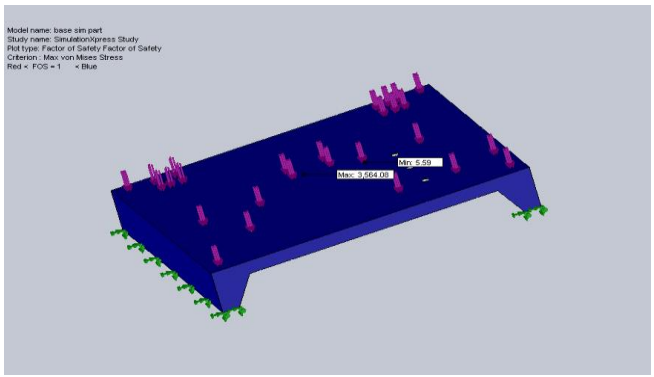

Figure 3. max. von mises stress of base

Cite this article as: Vijayan.S.N, Karthik.S, Maharaja.K. "PERFORMANCE ENHANCEMENT OF REFRIGERATED AIR DRYER CANOPY BASE." *International Conference on Systems, Science, Control, Communication, Engineering and Technology (2015)*: 92-97. Print.

The fig. 3 shows the maximum von mises stress acting on the canopy base. The maximum von mises stress is 62.6225 Mpa, which is greater than the strength of the material. So the canopy base will definitely deform under the given load.

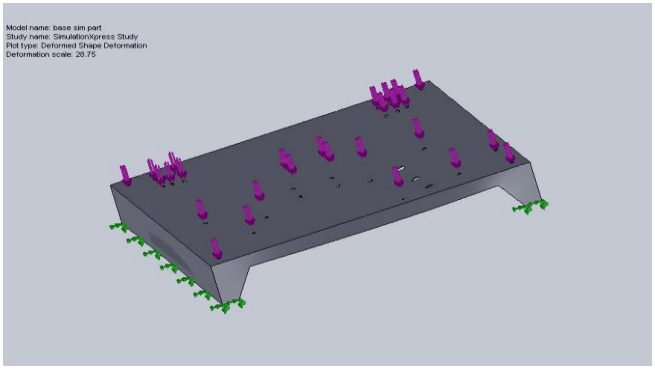

Figure 4.Deformation shape of base

The fig. 4 shows the deformation shape of the canopy base. It denotes the deformation of the surface under the given load.

Thickness Improvement of Canopy

By increasing thickness of base to 5 mm, the Deformation of the base has reduced to 0.18mm with increase the overall weight of the canopy to 25.9 Kg. fig. 5 shows the Deformation view of base for 5 mm thickness.

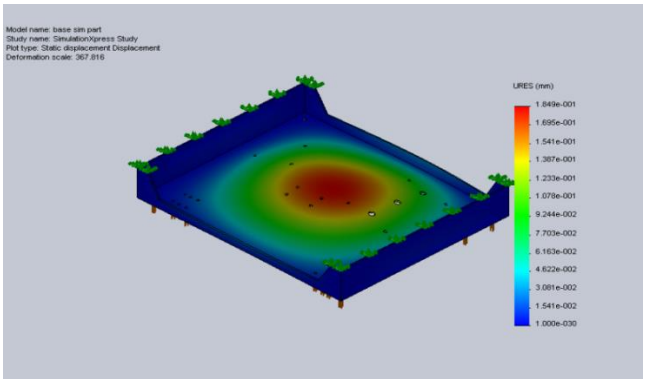

Figure 5. Deformation of base with 5mm thickness

Addition of Ribs

In this approaches number of ribs are added on the bottom side of the base from double rib to four ribs which is perpendicular to the base. The fig. 6 clearly shows the Deformation of base after addition of 4 ribs under the base has reduce the Deformation to 0.09 mm with 4.4 kg increase in weight of base.

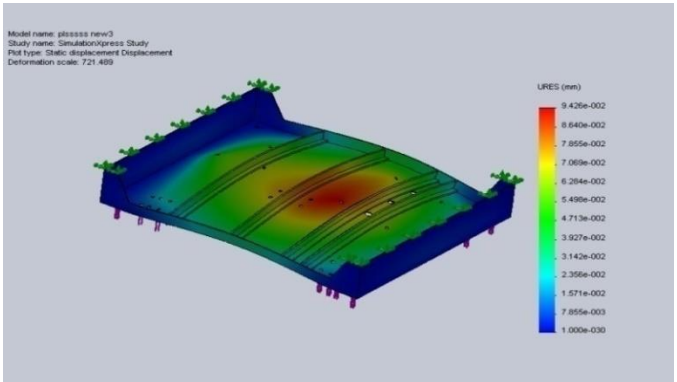

Figure 6. Deformation of base with 4 ribs

Cite this article as: Vijayan.S.N, Karthik.S, Maharaja.K. "PERFORMANCE ENHANCEMENT OF REFRIGERATED AIR DRYER CANOPY BASE." *International Conference on Systems, Science, Control, Communication, Engineering and Technology (2015)*: 92-97. Print.

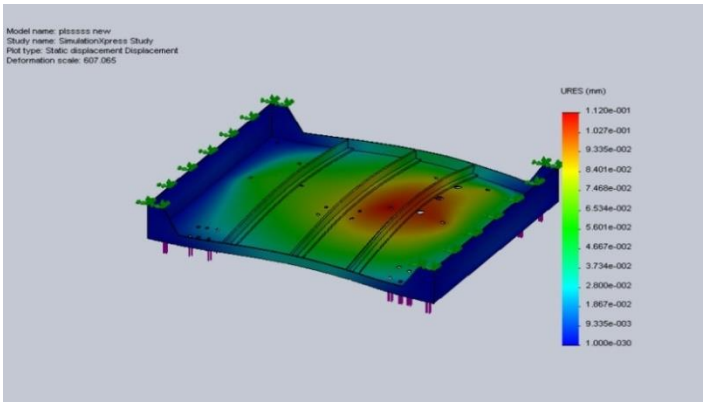

Figure 7. Deformation of base with 3 ribs

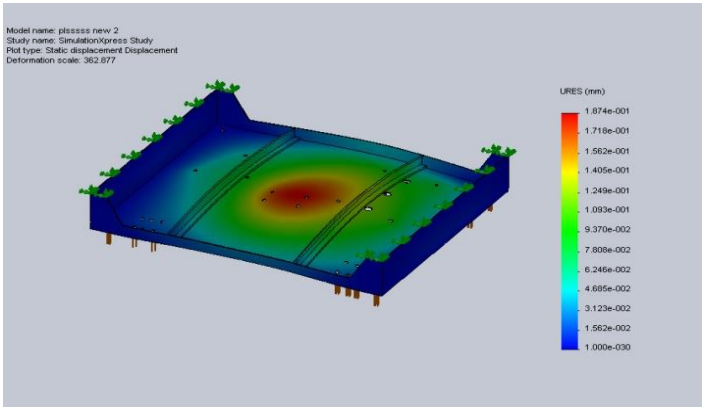

Figure 8. Deformation of Base with 2 Ribs

The weight of the canopy base becomes 24.9 kg, and by adding 3 ribs under the base has reduce the Deformation to 0.11 mm with 3.3 kg increase in weight of base which is shown in fig. 7 The weight of the canopy base becomes 23.8 kg, adding 2 ribs under the base has reduce the Deformation to 0.18 mm with 2.2 kg increase in weight of base. The weight of the canopy base becomes 22.7 kg it is shown in fig. 8.

Addition of Circular Structure

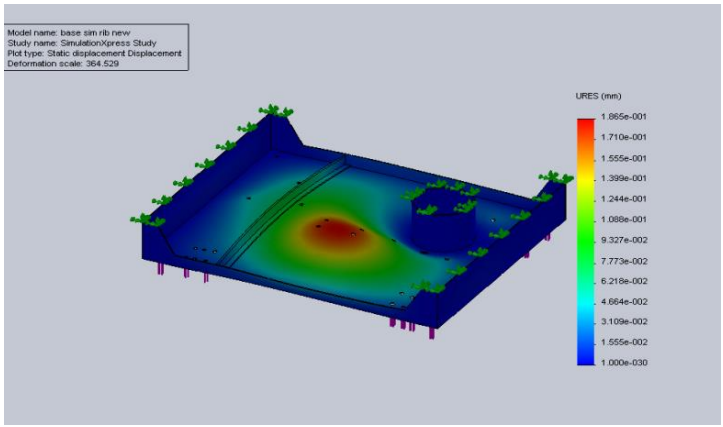

Figure 9. Deformation of base with circular structure

The fig. 9 shows the deformation results after adding a circular structure of 5mm thickness with single rib on the other side at the critical point where the load is maximum, the Deformation of the base will be reduced to 0.19mm with 1.84 kg increased in weight. The overall weight of the canopy becomes 22.3 kg.

Cite this article as: Vijayan.S.N, Karthik.S, Maharaja.K. "PERFORMANCE ENHANCEMENT OF REFRIGERATED AIR DRYER CANOPY BASE." *International Conference on Systems, Science, Control, Communication, Engineering and Technology (2015)*: 92-97. Print.

Table II shows the results obtained by using various alternative approaches used to overcome the Deformation of refrigerated air dryer canopy.

TABLE II
COMPARISON OF DEFORMATION VALUES AND WEIGHT

Sl No.	Approaches	Deformation in mm	Final weight in Kg
1	Adding 2 ribs	0.18	22.7
2	Adding 3 ribs	0.11	23.8
3	Adding 4 ribs	0.09	24.9
4	Improve thickness of base to 5mm	0.18	25.9
5	Rib with Circular Disc	0.19	22.3

From the results obtained using various approaches, by adding four rib can obtain very minimum value of deformation such as 0.09mm when compare with other approaches which is clearly shown in fig. 10.

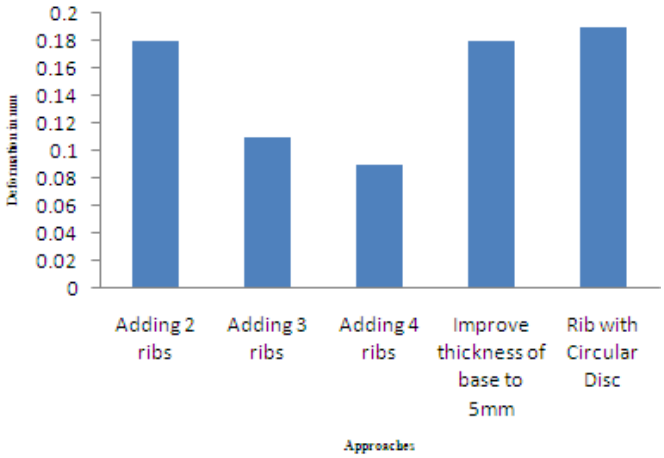

Figure 10. Alternative Approaches vs deformation of canopy base

The fig. 11 shows the results obtained by various alternative approaches with respect to weight of canopy base. By adding circular disc can obtained low weight of canopy with high deformation value when compare to other approaches.

Figure 11. Alternative Approaches vs Weight of canopy

Very minimum deformation value is obtained by adding four ribs on the bottom side of the refrigerated air dryer canopy with increase in overall weight of the canopy. But adding circular disc with one rib on the bottom side of the base give lenient deformation value when compare to other approaches, in this case the overall weight of the canopy is reduced.

Cite this article as: Vijayan.S.N, Karthik.S, Maharaja.K. "PERFORMANCE ENHANCEMENT OF REFRIGERATED AIR DRYER CANOPY BASE." *International Conference on Systems, Science, Control, Communication, Engineering and Technology (2015)*: 92-97. Print.

IV. CONCLUSION

The deformation value of the canopy base varies with respect to overall weight of the refrigerated air dryer and thickness of base plate. If the deformation value is maximum, it indicates the withstanding capacity of canopy is minimum, likewise if the deformation value is minimum it indicates the withstanding capacity of canopy as maximum. By introducing circular disc on the bottom of the canopy base can obtain high withstanding capacity of canopy.

Reference

[1]. A. Futakawa, K. Namura, H. Emoto, "Deformation and Stress of Refrigeration Compressor Flexible Ring Valve", International Compressor Engineering Conference, pp 266, 1978.

[2]. Pushpendra Mahajan, Prof. Abhijit L. Dandavate, "Analysis and optimization of Compressor Mounting Plate of Refrigerator using FEA", International Journal of Emerging Technology and Advanced Engineering, Volume 5, Issue 5, May 2015.

[3]. B. Sreedhar, U. Naga Sasidhar, "Optimization of Mounting Bracket", Simulation Driven Innovation, HTC 2012.

[4].Vyankatesh D. Pawade, Pushkaraj D. Sonawane, " Study of Design and Analysis of Air Conditioner Compressor Mounting Bracket", International Journal of Science and Research, Volume 4 Issue 1, January 2015.

[5].T.Ramachandran, K.P.Padmanaban, P.Nesamani, "Modeling and analysis of IC engine Rubber mount using FEM and RSM", procedia engineering, pp.1683-1692, 2012.

[6].Dr.Yadavalli Basavaraj, Manjunatha.T.H, " Design Optimization of Automotive Engine Mount System", International Journal of Engineering Science Invention, Volume 2, Issue 3, March. 2013, PP.48-53.

[7].K.Nagalakshmi, G. Marurhiprasad Yadav, "The Design and Performance Analysis of Refrigeration System Using R12 & R134a Refrigerants", Int. Journal of Engineering Research and Applications, Vol. 4, Issue 2, February 2014, pp.638-643.

Cite this article as: Vijayan.S.N, Karthik.S, Maharaja.K. "PERFORMANCE ENHANCEMENT OF REFRIGERATED AIR DRYER CANOPY BASE." *International Conference on Systems, Science, Control, Communication, Engineering and Technology (2015)*: 92-97. Print.

International Conference on Systems, Science, Control, Communication, Engineering and Technology 2015 [ICSSCCET 2015]

ISBN	978-81-929866-1-6
Website	icssccet.org
Received	10 - July - 2015
Article ID	ICSSCCET020

VOL	01
eMail	icssccet@asdf.res.in
Accepted	31- July - 2015
eAID	ICSSCCET.2015.020

Processing Techniques of Functionally Graded Materials – A Review

Saiyathibrahim.A[1], Mohamed Nazirudeen.S.S[1], Dhanapal.P[2]
[1]Department of Metallurgical Engineering, P.S.G College of Technology, Coimbatore, India
[2]Department of Mechanical Engineering, Karpagam Institute of Technology, Coimbatore, India

Abstract- *Functionally Graded Materials (FGMs) are a class of engineered materials characterized by a spatial variation of composition and microstructure aiming at controlling corresponding functional (i.e. mechanical, thermal, electrical, etc.) properties. The tailored gradual variation of microstructural features may be obtained through non-uniform distributions of the reinforcement phase(s) with different properties, sizes and shapes, as well as by interchanging the role of reinforcement and matrix materials in a continuous manner. Wide ranges of processing methods are considered on the production of FGMs. Each processing method has its own characteristics on the gradation phenomena which implies on the product. Processing parameters and their influences are presented with consideration of experimental investigations carried out earlier in this field. Also the processing steps to attain the desired gradation with limitations are discussed. Microstructural evaluation, wear mechanisms, porosity, stress distributions, etc. of various metal-metal, metal-ceramic and ceramic-ceramic FGMs are discussed to expose an overall view for carrying future research. Finally the applications of FGMs in various fields, which are still facing new innovations are considered. Improving the performance of processing techniques and extensive studies on material characterization on components produced will go a long way in bringing down the manufacturing cost of FGM and increase productivity in this regard.*

I. INTRODUCTION

FGMs exhibit gradual transition in the microstructure and/or the composition in a definite direction, the presence of which leads to variation in functional performance within the part through microstructural manipulation. FGMs possess a characteristic of tailoring of graded composition and micro structure according to the distribution of properties needed to achieve desired function which distinguishes it from the conventional materials. As we all know composite materials and cermets have been employed as a solution for the various engineering problems for the number of years. Though the development of new materials (FGMs) is due to mismatch occurs while applying them as a coating on the surface of the base material to withstand desired condition which leads to change in the properties like elastic modulli, thermal expansion and hardness. The gradual transition allows the creation of superior and multiple properties without any weak interface.

According to the material composition function specified, the volume fraction of one material constituent will be changed from 100% on one side to zero on another side, and that of another constituent will be changed the other way around as shown in Fig.1. The FGM helps to reduce stress, prevent peeling of the coated layer, prevent microcrack propagation, etc. For a component having a material region made of an FGM, its fabrication technology must be able to add different materials with certain volume fractions simultaneously for every pixel according to the specified composition function.

Cite this article as: Saiyathibrahim.A, Mohamed Nazirudeen.S.S, Dhanapal.P. "Processing Techniques of Functionally Graded Materials – A Review." *International Conference on Systems, Science, Control, Communication, Engineering and Technology (2015)*: 98-105. Print.

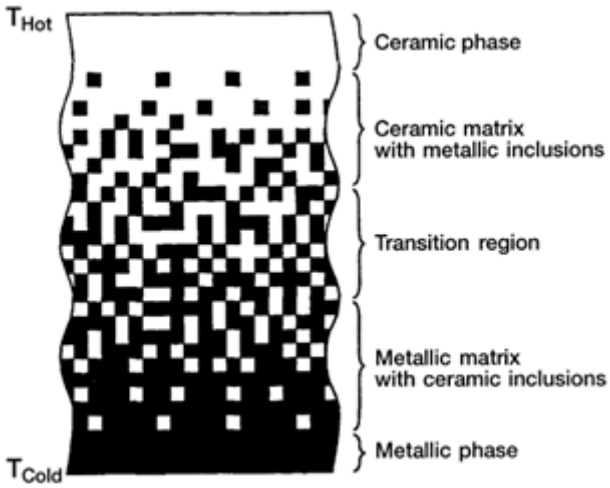

Figure 1. Structural view of continuously graded FGM

Various fabrication methods are available for the preparation of bulk FGMs and graded thin films. The processing methods are commonly classified into four ways like powder technology methods (dry powder processing, slip vesting, tape casting, infiltration process or electrochemical gradation, powder injection molding and self propagating high temperature synthesis, etc.), deposition methods (chemical vapour deposition, physical vapour deposition, electrophoretic deposition, slurry deposition, pulsed laser deposition, plasma spraying, etc.), in-situ processing methods(laser cladding, spray forming, sedimentation and solidification, centrifugal casting, etc.) and rapid prototyping processes (multiphase jet solidification, 3D-printing, laser printing, laser sintering, etc.)[1].

The manufacturing process of a FGM can usually be divided into two steps. Initial one is building up of the spatially inhomogeneous structure called Gradation. Another is the transformation of this structure into a bulk material called Consolidation. In detail gradation process can be categorized into constitutive, homogenizing and segregating processes. Stepwise build up of the graded structure from precursor materials is constitutive process. Homogenizing is a process of converting sharp interfaces between two materials into a gradient by material support. Segregation starts with a macroscopically homogeneous material, which is converted into graded material by material transport caused by an external field (i.e. gravitational, electrical field, etc). Normally sintering and solidification follows gradation process. Graded structure is of two types namely continuous and step wise. In continuous type structure, change in composition and/or microstructure occurs continuously with position. Powder metallurgical processed FGMs follow discrete (or) step wise structure. In detail their microstructure feature changes in a step wise manner with interfaces existing between discrete layers. Continuous graded structures are to be produced by centrifugal casting [2].

In this paper processing techniques of FGMs are presented with their experimental investigation of various materials. Some research works on functionally graded materials in recent times are presented and the future research needs are proposed. This work clearly demonstrates various possibilities available in FGM research and useful to gain background knowledge. Also some applications of functionally graded materials are presented here.

II. PROCESSING TECHNIQUES OF FGM

In this chapter a summary of the different technologies and process for the production of FGM is provided. This includes promising processes such as dry powder processing, Slip casting, tape casting, and centrifugal casting. The other processes mentioned in the introduction are still in developing stage.

A. Dry Powder Processing

Here the technique is used to produce functionally graded material through three basic steps namely: weighing and mixing of powder according to the pre-designed spatial distribution as dictated by the functional requirement, stacking and ramming of the premixed powders, and finally sintering as shown in Fig.2. This technique gives rise to a stepwise structure. Starting from the powder material it is possible to obtain nearly optimal conditions for graded materials varying in composition and microstructure. This performed by changing the chemical composition or average particle size of the applied powders. If continuous structure is desired, then centrifugal method is used. The powder metallurgy method is one of the most commonly employed techniques due to its wide range control on composition, microstructure and shape forming capability [3].

Mahmoud M. Nemat – alla et al. used steel/aluminium FGM with composition changing from 100% steel in one side to 100% aluminium in the other side. In their fabrication they found that the sintering temperature should not exceed 600°C, if it so a new component will be formed. Also increasing the number of layers in steel/aluminum FGM can decrease the sharp interface between the layers and produce FGM instead of functionally graded layers material. The fabricated steel/aluminum graded material specimen with very smooth transition will leads to disappearing of the thermal stresses singularities and minimizing the stress concentration values [4].

Xin jin et al. fabricated eleven layered ZrO_2/NiCr FGM in which the matrix phase varies from the metal to the ceramic and the inclusion phase varies from the ceramic to the metal. With the increase of ZrO_2, the hardness increases tediously and the ductility decreases gradually. Here the ceramic matrix provides the rigid skeleton and constrain the plastic flow of the metal.

Cite this article as: Saiyathibrahim.A, Mohamed Nazirudeen.S.S, Dhanapal.P. "Processing Techniques of Functionally Graded Materials – A Review." *International Conference on Systems, Science, Control, Communication, Engineering and Technology (2015)*: 98-105. Print.

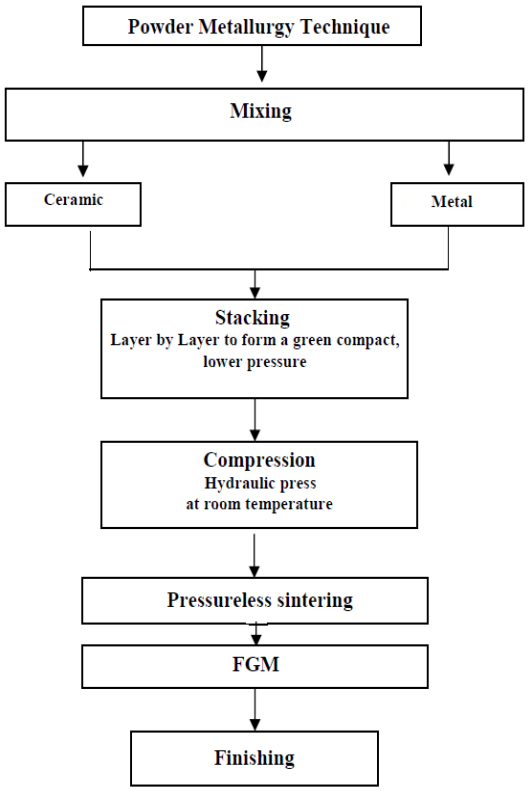

Figure 2. Flow chart of powder metallurgy technique for producing FGMs

The bending strength and elastic modulus firstly decrease as the volume fraction of ZrO_2 increase from 0% to 50%, and then increase as the volume fraction of ZrO_2 increase from 50% to 100%. These are mainly affected by the weakly bonded ceramic/metal interface. And the porosity does not seem to have an obvious effect on the distributions of the mechanical properties in the ZrO_2/NiCr FGMs [5].

B. Slip Casting

The slip casting is a powder based shaping method traditionally applied in the ceramic industry. In general slip casting is a filtration process where powder suspension is poured in a porous plaster mould. Due to the resulting capillary forces the liquid is removed from the suspension (slip) and the powder particles are forced towards the walls. A gradient will be formed by changing composition or grain size of the applied powder suspension during the slip casting procedure. This technique also requires subsequent consolidation step, where the powder is densified (sintered) and a gradient structure of the FGM results [6]. Tomoyuki Katayama et al. fabricated a functionally graded material (FGM) from tungsten and alumina powders. Two types of W powder, with different oxidizing properties, were used as the raw powders for the Al_2O_3–W FGM. "Oxidized W" was prepared by heat treatment at 200 °C for 180 min in air. The green compacts were subsequently dried, and then sintered using a vacuum furnace at 1600 °C for a fixed time. The green compact obtained with the as-received W powder showed a clear interface between Al_2O_3 and W as a result of the huge difference between the densities of the powders. However, with the oxidized W powder, the green compact revealed a W particle distribution which gradually varied, resulting in a microscopic compositional gradient [6].

C. Centrifugal Casting

Centrifugal force can be used to create a gradient composition in a metallic melt that contains another solid phase. Generally, fabrication of FGMs by the centrifugal method is classified into two categories based on the melting temperature of the reinforcement particle. If the melting point is significantly higher than the processing temperature, the reinforcement particle remains solid in a liquid matrix.

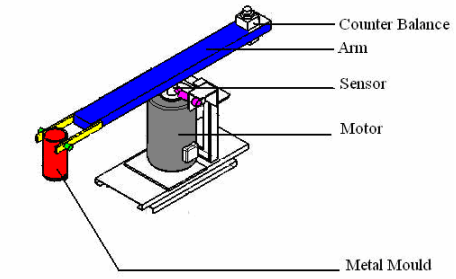

Figure 3. Vertical centrifugal casting setup

Cite this article as: Saiyathibrahim.A, Mohamed Nazirudeen.S.S, Dhanapal.P. "Processing Techniques of Functionally Graded Materials – A Review." *International Conference on Systems, Science, Control, Communication, Engineering and Technology (2015)*: 98-105. Print.

This method is named as a centrifugal solid-particle method (CSPM). The selective reinforcement of the component surface obtained by CSPM results in a higher wear resistance in the outer surface as well as maintaining high bulk toughness. On the other hand, if the melting point of the reinforcement particle is lower than the processing temperature, centrifugal force can be applied during the solidification both to the reinforcement particle and to the matrix. This solidification is similar to the production of in situ composites using the crystallization phenomena, and this method is, therefore, named as a centrifugal in situ method (CISM). The formation mechanism of the compositional gradient during the fabrication of FGM by the centrifugal in-situ method in the A–B alloy is, 1) Partial separation of A and B elements in the liquid state occurs due to the density difference. 2) A compositional gradient is formed before the crystallization of the primary crystal. 3) The primary crystals in the matrix appear according to local chemical composition. 4) The primary crystals migrate because of density difference, and a further compositional gradient is formed [7].

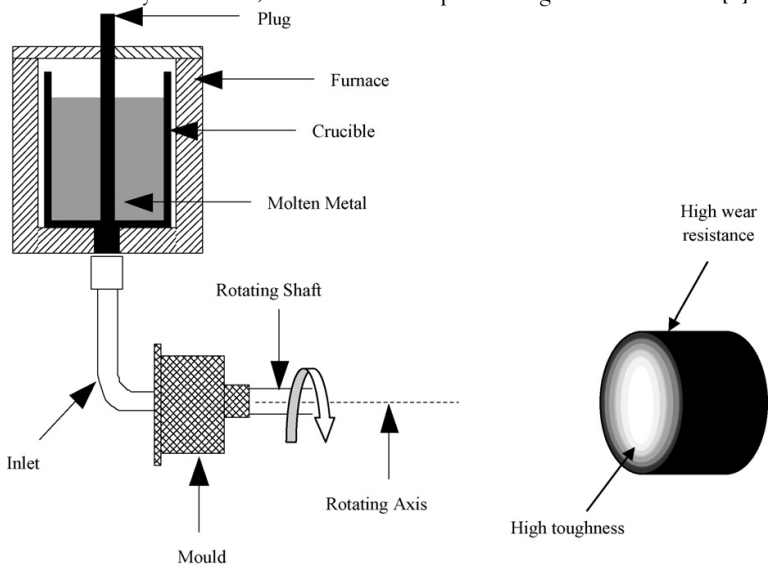

Figure 4. Schematic representation of: (a) the horizontal centrifugal casting process and (b) the final product obtained (Al - High toughness inner region and SiC – High wear resistance)

Usually, the density of the outer part of the FGM rings fabricated by the centrifugal in situ method is larger than that of the inner part of the ring. In general, steeper compositional gradient appears for the CSPM. Since the motion of the solid-particles under the centrifugal force is governed by stoke's law (Migration distance is greater for large particles). It is well known that, the mechanical properties depend on particle size distribution as well as the volume fraction of particles in particle reinforced or dispersion strengthened of any composite material. From the research works it is found that the extent of particle segregation and relative location of enriched and depleted particle zones within the casting are mainly dictated by the relative densities of the particle and liquid, teeming temperature, melt viscosity, cooling rate, particle size, solidification time and magnitude of centrifugal acceleration [8]. G. Chrita et al. studied the effect of centrifugal casting technique on castings as compared to the traditional gravity casting. They concluded that the centrifugal effect may produce an increase in rupture strength by 50%, rupture strain by 300% and young's modulus by 20%. Also an important and interesting finding in their study was, higher the distance in relation to the rotation centre (higher centrifugal force) the bigger the increase in mechanical properties. According to their study, the centrifugal effect on castings may be divided in three main features: centrifugal pressure, intrinsic vibration of the process, and fluid dynamics. The effect of each of these variables will be the responsible for the differences in both mechanical and/or metallurgical properties on the castings [9]. Yoshimi watanabe et al. conducted their examination to determine the particle size distributions in the FGM tubes were fabricated from plaster/corundum model materials by centrifugal solid - particle method. During solidification the reinforcement position is heavily depends on the 'G' number. Centrifugal force magnitude 'G' is given by,

$$G = \left(\frac{\omega^2 \times r}{g}\right) \quad (1)$$

Where 'R' is the radius of the arm in meters, 'ω' is the arm rotational speed in rad/sec and 'g' is the acceleration due to gravity. In here they considered three levels of centrifugal force listed as 15, 28 and 45 with five different corundum particle sizes for the fabrication of FGM cast tube. The particle size gradient in the FGM becomes steeper by increasing the 'G' number or by decreasing the mean volume fraction of particles [10].

In an study of Yoshimi watanabe et al. commercially available Mg alloy, ZK60A was used as a mater alloy to fabricate Mg based FGM with a mould temperature of 680°C with a cooling rate of 0.05°C/s. Results of EDX analysis showed that Zn concentration at each region was almost the same i.e weak peaks at middle and inner region, while Zr exists only in the outer region as strong peaks. Graded distribution of Zr phase is enhanced with increasing the 'G' number. Finally these graded structures are caused by the difference in the formation mechanisms of compositional gradient during the centrifugal method between Zr and Zn, since the solid Zr particles exist prior to the application of the centrifugal force. In case of hardness phenomena the maximum hardness value was attained at outer strong Zr phase region and it increased in the direction of centrifugal force [7]. Al-Al_2Cu functionally graded material (FGM) ring was fabricated from Al-3 mass%Cu initial master alloy by the centrifugal in-situ method. In the case of Al-3 mass%Cu alloy, the density of

Cite this article as: Saiyathibrahim.A, Mohamed Nazirudeen.S.S, Dhanapal.P. "Processing Techniques of Functionally Graded Materials – A Review." *International Conference on Systems, Science, Control, Communication, Engineering and Technology (2015)*: 98-105. Print.

the primary α-Al crystal is larger than that of the molten Al alloy. Therefore, the solid α-Al phase migrates towards the outer periphery of the ring when the centrifugal force is applied in the early stage of solidification. Consequently, since the Cu concentration within the FGM ring monolithically increases towards the ring's inner position, the FGM ring, whose density increases toward inner region, can be successfully fabricated by the centrifugal in-situ method from dilute Al-Cu alloy. It is also found that the hardness increases towards the inner region of the ring within the Al-Al_2Cu FGM ring [8]. A.S.Kiran et al. used centrifuge processing technique for the Al-Si FGM fabrication with consideration of the processing parameters like teeming temperature (900°C) and rotational speed of mould (400rpm). In the solidification primary Si particles moved in the direction opposite to the direction of the 'G' force as the density is less than that of liquid aluminium. Brinell hardness test shown that, the hardness is mainly affected by the content of primary Si content along the polished specimen [11].

Shimaa El-hadad et al. were fabricated Al-5mass%Zr functionally graded materials by centrifugal solid – particle method under applied centrifugal force of 30, 60 and 120G. Microstructural observation along the centrifugal force direction showed that Al_3Zr particles are almost oriented normal to the applied centrifugal force direction. Also increasing centrifugal force resulted in a steep particles distribution and decreased thickness of the intermetallics rich area. From the block-on-disk wear tests the anisotropy of wear property of the current Al/Al_3Zr FGMs was diminished with decreasing the applied centrifugal force and thence decreasing the particle orientation. An enhanced wear resistance was achieved in the Al/Al_3Zr FGMs by controlling the distribution of both the orientation and the volume fraction of Al_3Zr particles. Also they concluded plastic deformation induced wear was the dominant wear mechanism [12].

Xiaoyu huang et al. were fabricated Al-Si alloy based composite pistons reinforced with SiC particles locally at the head by centrifugal casting with parameters consideration as slurry temperature of the alloy, the mould temperature and the rotational speed of the mould on the particle segregation. By the SEM analysis, it is clear that a large quantity of SiC particles are in the piston head, which meets requirements such as hardness, wear resistance and thermal expansion behavior of pistons. The hardness values along the axis of piston gradually increased from the skirt to the head, which corresponds to the structure changing along the axis of the pistons. At a slurry temperature of 850°C, a mould temperature of 600°C and a rotation speed of 800rpm possessed the highest value of hardness with best wear resistance when compared with the piston fabricated by permanent gravity mould casting [13]. H.P Thirtha Prasad et al. used unidirectional solidification mould made up of graphite with the process considerations as slurry temperature of 750°C, rotational speed of the mould as 200rpm and maximum centrifugal acceleration of 54g for the fabrication of Al/ Al_2O_3 FGM. From their microstructural evaluation, most of the Al_2O_3 particles enriched in the external zone of the specimen under centrifugal force, and some congregated Al_2O_3 particles with low bulk density segregate to the inner reinforced zone of the cylinder. The mechanical properties of FGM were increased with increasing Al_2O_3 particles. Also the fracture surface of the FGM at the center was ductile nature and the outer was brittle nature [14]. Li chanyun et al. carried out hydraulic simulation experiments on vertical centrifugal casting machine with two different filling methods (top filling and bottom filling) and three kinds of rotational velocities (163, 245, and 375rpm) to determine the best filling method. A high speed camera photos taken in the experiment showed that in both top filling and bottom filling, liquids stick to back-wall of cavity or runner to filling due to the action of centrifugal force. Filling volume is rising with the increase of the filling time and rotational velocity of mold. Experiments on titanium alloy resulted that the bottom filling method is better than the top one, which can achieve stable filling, minimize turbulence and avoid drastic liquid collision [15].

R. Sivakumar et al. carried out their investigation on mullite-molybdenum graded cylinders by centrifugal molding technique with ceramic rich in inner surface and metal rich in outer surface were fabricated with the smooth increase of Mo content toward outer direction. Microstructural observation and EDX analysis performed showed linear gradation of Mo content along the radial direction of cylinders. The microstructures of graded hollow cylinders reveal that the methodology of slurry preparation has a vital influence on the gradation of Mo along the radial direction. Measured Vickers hardness values proved the continuous compositional change from inner to outer surface of graded cylinders and the hardness became constant in outer surface of graded specimens due to formation of interconnected Mo structures [16]. J.W. Gao et al. investigated the solidification process during the centrifugal casting of FGMs numerically and validated results against the experimental results. During solidification, the particles move to the outer or inner direction of the mould under centrifugal field depending on the particle density relative to that of the melt. Solidification is induced from the outer wall of the mould by convective cooling while the inner wall is assumed to be adiabatic. The model was used to investigate the solidification process in centrifugal casting of Al/SiC FGMs in a cylindrical mould. Three factors can be identified to be responsible for creation of the particle concentration gradient: the geometrical nature of particle flow in the cylindrical mould, the angular velocity, and the solidification rate, which captures the desired gradient — it is the interruption of particle migration by the solidification front that creates gradients in the particle concentration. By optimizing processing conditions, such as the particle size, initial particle concentration, rotational speed of the mould, cooling rate and superheat, one can engineer a desired gradient in the solidified part [17]. A.C. Vieira et al. have presented wear characteristics of Al/SiC_p FGM fabricated by centrifugal casting process with two different mould rotating speeds (1500 and 2000rpm). Under a constant acceleration, the velocity (V) of a spherical particle of size (R_p) may be estimated using stoke's law by,

$$v = \frac{2R_p{}^2(\rho_p - \rho_l)\gamma}{9\eta} \qquad (2)$$

Where, ρ_p and ρ_l are the densities of the particle and liquid and η are the viscosity of the liquid. From Eq. (2) it can be seen that a higher centrifugal force (acceleration) will result in a higher particle velocity, emphasizing the reinforcement gradient along the centrifugal direction. FGM cast at low centrifugal speed (1500 rpm) presented a smooth gradient on SiCp distribution, while FGM cast at higher centrifugal speed (2000 rpm) revealed a sharper gradient on the distribution of reinforcing particles. This gradient was controlled by the movement of the solidification front, blocking the mobility of SiC particles in the melt. For the aluminium based

Cite this article as: Saiyathibrahim.A, Mohamed Nazirudeen.S.S, Dhanapal.P. "Processing Techniques of Functionally Graded Materials – A Review." *International Conference on Systems, Science, Control, Communication, Engineering and Technology (2015)*: 98-105. Print.

FGM composites considered in this study, two-body abrasion wear, oxidative wear, adhesion and delamination were the main wear mechanisms identified [18].

D. Tape Casting

The tape casting process is shown in Fig.5. A slip, powder containing suspension is distributed on a carrier film in a thin casting type. The cast tape thickness is generally in the range of 25µm to 1mm. Minimal tapes down to 1µm could be produced.

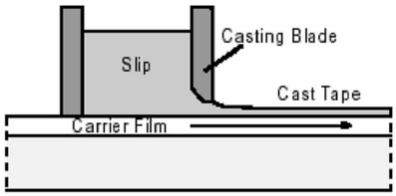

Figure 5. A tape casting process setup.

Different stages of tape casting are, 1) developing slip which contains water, powder particles and binder, 2) drying of green body or tape, 3) consolidating of dense material of tape. In order to achieve FGM, tapes of different composites were prepared. Square units were cut of the green tapes which were subsequently placed on top of each other. The thickness of the applied tapes is in the range of 200µm. The densification of tape is achieved by sintering. Stepped gradients of metal-ceramic and ceramic-ceramic materials are produced by casting of tapes of different composition and subsequent lamination. Anne-Laure Dumont et al. fabricated MoSi2/ Al_2O_3 FGM with alumina contents varying from 20 to 80 mol% using a combination of tape casting and self-propagating high-temperature synthesis (SHS). After debinding, the green samples were ignited at room temperature. The combustion reactions were conducted under a weak load to enhance the densification of the composition-graded composites. The porosity of the multilayer samples is significantly reduced when a low pressure (typically 3MPa) is applied during the SHS stage and when the green layer thickness is greater than 500 mm. The conservation of the multilayer structure is strongly dependent on the control of the amount of liquid formed during the SHS reaction [19]. Kongjun Zhu et al. were developed a piezoelectric actuator from the graded composition of PbO, Nb_2O_5, ZrO_2 and MgO powders. Results showed that sintering temperature has inverse effect in porosity and positive relation with the grain settlement. A non uniform grain size induces poor density of the ceramic [20].

III. Application of Functionally Graded Materials

Some of the applications of functionally graded materials are discussed below.

A. In Aerospace and Automotives

Space Shuttle utilizes ceramic tiles as thermal protection from heat generated during re-entry into the Earth's atmosphere. However, these tiles are prone to cracking at the tile / superstructure interface due to differences in thermal expansion coefficients. An FGM made of ceramic and metal can provide the thermal protection and load carrying capability in one material thus eliminating the problem of cracked tiles found on the Space Shuttle. The interest in graded materials like Aluminium/Silicon carbide (ceramic – metal) are focused primarily on the control of thermal stresses in elements exposed to high temperatures (to 1600°C) for instance aerospace structures and Cu/SiC for dynamic seal applications.

Thermal Barriers Coatings made up of ZrO_2 and NiCoCrAlY FGMs are very popular as thin layers protecting of aircraft engine components against the thermal shock (e.g. turbine blades). Boron additions to conventional titanium alloys have the potential to form lightweight, high modulus, dispersion strengthened, discontinuous-reinforced composite material structures enabling replacement for significantly more dense steel and nickel materials.

Exhaust and propulsion systems (e.g. Thrusters) that are required material properties like enhanced resistance to high temperature, thermal shocks, wear, oxidation and corrosion. Power transmission systems (e.g. Valves) that are required material properties like low specific weight, resistance to high temperature, resistance to wear and corrosion. Braking systems (e.g. Brake disks) that are required material properties like resistance to high temperature, friction and wear, high bending strength in room temperature and high temperature regimes, enhanced thermal conductivity, structural stability in temperature cycles, lower specific weight.

B. In medicine

In dental implantation a more realistic FGM is usually composed of collagen hydroxyapatite (HAP) and titanium is used [21]. Porous hydroxyapatite (HA) scaffolds with a functionally graded core/shell structure was fabricated for biomedical applications [22]. TiO_2 has also been used in combination with hydroxyapatite for developing biomaterials for implants because of its favourable biological effects and improved corrosion resistance. TiO_2 is also frequently and successfully used to reinforce Al_2O_3 wear resistant coating on metal substrate [23].

C. In defence

One of the most important characteristics of functionally graded material is the ability to inhibit crack propagation. Metal ceramic FGMs used in structures as fire retardant doors and penetration resistant materials for armour plates and bullet-proof vests. One of the available material compositions gradually shifts from titanium diboride to a combination of titanium and titanium diboride, combining the ceramic's ability to absorb energy with the toughness of a metal - ideal for vehicle armor solutions [22].

Cite this article as: Saiyathibrahim.A, Mohamed Nazirudeen.S.S, Dhanapal.P. "Processing Techniques of Functionally Graded Materials – A Review." *International Conference on Systems, Science, Control, Communication, Engineering and Technology (2015)*: 98-105. Print.

D. In Optoelectronics

Piezoelectric and thermoelectric devices, high density magnetic recording media, in optical applications as graded refractive index materials in audio-video discs.

E. In Industry

A ceramic roller suitable for various hybrid bearing applications in industries made up of silicon nitride as base material. This material possesses excellent mechanical properties, ideal for load bearing applications. In many cases, entire components are made of tungsten carbide, for an application requiring wear resistant properties. With a gradient, the use of expensive carbides can be minimized; thus lowering the total cost of the component. Functionally graded metal matrix composites (FGMMCs), especially gradient particulate composites with aluminum matrix, have been used in important applications such as in electronic packaging industry, for brake rotor assemblies in automobile industry and as armor materials [24].

IV. FUTURE SCOPE

Many research works carried out in the metal-ceramic FGMs such as (Al/ Al_2O_3, WC/Co, Mo/Mo_2C, Ni/ Al_2O_3, ZrO_2/NiCr and WC/Ni) for their proposed application. Based on the research history it is clear that the FGM processing stated with the ceramic compounds. Up to now so many processing technologies were discussed on the metal-ceramic type for the applications like which required high temperature resistance and toughness with light weight material. In contrast metal-metal combination having only least research works it may be due to the simplicity in the production processes of ceramic-ceramic and metal-ceramic combination. With the consideration of industrial needs new FGM families and their processing methods are to be developed especially with respect to real applications. In the field of FGM gradation forming is the critical step. To overcome this computer assisted modelling should be developed to improve forecasts for the proper gradient formation. Calculations related to the properties and combinations of the desire FGM should be done prior to the production. After the production of FGM, characterization is to be carried out by new testing methods in a non destructive way. Up scaling of laboratory route into industrial scale is necessary. In this regard a lot of works still needed to adopt the existing processing routes to industrial viable production routes. Industries are based on cost effective processes for the production either it may be mass or low volume. So technologies which transfer the FGM from laboratory to industry are to be invited. Also reproducibility in geometry, gradation and property of a FGM is very much important this has to be attained.

V. CONCLUSION

Functionally graded materials are very important in engineering and other applications which requires special properties which are not satisfied by the conventional materials like naturally available materials, alloys and metal matrix composites. Also we have discussed so many processing routes for making them to the special applications. In this regard here we present some of the deficiencies related to each processing technique for the further improvement. Commonly all the processing routes start with powders of base. During the consolidation for the gradient forming step, due to the lack in management of sintering temperature and time distortion in the final part arises with unequal density. To overcome this, a prior sintering step is to be implemented before the production in order to reach the desired part of final density.

REFERENCES

[1] Astrid rota (Editor), Technology and controlled tailoring of FGM.

[2] B. Kieback, A. Neubrand, and H. Riedel, "Processing techniques for functionally graded materials", Materials Science and Engineering A362 (2003), pp.81–105.

[3] M. S. El-Wazery, A. R. El-Desouky, O. A. Hamed, N. A. Mansour, and Ahmed. A. Hassan, "Preparation and Mechanical Properties of Zirconia / Nickel Functionally Graded Materials", Arab Journal of Nuclear Sciences and Applications, vol.45(2), 2012, pp.435-446.

[4] Mahmoud M. Nemat-Alla, Moataz H. Ata, Mohamed R. Bayoumi, and Wael Khair-Eldeen, "Powder Metallurgical Fabrication and Microstructural Investigations of Aluminum/Steel Functionally Graded Material", Materials Sciences and Applications, vol. 2, 2011, pp.1708-1718.

[5] Xin Jin, LinzhiWu, Yuguo Sun, and Licheng Guo, "Microstructure and mechanical properties of ZrO2/NiCr functionally graded Materials", Materials Science and Engineering A 509,2009, pp.63–68.

[6] Tomoyuki Katayama, Sohei Sukenaga, Noritaka Saito, Hajime Kagata, and Kunihiko Nakashima, Fabrication of Al2O3-W Functionally Graded Materials by Slip casting Method, IOP Conf. Series: Materials Science and Engineering 18, 2011, doi:10.1088/1757-899X/18/20/202023.

[7] Yoshimi Watanabe, Ryuho Sato, Ick-Soo Kim, Seiji Miura and Hiromi Miura, "Functionally Graded Material Fabricated by a Centrifugal Method from ZK60A Magnesium Alloy", Materials Transactions, Vol. 46, No. 5 ,2005,pp. 944-949.

[8] Yoshimi Watanabe, Hisashi Sato, Tetsuro Ogawa and Ick-Soo Kim, "Density and Hardness Gradients of Functionally Graded Material Ring Fabricated from Al-3 mass%Cu Alloy by a Centrifugal In-Situ Method", Materials Transactions, Vol. 48, No. 11, 2007, pp. 2945-2952.

[9] Chirita, G, Stefanescu, I, Soares, and D, Silva, F.S., "Centrifugal versus Gravity Casting Techniques over Mechanical Properties", Anales de Mecánica de la Fractura Vol. I, 2006, pp. 317-322.

[10] Yoshimi Watanabe, Akihiro Kawamoto and Koichi Matsuda, "Particle size distributions in functionally graded materials fabricated by the centrifugal solid-particle method", Composites Science and Technology 62, 2002, pp.881–888.

Cite this article as: Saiyathibrahim.A, Mohamed Nazirudeen.S.S, Dhanapal.P. "Processing Techniques of Functionally Graded Materials – A Review." *International Conference on Systems, Science, Control, Communication, Engineering and Technology (2015)*: 98-105. Print.

[11] A.S. Kiran, V. Desai, Narendranath and P.G. Mukunda, "Evolution of microstructure and hardness of Al-Si functionally graded material cast through centrifuge technique using hypereutectic and eutectic Al-Si", International Journal of Mechanical and Materials Engineering (IJMME), Vol.6, 2011, No.2, pp.275-279.
[12] Shimaa El-Hadada, Hisashi Sato, and Yoshimi Watanabe, "Wear of Al/Al3Zr functionally graded materials fabricated by centrifugal solid-particle method", Journal of Materials Processing Technology 210, 2010, pp.2245–2251.
[13] Xiaoyu Huang, Changming Liu, Xunjia Lv, Guanghui Liu, and Fuqiang Li, "Aluminum alloy pistons reinforced with SiC fabricated by centrifugal casting", Journal of Materials Processing Technology 211, 2011, pp.1540– 1546.
[14] Thirtha Prasad H.P and N.Chikkanna, "Experimental investigation on the effect of particle loading on microstructural, mechanical and fractural properties of Al/Al2O3 functionally graded materials", International Journal of Advanced Engineering Technology, Vol.II, Issue IV, October-December, 2011, pp.161-166.
[15] Li Changyun, Wu Shiping, Guo Jingjie, Su Yanqing, Bi Weisheng, and Fu Hengzhi, "Model experiment of mold filling process in vertical centrifugal casting", Journal of Materials Processing Technology 176, 2006, pp. 268–272.
[16] R. Sivakumar, T. Nishikawa, S. Honda, H. Awaji, and F.D. Gnanam, "Processing of mullite –molybdenum graded hollow cylinders by centrifugal molding technique", Journal of the European Ceramic Society 23, 2003, pp.765–772.
[17] J.W. Gao, and C.Y. Wang, "Modeling the solidification of functionally graded materials by centrifugal casting", Materials Science and Engineering A292, 2000, pp.207–215.
[18] A.C. Vieira, P.D. Sequeira, J.R. Gomes, and L.A. Rocha, "Dry sliding wear of Al alloy/SiCp functionally graded composites: Influence of processing conditions", Wear 267, 2009, pp. 585–592.
[19] Anne-Laure Dumont, Jean-Pierre Bonnet, Thierry Chartier, and Jose M.F. Ferreira, "MoSi2/Al2O3 FGM: elaboration by tape casting and SHS", Journal of the European Ceramic Society 21, 2001, pp.2353–2360.
[20] Kongjun Zhu, Hui Wang, Jinhao Qiu, Jun Luo, and Hongli Ji, "Fabrication of 0.655Pb(Mg1/3Nb2/3)O3-0.345PbTiO3 functionally graded piezoelectric actuator by tape casting", J Electroceram, 2011, vol.27, pp.197–202.
[21] Daniel Lin, Qing Li, Wei Li, Shiwei Zhou, and Michael V. Swain, "Design optimization of functionally graded dental implant for bone remodeling", Composites: Part B 40, 2009, pp.668-675.
[22] Young-Mi Soon, Kwan-Ha Shin, Young-Hag Koh, Jong-Hoon Lee, Won-Young Choi, and Hyoun-Ee Kim, "Fabrication and compressive strength of porous hydroxyapatite scaffolds with a functionally graded core/shell structure", Journal of the European Ceramic Society 31, 2011, pp.13–18.
[23] Siddhartha, Amar Patnaik, and Amba D. Bhatt, "Mechanical and dry sliding wear characterization of epoxy–TiO2 particulate filled functionally graded composites materials using Taguchi design of experiment", Materials and Design 32, 2011, pp. 615–627.
[24] Recep Ekici, M. Kemal Apalak, and M. Yildirim, "Indentation behavior of functionally graded Al–SiC metal matrix composites with random particle dispersion", Composites: Part B 42, 2011, pp.1497–1507.

Cite this article as: Saiyathibrahim.A, Mohamed Nazirudeen.S.S, Dhanapal.P. "Processing Techniques of Functionally Graded Materials – A Review." *International Conference on Systems, Science, Control, Communication, Engineering and Technology (2015)*: 98-105. Print.

International Conference on Systems, Science, Control, Communication, Engineering and Technology 2015 [ICSSCCET 2015]

ISBN	978-81-929866-1-6
Website	icssccet.org
Received	10 - July - 2015
Article ID	ICSSCCET021

VOL	01
eMail	icssccet@asdf.res.in
Accepted	31- July - 2015
eAID	ICSSCCET.2015.021

A Review on Characteristics and Mechanical Behavior of Metal Castings under Ultrasonic Vibration Technique

N.Suresh[1], P.Chandrasekar[2]

[1] Research Scholar, Department of Mechanical Engineering, Karpagam Institute of Technology, Coimbatore, Tamilnadu, India – 641105.

[2] Professor&Dean, School of Engineering, Professional Group of Institutions, Palladam, Tamilnadu, India – 641662.

Abstract- *The demanding problems for designers and engineers in the material science are to improve the quality of the castings. The several numbers of methods using external forces have been applied to introduce fluid flow during solidification of molten metal in casting process. These include mechanical, electromagnetic and ultrasonic vibration. Many technical journals describe the improvement in mechanical properties of castings under the vibration during solidification. In this paper, an attempt has been made to review the casting process to refine the microstructure of cast product during ultrasonic vibration technique. The awareness gain of these processes and application of the procedures offer the scope for better cost savings in design and manufacturing of cast products.*

Keywords: Ultrasonic Vibration; grain refinement; microstructure

I INTRODUCTION

Casting under vibratory conditions, moulds or work pieces are held rigidly on a vibratory table and the table is rigidly coupled to the vibration exciter which generates vibrations at different frequencies of oscillation and transmits them to the table and moulds which in turn vibrate at different frequencies of oscillation. The molten metal solidifies under these vibratory conditions. Inspection and testing of castings involve five main categories: casting ultimate, dimensional accuracy, mechanical properties, chemical substance and casting accuracy. Most of the research works are carried out to enhance casting soundness through micro structural analysis and mechanical property improvement for automobile and aerospace industries. During the process of solidifications, the vibration of moulding increases the properties of castings. In earlier studies, Campbell [1] noticed grain refinement to occur and mechanical properties improved in castings due to the application of vibration during casting. Fluidity is one of the most important factors in casting process. It is defined variously as the distance covered by quality liquid metal in a channel of fixed geometry before solidifying. That is the ability of a melt to flow and fill very narrow spaces, whether in a mould cavity grooves [2]. A coarse grained structure may result in a variety of surface defects in alloys used in rolled or extruded form, while the size of defects such as micro-porosity may reduce as a result of fine grain structures since the solidification of smaller grains will allow the mould to fill more completely and avoid unfavorable micro and macro- porosity thereby producing sound castings.

This paper gives a comprehensive review of the methods used for Ultrasonic vibration process with different materials, experimental investigation of vibration techniques, characterization such as microstructure examinations and mechanical properties.

Cite this article as: N.Suresh, P.Chandrasekar "A Review on Characteristics and Mechanical Behavior of Metal Castings under Ultrasonic Vibration Technique." *International Conference on Systems, Science, Control, Communication, Engineering and Technology (2015)*: 106-109. Print.

II PROCESSING

As can be seen in "Fig. 1," the experimental apparatus for ultrasonic treatment used in this study mainly consisted of a resistance furnace, an iron crucible, and a metallurgic ultrasonic system with power ranging from 0 to 2000 W. The ultrasonic system included an ultrasonic generator with a frequency of 20±2 kHz, a transducer, and a mild steel-made acoustic radiator [3].

Figure. 1. Experimental set-up: (a) conceptual model: 1 – US supply unit, 2 – US converter, 3 – waveguide, 4 – acoustic radiator, 5 – thermocouple, 6 – liquid alloy, 7 – melting furnace, 8 – positioning device; (b) laboratorial unit.

Al-Si alloys with 2%Fe materials were melted in a resistance furnace at 820-850° C. The melt was cooled down to a temperature of 750-780° C after degassing. The metal cup was preheated to 530-550° C by the heating furnace. Subsequently, about 600 g liquid metal was poured into the preheated metal cup. The USV was then applied on the melt with the ultrasonic vibrator immersed into the melt 15-20 mm in depth when the liquid metal cooled down to the predetermined temperature. The starting temperature of USV was 665° C, and ending temperature was 640° C. The USV treatment time was1.5 min [4].

The experimental setup for UST comprised a 5-kW ultrasonic generator, a 5-kW magnetostrictive transducer with water-cooling system and a niobium ultrasonic horn (sonotrode). Experiments were performed at the 4-kW generator power. The corresponding amplitude of vibrations was 40 μm, as measured by a contactless vibrometer. In each experiment, the amount of melt was 0.35 kg. The alloys were first molten in an electric furnace in graphite crucibles and then treated by ultrasound in different temperature ranges [5].

The various materials like AlSi9Cu3 alloy,7050 aluminium alloy,Mg-8Li-3Al alloy,AZ91 magnesium alloy ,A356 aluminium alloy were melted and applying Ultrasonic power source with different range[6-10] .

III CHARACTERIZATION

The below diagram referred to Microstructure of Ultrasonic vibration of castings with different frequencies. The implementation of ultrasonic vibration on the microstructure and mechanical properties of Al-17Si-2Fe-2Cu-1Ni alloys with 0.4% or 0.8% Mn were studied. The results show that the average grain size of primary Si in the alloys treated by USV could be refined to 21-24 μm[4]. Grain refinement (or) purification process of alloy with the help of Ultrasound the different powers was applied to treat AZ80 alloy melts to attain. The implement of ultrasonic powers from 0 W to 1400 W on microstructures of the AZ80 alloy with ultrasonic grain refinement treatment was investigated. The grain size of the alloy could be decreased from 387μm to 147μm after the ultrasound with the optimal power 600 W was applied to treat the melt [5].

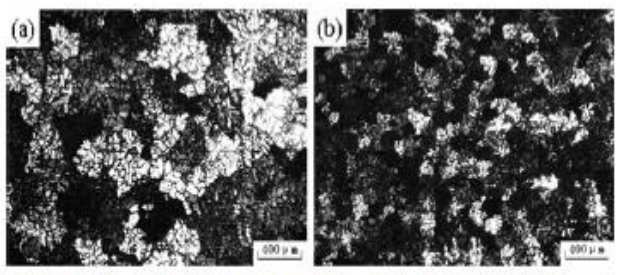

(Before vibration) (After vibration)

Figure.2.SEM Analysis of AZ80 alloy

Cite this article as: N.Suresh, P.Chandrasekar "A Review on Characteristics and Mechanical Behavior of Metal Castings under Ultrasonic Vibration Technique." *International Conference on Systems, Science, Control, Communication, Engineering and Technology (2015)*: 106-109. Print.

The effect of ultrasonic treatment on the formation of microstructure was systematically analyzed in hypo-eutectic, near-eutectic and hypereutectic Al-Si alloys, inclusive commercial piston alloys. The results show that UST usually results in the refinement of grains and primary Si particles when it is applied in a proper temperature range, while ultrasonic treatment during the whole solidification processing leads to coarsening effect on eutectic Si phase. An effective MMM (Multi-frequency, Multimode, Modulated) ultrasonic (US) technology was used to change the cast microstructure of the samples was analyzed by optical and scanning electron microscopy and energy dispersive spectrometry. Ultrasonic vibration developed the formation of small globular grains, changed the molecule size and morphology of intermetallic compounds and distributed them equally entire the castings [6].

Investigated the microstructures of 7050 aluminium alloys. Compared to the normal cast alloy, the ultrasonic cast ingot (UI) was characterized with a finer microstructure than that in the conventional cast ingot (CI). It was observed that the Ultrosonic Ingot alloy can be aged faster and aging-strengthened easier than the Conventional Ingot alloy[7]. Studied the effects of ultrasonic vibration on solidification structure of the alloy were investigated. Experimental results showed that the morphology of α- phase was modified from coarse rosette-like structure to fine globular one with the application of ultrasonic vibration [8].

The technique of ultrasonic vibration with different powers from 0W to 700W was applied during the solidification process of AZ91 alloy. The microstructures of alloy were characterized. Without apply to ultrasonic vibration (0W of ultrasonic power), the dendrites were coarse. Globular grains were obtained in AZ91 alloy subject to high intensive ultrasonic vibration. The grain size was reduced gradually from 202μm to 146μm with increasing ultrasonic power [9]. The impacts of high-energy ultrasonic field on the microstructure of A356 alloy are investigated. The result shows that the long dendritic silicon phases are split into number of particles [10].

IV MECHANICAL BEHAVIOR

A effective MMM (Multi-frequency, Multimode, Modulated) ultrasonic (US) technology was used to increase the mechanical properties of a AlSi9Cu3 alloy. Increased the value of Ultimate tensile strength and strain were to 332 MPa and 2.9%, respectively, which are 50% and 48% higher than the values derived for castings produced without vibration[3]. The implementation of ultrasonic vibration on the mechanical properties of Al-17Si-2Fe-2Cu-1Ni (mass %) alloys with 0.4% or 0.8% Mn were studied. With USV treatment, the UTS of A1 and A2 alloys are increased by 24.3% and 22.5% respectively at room temperature, compared to those of the alloys without USV treatment. The hardness of A1 and A2 alloys are also improved slightly after USV treatment [4].

Investigated the properties of ultrasonic 7050 aluminum alloys. When aged at 120 °C, the alloy attain its peak strength after 8 h, with tensile strength, yield strength and elongation of 602 MPa, of 547 MPa 12.7%,respectively. whereas the CI alloy plate had tensile strength of 536 MPa, yield strength of 462 MPa and elongation of 15.0%, after peak aged for 12 h [7]. The effects of ultrasonic vibration on solidification structure and properties of Mg-8Li-3Al alloy. Corrosion resistance and mechanical properties of the alloy were investigated. Corrosion resistance of the alloy with ultrasonic vibration for 90 seconds was improved compared with the alloy without ultrasonic vibration. Tensile strength and elongation of the alloy treated with ultrasonic vibration improved by 9.5 % and 45.7 % respectively [8].

The technique of ultrasonic vibration with different powers from 0W to 700W was applied during the solidification process of AZ91 alloy. Mechanical properties of the cured AZ91 alloy were characterized. The mechanical properties were improved by which the treated alloy. The ultimate tensile strength was increased from 145MPa to 195MPa and elongation to fracture from 2.3% to 5.2% correspondingly with increasing ultrasonic power [9]. The impact of high-energy ultrasonic field on the mechanical properties of A356 alloy is investigated. The acceptable improvement of mechanical properties can be reached due to the ultrasonic treating. The tensile strength yield stress and elongation are 293.85MPa, 207.34MPa and 6.98%, which are 1.55, 1.93 and 1.10 times to that of without high-energy ultrasonic treating, respectively[10].

V APPLICATIONS

The enhancement of mechanical properties due to the Ultrasonic vibration during the process of solidification has been widely applied in aerospace, automobile and industrial products. The composite materials are used in marine applications such as the construction of hull, connecting rod, and so on.

VI FUTURE SCOPE OF RESEARCH

The ultrasonic vibration technique may be used to improve the desirable characteristics of castings. By changing the process parameters such as frequency of vibration, time duration, pouring temperature, the castings can be fabricated thereby its mechanical properties and microstructure can be enhanced.

VII CONCLUSION

In this paper a review the effect of Ultrasonic vibration in various materials is discussed and its effects on the microstructure and mechanical properties are analyzed. Several researchers suggest vibration during casting with dendrite fragmentation, detachment have been identified as major factors which contributes the enhancement of grain structure and properties.

References

[1] Campbell, J., Effect of vibration during solidification, International Metals Review, vol. 26, no. 2, 1981, p.71-108.

Cite this article as: N.Suresh, P.Chandrasekar "A Review on Characteristics and Mechanical Behavior of Metal Castings under Ultrasonic Vibration Technique." *International Conference on Systems, Science, Control, Communication, Engineering and Technology (2015)*: 106-109. Print.

[2] Abdul-Karem, W., Kahlid F., Al-Raheem, F., Vibration improved the fluidity of aluminum alloys in thin wall investment casting, International Journal of Engineering Science and Technology, vol. 3, no. 1, 2011, p. 120 -135.

[3] H. Pugaa, S. Costaa, J. Barbosaa,*, S. Ribeirob, M. Prokicc., Influence of ultrasonic melt treatment on microstructure and mechanical properties of AlSi9Cu3 alloy, Journal of Materials Processing Technology ,vol.211, 2011, p. 1729– 1735.

[4] Chong Lin, Shusen Wu*, Shulin Lü, Ping An, Li Wan., Effects of ultrasonic vibration and manganese on microstructure and mechanical properties of hypereutectic Al-Si alloys with 2%Fe, Intermetallics ,vol.32, 2013,p. 176-183.

[5] Zhiwen Shao., Qichi Le., Zhiqiang Zhang., and Jianzhong Cui., Effect of Ultrasonic Power on Grain Refinement and Purification Processing of AZ80 Alloy by Ultrasonic Treatment, Met. Mater. Int., vol. 18, No. 2 2012, p. 209-215.

[6] L. Zhang., D.G. Eskin., A. Miroux., L. Katgerman., Formation of microstructure in al-si alloys under ultrasonic melt treatment, The Minerals, Metals & Materials Society, 2012 .

[7] Hua Shan, l., Xiang, Q., Zhi Hong, C., RongPiao, J., Xiao Quian, L., Effect of ultrasonic vibration during casting on microstructure and properties of 7050 Al alloy, Journal of Materials Science. vol. 46, no. 11, 2011, p. 3923 – 3927.

[8] Yao, L., Hao, H., Ji, S., Fang, C., Zhang, X., Effects of ultrasonic vibration on solidification structure and properties of Mg-8Li-3Al alloy. Transactions of Nonferrous Metals Society of China, vol. 21, 2011, p. 1241 –1246.

[9]. Deming Gao, Zhijun Li ., Qingyou Han., Qijie Zhai., Effect of ultrasonic power on microstructure and mechanical properties of AZ91 alloy, Materials Science and Engineering, vol.A 502, 2009, p. 2–5.

[10] Songli Zhang., Yutao Zhao., Xiaonong Cheng., Gang Chen., Qixun Dai., High-energy ultrasonic field effects on the microstructure and mechanical behaviours of A356 alloy, Journal of Alloys and Compounds, vol. 470 ,2009, p. 168–172.

Cite this article as: N.Suresh, P.Chandrasekar "A Review on Characteristics and Mechanical Behavior of Metal Castings under Ultrasonic Vibration Technique." *International Conference on Systems, Science, Control, Communication, Engineering and Technology (2015)*: 106-109. Print.

International Conference on Systems, Science, Control, Communication, Engineering and Technology 2015 [ICSSCCET 2015]

ISBN	978-81-929866-1-6
Website	icssccet.org
Received	10 - July - 2015
Article ID	ICSSCCET022

VOL	01
eMail	icssccet@asdf.res.in
Accepted	31- July - 2015
eAID	ICSSCCET.2015.022

Corrosion Behavior of Stainless Steel in Hydrochloric Acid and Nitric Acid Solutions

Dhanapal P[1], Dr. Ss. Mohammed Nazirudeen[2], Saiyath Ibrahim[3]
[1,3] Karpakam Institute of Technology
[2]PSG College of Technology.

ABSTRACT: *A detailed experimental study has been carried out to determine the pitting corrosion of 304 grade steel in acids like hydrochloric acid and nitric acid with different normalities. The corrosion rates have been calculated using weight loss method. In weight loss method without inhibitor, the sample pieces have been weighed and immersed into acids at different normalities like 4N, 5N, 6N, 7N, 8N for different time periods like 48 hours, 76 hours, 92 hours, 120 hours, 144 hours. The study reveals that maximum corrosion rate 0.64 mm/y of hydrochloric acid and 0.625mm/y in nitric acid occurred at the time period of 48 hours and at the normality of 8N. The inhibitor 2-Dimethyl amino ethanol for 8N is also applied to study the efficiency of the inhibitor. The results are also confirmed using the polarisation and FTIR studies.*

Keywords: **S**tainless steel; Corrosion; Hydrochloric acid; Polarization

1. INTRODUCTION

Austenitic stainless steels are among the most widely used types of stainless steel. The most commonly used grades are 300 series of alloys according the American Iron and Steel Institute (AISI). Starting from the basic 304 alloy (Fe-19Cr-10Ni), Mo is added to improve resistance to pitting (2-3 wt.% in the case of type 316 and 3-4 wt.% in type 317). Sensitization due to Cr depletion during welding and other heat treatments, and the possible resultant intergranular corrosion, can be avoided through the use of low-carbon grades (304L, 316L, 317L, in which C is limited to 0.03 wt.% max.) or by adding Ti (type 321) or Nb and Ta (type 347) to precipitate C at higher temperatures. The addition of Cr also imparts greater oxidation resistance, whilst Ni improves the ductility and workability of the material at room temperature (F. King, 2009). Stainless steel has important characteristics such as versatility, durability, attractiveness and high mechanical and corrosion resistance.

2. MATERIALS AND METHODS

Corrosion data here reported have been obtained through weight loss experiments of steel rod specimen.

Table 1. Composition of Stainless Steel (304)

Element	C	Mn	Si	P	S	Cr	Ni	N	Bal
%wt	0.08	2.00	0.75	0.045	0.03	18.00	9.00	0.1	Fe

Before weight loss and electrochemical measurements the sample were abraded with 600 grit SiC paper, washed with demonized water and acetone and dried. The dimensions of the samples are hexagon cross section of having 2.89 mm of side, Length 50 mm. Hydrochloric Acid and Nitric Acid both are used as 4N, 5N, 6N, 7N and 8N solution by mixing it with a specified ratio with the distilled water. And the solutions are made for 100 ml for every sample of testing.

Cite this article as: Dhanapal P, Dr. Ss. Mohammed Nazirudeen, Saiyath Ibrahim. "Corrosion Behavior of Stainless Steel in Hydrochloric Acid and Nitric Acid Solutions." *International Conference on Systems, Science, Control, Communication, Engineering and Technology (2015)*: 110-114. Print.

The samples are immersed into the acids for various time periods for testing. The time period taken into account for corrosion testing is 48 hrs, 72 hrs, 96 hrs, 120 hrs and 144 hrs. Diethyl amino ethanol is used as an inhibitor in stainless steel of grade 304. The usage of inhibitor on the corrosion medium is given below. Here the inhibitor has mixed in the solution by 10% that means 10 ml is added to the every 100 ml to get the various normality solutions. Polarization is an extremely important parameter because it allows useful statements to be made about the rates of corrosion process. In polarization studies 5%, 10%, 15% of inhibitor is mixed with the acid and inhibitor concentrations are tested. The polarization curves are drawn for the above said samples for stainless steel in the medium of 8N Hydrochloric Acid and 4N Nitric Acid.

A weighed sample of the metal or alloy under consideration is introduced into the process, and later removed after a reasonable time interval. The sample is then cleaned of all corrosion products and is reweighed. The weight loss is converted to a corrosion rate (CR) or metal loss (ML).The simplest way of measuring the corrosion rate of a metal is to expose the sample to the test medium and measure the loss of weight of the material as a function of time.

The weight loss is converted to a corrosion rate by the following formula.

$$\text{Corrosion rate} = \frac{K.W}{A.D.T}$$

Where,

K is a constant = 87.6

W is the weight loss in grams.

A is the surface area cm^2.

D is the density of the metal $gram/cm^3$.

T is the time in hours.

Fourier Transform Infrared Spectroscopy (FTIR) is a powerful tool for identifying types of chemical bonds in a molecule by producing an infrared absorption spectrum that is like a molecular "fingerprint".

FTIR is most useful for identifying chemicals that are either organic or inorganic. It can be utilized to quantify some components of an unknown mixture. It can be applied to the analysis of solids, liquids, and gasses. The term Fourier Transform Infrared Spectroscopy (FTIR) refers to a recent development in the manner in which the data is collected and converted from an interference pattern to a spectrum. Today's computerized FTIR instruments make them faster and more sensitive than the older dispersive instruments.

3. RESULTS AND DISCUSSION

3.1. RESULTS OF WEIGHT LOSS METHOD

The weight loss of the stainless steel in HCL and HNO_3 at different normalities is measured with and without inhibitor. The corrosion rate are calculated from the weight difference of the samples. The corrosion rate along with the weights before and after corrosion is tabulated in the following tables. Two samples in each category were considered and the average of the two is tabulated. Graphs are drawn based on the test timing. The graph is drawn between corrosion rate and normality of the acids where corrosion rate is taken in y-axis and normality of the acids are taken in x-axis. Two graphs are drawn for acids like HCL and HNO_3 separately.

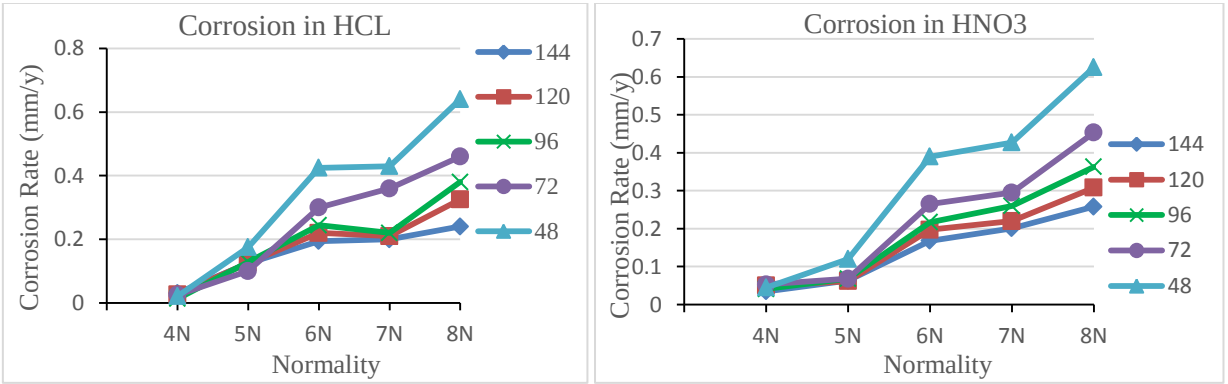

The above graph shows the rate of corrosion of 304 grade stainless steel in hydrochloric acid with respect to the normality of acid. The rate of corrosion is taken in Y-axis and the normality is taken in X-axis. Here the rate of corrosion for time period of 48 hours is very high as it reaches 0.65mm/y in 8N HCL solution and the corrosion rate value reduces as the normality reduces. The corrosion rate for time period 144 hours is very low when compared to other time periods. It reaches the corrosion rate of 0.23 mm/y in 8N solution and it further decreases when the normality decreases. The corrosion rate in 144 hours is less and more in 48 hours because at initial stage the colliding atoms will be very high and after the oxidation, the atoms will be less and the corrosion rate will be less when the time period increases.

Cite this article as: Dhanapal P, Dr. Ss. Mohammed Nazirudeen, Saiyath Ibrahim. "Corrosion Behavior of Stainless Steel in Hydrochloric Acid and Nitric Acid Solutions." *International Conference on Systems, Science, Control, Communication, Engineering and Technology (2015)*: 110-114. Print.

The above graph shows the rate of corrosion of 304 grade stainless steel in nitric acid with respect to the normality of acid. The rate of corrosion is taken in Y-axis and the normality is taken in X-axis. Here the rate of corrosion for time period of 48 hours is very high as it reaches 0.62 mm/y in 8N HCL solution and the corrosion rate value reduces as the normality reduces. The corrosion rate for time period 144 hours is very low when compared to other time periods. It reaches the corrosion rate of 0.258 mm/y in 8N solution and it further decreases when the normality decreases. The corrosion rate in 144 hours is less and more in 48 hours because at initial stage the colliding atoms will be very high and after the oxidation, the atoms will be less and the corrosion rate will be less when the time period increases.

3.2 POLARISATION CURVE (HCL)

3.2.1 RESISTANCE METHOD

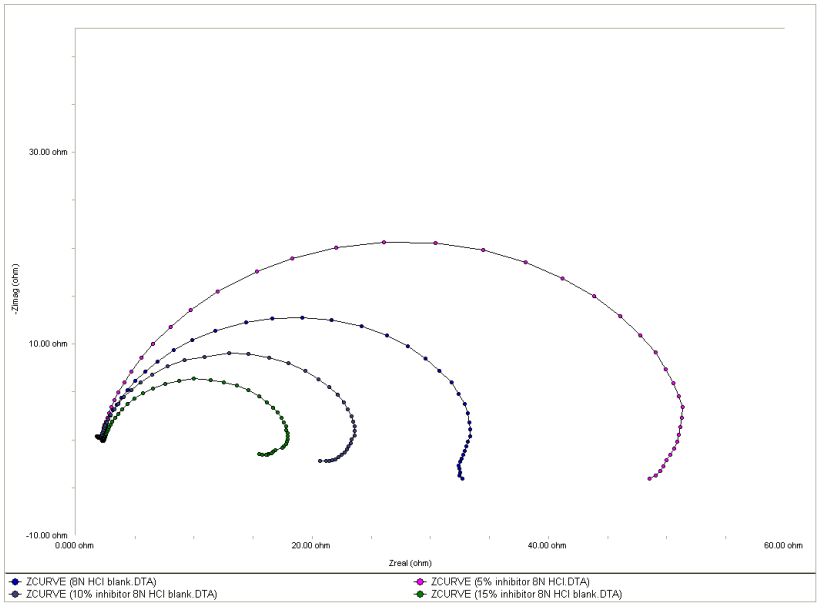

Figure 4.3 Polarisation curve for HCL (Resistance Method)

The above graph describes the polarisation curve by resistance method for various percentage of inhibitors mixed in hydrochloric acid. Here the resistance Zreal is taken in X-axis and the imaginary resistance Zimg is taken in Y-axis. Both the resistances are measured in ohms. When 5% of inhibitor is used, the real resistance value is higher which reaches nearly 52 ohms where the imaginary resistance value is also very high. When inhibitor is not used, the real resistance value reaches 35 ohms and the imaginary value also reaches more than 10 ohms. When 10% inhibitor is used, the real resistance value reaches 22 ohms and when 15% inhibitor is used, the resistance value is less than 20 ohms.

3.2.2 POTENTIAL METHOD

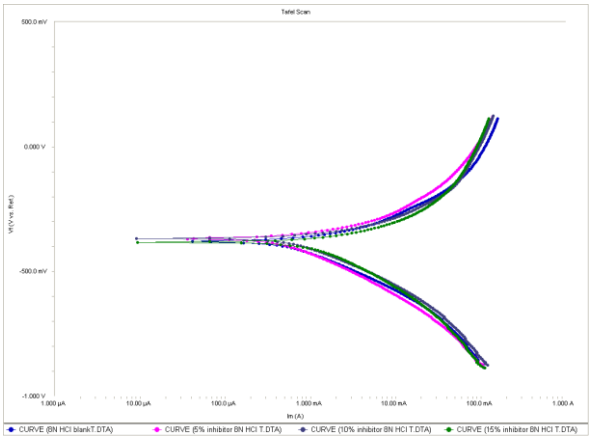

Figure 4.4 Polarisation curve for HCL (Potential Method)

Cite this article as: Dhanapal P, Dr. Ss. Mohammed Nazirudeen, Saiyath Ibrahim. "Corrosion Behavior of Stainless Steel in Hydrochloric Acid and Nitric Acid Solutions." *International Conference on Systems, Science, Control, Communication, Engineering and Technology (2015)*: 110-114. Print.

The above graph describes the polarisation curve by potential method for various percentage of inhibitors mixed in hydrochloric acid. Here the current I is taken in X-axis and the potential difference V is taken in Y-axis. Current is measured in ampere and potential difference is measured in voltage. This graph illustrates minimum difference in current value when any type of inhibitor is used. In every percentage of inhibitor the maximum current value of 120 milliampere is attained. Two curves are obtained in which one curve travels towards positive values of potential difference and another one travels towards the negative values of potential difference. The maximum value of potential value is 200 volts in positive side and 100 volts in negative side.

3.3 POLARISATION CURVE (HNO_3)

3.3.1 RESISTANCE METHOD

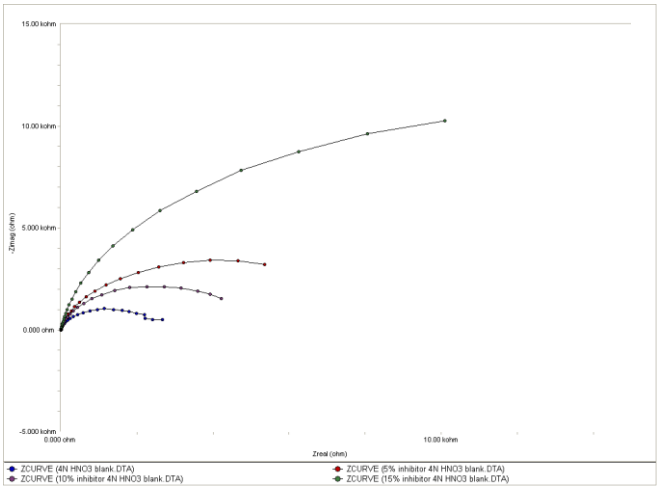

Figure 4.5 Polarisation curve for HNO_3 (Resistance Method)

The above graph describes the polarisation curve by resistance method for various percentage of inhibitors mixed in nitric acid. Here the resistance Zreal is taken in X-axis and the imaginary resistance Zimg is taken in Y-axis. Both the resistances are measured in ohms. When 15% of inhibitor is used, the real resistance value is higher which reaches nearly 11 kiloohms where the imaginary resistance value is also very high. When inhibitor is 5%, the real resistance value reaches 5 kiloohms and the imaginary value also reaches more than 10 ohms. When 10% inhibitor is used, the real resistance value reaches 5 kiloohms and when inhibitor is not used, the resistance value is less than 4 kiloohms.

3.3.2 POTENTIAL METHOD

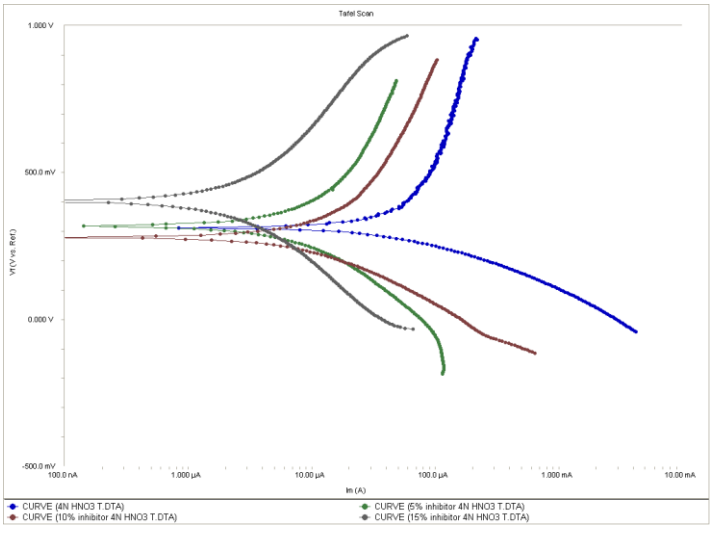

Figure 4.6 Polarisation curve for HNO_3 (Potential Method)

The above graph describes the polarisation curve by potential method for various percentage of inhibitors mixed in nitric acid. Here the current I is taken in X-axis and the potential difference V is taken in Y-axis. Current is measured in ampere and potential difference is measured in voltage. Here each percentage of inhibitor consists of two curves in which one travels towards positive value of potential difference and another one travels towards the negative value of the potential difference. When the inhibitor is not used, the

Cite this article as: Dhanapal P, Dr. Ss. Mohammed Nazirudeen, Saiyath Ibrahim. "Corrosion Behavior of Stainless Steel in Hydrochloric Acid and Nitric Acid Solutions." *International Conference on Systems, Science, Control, Communication, Engineering and Technology (2015)*: 110-114. Print.

current value reaches a maximum of 8 milliampere in negative side of potential difference. The minimum value of the current is attained when 5% inhibitor is used which is 80 micro ampere in positive side of potential difference.

3.4 Corrosion with Inhibitor

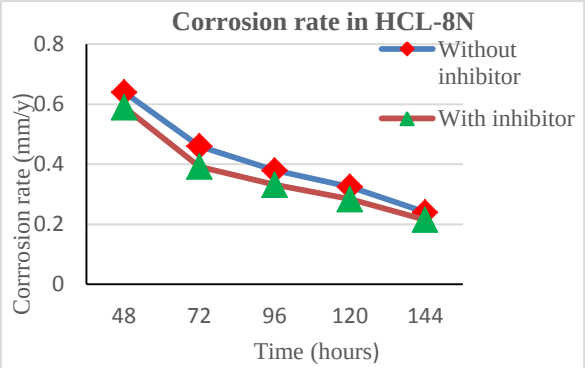

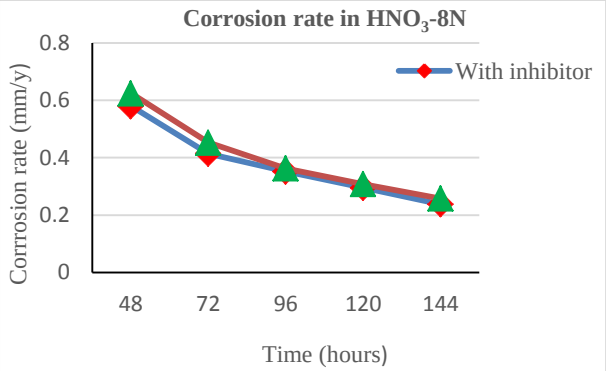

Figure 4.7 Corrosion rate in HCL-8N

Figure 4.8 Corrosion rate in HNO_3-8N

4. CONCLUSION

The corrosion effect of hydrochloric acid and nitric acid on stainless steel of grade 304 has been studied by using weight loss method.

- The study reveals that maximum corrosion rate 0.64 mm/year occurred at the time period of 48 hours and at the normality of 8N of hydrochloric acid and corrosion rate of 0.625 occurred at the time period of 48 hours and at a normality of 8N of nitric acid.
- The corrosion rate decreases if the test time increases and the normality decrease.
- Addition of inhibitor of 10% reduces an amount of 14.78% in corrosion rate.
- The polarisation studies also denote that higher normality has high real resistance value which shows high corrosion rate.

REFERENCE

1. Ehteram A. Noor, Aisha H. Al-Moubaraki, "Corrosion Behavior of Mild Steel in Hydrochloric Acid Solutions", Int. J. Electrochem. Sci., Vol. 3, 806 – 818, (2008).
2. Rohtash, Ajay K. Singh, Rajendra Kumar, "Corrosion Study of Stainless Steels in Peracetic Acid Bleach Media With and Without Chloride and Chelant", International Journal of Research and Innovations in Science and Technology, Vol. 1: Issue 1: 2014.
3. Bikic F.A and Mujagic D.B, "Investigation of possibility for reducing AISI 303 stainless steel pitting corrosion by microalloying with boron or zirconium", Bulletin of the Chemists and Technologists of Bosnia and Herzegovina, Vol. 42, pp 41- 46, 2014.
4. Henrique Ribeiro Piaggio Cardoso, Tiago Falcade, Sandra Raquel Kunst , Celia Fraga Malfatti, "Corrosion and Wear Resistance of Carbon Films Obtained by Electrode position on Ferritic Stainless Steel" Mat. Res. vol.18 no.2 Mar./Apr. 2015.
5. L.A. Dobrzański, Z. Brytan, M. Actis Grande, M. Rosso, "Corrosion resistance of sintered duplex stainless steel evaluated by electrochemical method" journal of Achievements in Materials and Manufacturing Engineering, Vol. 19, issue 1, pp 38-45, 2006.
6. Mohd Talha, C. K. Behera and O. P. Sinha, "Potentiodynamic polarization study of Type 316L and 316LVM stainless steels for surgical implants in simulated body fluids", Journal of Chemical and Pharmaceutical Research, 4(1):203-2082012.
7. Cheng-Hsun Hsu, Kuan-Hao Huang, Yi-Tsung Chen, Wei-Yu Ho, "The effect of electroless Ni–P interlayer on corrosion behavior of TiN-coated austempered ductile iron", Thin Solid Films, 529, (2013) 34–38.
8. T.J. Mesquita, R.P. Nogueira and I.N. Bastos, "Factorial design applied to corrosion of superduplex stainless steel", Lat. Am. appl. res. vol.41, no.4, 2011.

Cite this article as: Dhanapal P, Dr. Ss. Mohammed Nazirudeen, Saiyath Ibrahim. "Corrosion Behavior of Stainless Steel in Hydrochloric Acid and Nitric Acid Solutions." *International Conference on Systems, Science, Control, Communication, Engineering and Technology (2015)*: 110-114. Print.

International Conference on Systems, Science, Control, Communication, Engineering and Technology 2015 [ICSSCCET 2015]

ISBN	978-81-929866-1-6
Website	icssccet.org
Received	10 - July - 2015
Article ID	ICSSCCET023

VOL	01
eMail	icssccet@asdf.res.in
Accepted	31- July - 2015
eAID	ICSSCCET.2015.023

Analysis of Missile Bodies with Various Cross sections and Enhancement of Aerodynamic Performance

R.NALLAPPAN[1] , M.PRASATH[2], R.RAJKUMAR[3], K.UDHAYAN[4]
[1]Assitant Professor,Karpagam Institute of Technology
[2, 3, 4] Karpagam Institute of Technology
Coimbatore-641105,India

Abstract: *In order to optimize the geometry of the missile's cross-section for transportation purposes and also to obtain higher aerodynamic efficiencies, non-circular bodies have gained substantial attention by many researchers. In this work, we have compared the aerodynamic characteristics of three missiles having the same cross sectional areas, but different shapes (one circular , one square with round corners and one hexagonal with round corners). In order to differentiate the non-circularity and the fin effects, we have considered the bodies with no fins. A three dimensional, compressible, stationary, viscous, turbulent flow has been simulated using the FLUENT CFD code with the standard k-ε model. Our results indicate that, even though the square section missile has more friction drag, it produces less overall drag , similarly the hexagonal section has more frictional drag than square model , it produces less overall drag compared to both the square and circular section. Also, its lift is higher than that of the circular and square case and thus has a higher aerodynamic efficiency. Moreover, the rate of increase of the aerodynamic efficiency with increasing of the angle of attack is higher than that of circular and square section.*

keywords: Missiles configurations, CFD Analysis, Hexagonal Missiles

1 General Introduction

With increasing concern over security and exploitation of space plays a major role in the advancement of new technologies that are challenging each and every country in the field of rockets and missiles.
Various studies about the missiles are carried out in area to increase its efficiency and range of operation. In this content aerodynamic analysis of missile with different cross-sectional shapes in one such important task that helps to increase the ways for obtaining greater range and better aerodynamic efficiency.

1.1.MissileIntroduction.

Missiles are generally categorized by their launch platform and intended target. In broadest terms, these will either be surface (ground or water) or air, and then sub-categorized by range and the exact target type (such as anti-tank or anti-ship). Many weapons are designed to be launched from both surface and the air, and a few are designed to attack either surface or air targets (such as the ADATS missile). Most weapons require some modification in order to be launched from the air or ground, such as adding boosters to the ground launched version.

Cite this article as: R.NALLAPPAN, M.PRASATH, R.RAJKUMAR, K.UDHAYAN. "Analysis of Missile Bodies with Various Cross sections and Enhancement of Aerodynamic Performance." *International Conference on Systems, Science, Control, Communication, Engineering and Technology (2015)*: 115-119. Print.

Nomenclature

α	angle of attack
C_L	coefficient of lift
C_D	coefficient of drag
$M\infty$	free stream mach
C_p	pressure coefficient

2. Design of Missiles

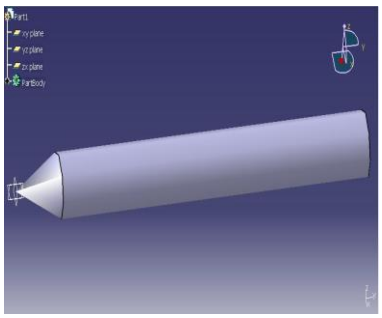

figure.1(a) circular missile

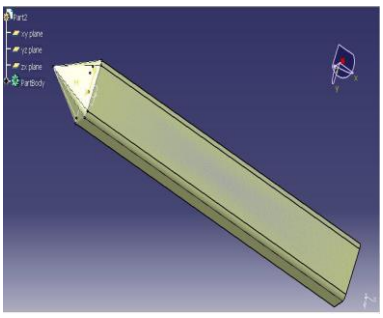

figure.1(b) . square missile

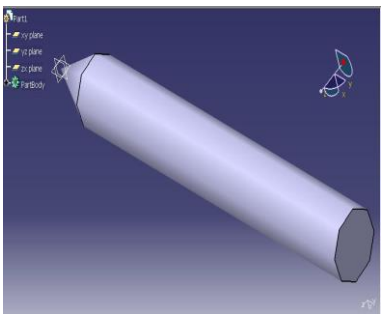

figure.1(c) hexagonal missile

First, a 3d missile model without fin was created in CATIA with the dimensions as shown in the fig.2.1.the non dimensional length of the missile is 36.44 including the conical region. The diameter is kept as 4.8.The non-dimensional scale considered is 1mm as the length scale and free stream velocity as the velocity scale

3.Computational analysis

The flow considered here is three-dimensional, compressible, stationary, viscous, turbulent and singlephase . The fluid is air, for which the viscosity is obtained using Sutherland relation.

3.1Turbulence modeling

The turbulence model used was a 2-equation model, the standard k-ε where k is the turbulent kinetic energy and ε is the dissipation rate. This is a semi-empirical model that uses constants determined from air and water experiments (FLUENT, Tannehill). The model assumes that the flow is fully turbulent. κ-ε model is a two-equation model, in which the averaged Reynolds stress is proportional to the averaged velocity gradient and the proportionality constant (μT) is to be found from the κ and the ε equations

3.2.Grid generation

For analysis domain considered is as follows, circumferential outer boundary is at a distance of 15D from the missile and in the axial direction domain boundaries are considered at 5D from the leading edge of the missile to 10D from the end of the missile. The grid over the missile and outer domain grid are generated using GAMBIT. The mesh used is Tri-primitive type(Triangular mesh).

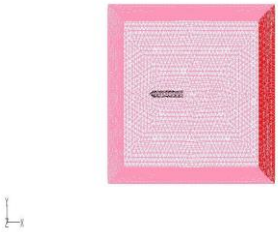

figure 2.(a) . 3D grid of Square missile

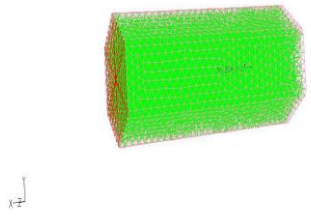

figure 2.(b) 3D grid of hexagonal missile

Cite this article as: R.NALLAPPAN, M.PRASATH, R.RAJKUMAR, K.UDHAYAN. "Analysis of Missile Bodies with Various Cross sections and Enhancement of Aerodynamic Performance." *International Conference on Systems, Science, Control, Communication, Engineering and Technology (2015)*: 115-119. Print.

figure 2.(c) 3D grid of circular missile

3.3. 3d Analysis Results

All 3D CFD cases were performed using the Fluent 3D double precision solver. Default criteria were used for most parameters. The convergence criteria for the residuals were again set at 1e-6. The residual tolerances were never achieved but were set to allow the solver to continue to iterate. The case was stopped after the lift and drag coefficients had reached steady values to at least 4 significant digits. The Courant number used for the cases was one.

3.3.(a) . circular missile

The 3D analysis of all missiles are computed and plotted for various mach numbers. The contours and vectors of all misiles are displayed in the following figures.

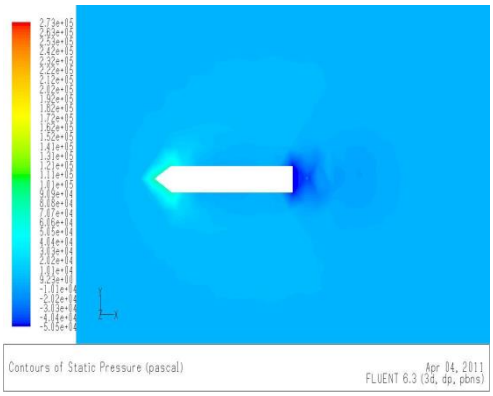

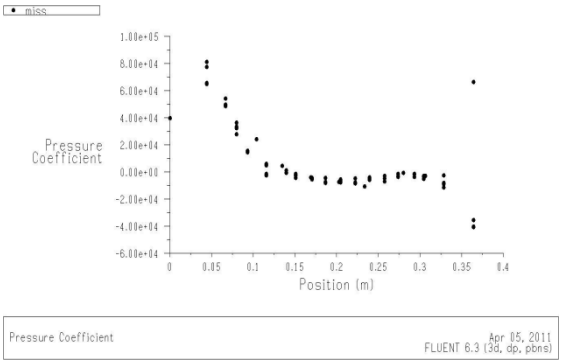

3.3.(b). Square missile

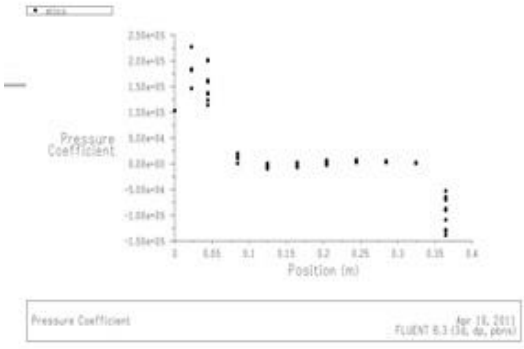

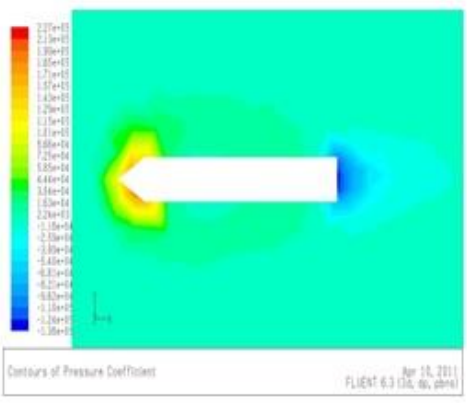

Cite this article as: R.NALLAPPAN, M.PRASATH, R.RAJKUMAR, K.UDHAYAN. "Analysis of Missile Bodies with Various Cross sections and Enhancement of Aerodynamic Performance." *International Conference on Systems, Science, Control, Communication, Engineering and Technology (2015)*: 115-119. Print.

3.3.(c).hexagonal missiles

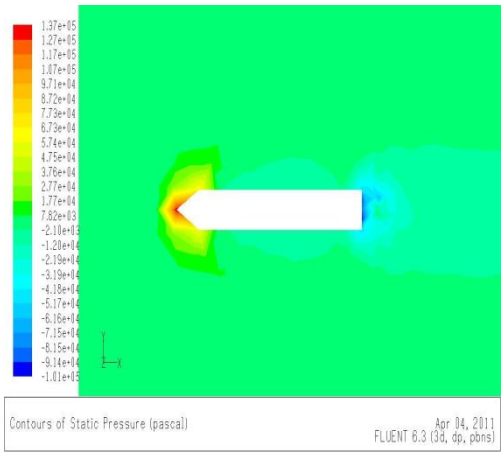

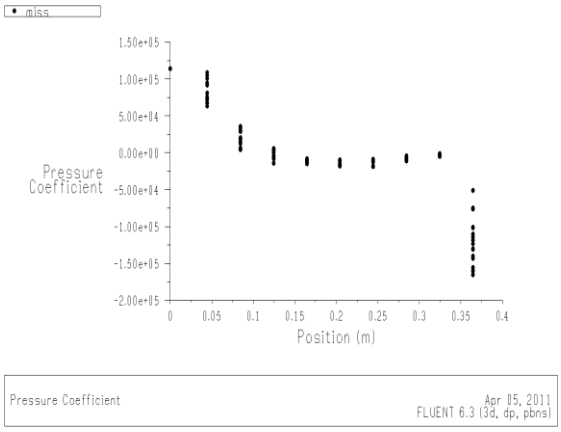

Result and discussion

The plots done for pressure distribution at various positions for different speeds. At mach number 1,the maximum Cp occurs at 0.1m. It shows, the velocity is minimum (345 m/s) compared to free stream velocity. This is due to the propagation of shock wave a head of the fore body. The Cp value decreases 0.25m and becomes negative at 0.25m of the missile body and it becomes constant at 0.4m of missile length. This is due to formation of expansion wave at the tail portion of the missile length. The static pressure over the length of missile decreases due to the presence of expansion waves, decreases at a distance of 0.4m from the leading edge of the missile length and the static pressure decreases below the free stream pressure, so Cp becomes negative, which can be obtained from

$$Cp = (P / P\infty - 1) / (1/2 * \gamma * M\infty 2)$$

At M∞=2 the Cp value increase is low compared to that of Cp at M∞=1 and its remains constant throughout the length of the missile body length. This is due to decrease of free stream mach number at the tip of the fore body.It shows the static pressure rise over the missile length. In this circumstance the point of inflection moves towards the downstream.

Further increase of free stream mach number (1 to 4), the cp distribution shows similarity i.e., the static pressure increases over the fore body. In all the cases the point of inflection keeps on increasing with free stream mach number. It shows that shock also moves with respect to point of inflection, mean while the prandtl-Meyer expansion takes place.

It is very tedious to predict the flow characteristics at M∞=4.Because it is a mixed flow of both supersonic and hypersonic flow.

Conclusion

Three missiles circular ,square and hexagonal of diameter 4.8cm and length 36.44cm (nose section 4.44cm and body 32cm length) with tapper of 5 degree for hexagonal and square section has been tested for supersonic mach number 1 to 4.This study will motivate the need of aerospace industry to quickly and inexpensively determine characteristics of missile without the need of wind tunnel experiments, which are difficult and expensive.

An analysis of the above results, has led to the following conclusions.

1. For allthe missile the shock is seen attached as the Mach number increases a detached shock wave is obtained.
2. In the case of circular missile have good lift characteristics but the over all drag is high compared to square missile.
3. As in the case of square missile the nose cone drag is high while the over all drag is low compared to that of the circular missile.
4. The Cp value for the hexagonal missile is low for all mach numbers compared to circular and square missiles.
5. When comparing all the missiles the hexagonal exhibit better aerodynamic characteristics for all the mach numbers.
6. With the attachments of fin a better aerodynamic characteristics and a good result can be obtained.

References

1. [1].Jackson, C.M. and Sawyer, W.C., "Bodies with Non-Circular Cross-Sections and Bank-to-Turn Missiles",Progress in Astronautics and aeronautics, Vol. 141, pp. 365-389, 1991.
2. [2]Graves, E.B., "Aerodynamic Characteristics of a Mono-Planar Missile Concept with Bodies of Circular and Elliptical Cross-Sections", NASA TM-74079, Dec. 1977
3. .[3] Sharma, R.K., "Experimental Aerodynamic Characteristics of Elliptical Bodies with Variation in Ellipticity Ratio", AIAA-2000-4505, 18th AIAA Applied Aerodynamics Conference & Exhibit., Aug. 2000.
4. [4] Sigal, A. and Lapidot, E., "The Aerodynamic Characteristics of Configurations Having Bodies with Square, Rectangular, and Circular Cross-Sections at a Mach Number of 0.75", AIAA, Inc., 1987

Cite this article as: R.NALLAPPAN, M.PRASATH, R.RAJKUMAR, K.UDHAYAN. "Analysis of Missile Bodies with Various Cross sections and Enhancement of Aerodynamic Performance." *International Conference on Systems, Science, Control, Communication, Engineering and Technology (2015)*: 115-119. Print.

5. .[5]Nielsen, J.N., "Problems Associated with the Aerodynamic Design of Missile Shapes, Proceedings of the Second Symposium on Numerical and Physical Aspects of Aerodynamic Flows, Long Beach, CA, Jan. 1983.
6. [6] Schneider, W., "Experimental Investigation of Bodies with Non-circular Cross-Section in Compressible Flow", AGARD-CP-336, Symposium on Missile Aerodynamics, Trondheim, Norway, pp. 19-1-19-15, Sept. 1982
7. .[7]Daniel, D.C., Yechout, T.R., and Zollars, G.J., "Experimental Aerodynamic Characteristics of Missiles with Square Cross-Sections", Journal of S&R, Vol. 19, 1982.
8. [8]Keimasi, M.R. and Taeibi-Rahni, M., "Numerical Simulation of Jets in a Cross-Flow Using Different Turbulence Models", AIAA Journal, vol. 39, Dec. 2001.
9. [9] "FLUENT 5 User's Guide", FLUENT Incorporated, July 1998.
10. [10] Birch, T.J., Wrisdale, I.E., and Prince, S.A., "CFD Predictions of Missile Flow-Fields", AIAA 2000-4211, 18th AIAA Applied Aerodynamics Conference & Exhibit., Aug. 2000.
11. [11] Bulbeck, C.J., Morgan, J., and Fairlie, B.D., "RANS Computations of High-Incidence Missile Flow Using Hybrid Meshes", AIAA 2000-4209, 18th AIAA Applied Aerodynamics Conference & Exhibit., Aug. 2000.

Cite this article as: R.NALLAPPAN, M.PRASATH, R.RAJKUMAR, K.UDHAYAN. "Analysis of Missile Bodies with Various Cross sections and Enhancement of Aerodynamic Performance." *International Conference on Systems, Science, Control, Communication, Engineering and Technology (2015)*: 115-119. Print.

International Conference on Systems, Science, Control, Communication, Engineering and Technology 2015 [ICSSCCET 2015]

ISBN	978-81-929866-1-6	**VOL**	01
Website	icssccet.org	**eMail**	icssccet@asdf.res.in
Received	10 - July - 2015	**Accepted**	31- July - 2015
Article ID	ICSSCCET024	**eAID**	ICSSCCET.2015.024

Efficient Implementation of Fast FCS Architecture using Viterbi Coders

R R Thirrunavukkarasu[1], R Satheeshkumar[2]
[1, 2] Assistant Professor, Department of ECE
[1]Karpagam Institute of Technology,
[2]KSR College of Technology, Coimbatore.

Abstract: *Viterbi algorithm is widely used as a decoding technique for convolutional codes as well as a bit detection method in storage devices. The design space for VLSI implementation of Viterbi decoders is huge, involving choices of throughput, latency, area, and power. This Paper propose Fast ACS architecture to reduce the area and power of the ACS unit in viterbi decoder. With the proposed structure it is possible to reduce the area and power of the ACS unit by 30% to 40% compare to conventional ACS architecture. The results are based on real designs for which actual synthesis and layouts are obtained using synopsys.*

Keywords: Viterbi algorithm, VLSI design.

I.INTRODUCTION

The Viterbi decoding algorithm, proposed in 1967 by Viterbi, is a decoding process for convolutional codes in memory-less noise. The algorithm can be applied to a host of problems encountered in the design of communication systems. In addition, the optimization criteria and the design figures keep on changing with the advancement in CMOS technology and design tools.
Different design aspects of the Viterbi decoder have been studied in a number of research papers [1]–[9]. However, most researchers concentrate on one specific component of the design (e.g., path metrics unit or survival memory unit). Somewhat more general studies are presented in [1], [8], and [9]. Still, in authors' view, a systematic and comprehensive analysis summarizing and characterizing as many of the trade-offs and implementation techniques as possible is missing. This contribution presents such a survey, providing designers with clear guidelines and references to find the best solution for every specific case.

II. GENERAL STRUCTURE OF THE VITERBI ALGORITHM

Viterbi decoding algorithm is the most popular method to decode convolutional error correcting codes. In a convolutional encoder, an input bit stream is passed through a shift register. Input bits are combined using the binary single bit addition (XOR) with several outputs of the shift register cells. Resulting output bit streams represent the encoded input bit stream. Generally speaking, every input bit is encoded using output bits, so the coding rate is defined as1/n (or k/n if input bits are used). The constraint length of the code K is defined as the length of the shift register plus one. Finally, generator polynomials G_x define which bits in the input stream have to be added to form the output. An encoder is completely described by n polynomials of degree k or less. A basic flow of viterbi decoder is shown below in Figure 1.

Cite this article as: R R Thirrunavukkarasu, R Satheeshkumar. "Efficient Implementation of Fast FCS Architecture using Viterbi Coders." *International Conference on Systems, Science, Control, Communication, Engineering and Technology (2015)*: 120-123 Print.

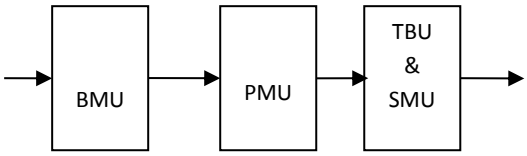

Fig 1 Block Diagram

A. Branch Metric Unit

A branch metric unit's function is to calculate branch metrics, which are average distances between every possible symbol in the code alphabet, and the received symbol.

B. Path Metric Unit

1). Design Space

PMU is a critical block both in terms of area and throughput. The key problem of the PMU design is the recursive nature of the add-compare-select (ACS). Figure 2 shows the ACS Block diagram. In order to increase the throughput or to reduce the area; optimizations can be introduced at algorithmic, word or bit level. To obtain a very high throughput, parallelism at algorithmic level is exploited. By algorithmic transformations, the Viterbi decoding is converted to a purely feed forward computation. This allows independent processing of input blocks. The algorithmic parallel block processing methods intend to achieve unlimited concurrency by independent block decoding of input stream. These techniques result in quite high area figures. But as technological advancements are making the devices shrink, they are getting more attractive. Still, for a specific case, if required throughput can be achieved by utilizing word or bit level optimization techniques, there is no specific need to use algorithmic transformations. Word level optimizations work on folding (serialization) or unfolding (parallelization) the ACS recursion loop. In the folding technique, the same ACS is shared among a certain set of states. This technique trades off throughput for area. This is an area efficient approach for low throughput decoders, though in case of folding, routing of the PMs becomes quite complex. With unfolding, two or more trellis stages are processed in a single recursion (this is called look ahead).

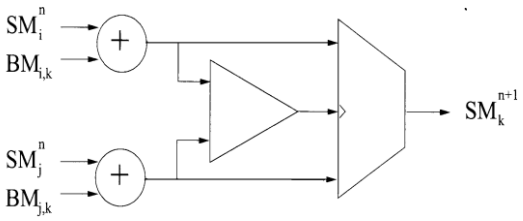

Fig 2 ACS unit for the Viterbi decoder

2). Path Metric Precision

The register temporarily storing path metrics should be wide enough to avoid overflow errors in the PMU operations. Modulo arithmetic is usually used for this purpose. PM bit width is determined as follows:

$PM_{BW} = [\log_2 B + \log_2(2x2x(K-1))]$

C. Trace Back Unit

Trace Back Unit restores a maximum-likelihood path from the decisions made by PMU. Since it does it in inverse direction, a viterbi decoder comprises a FILO (first-in-last-out) buffer to reconstruct a correct order.

D. Survivor Memory Unit

The survivor path storage block is necessary only for the trace back approach. The block records the survivor path of each state selected by the ACS module. It requires one bit of memory per state per stage to indicate whether the survivor path is the upper one or the lower one. The Combined TBU (TRACE BACK UNIT) and SMU (SURVIVOR MEMORY UNIT) generates the decoded outputs.

III. NEW STRUCTURE: DOUBLE STATE: FAST ACS METHOD

The proposed FAST ACS method uses clock gating technique for low power and also it replaces the existing ACS in path metric unit by placing new ACS architecture. The new method accepts the branch metric values with equal weights which are a single state architecture for the butterfly processing unit of the path metric unit it can also be calculated for Double state. The Fast ACS structure is shown in Figure 3.

Cite this article as: R R Thirrunavukkarasu, R Satheeshkumar. "Efficient Implementation of Fast FCS Architecture using Viterbi Coders." *International Conference on Systems, Science, Control, Communication, Engineering and Technology (2015)*: 120-123 Print.

For simplicity, we assume a binary input case (m=2). This result can be easily generalized to a multiple-input level case. Also, we continue explaining a new structure in the MLSD case. Applying the same structure to the ML convolutional decoder is straightforward.

First, note that the channel response polynomial H(D) of N order could be written as $H(D) = h_0+h_1D+\ldots.+h_ND^N+0.D^{N+1.}$ The numbers next to the states represent the input sequence. Also, the numbers on the arrow line show the ideal channel output associated with the transition.

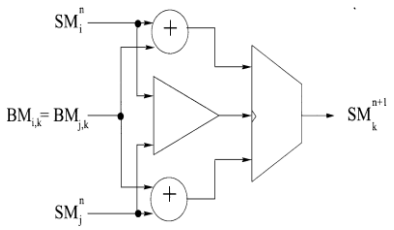

Fig 3 A Fast ACS unit

For a channel H (D) which has a zero coefficient for the last coefficient, the BMs for two transitions which have the same ending state are the same, because the two starting states are different in only the oldest bit position. In this case, the Viterbi processor 2^{N+1} has H (D) states, even though is actually a polynomial of order N (thus the term "double state").

By having the double state in a trellis, the BMs ending in one state are all the same. This means that when choosing the minimum of two possible SMs $SM_i^n + BM_{i,k}$ and $SM_j^n + BM_{j,k}$, we can select the less of two previous SMs SM_i^n and SM_j^n without waiting for an addition of the BMs. (In this case, $BM_{i,k} = BM_{j,k}$) Equivalently, we perform the following recursion.

$$SM_k^{n+1} = \min (SM^n_i) + BM_k^n$$

For example, in the current state 00 of Fig. 3, two incoming paths from the previous states 00 and 10 have the same BM 0. This applies to all the other states, since in the double state, the oldest input to the Viterbi processor makes no contribution on computing the BM for each state transitions.

Therefore, in the double-state structure, the "Add" operation which computes the SM can be carried out at the same time as the "Compare" operation. This new structure is shown in Fig. ---. As clearly shown in this diagram, two BMs $BM_{i,k}$ and $BM_{j,k}$ are the same. A combined ACS unit is shown below in Figure 4.

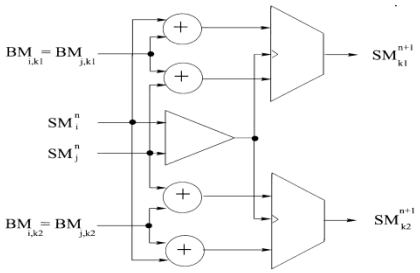

Fig 4 A combined ACS units.

IV.SIMULATION RESULTS

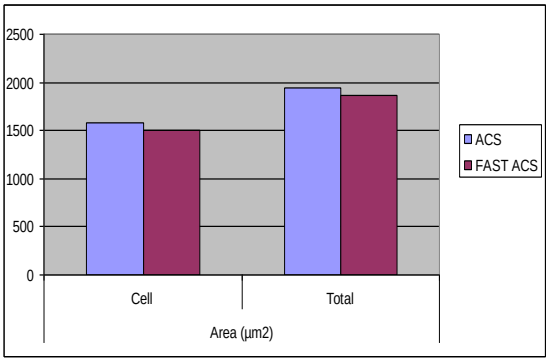

Fig 6 Power comparison of Decoder unit

Cite this article as: R R Thirrunavukkarasu, R Satheeshkumar. "Efficient Implementation of Fast FCS Architecture using Viterbi Coders." *International Conference on Systems, Science, Control, Communication, Engineering and Technology (2015)*: 120-123 Print.

V.CONCLUSIONS

In this paper, a comprehensive analysis of the Viterbi decoder design space is presented. Table I and II summarizes the importance of the different subunits of the decoder depending on the optimization criteria. The most significant contributions of the paper can be summarized as quantitative comparison of different ACS architectures; in particular, the Fast ACS unit and the conventional Radix 2 ACS are been Compared. For a better overview of the material, Table I and II summarizes the charts and tables related to different design aspects to choose the Fast ACS Viterbi decoder design over the conventional Radix 2 ACS.

REFERENCES

[1] Irfan Habib, Özgün Paker, *Member, IEEE*, and Sergei Sawitzki, *Member, IEEE* "Design Space Exploration of Hard-Decision Viterbi Decoding: Algorithm and VLSI Implementation" IEEE transactions on Very Large Scale Integration (VLSI) systems, vol. 18, no. 5, May 2010.

[2] inkyu lee senior member IEEE, and Jeff L. Sonntang"A New Architecture for the Fast Viterbi Algorithm"IEEE transactions on Communications vol 51.,no 10 october 2003.

[3] F. Angarita, M. J. Canet, T. Sansaloni AND J. Valls" Architectures for the Implementation of a OFDM-WLAN Viterbi Decoder" Springer ScienceJournal of Signal Processing Systems 52, 35–44, 2008.

[4] G. Fettweis, H. Meyr, "Cascaded feedforward architecture for parallel Viterbi decoding,"*IEEE ISCAS,* 978-81, *subm. Kluwer J. VLSI Sig. Proc.* 1990.

Cite this article as: R R Thirrunavukkarasu, R Satheeshkumar. "Efficient Implementation of Fast FCS Architecture using Viterbi Coders." *International Conference on Systems, Science, Control, Communication, Engineering and Technology (2015)*: 120-123 Print.

International Conference on Systems, Science, Control, Communication, Engineering and Technology 2015 [ICSSCCET 2015]

ISBN	978-81-929866-1-6	**VOL**	01
Website	icssccet.org	**eMail**	icssccet@asdf.res.in
Received	10 - July - 2015	**Accepted**	31- July - 2015
Article ID	ICSSCCET025	**eAID**	ICSSCCET.2015.025

Analysis of Different Routing Protocols for Wireless Sensor Networks

[1]C.H. Ram Manoger Lokiya, [2]S. Gopinath
1,2 Assistant Professor, Department of ECE
1Karpagam Institute of Technology, Coimbatore

ABSTRACT: *Wireless Sensor Networks (WSN) are an emerging and very interesting technology applied to different applications. They are formed by small, self organized devices that cooperate to form a large scale network with thousands of nodes covering a large area. The independent operation of the devices and the self-organization feature of the network present some challenges related to security, particularly regarding the security of the processed and routed data over the network. WSN are generally used to monitor activities and report events, such as fire,overheating etc. in a specific area or environment. It routs data back to the Base Station (BS). Data transmission is usually a multi-hop from node to node towards the BS. Sensor nodes are limited in power, computational and communication bandwidth.Primary goal of researchers is to find the energy efficient routing protocol.This study highlights the different routing protocol with advantages and limitations.*

Introduction

I. ENERGY EFFICIENT PROTOCOLS FOR WIRELESS SENSOR NETWORKS

SPIN (Sensor Protocols for Information via Negotiation)

- SPIN [18,22] is among the early work to pursue a data-centric routing mechanism. The idea behindSPIN is to name the data using high-level descriptors or meta-data. Before transmission, metadata are exchanged among sensors via a data advertisement mechanism, which is the key feature of SPIN. Each node upon receiving new data, advertises it to its neighbors and interested neighbors,i.e. those who do not have the data, retrieve the data by sending a request message.
- SPIN_s meta-data negotiation solves the classic problems of flooding such as redundant information passing,overlapping of sensing areas and resource blindness thus, achieving a lot of energy efficiency.There is no standard meta-data format and it is assumed to be application specific, e.g. using an application level framing.
- There are three messages defined in SPIN to exchange data between nodes. These are: ADV message to allow a sensor to advertise a particular meta-data, REQ message to request the specific data and DATA message that carry the actual data.

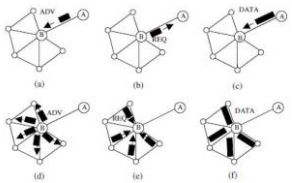

Cite this article as: C H Ram Manoger Lokiya, S Gopinath. "Analysis of Different Routing Protocols for Wireless Sensor Networks." *International Conference on Systems, Science, Control, Communication, Engineering and Technology (2015)*: 124-127. Print.

Fig 3.SPIN protocol.Node A starts by advertising its data to node B(a).Node B responds by sending a request to node A (b).After receiving the requested data(c).Node B then sends out advertisements to its neighbors (d),who in turn send requestsback to B (e–f).

- One of the advantages of SPIN is that topological changes are localized since each node needs to know only its single-hop neighbors.SPIN gives a factor of 3.5 less than flooding in terms of energy dissipation and meta-data negotiation almost halves the redundant data. However, SPIN_s data advertisement mechanism cannot guarantee the delivery of data. For instance, if the nodes that are interested in the data are far away from the source node and the nodes between source and destination are not interested in that data, such data will not be delivered to the destination at all. Therefore,SPIN is not a good choice for applications such as intrusion detection, which require reliable delivery of data packets over regular intervals.
- The simplest version of SPIN, referred to as SPIN-PP, is designed for a pointtopoint communications network. The three-step handshake protocol used bySPIN-PP is depicted in Figure 4(b). In step 1, the node holding the data, node A,issues an advertisement packet (ADV). In step 2, node B expresses interest inreceiving the data by issuing a data request (REQ). In step 3, node A responds tothe request and sends a data packet to node B[29].

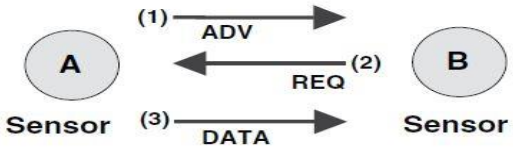

Fig 4 SPIN-PP three-way handshake protocol.[29]

- In point-to-point networks, the sender announces that it has new data with an advertisement message to each neighbor. When the neighbor receives the message, the node checks the metadata to know if it already stores the data item. If the neighbor is interested in the information, it responds with a request message. Upon receiving it, the sender transmits the information in a data message. The neighbor that receives the data, inform about its availability to its own neighbors with an advertisement message[28].
- The algorithm SPIN-EC introduces a technique in the nodes so when their current energy resources do not exceed a predetermined threshold that allows them to complete the three hand-shake protocol, they do not participate in the process. The SPIN-BC and SPIN-RL variants extend the algorithm to support broadcast transmissions. In this way, one advertisement message can reach all the neighbors. In this case, the neighbors do not respond immediately with a request message but they must wait a random time. To optimize the process, a node different from the advertising one cancels its own request message when it detects another similar message. Taking into account the broadcast transmission, the advertising node also responds with just one data message even when it has received multiple request messages[28].
- Additionally, SPIN-RL incorporates some reliability functionalities. Specifically, nodes keep track of the advertisement messages that they receive and their corresponding originators. If they send a request message, but the announcing node does not respond in a given interval, the node asks again for the data with a request message[28].

Directed Diffusion

- Directed Diffusion [18,24,25] is an important milestone in the data-centric routing research of sensor networks. The idea aims at diffusing data through sensor nodes by using a naming scheme for the data. The main reason behind using such a scheme is to get rid of unnecessary operations of network layer routing in order to save energy.
- Direct Diffusion suggests the use of attribute-value pairs for the data and queries the sensors in an ondemand basis by using those pairs. In order to create a query, an interest is defined using a list ofattribute-value pairs such as name of objects, interval, duration, geographical area, etc. The interest is broadcast by a sink through its neighbors.Each node receiving the interest can do caching for later use. The nodes also have the ability to do in-network data aggregation, which i modeled as a minimum Steiner tree problem [26].
- The interests in the caches are then used to compare the received data with the values in theinterests. The interest entry also contains several gradient fields. A gradient is a reply link to a neighbor from which the interest was received. It is characterized by the data rate, duration and expiration time derived from the received interest_s fields. Hence, by utilizing interest and gradients,paths are established between sink and
sources.
- Several paths can be established so that one of them is selected by reinforcement. The sink resendsthe original interest message through the selected path with a smaller interval hence reinforces thesource node on that path to send data more frequently.

Cite this article as: C H Ram Manoger Lokiya, S Gopinath. "Analysis of Different Routing Protocols for Wireless Sensor Networks." *International Conference on Systems, Science, Control, Communication, Engineering and Technology (2015)*: 124-127. Print.

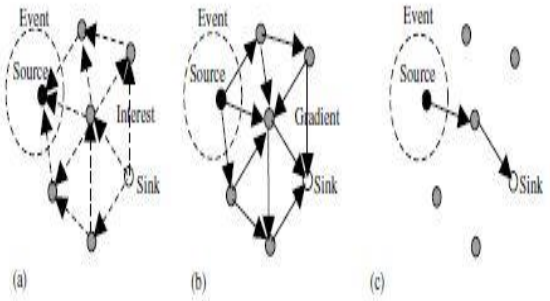

Fig 5. Directed Diffusion protocol phases. (a) Interest propagation, (b) initial gradients setup, (c) data delivery along reinforced

LEACH (Low Energy Adaptive Clustering Hierarchy)

- LEACH is based on a hierarchical clustering structure model and energy efficient cluster-based routing protocols for sensor networks. In this routing protocol, nodes self-organize themselves into several local clusters, each of which has one node serving as the cluster-head. In order to prolong the overall lifetime of the sensor networks, LEACH changes cluster heads periodically.
- LEACH has two main steps: the set-up phase and the steady-state phase. In the set-up phase, there are two parts, the cluster-head electing part and the cluster constructing part. After the cluster-heads have been decided on, sensor nodes (which are chosen as cluster-heads) broadcast an advertisement message that includes their node ID as the cluster-head ID to inform non-cluster sensor nodes that the chosen sensor nodes are new cluster-heads in the sensor networks. They use the carrier-sense multiple access (CSMA) medium access control (MAC) protocol to transmit this information.
- The non-cluster sensor nodes that receive it choose the most suitable cluster-head according to the signal strength of the advertisement message, and send a join request message to register on the chosen cluster-head. After receiving the join message, the cluster-heads make a time division multiple-access (TDMA) schedule for data exchange with non-cluster sensor nodes. Then, the cluster head informs the sensor nodes of its own cluster and the sensor nodes then start sending their data to the base station via their cluster-head during the steady-state phase[31].

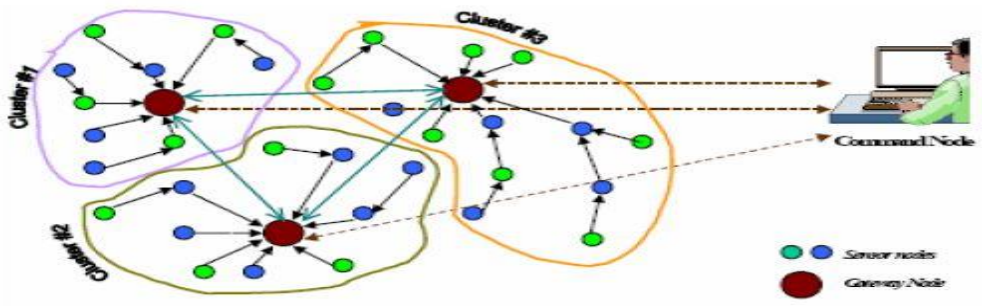

Fig: 6. clusters in LEACH network[13]

II. CONCLUSION

Wireless Sensor Network technology extends numerousapplication domains and it is crucial that WSNs perform in reliable and robust manner. One of the major issuesin the design of routing protocol for WSN is energy efficiency due to limited energy resources of sensors. Thispaper survey several different routing strategies for wireless sensor network. Therefore routing protocolsdesigned for WSN should be energy efficient as possible to prolong the life time of individual sensors..

REFERENCES

[1] http://www.cs.ucr.edu/~krish/lec7.pdf
[2] Wireless sensor network, http://http://en.wikipedia.org/wiki/wireless_sensor_network, January, 2008
[3] Chien-Chung Shen, Chavalit Srisathapornphat,Chaiporn Jaikaeo: Sensor Information Networking Architecture and Applications,IEEE Personal Communications, pp. 52-59 (August 2001).
[4] Kay Romer, Friedemann Mattern: The Design Space of Wireless Sensor Networks, IEEE Wireless Communications, pp. 54-61 (December 2004).
[5] Sarjoun S. Doumit, Dharma P. Agrawal: Self- Organizing and Energy-Efficient Network of Sensors, IEEE, pp. 1-6 (2002).

Cite this article as: C H Ram Manoger Lokiya, S Gopinath. "Analysis of Different Routing Protocols for Wireless Sensor Networks." *International Conference on Systems, Science, Control, Communication, Engineering and Technology (2015)*: 124-127. Print.

[6] Elaine Shi, Adrian Perrig: Designing Secure Sensor Networks IEEE Wireless Communications, pp. 38-43 (December 2004).
[7]Ian F. Akyildiz, Weilian Su, Yogesh Sankarasubramaniam, Erdal Cayirci: A Survey Special Issue on Ubiquitous Computing Security Systems
[8] José A. Gutierrez, Marco Naeve, Ed Callaway,Monique Bourgeois,Vinay Mitter, Bob Heile, IEEE 802.15.4: A Developing Standard for Low-Power Low-Cost Wireless Personal Area Networks, IEEENetwork, pp. 12-19(September/October 2001).
[9] Area Networks, IEEENetwork, pp. 12-19 (September/October 2001).
[10] Al-Karaki,J.N,Al-Mashagbeh: Energy-Centric Routing in Wireless Sensor Networks Computers and Communications, ISCC 06 Proceedings, 11th IEEE Symposium (2006).

Cite this article as: C H Ram Manoger Lokiya, S Gopinath. "Analysis of Different Routing Protocols for Wireless Sensor Networks." *International Conference on Systems, Science, Control, Communication, Engineering and Technology (2015)*: 124-127. Print.

International Conference on Systems, Science, Control, Communication, Engineering and Technology 2015 [ICSSCCET 2015]

ISBN	978-81-929866-1-6
Website	icssccet.org
Received	10 - July - 2015
Article ID	ICSSCCET026

VOL	01
eMail	icssccet@asdf.res.in
Accepted	31- July - 2015
eAID	ICSSCCET.2015.026

A Compact Multiband Fractal Antenna(CMFA) For Wireless Applications

A Manikandan[1], Dr S Uma Maheswari[2]
[1]Assistant Professor, Department of ECE,
Karpagam Institute of Technology, Coimbatore, Tamilnadu, India.
[2]Associate Professor, Department of ECE,
Coimbatore Institute of Technology, Coimbatore, Tamilnadu, India.

Abstract: In this paper, A compact Fractal antenna is designed and examining novel self-similar fractal geometry to reduce the size and to resonate for multiband frequencies. This antenna is microstrip line fed and its structure is based on fractal geometrics. . Design and Analysis of fractal antenna is done by using Software ADS (Advanced Design System). The proposed antenna exhibits multiband characteristics with a small return loss and high efficiency at design frequency of 2.2GHz. The ultimate aim of implementing self-similar fractal concept in antenna design makes it flexible in controlling the resonance and bandwidth. . It is very flexible, compact and has very small return loss at this design frequency. It covers WLAN IEEE 802.11b and IEEE802.15, PCS(1900), GSM lower band, GSM higher band DCS(1800), IMT(2000), UMTS(2100), Wi-Fi, DARS(digital audio radio service),WLAN and wireless applications.

Keywords: self similar geometry, ADS, return loss

I INTRODUCTION

Fractal is a rough or fragmented geometric shape that can be subdivided in parts, each of which is (at least approximately) a reduced- size copy of the whole. Fractals are generally self-similar and independent of scale. There are many mathematical structures that are fractals; e.g. Sierpinski gasket, Cantors comb, von Koch curves. Fractals also describe many real- world objects, such as clouds, mountains, turbulence, and coastlines that do not correspond to simple geometric shapes. As we see fractals have been studied for about a hundred years and antennas have been in use for as long.

Fractal antennas are new on the scene. That is, the antenna should keep similar radiation parameters through several bands. Second, because the space-filling properties of some fractal shapes (the fractal dimension) might allow fractal shaped small antennas to better take advantage of the small surrounding space These geometries have been used to characterize structures in nature that were difficult to define with Euclidean geometries. Examples include the length of a coastline, the density of clouds, and the branching of trees.

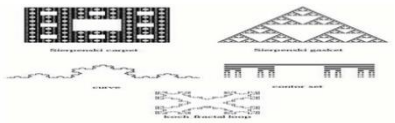

Fig.1 Examples of fractal antenna patte

Cite this article as: A Manikandan, Dr S Uma Maheswari. "A Compact Multiband Fractal Antenna(CMFA) For Wireless Applications." *International Conference on Systems, Science, Control, Communication, Engineering and Technology (2015)*: 128-131. Print.

These geometries have been used to characterize structures in nature that were difficult to define with Euclidean geometries. Examples include the length of a coastline, the density of clouds, and the branching of trees.

II ANTENNA DESIGN

The self-affine fractal structure in this project is constructed by scaling a rectangle as shown in Fig.1a. The initiator S0 by a factor of two along its width and two along its length, which leads to four rectangles of equal dimension, is presented. The upper topmost corner region is eliminated there by their retaining the remaining regions as shown in Fig.1b. ie. 75% of the total area is

Retained and 25% is eliminated. First, the initiator S0 is made to resonate at design frequency 2.4GHz by adopting coaxial feed technique. This process is a repetitive procedure and is continued up to nth iteration. The width of the Microstrip patch antenna is given by

$$W = \frac{C}{2 f_o \sqrt{(\varepsilon_r + 1)/2}}$$

- $c = 3x10^8$ m/s
- $\varepsilon_r = 4.4$
- $f_o = 2.2$ GHz

We calculated the width and it came out to be **W=41.5mm**

CALCULATION OF THE LENGTH

The formula for the Effective length is given as

$$L_{eff} = \frac{C}{2 f_o \sqrt{\varepsilon_{reff}}}$$

$L_{eff} = 32.6$ mm

SELF SIMILAR:

The phrase "self-similar" means that it looks same for all iterations and is super imposed of too many iterations and it portrays the self affinity property of fractal geometry. When the fractal iteration increases, then the original patch

reduces by 45% in size, thereby maintaining a radiation pattern comparable to that of a normal patch . A self similar structure is one in which the length and the width are scaled down by itself to a maximum number of possible iterations (n), through which the size of the geometry shrinks by maintaining its individuality. A Self-affine concept has been implemented in designing a low profile antenna which provides flexibility in obtaining a miniaturized antenna. By proper selection of scaling factor and optimization of the feed position, the antenna resonates for multiband covering the near bands

FRACTAL STRUCTURE

Cite this article as: A Manikandan, Dr S Uma Maheswari. "A Compact Multiband Fractal Antenna(CMFA) For Wireless Applications." *International Conference on Systems, Science, Control, Communication, Engineering and Technology (2015)*: 128-131. Print.

Fig 2.Self-Similar fractal structure

The self-affine fractal structure in this project isconstructed by scaling a rectangle as shown in Fig.1a. The initiator S0 by a factor of two along its width and two along its length, which leads to four rectangles of equal dimension, is presented. The upper topmost corner region is eliminated there by there retaining the remaining regions as shown in Fig.1b. ie., 75% of the total area is retained and 25% is eliminated. First, the initiator S0 is made to resonate at design frequency 2.4GHz by adopting coaxial feed technique. This process is a repetitive procedure and is continued upto nth iteration. Figures.1c. to 1d. shows that the number of iterations undergone by the initiator S0.

III RESULT AND DISCUSSIONS

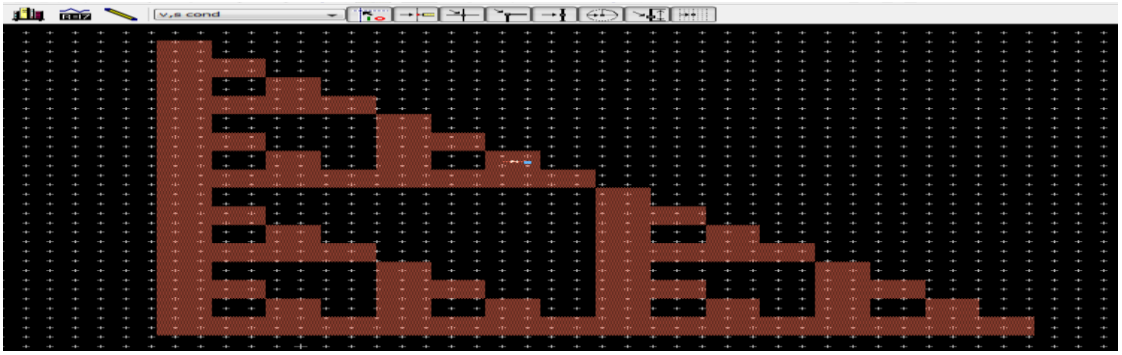

Fig3:Layout structure

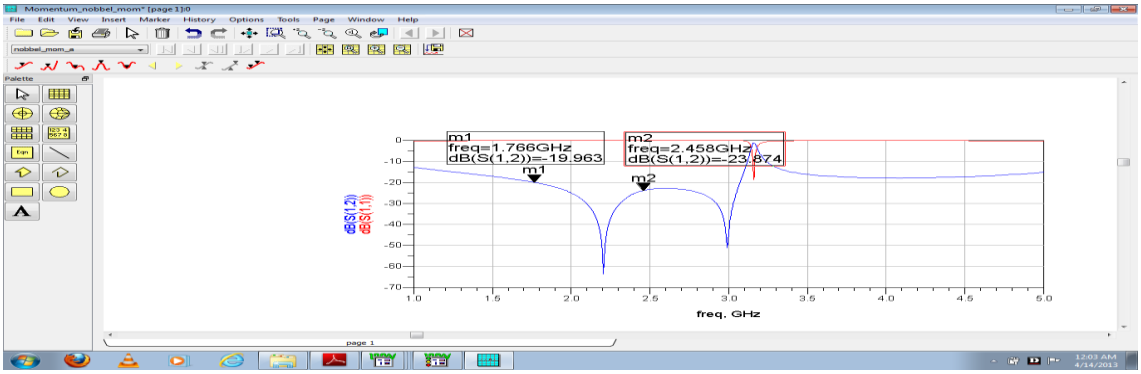

Fig.4 Simulated return loss against frequency for the proposed antenna.

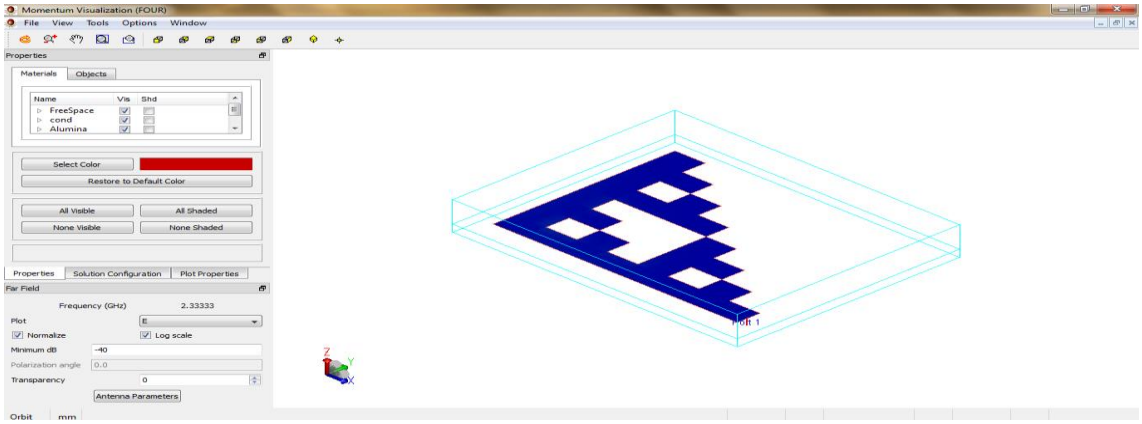

Fig.5 current distribution for the proposed antenna.

Cite this article as: A Manikandan, Dr S Uma Maheswari. "A Compact Multiband Fractal Antenna(CMFA) For Wireless Applications." *International Conference on Systems, Science, Control, Communication, Engineering and Technology (2015)*: 128-131. Print.

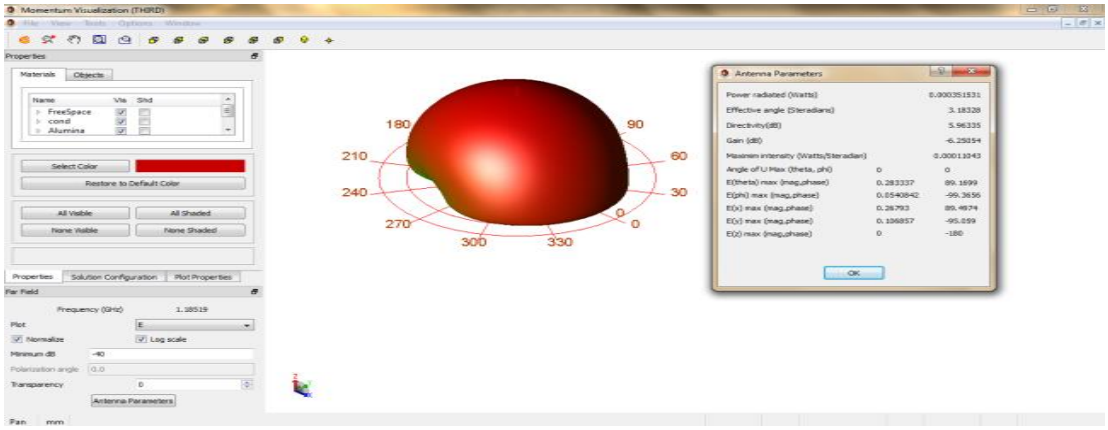

Fig.6 Radiation pattern and parameters of proposed antenna

IV CONCLUSION

A novel compact fractal antenna is proposed. Almost constant group delay is achieved. The good impedance matching characteristic, constant gain, and Omni directional radiation patterns over the entire operating bandwidth of 1.7GHz–2.4GHz (0.7GHz), 2.5 GHz-3GHz(0.5GHz) make this antenna a good candidate for wireless applications and systems. Return loss is -10 to -25 db and VSWR – 1-2 and impedance- 48 to 50 ohm. Microstrip line feeding is provided to proposed antenna which is simple and suitable for this.

V REFERENCES

[1].Neetu, Savina Bansal, R K Bansal, "Design and Analysis of Fractal Antennas based on Koch and Sierpinski Fractal Geometries." IJAREEIE Vol. 2, Issue 6, pp. 2110-2116, June 2013.

[2]. P. J. Soh, G. A. E. Vandenbosch, S. L. Ooi, and M. R. N. Husna, "Wearable dual-band Sierpinski fractal PIFA using conductive fabric," *Electronics Letters,* vol. 47, pp. 365-367, 2011.

[3] Yogesh Kumar Choukiker, S.K. Behera, "Design of Wideband Fractal Antenna with Combination of Fractal Geometries." ICICS, 2011.

[4] A. Ismahayati, P.J. Soh, R. Hadibah, G.A.E Vandenbosch, " Design and Analysis of a Multiband Koch Fractal Monopole Antenna." IEEE International RF and Microwave Confrence. pp. 58-62, 12th -14th December 2011.

[5] P. J. Soh, G. A. E. Vandenbosch, S. L. Ooi, and M. R. N. Husna, "Wearable dual-band Sierpinski fractal PIFA using conductive fabric," *Electronics Letters,* vol. 47, pp. 365-367, 2011.

[6].Amer Basim Shaalan, "Design of Fractal Quadratic Koch Antenna." International Multi- Conference on Systems, Signals and Devices, 2010.

[7] S. N. Shafie, I. Adam, and P. J. Soh, "Design and Simulation of a Modified Minkowski Fractal Antenna for Tri-Band Application," in *Mathematical/Analytical Modelling and Computer Simulation (AMS), 2010 Fourth Asia International Conference on*, 2010, pp. 567-570.

[8].D.D. Krishna, M. Gopikrishna, C.K. Aanandan, P. Mohanan, and K. Vasudevan, " Compact wideband Koac Fractal Printed slot antenna." IET Micro waves, Antennas and Propagation, Vol3, No. 5, pp. 782-789, 2009.

[9] N. A. Saidatul, A. A. H. Azremi, R. B. Ahmad, P. J. Soh, and F. Malek, "Multiband fractal planar inverted F antenna (F-PIFA) for mobile phone application," *Progress in lectromagnetic Research (PIER),* vol. 14, pp. 127-148, 2009.

[10] N. Abdullah, M. A. Arshad, E. Mohd, S. A. Hamzah, "Design of Minskowsi Fractal for Dual Band Application." IEEE, pp. 352-355, May 13-15, 2008.

[11] Raj Kumar, Yogesh B. Thakare and M. Bhattacharya, "Novel Design of Star Shaped Circular Fractal Antenna." IEEE, pp. 239-241, 2008.

[12] B.L. Ooi, "A modified contour integral analysis for Sierpinski fractal carpet antennas with and without electromagnetic band gap ground plane," IEEE Trans. Antennas Propag., Vol.52, pp. 1286-1293, May 2004.

[13] Introduction to antenna and near-field simulation in CST Microwave Studio Software By Jorge R.Costa Jerzy Guterman.

[14] Vinoy, K. J., "Fractal shaped antenna elements for wide and multi-band wireless applications," Thesis, Pennsylvania, Aug. 2002.

[15] Constantine A. Balanis, Antenna Theory Analysis & Design, John Wiley & Sons, 1997.

Cite this article as: A Manikandan, Dr S Uma Maheswari. "A Compact Multiband Fractal Antenna(CMFA) For Wireless Applications." *International Conference on Systems, Science, Control, Communication, Engineering and Technology (2015)*: 128-131. Print.

International Conference on Systems, Science, Control, Communication, Engineering and Technology 2015 [ICSSCCET 2015]

ISBN	978-81-929866-1-6	**VOL**	01
Website	icssccet.org	**eMail**	icssccet@asdf.res.in
Received	10 - July - 2015	**Accepted**	31- July - 2015
Article ID	ICSSCCET027	**eAID**	ICSSCCET.2015.027

A Multiband Microstrip Yagi Antenna for C band Applications

S Anbarasu[1], A Manikandan[2], A.G Paranthaman[3]
[1, 2, 3] Assistant Professor, Department of ECE,
Karpagam Institute of Technology, Coimbatore, Tamilnadu, India

***Abstract**: In this paper, the design of microstrip yagi uda antenna for multi bandwidth applications is proposed. The designed microstrip yagi uda antenna consists of double dipole, the pair of reflector and three parasitic elements that improve the results of antenna. The design antenna is simulated on substrate with dielectric constant of 4.4, loss tangent of 0.02 and height of 1.6 mm. The antenna has achieved directivity of 7.45 dBi, gain of 5.74 dB, return loss of -29.70 dB and high efficiency.*

Keywords: Yagi Uda antenna, Advanced Design System (ADS)

I. INTRODUCTION

The most common antenna used for the communication system is yagi uda antenna, it is preferred because of it's, low cost and directivity[2]. With the growth in communication system they are used in many applications such as in radar, medical, industrial and wireless communication, where there is a need of an antenna which provides a directional beam in particular direction, which is obtained by the yagi- uda antenna[3].In order to enhance the antenna characteristics, the driven element, reflector and parasitic element of microstrip yagi uda antenna are arranged on the same substrate[4]. To increase the gain of antenna the director is placed near the driven element[5]. The simple yagi uda antenna has, One reflector, one driven element and one or more parasitic elements, in which reflector reflects the power forward and highest gain is achieved at the axis of director and on its side. Most yagi uda antenna consists of large ground plane that act as the reflector which is not perfect for the radiation pattern optimization of yagi uda antenna. So, the proposed antenna consists of a pair of reflector, three directors and small ground plane[4]. The small ground plane is used as reflector for the suitable optimization of radiation pattern and the three directors are used to increase the gain of antenna. Compare to one and two director the gain had increase by the use of three directors. The small ground plane had increases the antenna efficiency compares to large ground plane. The designed antenna is simulated by Advanced Design System. The antenna has achieved good radiation pattern, high efficiency, gain and proper impedance matching with load. It yields better results at different bandwidth.

II. CONFIGURATTION AND DESIGN STRATEGY

The proposed microstrip yagi uda antenna is shown in figure 1. It is fabricated on FR-4 substrate with $\varepsilon r = 4.4$ with loss tangent of 0.02, thickness of 1.6 mm, the length and width of 100mm. The antenna consists of double dipole which is parallel to each other but different in length, and it is also designed with three directors each of different length and width placed above one another with

Cite this article as: S Anbarasu, A Manikandan, A.G Paranthaman. "A Multiband Microstrip Yagi Antenna for C band Applications." *International Conference on Systems, Science, Control, Communication, Engineering and Technology (2015)*: 132-135. Print.

different distance from each other and the dipole, the distance between the dipole and the first director is more when compared to the distance between the consecutive directors .It has very thin feed line[8]. The feeding technique used here is microstrip feed technique. Moreover thin feed line will tend to give better return loss when compared to thick ones. Due to absence of large ground plane it is easy to place the pair of reflectors which optimizes the radiation pattern[6]. The dimensions of proposed antenna given in table 1.

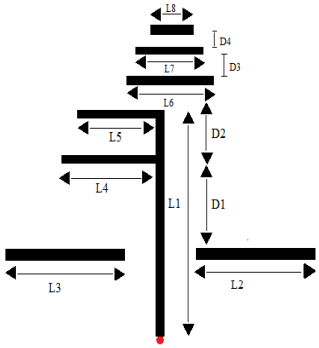

Figure 1: Schematic configuration of proposed Yagi uda antenna

Table1
Design Parameters of the proposed yagi uda antenna shown in Figure 1

Parameter	Dimension (mm)	Parameter	Dimension (mm)
L1	67	L9	103
L2	34	D1	10
L3	34	D2	12
L4	20.79	D3	5
L5	18	D4	4
L6	20	W1	2
L7	18	W2	22
L8	16		

L1 = length of microstrip connected to both dipole and fed point.
L2 & L3 = length of reflectors.
L4 & L5 = length of dipoles.
L6, L7 & L8 = length of parasitic element.

D1 = distance between reflector and second dipole.
D2 = distance between dipoles.
D3 & D4 = distance between parasitic element.
W1 = width of microstrip.
L9 & W2 = length and width of ground plane.

III. RESULTS AND DISCUSSIONS The proposed yagi uda antenna is simulated by using Advanced Design System(ADS) . As can be seen from the plot, the antenna operates from 4 GHz - to 8 GHz covering the required C band. The simulated result shows that the antenna is well matched using the Microstrip-fed structure whilst still achieving the required bandwidth covering the C-band .The gain of the antenna for frequencies from 4 GHz to 8 GHz is shown in

Cite this article as: S Anbarasu, A Manikandan, A.G Paranthaman. "A Multiband Microstrip Yagi Antenna for C band Applications." *International Conference on Systems, Science, Control, Communication, Engineering and Technology (2015)*: 132-135. Print.

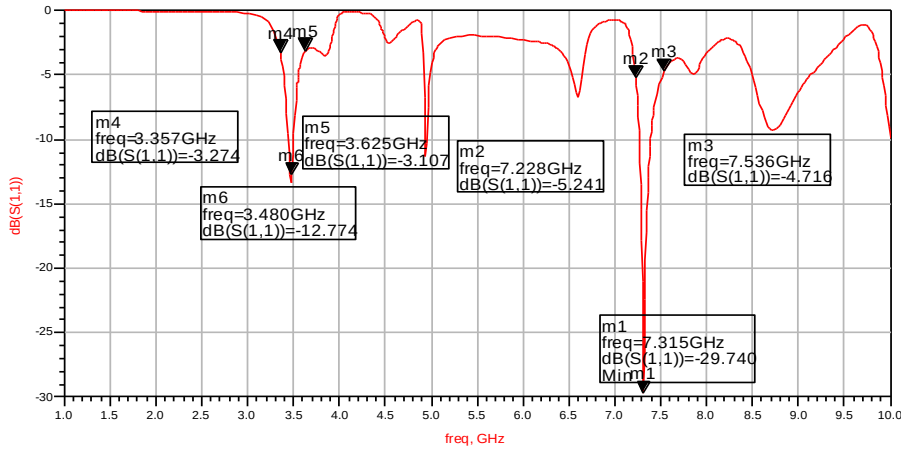

Figure2: Return loss performance of the antenna

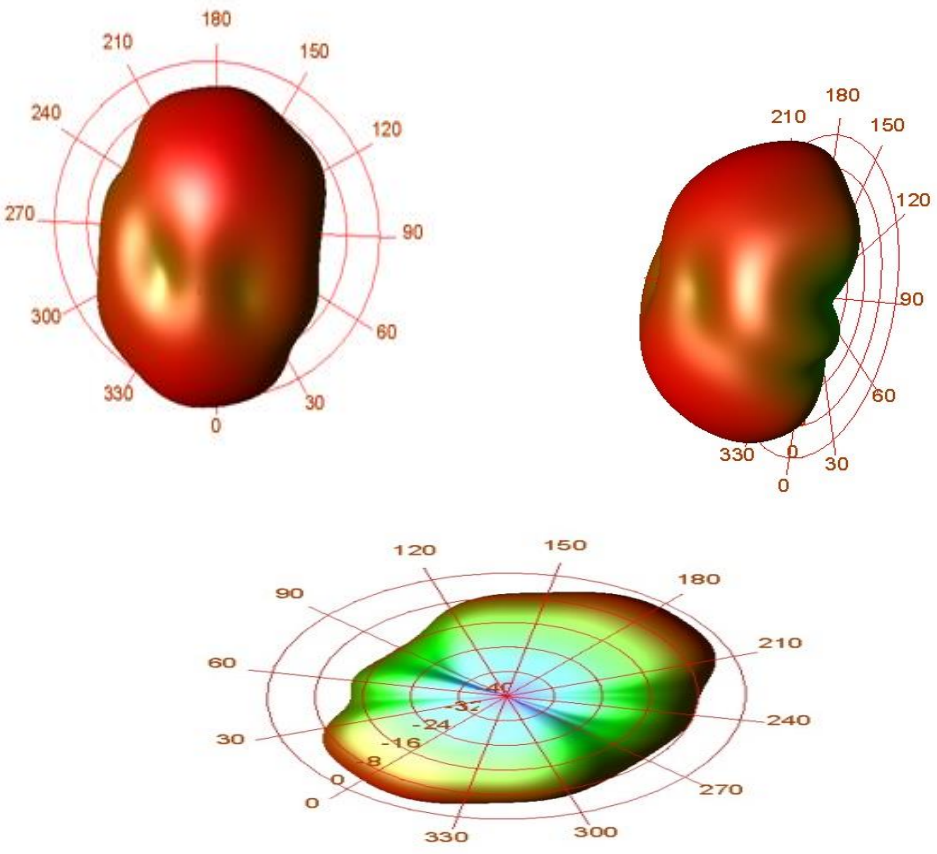

Figure3: Three Dimensional Radiation pattern

Cite this article as: S Anbarasu, A Manikandan, A.G Paranthaman. "A Multiband Microstrip Yagi Antenna for C band Applications." *International Conference on Systems, Science, Control, Communication, Engineering and Technology (2015)*: 132-135. Print.

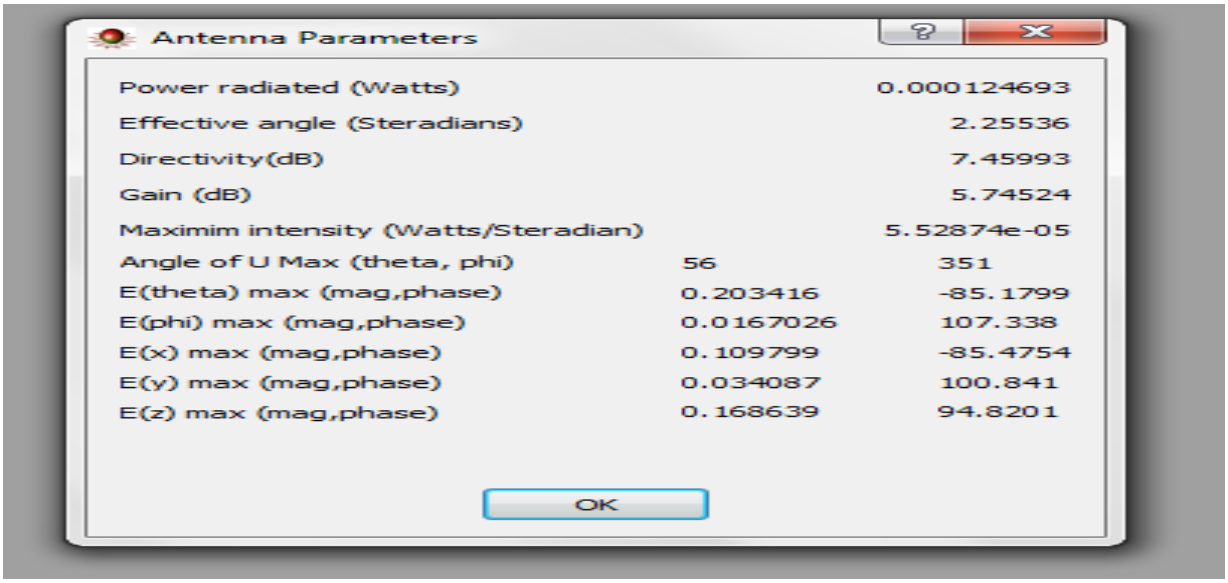

Figure 4: Antenna Parameters

IV.CONCLUSION

A Microstrip-fed antenna has been presented with two dipoles and three directors of different length has been simulated .The radiation pattern, return loss ,frequency, gain ,directivity of the antenna is measured and shown in the figure 2,3,4.This antenna operates in the C band frequency and has a wide range of applications .This antenna is small in size indicating that it is a good candidate for phased arrays.

V.REFERENCES

1. Sun, B.-H., S.-G. Zhou,Y.-F.Wei, and Q.-Z. Liu, "Modified two-element Yagi-Uda antenna with tunable beams," *Progress In Electromagnetics Research*, Vol. 100, 175-87, 2010.
2. Bemani, M. and S. Nikmeh, "A novel wide-band microstrip Yagi-Uda array antenna for WLAN applications," *Progress In Electromagnetics Research B*, Vol. 16, 389-406, 2009.
3. Misra, I. S., R. S. Chakrabarty, and B. B. Mangaraj, "Design,analysis and optimization of *V* -dipole and its three-element Yagi-Uda array," *Progress In Electromagnetics Research*, PIER 66, 137-156, 2006.
4. S.K. Padhi and M.E. Bialkowski, "Parametric Study of a Microstrip Yagi Antenna", Proceedings of the Asia-
5. Pacific Microwave Conference, PP: 715-718, Dec. 2000.
6. Lee, K. F., et al., "Microstrip antenna array with parasitic elements," *IEEE Antennas and Propagation Society Symposium Dig.*, 794-797, Jun. 1987.
7. Chen, C. A. and D. K Cheng, "Optimum element lengths for Yagi-Uda arrays," *IEEE Trans. Antennas and Propagation*, Vol. 23, Jan. 1975.
8. K.D.Prasad,"Antenna & Wave Propagation", 3rd Edition, Satya Prakashan, 2005.
9. David M. Pozar, "Microwave Engineering", 3rd Edition, John Wiley & Sons, 2004.

Cite this article as: S Anbarasu, A Manikandan, A.G Paranthaman. "A Multiband Microstrip Yagi Antenna for C band Applications." *International Conference on Systems, Science, Control, Communication, Engineering and Technology (2015)*: 132-135. Print.

International Conference on Systems, Science, Control, Communication, Engineering and Technology 2015 [ICSSCCET 2015]

ISBN	978-81-929866-1-6	**VOL**	01
Website	icssccet.org	**eMail**	icssccet@asdf.res.in
Received	10 - July - 2015	**Accepted**	31- July - 2015
Article ID	ICSSCCET028	**eAID**	ICSSCCET.2015.028

TECHNICAL RIVAL FOR GAS LEAKAGE

Saravan manikandan B[1], Neha R[2], Priyanka R[3]
[1]Assistant Professor, Department of ECE.
[2, 3] Students, Third Year, Department of ECE,
Karpagam Institute of Technology.

Abstract: *Nowadays, the accidents due to gas leakage are claiming the most number of lives. Almost, everyday, we come across incidents where the negligence of an individual living in an apartment, or any defect in the commercial gas pipelines have turned fatal to the people around. The negligence may result in fire or gas leakage accidents. The statistical growth of these types of incidents gave us an alarm that it's time to renew our existing alert systems and propose a novel one. Our proposed system consists of a number of nodes which can be placed in each flat of the apartment and the master node, located in the control center of the apartment. In case of a fire or gas leakage, the message is directly transmitted to the master node. Thereby, necessary action is taken automatically. In addition, it provides auto shut-off system for the gas leakage, thus conserving the gas and saving numerous lives.*

Keywords: MSP430 launch pad, sensors, RF booster pack, Energia software.

I. INTRODUCTION

Objective of the Project:

The primary objective of this project is to provide a novel means for safely detecting any malfunction of a pressurized gas system in order to prevent accumulation of combustible gases so that damage or explosion due such an accumulation to of gases can be prevented.
The gas leakage in industrial sectors causes loss of lives as well as huge financial loss. We may be familiar with the 'Bhopal Gas Leakage Tragedy' which occurred due the 'Methyl Iso - Cyanate' gas that claimed numerous lives. The aftermath of this tragedy is well known to all the Indians. Similar but less intense accidents are occurring even in the present world. In order to prevent such accidents there is a need to develop a novel security and alerting system with the facility of auto shut off.

II. THE PROPOSED SYSTEM

The system consists of several sub nodes and one Master node connected to the entire sub nodes. The sub node comprises of two sensors namely, a temperature sensor *LM 35*and a gas sensor *MQ 5*. This is connected to the processor *MSP EXP430G2*. The MSP-EXP430G2 Launch Pad is an easy-to-use flash programmer and debugging tool for the MSP430G2xx Value Line microcontrollers. This device is connected to a buzzer, an *Auto Shut down System*, and an *encoder HT12E* which in turn is connected to the *RF 430 BOOST CC11DC* which is used in the transmission of information. The Master node is made up of an *RF 430* which is connected to the *Decoder HT12D*. This is connected to *MSP EXP430G2* which is connected to several alerting devices like the *buzzers, LEDs* and *LCD Displays.*

Cite this article as: Saravan manikandan B, Neha R, Priyanka R. "TECHNICAL RIVAL FOR GAS LEAKAGE." *International Conference on Systems, Science, Control, Communication, Engineering and Technology (2015)*: 136-139. Print.

Software Description:

Energia is an open source software. The Energia IDE is cross platform and is supported on Mac OS, Windows and Linux. Energia uses the MSPGCC compiler. Energia includes an Integrated Development Environment (IDE) that is based on processing.Energia started out to bring the Wiring and Arduino framework to the Texas Instruments MSP430 Launch Pad.

Texas Instruments offers a MSP430, TM4C, C2000andCC3200 Launch Pad. The Launch Pad is a low-cost microcontroller board Together with Energia, Launch Pad can be used to develop interactive objects, taking inputs from a variety of switches or sensors, and controlling a variety of lights, motors, and other physical outputs [13]. Launch Pad projects can be stand-alone (only run on the Target Board, i.e. Launch Pad), or they can communicate with software running on your computer (Host PC).

Working Principle:

The sub nodes are placed in flats and master node is placed in control centre. The sub nodes detect for the presence of any gas leakage, abnormal rise in temperature.If any abnormalities are found, information from the sub node is transmitted to the master node with the help of RF booster pack (CC110L AIR INTERFACE). To alert about the problem, the buzzer rings at the corresponding region where leakage is found. At the master node the buzzer and LED are activated to intimate about the abnormality detected in the particular flat.

System Architecture Design:

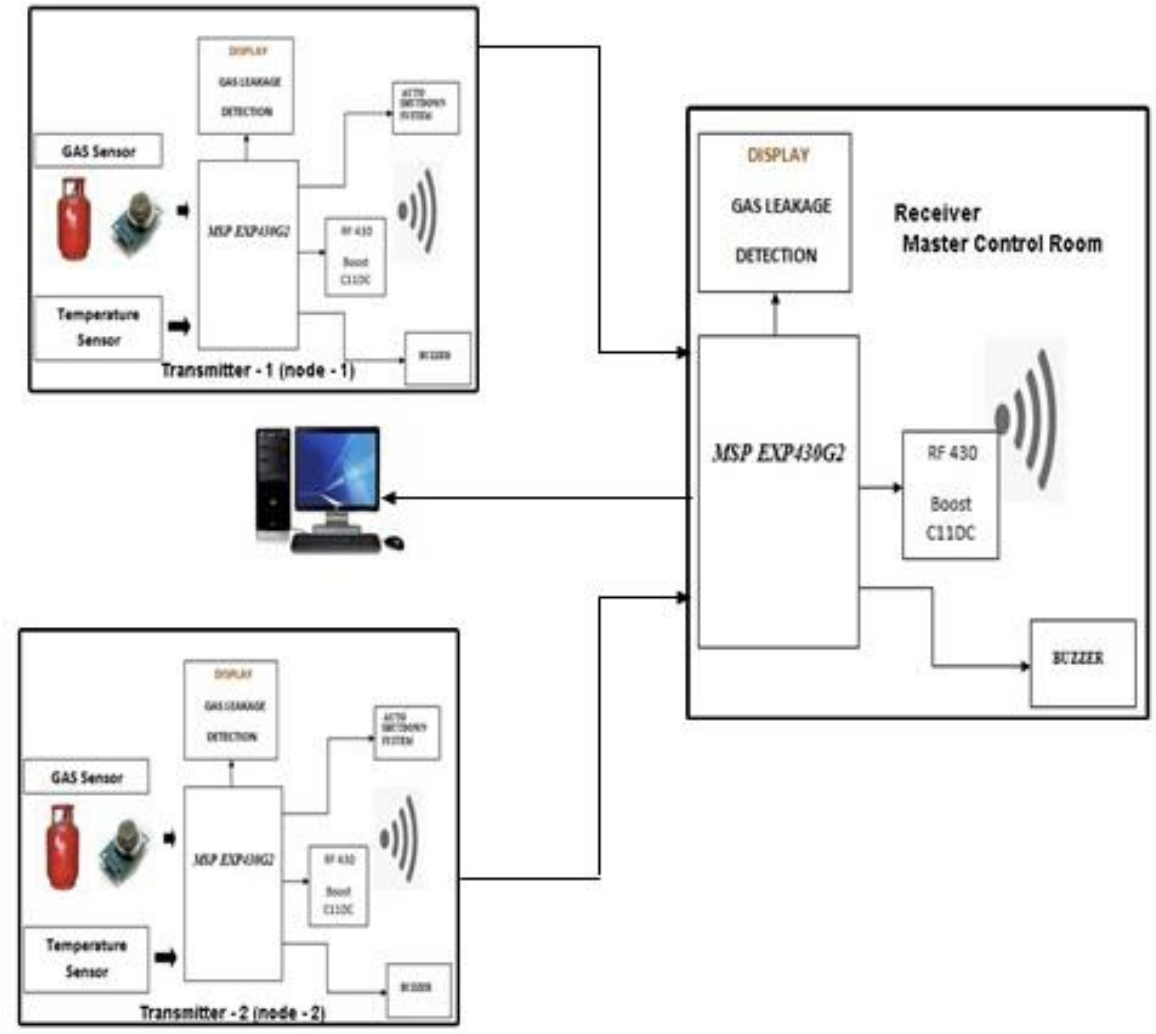

Cite this article as: Saravan manikandan B, Neha R, Priyanka R. "TECHNICAL RIVAL FOR GAS LEAKAGE." *International Conference on Systems, Science, Control, Communication, Engineering and Technology (2015)*: 136-139. Print.

FLOW CHART:

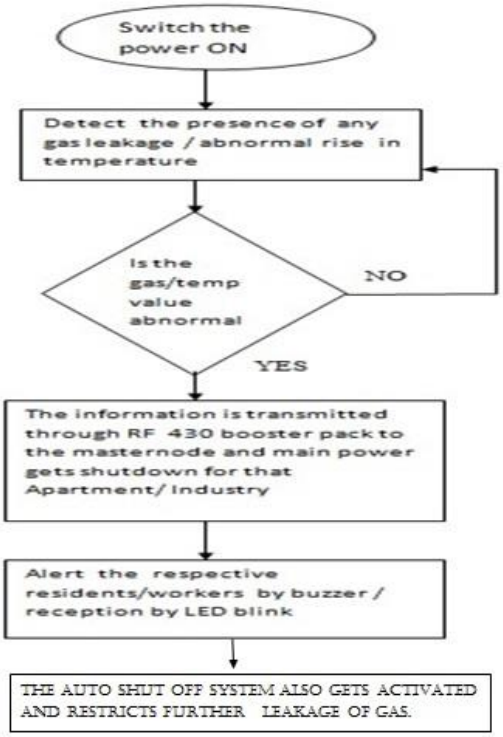

Figure 6.1 flow char

Circuit diagram:

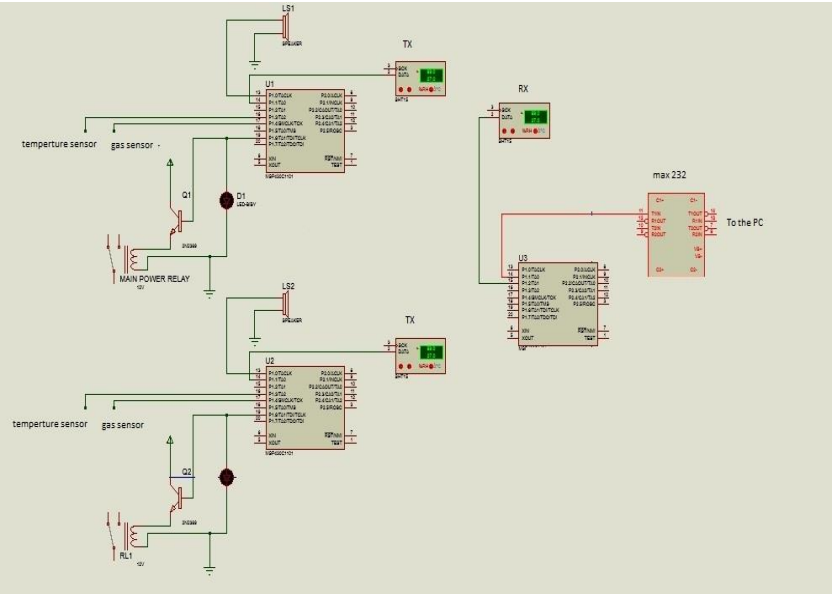

Cite this article as: Saravan manikandan B, Neha R, Priyanka R. "TECHNICAL RIVAL FOR GAS LEAKAGE." *International Conference on Systems, Science, Control, Communication, Engineering and Technology (2015)*: 136-139. Print.

III. CONCLUSION AND FUTURE ENHANCEMENTS

The occurrence of gas leakage can be sensed and immediate action can be taken. This prevents mass loss of lives, especially in areas where several gas terminals are activated within a small area. Implementation of this system may prevent replicas of past accidents. In future enhancement, we can modify the above system using RTOS (Real Time Operating System). If RTOS is used then any malfunctioning of the sensors or other elements can be easily detected and corrective actions can be taken accordingly and so the system can be made very efficient.

References:

[1]Breuer W, Becker W, Deprez J, Drope E, Schmauch H. United States Patent 4141800: Electrochemical gas detector and method of using same. Retrieved February 27, 2010.
[2]Figaro Sensor. General Information for TGS Sensors.Retrieved February 28, 2010. [11]Vitz, E. (1995). Semiconductor Gas Sensors as GC detectors and 'Breathalyzers'. Journal of Chemical Education.
[3]International Society of Automation..Point infrared gas detector design guide.Retrieved February 28, 2010.
[4]Muda R. Simulation and measurement of carbon dioxide exhaust emissions using an optical-fibre-based mid-infrared point sensor. Journal of Optics A: Pure and Applied Optics(2009).
[5] Lattuati-Derieux, Agnès; Bonnassies-Termes, Sylvette; Lavédrine, Bertrand (2004). "Identification of volatile organic compounds emitted by a naturally aged book using gas chromatography/mass spectrometry". *Journal of Chromatography A* **1026** (1–2): 9–18.
[6]Ailworth, Erin (July 7, 2014). "New Mass. law aims to speed repairs to gas leaks".*Boston Globe*.Retrieved 2014-07-18.
[7] Davies J H, Microcontroller Basics, Elsevier, 2011.
[8]Naranjo E. Ultrasonic Gas Leak Detectors. Retrieved February 27, 2010.
[9] Jackson C.N., Sherlock C.N.: Non-destructive Testing Handbook: Leak Testing, Library of Congress Cataloging-in-Publication Data, 2008
[10]API 1155: Evaluation Methodology for Software Based Leak Detection Systems. 1st Edition (February 1995). American Petroleum Institute. Replaced by API RP 1130.
[11] Berger, J.O.: Statistical Decision Theory and Bayesian Analysis. Springer Series in Statistics.2nd Edition (1985).
[12] Muhammad Ali Mazidi, RolinMcKinlay, Danny Causey, PIC Microcontroller and Embedded Systems: Using assembly and C, Pearson, 2008.
[13]Han-Way Huang, PIC Microcontroller: An Introduction to Software and Hardware Interfacing, Course Technology.
[14]R.P. Jain, Digital Electronics, Tata McGraw
[15]General Monitors. Infrared Point Detector for Hydrocarbon Gas Detection.Retrieved February 25, 2010.
[16]Fuchs H. V: Ten Year of Experience with Leak Detection by Acoustic Signal Analysis. Applied

Cite this article as: Saravan manikandan B, Neha R, Priyanka R. "TECHNICAL RIVAL FOR GAS LEAKAGE." *International Conference on Systems, Science, Control, Communication, Engineering and Technology (2015)*: 136-139. Print.

International Conference on Systems, Science, Control, Communication, Engineering and Technology 2015 [ICSSCCET 2015]

ISBN	978-81-929866-1-6
Website	icssccet.org
Received	10 - July - 2015
Article ID	ICSSCCET029

VOL	01
eMail	icssccet@asdf.res.in
Accepted	31- July - 2015
eAID	ICSSCCET.2015.029

An effective clock generator for Heterogeneous GALS in CMOS technology

A G Paranthaman[1], S Anbarasu[2], R Neethu[3]
[1, 2, 3] Assistant Professor, Department of ECE
Karpagam Institute of Technology, Coimbatore.

Abstract: *It is so complicate to present clock generator for GALS (Globally Asynchronous Locally Synchronous) MPSoCs (Multiprocessor Systems-on-chip) and here we are going to produce ADPLL (All-Digital Phase-Locked Loop) clock generator that consumes very low power of 2.7 mW and it has very small chip area of 0.0078 mm. These ADPLL clock generators are used in fine-grained power management such as DVFS per core and it contains phase rotation and frequency division blocks which are used to generate multiphase clock signal since that frequencies of core varies from 83 to 666 MHz with 50% duty cycle. Such clock should encounter the stipulation of DDR2/DDR3 memory interfaces and in addition it renders a devoted eminent-speed clock up to 4 GHz for serial data links of network-on-chip. And, in fast dynamic frequency scaling applications the core frequencies varies randomly in one clock cycle. Finally, a prototype in 65-nm CMOS technology varies the performance of statistical analysis of mismatch.*

Keywords: All-digital Phase-Locked Loop (ADPLL), Digitally Controlled Oscillator (DCO), Dynamic Voltage and Frequency Scaling (DVFS), Globally Asynchronous Locally Synchronous (GALS), Multiprocessor Systems- on-Chip (MPSoCs).

I.INTRODUCTION

MPSoCs (Multiprocessor systems-on-chip) render compromising solutions for baseband operations which support a broad range of radio standards are supported and eminent energy efficiency is compulsory for mobile terminals. [1]. In order to encounter such requirements, the heterogeneous MPSoCs let in dissimilar cores such as general purpose RISC processors, DSPs (digital signal processors), or hardware accelerator and in addition on-chip data transmission structures as though NoC (Network-on-Chip) eminent-speed links and I/O components such as DDR (double-data-rate) [2] memory interfaces or FPGA (Field-Programmable Gate Array) associations are division of complex MPSoCs and they possess differentiated necessitates for clock frequency and clock quality like jitter and duty cycle respectively. [3,4].

Usually, concentrated clock generators are employed that render clocks for multiple cores and I/O interfaces in heterogeneous Multiprocessor systems-on-chip and the 80 core processor [5] employs meso-synchronous clocking with an individual PLL only that does not permit single per core frequency scaling. In demarcation, GALS (Globally Asynchronous Locally Synchronous) clocking architectures render each and every core with a devoted clock deflecting global eminent-speed synchronous clock dispersion networks [6]. In order to provide further increase in energy efficiency, fine grained power management method like dynamic voltage and frequency scaling (DVFS) are necessitated[7], [8].

The independent local clocks are present in GALS MPSoCs in which per-core DVFS can be effectively implemented. Results for

Cite this article as: A G Paranthaman, S Anbarasu, R Neethu. "An effective clock generator for Heterogeneous GALS in CMOS technology." *International Conference on Systems, Science, Control, Communication, Engineering and Technology (2015)*: 140-143. Print.

extremist-fast provide voltage variations have been described [7]. Hence, a quick reacting clock generator is needed to recognize such fast DVFS approaches that minimize core idle times while varying the level of performance and enhance entire throughput of the system. [9] and [10] necessitates wide-eyed ring oscillators for Globally Asynchronous Locally Synchronous cores, that however are not desirable for DVFS. [11] employs locally graduated clock generators that are based on the controlled delay lines, but it does not have fast core frequency switching.

[8] employs an assembled ring oscillator for quick DVFS that cannot produce modest jitter clocks at determined frequencies because they are not locked to a mentioned clock. [12] proposed various clock generators that are based on flying adder (FA) frequency synthesis, that can produce a broad range of frequencies with modest jitter, but it necessitates prominent chip area. Believing the style for integration of several-core MPSoCs [5], compromising clocking solutions are needed to fulfill the requirements of clock quality and endure progressed fine-grained power management approaches. Thus, such operation provides a modest chip area, reduced power ADPLL (All-Digital Phase-Locked Loop)-based clock generator for per-core representation in heterogeneous GALS MPSoCs, rendering both a broad range of output frequencies and differentiated eminent-speed clocks. It modifies hyper-fast frequency switching for per-core DVFS systems.

II. ALL-DIGITAL PHASE-LOCKED LOOP (ADPLL)

The ADPLL of Fig. 1 has a structure and operation very similar to a second-order CPPLL. The principal difference is that the phase error information is processed in different domains. In the all-digital PLL, the UP and DN pulses are overlapped, and the result is digitized and processed by a digital filter. For the CPPLL, a charge pump (CP) is used to generate a charge which is proportional to the time difference between the UP and DN pulses. The resulting charge is pumped into the analog filter, the output voltage of which controls the VCO. This similarity allows one to extend the design procedure for a second-order CPPLL to a second-order ADPLL.

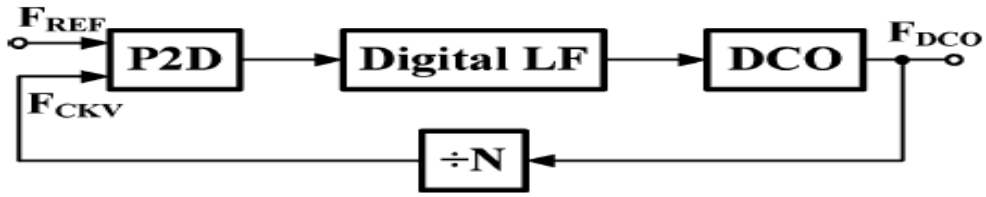

Figure 1: All Digital PLL

III. DYNAMIC VOLTAGE AND FREQUENCY SCALING

DVFS (Dynamic voltage and frequency scaling) is a generally employed proficiency to preserve power on a broad range of calculating systems such as embedded systems, laptop, desktop systems and eminent-performance server-category systems. DVFS can be able to minimize the consumption of power of CMOS integrated circuit, like a modern computing processor, by minimizing the frequency at that it works is shown by,

$$W = C_p f v^2 + P_{stat}$$

Where C_p is the transistor gate capacitance that reckons on boast size, f is the working frequency and v is the supplied voltage and the voltage necessitated for static operation is decided by the frequency of the circuit which is clocked. These can be minimized if the frequency is also minimized and this can be affording a substantial reduction in consumption of power since it has the v^2 relationship which is shown in above equation.

IV. GLOBALLY ASYNCHRONOUS LOCALLY SYNCHRONOUS

GALS (Globally Asynchronous Locally Synchronous) Systems merge the gains of systems such as synchronous and asynchronous systems and the modules are planned like modules in a globally synchronous plan, employing the similar tools and methodologies. Each and every block is severally clocked that assists to relieve clock skew and links among the synchronous blocks may be asynchronous. When data moves into a synchronous system from an asynchronous system, registers in that input are prostrate to metastability. In order to obviate this, the reaching of data is suggested by AHP (Asynchronous Handshaking Protocol). When the data reaches, the topically generated clock is hesitated: in exercise the arising edge of that clock is detained.

Once data is securely arrived, the clock is relinquished so data is connected with zero probability of the metastability on the path of data. [14] utilized ME components to intercede between the clock and the entering requests that assisted to excrete metastability. [15] presented wrappers of asynchronous systems, ideal components that can be located throughout synchronous modules to render the handshake signals and build them GALS modules and the local clock generator is fabricated from inverter and a delay line which is alike with an inverter ring oscillator. The trouble of utilizing such inverters is that which alone has a delay line and it is very difficult to exactly tune the clock period as operation variations and temperature impress the delay. Thus exact delay lines are formulated that can be able to maintain a static clock frequency [16], [17].

Cite this article as: A G Paranthaman, S Anbarasu, R Neethu. "An effective clock generator for Heterogeneous GALS in CMOS technology." *International Conference on Systems, Science, Control, Communication, Engineering and Technology (2015)*: 140-143. Print.

V. MULTIPROCESSOR SYSTEMS-ON-CHIP

MPSoCs (Multiprocessor systems-on-chips) have issued in past few decades as a significant class of VLSI (Very Large Scale Integration) systems and the MPSoC is a system on-chip, a VLSI system which integrates most of the components essential for an application and which utilizes MPP (Multiple Programmable Processors) as their system components. Multiprocessor systems-on-chips are widely employed in networking, communication systems, digital signal processing, multimedia and other applications.
MPSoCs substantiate as an essential and discrete branch of multiprocessors and they are not merely conventional multiprocessors reduced to a single chip but are planned to fulfill the unequalled necessities of embedded features. MPSoCs have been in production for much longer than multicore processors. We argue in this section that MPSoCs form two important and distinct branches in the taxonomy of multiprocessors: homogeneous and heterogeneous multiprocessors. The importance and historical independence of these lines of multiprocessor development are not always appreciated in the microprocessor community.

VI. DIGITALLY CONTROLLED OSCILLATOR

Phase-Locked loops (PLLs) are widely used in many communication systems to clock and data recovery or frequency synthesis. Traditional analog circuit design such as PLL shifts the design paradigm toward more digitally intensive techniques, easier testability and less parameter variability because of process migration. A digitally controlled oscillator (DCO) based architecture for RF frequency synthesizer was reported in [1]. The LC tank DCO achieves very fine frequency resolution (23 kHz) by using advanced 0.13- m CMOS process. The switchable capacitance of the finest pMOS varactor is 38 attofarads. However, this DCO suffers from one fundamental drawback. Due to the extremely small size of varactor, it requires intensive circuit layout and needs advanced lithography technology. A long design cycle will occur as product design transfers to different processes or the design specifications are changed. Thus, this work attempts to propose a high resolution DCO by using NOR/NAND gates as novel varactor.

VII. EXPERIMENTAL RESULTS

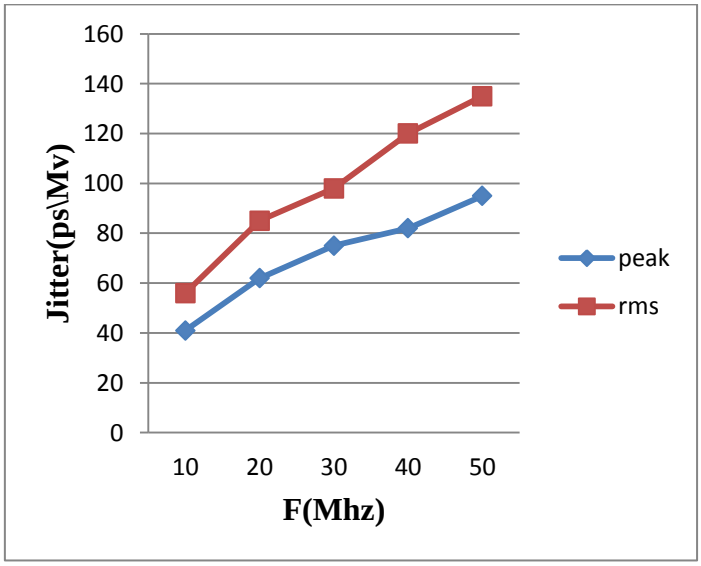

Fig 1:Performance Compared between Peak and Rms value according to Frequency and Jitter

VIII. CONCLUSION

Thus, we presented ADPLL (All-Digital Phase-Locked Loop) clock generator with low power consumption and very small chip area and such ADPLL contains DCO which only has analog custom components that guide to ultra small die area and in modern technologies these ultra small die area can scale well. The feature of DCO is to provide a new power-down strategy to assure save start-up and the open loop schemes are used to generate output clocks that permits instant variations in frequencies with no time-consuming ADPLL re-lock which renders fast frequency scaling in fine grained DVFS architectures. Moreover, such clock generators are renders a broad range of frequencies from 83MHz up to 4 GHz for core clocking, special purpose DDR2/3 clocks and high-speed NoC clocks. The performance is evaluated by test chip measurements in TSMC 65-nm LP CMOS technology and statistical measures demonstrate the robustness with respect to mismatch variations. Such phase mismatch effects in phase rotating frequency dividers is not an important effect for the directed application. The capacity of operation in MPSoC environments have been tested by noise sensitivity tests. Hence, our proposed circuit renders an effective new clocking solution for low-power consuming heterogeneous MPSoCs.

Cite this article as: A G Paranthaman, S Anbarasu, R Neethu. "An effective clock generator for Heterogeneous GALS in CMOS technology." *International Conference on Systems, Science, Control, Communication, Engineering and Technology (2015)*: 140-143. Print.

REFERENCES

[1]. U. Ramacher, "Software-defined radio prospects for multistandard mobile phones," Computer, vol. 40, no. 10, pp. 62–69, Oct. 2007.

[2]. D. Schinkel, E. Mensink, E. Klumperink, E. Ven Tuijl, and B. Nauta, "Low-power, high-speed transceivers for network-on-chip communication," IEEE Trans. Very Large Scale Integr. (VLSI) Syst., vol. 17, no. 1, pp. 12–21, Jan. 2009.

[3]. S. Scholze,H. Eisenreich, S. Höppner, G. Ellguth, S. Henker, M. Ander, S. Hänzsche, J. Partzsch, C.Mayr, and R. Schüffny, "A 32 GBit/s communication SoC for a waferscale neuromorphic system," Integr., VLSI J., vol. 45, no. 1, pp. 61–75, 2012.

[4]. T. Limberg,M.Winter, M. Bimberg, R. Klemm, E.Matus,M. Tavares, G. Fettweis, H. Ahlendorf, and P. Robelly, "A fully programmable 40 GOPS SDR single chip baseband for LTE/WiMAX terminals," in Proc. Solid-State Circuits Conf., 2008, pp. 466–469.

[5]. S. Vangal, J. Howard, G. Ruhl, S. Dighe, H. Wilson, J. Tschanz, D. Finan, A. Singh, T. Jacob, S. Jain, V. Erraguntla, C. Roberts, Y. Hoskote, N. Borkar, and S. Borkar, "An 80-tile sub-100-W teraflops processor in 65-nm CMOS," IEEE J. Solid-State Circuits, vol. 43, no. 1, pp. 29–41, Jan. 2008.

[6]. Z. Yu and B. Baas, "High performance, energy efficiency, and scalability with GALS chip multiprocessors," IEEE Trans. Very Large Scale Integr. (VLSI) Syst., vol. 17, no. 1, pp. 66–79, Jan. 2009.

[7]. W. Kim, M. Gupta, G.-Y.Wei, and D. Brooks, "System level analysis of fast, per-core DVFS using on-chip switching regulators," in Proc. IEEE 14th Int. Symp. High Perform. Comput. Arch. (HPCA), 2008, pp. 123–134.

[8]. D. Truong, W. Cheng, T. Mohsenin, Z. Yu, A. Jacobson, G. Landge, M. Meeuwsen, C. Watnik, A. Tran, Z. Xiao, E. Work, J. Webb, P. Mejia, and B. Baas, "A 167-processor computational platformin 65 nm CMOS," IEEE J. Solid-State Circuits, vol. 44, no. 4, pp. 1130–1144, Apr. 2009.

[9]. R. Jipa, "Dedicated solution for local clock programming in GALS designs," in Proc. Int. Semicond. Conf. (CAS), 2008, pp. 393–396.

[10]. A. Sobczyk, A. Luczyk, and W. Pleskacz, "Controllable local clock signal generator for deep submicron GALS architectures," in Proc. 11th IEEE Workshop Design Diagnose. Electron. Circuits Syst., 2008, pp. 1–4.

[11]. S. Moore, G. Taylor, P. Cunningham, R. Mullins, and P. Robinson, "Self calibrating clocks for globally asynchronous locally synchronous systems," in Proc. Int. Conf. Computer. Design, 2000, pp. 73–78.

[12]. L. Xiu, "A flying-adder on-chip frequency generator for complex SoC environment," IEEE Trans. Circuits Syst. II, Exp. Briefs, vol. 54, no. 12, pp. 1067–1071, Dec. 2007.

Cite this article as: A G Paranthaman, S Anbarasu, R Neethu. "An effective clock generator for Heterogeneous GALS in CMOS technology." *International Conference on Systems, Science, Control, Communication, Engineering and Technology (2015)*: 140-143. Print.

International Conference on Systems, Science, Control, Communication, Engineering and Technology 2015 [ICSSCCET 2015]

ISBN	978-81-929866-1-6	**VOL**	01
Website	icssccet.org	**eMail**	icssccet@asdf.res.in
Received	10 - July - 2015	**Accepted**	31- July - 2015
Article ID	ICSSCCET030	**eAID**	ICSSCCET.2015.030

A COMPACT PRINTED QUASI YAGI ANTENNA FOR WIRELESS APPLICATIONS

R Neethu[1], A Manikandan[2], S Anbarasu[3]
[1, 2, 3] Assistant Professor, Department of ECE,
Karpagam Institute of Technology, Coimbatore,Tamilnadu,India

Abstract: *A compact planar printed quasi-Yagi antenna is presented. The proposed antenna consists of a microstrip line to slotline transition structure, a driver dipole and two parasitic strips. The driverdipole is connected to the slotline through coplanar stripline (CPS). A compact planar printed quasi-Yagi antenna is presented. The proposed antenna consists of a microstrip line to slot line transition structure, a driver dipole and two parasitic strips. The driver dipole is connected to the slotline through coplanar stripline (CPS). This "quasi-Yagi" antenna achieves a measured 48% bandwidth for VSWR<2, better than 12 dB front-to-back ratio, smaller than -15 dB cross polarization, 3–5 dB absolute gain and a nominal efficiency of 93% across the operating bandwidth.and a nominal efficiency of 95%.*

Key words*:* Quasi-Yagi antenna, size reduction, unidirectional radiation pattern, wideband antenna.microstrip antennas.

I. INTRODUCTION

Yagi antennas have been widely used to obtain unidirectional radiation and high gain due to their simple structures [1]. Since the microstrip-fed quasi-Yagi antenna was first introduced by Huang in 1991[2], the planar printed quasi-Yagi antenna has attracted much attention owing to the advantages such as low profile, light weight, ease of fabrication and installation, etc., [3], [4].In this paper, we report a new type of planar Yagi–Uda antenna that is well suited to microwave and millimeter wave frequencies. Recently, planar quasi-Yagi antenna have received renewed interest due to its suitability for a wide range of application such as wireless communication systems, power combining, phased arrays, active arrays as well as millimeter-wave imaging arrays. Aim to increase the bandwidth of planar printed quasi-Yagi antennas,many designs have been reported in [5]–[11]. A quasi-Yagi antenna based onmicrostrip-to-slotline transition structurewas presented in [5]. Typical feeding methods utilizedinclude a microstrip feed [1 - 2] or a coplanar waveguide (CPW) feed [3] each requiring a balun to transform the transmission line mode at the input port of the antenna to the coplanar stripline [3]. A modified broadband microstrip-to-coplanar stripline (CPS) balun was used in quasi-Yagi antenna designs for increasing the antenna bandwidth [6], [7]. Approximately 48% and 38.3% bandwidth were achieved by using the microstrip-to-coplanar stripline transition structures in [6] and [7], respectively. However the bandwidths of the antennas are still restricted by the delay line used in the balun structures.

Coplanar waveguide feeding or ultrawideband balun were presented to improve the bandwidth in some designs [8], [9]. A broad bandwidth of 44% was obtained in [8]. The remainder of the communication is organized as follows. The geometry and parameters of the quasi-Yagi antenna are given in Section II. Simulation and measurement results are shown in Section III to demonstrate the effectiveness of the proposed antenna. Conclusions are drawn in the final section.

Cite this article as: R Neethu, A Manikandan, S Anbarasu "A COMPACT PRINTED QUASI YAGI ANTENNA FOR WIRELESS APPLICATIONS." *International Conference on Systems, Science, Control, Communication, Engineering and Technology (2015)*: 144-147. Print.

II.ANTENNA DESIGN

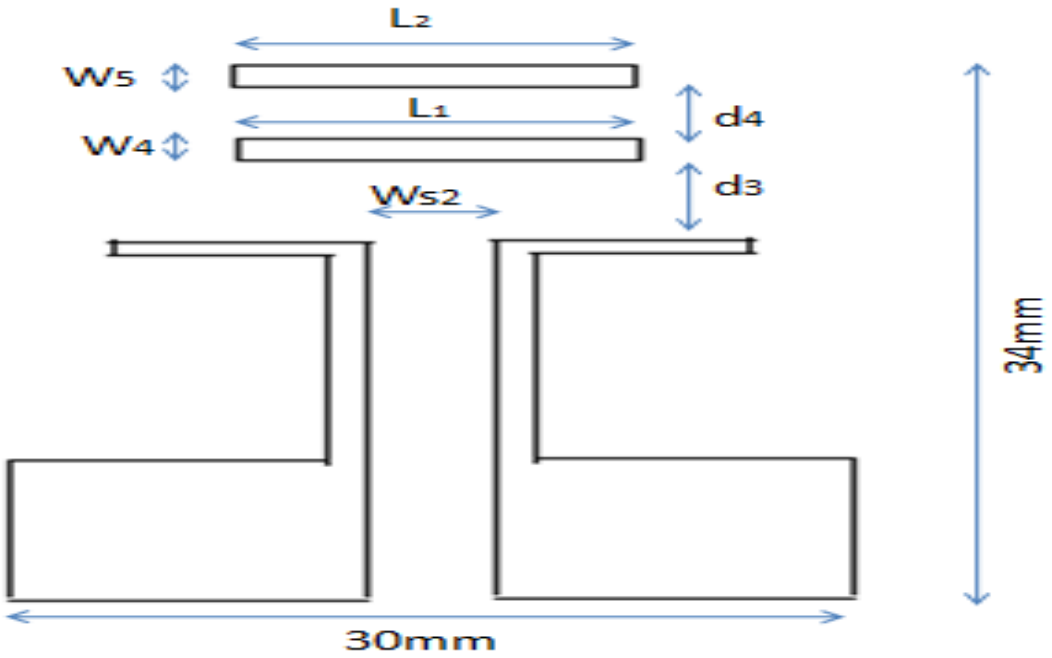

Fig. 1. Geometric structure and parameters of the proposed planar printed quasi-Yagi antenna

Fig. 1 shows the geometric structure and parameters of the proposed planar printed quasi-Yagi antenna. This antenna is printed on a FR-4 substrate with a dielectric constant of 4.4 and a thickness of 0.8 mm.The antenna is placed at xoy-plane. The xoy-plane is used as E-plane and the yoz-plane is set as H-plane. As can be seen from the figure, the antenna consists of two director elements, a driven element and a ground plane acting as a reflector. The antenna is fed by a CPW transmission line and as can be seen from Fig. 1 The top metallization consists of a microstrip feed, a broadband microstrip-to-coplanar stripline (CPS) balun and two dipole-elements, one of which is the driver element fed by CPS, and the second dipole being the parasitic director. The driver dipole is connected to the ground plane through coplanar stripline (CPS). The width of the ground plane equals to the lengthof the driver dipole. Compared with conventional planar quasi-Yagi antennas, the lateral size of the proposed antenna is reduced by modifying the ground plane. It is achieved by symmetrically adding two extended stubs to a flat ground plane. The microstrip line to slotline transition between the MS line and the CPS line is used to match the input impedance of the antenna to a 50- feeding line. In order to get agood impedancematching, a steppedmicrostrip feeding line is adopted. The width of the microstrip feeding line is fixed at 1.5 mm to achieve 50- characteristic impedance. The metallization on the bottom plane is a truncated microstrip ground, which serves as the reflector element for the antenna. The parasitic director element on the top plane simultaneously directs the antenna propagation toward the endfire direction, and acts as an impedance matching element.

Antenna Dimensions:
L=19.2 mm
W=29 mm
Ldir=3.73 mm
Sdirl=Sdir2=0.96 mm
Wdri Wdirl=Wdir2=0.96 mm
Ldir=11.5 mm
w=1 mm
L1=7.61 mm
L2=8.61 mm
Srd=9.69 mm
Sref=5.69 mm.

Cite this article as: R Neethu, A Manikandan, S Anbarasu "A COMPACT PRINTED QUASI YAGI ANTENNA FOR WIRELESS APPLICATIONS." *International Conference on Systems, Science, Control, Communication, Engineering and Technology (2015)*: 144-147. Print.

III.EXPERIMENTAL RESULTS

The designed antenna was fabricated with the optimized parameters. The difference between the simulated and the measured results is due to the effect of the SMA connector and fabrication imperfections. In order to demonstrate the radiation characteristics of the quasi-Yagi antenna, its radiation patterns are measured.

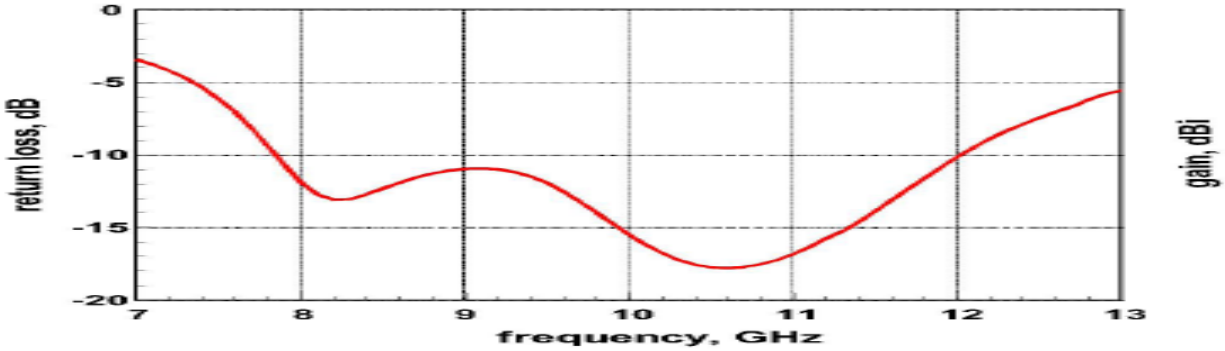

Figure 3:Return loss performance of the antenna

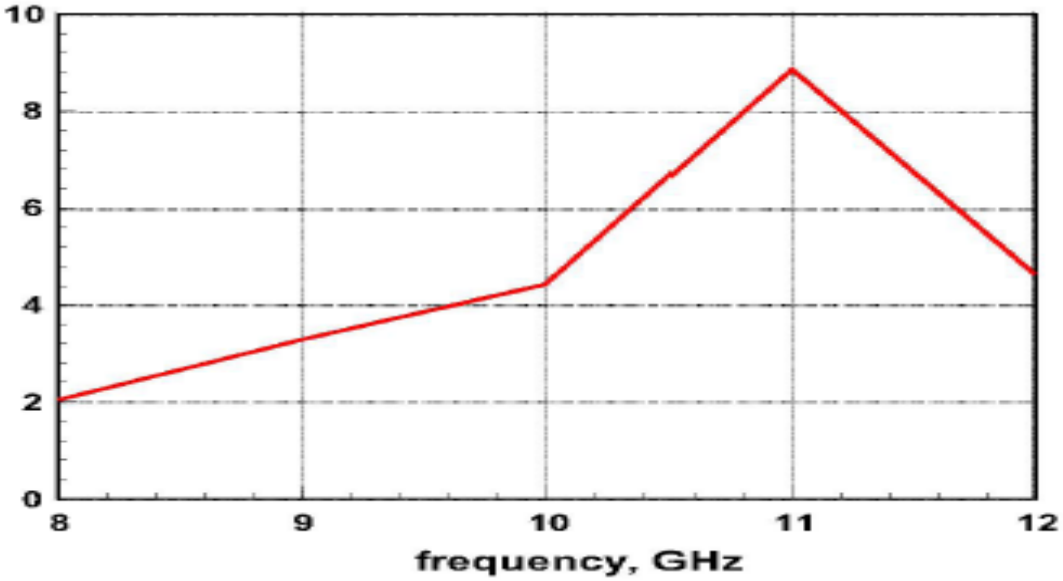

Figure 4:Gain of the antenna

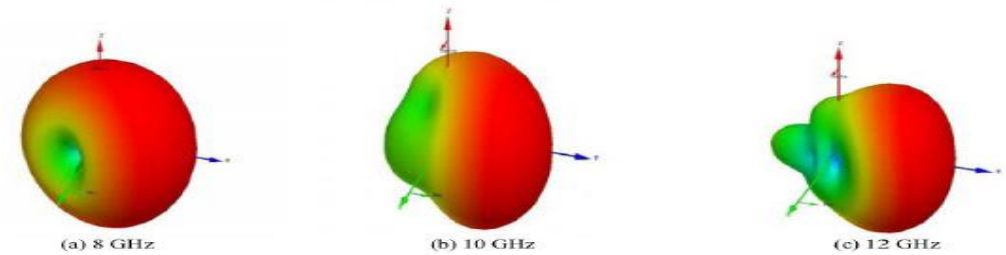

Figure 5:Three dimensional radiation pattern

IV.CONCLUSION

A planar printed quasi-Yagi antenna with size reduction is designed and experimentally studied in this communication. The antenna consists of a microstrip line to slotline transition structure, a driver dipole and two parasitic strips. Two extended stubs are symmetrically added to the ground plane. A coplanar waveguide-fed antenna has been presented. The antenna is the simplest form of a planar quasi-Yagi and it does not require any complicated balun structure and is unipolar. The 10 dB return loss bandwidth of the antenna is 40 % and showed directive radiation properties. In addition, the measured group delay of the antenna shows that this planar

Cite this article as: R Neethu, A Manikandan, S Anbarasu "A COMPACT PRINTED QUASI YAGI ANTENNA FOR WIRELESS APPLICATIONS." *International Conference on Systems, Science, Control, Communication, Engineering and Technology (2015)*: 144-147. Print.

quasi-Yagi antenna has a good time-domain characteristic, which means that a transmitted signal will not be seriously distorted by using this printed quasi-Yagi antenna.

V REFERENCES

[1] K. Han, Y. Park, H. Choo, and I. Park, "Broadband CPS-fed Yagi-Uda antenna," *Electron. Lett.*, vol. 45, no. 24, Nov. 2009.
[2] R. A. Alhalabi and G. M. Rebeiz, "Differentially-fed millimeter-waveNYagi-Uda antennas with folded dipole feed," *IEEE Trans. Antennas Propag.*, vol. 58, no. 3, pp. 966–969, Mar. 2010.
[3] S. X. Ta, S. Kang, and I. Park, "Closely spaced two-element foldeddipole- driven quasi-Yagi array," *J. Electromagn. Engrg. Sci.*, vol. 12, no. 4, pp. 254–259, Dec. 2012.
[4] P. T. Nguyen, A. Abbosh, and S. Crozier, "Wideband quasi-Yagi antenna with tapered driver," in *Proc. Asia-Pacific Conf. on Antennas and Propagation*, Singapore, Aug. 2012, pp. 138–139.
[5] K. Jiang, Q. G. Guo, and K. M. Huang, "Design of a wideband quasi- Yagi microstrip antenna with bowtie active elements," in *Proc. Int. Conf. onMicrowave andMillimeterWave Technology (ICMMT)*, 2010, pp. 1122–1124

Cite this article as: R Neethu, A Manikandan, S Anbarasu "A COMPACT PRINTED QUASI YAGI ANTENNA FOR WIRELESS APPLICATIONS." *International Conference on Systems, Science, Control, Communication, Engineering and Technology (2015)*: 144-147. Print.

International Conference on Systems, Science, Control, Communication, Engineering and Technology 2015 [ICSSCCET 2015]

ISBN	978-81-929866-1-6
Website	icssccet.org
Received	10 - July - 2015
Article ID	ICSSCCET031

VOL	01
eMail	icssccet@asdf.res.in
Accepted	31- July - 2015
eAID	ICSSCCET.2015.031

OPTIMIZATION OF PEER TO PEER CONTENT BASED FILE SHARING SYSTEM IN DISCONNECTED MANETS

Syed Jamaesha[1], T Boobalan[2]
[1, 2] Assistant Professor, Department of ECE
[1]Karpagam Institute of Technology.
[2]Sri Eshwar College of Engineering
Coimbatore.

ABSTRACT: *Current peer-to-peer (P2P) file sharing methods in mobile ad hoc networks (MANETs) can be classified into three groups: flooding-based, advertisement-based, and social contact-based. The first two groups of methods can easily have high overhead and low scalability. They are mainly developed for connected MANETs, in which end-to-end connectivity among nodes is ensured. The third group of methods adapts to the opportunistic nature of disconnected MANETs but fails to consider the social interests. SPOON groups common-interest nodes that frequently meet with each other as communities. It takes advantage of node mobility by designating stable nodes, which have the most frequent contact with community members, as community coordinators for intercommunity searching, and highly mobile nodes that visit other communities frequently as community ambassadors for intercommunity searching. An interest-oriented file searching scheme is proposed for high file searching efficiency. Additional strategies for file prefetching, querying-completion, and loop prevention, and node churn consideration are discussed to further enhance the file searching efficiency.*

INTRODUCTION

Mobile Ad Hoc Network (MANET) is a self-configuring system of mobile routers linked by wireless links which consequently combine to form an arbitrary topology. Thus, the topology may alter rapidly and unpredictably. However, due to the lack of any fixed infrastructure, it becomes complicated to exploit the present routing techniques for network services, and this provides some huge challenges in providing the security of the communication, which is not done effortlessly as the number of demands of network security conflict with the demands of mobile networks, largely due to the nature of the mobile devices e.g. low power consumption, low processing load.

LITERATURE REVIEW:

Cutting without Pain: Mitigating 3G Radio Tail Effect on Smartphones

Although having those applications mobile is quite appealing, high data rate transmission also poses huge demand for power. It has been revealed that the tail effect in 3G radio operation results in significant energy drain on smartphones. Recent fast dormancy technique can be utilized to remove tails but, without care, can degrades user experience. Propose a novel scheme SmartCut, which effectively mitigates the tail effect of radio usage in 3G networks with little side-effect on user experience. The core idea of SmartCut is to utilize the temporal correlation of packet arrivals to predict upcoming data, based on which unnecessary high-power-state tails of

Cite this article as: Syed Jamaesha, T Boobalan. "OPTIMIZATION OF PEER TO PEER CONTENT BASED FILE SHARING SYSTEM IN DISCONNECTED MANETS." *International Conference on Systems, Science, Control, Communication, Engineering and Technology (2015)*: 148-150. Print.

radio are cut out leveraging the Fast Dormancy mechanism.
Extensive trace-driven simulation results demonstrate the efficacy of SmartCut design. On average, SmartCut can save up to 56.57% energy on average while having little side-effect to user experience. SmartCut, which uses historical 3G traffic data to train ARMA models and further utilizes the predicted arrival time of future data transmission to effectively cut unnecessary tails while having little side effect to user experience.

Energy Consumption In Wireless
Networks Progress

Since the mobile phone relies on a limited power source and provides more demanding services today, minimizing the energy consumption is one of most important factors to consider. In this context, the focus will be set for two areas: modulation formats in the physical layer and the RRC-protocol in the network layer. The modulation formats section will be a literature study only, to show the energy advantages by using higher modulation combined with channel coding. Main focus will be set on the RRC-protocol and its functionality. The simulation chapter will show the importance of precise timer settings to gain energy efficiency as well as a comparison between the original RRC-protocol and a RRC-protocol proposed by us. The result shows decrease of 2.4 % for the proposal RRC and therefore seems to be more effective during web browsing utilization. Furthermore, the effect of the proposed RRC has to be confirmed in other utilization aspects as well as its impact on the transmission delay.

Energy Consumption of Always-On Applications in WCDMA Networks

Always-on applications, such as push email and voice-over-IP, are characterized by the need to be constantly reachable for incoming communications. In the presence of stateful firewalls or NATs, such applications require "keep-alive" messages to maintain up-to-date connection state in the firewall or NAT, and thus preserve reachability. Analyze how these keep-alive messages influence battery lifetime in WCDMA networks. Using measurements in a 3G network, we show that the energy consumption is significantly influenced by the Radio Resource Control (RRC) parameters and the frequency of keep-alive messages. The results suggest that especially UDP-based protocols, such as Mobile IPv4 and IPsec NAT Traversal mechanisms, require very frequent keep-alives that can lead to unacceptably short battery lifetimes. Especially UDP-based protocols with long sessions can lead to unacceptably short battery lifetimes. The most important factors influencing energy consumption are the RRC parameters and frequency of keep-alive messages, and thus 3G network.

Traffic-Aware Techniques to Reduce 3G/LTE Wireless Energy Consumption

The 3G/LTE wireless interface is a significant contributor to battery drain on mobile devices. A large portion of the energy is consumed by unnecessarily keeping the mobile device's radio in its "Active" mode even when there is no traffic. This paper describes the design of methods to reduce this portion of energy consumption by learning the traffic patterns and predicting when a burst of traffic will start or end. We develop a technique to determine when to change the radio's state from Active to Idle, and another to change the radio's state from Idle to Active. In evaluating the methods on real usage data from 9 users over 28 total days on four different carriers, find that the energy savings range between 51% and 66% across the carriers for 3G, and is 67% on the Verizon LTE network. When allowing for delays of a few seconds (acceptable for background applications), the energy savings increase to between 62% and 75% for 3G, and 71% for LTE. The increased delays reduce the number of state switches to be the same as in current networks with existing inactivity timers. The key idea in this paper is to adapt the state of the radio to network traffic. To put the 66% saving (without any delays) or 75% saving (with delay) .

OUR PROPOSAL

Dual Queue Scheduling Algorithm

- In telecommunication a distributed multi-access network that (a) supports integrated communications using a dual bus and distributed queuing, (b) provides access to local or metropolitan area networks, and (c) supports connectionless data transfer connection-oriented data transfer, and isochronous communications, such as voice communications.
- Dual queue scheduling algorithm for scheduling these two categories of requests.
- TailTheft schedules requests by maintaining two queues:
- (1) the real-time queue for requests that must be scheduled instantaneously, and (2) the TailTheft queue for TailTheft requests.
- TailTheft schedules requests in the real-time queue if requests are present in this queue and schedules those in the TailTheft queue if the real-time queue is empty or if the deadline of the first request in the TailTheft queue approaches.

Virtual Tail Time

Achieving batching and prefetching in the tail time requires identification of the time during which these tasks can be performed. The types of demotion, namely, DCH→FACH→IDLE or DCH→IDLE, can be accurately determined. The former demotion type has two tail times (T1 and T2), and the latter has only one tail time (T1). The mechanism of the two tail times can be directly applied to one tail time. Thus, we consider only the former. i separate the two tail times primarily because the scheduling rates in these two periods are distinct. Two mechanisms are employed for online determination of whether now is the tail time. Power-based state inference mechanism is used to infer the current RRC state based on power consumption.

Cite this article as: Syed Jamaesha, T Boobalan. "OPTIMIZATION OF PEER TO PEER CONTENT BASED FILE SHARING SYSTEM IN DISCONNECTED MANETS." *International Conference on Systems, Science, Control, Communication, Engineering and Technology (2015)*: 148-150. Print.

Handling TailTheft Requests

TailTheft is feasible if and only if it not only transmits requests in the real-time queue as soon as they are inserted, but also processes requests in the TailTheft queue before their deadlines. Specifically, delay-tolerant requests should be scheduled before their deadlines, and previous attempts should be scheduled before their deadlines or discarded as their deadlines approach. To meet the deadlines indicated by requests, the dual queue scheduling algorithm introduces a new timer θ. After being delivered by applications, TailTheft requests are added to the queue from small to large, according to the time between tnow and di, where tnow is the current time, and di equals to the sum of the arrival time ai and the absolute value of **r_delay** of request i. The first request in the TailTheft queue is assigned with the latest deadline and is the first to be transmitted. After each enqueue operation, TailTheft derives the latest deadline, denoted as dl, and restarts the timer θ, the end time of which is dl −tnow. When now is the virtual tail time, the first request in the queue is dequeued first. Timer θ is cancelled before the first request is dequeued and reactivated according to the deadline of the next request in the queue after dequeuing.

RESULTS &CONCLUSION

Inactivity timers in cellular networks are used to balance the trade-offs between resource efficiency for enhanced user experience and low management overhead. However, considerable radio resources and battery energy are wasted in the tail time. Proposed TailTheft, which leverages the tail time for batching and prefetching. Our work is the first to consider using rather than eliminating the tail time for saving energy. To utilize the tail time, TailTheft uses a virtual tail time mechanism to determine the amount of tail time that can be used and a dual queue scheduling algorithm to schedule transmissions. Given that numerous transmissions are scheduled in the tail time, energy consumption is significantly decreased. TailTheft can benefit a number of common applications, including delay-tolerant applications (e.g., e-mail, RSS feeds, and software updates), and prefetchable applications (e.g., news, social networking, browsing, media and maps). We have simulated TailTheft in NS-2 and evaluated its performance under various conditions. The experimental results show that TailTheft achieves more significant savings on battery energy and radio resources than existing methods.

REFERENCE

[1] "The State of the Smartphone Market," http://www.allabout symbian.com/news/item/6671_The_State_of_the_Smartphone_ Ma.php, 2013.
[2] "Next Generation Smartphones Players, Opportunities & Forecasts 2008-2013," technical report, Juniper Research, 2009.
[3] "A Market Overview and Introduction to GyPSii," http:// corporate.gypsii.com/docs/MarketOverview, 2013.
[4] "Bittorrent," http://www.bittorrent.com, 2013.
[5] "Kazaa," http://www.kazaa.com, 2013.

Cite this article as: Syed Jamaesha, T Boobalan. "OPTIMIZATION OF PEER TO PEER CONTENT BASED FILE SHARING SYSTEM IN DISCONNECTED MANETS." *International Conference on Systems, Science, Control, Communication, Engineering and Technology (2015)*: 148-150. Print.

International Conference on Systems, Science, Control, Communication, Engineering and Technology 2015 [ICSSCCET 2015]

ISBN	978-81-929866-1-6
Website	icssccet.org
Received	10 - July - 2015
Article ID	ICSSCCET032

VOL	01
eMail	icssccet@asdf.res.in
Accepted	31- July - 2015
eAID	ICSSCCET.2015.032

Equity Portfolio Optimization Algorithm for Neural Networks

Dr K Keerthivasan[1], S Gopinath[2]
[1]Professor & Head and [2] Assistant Professor, Department of ECE,
Karpagam Institute of Technology, Coimbatore

Abstract *- Stock trading point's detection is a very interesting subject arising in numerous financial and economic planning problems. Here a Hybrid Intelligent system (HIS) method with dynamics time warping system for stock trading point's detection is presented. The Hybrid intelligent system is able to generate numerous stocks trading points from the historic data base, and then the dynamic time warping system will be applied to retrieve similar stock price patterns from historic data for training the system. These trading points represent short-term trading signals for selling or buying stocks from the market. A Back-Propagation neural network and Genetic Algorithm is further applied to learn the connection weights from these historic trading points and afterwards it is applied to forecast the future trading points from the set of test data. Experimental results demonstrate that the Hybrid Intelligent system with genetic algorithm can make a significant amount of profit when compared with other approaches using stock data.*

Keywords - Hybrid Intelligent system; Genetic Algorithm; Neural Network; Fuzzy Inference System

I. INTRODUCTION

Trading Points are difficult to predict to a particular Stock because they don't have much information about the trading points of a particular Stock. The Hybrid Intelligent System is used to decompose the particular Trading points and the result would be passed on to the back propagation neural network to train the entire Model. A hybrid intelligent system is developed with the genetic algorithm to be integrated with the neural network to improve the threshold value to further increase the profitability of the model. The refinement of data using genetic algorithm and the BPN models are used to predict the Trading Points. A genetic algorithm (GA) is a search technique used in computing to find exact or approximate solutions to optimization and search problems. Genetic algorithms are categorized as global search heuristics. Genetic algorithms are a particular class of evolutionary algorithms (EA) that use techniques inspired by evolutionary biology such as inheritance, mutation, selection, and crossover.

II. DEVELOPMENT OF HYBRID INTELLIGENT SYSTEM

The HIS is started up with the retrieval of the data from the specified server. The data taken out is used to develop the pattern and the template. The pattern and template are the training data and they are passed on to the HIS .The HIS comprises of the Neural Network and the Genetic Algorithm. In the Neural Network the training data is checked along with the testing data .They are assigned weights

Cite this article as: Dr K Keerthivasan, S Gopinath. "Equity Portfolio Optimization Algorithm for Neural Networks." *International Conference on Systems, Science, Control, Communication, Engineering and Technology (2015)*: 151-154. Print.

and if the weights do not satisfy the neural condition they are again trained unless they attain the required weight to pass on to the next phase. The next Phase would be the genetic algorithm where the stock trading points are predicted. The Crossover pattern is used here to predict the future trading points. Entire HIS operation in predicting the stock trading points is represented in Fig.1.

A. Back Propagation Neural Network

Neural networks are applicable in virtually every situation in which a relationship between the predictor variables (independents, inputs) and predicted variables (dependents, outputs) exists, even when that relationship is very complex and not easy to articulate in the usual terms of "correlations" or "differences between groups. Fluctuations of stock prices and stock indices are another example of a complex, multidimensional, but in some circumstances at least partially-deterministic phenomenon. Neural networks are being used by many technical analysts to make predictions about stock prices based upon a large number of factors such as past performance of other stocks and various economic indicators. The ability of the non linear relationships in input data makes them ideal for modeling the non linear dynamic systems such as the stock market. The Neural Networks are examined in three areas they are

1. Network Environment and training data
2. Network Organization
3. Network Performance.

The Neural Network must be trained on some Input Data. The two major problems in it are

1. Defining set of input used.

2. Deciding an algorithm to train the data.

Neural networks process numeric data in a fairly limited range. This presents a problem if data is in an unusual range, if there is missing data, or if data is non-numeric. Fortunately, there are methods to deal with each of these problems. Numeric data is scaled into an appropriate range for the network, and missing values can be substituted for using the mean value (or other statistic) of that variable across the other available training cases. After generating the sub segments through the PLR the trading points are needed to transformed into 0 and1 before they are fed to the BPN. The sub segments are divided and the time series data are defined as

If Ci=C+d; trend=upward;

If Ci=C-d; trend=downward;

If Ci=d<c; trend =steady;

Where

Ci is the stock Price at the ith trading point .

C is the stock price at the current trading point.

D is the threshold for checking the stock Price.

The trend is transferred as an output value of BPN. If the trend changes from up to down, the trading signal is changed from 0 to 1; if the trend changes from down to up, the trading signal is changed from 1 to 0; otherwise, the signal does not change. The trading Signals are not quite related to the Price Variation. The Trading signal should be able to react to the price variation and provide more detailed information. The trading points are redefined according to the tendency of the stock.

B. Back Propagation Algorithm

If the trend is up ward

$$Ti=Ci - \min\{Ci,Ci+1,Ci+c\} - \max\{Ci,Ci+1,Ci+c\} - \min\{Ci,Ci+1,Ci+c\} * 0.5$$

If the trend is downward

$$Ti=Ci - \min\{Ci,Ci+1,Ci+c\} - \max\{Ci,Ci+1,Ci+c\} - \min\{Ci,Ci+1,Ci+c\} * 0.5+0.5.$$

Ci means the Stock price of the ith Transaction Day.

The Back Propagation Leaning algorithm has two procedures. They are

Cite this article as: Dr K Keerthivasan, S Gopinath. "Equity Portfolio Optimization Algorithm for Neural Networks." *International Conference on Systems, Science, Control, Communication, Engineering and Technology (2015)*: 151-154. Print.

1) Feed forward step

2) Back propagation weight training step.

In back propagation, the gradient vector of the error surface is calculated. This vector points along the line of steepest descent from the current point, so we know that if we move along it a "short" distance, we will decrease the error. A sequence of such moves (slowing as we near the bottom) will eventually find a minimum of some sort. The difficult part is to decide how large the steps should be. A classic example of this in neural network training is where the algorithm progresses very slowly along a steep, narrow, valley, bouncing from one side across to the other. In contrast, very small steps may go in the correct direction, but they also require a large number of iterations. In practice, the step size is proportional to the slope and to a special constant: the learning rate. The correct setting for the learning rate is application-dependent, and is typically chosen by experiment; it may also be time-varying, getting smaller as the algorithm progresses.

C. Genetic Algorithm

A genetic algorithm has three major components. The first component is related with the creation of an initial population of m *randomly* selected individuals. The initial population shapes the first generation. The second component inputs m individuals and gives as output an evaluation for each of them based on an objective function known as fitness function. This evaluation describes how close to our demands each one of these m individuals is. Finally the third component is responsible for the formulation of the next generation. A new generation is formed based on the fittest individuals of the previous one. This procedure of evaluation of generation N and production of generation N+1(based on N) is iterated until a performance criterion is met.
A typical genetic algorithm requires:

1. A genetic representation of the solution domain,

2. A fitness function to evaluate the solution domain.

III. RESULT

The data retrieval would be from any server and then the generated pattern and the template are created with the data retrieved. The moving averages help out in a large scale for the using of the linear rise and fall in the retrieved points. The training process is only needed when a neural network is used. The genetic is used to search the best threshold value of the entire process. Using the HIS future trading points are predicted in an significant period of time.

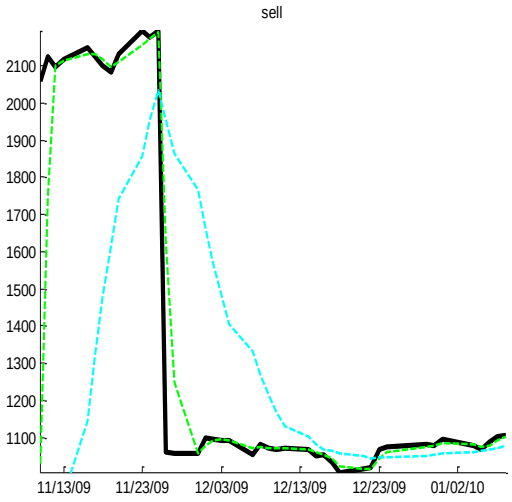

Figure 1. Compare moving average with current data.

The moving average would be useful in checking the input data because a graph would be plotted along with the data about the rise and the fall and it was shown in Fig. 1. Comparison between the genetic algorithm and the multi start search shows that the genetic algorithm can show improvements further. The risk of false prediction is completely eliminated by the algorithm and the conditions which are used in the Hybrid Intelligent System. The generated portfolio would say the entire details of the company along with the prediction in the stock trading points. The system is time efficient and with the usage of the neural and the genetic algorithm

Cite this article as: Dr K Keerthivasan, S Gopinath. "Equity Portfolio Optimization Algorithm for Neural Networks." *International Conference on Systems, Science, Control, Communication, Engineering and Technology (2015)*: 151-154. Print.

would help in more accurate prediction. The important fact of this system is it can work out in both the online and the offline mode. Offline mode is the process of manually selecting the trading points and predict based on them.

IV. CONCLUSION

The usage of the Back Propagation neural network and the algorithm in the HIS would help in analyzing the data through various conditions and also would generate a moving average before the algorithm. The main work of the algorithm is to select the trading points and pass on to the next algorithm. The Genetic Algorithm is the one where the process of prediction occur which would be more accurate and the time efficiency is also higher. The proposed system with the genetic algorithm and the crossover pattern would help the stock traders in predicting the points for the current data and the old data. By which the system operation can be certainly understandable by the prediction of the trading point for the earliest of the day and the predicting capability of the system can also be checked at any time and for any kind of the stock data. Hence the investors in the stock market can be given a certain indication of the future points whether to buy or sell it. Hence with this system the prediction can be more helpful for the traders to make an affinitive decision on a company stock on the current day whether to buy the stock or sell the stock of the particular company which is with in their hands.

REFERENCES

1. Norio Baba, Naoyuki Inoue."Utilization of neural networks and GA for constructing reliable decision support for stock trade points".2000 IEEE pages:111-116.
2. V.Srikanth "A Multi agent hybrid Architecture ".CIFER 1999 pages:64-73
3. Paul bao, Hakman Wong "A hybrid portfolio theory model based on genetic algorithm and vector quantization". 1998 IEEE pages;4301-04
4. Meng-feng Yen; Tsung-nan Chou; Hung-chih Li; Ying-yue Ho "Using neural network and genetic algorithm to predict Inter commodity spreads"ICICIC 2007 page:192
5. Dr. Dennis ettes. "Trading the stock markets using the genetic fuzzy modeling". 10.1109/CIFER.2000 pages:22-25
6. Khan A.U, Bandopadhyaya T.K, Sharma, S "Classification and identification of stocks using som and genetic algorithm based back propagation neural network". IEEE 2008 in IIT pages: 292-296.
7. Jeurissen. R, van den Berg.J."Optimized index tracking using hybrid genetic algorithm". IEEE 2008 pages-2327-2334.
8. Fengming Ye Mahn,S, Lutao Wang Eto. S, Hirasawa. K."Genetic network programming with reconstructed individuals".IEEE2009 pages: 854-859

Cite this article as: Dr K Keerthivasan, S Gopinath. "Equity Portfolio Optimization Algorithm for Neural Networks." *International Conference on Systems, Science, Control, Communication, Engineering and Technology (2015)*: 151-154. Print.

International Conference on Systems, Science, Control, Communication, Engineering and Technology 2015 [ICSSCCET 2015]

ISBN	978-81-929866-1-6
Website	icssccet.org
Received	10 - July - 2015
Article ID	ICSSCCET033

VOL	01
eMail	icssccet@asdf.res.in
Accepted	31- July - 2015
eAID	ICSSCCET.2015.033

A Level-up Shifter using MTCMOS Technique for Power Minimization

T.Arthi[1], N.Preetha[2]
[1, 2]Assistant Professors, Department of ECE
Karpagam Institute of Technology, Coimbatore

Abstract- Level shifter is an interfacing circuit which can interface low core voltage to high input-output voltage. It allows communication between different modules without adding up any extra supply pin. The main objective of the work is to minimize power dissipation in shifter circuit, which is due to different supply voltages in the circuit. The proposed method uses MTCMOS technique, which is one of the low power design technique to achieve power minimization. The new circuit uses the multi-threshold CMOS technique to provide a wide voltage conversion . The proposed design is implemented in CADENCE Virtuoso 180-nm CMOS technology. The new LS reaches a propagation delay value of 17 ns, a static power dissipation of only 115.3 pW, for a 1-MHz input pulse.

Keywords- Level Shifter, Sub-threshold, MTCMOS, low power, low voltage.

I. INTRODUCTION

The most direct way to reduce power dissipation in digital LSIs is to reduce supply voltage. Several low power design techniques were used. Sub-threshold LSI is the most widely used in power aware applications. However there are a number of design challenges imposed and several studies were carried out. Among the techniques known in the literature to reduce power consumption, those based on power supply voltage reduction are considered very effective even though they can severely penalize speed performances . An alternative approach, known as the multi-supply voltage domain technique , consists of partitioning the design into separate voltage domains (or voltage islands), each operating at a proper power supply voltage level depending on its timing requirements.
A key challenge in the design of efficient multiple-supply circuits is minimizing the cost of the level conversion between different voltage domains while maintaining the overall robustness of the design. To such a purpose, level shifter (LS) circuits have to be used. Traditionally, level shifter circuits were used to allow chip core signals to be transmitted to the outside world through the pad ring, which often operated with different voltage levels.

II. CONVENTIONAL LEVEL SHIFTER METHOD

The conventional LS (Level Shifter) circuit consists of level conversion circuit and a logic error correction circuit (LECC) [3]. The complementary input signals (IN and INB) and the output signal (OUT) are applied to the LECC. Figure 1 shows the schematic of the conventional level shifter circuit. The operation principles of the circuits are described in the following sections.

Cite this article as: T Arthi, N Preetha. "A Level-up Shifter using MTCMOS Technique for Power Minimization." *International Conference on Systems, Science, Control, Communication, Engineering and Technology (2015)*: 155-158. Print.

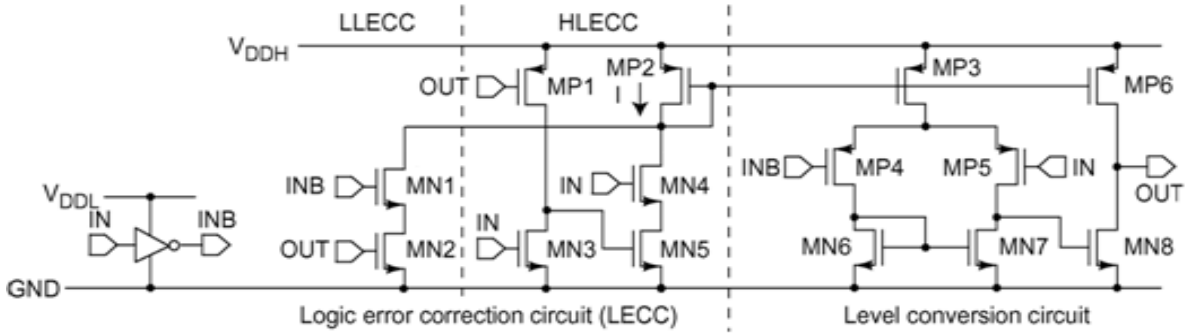

Fig. 1 Schematic of conventional Level Shifter Circuit

The LECC, which is shown on the left in Fig. 1, consists of two circuit blocks:

- a low logic error correction circuit (LLECC) and
- a high logic error correction circuit (HLECC).

The LECC generates an operating current such that IN and OUT correspond to each other. When the output logic level of the LS circuit corresponds to the input logic level, the LECC does not supply current . When they do not correspond, the LECC detects the logic error, and the LLECC or HLECC supplies an operating current. In other words, the LECC supplies an operating current only when the input and output logic levels do not correspond to each other. When IN and OUT correspond, the LECC does not supply any current to the level conversion circuit. However, in fact, leakage current flows in the circuit. However, when the input voltage signal is high, the output node of the current mirror floats, thus negatively impacting the overall power consumption.

The level conversion circuit, is based on a conventional two-stage comparator circuit which generates output voltage signal, OUT, according to the difference in the voltage of IN and INB. The output voltage is determined by the drive currents of pull-up transistor MP6 and pull-down transistor MN8, and the currents flowing in MP6 and MN8 depend on current flowing through MP2.

A. Drawbacks

In this conventional comparator design, a current reference circuit needs to operate steadily. However, because the current reference circuit dissipates static current and increases power dissipation , it proves impractical to use.

III. PROPOSED LEVEL SHIFTER CIRCUIT WITH MTCMOS TECHNIQUE

The circuit diagram of proposed level shifter circuit based on MTCMOS technique is shown in figure 2.

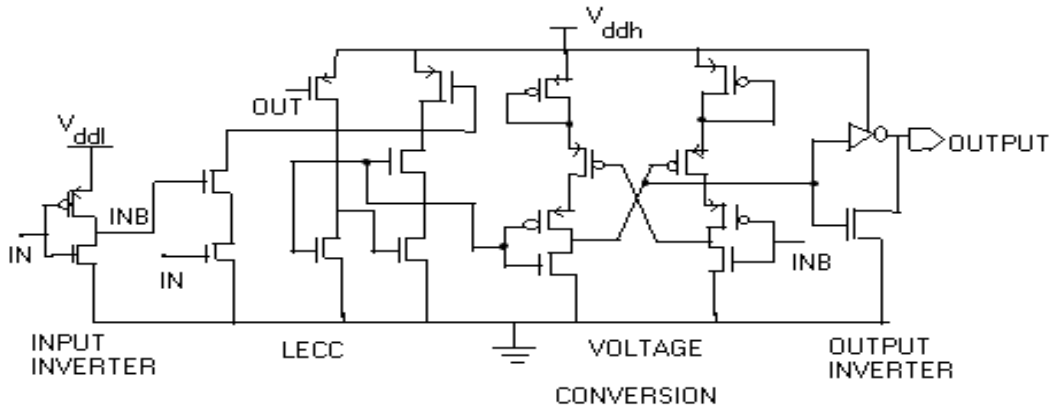

Figure 2. Schematic of Proposed Level Shifter Circuit based on MTCMOS Technique

A. Input Inverter

The input inverter consists of PMOS and NMOS transistors. They are driven by a lower supply voltage VDDL . The source of the PMOS transistor is connected to low supply voltage and the drain of NMOS is connected to ground.

B. LECC (Logic Error Correction Circuit)

The LECC is driven by IN, INB, and OUT. The LECC generates an operating current such that IN and OUT correspond to each other. When the output logic level of the LS circuit corresponds to the input logic level, the LECC does not supply current . When they do not correspond, the LECC detects the logic error.

C. Voltage Conversion Stage

The voltage conversion circuit is based on DCVS (Differential Cascode Voltage Switch) logic. The circuit is designed with low-voltage threshold (lvt), standard voltage threshold (svt), and high-voltage threshold (hvt) transistors. To provide fast differential low-voltage input signals and to increase the strength of the pull-down network of the main voltage conversion stage, the input inverter was created using lvt devices. To reduce the effect of cross bar current flowing in the nodes NH and NL, two lvt PMOS devices are adopted.

D. Output Inverter

Cite this article as: T Arthi, N Preetha. "A Level-up Shifter using MTCMOS Technique for Power Minimization." *International Conference on Systems, Science, Control, Communication, Engineering and Technology (2015)*: 155-158. Print.

The voltage conversion stage is connected to the output inverter so as to measure the required output of the proposed circuit.

IV. RESULTS

The proposed circuit is implemented in CADENCE – Virtuoso tool and implemented in 180 nm CMOS technology. Figure 3 shows the schematic drawn in Cadence tool. The circuit dissipates 115.3pW of static power with the supply voltage of less then 2V(1.8V). The fig.4 and fig. 5 shows the simulated waveform in Cadence and power spectral graph. Table 1 shows the performance comparison of various level shifter circuits. The table shows a considerable reduction in static power.

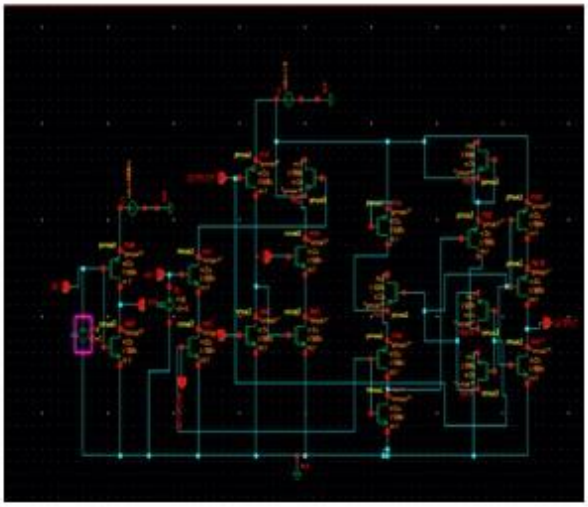

Figure 3. Schematic Circuit drawn in Cadence

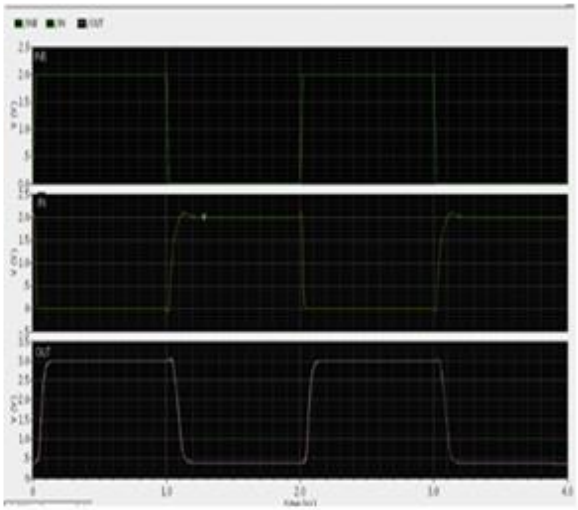

Figure 4. Level Shifted Waveform in Cadence

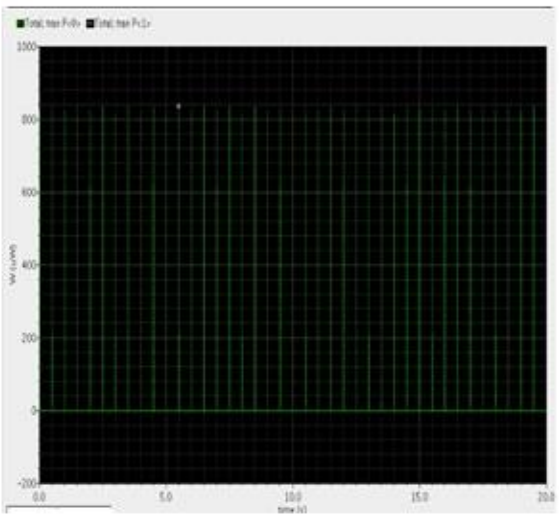

Figure 5. Power Spectral Graph of Proposed Circuit

Parameter	Conventional LS	Proposed LS
Type of technology	350 nm	180 nm
Type	Comparator	DCVS
V_{DD} (V), f_{IN} (Hz)	0.4, 10 kHz	0.23, 1 kHz
V_{DDL} (V)	0.23 V	0.2 V
V_{DDH} (V)	3 V	2.5 V
Static Power (nW)	58 nW	115.3 pW

Table 1. Performance Comparison Table

The power dissipation of the proposed LS circuit can be expressed as

$$P = P_{dyn} + P_{int}$$
$$= C_L V_{DDH}^2 f_{IN} + I_{AVG} V_{DDH} \quad (1)$$

where I_{AVG} is the average current flowing through the circuit.

V. CONCLUSION

Cite this article as: T Arthi, N Preetha. "A Level-up Shifter using MTCMOS Technique for Power Minimization." *International Conference on Systems, Science, Control, Communication, Engineering and Technology (2015)*: 155-158. Print.

The proposed level shifter circuit with MTCMOS circuit is presented and it is simulated in Cadence Virtuoso tool. The proposed circuit with MTCMOS technique is implemented in 180-nm CMOS technology. The static power dissipation achieved was 115.3 pW with the supply voltage of 0.2 V.

REFERENCES

[1]. J. C. Chi, H. H. Lee, S. H. Tsai, and M. C. Chi,(2007), " Gate level multiple supply voltage assignment algorithm for power optimization under timing constraint", IEEE Trans. Very Large Scale Integr. (VLSI) Syst., vol. 15, no. 6, pp. 637–648.
[2]. T.-H. Chen, J. Chen, and L. T. Clark, (2006)," Sub-threshold to above threshold level shifter design, J. Low Power Electron., vol. 2, no. 2, pp. 251–258.
[3]. K.-H. Koo, J.-H. Seo, M.-L. Ko, and J.-W. im, (2005),"A new level-up shifter for high speed and wide range interface in ultra deep sub-micron," in Proc. IEEE Int. Symp. Circuits Syst., Kobe,Japan, pp. 1063– 1065.
[4]. S. N. Wooters, B. H. Calhoun, and T. N. Blalock,(2010)," An energy-efficient subthreshold level converter in 130- nm CMOS", IEEE Trans. Circuits Syst. II, Exp. Briefs, vol. 57, no. 4, pp. 290– 294.
[5]. A. Chavan and E. MacDonald, "Ultra low voltage level shifters to interface sub and super threshold reconfigurable logic cells", in Proc. IEEE Aerosp. Conf., 2008, pp. 1–6.
[6]. A. Hasanbegovic and S. Aunet, "Low-power subthreshold to above threshold level shifter in 90 nm process", in Proc. NORCHIP Conf., Trondheim, Norway, 2009, pp. 1–4.
[7]. S. Lütkemeier and U. Rückert, "A subthreshold to above-threshold level shifter comprising a wilson current mirror", IEEE Trans. Circuits Syst. II, Exp. Briefs, vol. 57, no. 9, pp. 721– 724, Sep. 2010.
[8]. Y. Osaki, T. Hirose, N. Kuroki, and M. Numa," A low-power level shifter with logic error correction for extremely low-voltage digital CMOS LSIs, IEEE J. Solid-State Circuits, vol.47, no. 7, pp. 1776–1783, Jul. 2012.
[9]. T. Hirose N. Kuroki, M. Numa and Y. Osaki,(2011), A level shifter circuit design by using input/output voltage monitoring technique for ultra-low voltage digital CMOS LSIs, in Proc.NEWCAS Conf., pp. 201–204.
[10]. D. Blaauw ,Y. Kim, and D. Sylvester, (2011),"LC2 : Limited Contention level converter for robust wide-range voltage conversion, in Dig. Symp. VLSI Circuits, pp. 188–189.

Cite this article as: T Arthi, N Preetha. "A Level-up Shifter using MTCMOS Technique for Power Minimization." *International Conference on Systems, Science, Control, Communication, Engineering and Technology (2015)*: 155-158. Print.

International Conference on Systems, Science, Control, Communication, Engineering and Technology 2015 [ICSSCCET 2015]

ISBN	978-81-929866-1-6
Website	icssccet.org
Received	10 - July - 2015
Article ID	ICSSCCET034

VOL	01
eMail	icssccet@asdf.res.in
Accepted	31- July - 2015
eAID	ICSSCCET.2015.034

INTELLIGENT TICKETING MECHANISM FOR PUBLIC TRANSPORT

Ms.R.Monisha,[1] Ms.P.Sandhiya[2].
[1, 2] Assistant Professor (Karpagam institute of technology)
Department Of Electronics And Communication Engineering

ABSTRACT: *We often come across the pathetic scene of roadside bystanders patiently waiting at the bus stop for a bus to take them to their destination in time safely. The anxious, tired and pathetic face tells the entire story behind the misery and fate. The helplessness of the authorities is another story difficult to gulp. The proposed project work will totally eradicate this problem by taking care of the scheduling of vehicles. With the modern device possessed by the conductors of the vehicles, the owners can get instant collection details, scheduling other vehicles, tracking the movement, etc. Further using GPS technologies, position, arrival and departure of the vehicle can be flashed to all stake holders at all bus stations. While deciding the logic and coding, focus is laid on user friendly approach. Since the days are not far off for remote operated vehicle this can be the first step to prepare the citizen to adopt for a sea change in futuristic passenger travel The additional part of the same project work is presented here. Use of paper tickets in public transport is a prevalent practice. However, this system has its own drawbacks; the exact amount has to be tendered, keep the small ticket safely till the journey end. It is said that the job of a town bus conductor is the most difficult job to perform. The conductors' plight cannot be surmounted with words, his brain is a live CPU doing all the multitasking and still stay cool, (even computers get hot and has a fan) towards all kinds of passenger behavior and comments. Should ask for the destination, ticketing, collecting and tendering changes in rupee notes and coins, announcing the place of arrival, directing the passengers to get packed properly, answering unruly passengers, ensuring the door step people on safety thereby ensuring escape from penalties, self recording the transactions while jolting, rocked to face the inspectors, and the list goes on. This project work seeks out a visible technical solution using modern technologies to come out of these chaoses. It is proposed to use smart cards to avoid ticketing and money collection and tendering of changes. The destination is to be entered and all relevant details of the journey are displayed in the handheld device which is available with the conductor. The passenger upon swiping his ticketing smart card will immediately get a message on his registered mobile detailing the journey particulars, the balance amount in his travel card and its validity.*

INTRODUCTION

A significant proportion of the population depends on public transport for their daily commute. The use of paper tickets has its own drawbacks. Firstly, there is a lot of confusion between the passengers regarding fares which lead to corruption; secondly due to mismanagement of public transport the passengers face a lot of problems; thirdly the entire responsibility of distributing tickets, maintaining the record of the sold tickets and handling money transactions is that of the ticket distributor. Further, paper tickets manufacturing uses wood pulp. This motivates the design of an eco-friendly electronic ticketing system. This project describes the implementation of a system, which enables the use of mobile phones for acquiring public transport ticket and information will be stored in server. Automated accounting of public transport can be used to provide useful estimates of the cost of travelling from one

Cite this article as: Ms R Monisha Ms P Sandhiya. "INTELLIGENT TICKETING MECHANISM FOR PUBLIC TRANSPORT." *International Conference on Systems, Science, Control, Communication, Engineering and Technology (2015)*: 159-162. Print.

bus stop to another as well as the crowd density can be measured. Using GPS technology current location of the buses which is around the bus stop has to be identified by server and this information will be displayed in the bus stop unit. This eliminates the need of man power to verify the bus timings and reduces the waiting time of passengers in all the bus stops.

WORKING PRINCIPLE

The Intelligent Ticketing Mechanism consists of a GPS module with swipe function. The passengers are given a travel card just like a debit card which can be issued after verification of proof of identity/Ration card. The passengers can recharge this card online or through mobile recharge retailer. The passenger swipes the card with the module available with the conductor. The conductor enters the destination and amount will be automatically deducted from the travel card. This information gets stored in the server and the passenger receives a message which can be used as ticket. This helps the transport corporation to track the bus timings. It even checks whether fare is collected or not, if fare is not collected a fine can be imposed on the conductor. This intelligent system can help the transport corporation to analyses the passenger rush and buses can be allocated efficiently. The head of the family can track even the members especially his/her children through the online unique ID and get information about their boarding on bus. This ticketing system can also be implanted in trains and cabs.

COMPONENTS USED

The following components are used for this project,

- PIC 16F877A
- GSM Modem
- GPS
- RF Transmitter and Receiver
- RFID card
- RFID Reader
- LCD Display

BLOCK DIAGRAM:

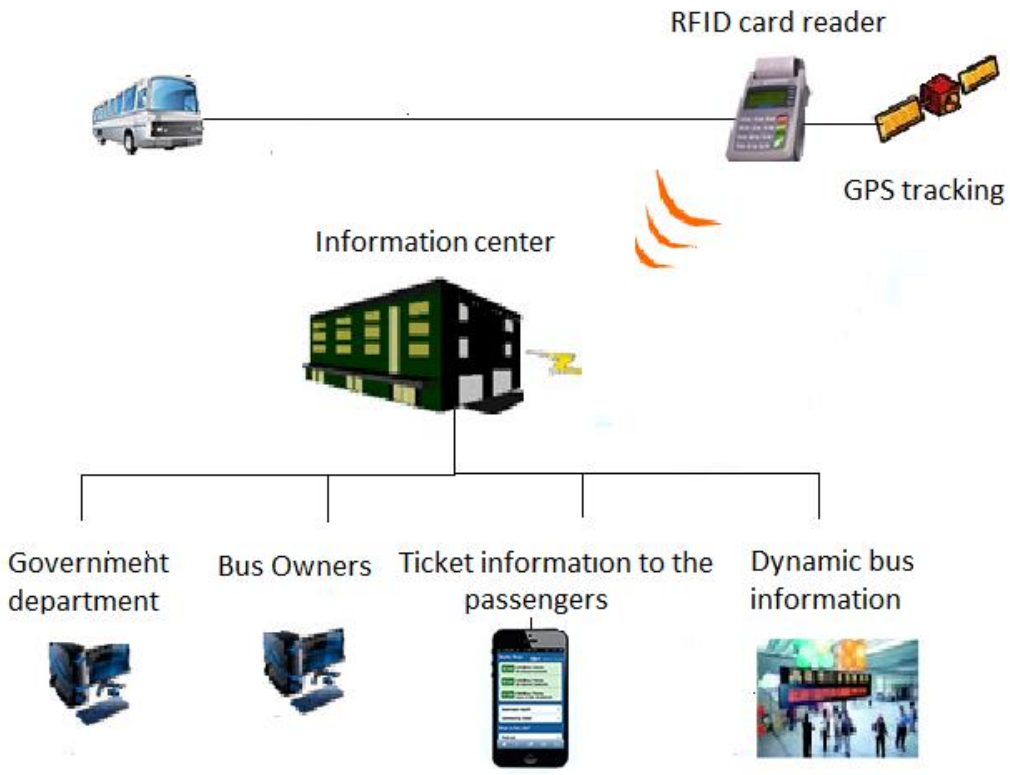

BLOCK DIAGRAM DESCRIPTION

RFID card reader is used for swiping function. With the help of keypad the details of travel can be entered manually by the conductor. Automatic fare collection algorithm is used, so extra amount detection is not at all possible in this system. The processed information will be displayed in the LCD. The information will be encoded and transmitted by the RF transmitter. Here the GSM is used to send the text message and the GPS is used to track the exact coordinates of the bus. In server unit the information is received using the RF

Cite this article as: Ms R Monisha Ms P Sandhiya. "INTELLIGENT TICKETING MECHANISM FOR PUBLIC TRANSPORT." *International Conference on Systems, Science, Control, Communication, Engineering and Technology (2015)*: 159-162. Print.

receiver and then decoded for further processing. This information will be used by the transport corporation to manage the bus in an efficient manner. Automatic fare calculation algorithm is used to verify the fare collection and also ensure that correct amount is collected from the passenger. The details of the travel are sent to the passenger's mobile number which is registered with the card.
Using GPS, the current location of the buses has to be identified and the arrival of buses will be displayed in the bus stops. The dynamic bus display reduces the waiting time of the passengers in bus stand to catch the next bus.

The card ensures the safety of the passenger. Nowadays children and ladies were travelling alone in taxis, autos and trains; the major issue is their safety. This system provides the solution for the above problem by the way of obtaining the last transaction of their travel card. Using the GPS module bus timings has been monitored. The same travel card can be implemented in all autos, taxis and trains. In case of card missing, the user is allowed to block the card by simply sending a request to the server from his registered mobile.

7. CONCLUSION

Thus the project provides a new portable ticketing system that will improve transactions and sales documentation and reduce paper wastages. Traditional systems have a number of drawbacks. The current trend is moving away from traditional ticketing systems and towards smart and intelligent ticketing systems. The entire process involves the use of technology in a smart way. This system, if implemented, avoids the use of paper tickets and reduces the confusion between the passengers regarding the fares. Upon implementation, it was found that the system is scalable. The proposed system is simple, efficient and foolproof. It is also eco-friendly since there is no wastage of paper. The system is automated so it reduces the conductor burden. The cards being reusable, this methodology is much more convenient compared to the paper based ticketing system. This system will improve on the current system's deficiencies by ensuring accurate money transactions, making sales data readily available, reducing the amount of paperwork, the margin for error and effectively running the buses in needed routes.

FEATUTRES OF THE PROJECT

1. Huge amount of paper can be saved by implementing this system.
2. Eliminates usage of coins and the need for carrying the exact amount of fares.
3. Conductor cannot cheat the passenger by collecting money and not issuing the ticket.
4. Bus location and timings can be obtained when the passenger swipes the travel card.
5. Using the details, buses can be allocated efficiently by sorting regular and irregular passengers.
6. Recharging can be done online or through any mobile recharge retailer.
7. The details of unreserved passengers can be collected when this card is implemented in train ticketing system and also it can be useful in case of any accident.
8. In cabs also this system can be implemented, if so the details of fare and locations of the cabs can be sent to the owner.
9. Eliminates the long waiting time of the passengers in bus stand.

ACKNOWLEDGMENT

Heartfelt thanks to MR. Prof. Dr. K. KEERTHIVASAN, for his guidance in this project. His years of experiences in the communication field have given me much required knowledge for this project. The suggestions and comments of his guidance, which have greatly helped to improve the quality of this paper, are acknowledged. And we would like to thank Karpagam institute of technology ,Coimbatore for providing necessary facilities to carry out this work.

REFERENCES

[1] Antero Juntunen and Sakari Luukkainen,Virpi Kristiina Tuunainen. "Deploying NFC Technology for Mobile Ticketing Services.",*2010 Ninth International Conference on Mobile Business / 2010 Ninth Global Mobility Roundtable*
[2] G. Madlmayer, J. Langer, and J. Scharinger, "Managing an NFC ecosystem," *Proc. 7th International Conference on Mobile Business (ICMB '08)*, Jul. 2008, pp. 95-101, doi:10.1109/ICMB.2008.30.
[3] J. Ondrus, and Y. Pigneur, "An assessment of NFC for future mobile payment systems," *Proc. 6th International Conference on the Management of Mobile Business (ICMB 2007*), pp. 43-43, Jul. 2007.
[4] Li Bai, Gerald Kane, and Patrick Lyons." Open Architecture for Contactless Smartcard-based Portable Electronic Payment Systems "*4th IEEE Conference on Automation Science and Engineering*, pp.715-719, August 23- 2008.
[5] Niina Mallat, Matti Rossi, Virpi Kristiina Tuunainen, Anssi Öörni "The Impact of Use Situation and Mobility on the Acceptance of Mobile Ticketing Services "(ICSS- 2006)
[6] Luxiong XuI Na Wang, and Chenglian Liu "Security of Electronic Ticketing," *International Conference on computerand communication technologies in agriculture engineering.*vol.3,pp.372-379,june-2010.
[7]. Marchau, W. Walkera and R. van Duin. An adaptive approach to implementing innovative urban transport solutions. Transport

Cite this article as: Ms R Monisha Ms P Sandhiya. "INTELLIGENT TICKETING MECHANISM FOR PUBLIC TRANSPORT." *International Conference on Systems, Science, Control, Communication, Engineering and Technology (2015)*: 159-162. Print.

Policy, Volume 15, Issue 6, November 2008, Pages 405-412.
[8] LV ZHIAN HU HAN ."A Bus Management System Based on ZigBee and GSM/GPRS "*2010 International Conference on Computer Application and System Modeling (ICCASM 2010)* .[9] Md. Feisal Mashed Hasan, Golem Tangy, Md. Kafiul Islam, Md. Rezwanul Haque Khandokar,And Alam. "Rfid-Based Ticketing For Public Transport System: Perspective Megacity Dhaka", *3rd IEEE International conference on computer science and information technology (ICCSIT),*vol.6,pp.459-462,july-2010.
[10] Rainer Widmann, Stefan Gr¨unberger, Burkhard Stadlmann,and Josef Lange,"System Integration of NFC Ticketing into an Existing Public Transport Infrastructure" *Fourth International Workshop with Focus on Near Field Communication,*pp 13-18,March-2012.
[11] Luka Finžgar, and Mira Treba."Use of NFC and QR code Identification in an Electronic Ticket System for Public Transport," *19th international conference on software telecommunications and computer networks* ,pp.1-6 september-2011.
[12] Lada Rodzina, and Olga Ionova."Universal Devices for Public Transport," *international conference on collaboration technologies and systems(CTS),pp. 646-647,*May-2011.
[13] VN Kamalesh ,Vikram Ravindra, Pradeep P Bomble, and Pavan MP ." Virtual ticketing system,"*2011 International Conference on e-Education, Entertainment and e-Management,*pp. 151-154,December-2011.
[14] Torode,R.B."Prestige - Contactless Smartcard Ticketing On London Transport," *International Conference on public transport electronic systems,*pp .72-73,May-1996.

Cite this article as: Ms R Monisha Ms P Sandhiya. "INTELLIGENT TICKETING MECHANISM FOR PUBLIC TRANSPORT." *International Conference on Systems, Science, Control, Communication, Engineering and Technology (2015)*: 159-162. Print.

International Conference on Systems, Science, Control, Communication, Engineering and Technology 2015 [ICSSCCET 2015]

ISBN	978-81-929866-1-6	**VOL**	01
Website	icssccet.org	**eMail**	icssccet@asdf.res.in
Received	10 - July - 2015	**Accepted**	31- July - 2015
Article ID	ICSSCCET035	**eAID**	ICSSCCET.2015.035

MODIFIED KERNEL ANISOTROPIC DIFFUSION DESPECKLE FILTER FOR MEDICAL ULTRASOUND IMAGING

N Preetha[1], T Arthi[2], M Venkateswari[3]
[1, 2, 3] Dept of Electronics and Communication Engineering,
Karpagam Institute of Technology, Coimbatore, India

Abstract: *Speckle is a primary factor which degrades the contrast resolution and masks the meaningful texture information present in an ultrasound image. Its presence severely hampers the interpretation and analysis of ultrasound images. Speckle noise is produced by the mutual interference of a set of scattered wavefronts. Depending on the phase of the wavefronts, the interference may be constructive or destructive resulting in brighter or darker pixels. The proposed filter is based on steps to attenuate the resultant brighter and darker pixels. Anisotropic diffusion minimizes the noise fluctuation while simultaneously preserving the edges of the image.In this paper, a detailed description of Modified kernel Anisotropic diffusion despeckle filter(MKAD) is proposed. MKAD performance is compared with 5 other diffusion filters in medical ultrasound quantitatively and functionally. The proposed filter has presented the greatest structural similarity, 0.95.For better analysis, field II simulation is done on ultrasound images.*

Keywords: ultrasound, speckle noise, diffusion, median, anisotropic diffusion

I.INTRODUCTION

Ultrasound imaging is an important and frequently used diagnostic tool in medical imaging. It uses high-frequency inaudible sound waves to assess images of the soft tissues. The accurate interpretation of ultrasound image is hampered by two signal processing roadblocks. First, subresolution scatterers lead to image speckle that plagues imaging applications by obscuring the underlying tissue properties. Second, the imaging system itself has a point spread function that creates blurring of image features. Both these factors degrade the image quality. As a result, image processing for reducing the speckle noise and blurring is required. Speckle is not truly a noise in the typical engineering sense because its texture often carries useful information about the image being viewed.So speckle reduction should be designed such that it smoothens the image in a controlled fashion without significant loss of information.

Several speckle denoising filters are proposed, of which anisotropic based filters are significant. Several researchers proposed anisotropic diffusion methods based on the original study of Perona and Malik [2], where the anisotropic diffusion equation provides a technique for selective image smoothing. The development of research for anisotropic diffusion via the partial differential equation has taken place in such a way that important structures in the images remain preserved. Speckle reduction method should be a balance between speckle suppression and feature preservation .The Proposed filter enhance objects by suppressing the speckle pattern, while preserving the edges of the objects.

Cite this article as: N Preetha, T Arthi, M Venkateswari. "MODIFIED KERNEL ANISOTROPIC DIFFUSION DESPECKLE FILTER FOR MEDICAL ULTRASOUND IMAGING." *International Conference on Systems, Science, Control, Communication, Engineering and Technology (2015)*: 163-166. Print.

The organization of the paper is as follows. Section II describes the proposed filter(MKAD).Evaluation methods are detailed in Section III, including filtering of Field II simulated ultrasound images, use of quantitative quality metrics, and functional evaluation based on object segmentation. Results and Discussions are presented in Section IV, and Section V concludes the paper.

II.PROPOSED FILTER

Let speckled image be the B-mode ultrasound image. The Modified Kernel Anisotropic Diffusion(MKAD) Filter can be divided into three steps, namely: median filter, destructive interference suppression and constructive interference suppression and modified kernel anisotropic diffusion.The block diagram of the proposed filter is shown in fig 1,

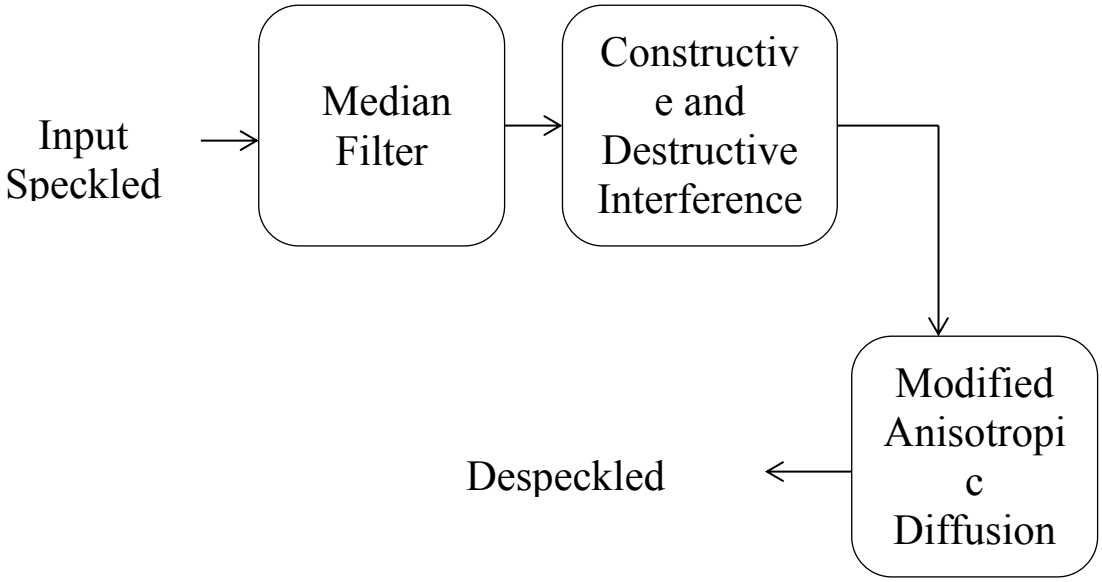

Fig.1.Block Diagram of the MKAD method for Ultrasound Speckle Reduction

Median Filter

A median filter is first applied to the speckled image to smooth the image. Here, a circular window was used rather than a square window to avoid ''blocking'' artifacts. Generally, the larger the window radius, the smoother the image texture becomes. However, to avoid over-smoothing, the selected radius should not be bigger than image structures. Several window radii were tested, ranging from 3 to 40 pixels.

Destructive interference suppression.

The primary purpose of this filter is to smooth an ultrasonography image through the suppression of the gray values caused by destructive interferences, for each position (x, y) , the maximum value between the median filtered image and the speckled image is selected.

$$I_c(x,y) = \max\{I(x,y), I_{med}(x,y)\} \quad (1)$$

where I is the speckled image, I_{med} is the median-filtered image and I_C is the constructive interference only image. For each position (x,y), the brighter pixel between I(x,y) and $I_{med}(x,y)$ is chosen. Hence, step 2 suppresses the darker pixels, which are related to destructive interference (Burckhardt 1978).

Constructive interference suppression.

As only bright speckles remain in the resulting constructive interference image from step 2, a small-windowed (3 pixels radius) median filter is applied to eliminate the remaining extreme single pixels.

Modified Kernel Anisotropic Diffusion Filter

Given the interference suppressed images are good candidates for anisotropic diffusion. The kernel is modified as shown in the fig 2.The discretised filter equation for modified kernel is given in equation (13),

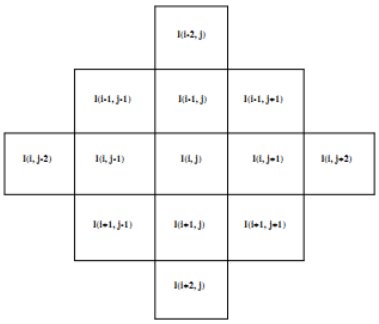

Cite this article as: N Preetha, T Arthi, M Venkateswari. "MODIFIED KERNEL ANISOTROPIC DIFFUSION DESPECKLE FILTER FOR MEDICAL ULTRASOUND IMAGING." *International Conference on Systems, Science, Control, Communication, Engineering and Technology (2015)*: 163-166. Print.

Fig.2.Kernel of the proposed filter

$$I(x,y,t+1) = I(x,y,t) + \frac{\nabla t.\lambda}{|\overline{n_s}|}(cN.\nabla I_N + cE.\nabla I_E + cW.\nabla I_W + cS.\nabla I_S + cNE.\nabla I_{NE} + cSE.\nabla I_{SE} + cNW.\nabla I_{NW} + cSW.\nabla I_{SW} + cN1.\nabla I_{N1} + cE1.\nabla I_{E1} + cW1.\nabla I_{W1} + cS1.\nabla I_{S1} \quad (2)$$

where c(x,y,t) represents value of diffusion co-efficient for the pixels in all possible directions. ∇I represents the image gradient in the respective directions.

III EVALUATION METHODOLOGY

The proposed method is compared with five existing diffusion filtering methods which are Perona and Malik filter, MGAD filter, SRAD filter, RTFAD filter and Interference suppressed speckle filter followed by Anisotropic Diffusion(ISFAD) filter. The proposed method of speckle reduction and edge preservation is tested using Field II speckle simulated ultrasound image (Fig.3(a)).The filtered images are functionally evaluated by object segmentation algorithm like level set (Fig.4(a)-4(g)).

Table. 2 summarizes the quantitative results for the simulated ultrasound image.Comparing Fig. 3 and Fig.4 with Table II, we realized that our proposed method successfully improved the speckle reduction and edge preservation and better structural similarity index of 0.95.

IV RESULTS AND DISCUSSION

For experimentation, cyst field II image is taken.The speckled image is be obtained for a scattering distribution of 10,000 and transducer frequeny of 5MHz.The field II speckle simulated medical ultrasound images are subjected to five speckle reducing diffusion filters and the proposed MKAD filter.Level Set object segmentation technique is applied to filtered images .Levelset images shows that the proposed filter preserves the edges and local gray level information of ultrasound image. Table II shows that MKAD filter gives better structural similarity index and reduced error.

CYST PHANTOM –Simulation I

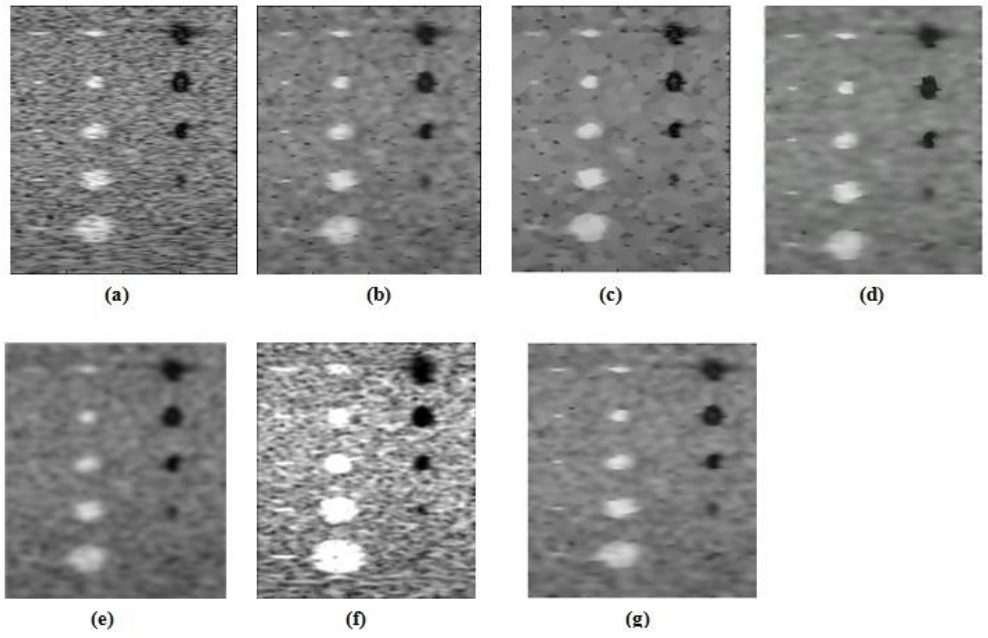

Table II A.Numerical Performances of the filters

Filter	σ	RMSE x 100	SSIM x 100	CSR x 100	Filter	σ	RMSE x 100	SSIM x 100	CSR x 100
Gold Standard	0	0	100	α	MGAD	21.4	81.57	50	837.1
Speckled	12.7	14.46	-64	100	SRAD	22.6	214.0	18	406
					ISFAD	20.6	5.69	90	250.2
AD	24.5	5.70	33.58	88.04	MKAD	63.8	4.06	95	739
RTAD	18.7	0.320	93	0.397					

Cite this article as: N Preetha, T Arthi, M Venkateswari. "MODIFIED KERNEL ANISOTROPIC DIFFUSION DESPECKLE FILTER FOR MEDICAL ULTRASOUND IMAGING." *International Conference on Systems, Science, Control, Communication, Engineering and Technology (2015)*: 163-166. Print.

CONCLUSION

The experimental results shows that the proposed algorithm can denoise the speckle images more effectively. The main advantage of the MKAD filter is that the image features are retained without any information loss. Median filtering is used to suppress the constructive and destructive interference pixels. Further anisotropic filter with hybrid kernel preserves the edges and the local gray level information. Results reveal that our method performs superior to the other method, indicating it's potential to speckle reduction in ultrasound images.

REFERENCES

[1] Fernando M. C Ardoso, Monica M. S. M Atsumoto, Y And Sergio S. Furuie,2012, "Edge Preserving Speckle Texture Removal by Interference based speckle filtering followed by anisotropic diffusion",Ultrasound in Med. And Biology,Vol 36,No 8,pp 1414-1428.
[2] Perona P, Malik J. "Scale-space and edge detection using anisotropic diffusion". IEEE Trans Pattern Anal Mach Intell 1990;12(7): 629–639.
[3] Yang Z, Fox MD. ''Speckle reduction and structure enhancement by multichannel median boosted anisotropic diffusion''. EURASIP JAppl Signal Process 2004;1:2492–2502.
[4] Yu Y, Acton S. "Speckle reducing anisotropic diffusion" IEEE Trans Image Process 2002;11:1260–1270.Median guided anisotropic diffusion
[5] Yinhui Deng, Yuanyuan Wang , Yuzhong Shen 2012 "Speckle reduction of ultrasound images based on Rayleigh-trimmed anisotropic diffusion filter", Pattern Recognition Letters 32 (2011) 1516–1525
[6]Jensen.J.A 1996, "Field:A Program for Simulating Ultrasound Systems",Med Biol Eng Comput, Volume 34,351-353
[7] Jensen JA (2011, Mar 25).Field II Simulation Program [Online].Available:http://server.electro.dtu.dk/personal/jaj/field/?downloading. html
[8] R. F. Wagner, S. W. Smith, J. M. Sandrik and H.Lopez, 1983, "Statistics of Speckle in Ultrasound B-Xcans,"IEEE Trans. Sonics Ultrasonics 30, 156–163.

Cite this article as: N Preetha, T Arthi, M Venkateswari. "MODIFIED KERNEL ANISOTROPIC DIFFUSION DESPECKLE FILTER FOR MEDICAL ULTRASOUND IMAGING." *International Conference on Systems, Science, Control, Communication, Engineering and Technology (2015)*: 163-166. Print.

International Conference on Systems, Science, Control, Communication, Engineering and Technology 2015 [ICSSCCET 2015]

ISBN	978-81-929866-1-6	**VOL**	01
Website	icssccet.org	**eMail**	icssccet@asdf.res.in
Received	10 - July - 2015	**Accepted**	31- July - 2015
Article ID	ICSSCCET036	**eAID**	ICSSCCET.2015.036

STRONGLY g*-CLOSED SETS IN BITOPOLOGICAL SPACES

J. Logeshwari[1], J. Manonmani[2], S. Padmanaban[3], S. Gowri Sankar[4]
[1, 2, 3, 4] Assistant Professors, Department of Mathematics,
Karpagam Institute of Technology, Coimbatore.

Abstract: *The purpose of this paper is to define and study sg^*-closed sets in bitopological spaces*

Keywords: Strongly g^*-closed sets

1. INTRODUCTION AND PRELIMINARIES

A triple (X, τ_1, τ_2) where X is a non-empty set and τ_1 and τ_2 are topologies on X is called a bitopological space and Kelly [3] initiated the study of such spaces.

Throughout this paper (X, τ_1, τ_2) or simply X represents the bitopological spaces on which no seperaxion axioms are assumed unless otherwise mentioned. For any subset $A \subseteq X$, τ_i-$int(A)$ and , τ_i-$cl(A)$ denote the interior and closure of a set A with respect to the topology τ_i, respectively.

Definition 1.1: A subset A of a topological space (X, τ) is said to be

(1) Semi-open [4] if $A \subseteq cl(int(A))$

(2) Regular open if $A = int(cl(A))$

Definition 1.2: A subset A of a topological space (X, τ) is said to be generalized closed **(briefly g-closed)** [1] if $cl(A) \subseteq U$ whenever $A \subseteq U$ and U is open in X.

Definition 1.3: A subset A of a topological space (X, τ) is said to be generalized* closed **(briefly g^*-closed)** [6] if $cl(A) \subseteq U$ whenever $A \subseteq U$ and U is g-open in X.

Definition 1.4: A subset A of a bitopological space (X, τ_1, τ_2) is said to be

(1) $\tau_1\tau_1$-Semi-open [2] if $A \subseteq \tau_2 - cl(\tau_1 - int(A))$

(2) $\tau_1\tau_2$ -Regular open if $A = int(cl(A))$

Definition 1.5: A subset A of a bitopological space (X, τ_1, τ_2) is said to be $\tau_1\tau_2$-generalized closed ($\tau_1\tau_2$-g- closed) [ ] if $\tau_2 cl(A) \subseteq U$ whenever $A \subseteq U$ and U is τ_1-open.

Definition 1.6: A subset A of a bitopological space (X, τ_1, τ_2) is said to be $\tau_1\tau_2$-generalized* closed ($\tau_1\tau_2$-g^*- closed) [ ] if $\tau_2 - cl(A) \subseteq U$ whenever $A \subseteq U$ and U is τ_1-g open.

2. STRONGLY g*-CLOSED SETS

Cite this article as: J Logeshwari, J Manonmani, S Padmanaban, S Gowri Sankar. "STRONGLY g*-CLOSED SETS IN BITOPOLOGICAL SPACES." *International Conference on Systems, Science, Control, Communication, Engineering and Technology (2015)*: 167-169. Print.

Definition 2.1: Let (X, τ_1, τ_2) be a bitopological space and A be its subset, then A is a strongly g^*-closed set (briefly sg^*-closed) if $\tau_2\text{-}cl(\tau_1 - int(A)) \subseteq U$ whenever $A \subseteq U$ and U is τ_1- g open

Theorem 2.2: Let (X, τ_1, τ_2) be a bitopological space. Every closed set is strongly g^*-closed set, but not conversely.

Proof: Suppose that A is closed. Let U be an open set containing A. Then $\tau_2\text{-}cl(\tau_1 - int(A)) \subseteq \tau_2 - cl(A) = A$, which implies, $\tau_2\text{-}cl(\tau_1 - int(A)) \subseteq U$. Hence, A is a strongly g^*-closed set.

Example 2.3: Let $X = \{a, b, c\}$, $\tau_1 = \{\emptyset, \{a\}, \{b\}, \{a, b\}, X\}$ and $\tau_2 = \{\emptyset, \{a\}, \{a, b\}, X\}$. Then the set $\{a, c\}$ is a strongly g^*-closed set but not a closed set.

Theorem 2.4: If a subset A of a bitopological space (X, τ_1, τ_2) is g^*-closed then it is strongly g^*-closed in X, but not conversely.

Proof: Suppose A is g^*-closed in (X, τ_1, τ_2). Let G be an open set containing A in X. Then G contains $\tau_2 - cl(A)$ and $G \supseteq \tau_2 - cl(A) \supseteq \tau_2 - cl(\tau_1 - int(A))$. Thus, A is strongly g^*-closed in X.

Example 2.5: Let $X = \{a, b, c\}$ with topologies $\tau_1 = \{\emptyset, \{b\}, \{c\}, \{b, c\}, X\}$ and $\tau_2 = \{\emptyset, \{a, c\}, X\}$. In this topological space the subset $\{a\}$ is strongly g^*-closed but not a g^*-closed set.

Theorem 2.6: If a subset A of a topological space (X, τ_1, τ_2) is both open and strongly g^*-closed, then it is closed.

Proof: Suppose a subset A of X is both open and strongly g^*-closed. Then $A \supseteq \tau_2 - cl(\tau_1 - int(A)) \supseteq \tau_2 - cl(A)$ and so $A \supseteq \tau_2 - cl(A)$. Since $\tau_2 - cl(A) \supseteq A$, we have, $A = \tau_2 - cl(A)$. Thus A is closed in X.

Theorem 2.7: If a subset A of a bitopological space (X, τ_1, τ_2) is both strongly g^*-closed and semi-open then it is g^*-closed.

Proof: Suppose A is both strongly g^*-closed and semi-open in X, let G be an open set containing A. As A is strongly g^*-closed, $G \supseteq \tau_2 - cl(\tau_1 - int(A))$. Now, $G \supseteq \tau_2 - cl(A)$, since A is semi-open. Thus A is g^*-closed in X.

Corollary 2.8: If a subset A of a bitopological space (X, τ_1, τ_2) is both strongly g^*-closed and open then it is a g^*-closed set.

Proof: Suppose A is both strongly g^*-closed and open in X, let G be an open set containing A.

As A is strongly g^*-closed, $G \supseteq \tau_2 - cl(\tau_1 - int(A))$ and $G \supseteq \tau_2 - cl(A)$, since A is open. Thus, A is g^*-closed in X.

Theorem 2.9: A subset A is strongly g^*-closed if and only if $\tau_2 - cl(\tau_1 - int(A)) - A$ contains no non-empty closed set.

Necessity: Suppose that F is a non-empty closed subset of $\tau_2 - cl(\tau_1 - int(A)) - A$. i.e., $F \subseteq \tau_2 - cl(\tau_1 - int(A)) \cap (X - A)$. Then $F \subseteq \tau_2 - cl(\tau_1 - int(A))$ and $F \subseteq (X - A)$. Since $X - F$ is an open set and A is strongly g^*-closed, $\tau_2 - cl(\tau_1 - int(A)) \subseteq (X - F)$. i.e., $F \subseteq (X - \tau_2 - cl(\tau_1 - int(A)))$. Hence, $F \subseteq \tau_2 - cl(\tau_1 - int(A)) \cap (X - (\tau_2 - cl(\tau_1 - int(A)) = \emptyset$. i.e., $F = \emptyset$. Thus, $\tau_2 - cl(\tau_1 - int(A)) - A$ contains no non-empty closed set.

Sufficiency: Conversely, assume that $\tau_2 - cl(\tau_1 - int(A)) - A$ contains no non-empty closed set. Let $A \subseteq U, U$ is g-open. Suppose that $\tau_2 - cl(\tau_1 - int(A))$ is not contained in U. Then $\tau_2 - cl(\tau_1 - int(A)) \cap (X - U)$ is a non-empty closed set and contained in $\tau_2 - cl(\tau_1 - int(A)) - A$ which is a contradiction. Therefore, $\tau_2 - cl(\tau_1 - int(A)) \subseteq U$ and hence A is strongly g^* - closed.

Corollary 2.10: A strongly g^* - closed set A is regular closed if and only if $\tau_2 - cl(\tau_1 - int(A)) - A$ is closed and $\tau_2 - cl(\tau_1 - int(A)) \supseteq A$.

Proof: Assume that A is regular closed. Since $\tau_2 - cl(\tau_1 - int(A)) = A$, $\tau_2 - cl(\tau_1 - int(A)) - A = \emptyset$ is regular closed and hence closed.

Conversely, assume that $\tau_2 - cl(\tau_1 - int(A)) - A$ is closed. By Theorem 9, $\tau_2 - cl(\tau_1 - int(A)) - A$ contains no non-empty closed set. Therefore, $\tau_2 - cl(\tau_1 - int(A)) - A = \emptyset$. Thus, A is regular closed.

Theorem 2.11: Suppose that $B \subseteq A \subseteq X$, B is a strongly g^*- closed set relative to A and that both open and strongly g^*-closed subset of (X, τ_1, τ_2) then B is a strongly g^* - closed set relative to (X, τ_1, τ_2).

Proof : Let $B \subseteq G$ and G be an open set in (X, τ_1, τ_2). But given that $B \subseteq A \subseteq X$, therefore $B \subseteq A$ and $B \subseteq G$. This implies, $B \subseteq A \cap G$. Since B is strongly g^* - closed relative to A, $\tau_2 - cl(\tau_1 - int(B)) \subseteq A \cap G$. i.e., $A \cap \tau_2 - cl(\tau_1 - int(B)) \subseteq A \cap G$. This implies, $A \cap \tau_2 - cl(\tau_1 - int(B)) \subseteq G$. Thus, $A \cap \tau_2 - cl(\tau_1 - int(B)) \cup (X - (\tau_2 - cl(\tau_1 - int(B)))) \subseteq G \cup (X - \tau_2 - cl(\tau_1 - int(B)))$. Also, $B \subseteq A$ which implies $\tau_2 - cl(\tau_1 - int(B)) \subseteq \tau_2 - cl(\tau_1 - int(A))$

Corollary 2.12: Let A be strongly g^*-closed and suppose that F is closed then $A \cap F$ is a strongly g^*-closed set.

Proof: To show that $A \cap F$ is strongly g^*-closed, we have to show $\tau_2 - cl(\tau_1 - int(A \cap F)) \subseteq G$ whenever $A \cap F \subseteq G$ and G is g-open. Since $A \cap F$ is closed in A, we have $A \cap F$ is strongly g^*-closed in A. By Theorem 4.11, $A \cap F$ is strongly g^*-closed in (X, τ_1, τ_2), since $A \cap F \subseteq A \subseteq (X, \tau_1, \tau_2)$.

Theorem 2.13: If A is strongly g^*-closed and $A \subseteq B \subseteq \tau_2 - cl(\tau_1 - int(A))$, then B is strongly g^*-closed.

Proof: Given that $B \subseteq \tau_2 - cl(\tau_1 - int(A))$ then $\tau_2 - cl(\tau_1 - int(B)) \subseteq \tau_2 - cl(\tau_1 - int(A))$, $\tau_2 - cl(\tau_1 - int(A)) - B \subseteq \tau_2 - cl(\tau_1 - int(A)) - A$. Since $A \subseteq B$, and A is strongly g^*-closed, by Theorem 4.9, $\tau_2 - cl(\tau_1 - int(A)) - A$ contains no non-empty closed set and $\tau_2 - cl(\tau_1 - int(B)) - B$ contains no non-empty closed set. Again by Theorem 4.9, B is a strongly g^*-closed set.

Theorem 2.14: Let X and Y are bitopological spaces and let $A \subseteq Y \subseteq X$ and suppose that A is strongly g^*- closed in X then A is strongly g^*- closed relative to Y.

Cite this article as: J Logeshwari, J Manonmani, S Padmanaban, S Gowri Sankar. "STRONGLY g*-CLOSED SETS IN BITOPOLOGICAL SPACES." *International Conference on Systems, Science, Control, Communication, Engineering and Technology (2015)*: 167-169. Print.

Proof: Given that $A \subseteq Y \subseteq X$ and A is strongly g^*-closed in X. To show that A is strongly g^*-closed relative to Y, let $A \subseteq Y \cap G$, where G is g-open in X. Since A is strongly g^*-closed in X, $A \subseteq G$ implies $\tau_2 - cl(\tau_1 - int(A)) \subseteq G$. i.e., $A \subseteq Y \cap G$, where $Y \cap \tau_2 - cl(\tau_1 - int(A)) \subseteq Y \cap G$, where $Y \cap \tau_2 - cl(\tau_1 - int(A))$ is the closure of interior of A in Y. Thus A is strongly g^*-closed relative to Y.

REFERENCES

1. Fukutake. T, On generalized closed sets in bitopological spaces, Bull. Fukuoka. Univ. Ed. Part III, 35(1986), 19-28.
2. Fukutake. T, Semi open sets in bitopological spaces, Bull. Fukuoka. Uni. Education, 38(3) 35(1986), 19-28.
3. Kelly. J.C, Bitopological spaces, Proc. London Math. Society, 13(1963), 71-89.
4. Levine. N, Semi-open sets and semi-continuity in topological spaces, Amer. Math. Monthly, 70(1) (1963), 36-41.
5. Levine. N, Generalized closed sets in topology, Rend. Circ. Mat. Palermo, 19(2) (1970), 89-96.
6. Sheik John. M and Sundaram. P, g^*-closed sets in bitopological spaces, Indian J. Pure. Appl. Math., 35(1), 2004, 71-80.

Cite this article as: J Logeshwari, J Manonmani, S Padmanaban, S Gowri Sankar. "STRONGLY g*-CLOSED SETS IN BITOPOLOGICAL SPACES." *International Conference on Systems, Science, Control, Communication, Engineering and Technology (2015)*: 167-169. Print.

International Conference on Systems, Science, Control, Communication, Engineering and Technology 2015 [ICSSCCET 2015]

ISBN	978-81-929866-1-6	**VOL**	01
Website	icssccet.org	**eMail**	icssccet@asdf.res.in
Received	10 - July - 2015	**Accepted**	31- July - 2015
Article ID	ICSSCCET037	**eAID**	ICSSCCET.2015.037

A Cross Layer Based Secure Multipath Neighbor Routing Protocol in MANET

H INDRAPRIYADARSINI[1], T ARTHI[2]
[1, 2] Assistant Professors, Department of Electronics and Communication Engineering,
Karpagam Institute of Technology, Coimbatore.

Abstract: *A mobile ad hoc network is a collection of mobile nodes forming an ad hoc network without the assistance of any centralised structures or administration. It is a wireless network and a self-configuring one. Due to high mobility of nodes in mobile ad hoc networks (MANETs), there exist frequent link breakages which lead to frequent path failures and route discoveries. The overhead of a route discovery cannot be neglected. In a route discovery, broadcasting is a fundamental and effective data dissemination mechanism, where a mobile node blindly rebroadcasts the first received route request packets unless it has a route to the destination, and thus it causes the broadcast storm problem. In this phase, cross layer is deployed to improve lifetime and quality of service (QoS). By deploying secret sharing scheme have provided message integrity and authentication. By using the experimental result of CLSMRSCA achieves more path reliability rate, lifetime, end to end delay and less overhead than the existing scheme CLMNRP.*

Keywords: CLSMRSCA -Cross Layer Based Secure Multipath Routing Scheme for Collision Avoidance, CLMNRP -Cross Layer Based Multipath Neighbor Routing Protocol.

1. INTRODUCTION

Mobile Ad Hoc Network

Mobile Ad Hoc Network (MANET) is a self-configuring system of mobile routers linked by wireless links which consequently combine to form an arbitrary topology. Thus, the network's wireless topology may alter rapidly and unpredictably. However, due to the lack of any fixed infrastructure, it becomes complicated to exploit the present routing techniques for network services, and this provides some huge challenges in providing the security of the communication, which is not done effortlessly as the number of demands of network security conflict with the demands of mobile networks, largely due to the nature of the mobile devices .e.g. low power consumption, low processing load.

Cite this article as: H INDRAPRIYADARSINI, T ARTHI. "A Cross Layer Based Secure Multipath Neighbor Routing Protocol in MANET." *International Conference on Systems, Science, Control, Communication, Engineering and Technology (2015)*: 170-174. Print.

II.A CROSS LAYER BASED MULTIPATH NEIGHBOR ROUTING PROTOCOL

II.1 Cross layer design

A cross layer based multipath neighbor routing protocol is developed to attain network connectivity. Here this protocol is deployed to overcome the link and path breakages. Cross layer design is said to be the violation of layered communication architecture in the protocol design with respect to the original architecture. Distributed algorithms can exploit a cross-layer design to enable each node to perform fine-grained optimizations locally whenever it detects changes in network state.

II.2 Multipath Routing

Multipath routing has been explored in several different contexts. Traditional circuit switched telephone networks used a type of multipath routing called alternate path routing. In alternate path routing, each source node and destination node have a set of paths (or multipaths) which consist of a primary path and one or more alternate paths. Alternate path routing was proposed in order to decrease the call blocking probability and increase overall network utilization.

In alternate path routing, the shortest path between exchanges is typically one hop across the backbone network; the network core consists of a fully connected set of switches. When the shortest path for a particular source destination pair becomes unavailable (due to either link failure or full capacity), rather than blocking a connection, an alternate path, which is typically two hops, is used. Multipath routing increases fault-tolerance and reliability. The router can split the same label traffic flow into different paths with the given traffic engineering constraint. QoS constraints like minimum delay and maximum bandwidth are considered for splitting a given flow dynamically into

these multiple paths. The steps for achieving load distribution through the multipath routing is follows.

Step 1: Calculate the ℓ, a set of disjoint path from source to destination. The path is considered as a loop less path.

Step 2: Find the path χ from ℓ based on the bandwidth and (least hop) shortest path distance i.e.

$Bw(p_m) = Bw(p_k)$ and the distance $S_d(m) = S_d(l)$.

Step 3: If (Path failure occurs)

Choose the alternative backup path form the set ℓ $\{P_l, P_m, \ldots\ldots\ldots P_n\}$ with least hop distance. If the source is l and the destination n.

Else

Stop the transfer of the data form source to destination.

Step 4:

Select the path from the maximum number of edge disjoint paths which satisfies the bandwidth and delay requirements

$BW(p_l) + BW(p_m) + \ldots\ldots\ldots BW(p_k) = BW_t(P_T)$

$DE(p_l) + DE(p_m) + \ldots\ldots\ldots DE(p_k) = DE_t(P_T)$

Step 5:

Establishing the multipath routing among all the mobile nodes in the network.

Step 6:

Achieving the load balancing to improve the throughput and network connectivity.

Cite this article as: H INDRAPRIYADARSINI, T ARTHI. "A Cross Layer Based Secure Multipath Neighbor Routing Protocol in MANET." *International Conference on Systems, Science, Control, Communication, Engineering and Technology (2015)*: 170-174. Print.

II.3 Energy Consumption Model

In MANETs, the topology is dynamic not static. Due to the dynamic topology, node consumes more energy while roaming.The energy model of proposed algorithm is given below. In this model energy consumption for transmitting M bit is equal to:

$E_{tr}(M, d) = E_{elec} \times M + \delta_{amp} \times M \times d^2 - E_{wast}(P_{drop})$
M = bit contain some information like current energy level of the node, data label, node's location and hop count.
E_{elec} = Energy to be Transmitted and Received electronic device module (75 nJ/bit).
δ_{amp} = Transmitter Amplifier (150 pJ/bit/m^2)
d = distance between the two nodes.
$E_{wast}(P_{drop})$ = Energy wasted on packet dropping.
And the energy for receiving K bit is equal to:
$E_{rr} = E_{elec} \times M$

II.4 Secret Sharing Scheme

Use the concept of Proactive Secret Sharing (PSS) to provide data authenticity and confidentiality. In the PSS implementation, each share holder randomly generates own sub-shares (e.g., (s_{i1}, s_{i2}, . . . , s_{in}) on node i), and each sub-share is mutually exchanged to refresh own share. More precisely, the PSS procedure can be performed in the following steps:

1) Let (s_1, s_2, . . . , s_n) be an (n, t) sharing of the secret key S of the service, with node *l* having S_l.
2) Node *l* (i {1 . . . n}) randomly generates s_l's sub shares (s_{l1}, s_{l2}, . . . , s_{ln}) for an (n, t) sharing.
3) Every sub-share s_{lk} (k {1 . . . n}) is distributed to node k through secure link.
4) When node k gets the sub-shares (s_{1k}, s_{2k}, . . . , s_{nk}), it computes a new share from these sub-shares and its old share with an equation,

$$s'_k = s_k + \sum_{k=1}^{n} s_{lk}$$

III. RESULTS

In our simulation, 350 mobile nodes move in a 1000 meter x 1000 meter square region for 60 seconds simulation time. All nodes have the same transmission range of 500 meters.

Fig.1 shows the the comparison of overhead and mobility. It is clearly shown that the overhead of CLSMRSCA has low overhead than the CLMNRP protocol while varying mobility range from 20.0000 to 100.0000.
Figure.2 shows the results of Throughput Vs Network Lifetime. From the results, we can see that CLSMRSCA scheme has higher Network Lifetime than the CLMNRP while varying the Throughput from 100.0000 to 500.0000(pkts).
Figure.3 presents the comparison of End to end delay while varying the Speed from 20.0000 to 100.0000. It is clearly shown that the delay of CLSMRSCA lower than the CLMNRP protocol.

Figure.4 presents the comparison of No.of nodes Vs path reliability rate while varying the No.of nodes from 20.0000 to 100.0000. It is clearly shown that the path reliability rate of CLSMRSCA higher than the CLMNRP protocol.

Figure 5. presents the comparison of Simulation time Vs energy consumption while varying the time from 10.0000 to 50.0000. It is clearly shown that the energy consumption of CLSMRSCA lower than the CLMNRP protocol.

Cite this article as: H INDRAPRIYADARSINI, T ARTHI. "A Cross Layer Based Secure Multipath Neighbor Routing Protocol in MANET." *International Conference on Systems, Science, Control, Communication, Engineering and Technology (2015)*: 170-174. Print.

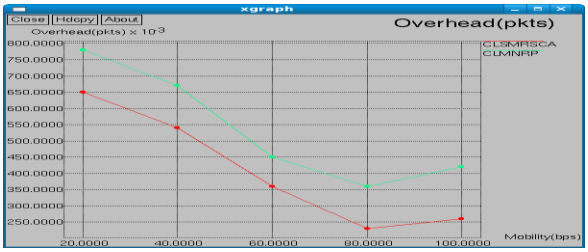

Figure.1 Mobility Vs Overhead

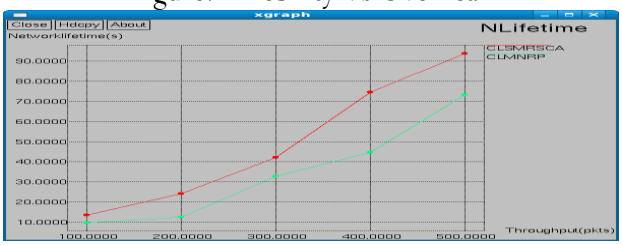

Figure.2ThroughputVsNetwork Lifetime

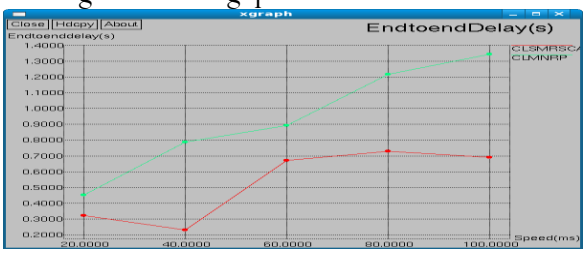

Figure.3: End to End delay Vs Speed

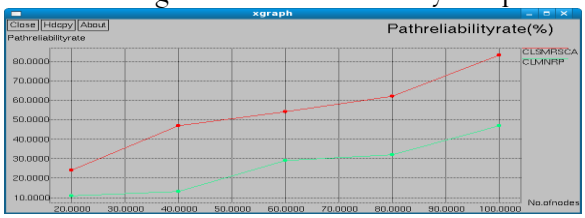

Figure.4: No.of nodes Vs path reliability rate

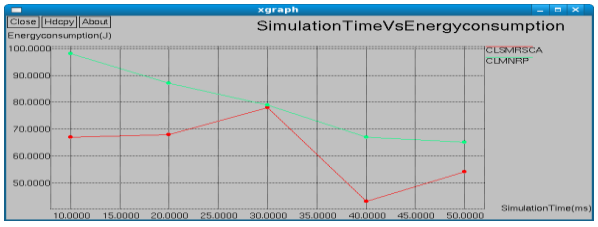

Figure 5: Simulation Time Vs Energy Consumption

V.CONCLUSION AND FUTURE WORK

In this project, a cross layer based secure multipath routing scheme has been proposed for mobile ad hoc networks. This cross layer increases additional network lifetime. Here, secure multipath routing is deployed to overcome the failures of links and paths as well as provide security from the intruders. For reducing the effect of attackers secret sharing scheme provides authentication. The simulation results also show that the proposed scheme has good performance and achieves more connectivity, lifetime, less overhead, path reliability rate and energy consumption.In future, integration of symmetric key cryptography model with energy consumption can be implemented. Efficient link aware scheduling can be done with authentication scheme to achieve high integrity and authentication

Cite this article as: H INDRAPRIYADARSINI, T ARTHI. "A Cross Layer Based Secure Multipath Neighbor Routing Protocol in MANET." *International Conference on Systems, Science, Control, Communication, Engineering and Technology (2015)*: 170-174. Print.

REFERENCES

[1] Kalpana Sharma and M.K. Ghose,(2011),' Cross Layer Security Framework for Wireless Sensor Networks' proceeding of International Journal of Security and Its Applications Vol. 5 No. 1, pp.No.1-14.
[2] Asmidar Abu Bakar , Roslan Ismail , Abdul Rahim Ahmad and Jamalul-Lail Abd Manan,(2012),' Ensuring Data Privacy and Security in MANET: Case in Emergency Rescue Mission' proceeding of International Conference on Information and Knowledge Management (ICIKM 2012) IPCSIT vol.45, pp.No.1-5.
[3] D. N. Goswami and Anshu Chaturvedi,(2012),' Cross Layer Integrated Approach for Secured Cluster Selection in Ad Hoc Networks', proceeding of International Journal of Computer and Communication Engineering, Vol. 1, No. 3, pp.No.1-4.
[4] G. S. Mamatha,(2012),' A Defensive Mechanism Cross Layer Architecture for MANETs to Identify and Correct Misbehavior in Routing', proceeding of International Journal of Network Security & Its Applications (IJNSA), Vol.4, No.1, pp.No.1-10.

Cite this article as: H INDRAPRIYADARSINI, T ARTHI. "A Cross Layer Based Secure Multipath Neighbor Routing Protocol in MANET." *International Conference on Systems, Science, Control, Communication, Engineering and Technology (2015)*: 170-174. Print.

International Conference on Systems, Science, Control, Communication, Engineering and Technology 2015 [ICSSCCET 2015]

ISBN	978-81-929866-1-6	**VOL**	01
Website	icssccet.org	**eMail**	icssccet@asdf.res.in
Received	10 - July - 2015	**Accepted**	31- July - 2015
Article ID	ICSSCCET038	**eAID**	ICSSCCET.2015.038

ON r δ-CLOSED SETS IN TOPOLOGICAL SPACES

S Padmanaban[1], B Anand[2], S Sharmila Banu[3], S Faridha[4]
Assistant Professors, Department of Mathematics,
Karpagam Institute of Technology, Coimbatore

Abstract: *A new set called regular δ-closed (briefly rδ) sets is introduced in this research which arises between the class of δ-closed sets and the class of all regular g-closed sets. In addition we study some of its vital properties and examine the relations between the associated topology.*

Keywords: Topological spaces, closed sets, separation axioms, δ-closed sets, generalized closed sets, regular generalized closed sets

1. INTRODUCTION AND PRELIMINARIES

Norman Levine introduced and studied generalized closed (briefly g-closed) sets [11] and semi-open sets [12] in 1963 and 1970 respectively. Arya and Nour [3] defined generalized semi-closed (briefly gs-closed) sets for obtaining some characterizations of s-normal spaces in 1990.

Njåstad [17] introduced the concepts of α-sets (known as α-open sets) and β-Sets (known as β-open sets) for topological spaces. Andrijević [1] called β-sets as semi-preopen sets. H. Maki called generalized α-open sets in two ways and introduced generalized α-closed(briefly gα-closed) sets[13] and α-generalized closed(briefly αg-closed) sets[14] in 1993 and 1994 respectively. Dontchev [6] introduced generalized semi-preclosed (briefly gsp-closed) sets in 1995. Palaniappan and Rao [18] introduced regular generalized closed (briefly rg-closed) sets in 1993. Gnanambal [10] introduced generalized pre regular closed (briefly gpr-closed) sets. In this paper, we study the relationships of δ-closed sets with regular generalized closed sets.We obtain basic properties of regular δ -closed sets.

Throughout this paper $(X,\tau),(Y,\sigma)$ and (Z,η) $(or\ X,Y,Z)$ represents topological spaces on which no seperaxion axioms are assumed unless otherwise mentioned. For a subset A of a space (X,τ), $cl(A)$, $int(A)$ and A^c $(or\ X - A)$ denote the closure of A, the interior of A and the complement of A in X, respectively.

Definition:1.1 A subset A of a topological space (X,τ) is called:

1. pre open [16] $A \subseteq int(cl(A))$,
2. semi open[12] $A \subseteq cl(int(A))$,
3. regular open [19] $A = int(cl(A))$.

Cite this article as: S Padmanaban, B Anand, S Sharmila Banu, S Faridha. "ON r δ-CLOSED SETS IN TOPOLOGICAL SPACES." *International Conference on Systems, Science, Control, Communication, Engineering and Technology (2015)*: 175-178. Print.

Definition:1.2 A subset A of a topological space (X, τ) is called:

1. a generalized closed set (briefly g-closed) [11] if $cl(A) \subseteq U$ whenever $A \subseteq U$ and U is open in (X, τ),
2. a αg-closed [13] if $\alpha cl(A) \subseteq U$ whenever $A \subseteq U$ and U is open set in (X, τ),
3. a $\hat{g}$ –closed [20] if $cl(A) \subseteq U$ whenever $A \subseteq U$ and U is semi open set in (X, τ).
4. a gs –closed [3] if $scl(A) \subseteq U$ whenever $A \subseteq U$ and U is open set in (X, τ).

The complements of above sets are called their respective open sets.

Definition 1.3 A subset A of a topological space (X,τ) is called Regular δ-closed (rδ-closed) if $A = cl_\delta(A)$ where

$cl_\delta(A) = \{x \epsilon X : int(cl_\delta(U)) \cap A \neq \emptyset, U \in \tau \text{ and } x \epsilon U\}$ whenever $A \subseteq U$ and U is regular open in (X,τ).

2. R δ - closed sets

Theorem : 2.1 Every rδ- closed set is a g- closed set.

Proof: Obvious.

The converse of the above theorem is not true in general as it can be seen from the following example.

Example: 2.2 Let X = {x, y, z} = τ = {∅, X, {x}, {y, z}} and D = {y}. D is not a g- closed set since {y} is a g-open set of (X,τ) such that $D \subseteq \{y\}$ but $cl_\delta(D) = cl_\delta\{\{y\}\} = \{y, z\} \subseteq \{y\}$

The following theorem shows that the class of rg-closed sets is properly contained in the class of αg-closed sets, the class of gs-closed sets, the class of gsp-closed sets, the class of gp-closed sets, the class of gpr-closed sets, the class of αg-closed.

Corollary: 2.3 Union (intersection) of any rδ -closed sets is again rδ -closed.

Corollary: 2.4 Let A be a rδ -closed of (X, τ). Then A is closed if and only if cl(A)-A is semi-closed.

Corollary:2.5 In a submaximal space (X, τ), every rδ -closed set is closed.

Theorem :2.6 Let A be a rδ -closed set of (X, τ). Then cl(A)-A does not contain any non-empty semi-closed set.

Proof: Let F be a semi-closed subset of (X, τ) such that F ⊆ cl(A)-A. Then F ⊆ X-A. This implies A ⊆ X-F. Now X-F is semi-open set of (X, τ) such that A ⊆ X-F. Since A is a rδ -closed set of (X, τ), then cl(A) ⊆ X-F. Thus F ⊆ X-cl(A). Now F ⊆ cl(A) ∩ (X-cl(A)) =∅.Therefore F = ∅.

Theorem :2.7 Every rδ-closed set is rg-closed set but not conversely.

Proof: Let A be rδ -closed set of (X, τ). Let G be a regular open set such that A ⊆ G. Then A ⊆ int(cl(G)). Since int(cl(G)) is semi-open set containing the rδ -closed set, then cl(A) ⊆ int(cl(G)). Therefore A is an rg-closed set.

Theorem :2.8 Every closed (resp. ĝ-closed) set is an r δ-closed set.

Proof: From the following example we will prove that the converse of the above theorem is not true.

Example :2.9 Let X = {a, b, c} and τ = {∅, X, {a}, {b, c}}. Consider A = {b}. A is not a closed set. However, A is an rδ-closed set.

Example :2.10 Let X = {a, b, c} and τ = {∅, X, {a}, {a, c}}. Consider A = {a, b}. A is not an rδ -closed set. However, A is a g-closed set.

Therefore, the class of rδ-closed sets is properly contained in the class of g-closed sets and properly contains the class of closed sets.

Theorem :2.11 Every rδ-closed set is αg-closed, gα-closed, and gs-closed set but not conversely.

Cite this article as: S Padmanaban, B Anand, S Sharmila Banu, S Faridha. "ON r δ-CLOSED SETS IN TOPOLOGICAL SPACES." *International Conference on Systems, Science, Control, Communication, Engineering and Technology (2015)*: 175-178. Print.

Proof: Follows from the previous theorem and the fact that every rδ-closed set is an αg-closed set, gs-closed set and scl(A) ⊆ αcl(A) ⊆ cl(A) for any subset A of a space (X, τ).

Consider the space (X, τ) in the Example. The set B = {c} is αg-closed and gα-closed and hence sg-closed and gs-closed. But B is not an rδ -closed set.

Thus the class of rδ-closed sets properly contains the class of αg-closed sets, the class of gα-closed sets, the class of gs-closed sets and the class of sg-closed sets. Next we show that this new class also properly contains the class of rg-closed sets, the class of gpr-closed sets and the class of gsp-closed sets.

Theorem :2.12 Let A be a rδ- closed set of a topological space (X,τ), Then, $pcl_\delta(A)$is rδ- closed.

Proof:A subset A of (X,τ), $scl_\delta(A) = A \cup int(cl_\delta(A))$and $pcl_\delta(A) = A \cup int(cl_\delta(A))$.

Since $pcl_\delta(A)$ is the union of two rδ- closed sets A and $cl_\delta(int(A))$.

Example:2.13 Let X = {a, b, c} τ = {∅,X,{a},{b},{a, b} {a, c}}. Consider A = {c}. Here A is not regular open. This A is δ-closed and$scl_\delta(A) = pint(A) = \emptyset$ is rδ- closed.

Theorem : 2.14 If A is a rδ- closed set of (X), such that. $A \subseteq B \subseteq cl_\delta(A)$, then B is also rδ- closed set of (X,τ).

Proof: Let U be a regular open set of (X,τ) such that $B \subseteq U$ Then $A \subseteq U$ since A is δ- closed the $cl_\delta(A) \subseteq U$.

$cl_\delta(B) \subseteq cl_\delta\big(cl(A)\big) = cl_\delta(A) \subseteq U$. B is rδ- closed set of (X,τ). $B \subseteq U$

Theorem :2.15 Let A be a locally closed set of (X, τ). Then A is rδ -closed if and only if A is closed.

Proof: Obvious.

Theorem :2.16 If A is regular open, then sint(A) is rδ -closed.

Proof: First we note that for a subset A of (X, τ), scl(A) = A ∪ int(cl(A)) and pcl(A) = A ∪ cl(int(A)). Moreover, sint(A) = A ∩ cl(int(A)) and pint(A) = A ∩ int(cl(A)).

(1) Since cl(int(A)) is a closed set, then A and cl(int(A)) are rδ -closed sets. By the Theorem 3, A ∩ cl(int(A)) is also a rδ -closed set.

Theorem :2.17 If A is regular open ,then pcl(A) is rδ -closed.

Proof: pcl(A) is the union of two rδ -closed sets A and cl(int(A)). Again by the Theorem 3,

pcl(A) is rδ -closed.

Theorem :2.18 If A is regular open, then pint(A) and scl(A) are also rδ -closed sets.

Proof: Since A is regular open, then A = int(cl(A)). Then scl(A) = A ∪ int(cl(A)) = A. Thus scl(A) is rδ -closed. Similarly pintA is also an rδ -closed set.

Theorem :2.19 A is a rδ- closed of (X,τ) such that if and only if $cl_\delta(A)$ -A does not contain any non-empty δ- closed set.

Proof: Let U be a δ –regular open set of (X, τ) such that A ⊆U. If cl $_\delta$ (A) ⊆ U, then cl $_\delta$ (A) ∩ C(U) = ∅ . Since cl $_\delta$ (A) is a closed set, then by **[12]**, ∅= cl $_\delta$ (A) ∩ C(U) is a δ -closed set of (X, τ). Then ∅= cl (A) ∩ C(U) ⊆ cl$_\delta$(A)-A. So cl $_\delta$ (A)-A contains a non-empty δ -closed set. A contradiction. Therefore A is r δ -closed.

References

1. D.Andrijevic, Semi-preopen sets, Mat. Vesnik, 38(1)(1986), 24-32.
2. I.Arokiarani, K.Balachandran and J.Dontchev, Some characterizations of gp-irresolute and gp-continuous maps between topological spaces, Mem. Fac. Sci. Kochi. Univ. Ser.A. Math., 20(1999),93-104.

Cite this article as: S Padmanaban, B Anand, S Sharmila Banu, S Faridha. "ON r δ-CLOSED SETS IN TOPOLOGICAL SPACES." *International Conference on Systems, Science, Control, Communication, Engineering and Technology (2015)*: 175-178. Print.

3. S. P. Arya and T.M. Nour, characterizations of S-normal spaces, Indian J. Pure Appl. Math., 21(1990), 717-719.

4. K.Balachandran, P.Sundaram and H.Maki, On generalized continuous maps in topological spaces, Mem. Fac. Kochi Univ. Ser.A, Math., 12(1991), 5-13.

5. N.Bourbaki, General Topology, Part I, Addision-Wesley, Reading, Mass., 1966.

6. J.Dontchev, On generalizing semi-preopen sets, Mem.Fac.Sci.Kochi Ser.A, Math., 16(1995), 35-48.

7. J.Dontchev and M.Ganster, On δ -generalized closed sets and T3/4-spaces, Mem.Fac. Sci. Kochi Univ. Ser.A, Math., 17(1996), 15-31.

8. J.Dontchev and H.Maki, On δ-generalized closed sets, Internet. J. Math. Math.Sci..

9. M.Ganster and I.L.Reilly, Internat. J. Math., & Math. Sci.,12(3)(1989), 417-424.

10. Y.Gnanambal, On generalized preregular closed sets in topological spaces, Indian J.Pure. Appl. Math., 28(3)(1997), 351-360.

11. N.Levine, Generalized closed sets in topology, Rend. Circ. Math. Palermo, 19(2)(1970), 89-96.

12. N.Levine, Semi-open sets and semi-continuity in topological spaces, Amer. Math. Monthly, 70(1963), 36-41.

13. H.Maki, R.Devi and K.Balachandran, Generalized α-closed sets in topology, Bull. Fukuoka.Univ.Ed.Part III, 42, (1993), 13-21.

14. H.Maki, R.Devi and K.Balachandran, Associated topologies of generalized δ-closed sets and δ-generalized closed sets, Mem. Fac. Sci. Kochi Univ. Ser.A, Math., **15**(1994), 51-63.

15. A.S.Mashhour, I.A.Hasanein and S.N.El-Deeb, δ-continuous and δ-open mappings.,Acta Math. Hung.**,** 41(3-4)(1983), 213-218.

16. A.S. Mashhour, M.E.Abd. El-Monsef and S.N. El.deep, on pre continuous and weak precontinuous mappings, Proc. Math. and Phys. Soc. Egypt., 53(1982), 47-53.

17. O.Njastad, On some classes of neraly open sets, Pacific J.Math., **15**(1965), 961-970.

18. N.Palaniappan and K.C.Rao, Regular generalized closed sets, Kyungpook Math.J., 33(2)(1993), 211-219.

19. M. Stone, Application of the theory of Boolean rings to general topology, Trans. Amer. Math. Soc. 41(1937), 374–481.

20. M.K.R.S .Veerakumar, $\hat{g}$-closed sets and G $\hat{L}$C-functions, Indian J.Math.,43(2)(2001), 231-247.

21. N.V.Velicko, H-closed topological spaces, Amer. Math. Soc. Transl.,78(1968),103-118

.

Cite this article as: S Padmanaban, B Anand, S Sharmila Banu, S Faridha. "ON r δ-CLOSED SETS IN TOPOLOGICAL SPACES." *International Conference on Systems, Science, Control, Communication, Engineering and Technology (2015)*: 175-178. Print.

International Conference on Systems, Science, Control, Communication, Engineering and Technology 2015 [ICSSCCET 2015]

ISBN	978-81-929866-1-6	**VOL**	01
Website	icssccet.org	**eMail**	icssccet@asdf.res.in
Received	10 - July - 2015	**Accepted**	31- July - 2015
Article ID	ICSSCCET039	**eAID**	ICSSCCET.2015.039

Language Translator Application using Image In Android

V.Renupriya[1], K.Vignesh[2]
[1, 2] Assistant Professor, Computer Science and Engineering,
Karpagam Institute of Technology.

Abstract: *This paper provides a new idea to the people when they want to transcript the other language text into their known language. Language Translator is an application that can be installed in user's mobiles like other mobile application. Using this they can transcript their unknown language text into their known language text format. User has to take a photo image of the unknown language text and they have to give this image as an input for the software and the software will give the output as their known text. Tesseract is an open source Optical character recognition (OCR) technology used to extract the text from the image and Google API is used for translation of language. This application software is very useful in the emergency situation (If the user moves to the different states).*

I. INTRODUCTION

Text extraction from image is one of the complicated areas in digital image processing. It is a complex process to detect and recognize the text from image. It's possible of computer software only can provide extracted text from image using most complicated algorithm. So it can't be use anywhere in this existing environment. Here different types of language translators are available such as voice based translator, keyboard based translator etc. But those translators are not easy to use.

The purpose of this work is to demonstrate that a tight dynamical connection may be made between text and interactive visualization imagery. The Android device camera can prove this type of extraction and also we can easily to implement algorithm using java language. Millions of mobile users in this world and they always have mobile in their hand, so simply they can capture the image to extract the text.

A. OPTICAL CHARACTER RECOGNITION

Image translation is a term related to machine translation services for mobile devices (mobile translation). Image translation refers to an additional service provided by mobile translation applications where the user can take a photo of some printed text (menu list, road sign, document etc.), apply optical character recognition (OCR) technology to it to extract any text contained in the image, and then have this text translated into a language of their choice.

Optical character recognition (OCR) is the mechanical or electronic conversion of images of typewritten or printed text into machine-encoded text. OCR has a high degree of recognition accuracy for most fonts are now common. Some systems are capable of reproducing formatted output that closely approximates the original page including images, columns, and other non-textual components.

Many valuable paper documents are usually scanned and kept as images for backup. Extracting text from the images is quite helpful and thus a need for some tool for this extraction is always there. To achieve this the Image Translator application will be very useful.

Cite this article as: V.Renupriya, K.Vignesh. "Language Translator Application using Image In Android." *International Conference on Systems, Science, Control, Communication, Engineering and Technology (2015)*: 179-182. Print.

B. LANGUAGE TRANSLATOR

After extracting the words from image by using the OCR (Optical Character recognition) Engine, those words are translated into known language to do this the GOOGLE TRANSLATE API service is used. This is a paid service. It provides many libraries for translation. The first thing to remember is that translation is the transfer of meaning from one language to another. It is not the transfer of words from language to language. You must translate the meaning of what is being said, rather than do it word-for-word. This is because languages are not just different words. Different languages also have different grammar, different word orders, sometimes even words for which other languages do not have any equivalents.

For this case the Google API translation service will be very useful that provides instant translations between dozens of different languages. It can translate words, sentences and web pages between any combinations of our supported languages. With Google Translate, the information can be made universally accessible and useful, regardless of the language in which it's written.

It can make intelligent guesses as to what an appropriate translation should be. This process of seeking patterns in large amounts of text is called "statistical machine translation". Since the translations are generated by machines, not all translation will be perfect. The more human-translated documents that Google Translate can analyze in a specific language, the better the translation quality will be. This is why translation accuracy will sometimes vary across languages.

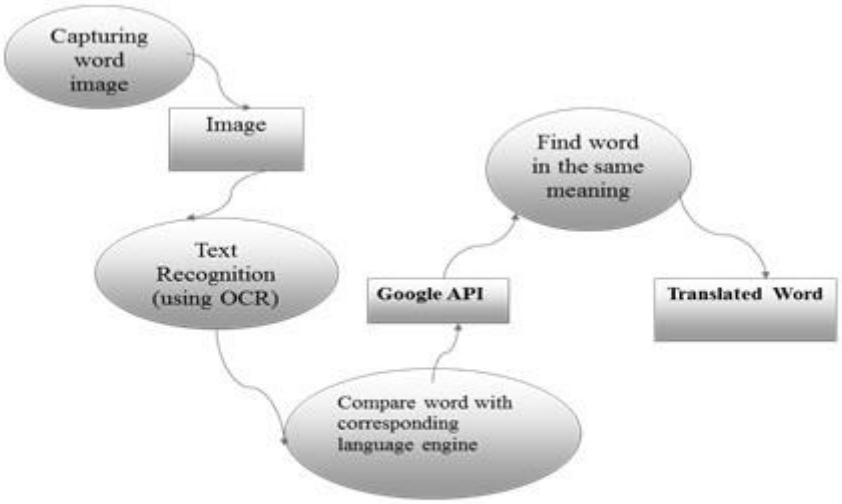

Figure 1: Language Translator application process

II. PROPOSED WORK

A. TESSERACT ENGINE INTEGRATION

Optical character recognition (OCR) is the mechanical or electronic translation of scanned images of handwritten, typewritten, or printed text, to machine encoded text. The open source OCR API called Tesseract is used as a basis for Image Recognition. Tesseract is considered the most accurate free OCR engine in existence. Google has benefitted extensively from Tesseract in their Google books project, which has attempted to digitize the world's libraries.

Tesseract works with independently developed Page Layout Analysis Technology. Hence Tesseract accepts input image as a binary image. Tesseract can handle both, the traditionalBlack on White text and also inverse-White on Black text. Outlines of component are stored on connected Component Analysis. Nesting of outlines is done which gathers the outlines together to form a Blob. Such Blobs are organized into text lines. Text lines are analyzed for fixed pitch and proportional text. Then the lines are broken into words by analysis according to the character spacing.

Fixed pitch is chopped in character cells and proportional text is broken into words by definite spaces and fuzzy spaces. Tesseract performs activity to recognize words. This recognition activity is mainly consists of two passes. The first pass tries to recognize the words. Then satisfactory word is passed to Adaptive Classifier as training data, which recognizes the text more accurately. During second pass, the words which were not recognized well in first pass are recognized again through run over the page.

Line Finding Algorithm : Lines of text are found by analyze the image space adjacent to potential characters. This algorithm does a Y projection of the binary image and finds locations having a pixel count less than a specific threshold. These areas are potential lines, and are further analyzed to confirm.

Cite this article as: V.Renupriya, K.Vignesh. "Language Translator Application using Image In Android." *International Conference on Systems, Science, Control, Communication, Engineering and Technology (2015)*: 179-182. Print.

Baseline Fitting Algorithm : Finds baselines for each of the lines from the picture. After each line of text is found, Tesseract examines the lines of text to find approximate text height across the line. This process is the first step in determining how to recognize characters.

Fixed Pitch Detection : The other half of setting up character detection is finding the approximate character width. This allows for the correct incremental extraction of characters as Tesseract walks down a line.

Word Recognition : After finding all of the possible character "blobs" in the document, Tesseract does word recognition word by word, on a line by line basis. Words are then passed through a contextual and syntactical analyzer which ensures accurate recognition

B. TRANSLATE USING GOOGLE API

Google Translate API gives free translation service that provides instant translations between dozens of different languages. It can translate words, sentences and web pages between any combinations of our supported languages. With Google Translate, the information can be made universally accessible and useful, regardless of the language in which it's written.

It can make intelligent guesses as to what an appropriate translation should be. This process of seeking patterns in large amounts of text is called "statistical machine translation". Since the translations are generated by machines, not all translation will be perfect. The more human-translated documents that Google Translate can analyze in a specific language, the better the translation quality will be. This is why translation accuracy will sometimes vary across languages.

III. IMPLEMENTATION

Android is a software stack for mobile devices that includes an operating system, middleware and key applications. The Android SDK provides the tools and APIs necessary to begin developing applications on the Android platform using the Java programming language. Android applications are developed using Java and can be ported rather easily to the new platform. If you have not yet downloaded Java or are unsure about which version you need, I detail the installation of the development environment. Other features of Android include an accelerated 3-D graphics engine (based on hardware support), database support owner by SQLite, and an integrated web browser. Android Market filters the applications that are visible to users, so that users can see and download only those applications that are compatible with their devices. One of the ways Market filters applications is by feature compatibility.

Figure 2 capturing the word

Figure 3 Translated word

IV. FUTURE ENHANCEMENT

In future the language translator application can be enhanced by including many features such as voice based input method, handwritten method, keyboard based input method. It will achieve translate between 90 languages. It will provide translation while travelling without internet connection. Particularly useful features will include instant language recognition, batch processing of file folders full of documents, text-to-speech capability to help you learn correct pronunciation and an integrated spell-checker.

V. CONCLUSION

Language translator using image application offers a variety of languages to choose from and provides good support and a user-friendly interface. To achieve this, the user needs to take a picture from our phone camera and translate it directly to any language. The

Cite this article as: V.Renupriya, K.Vignesh. "Language Translator Application using Image In Android." *International Conference on Systems, Science, Control, Communication, Engineering and Technology (2015)*: 179-182. Print.

application will recognize the text from your picture and translate it automatically. User can use this application in restaurants, airports, train stations, buses, etc. This application supports the variety of languages. It provides very accurate guesses.

VI. REFERENCES

[1] Programming Android: Java Programming for the New Generation of Mobile Devices.
[2] Elias. M. Award, 1991, 'System Analysis and Design' Galgotia Publication Pvt. Ltd.
[3]Professional Android Application Development (Wrox Programmer to Programmer) Paperback – November 24, 2008
[4] Creating Android Applications: Develop and Design by Chris Haseman (Author).
[5] The Busy Coder's Guide to Advanced Android Development by Mr. Mark L Murph 20 Jul 2011
[6] Mike Gunderloy,JosephL.Jorden (2001), 'Mastering MYSQL Server', BPB Publications.
[7] Mridula Parihar, 2002, 'professional Android 4 Application Development', Second Edition, By Mr. Mark L Murphy.
[8] Rogers Pressman, 2001, 'Software Engineering', Fifth Edition, McGraw-Hill Publication.
[9] R. E. Blahut. The theory and practice of error control codes. Addison-Wesley, 1983.
[10] R. D. Brandt and F. Lin. Representations that uniquely characterize images modulo translation, rotation and scaling. Pattern Recognition Letters, 17:10011015, August 1996.
[11] G. Caronni. Assuring Ownership Rights for Digital Images. In H. H.

Cite this article as: V.Renupriya, K.Vignesh. "Language Translator Application using Image In Android." *International Conference on Systems, Science, Control, Communication, Engineering and Technology (2015)*: 179-182. Print.

International Conference on Systems, Science, Control, Communication, Engineering and Technology 2015 [ICSSCCET 2015]

ISBN	978-81-929866-1-6
Website	icssccet.org
Received	10 - July - 2015
Article ID	ICSSCCET040

VOL	01
eMail	icssccet@asdf.res.in
Accepted	31- July - 2015
eAID	ICSSCCET.2015.040

DECENTRALIZED ACCESS CONTROL WITH ADVANCED ENCRYPTION STANDARD AND ANONYMOUS AUTHETICATION FOR USERS IN CLOUD

T.Yawanikha[1], Bavithra Madhuranjani.K.S[2], S.Ganapathiammal[3]
[1]Assistant Professor-IT, Karpagam Institute of Technology, Coimbatore, India
[2]PG Scholar, Hindusthan College of Engineering & Technology, Coimbatore, India
,[3]Assistant Professor-IT, Karpagam Institute of Technology, Coimbatore, India

ABSTRACT: *Cloud computing is one of the recent trends emerging in the field of Information Technology, it mainly focuses on global access of data. Data sharing is an important functionality in cloud storage at the same time, threat is an issue. This system proposes an access control scheme for secure and scalable data storage in cloud and supports anonymous authentication. In the proposed system the cloud verifies the authenticity of the user without knowing the user's identity. The Advanced Encryption Standard algorithm is used to for scalable data sharing where a set of secret keys are comprised as a single key encompassing the power of all secret keys. Access policies with several forms are used securely and they decide who can access the data stored in the cloud. Most systems do not support many users to have write permission which is supported by this system and access policies are hidden. System will process only the encrypted data so that confidentiality will be maintained. This system will also prevent replay attacks. The Key Aggregate mechanism will decrease the bandwidth used for the communication and reduce the rounds of communication.*

Keywords: ***Advanced Encryption Standard, String matching algorithms, Attribute based encryption.***

I INTRODUCTION

Cloud is a market-oriented distributed computing system consisting of a collection of inter-connected and virtualized computers that are dynamically provisioned and presented as one or more combined computing resources based on service-level agreements (SLAs) recognized through intervention between the service provider and consumers. In cloud computing, users can farm out their computation and cargo space to servers (also called clouds) using Internet.

Clouds can afford several types of services like applications (e.g., Google Apps, Microsoft online), infrastructures (e.g., Amazon's EC2, Eucalyptus, Nimbus), and platforms to help developers write applications (e.g., Amazon's S3, Windows Azure).Security is needed because data stored in clouds is greatly sensitive, for example, medical records and social networks. User privacy is also required so that the cloud or other users do not know the identity of the user. Thus it is a complex system which possesses highly securable processes. So it must need a proper systematic scheme to manage data.

Transactions done in the cloud should also be noted periodically. The user should be confirmed and should give suitable permission for them. Permission criteria are carefully handled because users may change the data unnecessarily. Adding this kind of feature may automatically reduce the effectiveness of the algorithm, so the algorithm designed must be very efficient.

Cite this article as: T.Yawanikha, Bavithra Madhuranjani.K.S, S.Ganapathiammal. "DECENTRALIZED ACCESS CONTROL WITH ADVANCED ENCRYPTION STANDARD AND ANONYMOUS AUTHETICATION FOR USERS IN CLOUD." *International Conference on Systems, Science, Control, Communication, Engineering and Technology (2015)*: 183-186. Print.

Consider the following situation: A student from a college found out some malpractices done by some employees in college. Then the student takes steps to tell the details about the malpractice done in the college. Now he will report the malpractice done by the employees of the college to the university which controls the college. While reporting there are some conditions to be checked seriously. First the student should prove the identity because the university should believe that the message came from an authorised person. Second there should not be any interference. Also if any change is done for the original message then it should be found out and the file is recovered. Thus in this paper the above problems are described and rectified.
Existing concepts in cloud are centralized nature so security can't be provided in a perfect manner. The schemes which use symmetric key encryption also not a better choice. Earlier work by Zhao provides privacy preserving authenticated access control in cloud. However, the authors take a centralized approach where a single key distribution center (KDC) distributes secret keys and attributes to all users. Unfortunately, a single KDC is not only a single point of failure but difficult to maintain because of the large number of users that are supported in a cloud environment.

1.1 OUR CONTRIBUTIONS

The main contribution of this paper is
1) Access control with powerful scheme is used so that only valid users can enter/
2) Authentication of users is done during the registration phase itself.
3) The identity of the user is protected from the cloud during authentication.
4) Encryption is based upon aggregate key encryption which is highly secure.
5) The protocol supports multiple read and write on the data stored in the cloud.
6) Access policies are assigned to users during the registration phase itself.

II RELATED WORK

Attribute based encryption (ABE) was proposed by Sahai and Waters. In ABE, a user has a set of attributes based on the user in addition to its unique ID. In Key-policy ABE or KP-ABE (Goyal et al), the sender has an access policy to encrypt data. A writer whose attributes and keys have been revoked cannot write back stale information. The receiver receives attributes and secret keys from the attribute authority and is able to decrypt information if it has matching attributes. In Cipher text-policy, CP-ABE, the receiver has the access policy in the form of a tree, with attributes as leaves and monotonic access structure with AND, OR and other threshold gates.

All the approaches take a centralized approach and allow only one KDC, which is a single point of failure. Chase proposed a multi-authority ABE, in which there are several KDC authorities (coordinated by a trusted authority) which distribute attributes and secret keys to users. Multi-authority ABE protocol was studied in which required no trusted authority which requires every user to have attributes from at all the KDCs. Recently, Lewko and Waters proposed a fully decentralized ABE where users could have zero or more attributes from each authority and did not require a trusted server. In all these cases, decryption at user's end is computation intensive. So, this technique might be inefficient when users access using their mobile devices. To reduce or block replay attack we use string matching algorithms which are more efficient and perfect in security. It works more efficient than all other matching algorithms.

III BACKGROUND

In this section, we describe our cloud storage model, adversary model and the assumptions we have made in the paper.
We make the following assumptions in our work.
1) The cloud is insecure and to make it secure, the data is classified and given class indexes.
2) Users can have either read or write or both accesses to a file stored in the cloud.
3) All communications between users/clouds are secured by Secure Shell Protocol, SSH.
4) The cloud supports all sorts of traffics.

IV PROPOSED SCHEME

We explain public-key cryptosystems which produce a set of constant-size cipher texts such that efficient delegation of decryption rights for any set of cipher texts is possible. The best thing is that it is very easy to combine encryption key into a single key, but encompassing the power of all the keys being aggregated. The secret key holder can release a constant-size aggregate key for flexible choices of cipher text set in cloud storage, but the other encrypted files outside the set remain confidential and very much authenticated. This matching aggregate key can be easily send to others or be stored in a storage media with very limited secure storage. We provide formal security analysis of our schemes in the standard model. Our schemes give the first public-key patient-controlled encryption for flexible hierarchy and security, which was yet to be described.
Advanced encryption standard scheme consists of five polynomial-time algorithms as follows. The data owner establishes the public system parameter via Setup and generates a public/master-secret key pair via KeyGen. Messages can be encrypted via Encrypt by anyone who also decides what cipher text class is associated with the plaintext message to be encrypted. The data owner can use the master-secret to generate an aggregate decryption key for a set of cipher text classes via Extract.

Cite this article as: T.Yawanikha, Bavithra Madhuranjani.K.S, S.Ganapathiammal. "DECENTRALIZED ACCESS CONTROL WITH ADVANCED ENCRYPTION STANDARD AND ANONYMOUS AUTHETICATION FOR USERS IN CLOUD." *International Conference on Systems, Science, Control, Communication, Engineering and Technology (2015)*: 183-186. Print.

The generated keys can be passed to delegates securely (via secure e-mails or secure devices) finally; any user with an aggregate key can decrypt any cipher text provided that the cipher text's class is contained in the aggregate key via Decrypt.
The aggregate key cryptosystem is explained as follows the Figure 2 shows the flow of variables for generating the aggregate key and decryption of the messages using the aggregate key. Setup (1^{λ}; n): executed by the data owner to setup an account on an untrusted server. On input a security level parameter $1^{\lambda}$and the number of cipher text classes n (i.e., class index should be an integer bounded by 1 and n), it outputs the public system parameter *param,* which is omitted from the input of the other algorithms for brevity. KeyGen: executed by the data owner to randomly generate a public/master-secret key pair (pk; msk). Encrypt (pk; i;m): executed by anyone who wants to encrypt data. On input a public-key pk, an index i denoting the cipher text class, and a message m, it outputs a cipher text C. Extract (msk; S)*:* executed by the data owner for delegating the decrypting power for a certain set of cipher text classes to a delegatee. On input the mastersecret key msk and a set S of indices corresponding to different classes, it outputs the aggregate key for set S denoted by KS. Decrypt (KS; S; i; C): executed by a delegate who received an aggregate key KS generated by Extract. On input KS, the set S, an index i denoting the cipher text class the cipher text C belongs to, and C, it outputs the decrypted result , m if i is an element of S.

4.1 Setting Up The Cloud And Enabling Data Transfer

The cloud is setup using the Amazon EC2™ and the security configurations are made. The cloud instances are setup in such a way that it will support all types of traffic like TCP, UDP etc. The various instances in the Amazon cloud communicates each other using socket programming. Initial module is setup using AES encryption for generating keys for the users. Basic file upload and download is done using socket programming.

4.2 User Authentication and enabling Advanced Encryption Standard

The data in the cloud is classified, and each class of data will be given a class index. All the keys of the data associated with the same class will be combined using the algorithm so that the data in the same class can be accessed using the aggregate key. When registering, the user will provide the keyword for authentication purpose. The users who are registered will be divided into several levels and these levels will be given separate key for data access. The keys will be generated based on the access rights of the user. Since the users with the same access rights will be given same keys, the number of keys used will be reduced.

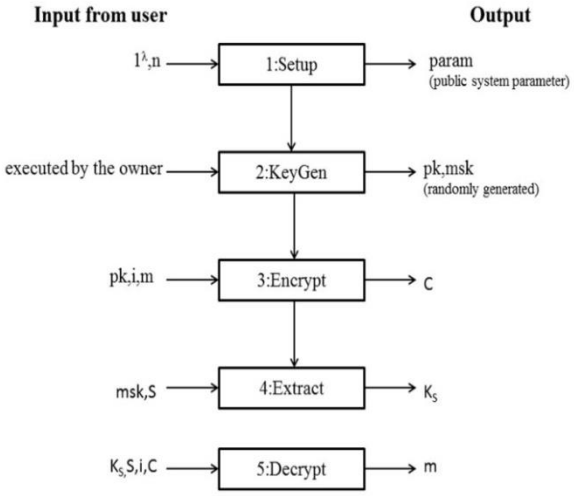

4.3 User Revocation

The users with same access rights will have same set of keys. Before revoking the access rights of the user, it should be ensured that the user is not having the ability to access the data even if they possess the matching aggregate keys. So for doing that the data will be clustered again and the aggregate key will be generated. This aggregate key will be send to all users excluding the revoked user. So the previous set of aggregate keys will become useless. In doing the process, the security features will be enhanced and the system can be trusted more

V CONCLUSION

The data security is the highest discussed topic. As more crypto graphical tools come into existence, more it secure but at the same time, data security is threatened by attackers who can break through any kind of algorithm. The proposed scheme is secure like any algorithm that is used. The only difference is that the algorithm will reduce the rounds of communication, thereby enhancing the cloud environment. The scheme used here only tries to compress the set of secret keys and to make an aggregate key. Since users with same access rights will have same set of encryption keys, the complexity of the system will also get reduced. Since the keys are generated for a scalable amount of data, if the amount of data to be shared is increased, the number of classes of data will change and the aggregate

Cite this article as: T.Yawanikha, Bavithra Madhuranjani.K.S, S.Ganapathiammal. "DECENTRALIZED ACCESS CONTROL WITH ADVANCED ENCRYPTION STANDARD AND ANONYMOUS AUTHETICATION FOR USERS IN CLOUD." *International Conference on Systems, Science, Control, Communication, Engineering and Technology (2015)*: 183-186. Print.

keys generated will also differ. The limitation in the scheme is the predefined number of cipher text classes. As far as cloud is concerned, the amount of data to be shared is increasing at a rapid and exponential rate. This problem can be rectified by registering additional key pairs for future purpose.

VI REFERENCES

1) SushmitaRuj, Milos Stojmeovic, Amiya Nayak" Decentralized Access Control with Anonymous Authentication of Data Sharing in Cloud"IEEE Transaction on Parallel and Distrinbuted System, Vol.25,no.2,2014.
2) Cheng-Kang Chu, Sherman S. M. Chow, Wen-GueyTzeng, Jianying Zhou, Robert H. Deng "Key-Aggregate Cryptosystem for Scalable Data Sharing in Cloud Storage" Vol.25,pp.468-477,2014
3) J. Bethencourt, A. Sahai, and B. Waters, "Ciphertext-Policy Attribute-Based Encryption," Proc. IEEE Symp. Security and Privacy, pp. 321-334, 2007.
4) B. Wang, S. S. M. Chow, M. Li, and H. Li, "Storing Shared Data on the Cloud via Security-Mediator," in International Conference on Distributed Computing Systems - ICDCS 2013. IEEE, 2013.
5) S. G. Akl and P. D. Taylor, "Cryptographic Solution to a Problem of Access Control in a Hierarchy," ACM Transactions on Computer Systems (TOCS), vol. 1, no. 3, pp. 239–248, 1983.
6) F. Guo, Y. Mu, and Z. Chen, "Identity-Based Encryption: How to Decrypt Multiple Ciphertexts Using a Single Decryption Key," in Proceedings of Pairing-Based Cryptography (Pairing '07), ser. LNCS, vol. 4575. Springer, 2007, pp. 392–406.
7) S. Ruj, M. Stojmenovic, and A. Nayak, "Privacy Preserving Access Control with Authentication for Securing Data in Clouds," Proc. IEEE/ACM Int'l Symp. Cluster, Cloud and Grid Computing, pp. 556- 563, 2012.
8) S. Yu, C. Wang, K. Ren, and W. Lou, "Attribute Based Data Sharing with Attribute Revocation," Proc. ACM Symp. Information, Computer and Comm. Security (ASIACCS), pp. 261-270, 2010.

Cite this article as: T.Yawanikha, Bavithra Madhuranjani.K.S, S.Ganapathiammal. "DECENTRALIZED ACCESS CONTROL WITH ADVANCED ENCRYPTION STANDARD AND ANONYMOUS AUTHETICATION FOR USERS IN CLOUD." *International Conference on Systems, Science, Control, Communication, Engineering and Technology (2015)*: 183-186. Print.

International Conference on Systems, Science, Control, Communication, Engineering and Technology 2015 [ICSSCCET 2015]

ISBN	978-81-929866-1-6
Website	icssccet.org
Received	10 - July - 2015
Article ID	ICSSCCET041

VOL	01
eMail	icssccet@asdf.res.in
Accepted	31- July - 2015
eAID	ICSSCCET.2015.041

APPLICATION OF NANO POROUS CARBON FOR THE UPTAKE OF PHENOL AND 2-CHLOROPHENOL AS BISOLUTE FROM WATER

R. Subha[1], C. Namasivayam[2]
[1] Karpagam Institute of Technology, Coimbatore-641105, India
[2] Environmental Chemistry Division, Department of Environmental Sciences
Bharathiar University, Coimbatore - 641046, India

ABSTRACT: *Nano porous activated carbon prepared from coir pith using $ZnCl_2$ (ZnCPC) was investigated to find the feasibility of its application for mixture of phenol and 2-chlorophenol in aqueous solution through sequential adsorption/desorption process by HPLC C-18 column. Nano porous carbon was characterized using standard physio-chemical methods, BET surface area, pore diameter, SEM and XRD studies. Adsorption of 2-CP in bisolute systems showed that 2-CP were adsorbed preferentially, but phenol was adsorbed competitively. This result was further confirmed by η_1 and η_2 values obtained from extended Langmuir model. The cost of ZnCPC is economically effective compared to commercial activated carbon.*

Keywords*:* Nano porous activated carbon, Bisolute system, Sequential adsorption/desorption

1. INTRODUCTION

Phenol is present in the surface water of industrial effluents such as coal tar, gasoline, plastic, rubber-proofing, coking, pharmaceutical, petrochemical and steel industries, domestic wastewaters and chemical spillage [1]. Phenol presence in natural water can lead further to the formation of chlorophenols during disinfection and oxidation processes, which are carcinogenic compounds[2]. Chlorophenols are listed as priority environmental pollutants by US EPA because of their higher toxicity, carcinogenicity and recalcitrant properties [3]. Long term ingestion of water containing phenols in the human body causes protein degeneration, tissues erosion and paralysis of the central nervous system, and also damages the kidney, liver and pancreas [4]. The World Health Organization (WHO) guideline for maximum admissible concentration in drinking water is 10 µg/L for 2-chlorophenol (2-CP) and phenol 1mg/L[5]. In India, Coir pith is a lignocellulosic light fluffy biomaterial generated as a byproduct during separation of fiber from ripened coconut husk contains mainly cellulose, lignin and pentosans. The production of coir pith in India is estimated to be about 7.5 million tons annually and this often causes serious disposal problems [6].Usually, the industrial effluents present a mixture of phenols which compete between itself for the active adsorbed sites, that is important for a determination of the phenols selectivity in the solution by adsorbent material. The conventional treatment method available for the treatment of mixture of phenols are sol –gel method [7] and competitive adsorption [8]. Studies of competitive adsorption reveals that different adsorbates compete for adsorption sites characterized by maximum heat of adsorption and minimum free energy of adsorption[9]. Very few adsorbents are reported in literature for the simultaneous adsorption

Cite this article as: R. Subha, C. Namasivayam. "APPLICATION OF NANO POROUS CARBON FOR THE UPTAKE OF PHENOL AND 2-CHLOROPHENOL AS BISOLUTE FROM WATER." *International Conference on Systems, Science, Control, Communication, Engineering and Technology (2015)*: 187-190 Print.

of phenol and 2-CP such as hydrophobic FAU zeolites[10], Amberlite XAD-4 and NDA-100[11], granular activated carbon[8], layered hexaniobate [12], montmorillonite modified with hexadecyl trimethylammonium cation [13], polymeric resin MN200[14], CF_2, a pure powdered activated carbon [15] and Duolite ES – 86 [16], respectively. The objective of the work is to explore the feasibility of using the $ZnCl_2$ activated nano porous coir pith carbon as an adsorbent for the removal and recovery of toxic phenol and 2-chlorophenol (2-CP) as binary adsorbate from water using HPLC C-18 column.

2. MATERIAL & METHODS

Coir pith was dried in sunlight for 5 h. The dried coir pith (200 g) was stirred in a boiling solution of anhydrous $ZnCl_2$ (100 g in 1 liter of distilled water) for 1h, then the remaining solution was drained off and dried at 60° C for 12 h. The whole set up was placed in a muffle furnace at 700°C and carbonization was done for 1 h. After cooling the excess zinc chloride present in the carbonized material was leached out by immersing in 1 M HCl solution for 24 h in an oven at 80°C. Then the carbon was repeatedly washed with water to get rid of traces of HCl and $ZnCl_2$.The carbonized material was sieved to 250 to 500 µm size and characterized using physico-chemical methods and used for adsorption studies[6].

Procedure

Equilibrium isotherms in two component system Phenol+2-chlorophenol at a constant pH was determined using sequential adsorption/desorption method[17] as follows: To 100 mg of the adsorbent, added 50 ml of 40 mg/L of phenol at pH 2.0, agitated for 2 h. After agitation, the supernatant was removed and analyzed for phenol at 270 nm using HPLC. To the phenol loaded adsorbent, added 50 ml of 120 mg/L of 2-chlorophenol at pH 2.0 and agitated for 2 h. Then the supernatant was analyzed both for phenol and 2-chlorophenol using HPLC at 270 and 273 nm, respectively. The mobile phase was methanol-water-acetic acid in the ratio 60:39:1. The analysis was carried out in an elution gradient mode with 60 % methanol using a flow rate of 1 ml/min at 35 °C [18]. The residual concentrations of phenol and chlorophenol were obtained from calibration curves. The same procedure was repeated for other combinations of phenol and 2-chlorophenol (120 mg/L of P+40 mg/L of 2-CP; 40 mg/L of 2-CP +120 mg/L of P) in two component system.

3. RESULTS AND DISCUSSIONS

The physio-chemical characteristics of $ZnCl_2$ activated coir pith nano porous carbon in comparison with coir pith carbon in the absence of $ZnCl_2$ activation have already been reported [19].

SEM study

In SEM studies, $ZnCl_2$ activated coir pith carbon before adsorption (250 X magnification) revealed honeycomb voids with a large number of pores (Fig.1a). After adsorption the pores were filled by 2- CP (Fig. 1b). Coverage of the surface of the adsorbent due to adsorption of the adsorbate molecule presumably leading to formation of a monolayer of the adsorbate molecule over the adsorbent surface is evident from the formation of white layer (molecular cloud) of uniform thickness and coverage (spread).The preparation of activated carbon from Tectona grandis sawdust with 10% $ZnCl_2$ after mixing and subjected to vaccum drying with 1000 times magnification reveals pores of different size and shapes and there was a scattering of salt particles on the surface of the activated carbon [20].

XRD study

Fig. 2 shows that the XRD pattern of the $ZnCl_2$ activated coir pith carbon is crystalline in nature and shows sharp peaks corresponding to 2θ = 26.56 (d= 3.06056) and 42.0 (d= 2.14006). Measured inter planar distances agreed with the values reported for cellulose in literature [21]. The XRD data of the adsorbate loaded carbons have an evidence of crystalline nature of carbon changing into amorphous nature after adsorption and this suggests that the phenol molecules diffuse into micro pores and macropores.

Batch mode studies

Bisolute sequential adsorption experiments were conducted until a less strongly adsorbed solute desorbed from ZnCPC due to competition.

(i) 40 mg/L of P + 120 mg/L of 2-CP

In this case, phenol was added first and 2-CP was added second to the adsorbent. The phenol which was adsorbed to the extent of 87.54 %, was desorbed up to 43.60 % on the addition of 2-CP solution, while 2-CP adsorption did not change in the presence of phenol. It shows that 2-CP was preferentially adsorbed in comparison with the phenol. The adsorbed quantity of 2-CP (55.87 mg/g) in the presence of phenol is almost the same as that of 2-CP when present as the sole adsorbate (56.07 mg/g)[6,22].

(ii)120 mg/L of 2-CP + 40 mg/L of P

When the order of addition was reversed, i.e. 2-CP first and phenol second, 2-CP, which was adsorbed to the extent of 93.45 % was desorbed up to 9.42 % on the addition of P, while P was adsorbed up to 75.40 % in the presence of 2-CP compared to 87.54 % in the absence of 2-CP. The adsorbed quantity of 2-CP (55.79 mg/g) in the presence of phenol is almost the same as that of 2-CP when present as the sole adsorbate (56.07 mg/g)[6]. In both the cases (i) & (ii) (ie. when the order is reversed), the presence of phenol does not influence the adsorption of 2-CP, whereas presence of 2-CP desorbed P from the P loaded adsorbent. Similarly, the effect of thermally activated carbons were found to be better adsorbers for the bisolute mixture of phenol and 2-chlorophenol compared with chemically activated carbons, but adsorption of phenol was strongly suppressed in the presence of 2-chlorophenol[8].

Cite this article as: R. Subha, C. Namasivayam. "APPLICATION OF NANO POROUS CARBON FOR THE UPTAKE OF PHENOL AND 2-CHLOROPHENOL AS BISOLUTE FROM WATER." *International Conference on Systems, Science, Control, Communication, Engineering and Technology (2015)*: 187-190 Print.

Modified Langmuir model in bisolute system

In the modified Langmuir model, an interaction term η which is a characteristic of each species and depends on the concentrations of the other components[23]. The modified Langmuir isotherm is written as

$$q_{eq\,i} = \frac{Q^{o}_{i}\, b_i\, (Ceqi/\eta i)}{1 + \sum^{N}_{J=1} b_j\, (C_{eqi}/\eta_j)} \quad (1)$$

where

b_1, b_2 = individual Langmuir adsorption constants of the first and the second solute related to the affinity of the binding sites, respectively, C_{eq1}, C_{eq2} is the unadsorbed concentrations of the first and the second solute, respectively, at equilibrium (mg/L), q_{eq1}, q_{eq2} is the adsorbed quantities of the first and the second solutes per gram at equilibrium, respectively (mg/g), Q^{o}_{1}, Q^{o}_{2} is the individual Langmuir adsorption capacity of the first and the second solutes respectively and η_1, η_2 is the multicomponent Langmuir adsorption capacity of the first and the second solute, respectively. The η values of chlorophenol (η_2) is higher than that of phenol (η_1) in any combination of phenol and 2-chlorophenol. The calculated qe values of Langmuir multicomponent system agreed well with the experimental qe values in P+2-CP system. These results show that the competitive, modified Langmuir isotherm provided a more realistic description of the adsorption process in bisolute system.

4. CONCLUSIONS

The present study shows that $ZnCl_2$ activated carbon developed from an agricultural waste, coir pith, is an effective adsorbent and phenol adsorption was suppressed to a great extent in the presence of 2-CP. Adsorption of 2-CP in bisolute and single solute systems showed that 2-CP was adsorbed preferentially, but phenol was adsorbed competitively. This result was further confirmed by η_1 and η_2 values obtained from extended Langmuir model. Lower solubility, molecular weight, nature and position of the substituent group, greater electron density and lower pKa value are responsible for preferential adsorption of 2-CP over phenol. These results would be useful for designing the removal of phenol/2-chlorophenol from wastewaters in the treatment plants.

Acknowledgements

The authors are grateful to DST, Government of India for FIST which provided HPLC, FT-IR and Nanopure water system that facilitated my research work. One of the authors (R.S) gratefully acknowledges CSIR for the award of Senior Research fellowship.

References

[1] S.Kumar, M. Zafar, J.K. Prajapati, S.Kumar, S.Kannepalli, "Modeling studies on simultaneous adsorption of phenol and resorcinol onto granular activated carbon from simulated aqueous solution", J Haz Mat, vol: 185, pp:287-294, 2011.

[2] A. Hasanoglu, "Removal of phenol from wastewaters using membrane contactors: Comparative experimental analysis of emulsion protraction", Desal, vol: 309, pp:171-180, 2013.

[3] W.Oh, P.Lim, C. Seng, A.N.A Sujari, "Bioregeneration of granular activated carbon in simultaneous adsorption and biodegradation of chlorophenols", Biores Tech, vol:102,pp: 9497-9502, 2011.

[4] Y.Li, Q.Du, T.Liu, J.Sun, "Equilibrium, kinetic and thermodynamic studies on the adsorption of phenol onto grapheme", Mat Res Bull, vol:47, pp:1898-1904, 2012.

[5] WHO. Guidelines for drinking water quality, Third edition incorporating the 1st and 2nd addenda, Geneva, WHO Press, World Health Organisation, Switzerland, 2008.

[6] R.Subha, C. Namasivayam, " $ZnCl_2$ - modified activated carbon from biomass coir pith for the removal of 2-Chlorophenol by adsorption process". Bioremediation J, vol: 14, pp:1-9, 2010.

[7] J.M.Palacois-Santander, L.M Cubillana-Aguilera, M. Cocchi, A. Ulrici et al., "Multi component analysis in the wavelet domain of highly overlapped electrochemical signals: Resolution of quaternary mixtures of chlorophenols using a peg-modified Sonogel-Carbon electrode", Chem. Intel Lab Syst, vol: 12, pp: 34-38, 2007.

[8] O. Aktas, F. Cecen, "Competitive adsorption and desorption of a bi-solute mixture: effect of activated carbon type", Adsorption, vol: 13, pp:159-169, 2008.

[9] V.M.Gunko, "Competitive adsorption", Thero. Exp. Chem, vol: 43, pp:139-179, 2007.

[10]D.M.Nevskaia, E.Castillejos-Lopez, V.Munoz, Guerrereo-ruiz, "Adsorption of aromatic compounds from water by treated carbon materials", Environ Sci Technol, vol:38,pp: 5786-5796, 2004.

[11] B. Koubaissy, G. Joly, P. Manoux, " Adsorption and competitive adsorption on zeolites of nitrophenol compounds present in wastewater", Ind Eng Chem Res, vol:47, pp: 9558-9565, 2008.

[12] W.Zhang, C. Hong, B.Pan, Z.Xu, Q.Zhang,L.V. Lu, " Removal enhancement of 1-naphthol and 1-naphthylamine in single and binary aqueous phase by acid-basic interactions with polymer adsorbents" J Haz Mat,vol:158, pp: 293-299, 2008.

[13]J.H. Kim,W.S. Shin, D.I.Song, S.J. Choi, "Multi-step competitive sorption and desorption of chlorophenols in surfactant modified montmorillonite" Water Air Soil Poll, vol: 166, pp:367-380, 2005.

[14] C.Valderrama, J.I. Barios, M.Caetano, A. Farran, J.L.Cortina, "Kinetic evaluation of phenol/aniline mixtures adsorption from aqueous solutions onto activated carbon and hypercrosslinked polymeric resin (MN200)", React Funct polym, vol:70,pp:142-150, 2010.

Cite this article as: R. Subha, C. Namasivayam. "APPLICATION OF NANO POROUS CARBON FOR THE UPTAKE OF PHENOL AND 2-CHLOROPHENOL AS BISOLUTE FROM WATER." *International Conference on Systems, Science, Control, Communication, Engineering and Technology (2015)*: 187-190 Print.

[15] R. Mihalache, I. Pelanu, I.Meghea, A.Tudorache, "Competitive adsorption models of organic pollutants from bi and tri solute systems on activated carbon" J Radioanalytical Nuclear Chem, vol:229,pp:133-137, 1998.
[16] A.Garcia, L.Ferreria, A. Leitao, A.Rodrigues, "Binary adsorption of phenol and m- cresol mixtures onto a polymeric adsorbent" Adsorption, vol:5,pp:359-368, 1999.
[17] F.Pagnanelli, M.Trifoni, F.Belochini, A.Esposito, L.Toro, F.Veglio,"Equilibrium biosorption studies in single and multi-metal systems", Process Biochem, vol:37, pp:115-124, 2001.
[18] H.S.Bae, T.Yamagishi, Y.Suwa,"Evidence for degradation of 2-chlorophenol by enrichment cultures under denitrifying conditions", Microbiology, vol: 148, pp:221-227, 2002.
[19]R.Subha, C.Namasivayam, "Removal and Recovery of PCP onto low cost nano porous carbon surface: Kinetics and Isotherms", J Solid Waste tech Manage,vol:37, pp:168-178, 2011.
[20] K.Mohanty, D.Das, M.N.Biswas, "Adsorption of phenol from aqueous solutions using activated carbons prepared from Tectona grandis sawdust by $ZnCl_2$ activation", Chem Eng J, vol:115,pp: 121-131, 2005.
[21] A.Mihranyan, A.P. Llagostera, R.Karmhag, M. Stomme, R. Ek, "Moisture sorption by cellulose powders of varying crystallinity", Int J Pharmaceutics, vol:269, pp:433-442, 2009.
[22]R.Subha, C. Namasivayam, "Kinetics and isotherm studies for the adsorption of phenol using low cost micro porous $ZnCl_2$ activated coir pith carbon", Can. J Civ. Eng, vol:8,pp: 1-12, 2009.
[23] J.C.Bellot, J.S.Condoret, „Modelling of liquid chromatography equlibria. Process Biochem, vol: 28, pp: 365, 1993.

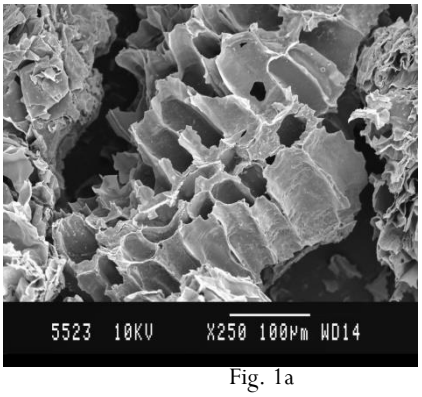

Fig. 1a

SEM Micrograph of ZnCPC before adsorption (250X)

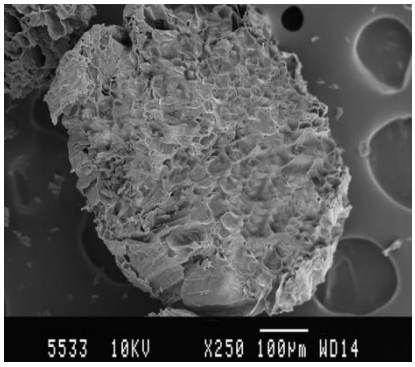

Fig. 1b

SEM Micrograph of ZnCPC after adsorption (250X)

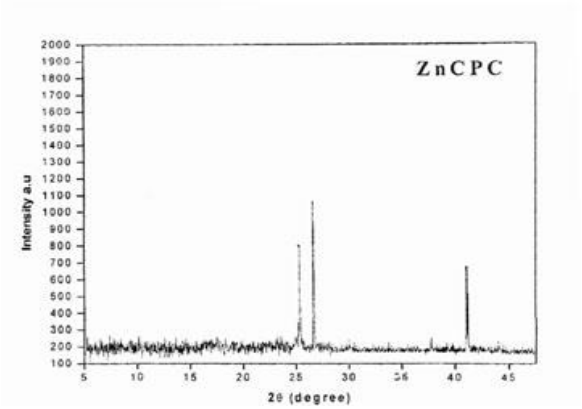

Fig. 2 XRD spectrum of unloaded adsorbent

Cite this article as: R. Subha, C. Namasivayam. "APPLICATION OF NANO POROUS CARBON FOR THE UPTAKE OF PHENOL AND 2-CHLOROPHENOL AS BISOLUTE FROM WATER." *International Conference on Systems, Science, Control, Communication, Engineering and Technology (2015)*: 187-190 Print.

International Conference on Systems, Science, Control, Communication, Engineering and Technology 2015 [ICSSCCET 2015]

ISBN	978-81-929866-1-6
Website	icssccet.org
Received	10 - July - 2015
Article ID	ICSSCCET042

VOL	01
eMail	icssccet@asdf.res.in
Accepted	31- July - 2015
eAID	ICSSCCET.2015.042

2-Dimethyl amino ethanol as a non toxic corrosion inhibitor for austenitic stainless steel 304 in 1 M HCl solution

R.Subha[1], D.Sudha[2], K.Murugan[3]
[1]Assistant Professors, Department of Chemistry
Karpagam Institute of Technology, Coimbatore

ABSTRAC: *The inhibiting action of 2-dimethyl amino ethanol (DMAE) on stainless steel type 304 grade in 1.0 M HCl solution within the temperature of 303 K and 333 K was studied using weight loss method. The inhibition efficiency was found to increase with the inhibitor concentration and decrease with temperature.. Thermodynamic calculations reveal physiochemical interactions and spontaneous adsorption mechanism.*

Keywords: Austenitic stainless steel, DMAE, Free energy, enthalpy, enthropy

1. INTRODUCTION

It is well known that the corrosion of metallic structures has a significant impact on economy, including infrastructure, transportation, utilities, production, manufacturing, and government [1]. Austenitic steels are non magnetic stainless steels that contain high levels of chromium and nickel, low levels of carbon. They have good formability and weldability, as well as excellent toughness, particularly at low or cryogenic temperatures [2]. The annual world production of the steel is approximately 400 million, and of this about 2% is stainless. Demand for stainless steel increases by 3-5% per annum with major applications in extractive industries, petrochemicals, chemical processing plants, automotive and aerospace structural alloy, construction materials, petroleum industry, marine environments, sugar industries, food industry and breweries, energy production, pulp and paper and textile industry [3]. The poor wear properties and low surface hardness make extreme limits in many cases. The surface modification is needed to decrease the coefficient of friction of substrate and increase the mechanical and tribiological properties [4, 5]. It is necessary to use acid solutions to remove undesirable scale and corrosion products from metals. This corrosion can cause serious damage to the metal and degrade its properties, thereby limiting its applications [6]. The use of inhibitors is one of the most convenient means for protection of steel corrosion in acidic solution as they can prevent metal from dissolution and consequently reduce the operation cost [7].
Organic compounds have shown good application as corrosion inhibitors for steel in acidic environments [8-17,1]. So it is necessary for the development of new approach to introduce environmentally friendly corrosion inhibitors, which can provide prolonged and even smart release of inhibiting species on demand and adequate corrosion protection is needed [18]. 2-dimethyl amino ethanol (DMAE) is a primary alcohol with a 4-carbon structure and the molecular formula is $C_4H_{11}NO$, belonging to the higher and branched chain alcohols

Cite this article as: R.Subha, D.Sudha, K.Murugan. "2-Dimethyl amino ethanol as a non toxic corrosion inhibitor for austenitic stainless steel 304 in 1 M HCl solution." *International Conference on Systems, Science, Control, Communication, Engineering and Technology (2015)*: 191-194 Print.

without any record of harm to humans and the environment. This investigation aims to assess the inhibitive effect of 2-dimethyl amino ethanol as non toxic inhibitor on the type 304 stainless steel in dilute HCl.

2. MATERIALS & METHODS

Commercially available type 304 stainlesss steel was used for all experiments of average nominal composition; 18.21 % Cr, 8.42 % Ni, 68.12 % Fe, 0.08% C, 2% Mn, 0.75 % Si, 0.045% P and 0.03% S respectively. 2-dimethyl amino ethanol (DMAE), a yellowish translucent liquid is the inhibitor used. The structural formula is shown in Fig.1. The molecular formula is $C_4H_{11}NO$, while the molar mass is 89.14 g/mol.

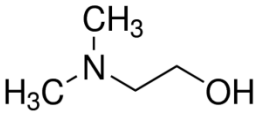

Fig.1 **Structure of 2-dimethyl amino ethanol**

DMAE was prepared in volumetric concentrations of 2.5 %, 5 %, 7.5% and 10 % per 100 ml of the acid solution respectively. Solutions of 1 M HCl of analytical grade was used as the corrosion test media.

Stainless steel specimen of the required size was used for measurement of weight loss study. The strips were mechanically polished using 1/0, 2/0, 3/0 and 4/0 emery paper and finally degreased with the organic solvent like trichloroethylene and dried before use.

Weight loss measurements were carried out by weighing the specimens in triplicate before and after immersion in 100 ml of 1 M HCl for 24, 48 and 72h at optimum temperature. Each of the test specimen was taken out every 24 h, washed with distilled water, dried and re-weighed. The corrosion rate (R), inhibition efficiency (% IE) and surface coverage (θ) were calculated from the following equations;

$$R(mpy) = \frac{534 \times W}{AxDxT} \quad (1)$$

$$\%\ IE = \frac{W_b - W_i}{W_b} \quad (2)$$

$$\Theta = \%\ IE / 100 \quad (3)$$

Where W is the weight loss in milligrams, D is the density in g/cm^2, A is the surface area in cm^2, T is the immersion time, W_b and W_i are the corrosion rates of 304 stainless steel without and with inhibitor, respectively. The same procedure was carried out at 298 K and 353 K using thermostat to study the inhibition efficiency of inhibitor. This study gives details about the rate of adsorption and activation energy.

3. Results & Discussions

3.1 Weight loss measurements

The weight loss (W), Corrosion rate(R) and the % Inhibition efficiency (IE) and surface coverage (θ) of austentic stainless steel in 1 M HCl solution without(Blank) and with different concentrations of inhibitor for 24, 48 and 72 h at optimum temperature are provided in Table 1. It obviously shows that the corrosion rate decreases with increase inhibitor concentration at optimum temperature, the % IE increases with the presence of higher concentration of inhibitor. As inhibitor concentration increases, the barrier film formed on the steel surface becomes more compact, effectively separating the specimen from aggressive anionic species within the test solution while at the same time, stifling the redox reactions associated with the corrosion process. The diffusion of Fe^{2+} and Cl^-/SO_4^{2-} is thus effectively inhibited [19]. The barrier film is strongly adsorbed through physisorption mechanism by weak van der waal's force. Effective inhibition occurred from 7.5- 10.0 % inhibitor concentration, most probably through the adsorption of the functional hydroxyl group of the inhibitor on the steel surface by the interaction of π- electrons or lone pair of electron of hetero atom with the metal [17].

3.2 Effect of temperature

The inhibition efficiency is reduced to 63.84% for 72 h at 333 K as compared to 70.26% for 72 h at 298 K. As the temperature of the inhibitor's free solution increases above 298 K, the corrosion rate of austentic steel increases and the rate in 1 M HCl solution with low concentration of inhibitor were even higher than that in the blank solution. Similarly, the rate of corrosion increases and inhibition efficiency decreases with increase in temperature above 303 K for non ionic surfactant TRITON-X-405 on ferritic stainless steel in 1 M H_2SO_4solution [1].

3.3 Activation energy

Corrosion rate increases exponentially with temperature because the hydrogen evolution decreases; therefore the dependence of a corrosion rate (R) on temperature can be expressed by the Arrhenius equation,

$$\ln R = E_a/RT + A \quad (4)$$

Cite this article as: R.Subha, D.Sudha, K.Murugan. "2-Dimethyl amino ethanol as a non toxic corrosion inhibitor for austenitic stainless steel 304 in 1 M HCl solution." *International Conference on Systems, Science, Control, Communication, Engineering and Technology (2015)*: 191-194 Print.

Where E_a represents the apparent activation energy, R is the general gas constant, T is the absolute temperature, A is the Arrhenius pre-exponential constant depending on the metal type and the electrolyte [20]. The activation energy can be calculated from the slope, by plotting the natural logarithm of the corrosion rate against 1/T. The values of apparent activation energies obtained for various concentrations of DMAE at 298 and 333 K are 11.26 , 13.98, 14.21, 14.98KJ, respectively. The greater increase for the activation energy in the presence of the inhibitor indicates physisorption or weak chemical bonding between the inhibitor molecules and the metal surface. Mazhar et al. [21]explained that the increase in the activation energy with respect to uninhibited solution was due to diffusion of metal ions through the protective film on the metal surface.

3.5 Thermodynamic parameters

Free energy of adsorption (ΔG) can be calculated using the equation,

$$\Delta G = RT \ln(C_{solvent} K) \quad (5)$$

$$\text{ie } K = \theta / C(1-\theta) \quad (6)$$

Where R is the universal gas constant, $C_{solvent}$ is the molar concentration of the solvent, which in the case of water is 55.5 mol/L, C is the concentration of the inhibitor and θ, the degree of surface coverage of the metal surface. The ΔG values calculated from equation (5) were found to be -4.98 KJ and -3.55 KJ at 298 and 333 K respectively, which ensures the spontaneity of the adsorption process. The standard adsorption heat (ΔH) and standard adsorption entropy (ΔS) were calculated according to van't Hoff equations. The plot of ln K versus 1/T gives a straight line with a slope of ($-\Delta H/R$) and intercept. The ΔH and ΔS values calculated were found to be -47.34 KJ and -19.32 KJ respectively. The negative value of ΔH and ΔS indicates that the adsorption of the non toxic inhibitor on the steel surface in 1.0 M HCl solution is an exothermic process and accompanied by decrease in entropy. Similarly, the adsorption of TRITON-X-405 on the steel surface throughout the process showed that the inhibitor molecules were orderly adsorbed onto the surface, $\Delta S < 0$ and the diffusion of metal ions through the protective film on the metal surface is rate controlling [1].

4. Conclusions

Experimental analysis of the corrosion inhibition properties of 2-dimethyl amino ethanol showed that the compound to be an efficient inhibitor in the acidic environment at 298 K and 333 K respectively, giving a maximum inhibition efficiency from weight loss analysis. The maximum inhibition efficiency of DMAE on stainless steel was found to be 70 % and 63.6 % at 298 and 333 K respectively. Inhibition efficiency values increased with increase in inhibitor concentration and decrease with temperature. Thermodynamic variables of adsorption deduced revealed a physisorption with the steel surface and spontaneous adsorption of DMAE.

Acknowledgement

The authors are grateful to the Management, Principal and Head of department, Karpagam Institute of technology for their continuous support and providing us lab facilities to carry out the research work

References

[1] R.F.Godec, M.G.Palvoic and M.V.Tomic, "Effect of temperature on the corrosion inhibition of non ionic surfactant TRITON- X 405 on ferritic stainless steel in 1.0M H_2SO_4", Industrial Engineering and Chemical Research, Vol: 51, pg:274-284, 2012.

[2] B.Terence, Austenitic stainless, www.metals.about.com. Retrieved on 3 April 2014.

[3] L.Bela, Stainless steel and their properties, www. Outokumpu.com. Retrieved on 3 April 2014.

[4] S. Baradaran, W.J.Basirun, E.Zalnezhad, M.Hamdi, A.D.Sarhan, Y.Alias, "Fabrication and deformation behavior of multilayer Al2O3/Ti/TiO2 nano tube arrays", J Mech. beha and biomed. material, Vol:20,pp: 272-282, 2013.

[5] E.Zalnezhad, S.Baradaran, A.R. Bushora, A.D.Sarhan, "Mechanical property enhancement of Ti-6Al-4V by multilayer thin solid film Ti/TiO2 nanotubular array coating for biomedical application", Metal. Mat. trans, Vol:45, pp: 785-797, 2014.

[6] R.Yildiz, "An electrochemical and theoretical evaluation of 4,6-diamino-2-pyrimidinethiol as a corrosion inhibitor for mild steel in HCl solutions", Corr sci, Vol: 90, pp: 544-555, 2015.

[7] M.M.A. El-Sukkary, E.A. Soliman, D.A. Ismail, S.M. El Rayes, M.A. Saad, J. Tenside, Surface determination, Vol:48,pp:, 82-86, 2011.

[8] F.C.Giacomelli, C.Giacomelli, M.F. Amadori, V.Schmidt, A.Spinelli, "Inhibitor effect of succinic acid on the corrosion resistance of mild steel: electrochemical, gravemetric and optical microscopic studies", Mat Chem phy, Vol:83, pp:, 124, 2014.

[9] A.K.Satapathy, G. Gunasekaran, S.C.Sahoo, K.Amit, P.V.Rodrigues, "Corrosion inhibition by Justicia gendarussa plant extract in hydrochloric acid solution", Corr Sci, Vol: 51, pp: 2848-2850, 2009.

[10] X.H.Li, S.D.Deng, H.Fu, "Inhibition by Jasminum nudiflorum lindl.leaves extract of the corrosion of cold rolled steel in hydrochloric acid solution", J App Electrochem, Vol:40, pp: 1641-1647, 2010.

[11] P.Lima-Neto, A.P. Araujo, W.S.Araujo, A.N.Correia, Progress in organic coatings, Progress organic coatings, Vol:62,pp: 344-346, 2008.

[12] J.Mathiyamsu, I.C.Nebru, P.Subramania, N.Palaniswamy, N.S.Rengaswamy, 2001

[13] N.Ochao, F.Moran, N.Pebre, "The synergistic effect between phosphonocarboxylic acid salts and fatty amines for the corrosion protection of a carbon steel", J App Electrochem, vol:34, pp: 487-489, 2009.

[14]E.E. Oguzie, "Influence of halide ions on the inhibitive effect of congo red dye on the corrosion of mid steel in sulphuric acid solution", Mat Chem Phy, vol:87,pp:212-215, 2004.

Cite this article as: R.Subha, D.Sudha, K.Murugan. "2-Dimethyl amino ethanol as a non toxic corrosion inhibitor for austenitic stainless steel 304 in 1 M HCl solution." *International Conference on Systems, Science, Control, Communication, Engineering and Technology (2015)*: 191-194 Print.

[15]M.N.Shalaby, M.M.Osman, "Synergistic inhibition of anionic and non ionic surfactants on corrosion of mild steel in acidic solution", Anticorr mat, vol: 48,pp: 309-312, 2001.
[16] E.E.Ebenso, "Synergistic effect of halide ions on the corrosion inhibition of aluminium in H_2SO_4 using 2-acetylphenothiazine", Mat Chem phy,Vol: 79,pp: 58, 2003.
[17] R.T.Loto, C.C.Loto, A.P.I. Popoola and T.I Fedotova," Inhibition effect of butan-1-ol on the corrosion behavior of austenitic stainless steel type 3040 in dilute sulphuric acid", Arab J Chem in press, 2014.
[18] M.L. Zheludkevich, D.G. Shchukin, A. Kiryl, Y.H. Mohwald and M.S.S. Ferreria, "Anticorrosion coatings with self healing effect base on nano containers impregnated with corrosion inhibitor", Chem Mat,Vol: 19, pp: 402-411, 2007.
[19] X.Zheng, S.Zhang, W.Li, M.Gong, L.Yin, "Experiemental and theoretical studies of two imidazolium-based ionic liquids as inhibitors for mild steel in sulfuric acid solution" Corrosion science, in press 2015.
[20] N.A.Negum, A.M. Al Sabagh, M.A. Mighaded, H.M. Abdel Bary, H.M. El-Din, "Effectiveness of some diquaternary ammonium surfactants as corrosion inhibitor for carbon steel in 0.5 M HCl solution", Corr Sci, Vol:52,pp: 2122, 2010.
[21] A.A. Mazhar, S.T. Arab, E.A. Noor, "Influence of N-hetero cyclic compounds on the corrosion of Al-Si alloy in hydrochloric acid-effect of pH and temperature", Cor Sci,Vol:58,pp: , 192, 2002.
[22] M.Behopur, S.M. Ghoreishi, N.Soltani, M.Salavati-Niasari, M.Hamadanian, A.Gandomi, Cor Sci, Vol:50,pp: 2172, 2008.

Table 1 Corrosion parameters obtained from weight loss measurements for stainless steel 304 in 1M HCl solution without and with different concentrations of inhibitors for different time intervals at 298 K and 333 K

Time (h)	Concentration (mM)	298 K				333 K			
		Weight loss (mg)	Corrosion rate (mY)	% IE	θ	Weight loss (mg)	Corrosion rate (mY)	% IE	θ
24	Blank	7.186	110.62	-	-	9.346	143.87	-	-
	2.5	5.912	91.01	17.73	0.1773	7.234	111.36	22.60	0.2260
	5	3.793	58.34	35.84	0.3584	5.486	84.85	41.30	0.4130
	7.5	2.056	31.65	47.79	0.4779	4.007	61.68	44.61	0.4461
	10	1.386	16.72	47.18	0.4718	2.104	32.39	61.65	0.6165
48	Blank	11.237	86.49	-	-	13.189	101.51	-	-
	2.5	7.316	56.31	21.38	0.2138	11.567	89.03	12.30	0.1230
	5	5.014	38.59	55.38	0.5538	8.986	69.16	37.81	0.3781
	7.5	2.913	22.44	60.18	0.6018	5.032	38.73	56.50	0.5650
	10	1.905	14.66	62.01	0.6201	2.989	23.01	66.74	0.6674
72	Blank	15.187	77.93	-	-	17.487	89.73	-	-
	2.5	11.463	58.82	24.52	0.2452	14.984	76.89	14.31	0.1431
	5	8.106	41.59	46.63	0.4663	11.087	56.89	36.60	0.3660
	7.5	3.751	19.25	67.28	0.6728	8.432	43.27	43.73	0.4373
	10	2.195	12.37	70.26	0.7026	4.009	20.57	63.84	0.6384

Cite this article as: R.Subha, D.Sudha, K.Murugan. "2-Dimethyl amino ethanol as a non toxic corrosion inhibitor for austenitic stainless steel 304 in 1 M HCl solution." *International Conference on Systems, Science, Control, Communication, Engineering and Technology (2015)*: 191-194 Print.

International Conference on Systems, Science, Control, Communication, Engineering and Technology 2015 [ICSSCCET 2015]

ISBN	978-81-929866-1-6	**VOL**	01
Website	icssccet.org	**eMail**	icssccet@asdf.res.in
Received	10 - July - 2015	**Accepted**	31- July - 2015
Article ID	ICSSCCET043	**eAID**	ICSSCCET.2015.043

Removal of mercury from aqueous solution- Review on current status and development

D.Anitha[1], O.A.Sridevi[2], R.Subha[3]
[1,2,3] Assistant Professor, Department of Chemistry,
Karpagam Institute of Technology, Coimbatore

ABSTRACT: *Environmental pollution due to heavy metals like mercury is of serious concern throughout the world. Due to anthropogenic activities, the concentration of mercury has increased in the environment. Though many methods are available for mercury removal, adsorption is considered as simple, economical and versatile method. In this paper the efficiency of mercury removal from aqueous solution using agricultural waste, polymers and nano material were reviewed.*

Keywords: Heavy metal; Modification; Adsorption; Isotherm

1. INTRODUCTION

Heavy metals are abundant in our drinking water, air and soil because they are present in every area of modern consumerism like construction materials, cosmetics, medicines, processed foods and personal care products [1]. Natural inputs of mercury to the environment are related to weathering of mercuriferous area, the degassing from surface water and from the earth's crust through volcanic eruptions, naturally caused forest fires, and biogenic emissions [2]. Mercury is a pervasive contaminant that is highly toxic and is readily accumulated by organisms [3,4]. Mercury may enter a human body by inhalation of mercury vapor as Hg^0, drinking water as inorganic mercury, Hg^{2+}, and/or by the consumption of fish and fish products as methyl mercury, CH_3Hg^+ in the diet [5,6]. In small quantities, certain heavy metals are nutritionally essentially for a healthy life, but in large amounts they may cause acute or chronic toxicity (poisoning). The absorption of this hazardous substance into the bloodstream, distribution to the entire tissues and bioaccumulation in the receptive sites leads to adverse effects, such as potent neurotoxicity, blood vessel congestion and kidney damages [7].

Various methods exist for the removal of mercury from water which include chemical precipitation/ coagulation, membrane technology, electrolytic reduction, ion exchange and adsorption [8, 9].Among various available methods for the removal of Hg, adsorption has been shown to be an economically feasible and easily applicable alternative using various adsorbents [10-12]. The other methods are not to be effective and least possible for treatment of mercury form water. More number of studies on mercury removal has been reported in the literature. In the present work, we have reviewed the recent articles on the mercury removal from aqueous solution by considering the effect of various parameters such as pH, temperature, metal ion concentration, contact time, and

Cite this article as: D.Anitha, O.A.Sridevi, R.Subha. "Removal of mercury from aqueous solution- Review on current status and development." *International Conference on Systems, Science, Control, Communication, Engineering and Technology (2015)*: 195-198. Print.

adsorbent dosage on mercury uptake. These factors are of the utmost significance, as any change in these parameters may considerably change the mercury removal efficiency of an adsorbent.

2. GENERAL OBSERVATIONS

Most of the studies have been performed in batch mode operation. Synthetic stock solutions were prepared by dissolving mercury compounds (mercury nitrate, mercury chloride etc) for adsorption studies. Adsorption and kinetic plots were noted. Few authors have performed thermodynamic and column studies also.

2.1 Effect of temperature

Temperature plays a significant role in the uptake of mercury ion from the surface at ambient temperatures. Depending upon the adsorption mechanism, the rate may either increase or decrease with temperature [13]. Xincheng et al., observed a significant decline in adsorption with increasing temperature indicating that the process is endothermic [18]. Rajamohan, observed an increase in mercury adsorption capacity with increase in temperature indicating the process to be exothermic [20].

2.2 Effect of pH

Adsorption of mercury is very sensitive to the pH. The adsorption capacities were found to be low at low pH values and increased with increase in pH. The mechanism of adsorption can be explained based on pH. The mercury ions were bound to the adsorbent surfaces mainly by the process of the ion exchange and physico-chemical adsorption as the ionic mobility plays an important role. The mobility of ions and rate of interactions between oppositively charged ions and adsorbent surfaces are more pronounced in dilute solutions. Anurudhin et al observed the percentage removal to increase gradually with increasing pH and reach an optimum value of 6.The solution pH affects the surface charge of the adsorbent, the degree of ionization and the speciation of the surface functional group [16].

2.3 Effect of Contact time and initial metal ion concentration

The initial concentration of metal ions provides an important driving force to overcome all mass transfer resistances of the metal ion between the aqueous and solid phases [28]. Equilibrium time is one of the important parameters for selecting a wastewater treatment system [29]. Equlibrium concentration increases with increase in adsorbate concentration due to saturation of sorption sites on the adsorbent [26]. Anirudhan et al carried out adsorption experiments at concentrations from 25 to 100 mg/L and found an increase in adsorption of metal ion with increase in contact time of 3 hr [16]. Syed and Ganesan indicate that the increase in initial concentration of Hg(II) ions resulted in a reduction in the percentage removal using Eucalyptus globules bark as adsorbent It was observed that, the percentage removal of Hg (II) ions decreases exponentially with the increase in the initial concentration of Hg(II) ions. This may be due to reduction in immediate solute adsorption, owing to the lack of available active sites on the adsorbents surface compared to the relatively large number of active sites required for high initial concentration of Hg (II) ions [25].

2.4 Effect of Adsorbent Dose

Dosage of adsorbent is a key parameter to control both availability and accessibility of adsorption sites [30].Adsorption has been found increasing with the increase in dose of adsorbent. But with the higher dose of adsorbent in the solution, the mobility of the ion reduces and there results a decrease in the rate of adsorption. Syed and Ganesan found an increase in removal of Hg (II) with increase in dose of adsorbent due to increase in availability of active sites [25].

2.5 Adsorption and Kinetics equilibrium

The equilibrium relationships between adsorbent and adsorbate are best explained by adsorption isotherms [31].Several equilibrium isotherm models were employed in order to study the nature of adsorption process. These include two parameter isotherms such as the Langmuir, Freundlich, Temkin, Dubinin-Radushkevich and three parameter isotherms such as the Sips and Redlich Peterson respectively.

The adsorption kinetics is significant in the treatment of wastewater, as it provides valuable insights into the reaction pathways and rate of reactions [32]. These models include the pseudo-first order, pseudo-second order, Elovich, intraparticle diffusion and Baughman's plot. The adsorption capacities, isotherm and kinetics of various adsorbents were given in Table 1.

Conclusion

The present review has established that adsorption offers a great opportunity for a cheap and highly effective process for the removal of mercury (II) ions from aqueous solution. Experimental parameters like temperature, solution pH ,metal ion concentration, adsorbant dose, contact time and adsorption kinetics influence adsorption process. On the basis of evidences presented in this review there exist a significant potential for future research in utilizing the adsorbent in industries, agriculture as well as for domestic puropose.

Acknowledgement

The authors are grateful to the Management, Principal and Head of department Karpagam Institute of technology for their continuous support and providing us facilities to carry out the research work.

References

[1] A.A.Abia, O.B Didi and E.D Asuquo "Modelling of Cd^{2+} sorption kinetics from aqueous solutions onto some thiolated agricultural waste adsorbents", J. Appl Sci, Vol: 6, pg: 2549–2556, 2006.

{2] F.M.M.Morel, A.M.L.Kraepiel, M.Amyot, "The chemical cycle and bioaccumulation of mercury", Annu. Rev. Ecol. Syst Vol: 29, pg: 543–566, 1998

Cite this article as: D.Anitha, O.A.Sridevi, R.Subha. "Removal of mercury from aqueous solution- Review on current status and development." *International Conference on Systems, Science, Control, Communication, Engineering and Technology (2015)*: 195-198. Print.

[[3] M.Ghaedi, M.R.Fathi, A.Shokrollahi, F.Shajarat, "Highly selective and sensitive preconcentration of mercury ion and determination by cold vapor atomic absorption spectroscopy", Anal. Lett. Vol: 39, pg: 1171–1185, 2006.
[4] A.Shokrollahi, M.Ghaedi, M.Shamsipur, "Highly selective transport of mercury(II) ion through a bulk liquid membrane", Quim. Nova Vol: 32 ,pg: 153–157, 2009.
[5] H.Seiler,H.Sigel, "Handbook on Metals in Clinic and Analytical Chemistry,Marcel Dekker", pg: New York, 1994.
[6] J.C.A.Wuilloud, R.G.Wuilloud, R.A.Olsina, L.D.Martinez, "Separation and preconcentration of inorganic and organomercury species in water samples using a selective reagent and an anion exchange resin and determination by flow injection-cold vapor atomic absorption spectrometry", J. Anal. Atom. Spectrom. Vol: 17, pg: 389–394, 2002.
[7] K.Kidd, K.Batchelar, Mercury, in: C.Wood, A.P.Farrell, C.J Brauner (Eds.), "Homeostasis and Toxicology of Non-Essential Metals", Elsevier Ltd., US, pg: 237–295, 2012.
[8] T.A.Kurniawan,G.Y.S.Chan,W.H.Lo,S.Babel, "Physicochemical treatment techniques for wastewater laden with heavy metals",Chem Eng J ,Vol: 118 (1–2), pg: 83–98, 2006.
[9] Y.H.Wang, S.H.Lin, R.S.Juang "Removal of heavy metal ions from aqueous solutions using various low-cost adsorbents", J Hazard Mater Vol: 102 (2–3), pg: 291–302 2003.
[10] C.P.Huang "Chemical interactions between inorganic and activated carbon. In: Cheremisinoff PN, Ellerbush F (eds) Carbon adsorption handbook. Ann Arbor Science, Ann Arbor,pg: 281–329,1978.
[11] Koshima H, Onishi H "Collection of mercury from artificial sea-water with activated carbon".. Talanta Vol: 27: pg: 795–799, 1980.
[12] X.Ma, K.S.Subramanian, C.L.Chakrabarti, R.Guo, J.Cheng, Y.Lu, W.F.Pickering "Removal of trace mercury (II) from drinking water: sorption by granular activated carbon". J Environ Sci Health Vol: 27: pg: 1389–1404, 1992.
[13] W. R. Knooke and L. H .Hemphin "Mercury sorption by waste rubber". Wat. Res., Vol: 18, pg: 175 1981.
[14] M. Zabihia, A. Ahmadpourb,*, A. Haghighi Asla,"Removal of mercury from water by carbonaceous sorbents derived from walnutshell".J Hazard Mater Vol: 167, pg: 230–236, 2009.
[15] Mustafa Tuzena, Ahmet Sari a, Durali Mendila, Mustafa Soylakb,* "Biosorptive removal of mercury(II) from aqueous solution using lichen (Xanthoparmelia conspersa) biomass: Kinetic and equilibrium studies",J Hazard Mater Vol: 169 , pg: 263–270 ,2009
[16] T. S. Anirudhan*, S. S. Sreekumari, "Adsorptive removal of heavy metal ions from industrial effluents using activated carbon derived from waste coconut buttons".,J Environ Sci , Vol: 23(12), pg: 1989–1998,2011.
[17] Dilip Kumar Mondal , Barun Kumar Nandi , M.K. Purkait, "Removal of mercury (II) from aqueous solution using bamboo leaf powder:Equilibrium, thermodynamic and kinetic studies". Journal of Environmental Chemical Engineering Vol: 1, pg: 891–898,2013.
[18] Xincheng Lu, Jianchun Jiang , Kang Sun, Jinbiao Wang, Yanping Zhang, "Influence of the pore structure and surface chemical properties of activated carbon on the adsorption of mercury from aqueous solutions".. Mar. Pollut. Bull. 2013.
[19] Zahra Aghajani1, Mohamad-Reza Zand-Monfared 1,Somaye Bahmani-Androod, "Removal of lead (II) and mercury (II) from aqueous solutions and waste water using pistachio soft shell as agricultural by-products ", J. Bio. & Env. Sci. pg: 170-176, 2014.
[20] N. Rajamohan,"Biosorption of Mercury onto Protonated Pistachio Hull Wastes – Effect of Variables and Kinetic Experiments". International J Chem Eng App, Vol: 5, pg: 5, 2014.
[21] Renjie Li, Lifen Liu, Fenglin Yang, "Removal of aqueous Hg(II) and Cr(VI) using phytic acid dopedpolyaniline/cellulose acetate composite membrane". J Hazard Mater Vol: 280, pg: 20–30, 2014.
[22] Kunawoot Jainae , Nipaka Sukpirom , Saowarux Fuangswasdi , Fuangfa Unob, "Adsorption of Hg(II) from aqueous solutions by thiol-functionalized polymer-coated magnetic particles ",J. Ind. and Eng. Chem., In Press, 2014.
[23] Sh. Mokhtari, H. Faghihian, "Modification of activated carbon by 2,6-diaminopyridine for separation of Hg^{2+} from aqueous solutions J. Environ. Chem. Eng, In Press, 2015.
[24] M. Arshadi ",Manganese chloride nanoparticles: A practical adsorbentfor the sequestration of Hg(II) ions from aqueous solution". Chem.Eng.J, Vol: 259, pg: 170–182, 2015.
[25] M. Syed Meeral, T.K. Ganesan, " Removal of Mercury Ions from Aqueous Solutions using Eucalyptus Globules Bark Carbon – A Low Cost Material Alternate to Commercial Activated Carbon",J Advanced Chem Sci Vol: 1(3), pg: 89–92 2015.
[26] Akbar Esmaeili, Betsabe Saremnia, Mona Kalantari, "Removal of mercury (II) from aqueous solutions by biosorption on the biomass of Sargassum glaucescens and Gracilaria corticata".Arabian J Chem, Vol: 8, pg: 506–511, 2015.
[27] Limei Cui , Xiaoyao Guo , Qin Wei , Yaoguang Wang , Liang Gao , Liangguo Yan , Tao Yan , Bin Du ,"Removal of mercury and methylene blue from aqueous solution byxanthate functionalized magnetic graphene oxide: Sorption kinetic and uptake mechanism". J. Colloid Interface Sci., Vol: 439 , pg: 112–120,2015.
[28] Malkoc, E., J. Hazard. Mater, Vol: 142, pg: 219, 2007
[29] Abdel-Ghani N, Hefny M, El-Chaghaby G. "Removal of lead from aqueous solution using low cost abundantly available adsorbents " ,Vol: 4:, pg: 67.73,2007.
[30] Li F., Du P. and Zhang S. "Preparation of silica-supported porous sorbent for heavy metal ions removal in wastewater treatment by organic-inorganic hybridization combined with sucrose and polyethylene glycol imprinting". Anal. Chim. Acta, Vol: 585, pg: 211-218 (2007).
[31] Mittal A, Mittal J, Malviya A, Kaur D, Gupta VK. "Adsorption of hazardous dye crystal violet from wastewater by waste materials". J.Colloid Interface Sci 2010; Vol: 343, pg: 463.73.

Cite this article as: D.Anitha, O.A.Sridevi, R.Subha. "Removal of mercury from aqueous solution- Review on current status and development." *International Conference on Systems, Science, Control, Communication, Engineering and Technology (2015)*: 195-198. Print.

[32] V.K.Gupta, A.Rastogi, A.Nayak "Biosorption of nickel onto treated alga(Oedogonium hatei): Application of isotherm and kinetic models". J Colloid Interface Sci; Vol: 34, pg: 533.9, 2010.

Table 1 Removal of mercury from aqueous solution using agro waste, polymers and nano material from selected literature.

Adsobent	Activation	Q_{max} ($mg\,g^{-1}$)	pH	Isotherm model	Kinetics studied	Reference
Wal nut	Zinc chloride	151.51	2	L,F, Langergren	Pseudo first order, Second order	Zabihi et al. (2009) [14]
Bio masslichen (*Xanthoparmelia conspersa)*	Un Modified	82.5	6	L,F	Pseudo first order, Pseudo second order	MustafaTuzen et al. |(20009)[15]
Coconut buttons	Acid activation(H_2SO_4)	41.83	7	L,F	Pseudo first order, ,Second order	Anirudhan et al. (2011) [16]
Bamboo Leaf Triton X-100 Modified SDS Modified	Surfactant modification	 27.1 28.1 31.05	 8	L,F,Temkin Langergren	Pseudo first order, Second order, Elovich	Dilip Kumar Mondal et al. (2013) [17]
Coconut	H_2O_2	5.236		L,F, Langergren	First order, Second, order, Pseudo second order	Xincheng et al. (2013) [18]
Pistachio shell	Un Modified	2.299	6	L,F	Second order	Zahar Aghajani et al.(2014) [19]
Pistachio Hulls	Acid activation(HCl)	113.64	7		Pseudo second order, Intra particle diffusion	Rajamohan et al. (2014) [20]
Polyaniline/ cellulose acetate composite	Chemical polymerization	280.11	5	L	Pseudo first order, Second order	Renjie Li et al .(2014)[21]
Polymer	polystyrene coated $CoFe_2O_4$ modified with 2-(3-(2-aminoethylthio)propylthio)ethanamine (AEPE-PS-MPs)	-	7-8	-	Pseudo first,order, Second order	Kunawoot Jainae et al. (2014)[22]
Pine Cone	chemically activated by H_3PO_4 and then modified with 2,6-diaminopyridine.	384.62 mg/g	1.5	L,F	Pseudo first, order, second order	Mokhtari et al. (2015)[23]
Manganese chloride nanoparticle	Sol gel	311	6	L,F	Pseudo first order, Second order, Intra-particle diffusion	Arshadi et al. (2015)[24]
Eucalyptus globules bark	Acid activation (HNO_3)	4.014	7	L,F	First order, Intra particle diffusion	Syed Meera et al. (2015) [25]
Bio mass S. glaucescens G. corticata,	Un Modified	 147.05 -4.71	 5 7	L,F	First,Second order	AkbarEsmaeili et al. (2015) [26]
Graphite	Hummer modification	181.8	7	L,F. Henry, Dubinin-Radshkevich,	Pseudo first Second,order, Elovich,Bangham	Limei Cui et al. (2015)[27]

L,Langmuir;F,Friendlich

Cite this article as: D.Anitha, O.A.Sridevi, R.Subha. "Removal of mercury from aqueous solution- Review on current status and development." *International Conference on Systems, Science, Control, Communication, Engineering and Technology (2015)*: 195-198. Print.

International Conference on Systems, Science, Control, Communication, Engineering and Technology 2015 [ICSSCCET 2015]

ISBN	978-81-929866-1-6	**VOL**	01
Website	icssccet.org	**eMail**	icssccet@asdf.res.in
Received	10 - July - 2015	**Accepted**	31- July - 2015
Article ID	ICSSCCET044	**eAID**	ICSSCCET.2015.044

Treatment methods for the removal of phenol from water- A Review

R. Subha[1], O.A.Sridevi[2], D.Anitha[3], D.Sudha[4]
[1, 2, 3, 4] Assistant Professors, Department of Chemistry,
Karpagam Institute of Technology, Coimbatore

ABSTRACT: *In recent years, there has been an enormous amount of research and development in the area of removal of phenol by various physio-chemical methods due to their carcinogenic nature and pungent odour. The MOEF has set a maximum concentration level of 1 mg/L of phenol in industrial effluents for safe discharge into surface waters, the WHO recommends a permissible phenolic concentration of 0.001 mg/L in potable water. Recent findings suggested that advances in nanotechnology and nano structured materials have allowed the modification of existing adsorbents which increase the potential of these technologies. Among various methods, adsorption is effective method due to simplicity, less economic and easy design.*

Key words: Phenol, Physio-chemical methods, Adsorption

1. INTRODUCTION

Water pollution by organic chemicals is a major problem over decades. The removal of organic contaminants from ground water or separation of contaminants present in polluted water has become a major focus of research and policy debate [1]. The presence of harmful organic compound such as phenols and their derivatives in water supplies and from industrial effluents is an ever increasing problem for the global concern[2]. Total phenol concentration in the wastewater of a typical Indian refinery processing 5.0 million tonnes of crude per year is around 135 mg/L and the discharge rate of wastewaters varies from 125 to 250 m^3 with pH being in the range of 8.8-9.4[3]. The ministry of environment and forests (MOEF), Government of India and EPA, United states have listed phenol and phenolic compounds on the priority pollutants list [4]. The MOEF has set a maximum concentration level of 1 mg/L of phenol in industrial effluents for safe discharge into surface waters, the WHO recommends a permissible phenolic concentration of 0.001 mg/L in potable water [3,5]. The major sources containing phenols are the wastewaters from processing, manufacturing industries engaged in oil refining, coal tar processing, petrochemical production, coke oven by products, plastic industry, textile processing, leather processing, insecticides production, manufacture of dyes and dyeing, glass production, etc[6]. Removal of phenol from industrial effluents is an important and dynamic area of research as well as being an important challenge, because environmental laws and regulations governing safe discharge levels are becoming increasingly stringent [7]. Several technologies including advance oxidation processes like Fenton, photo fenton, ozone oxidation, sono photo fenton and photo catalytic oxidation[8], membrane filtration [9], biological treatment [10], photocatalytic degradation [11], nanofiltration and adsorption[12]. Over the last decades, advances in nanotechnology and nanostructured materials have allowed the modification of existing adsorbents which increase the potential of these technologies [13]. This paper aims to review and summarize the various physiochemical methods for the treatment of phenol from water. Recent research on nano composites for improving phenol removal in water by means of metal, non metal and ion doping is also highlighted in this review.

Cite this article as: R. Subha, O.A.Sridevi, D.Anitha, D.Sudha. "Treatment methods for the removal of phenol from water- A Review." *International Conference on Systems, Science, Control, Communication, Engineering and Technology (2015)*: 199-203. Print.

2. TREATMENT METHODS

The fate of phenols in the environment and their removal from aqueous media is complicated by their low solubility, ability to ionize, low vapor pressure and tendency to undergo oxidation and oxidative polymerization with humic acid and fulvic acid-type products. The recent awareness of the toxic organic substances in wastewaters has generated interest in establishing effective treatment technologies.

A. Membrane filtration

B.

(i) Reverse osmosis

Separation methods for phenols which involve membranes are energy saving and can operate at room temperature. The separation of organic solutes from aqueous solutions by reverse osmosis has attracted attention, because of its energy saving nature. Typical operating pressures are in the range 15–50 bar, depending on the application. Reverse osmosis rejects monovalent ions and organics of molecular weight greater than about 50 (membrane pore sizes are less than 2 nm). The most common application of reverse osmosis is desalination of brackish water and seawater [14]. The rejection data of phenol using a commercial thin film composite polyamide reverse osmosis membrane are analyzed with the help of the combined film theory–solution–diffusion (CFSD) model and the combined film theory- Spiegler-Kedem. Although both the models can represent the experimental data available, the combined film theory- Spiegler-Kedem model predicted the rejection more accurately (max error ± 3%) than combined film theory–solution–diffusion (max error ± 10 %) model in phenol-water system. The $R_{o,max}$ predicted from both models are different, but there was no experimental verification as to which is more accurate. This analysis may be used to characterize reverse osmosis and nano filtration membranes[14].

(ii) Ultrafiltration

Ultrafiltration is similar in principle to reverse osmosis, but the membranes have much larger pore sizes (typically 0.002–0.03 mm) and operate at lower pressures. Ultrafiltration membranes reject organic molecules of molecular weight above 800 and usually operate at pressures less than 5 bar. The effectiveness of Membrane Ultra Filtration in removing organic compounds from aqueous stream owes to the fact that surfactant micelles containing these contaminants are too large to pass through the pores of the ultra filter [15,16,17] . Zeng et al. developed a micellar enhanced ultrafiltration of phenol in synthetic wastewater using two polysulfone spiral membranes of 6- and 10-kDa molecular weight cut–off and cetylpyridinium chloride as cationic surfactant. Polysulfone membranes could adsorb free phenol so that the concentration of permeate phenol was lower than that of free phenol. It was found that the phenol concentration of the feed, the permeate and the retentate cannot meet the material balance. The retenate phenol concentration kept increasing, and then decreased slightly with the increase of the feed cetylpyridinium chloride concentration [18].

(iii) Nanofiltration

Nanofiltration uses a membrane with properties between those of reverse osmosis and ultrafiltration membranes; pore sizes are typically 1-100 nm. Nanofiltration membranes allow monovalent ions such as sodium or potassium to pass but reject a high proportion of divalent ions such as calcium and magnesium and organic molecules of molecular weight greater than 200. Operating pressures are typically about 5 bar. Nanofiltration may be effective for the removal of color and organic compounds. Bodalo et al. studied the removal of phenol from aqueous solutions by nanofiltration using three experimental conditions and different membranes (NF-97, NF-99 and DSS-HR98PP). Three experimental conditions were carried out with different operating pressures: 10, 15 and 20 x 10^5 N/m^2, feed flow was kept constant at 2.78 x 10^{-5} m^3/s, pH=8 and T= 25°C. For each pressure feed phenol concentration was varied between 50 and 200 x 10^{-3} x kg/m^3. The different percentages rejection obtained between the nanofiltration membranes with feed phenol concentration variation can be attributed to the molecular characteristic of organic compounds such as acidity, solubility, ability to hydrogen bonding, etc. For the membrane NF-99, maximum value of water flux was obtained at pH 7. For membranes NF-97 and DSS-HR98PP the pH variation did not have a clear effect on the rejection percentages and solvent flux obtained[19].

B. Solvent extraction

Solvent extraction is the most often used technique to recover phenols from various aqueous effluents[20]. In membrane solvent extraction (MSE), there are two main kinds of membranes used: porous and nonporous. The solute within the membrane is transported from one side to the other side by a driving force, such as chemical potential differences across the membrane. Among porous membranes, microfiltration membranes have widely been applied for MSE process. Microfiltration membranes have pore sizes in the range of 0.1 to 10 microns, and so offer relatively low mass transfer resistance. Yang et al. developed a phenol removal process for the coal gasification wastewater. Based on the theoretical study and experiments, methyl isobutyl ketone was selected as the extracting solvent for the treatment of the coal gasification wastewater containing 5000 mg/L phenols and 20,000 mg/L COD. The results of the trial plant showed that more than 93% of the phenol in the wastewater was recovered, which was a by-product with economic benefit[21].

C. Ion exchange process

Cite this article as: R. Subha, O.A.Sridevi, D.Anitha, D.Sudha. "Treatment methods for the removal of phenol from water- A Review." *International Conference on Systems, Science, Control, Communication, Engineering and Technology (2015)*: 199-203. Print.

Ion exchange is a unit process in which ions of a given species are displaced from an insoluble exchange material by ions of a different species in solution. Ion exchange processes can be operated in batch mode or continuous mode. In a batch mode process, the resin is stirred with the water to be treated in a reactor until the reaction is complete. The spent resin is removed by settling, regenerated and reused. In a continuous process, the exchange material is placed in a bed of a packed column and the water to be treated is passed through it. When the resin is exhausted, the column is back-washed to remove trapped ions and the ion exchange resin is regenerated.

Lu et al. explored the proton exchange between phenol and ammonia or ammines based on density functional theory to show intracomplex proton exchange mechanism. The phenol-ammonia (parent) system possesses a barrier height (34.6 kcal/mol) of proton exchange. The results showed that the phenol tends to exchange hydrogen with the amines, preferably the secondary amines and the steric effect was favorable for the proton exchange. Finally, the calculations showed that the phenols radical cation $-NH_3$ system represented a barrierless proton transfer and remarkably low barrier (5.2 kcal/mol) of proton exchange, which support the importance of proton transfer in the proton exchange[22].

D. Advanced oxidation process

Advanced oxidation process (AOP) can be broadly defined as aqueous phase oxidation methods based on the intermediacy of highly reactive species such as hydroxyl radicals in the mechanism leading to the destruction of the target pollutant. Over the past 30 years, research and development concerning AOPs had been immense particularly for two reasons, namely the diversity of technologies involved and the areas of potential application. Key AOPs include heterogeneous and homogenous photo catalysis based on near ultraviolet (UV) or solar visible irradiation, electrolysis, ozonation, the Fenton's reagent, ultra sound and wet air oxidation, while less conventional but evolving processes include ionizing radiation, microwaves, pulsed plasma and the ferrate reagent. Depending on the properties of the waste stream to be treated and the treatment objective itself, AOPs can be employed either alone or coupled with other physiochemical and biological processes.

Chairez et al. proposed a new technique- differential neural network to estimate decomposition dynamics of phenols, byproducts accumulation and decomposition, and final products accumulation. The effect of increase in pH on the decomposition dynamics of phenol and 4-CP. 2, 4- DCP was very significant. It reduced the total decomposition time by a factor of 10. The presence of the chloro species in the phenol molecules also reduced the degradation time in ozonation[23].

Catalytic wet air oxidation of phenol with pelletized catalyst Ru/ZrO_2-CeO_2 was performed in a continuous packed bubble column reactor. The fresh and used Ru/ ZrO_2-CeO_2 catalysts were compared and it showed that introduction of ZrO_2 into Ru/CeO_2 increased the mechanical strength, specific surface area and adsorption capacity of pelletized catalyst. In the experiment of wet air oxidation of phenol with Ru/ ZrO_2-CeO_2 for 100 h, phenol and TOC removal stabilized around 100 and 96%, respectively[24].

Zairuddin et al. studied the degradation of phenol over the synthesized photo catalyst under the UV radiation in a batch reactor. The optimum formulation of supported nano TiO_2/ZSM-5/silica gel which consists of mixture of nano TiO_2, zeolite-5 supported in silica gel using colloidal silica gel as binder was found to be in the ratio of 1:0.6:0.6:1. 90 % of the phenol was degraded due to high surface area , low electron hole pairs, recombination rate and high crystalline quality of the synthesized catalyst[2]. Nanometric size Zn-doped TiO_2 photocatalyst was obtained by the oil/ water microemulison method. The increased photocatalytic activity in zn-doped TiO_2 with optimal zinc amount (5%) leads to the generation of surface oxygen vacancies in doped material promoting a decrease in the hole electron charge and the formation of tetracordinated Ti on nanomateral particles[13].

The degradation of phenol in air–equilibrated aqueous media was investigated using coupled sonochemistry and Fenton's reagent for a variety of operating conditions. The enhancement in the phenol degradation was mainly due to the contribution of additional hydroxyl radicals generated by Fenton's reagent as Fe (II) reacted with H_2O_2 (formed on sonolysis) enabling further production of $OH^{\cdot}$. The decomposition rate of aqueous phenol using coupled ultrasound and Fenton's reagent was strongly dependent on the initial concentration of reactant, Fe (II) concentration as well as pH[25].

E. Adsorption

Adsorption arises as a result of the unsaturated and unbalanced molecular forces that are present on every solid surface. Thus, when a solid surface is brought into contact with a liquid, there is an interaction between the fields of forces of the surface and that of the liquid. The solid surface tends to satisfy these residual forces by attracting and retaining on its surface the molecules, atoms, or ions of the liquid. Subha and Namasivayam, examined the feasibility of zinc chloride activated nano porous coir pith carbon for the removal of phenol from aqueous solution. Langmuir adsorption capacity was found to be 92.59 mg g^{-1} which was higher when compared to coir pith carbon in the absence of $ZnCl_2$ activation. Tests with synthetic wastewater showed that per cent removal of phenol by $ZnCl_2$ activated carbon was lower compared to pure phenol solutions due to the presence of other impurities that competed for adsorption sites[26]. Massalha et al. investigated the composite hydrophilic polyurethane (HPU) foams, which were enriched with various additives including dry biomass, clay and powdered activated carbon(PAC). The phenol adsorption capacity of the non-enriched foams was very low (2-8-5-4 mg/g foam).The enrichment of the foams by immersing in PAC aqueous solution, the maximal adsorption capacity of the adherent PAC on the foam was about 65% lower in average compared to free PAC[27]. Parker et al. revealed that the materials exhibited high efficiency to remove phenols from aqueous media due to the high mesoporous nature. The adsorption process was described well by Langmuir and Freundlich isotherms. Regeneration of starbon was attempted using a range of P^H with phenol recovery of upto 40% achieved[28]. Mohanty et al. investigated the nuts of Terminalia Arjuna,an agricultural waste were used to

Cite this article as: R. Subha, O.A.Sridevi, D.Anitha, D.Sudha. "Treatment methods for the removal of phenol from water- A Review." *International Conference on Systems, Science, Control, Communication, Engineering and Technology (2015)*: 199-203. Print.

prepare activated carbons by zinc chloride activation under four different activation atmospheres. The carbons showed surface area and microporous volumes of around 1260 m^2/g and 0.522 cm^3/g, respectively. The maximum removal of phenol was obtained at P^H 3.5, above 93% for adsorbent dose of 10 g/L and 100 g/L initial concentration[6].

3.CONCLUSIONS

Todate, adsorption as well as photocatalytic degradation are widely explored as highly efficient adsorbent/metal oxides for removal of phenol from water. They exhibit various advantages such as fast kinetics, high capacity and preferable sorption/degradation towards phenol in water. Neverthless, the application of nano metal oxides (NMO) as adsorbent can be used for removal of phenol but the NMOs tend to aggreagate into large size particles and their capacity loss seems inevitable. Fortunately, fabrication of new NMO's based composite adsorbents seem to be an effective approach to respond to all the above technical problems.

Acknowledgement

The authors are grateful to the Management, Principal and Head of department of Karpagam Institute of technology for their continuous support and providing us lab facilities to carry out the research work

References

[1] P.A.Mangruklar, S.P.Kamble, J.Meshram, S.S. Raylu, "Adsorption of phenol and o-chlorophenol by mesoporous MCM-41", J.Haz Mat, vol: 160, pp: 414-421, 2008

[2] N.F.Zairuddin, A.Z.Abdullah, A.R.Mohamed, "Characteristic of supported nano TiO2/ZsM-5/Silica gel (SNT-2s) photocatalytic degradation of phenol, J Haz Mat, vol:174, pp:299-306, 2010.

[3]S.Mukherjee, S.Kumar, A.K. Misra, M.Fan, "Removal of phenol from water environment by activated carbon, bagasse ash and wood charcoal ", Chem Eng J, vol: 129, pp:133-142, 2007.

[4]M.Ahmaruzzaman, " Role of fly ash in the removal of organic pollutants from wastewater", Energy & fuels, vol: 23, pp: 1494-1511, 2009.

[5] WHO. Guidelines for drinking water quality, Third edition incorporating the 1st and 2nd addenda, Geneva, WHO Press, World Health Organisation, Switzerland, 2008.

[6] K. Mohanty, M.Jha, B.C.Meikap, M.N.Biswas, " Preparation and characterization of activated carbons from Terminalia Arjuna Nut with zinc chloride activation for the removal of phenol from wastewater, Ind Eng Chem Res, vol:44, pp:4128-4138, 2005.

[7] A.Hasanoglu, " Removal of phenol from wastewaters using membrane contactors: Comparative experimental analysis of emulsion pertraction", Desalination, vol: 309, pp:171-180, 2013.

[8] S.Bae,D.Kim,W.Lee, "Degardation of diclofenac by pyrite catalysed Fenton oxidation",Appl.Catal.B.Envion. , vol: 134-135, pp:93-102, 2013.

[9]K.Rzeszutek,A.Chow, " Extraction of phenol using polyurethane membrane",Talanta, , vol: 46, pp:507-519, 1998.

[10] A.P.Annachhatre,S.H.Gheewala, " Biodegradartion of chlorinated phenolic compounds", Biotechnol.Adv. , vol: 14, pp:35-36, 1996.

[11] A.Ahiileos,E.Hapeshi,N.P.Xekoukoulotakis,D.Mantzavinos,D.Fatta-Kassinos, "Factors affecting dichlofenac decomposition n water by UV-Tio2 photocatalysis"Chem.Eng.J, vol: 161, pp:53-59, 2010.

[12]T.X.Bui,S.Y.Kang,S.H.Lee,H.Choi, "Organically functionalized mesoporous SBA-15 as sorbents for removal of selected pharamecuticals from water",J.Hazard.Mater, , vol: 193, pp:156-163, 2011.

[13]M.S.D.G.Maria, C.Rodriguez, A.I.Arturo, V.Rodriguez, S.A. Vela-gonzalez, " Synthesis of Zn doped TiO_2 nano particles by the novel oil in water microemulsion method and their uses for the photolytic degradation of phenol", J.Env Chem Eng, in press , 2015.

[14]Z.V.P. Murthy, S.K Gupta, "Thin film composite polyamide membrane parameters estimation for phenol-water system by reverse osmosis", Sep Sci Technol, vol:33, pp:2541-2557,1998.

[15]B.R. Fillipi,J.F. Scamehorn and S.DChristian and R.W.Taylor , " A comparative economic analysis of copper removal from water by ligand-modified micellar-enhanced ultrafiltration and by conventional solvent extraction J Membr Sci, , vol:145,pp: 27-44,1998.

[16]L.L.Gibbs, J.F.Scamehorn , and S.D.Christian, "Removal of n-alcohols from aqueous streams using micellar enhanced ultrafilltration", J.Membr.Sci, vol:30, pp:67-74,1987.

[17]H.Adamczak,K. Materna, R.Urbanski, H.Szymanowski, " Ultrafiltration of micellar solution containing phenols", J.Coll.Interf.Sci, vol:218, pp:359-368,1999.

[18]G.M. Zheng, K.Xu, J.H.Huang, L.Xue, Y.Y.Fang, Y.H.Qu, " Micellar enhanced ultrafiltration of phenol in synthetic wastewater using polysulfone spiral membrane", J.Mem.Sci, vol:310, pp:149 – 160,2008.

[19] A.Bodalo, E.Gomez, A.M.Hidalgo, M. Gomez, M.D. Murcia, I. Lopez," Nanofiltration membranes to reduce phenol oncentration in wastewater". Desalination, vol:245, pp: 680-686,2009.

[20] M.Bielska,K.Materna,J. Szymanowski, "Cross-flow ultrafiltration of micellar solutions containing selected phenols" J. Env. Sci, vol:12, pp.233-258,2003.

Cite this article as: R. Subha, O.A.Sridevi, D.Anitha, D.Sudha. "Treatment methods for the removal of phenol from water- A Review." *International Conference on Systems, Science, Control, Communication, Engineering and Technology (2015)*: 199-203. Print.

[21] C.Yang, Y.Qian,L. Zhang,J.Feng, "Solvent extraction process development and on- site trial plant for phenol removal from industrial coal-gasification wastewater"Chem.Eng.J, vol:117,pp: 179-185,2006.
[22] Y.X.Lu, J.W.Zou,Z.M. Jin, Y.H.Wang,H.X. Zhang,Y.J. Jiang,Q.S. YU," Proton exchangers between phenols and ammonia or amines: A computational study" J. Phys. Chem. A, vol:110, pp:9261-9266,2006.
[23] J.Chairez , A.Poznyak, T.Poznyak ," Reconstruction of dynamics of aqueous phenols and their products formation in ozonation using differential neural network observers", Ind. Eng. Chem .Res,vol: 46, pp: 5855-5866,2007.
[24] H.Wang,F. Zhao,S.I. Fujita, M.Arai, "Hydrogenation of phenol in $SCCO_2$ over carbon nanofiber supported Rh catalyst", Cat. comm, vl:9,pp: 362- 368,2008.
[25] Y.Jiang, T.D. Waite, " Degradation of trace contaminants using coupled sonochemistry and Fenton's reagent" Water Sci Technol,vol: 47,pp: 85-92,2003.
[26] R.Subha and C.Namasivayam, "Kinetics and isotherm studies for the adsorption of phenol using low cost micro porous $ZnCl_2$ activated coir pith carbon", *Can J Civ Eng* (NRC Research Press, Canada),vol: 8, pp:1-12,2009.
[27] N.Massalha, A.Brenner, C.Sheindorf, Y.Haimov, I.Sabbah, "Enriching composite hydrophilic polyurethane foams with PAC to enhance adsorption of phenol from aqueous solution, Chem Eng J, vol:280, pp:283-292, 2015.
[28] H.Parker, V.L.Budarin, J.H.Clark, A.J.Hunt, " Use of starbon for the adsorption and desorption of phenol", Sus Chem Eng J, vol:1,pp:1311-1318, 2013.

Cite this article as: R. Subha, O.A.Sridevi, D.Anitha, D.Sudha. "Treatment methods for the removal of phenol from water- A Review." *International Conference on Systems, Science, Control, Communication, Engineering and Technology (2015)*: 199-203. Print.

International Conference on Systems, Science, Control, Communication, Engineering and Technology 2015 [ICSSCCET 2015]

ISBN	978-81-929866-1-6
Website	icssccet.org
Received	10 - July - 2015
Article ID	ICSSCCET045

VOL	01
eMail	icssccet@asdf.res.in
Accepted	31- July - 2015
eAID	ICSSCCET.2015.045

Synthesis and characterization of spherical silica nanoparticles by Sol-Gel method

R.Sumathi[1], R.Thenmozhi[2]
[1]Assitant Professor, Karpagam Institute Technology,
Coimbatore, Tamilnadu, India.
[2]Assitant Professor, Sakthi College of Arts and Science for Women, Oddanchathram,
Dindigul, Tamilnadu, India.

Abstract: Silica nanoparticles were synthesized by sol gel method from tetraethyl orthosilicate (TEOS), ethanol (C_2H_5OH), water (H_2O) and ammonoium hydroxide (NH_4OH)as catalyst. The morphology and structure of colloidal silica particles formed depend on the molar ratio of reagents. The XRD patterns show the amorphous nature of the particles. FTIR spectra confirm the presence of functional group in the bulk and at the surface of the silica particles. SEM image shows that spherical structure of silica nano particles, whose particle is varied by using different molar ratio TEOS, C_2H_5OH and NH_3. The FTIR and EDAX analyses prove the successful synthesis of silica material.

1. Introduction

Silica nanoparticles are widely used in industrials such as electronic devices, insulator, catalysis or pharmaceuticals [1, 2] due to their attractive properties in optical properties.The most popular process of obtaining silica nanoparticles is through sol gel technique [3-7]. It involves the simultaneous hydrolysis and condensation reaction of the metal alkoxide. The resultants desired particles size and morphology of silica particles are produced through controlling parameters such as concentration of alkoxide, amount of water and concentration of ammonia or acid and solvent and aging time.

2. Experimental methods

2.1. Preparation of silica (SiO_2) nano powder

Chemicals used in this experiment are Tetraethyl Orthosilicate (TEOS), concentrated Ammonia (NH_3) and Ethanol (C_2H_5OH) solution. Tetraethyl Orthosilicate (TEOS) is used as the silica source. Aqueous ammonia solution was used as the catalyst. All the chemicals are purchased from Aldrich without further purification. Distilled water was used throughout the experimentSilica nanoparticles were synthesized using a standard procedure with experimental conditions provided in Table 1. The product was grained to get the silica nanoparticle.

Cite this article as: R.Sumathi, R.Thenmozhi. "Synthesis and characterization of spherical silica nanoparticles by Sol-Gel method." *International Conference on Systems, Science, Control, Communication, Engineering and Technology (2015)*: 204-208. Print.

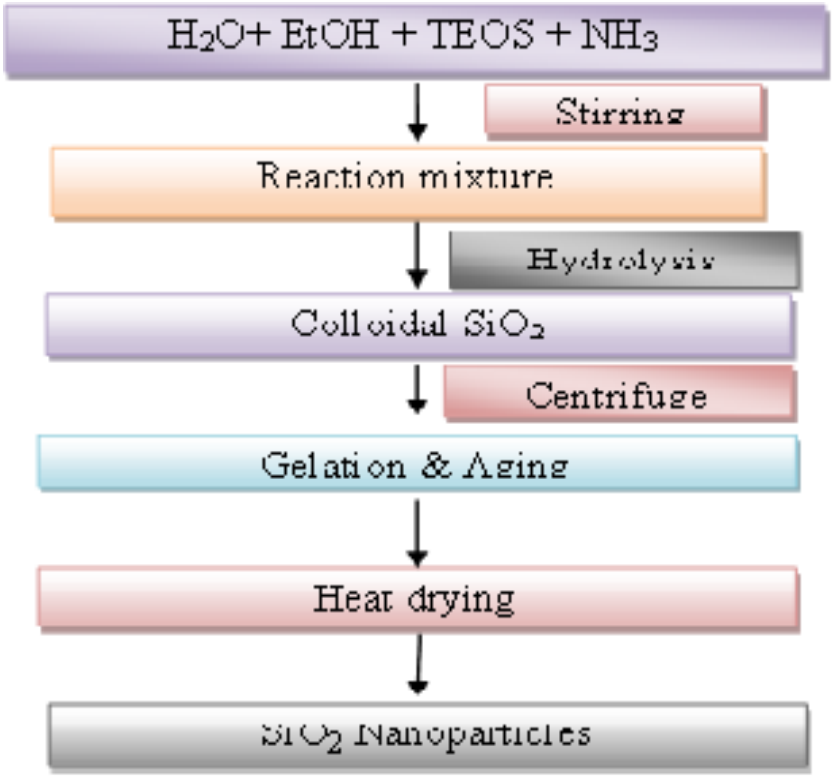

Flow chart for the Synthesis of silica nanoparticles by sol-gel method

Table 1: Molar ratios for the preparation of silica nanoparticles

Sample	Molar Ratio			
	H_2O	TEOS	NH_3	EtOH
a.	1	5	7	14
b.	1	5	9	7
c.	1	7	7	7

2.2. Characterization

The characterization of nanoparticles is done by using different techniques. The crystalline structure, morphology and compositional analysis of the prepared samples are examined by that the X-ray Diffraction (XRD), Scanning Electron Microscope(SEM), and Energy Dispersive Analysis using X-rays (EDAX) respectively. Nature of bonding and the chemical composition were analyzed by Fourier Transfer Infrared spectra (FTIR).

3. Results and Discussion

3.1. X-ray diffraction analysis

The crystal structures and phases of all the synthesized nanomaterials were ascertained from the XRD pattern. The figure shows that the XRD patterns of silica nanopowder prepared by sol-gel method for different molar ratios of ammonia, TEOS and ethanol concentration. From the three graphs (Fig 1) shows that the particles are amorphous in nature. The intense peak at $\theta = 23^{\circ}$ indicates, that the silica particles are formed by small nanocrystals. The broadening of peak is high owing to the smaller grain size effect. Other peaks are not present which represents the amorphous in nature due to the smaller particle size effect and incomplete inner structure of the nanoparticles [8]. XRD peaks which represent that silica nanoparticles structure is not changed entirely with small variation in ammonia, TEOS and ethanol concentration. By changing the different concentration, there is no phase change which represents the high purity of the silica nanoparticles. This demonstrates that high percentages of these particles are amorphous [9].

Cite this article as: R.Sumathi, R.Thenmozhi. "Synthesis and characterization of spherical silica nanoparticles by Sol-Gel method." *International Conference on Systems, Science, Control, Communication, Engineering and Technology (2015)*: 204-208. Print.

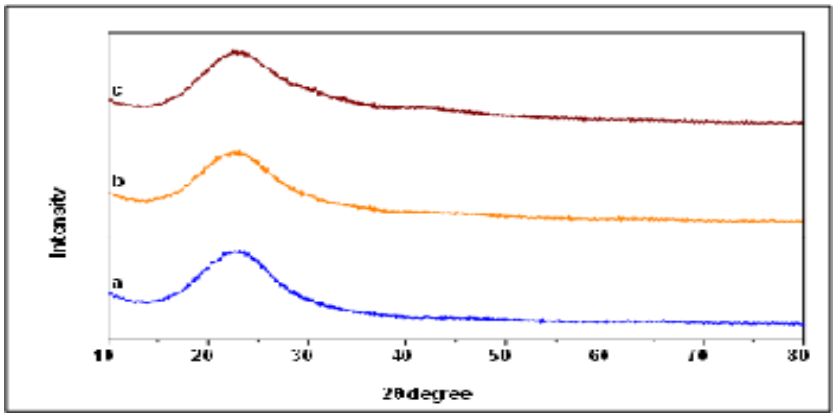

Fig 1: XRD spectrum of silica nanoparticle at different molar ratio of water, TEOS, NH_3, EtOH a) 1:5:7:14 b) 1:5:9:14 c)1:7:7:7

3.2. Morphological analysis (SEM) & Compositional analysis (EDAX)

The surface morphology of the silica nanopowder is analyzed using scanning electron microscope at the molar ratios of Water: TEOS: NH_3: EtOH as shown in Figure (2-4). The reaction was performed at lower water molecules in the solution to avoid aggregation of the silica nanoparticles at constant temperature. Therefore, hydrolysis and condensation of the reaction is carried out in alcohol with the presence of basic medium to get uniform distribution of silica nanoparticles. Figures 2-4 shows the spherical and agglomerated silica nanoparticles, which were obtained using different molar ratios of reagents and solvents.

The figure 2 shows that for preparing smaller silica nanoparticles, the reaction mixture should have higher concentration of ethanol and lower concentration of ammonia. Aggregation is always energetically favoured over nanoparticles since it minimizes surface areas and saturates the bonding and co-ordination sites and therefore, in order to prevent the nanoparticles from further growth or aggregation, the particle surfaces should be saturated immediately after nucleation by electrostatic or steric stabilization. Thus, the ammonia and solvent molecule of ethanol plays an important role to produce small size of silica nanoparticles with monodispersed spherical shape.

The figure 3 shows increase in particle size compared to sample 1. The base medium of ammonia is increased where as the amount of ethanol is decreased compared to sample 1. When the concentration of ammonia was changed corresponding decrease in the amount of solvent, many particles agglomerated, although few smaller spheres starts to form bigger silica nanoparticles. With the increase in the amount of ammonia, the sizes of the particle gradually increased and produce irregular spherical nanoparticles with high aggregation effect. The irregular shape of silica particles is obtained due to the fast nucleation process which is difficult to control the reaction by high concentration of basic medium and less solvent effect. And also decrease in the amount of ethanol the particle size increases [10]. Hence the SEM shows an increase in the size and irregular shape of the silica nanoparticles compared to SEM 1.

Figure 4 shows the silica nanoparticles were synthesized with same molar ratio of TEOS, Ammonia and Ethanol giving rise to larger silica nanoparticles with a broad distribution of particle sizes. Uniform orientation of the silica nanoparticles without aggregation is obtained is due to the covalent bond between the neighboring nanoparticles. Synthesis time was necessary because TEOS must be added very slowly to avoid any second nucleation or chemical aggregation. Second or multi nucleation could be avoided by three ways:1) increase of the ionic force in order to reduce the number of nucleation centers, 2) increase of particle surface in solution, 3) limiting TEOS concentration. Different concentration of TEOS, ammonia and ethanol, spherical silica nanoparticles is formed in different size which is not only alter the particle size and shape, also dramatically affects the optical properties of resultant nanoparticles.Finally we concluded, the particle size decreases with increasing molar ratio of ethanol and the particle size increases with increasing molar ratio of TEOS and ammonia.

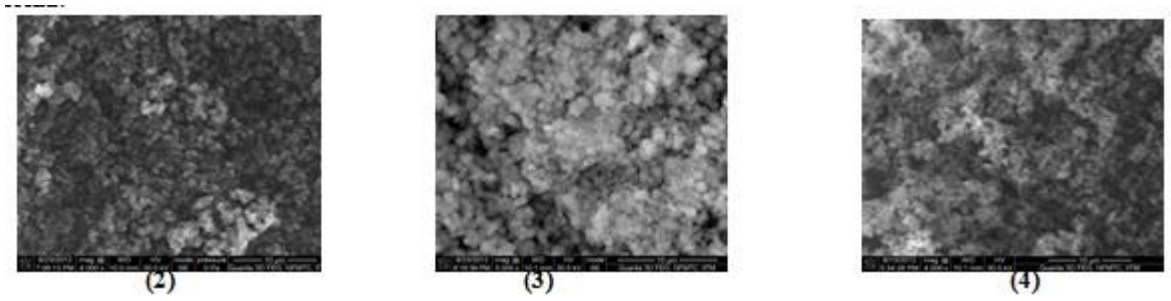

Fig 2, 3 and 4 shows SEM micrographs of silica nanoparticles obtained from a molarratio of Water: TEOS: NH_3: EtOH a) 1:5:7:14 b) 1:5:9:7 c) 1:7:7:7.

The elements of silica nanoparticles are confirmed by EDAX analysis, this is shown in figures 5,6 and 7. The

Cite this article as: R.Sumathi, R.Thenmozhi. "Synthesis and characterization of spherical silica nanoparticles by Sol-Gel method." *International Conference on Systems, Science, Control, Communication, Engineering and Technology (2015)*: 204-208. Print.

Composition is given in table 2 [11].

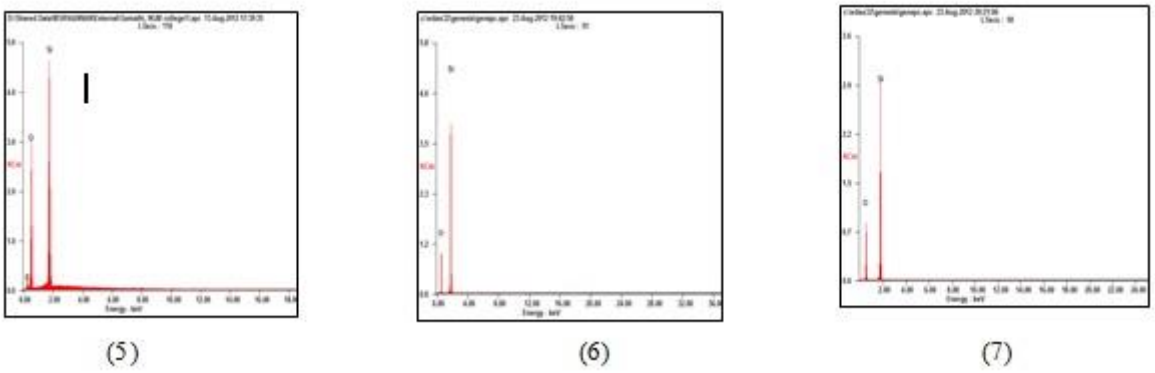

(5) (6) (7)

Fig 5,6 and 7 shows EDAX spectrum of Si particles of molar ratio a)1:5:7:14 b)1:5:9:7c)1:7:7:7

Table 2: EDAX result of silica nanoparticleswith different molar ratio

S.No	Molar Ratio				Elements	Atomic %
	H_2O	TEOS	NH_3	EtOH		
a.	1	5	7	14	Si : O	24.43 : 75.70
b.	1	5	9	7	Si : O	36.12 : 63.88
c.	1	7	7	7	Si : O	31.15 : 68.85

3.3 Fourier Transform Infrared Spectroscopy

FTIR results of present study in figure 8 shows the spectrum of silica nanoparticles at different molar ratio of Water, TEOS, NH_3, EtOH. The Band values of Sample a, b and c are summarized and are given in Table 3.[12-15].

Table 3: FT-IR spectra of Sample a, b and c

Name of the Sample	Adsorption bands (cm^{-1})	Functional groups
Sample a	457	Si-O-Si bond of bending vibration
	798	symmetric vibration of Si-O
	950	stretching vibration of Si-OH
	1633	bending vibration of water
	2856 and 2960	stretching and bending vibrations of C-H bond
	3448	H-bonded silanol OH group
Sample b	476	Si-O-Si bond of bending vibration
	800	symmetric vibration of Si-O
	950	SiO_2 stretching vibration of Si-OH bond
	1633	bending vibration of molecular water
	2856 and 2957	stretching and bending vibrations of C-H bonds
	3632	H-bonded silanol OH groups
Sample c	464	Si-O-Si bond shows bending vibration
	798	symmetric vibration of Si-O
	950.	SiO_2 stretching vibration of Si-OH bond
	1632	bending vibration of molecular water
	2856 and 2957	stretching and bending vibrations of C-H bond
	3454	H-bonded silanol OH group

Cite this article as: R.Sumathi, R.Thenmozhi. "Synthesis and characterization of spherical silica nanoparticles by Sol-Gel method." *International Conference on Systems, Science, Control, Communication, Engineering and Technology (2015)*: 204-208. Print.

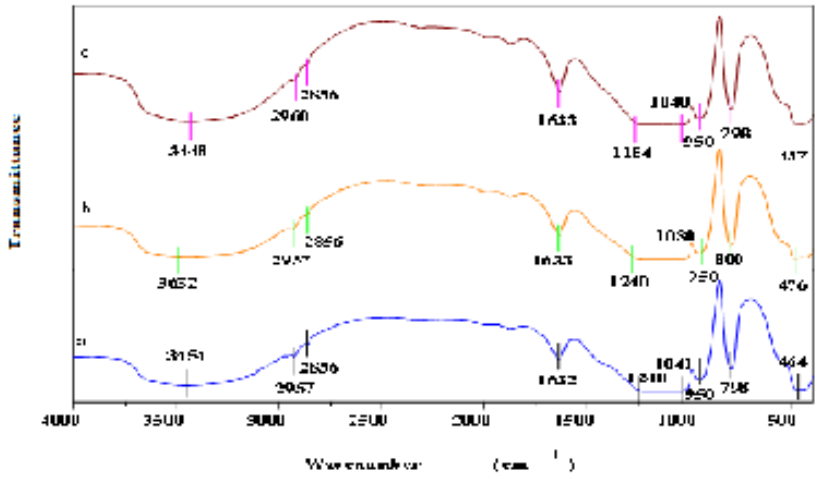

Fig 8: FTIR spectrum of Si-nanoparticles of molar ratio a) 1:5:7:14 b) 1:5:9:7c) 1:7:7:7.

Conclusion

We have successfully synthesized monodisperse silica spheres with the size ranging from >100 nm through sol-gel method. The reaction parameters can be used effectively for the synthesis of spherical silica nanoparticles at different molar ratio of Water, TEOS, NH_3, EtOH. The influence of the matrix obtained from the TEOS precursors and ammonia plays a major role in the evolution of the processes. The morphology and average diameter of colloidal silica particles depend on the proportion of reactants. XRD pattern shows the amorphous nature of silica nanoparticles. The SEM image shows the spherical structure of nanoparticles, whose particle size decreased with increasing molar ratio of ethanol in sample a. The particle size increased with increasing molar ratio of ammonia and decreasing molar ratio of EtOH in sample b. The particle size is increased for equal molar ratio of TEOS, NH_3, EtOH, in sample c. The FTIR and EDAX analyses prove the successful synthesis of the silica material. The resultant spherical silica nanoparticles synthesized can be used for various photocatalytic activity, assembly of photonic structures and these microspheres have potential for biomedical applications.

References

1. K.J. Klabunde, Nanoscale Materials in chemistry, Wiley-Interscience, USA 2001.
2. Y.T.Chen. Tamkang J.Sci.Eng. 5(2002) 99.
3. W.Stober, A. Fink, E.Bohn, J. Colloid Interface Sci. 26 (1968) 62-69.
4. N. enomoto. T.Koyano, Z. Nakagawa, Ultrason. Sonochem. 3 (1996) 105-109.
5. G. Buchel, M.Gurnn, K.K. Unger, A. Matasumoto, K.Tsutnami, S-pramol. Sci. 5(1998) 532-559.
6. D. Nagoo, H. Osuzu, A. Yamada, E. Mine, Y. Kobayashi, M. Konno, J. Colloid Interface Sci.274 (2004) 143-149.
7. S. Tatabaei, A. Shukohfar, R. Aghababazadeh, A.Mirhabibi, j. Phys. Confer. Series 26 (2006) 371-374.
8. E. R. Jisha et al, International Journal of Pharm Tech Research, 4 (2012) 1323-1331.
9. NoorsaiyyidahDarmonSingho, MohdRafie John, Int. J. ElectrochemSci, 7 (2012 5604-5615).
10. AldonaBeganskiene et al,Materials Science, 10 (2004) 287-290.
11. Binary K. Dutta et al, World Academy of Science Engineering and Technology, 73 (2011) 443-447.
12. Y. Shan, L. Guo and S. Zheng, Mater ChemPhys, 88 (2004) 192.
13. W. Posthemus, P. C. M. M. Magusin, J. C. M. Brokken-Zijp, A. H. A. Tinnemans and R. Vander linde, Surface Modification of oxide nanoparticles using 3-methacryloxy propyltrimethoxysilane, Journal of Colloid and Interface Science, 269 (2004) 109-116..
14. J. R. Agger, M. W. Anderson, M. E. Pemble, O. Terasaki and Y. Nozue, J PhysChem B,102 (1998) 3345.
15. J. M. Berquier, L. Teyssedre, C. Jacquiod, Journal of Sol-Gel Science Technology, 13 (1998) 739.

Cite this article as: R.Sumathi, R.Thenmozhi. "Synthesis and characterization of spherical silica nanoparticles by Sol-Gel method." *International Conference on Systems, Science, Control, Communication, Engineering and Technology (2015)*: 204-208. Print.

International Conference on Systems, Science, Control, Communication, Engineering and Technology 2015 [ICSSCCET 2015]

ISBN	978-81-929866-1-6
Website	icssccet.org
Received	10 - July - 2015
Article ID	ICSSCCET046

VOL	01
eMail	icssccet@asdf.res.in
Accepted	31- July - 2015
eAID	ICSSCCET.2015.046

Development and Testing of Coir Fiber Reinforced Sandwich Panel

Sasi Kumar M, Raghul R, I Balaguru, K Madhan Muthu Ganesh
Karpagam Institute of Technology, Coimbatore, Tamilnadu
India

Abstract- *Sandwich panels are the composite materials consist of a core at the centre covered by skin material on the upper and lower surface of the core. Sandwich structures have recently been investigated for their lightweight and multifunctional Characteristics, as well as their resistance to blast. This paper deals with increment of strength to weight ratio in natural fiber composites. For this a sandwich panel is developed using Coir fiber and polyester resin to prepare skin material and aluminium honeycomb is used as core in the panel. In this work, coir composites are developed and their mechanical properties are evaluated. The results indicate that coir can be used as a potential reinforcing material for many structural and non-structural applications.*

I. INTRODUCTION

Composites have wide range of applications because of their adaptability to different situations and the relative ease of combination with other materials to serve specific purposes and desirable properties [1]. Composites provide ample scope and receptiveness to design materials and processes. The strength-weight ratio is higher when compared with other materials. Their mechanical properties like stiffness, cost effectiveness, apart from easy availability of raw materials, make them the obvious choice for various applications. Sandwich panels are the composite materials consist of a core at the centre covered by skin material on the upper and lower surface of the core. Sandwich structures are recently investigated for their lightweight and multifunctional Characteristics [2]. Various types of cores and skins are used for sandwich panels and are explained below.

Core forms the major portion of the sandwich panels. Usually it will be light in weight but supports make them stronger when loaded. The major types of cores are Polymer foam cores, Wood cores, Syntactic cores and Honeycomb/corrugated cores

The covering material on the upper and lower surface of the core is the skin. It will be of any of the composite material. Usually the composite materials are used as skin materials are Metal matrix composites, Ceramic matrix composites, Polymer matrix composites and Elemental matrix composites. The use of sandwich structures is steeply increasing in recent years as a result of their light weight and high stiffness [3]. Sandwich Panel Composites have been used in a variety of applications such as automotive bodywork, marine hulls, aircraft wing skins and satellite bodies and their solar panels. Special attention is contributed for improving the performance of those structures.

Basically two main tasks that were carried out to achieve the objectives of the paper. In the first task, a composite material has prepared by combining the polyester and coconut coir at various strength to weight ratios of fiber. Then it was continued by

Cite this article as: Sasi Kumar M, Raghul R, I Balaguru, K Madhan Muthu Ganesh. "Development and Testing of Coir Fiber Reinforced Sandwich Panel." *International Conference on Systems, Science, Control, Communication, Engineering and Technology (2015)*: 209-215. Print.

performing the mechanical test along with aluminium honeycomb as core to determine the physical characteristics of the studied composite.

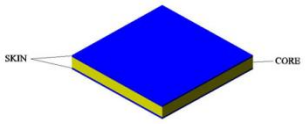

Figure 1: Structure of a Sandwich Panel

II. LITERATURE REVIEW

According to Bujang I.Z, et al, the influence of fibers volume on the mechanical properties and dynamic characteristic of the composites has analysed. The sheets are prepared for the variable volume from 5% to 15% and mechanical test is carried to prove that the volume of the fiber has great influence in the strength of the composite, i.e., whenever the volume of fiber increases the strength of the composite also will increase [4]. Flavio de Andrade Silva, et al explained that the need for cheap, sustainable, harmless, and secure shelter is an inherent global problem and numerous challenges remain in order to produce environmentally friendly construction products which are structurally safe and durable. The use of natural fiber with enhanced mechanical performance reinforcement in a cement based matrix is a promising opportunity. Sisal fibers were used as a fabric to reinforce a multi-layer cementitious composite with a low content of Portland cement [5]. Dr. Navdeep Malhotra, et al, explained that composites are one of the most advanced and adaptable engineering materials. The work reports the use of bio-fibers as reinforcement in developing polymer composites. Natural fiber offer many technical and ecological benefits for its use in reinforcing composites. Many types of natural fibers have been investigated for use in plastics including jute, straw, Flax, hemp, wood, sugarcane, bamboo, grass , kenaf, sisal, coir, rice husks, wheat, barley, oats, kapok, mulberry, banana fiber, raphia, pineapple leaf fiber and papyrus etc. and the matrix material used for reinforcing the fibers are classified as thermo sets, thermoplastics and elastomers. This study leaves an excellent knowledge to know about the Natural fiber polymer composites (NFPC) [6]. Olusegun David Samuel, et al, discussed the mechanical properties of banana, sisal, coconut, hemp and E-glass fiber reinforced laminates were evaluated to assess the possibility of using it as new material in engineering applications. Natural fibers form an interesting option for the most widely applied fiber in the composite technology. They possess desirable properties such as bio-degradability, renewability, combustibility, lower durability, excellent mechanical properties, low density and low price. Thus it is very important to study the mechanical properties of these natural fibers [7].Dixit S. et al, discussed the three most important and effective fibers among all the natural fibers are the coir, sisal and jute. The properties of these fibers are studied and the effect of hybridization on mechanical properties on Coir and Sisal Reinforced Polyester composite (CSRP), Coir and Jute Reinforced Polyester composite (CJRP), Jute and Sisal Reinforced Polyester composite (JSRP) were evaluated experimentally. The results demonstrate that hybridization play an important role for improving the mechanical properties of composites [8]. Sreekala M S et al, said that material selection is an important process in developing a new composite material. For this the database of the material properties of the various natural fibers are organized. The major material properties of the natural fiber includes density, tensile strength, cost, Young's modulus and durability are studied before selecting the material. Each of the fiber has its own properties which differ from others and thus the fibers are selected according to its application [9]. Mohd Yussni Hashim et al, explained that Natural fibers are available in abundance, low cost, lightweight polymer composite and most importance its biodegradability features, which often called "eco-friendly" materials. However, their applications are still limited due to several factors like moisture absorption and poor wet-ability. Therefore, to overcome this challenge, fiber treatment process is one common alternative that can be use to modify the fiber surface by chemically, physically or mechanically technique. Nevertheless, the focus onthe effect of mercerization treatment on mechanical properties enhancement of natural fiber reinforced composite. It specifically discussed on mercerization parameters, and natural fiber reinforced composite mechanical properties enhancement [10]. Henrik Herranen et al , discussed that sandwich composites have high strength to weight ratio, extended operational life, lower maintenance cost (due to less corrosion, and resistance to marine boring organisms), as well as a range of integrated functions, such as thermal and sound insulation, excellent signature properties, fire safety, good energy absorption, directional properties of the face sheets enabling optimized design and production of complex and smooth hydrodynamic surfaces [11].

Cite this article as: Sasi Kumar M, Raghul R, I Balaguru, K Madhan Muthu Ganesh. "Development and Testing of Coir Fiber Reinforced Sandwich Panel." *International Conference on Systems, Science, Control, Communication, Engineering and Technology (2015)*: 209-215. Print.

Table I . Cellulose and Lignin Content of Natural Fibers

Sl.No	Fiber	Cellulose content (%)	Lignin content (%)	Diameter (µm)	Elongation Max.
1	Banana	64	5	50-250	3.7
2	Sisal	70	12	50-200	5.1
3	Pineapple	85	12	20-80	2.8
4	Coir	37	42	100-450	47
5	Polymer	40-50	42	70-1300	2.8

From the Table No 1 it is clear that the coir has effective amount of cellulose and lignin content [12]. Naveen et al. carried out an investigation to make use of coconut coir, a natural fiber abundantly available in India. Natural fibers are strong, lightweight, very low cost and easily available when compared with the other materials [13]. The literature review shows that the density of the coir fiber is very less, it is the lowest among cost, it is highly durable and its elongation is comparatively high when compared to other natural fibers, hence this fiber is selected for this research, which is effective with polyester resin [14].

III. MATERIALS AND METHODS

In this section we will discuss about the extraction of the coir, mould preparation, and preparation of composites. These materials will be used for the testing. The studied composite material has made by polyester reinforced matrix with coconut fibers which were arranged in chopped configuration. The coir fibers can obtain from coconut husk which was extracted from coconut fruit. After they had been extracted, the coir fibers were dried at 70°C to 80°C. The coir were treated to avoid the degradation factor. This process consists of immersing the coir fibers into 5% sodium Hydroxide (NaOH) solution for 24 hours to remove the first layer. The obtained fibers are washed abundantly with water to remove the NaOH , dried again in furnace at 70°C to 80°C for next 24 hours. The coir fibers were then soaked into 5% of silicone and 95% of methanol solution for 4 hour and dried at 70°C for next 24 hours curing time. The physical properties of coir fibers are shown in Table II [4].

Table II . Mechanical Properties of Coir Fiber

Sl.No	PROPERTY	RANGE
1	Density (kg/m^3)	1.15 – 1.33
2	Elongation at break (%)	18–30
3	Tensile strength (MPa)	140 – 150
4	Young modulus (GPa)	4 – 5
5	Water absorption (%)	130-180

The usage of polyester resin as a matrix was chosen because it is the standard economic resin commonly used [12]. The physical properties of polyester resin are shown in Table III.

Table No III . Mechanical Properties of Polyester Resin

Sl.No	PROPERTY	RANGE
1	Density (kg/m^3)	1.2 - 1.5
2	Young Modulus (GPa)	2 - 4.5
3	Tensile Strength (MPa)	40 – 90

Cite this article as: Sasi Kumar M, Raghul R, I Balaguru, K Madhan Muthu Ganesh. "Development and Testing of Coir Fiber Reinforced Sandwich Panel." *International Conference on Systems, Science, Control, Communication, Engineering and Technology (2015)*: 209-215. Print.

4	Compressive Strength (MPa)	90 -250
5	Tensile Elongation at break (%)	2
6	Water Absorption 24h at 20 °C	0.1 - 0.3

The mould used for coir fiber composite is made from mild steel, it was fabricated in machining lab whose length and width are 270 mm as shown as in Figure 2.

Figure 2. Mould for the composites and Coir fiber composite

Composites having different fibers content were prepared by varying the fiber volume as 25%, 30% and 35%. In the process of preparing the composite, a mould release agent was used to clean and dry the mould before the polyester can be laid up on the mould. The polyester was mixed uniformly with the coconut fibers by using a special brush in the mixed container [4]. The mixture was transferred carefully into the moulds and flattened appropriately by using the roller before being dried for 24 hours [13]. After the composite mixture was fully dried, they were separated from the moulds. In the similar manner two specimens are prepared at each weight fraction of the fiber. The specimens are shown in the Figure 2.

The aluminium honeycomb is light in weight but have high strength, since it is a honeycomb structure it is very low in density. The skin material is used with this aluminium to form the sandwich panel[11]. The Mechanical Properties of the Aluminium Honeycomb is shown in Table IV.

Table No IV . Mechanical properties of Aluminium Honeycomb

Sl.No	PROPERTY	VALUE
1	Density(kg/m^3)	91.2
2	Young's modulus(GPa)	1.288
3	Shear modulus(KPa)	42.6
4	Poisson's ratio	0.4

IV. ANALYTICAL CALCULATION

In the analytical calculation we calculate the weight fraction calculation for the composite material from the properties of the fiber and the matrix, using the rule of mixtures.

Table No V . Weight fraction of coir and polyester matrix

S.No	The entire weight of the single layer of the skin specimen is 300 g			
1	Fiber %	25	30	35
2	Weight of the coir (g)	75	90	105
3	Weight of the polyester (g)	225	210	195

Cite this article as: Sasi Kumar M, Raghul R, I Balaguru, K Madhan Muthu Ganesh. "Development and Testing of Coir Fiber Reinforced Sandwich Panel." *International Conference on Systems, Science, Control, Communication, Engineering and Technology (2015)*: 209-215. Print.

The properties of composite is related to fiber and matrix by the Rule of mixture:

Young's modulus of the composites:

$E_c = E_f W_f + E_m W_m$ [15] (1)

Where –E_c, E_f and E_m are the young's modulus of the composite, fiber and matrix respectively and W_f and W_m are the weight fraction of the fiber and matrix respectively.

Density of the composite:

$\rho_c = \rho_f W_f + \rho_m W_m$ [15] (2)

Fiber and matrix respectively and W_f and W_m are the weight fraction of the fiber and matrix respectively.

V. MATERIAL TESTING

A. Tensile Testing

Tensile testing is the most common mechanical testing for determining the elongation property and elastic modulus of the material. The tests consist of applying a constant strain on the panel and measure the load. Universal Testing Machine with strain speed of 10 mm/min used for testing. The panels were cut in accordance with ASTM D790 (100mm x 25mm) standards [4] at each of the three specimens and the test is done. The Tensile testing is shown in the Figure 3 a.

B. Compression Testing

Compression testing is carried for determining the properties of materials such as strength, ductility, toughness and strain hardening. The compression test consists of applying a constant strain on the panel and measure the load. Universal testing machine was used with a constant load applied gradually. The panels were cut in accordance with ASTM C297-94 (25mm x 25mm) standards [10] at each of the three specimens and the test is done. The Compression testing is shown in the Figure 3 b.

C. Impact Testing

Impact test is carried to find the amount of sudden impact of energy applied to the specimen. This testing method consists of applying sudden impact of over the panel, which is done by charpy test. The panels were cut in accordance with ASTM D638M (100mm x 20mm) standards [10] at each of the specimen and the test is carried. The Impact testing is shown in the Figure3 c.

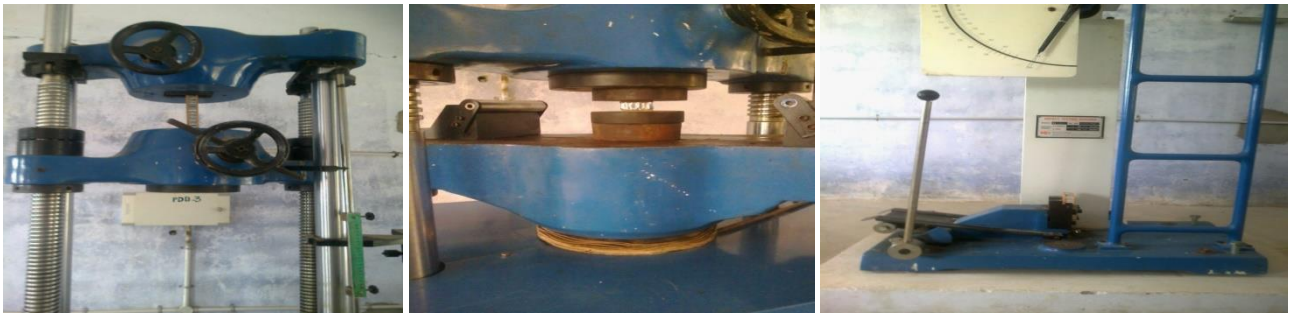

Figure 3. a) UTM Tensile Testing, b)UTM Compression c)Testing Charpy Impact Testing

VI. RESULTS AND DISCUSSIONS

The mechanical properties of the coir fiber reinforced composites are expected to depend on the content or volume or weight fraction of the fibers in the composites**.** Even a small change in the physical nature of fibers for a given Weight content of fibers may result in distinguished changes in the overall mechanical properties of composites. Therefore the influence of natural fibers content on mechanical properties of coir fibers reinforced composites was investigated and the mechanical properties of coir fibers reinforced sandwich panel with fibers weight changing from 25% to 35%. High

Cite this article as: Sasi Kumar M, Raghul R, I Balaguru, K Madhan Muthu Ganesh. "Development and Testing of Coir Fiber Reinforced Sandwich Panel." *International Conference on Systems, Science, Control, Communication, Engineering and Technology (2015)*: 209-215. Print.

percentage of coir fiber will result in poor wetting between the coir fiber and polyester matrix. The result indicates that the tensile, compression and the impact strength of the composite increases with the increase in weight of the fiber and those results are shown Table VI

Table No VI. Mechanical properties of fabricated composite result

S.No	Mechanical Properties	Fiber 25%	Fiber 30%	Fiber 35%
1	Young's modulus(MPa)	2500	2600	2700
2	Tensile strength (Newtons)	882.9	981	1079.1
3	Compression strength (Newtons)	2746.8	2844.9	2943
4	Impact Energy (joules)	40	58	68

Table VI shows that 30% fiber composite panel withstand 40% more impact strength than the 25% fiber composite panel and the 35% fiber composite panel withstand 25% more impact strength than the 30% fiber composite panel. From the above results of the various test conducted to the Coir fiber reinforced sandwich panel it is clear that it has better strength to weight ratio than the other natural fiber composites. It also proves that whenever the amount of fiber increases to certain extend in a composite material, the strength of the material also increased

VII. CONCLUSION

The project work carried to develop a natural fiber composite, the effective fiber among the various natural fiber i.e. coir fiber is selected, similarly cheap and effective resin in combination with the coir fiber is found to be polyester resin. Using this coir fiber and polyester resin, composite material is made in three different ratios of weight fraction of the fiber as 25%, 30% and 35%. In each ratio two specimens is made and each of which is used as skin material along with the core which is Aluminum honeycomb to form sandwich panels. Thus the Coir fiber reinforced sandwich panel is made. Then each of this panel is tested for its mechanical strength. The result of the tensile, compression and impact test proves that it has better strength to weight ratio than the other natural fiber composites and whenever the amount of fiber increases to a certain extend in a composite material, the strength of the material also increases. Since there is no end for invention and innovative ideas, this project work can be further developed by changing the types of fiber and resin, the thickness for the core and the skin material can also be changed and the tests can be carried and the results can be produced.

ACKNOWLEDGMENT

With great pleasure and deep gratitude, The authors wish and express their sincere gratitude to beloved Principal **Dr. T. Ramachandran** for providing an opportunity and necessary facilities in carrying out this work and express their sincere thanks to Head of department Mr.S.Sendhil Kumar, staff Mr.K.M. Kiran babu and all the staff members of Aeronautical Engineering whose assistance played a big role in this work and have been of immeasurable value.

REFERENCES

1. Jenarthanan M P, Jeyapaul R. Optimisation of machining parameters on milling of GFRP composites by desirability function analysis using Taguchi method. International Journal of Engineering, Science and Technology. 2013; 5(4): 23-36.
2. Rathbun H J, Zok F W, Evans A G. Strength optimization of metallic sandwich panels subject to bending. International Journal of Solids and Structures. 2005; 42:6643-6661.
3. Boruszewski W, Kataoka-Filho M. Designing optimum fibre layout for composite sandwich panels. Instituto Nacional de Pesquisas Espaciais. 2000; 51: 1-6.
4. Bujang, I.Z., Awang, M.K, Ismail, A.E. Study on dynamic characteristics of coconut fibre reinforced composites. Regional Conference on Engineering Mathematics, Mechanics, Manufacturing & Architecture. 2007; 185-202.
5. Flavio de Andrade Silva, Barzin Mobasher, Romildo Dias de Toledo Filho. Advances in Natural Fiber Cement Composites. Visiting Researcher D.Sc. Institute of Construction Materials. 4th Colloquium on Textile Reinforced Structures. 2008; 377-388.
6. Navdeep Malhotra, Khalid Sheikh, Sona Rani. A review on mechanical characterization of natural fiber reinforced polymer composites. A Journal of Engineering Research and Studies. 2012; 3(1):75-80.
7. Olusegun David Samuel, Stephen Agbo, Timothy Adesoye Adekanye. Assessing Mechanical Properties of Natural Fiber Reinforced Composites for Engineering Applications. Journal of Minerals and Materials Characterization and Engineering. 2012; 11: 780-784.

Cite this article as: Sasi Kumar M, Raghul R, I Balaguru, K Madhan Muthu Ganesh. "Development and Testing of Coir Fiber Reinforced Sandwich Panel." *International Conference on Systems, Science, Control, Communication, Engineering and Technology (2015)*: 209-215. Print.

8. Dixit S and Verma P. The Effect of Hybridization on Mechanical Behavior of Coir/Sisal/Jute Fibers Reinforced Polyester Composite Material. Research Journal of Chemical Sciences. 2012; 2(6): 91-93.
9. Sreekala M S, Kumaran M G, Joseph S, Jacob M and Thomas S. Oil palm fiber reinforced phenol formaldehyde composites. Influence of fiber surface modifications on the mechanical performance. Applied Composite Materials. 2000; 7:295-329.
10. Mohd Yussni Hashim, Mohd Nazrul Roslan, Azriszul Mohd Amin, Ahmad Mujahid Ahmad Zaidi and Saparudin Ariffin. A Review Mercerization Treatment Parameter Effect on Natural Fiber Reinforced Polymer Matrix Composite. A Journal by World Academy of Science, Engineering and Technology. 2012; 68:1382 – 1388.
11. Henrik Herranen, Ott Pabut, Martin Eerme, Juri Majak, Meelis Pohlak, Jaan Kers, Mart Saarna, Georg Allikas, Aare Aruniit. Design and Testing of Sandwich Structures with Different Core Materials. Journal on Materials Science. 2012; 18(1):45-80.
12. M P Westman, S G Laddha, L S Fifield, T A Kafentzis, K L Simmons. Natural fiber composites: A Review. Pacific Northwest National Laboratory. U.S. Department of Energy, 2010.
13. Naveen P N E, Dharma Raju T. Evaluation of Mechanical Properties of Coconut Coir Fiber Reinforced Polymer Matrix Composites. Journal of Nano Research. 2013; 24:34-45.
14. Shabnam Sadeghi Esfahlani, Hassan Shirvani, Ayoub Shirvani, Habtom Mebrahtu and Sunny Nwaubani. Design, Development and Numerical analysis of honeycomb core with variable crushing strength. American Journal of Engineering and Applied Sciences. 2012; 6 (1): 8-19.
15. Autur K Kaw. 'Structure of Composite Materials', CRC Press Second edition.

Cite this article as: Sasi Kumar M, Raghul R, I Balaguru, K Madhan Muthu Ganesh. "Development and Testing of Coir Fiber Reinforced Sandwich Panel." *International Conference on Systems, Science, Control, Communication, Engineering and Technology (2015)*: 209-215. Print.

International Conference on Systems, Science, Control, Communication, Engineering and Technology 2015 [ICSSCCET 2015]

ISBN	978-81-929866-1-6	**VOL**	01
Website	icssccet.org	**eMail**	icssccet@asdf.res.in
Received	10 - July - 2015	**Accepted**	31- July - 2015
Article ID	ICSSCCET047	**eAID**	ICSSCCET.2015.047

CHARACTERIZATION OF NICKEL OXIDE NANOPARTICLES SYNTHESIZED VIA SOLUTION-PHASE PRECURSOR ROUTE

A Lathamaragatham
Department of Science and humanities (Physics),
Karpagam Institute of Technology, Coimbatore, India

Abstract: *Nickel oxide (NiO) nanoparticles were produced via a solution-phase precursor route by adding solid Guanidium carbonate in citric acid and nickel nitrate hexahydrate solution at the temperature of 95 °C in water bath. High purity NiO nanoparticles were obtained by calcinating the precipitated powders at different temperatures. Thermal analysis reveals the phase formation temperature by degrading the citrates and water content before 500°C. The strong absorption band at 419 cm^{-1} is corresponding to the stretching vibration of NiO are confirmed by FTIR spectrum. X-ray diffraction patterns revealed that the well-crystallized/high-purity nanostructure with grain size ~35 nm of NiO nanoparticles. Scanning electron microscope and FESEM images showed that the synthesized NiO nanopowder had porous structure with pore size of ~90 nm. Nowadays porous nanopowders are using for the applications of super capacitors*

I. INTRODUCTION

Nanoparticles of transition metal oxides have attracted the attention of many materials researchers due to their exceptional properties stimulating advanced applications [1-2]. Nickel oxide (NiO) is a p-type semiconductor with a wide band gap (3.6−4.0 eV) and large exciton binding energy [3, 4]. Nanostructural NiO is considered as a promising candidate for optical, electronic, catalytic, superparamagnetic, transparent conductor film, gas sensor, alkaline battery cathode, dye-sensitized solar cell and solid oxide fuel cell anode applications [3].

Among the various preparation techniques, the solution-phase precursor route has many advantages and much promising. The advantages of this solution based technique are that it is simple, cost effective, appreciable reduction in the processing temperature and the resulting material being of nanostructure. Also, it provides excellent stoichiometry, low impurity content compared to the other methods. In this work, Guanidine metal citrate precursor was first produced by solution-phase precursor route method. Then it was post heated to form nickel oxide nanopowders. Morphological and structural characteristics of the nickel oxide were subsequently determined by SEM, FESEM and XRD.

II. EXPERIMENTAL PROCEDURE

Sample preparation

Solution-Phase Precursor Route synthesis of NiO nanopowder was composed of two stages: (a) the formation of guanidine nickel citrate precursor and (b) subsequent heat treatment of precursor to transform into NiO. To synthesis the precursor, solid

Cite this article as: A Lathamaragatham. "CHARACTERIZATION OF NICKEL OXIDE NANOPARTICLES SYNTHESIZED VIA SOLUTION-PHASE PRECURSOR ROUTE." *International Conference on Systems, Science, Control, Communication, Engineering and Technology (2015)*: 216-220. Print.

Guanidinium carbonate was added to an aqueous solution of Citric acid with continuous stirring. To this acid-base solution an aqueous solution of Nickel nitrate hexahydrate was added. Here the metal, acid and base ratio was maintained at 1:1:4. There is a precipitate formation taking place while adding the metal to acid base solution. During the reaction the pH =9 was measured. This precipitated solution became clear with the prolonged stirring. The resulting clear solution with pH = 9 was evaporated in the water bath to reduce half of its volume. The concentrated solution was left aside over night at room temperature for re-crystallization. Finally a highly crystalline substance was separated from the solution and dried in air. Formation mechanism for metal complex,

$$Ni(NO_3)_2.6H_2O + H_4Cit + 2Gu.H_2CO_3$$

$$\downarrow \Delta\ 90\ ^{\circ}C, \text{ on water bath}$$

$$(Gu)_2[Ni(Cit)].2H_2O + 2HNO_3 + 6H_2O + 2CO_2$$

By heating this citrate prcursor at various temperature from 600°C to 1000°C, nickel oxide nanoparticles have been obtained.

Results and discussions:

TG/DTA Analysis

As shown in Fig (i), the TG/DTA analysis confirmed that the transformation of NiO from its metal complexes taking place after 500°C. It showed that dehydration takes place at 170°C and removal of base followed by citrate takes place around 320-460°C.

Then the formation of NiO by thermal decomposition of the metal complex has been confirmed by the IR spectrum of the residues. The IR spectrum for NiO is shown in Fig (ii). The strong absorption band at 419 cm^{-1} is corresponding to the stretching vibration of NiO.

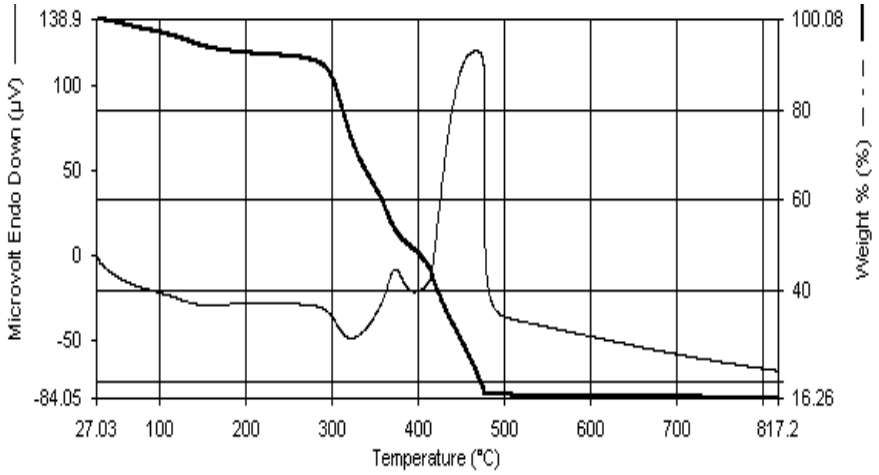

Fig (i) TG/DTA curves for the metal complex

The band at 3419 and 1383 cm^{-1} are due to the calcinated powder tends to physically absorb water and carbonated ions [5,6].

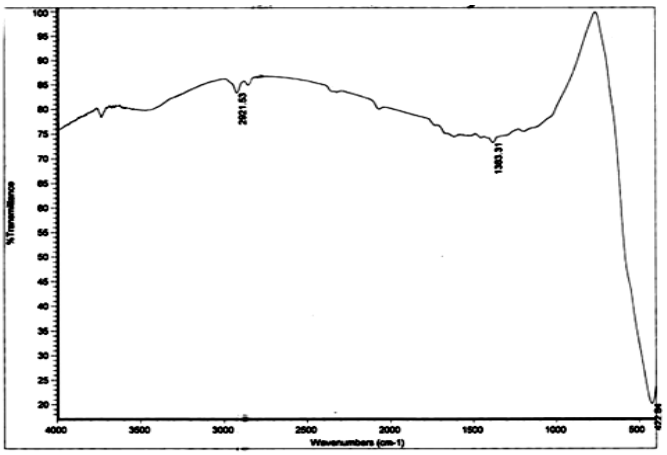

Fig (ii). IR spectrum of NiO nanopowders

The phase purity and crystallinity of the prepared samples were studied through the powder X-ray diffraction method. The powder XRD pattern of NiO nanoparticles is shown in Fig (iii). It shows that NiO nanoparticles obtained by thermal decomposition of the complex precursor with different calcinations temperatures, varied from 600 to 1000 °C at zero hour. The XRD pattern for the 600 to 800°C calcinated sample shows, few hydroxide peak in the product sample. This confirms the sample in the form of nickel

Cite this article as: A Lathamaragatham. "CHARACTERIZATION OF NICKEL OXIDE NANOPARTICLES SYNTHESIZED VIA SOLUTION-PHASE PRECURSOR ROUTE." *International Conference on Systems, Science, Control, Communication, Engineering and Technology (2015)*: 216-220. Print.

hydroxide upto 800°C calcinations. While increasing the temperature from 900 to 1000 °C the hydroxyl group disappears from the complex precursor and it form a single phase *face centered cubic* (*fcc*) structure of NiO. The prominent and sharp peaks of the diffractogram indicate the formation and high crystallinity of the prepared NiO. These peaks are very well match with the JCPDS # 78-0423. The average crystallite sizes of the samples were calculated by using the (111), (200), (220), (311), and (222) planes. The average crystallite size of the NiO prepared by thermal decomposition of complex precursors are calculated by using Scherer's formula and compared with the William-Hall plot method.

Scherrer's formula is given by, $$D = \frac{K\lambda}{\beta \cos\theta}$$

Where, **λ** is the wavelength of the X-rays used, **θ** is a Bragg angle, **K** is the geometrical shape factor and **β** be the full width half maximum of the sample in radian.

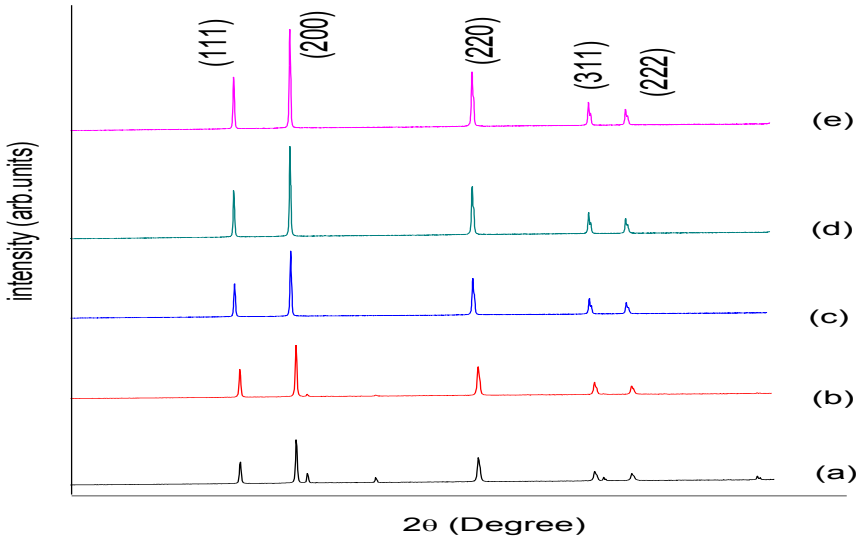

Fig (iii) Powder XRD pattern for the different calcination temperatures (a) 600°C, (b) 700°C, (c) 800°C, (d) 900°C and (e) 1000°C

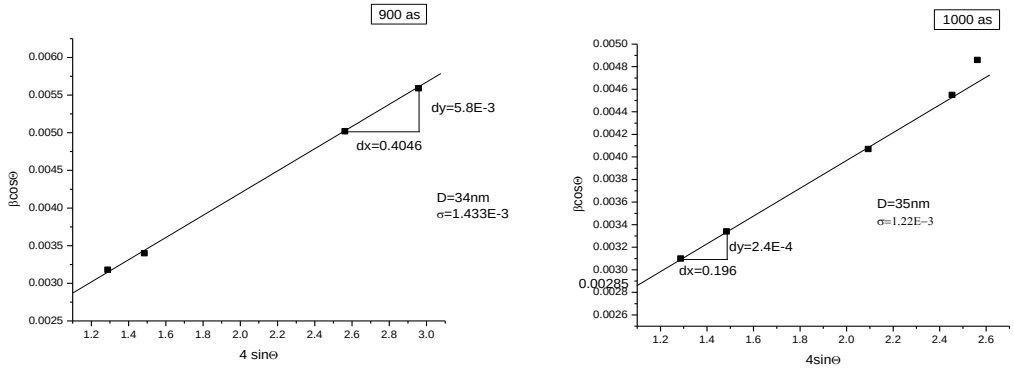

William and Hall plot for the samples prepared at 900°C & 1000°C

The calculated average crystallite sizes, strain and dislocation density were tabulated.

Samples calcination temperatures (°C)	Avg. Grain size calculated from (nm)		Strain $lin^{-2}m^{-4}$	Dislocation Density lines/m^2
	Scherrer formula	W-H plot method		
900	36	34	1.43E-03	7.70E-04
1000	37	35	1.22E-03	7.30E-04

In both cases the increase in the calcination temperature the reduction in the lattice strain is observed.

The SEM images for the samples calcinated at different temperatures are shown in fig (iv).

Cite this article as: A Lathamaragatham. "CHARACTERIZATION OF NICKEL OXIDE NANOPARTICLES SYNTHESIZED VIA SOLUTION-PHASE PRECURSOR ROUTE." *International Conference on Systems, Science, Control, Communication, Engineering and Technology (2015)*: 216-220. Print.

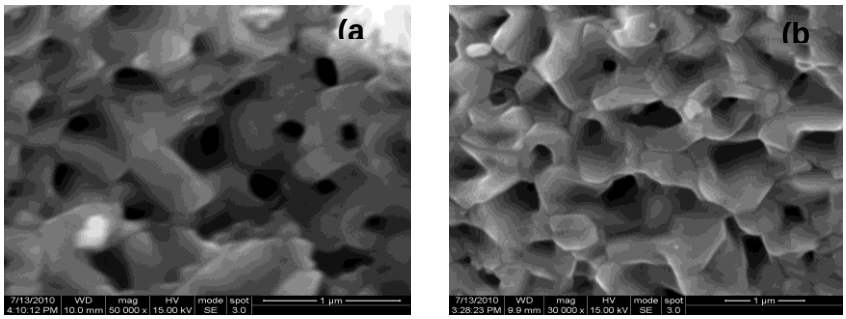

Fig (iv) SEM image for the calcination temperatures of (a) 900 °C and (b)1000°C

While increasing the calcinations temperature, the clear and smooth surface morphologies were obtained. Due to their nanoscale size and surface properties, also nanoparticles tend to aggregate or precipitate in suspensions. The increase in the calcination temperature leads to the formation of porous like structure in the morphology [7]. Further increase in the calcination temperature also yields smooth porous like morphologies. The morphology of the 1000 °C calcinated sample shows the piled up plates. This particular morphology is considered as an optimized sample for further analysis. Based on the scanning electron micrographs, the pore size histograms can be drawn and mean pore size can be determined. Fig (v) shows the pore size distribution for NiO nanoparticles at 1000 °C. The average pore size of the 1000 °C sample is in the range 90 to 300 nm.

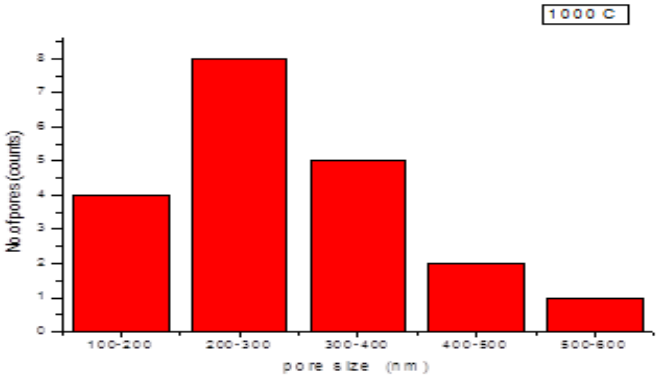

Fig (v) Pore size distribution of 1000 °C calcinated sample

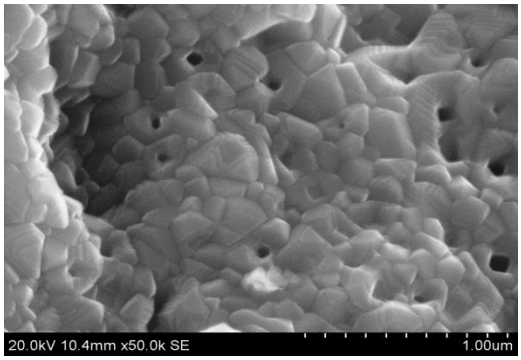

Fig (vi) FESEM image of 1000°C Calcinated sample in air.

The FESEM image of the sample is shown in fig (vi). It shows a fascinating structure for the optimized sample. The image shows the triangle like plates are piled up and the particles are in uniform in size with the prism like grains which are well connected to provide porous structure which is much required for device applications, for instance super capacitors. Since electric double-layer capacitance and pseudocapacitance are interfacial phenomena, the materials for electrochemical capacitors should possess a high specific surface area with a suitable pore-size distribution to enhance the charge-storage capability. In this work we have developed a mesoporous Nickel Oxide with a very high surface area is developed by an anionic template.

Conclusion:

Cite this article as: A Lathamaragatham. "CHARACTERIZATION OF NICKEL OXIDE NANOPARTICLES SYNTHESIZED VIA SOLUTION-PHASE PRECURSOR ROUTE." *International Conference on Systems, Science, Control, Communication, Engineering and Technology (2015)*: 216-220. Print.

Highly-crystallized porus nickel-oxide nanoparticles with average crystallite size of ~35nm were synthesized by a solution-phase precursor route method. Morphology of the resulted powder showed triangle like plates are piled up with lots of pores on the suraface. This method resulted in formation of a well-shaped crystalline and mesoporous product. This phenomenon could be attributed to stoichiometry of the nanoparticles obtained.

References:

[1]. P. Duran, J. Tartaj, C. Moure, J. Am. Ceram. Soc., Vol. 86 (8), 2003, pp. 1326–1329.
[2]. M. Mazaheri, A.M. Zahedi, M.M. Hejazi, Mater. Sci. Eng. A, Vol. 492, 2008, pp. 261–267.
[3]. J. Bahadur, D. Sen, S. Mazumder, S. Ramanathan, J. Sol. Sta. Chem., Vol. 181, 2008, pp. 1227–1235.
[4]. H. Sato, T. Minami, S. Takata, T. Yamada, Thin Solid Films, Vol. 236, 1993, pp. 27.
[5]. Hongxia Qiao, Zhiqiang wei, Hua yang, Lin Zhu, and Xiaoyan yan, journal of Nanomaterials. Volume 2009.
[6]. Y. Bahari Molla Mahaleh, S.K.sadrnezhaad, and D. Hosseini, Journal of nanomaterials, volume 2008.

Cite this article as: A Lathamaragatham. "CHARACTERIZATION OF NICKEL OXIDE NANOPARTICLES SYNTHESIZED VIA SOLUTION-PHASE PRECURSOR ROUTE." *International Conference on Systems, Science, Control, Communication, Engineering and Technology (2015)*: 216-220. Print.

International Conference on Systems, Science, Control, Communication, Engineering and Technology 2015 [ICSSCCET 2015]

ISBN	978-81-929866-1-6
Website	icssccet.org
Received	10 - July - 2015
Article ID	ICSSCCET048

VOL	01
eMail	icssccet@asdf.res.in
Accepted	31- July - 2015
eAID	ICSSCCET.2015.048

Zeta potential measurements in colloidal suspensions

S. Prabhu[1], K. Murugan[2]
[1, 2] Assistant Professor, Karpagam Institute of Technology, Coimbatore

Abstract: *A parameter determining the stability of colloidal suspensions is the amount of surface charge on the particle. Higher the repulsion between like charged particles, better is the stability of the suspension. A method to quantify the suspension stability is its zeta potential which is a measure of the charges on the surface of the particle. This articles describes the measurement of zeta potential and the various factors affecting the zeta potential of suspensions.*

Keywords: Zeta Potential, electro-phoresis, iso-electricpoint

1. Introduction

Particles in colloidal suspensions have positive or negative charges on their surface.This is mainly due to the ionization of chemical groups on the particle surface that produce a charged surface or the preferential adsorption of ions. Deliberately added chemical compounds can also absorb onto the particle surface thus rendering them charged. The amount of charge on the particles is an important characteristic of the particle which determines the properties of the colloidal suspension.

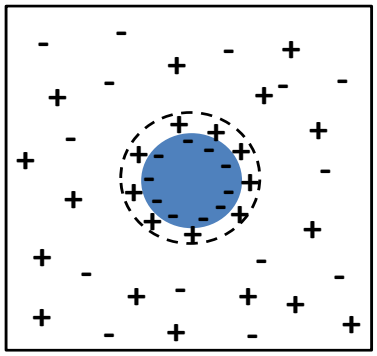

Figure 1: Distribution of charge around a negatively charged particle.

Though particles are electrically neutralthe charge on the surface of each particle is counter balanced by charges(ions) of opposite sign in the surrounding solution.The suspension is neutral overall and also on a scale somewhat larger than the particles themselves.The

Cite this article as: S. Prabhu, K. Murugan. "Zeta potential measurements in colloidal suspensions." *International Conference on Systems, Science, Control, Communication, Engineering and Technology (2015)*: 221-224. Print.

charges on the particle surface are normally considered to be attached ratherfirmly to it and to remain there more or less indefinitely (though they may be exchanging with charges of similar type in the solution). The surrounding (balancing)charge, by contrast, is much more loosely associated with the particle.Because of the thermal motions of the solvent molecules and ions, this counter charge is spread in a diffuse layer which stretches out for some distance (of order nanometres) from the particle surface **(Figure 1).**

The oppositely charged ions (called counter-ions) tend to accumulate around the particle and very few negatively charged (co-ions) can get close to the surface because of the repulsion from the charges on the particle. Farther away from theparticle the co-ions suffer less repulsion and eventually, at distances of at most a few tens of nanometres, the numbers of cationic and anionic charges are evenly balanced.

2.Measuring the Charge on the surface of the particle

Though there are various ways to measure the particle charge the most effective methods is to apply an electric field to the suspension and to measure how fast the particles move as a result. This process is called **electro-phoresis.**

Particles carrying bigger charge move faster.The electrostatic potential near the particle surface is shown in **Figure 2**. The electric field pulls the particle in one direction but it will also be pulling the counter ions in the opposite direction. Some of the counter ions will move with the particle (those within the dotted circle) so the measured charge will be a net charge taking that effect into account.

It changes very quickly (and linearly) from its value at the surface through the first layer of counter ions and then changes more or less exponentially through the diffuse layer.The junction between the bound charges and the diffuse layer is again marked by the broken line.

That surface, which separates the bound charge from the diffuse charge around the particle, marks where the solution and the particle move in opposite directions when an external field is applied. It is called the surface of shear or the slip surface.The electrostatic potential on that surface is called the **zeta potential** and it is that potential which is measured, when one measures the velocity of the particles in a d.c.electric field.The velocity (in metre/second) for a unit field strength (1 Volt per metre) is called the electrophoretic mobility, and is given the symbol U_E. It is related to the zeta potential(ξ), and is usually assumed to measure the potential at the point marked by thebroken line in **Figure 2.**

The velocity is dependent on thestrength of electric field or voltagegradient, the dielectric constant of themedium, the viscosity of the mediumand the zeta potential.The velocity of a particle in a unitelectric field is referred to as itselectrophoretic mobility. Zeta potentialis related to the electrophoretic mobility by the **Henry equation**

$$\mathbf{U_E = 2\,\varepsilon\,\xi f(\kappa a)/3\eta}$$

where U_E = electrophoretic mobility, ξ= zeta potential, ε = dielectricconstant, η = viscosity and f(κa) =Henry's function.

The units of κ, termed the Debyelength, are reciprocal length and κ^{-1} isoften taken as a measure of the"thickness" of the electrical doublelayer. The parameter 'a' refers to theradius of the particle and therefore κameasures the ratio of the particleradius to electrical double layerthickness

When the charge is measured in this way it reflects more realistically what one particle "sees" as it approaches another particle and that is what determines theproperties of the suspension. If the repulsion between approaching particles is largeenough they will bounce away from one another and that will keep the particles in a state of dispersion.

If the repulsive force is not strong enough, the particles will come together and may stick in a permanent doublet. Then other particles may comealong and also be caught in the growing aggregate.The suspension is then unstable and the aggregates will quickly settle out from the surrounding medium. If electric charge alone is relied upon to keep thesystem in a disperse state then the zeta potential will usually need to be kept above25 mV (positive or negative).

The higher the absolute value of the zeta potential, the more stable the system will be. That means it will be better able to withstand additions of salt (which might otherwise destabilize it). It will also usually show a lower viscosity.On the other hand, if one wants to separate the particles and remove them from the surrounding fluid, it will pay to reduce the magnitude of the zeta potential.

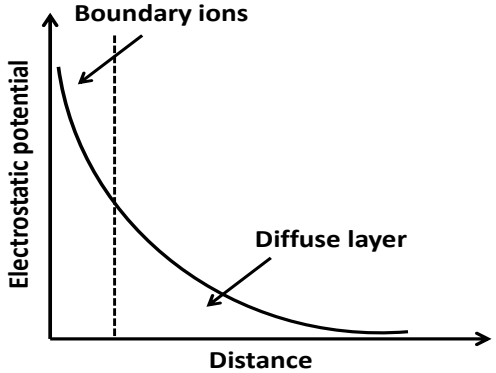

Figure 2: Electrostatic potential around a negatively charged spherical particle.

Cite this article as: S. Prabhu, K. Murugan. "Zeta potential measurements in colloidal suspensions." *International Conference on Systems, Science, Control, Communication, Engineering and Technology (2015)*: 221-224. Print.

3.Factors Affecting Zeta Potential

3.1.pH

In aqueous media, the pH of the sample is one of the most important factors that affects its zeta potential. Azeta potential value on its own without defining the solution conditions is a virtually meaningless number.Imagine a particle in suspension with a negative zeta potential. If more alkali is added to this suspension then the particles tend to acquire more negative charge.

If acid is added to this suspension then a point will bereached where the charge will be neutralised. Further addition of acid will cause a build up of positive charge. Therefore a zeta potential versus pH curve will be positive at lowpH and lower or negative at high pH.There may be a point where the plot passes through zero zeta potential.This point is called the **iso-electricpoint** and is very important from a practical consideration. It is normally the point where the colloidal system isleast stable.

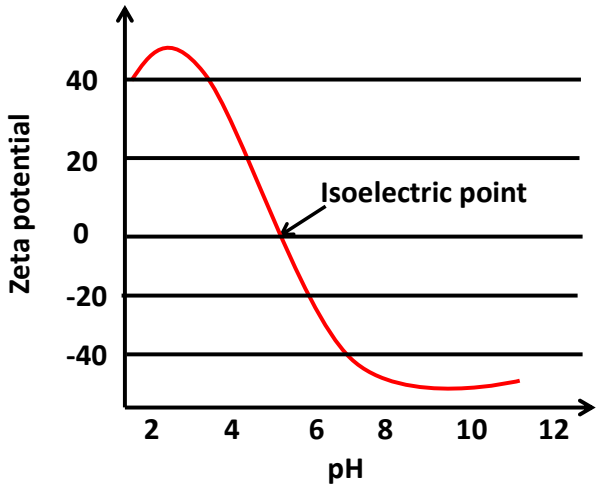

Figure 3: Typical plot of zeta potentialversus pH showing the position of theisoelectric point

A typical plot of zeta potential versus pH is shown in figure 3. In this example, the isoelectric point of the sample is at approximately pH 5.5. In addition, the plot can be used topredict that the sample should be stable at pH values less than 4(sufficient positive charge is present) and greater than pH 7.5 (sufficient negative charge is present). Problems with dispersion stability would be expected at pH values between 4 and7.5 as the zeta potential values are between +30 and -30mV.

3.2. Conductivity

The thickness of the double layer (κ^{-1}) depends upon the concentration of ions in solution and can be calculated from the ionic strength of the medium.The higher the ionic strength, the more compressed the double layer becomes. The valency of the ions will also influence double layer thickness.A trivalent ion such as Al^{3+} willcompress the double layer to a greater extent in comparison with amonovalent ion such as Na^{+}.

Inorganic ions can interact with charged surfaces in one of two distinct ways (i) non-specific ion adsorption where they have no effecton the isoelectric point. (ii) specific ion adsorption, which will lead to achange in the value of the iso-electricpoint. The specific adsorption of ions on to a particle surface, even at low concentrations, can have a dramatic effect on the zeta potential of the particle dispersion. In some cases,specific ion adsorption can lead to charge reversal of the surface.

3.3 Concentration of a formulation component

The effect of the concentration of a formulation component on the zetapotential can give information to assist in formulating a product to give maximum stability. The influence of known contaminants on the zetapotential of a sample can be a powerful tool in formulating the product to resist flocculation for example.

4.Conclusion

This article discusses the method to measure the zeta potential in colloidal suspensions. Zeta potential is an important parameter that determines the stability of colloidal suspensions. It is important to measure the zeta potential of suspensions to get an idea about the properties of the suspensions and to devise methods to enhance their stability.

References

1. Derjaguin, B.V. and Landau, L. (1941)ActaPhysiochim. URSS, 14, 633.
2. Verway, E.J.W. and Overbeek, J. Th.G. (1948) Theory of the Stability ofLyophobic Colloids, Elsevier,Amsterdam.
3. Hunter, R.J. (1988) Zeta Potential InColloid Science: Principles AndApplications, Academic Press, UK.
4. Shaw, D.J. (1992) Introduction ToColloid And Surface Chemistry,Butterworth Heinemann, UK.
5. Everett, D.H. (1994) Basic PrinciplesOf Colloid Science, The Royal Societyof Chemistry, UK.

Cite this article as: S. Prabhu, K. Murugan. "Zeta potential measurements in colloidal suspensions." *International Conference on Systems, Science, Control, Communication, Engineering and Technology (2015)*: 221-224. Print.

6. Ross, S. and Morrison, I.D. (1988)Colloidal Systems and Interfaces,John Wiley and Sons, USA.
7. Lyklema, J. (2000) Fundamentals ofInterface and Colloid Science: Volume1 (Fundamentals), Academic Press,UK.
8. Measuring Zeta Potential: LaserDoppler Electrophoresis, TechnicalNote available fromwww.malvern.co.uk
9. Measuring Zeta Potential UsingPhase Analysis Light Scattering(PALS), Technical Note available fromwww.malvern.co.uk
10. Measuring Zeta Potential: A NewTechnique, Technical Note availablefrom www.malvern.co.uk

Cite this article as: S. Prabhu, K. Murugan. "Zeta potential measurements in colloidal suspensions." *International Conference on Systems, Science, Control, Communication, Engineering and Technology (2015)*: 221-224. Print.

International Conference on Systems, Science, Control, Communication, Engineering and Technology 2015 [ICSSCCET 2015]

ISBN	978-81-929866-1-6
Website	icssccet.org
Received	10 - July - 2015
Article ID	ICSSCCET049

VOL	01
eMail	icssccet@asdf.res.in
Accepted	31- July - 2015
eAID	ICSSCCET.2015.049

Isolation and characterisation of phytoconstituents using low polar solvents from the flowers of *Couroupita guianensis*

Velliangiri Prabhu[1], Subban Ravi[2], S. Elamaran[3], Murugan kamayan[4]
[1]Department of Chemistry, Karpagam College of Engineering, Coimbatore-641032
[2]Department of Chemistry, Karpagam University, Coimbatore-641021
[3]Department of Chemistry, Karpagam Institute of Technology, Coimbatore-641050
[4]Department of Chemistry, Karpagam College of Engineering, Coimbatore-641032

Abstract- *Couroupita guianensis is used extensively as an ingredient in many ayurvedic preparations which cure gastritis, scabies, bleeding piles, dysentery, and scorpion poison. The flower was subjected to extraction with petroleum ether and chloroform solvents. Compounds* ***(CGA-I)*** *octyl 4-(nonanoyloxy) benzoate along with myristoleic acid* ***(CGA-II)****, linoleic acid* ***(CGA-V)*** *and (8E, 10E, 12E)-icosa-8, 10, 12-triene)* ***(CGA-VIII)*** *were isolated by column chromatography and characterised with IR, ^{1}H-NMR, ^{13}C-NMR spectral data.*

Keywords- *Couroupita guianensis, Lecythidaceae, flower, octyl 4-(nonanoyloxy) benzoate, myristoleic acid, linoleic acid, (8E, 10E, 12E)-icosa-8, 10, 12-triene)*

I. INTRODUCTION

During the past decade, the indigenous or traditional system of medicine has gained importance in the field of medicine. In most of the developing countries, a large number of populations still depend on traditional practitioners, who in turn are dependent on medicinal plants, to meet their primary health care needs. Thus, it is clear that herbal medicine plays a pivotal role in therapeutic strategies in the modern world. One such plant that has been used widely in traditional medicine is *Couroupita guianensis* Aubl. belonging to the family *Lecythidaceae*. It is grown in Indian gardens as an ornamental tree. *C. guianensis*, also called as Cannonball tree is native to South India and Malaysia and is commonly known as Nagalinga pushpam in Tamil. In *Ayurveda*, it is called as ayahuma, it is used extensively as an ingredient in many preparations which cure gastritis, scabies, bleeding piles, dysentery, scorpion poison and many [10,4]. It has rubefacint and anti rheumatic properties used in Ayurvedic concepts, cold relief balm. The fruit pulp is used to cure headache. In folk medicine, the flowers are used to cure cold, intestinal gas formation and stomach ache, and also for treating diarrhoea, and when dried and powdered, used as a snuff. The fragrance of flowers is used for curing asthma. The shell of the fruit is used as a utensil. The flowers of *C. guianensis* showed analgesic and anti-inflammatory activity and immunomodulatory activity, anthelmintic activity, antimicrobial, wound healing and antioxidant activity, antinociceptive activity Geetha et al. [3], Pradhan et al. [6], Farrukh Aqil et al. [2], Rajamanickam et al. [7], Umachigi et al. [11] and Pinheiro et al.[5]. Previous work on *C. guianensis* has showed that the plant consists of several chemical constituents with novel structures and possesses bio-active moieties. This includes eugenol, linalool,

Cite this article as: Velliangiri Prabhu, Subban Ravi, S. Elamaran, Murugan kamayan. "Isolation and characterisation of phytoconstituents using low polar solvents from the flowers of Couroupita guianensis." *International Conference on Systems, Science, Control, Communication, Engineering and Technology (2015)*: 225-228. Print.

farnesol, nerol, tryptanthrine, indigo, indirubin, isatin, linoleic acid, α, β- amyrins, carotenoids and sterols [12], Rane et al.[8], Bergman et al. [1] and Sen et al. [9]. Albeit, the known uses of the plant parts and their extracts in various disorders, especially those against microbial infections, none of the studies aimed at isolation and identification of the constituents from the flowers of *C. guianensis*. This prompted us to undertake the present work and we have isolated and identified the four compounds **CGA-I**, **CGA- II**, **CGA- V** and **CGA-VIII** from *C. guianensis* by chromatographic and spectral methods.

Experimental

A. Plant material

Fresh flowers of *C. guianensis* was collected in February, 2010, from Palakkad district, Kerala and the plant species was authenticated in the Department of life science, Karpagam University, Coimbatore-21. Voucher specimen was preserved in our Department (No. KU11CHE1934).

B. Extraction and Isolation

The 5.2 Kg of powdered, dried flower was extracted thrice (3X72 hrs) with petroleum ether under cold percolation. The combined extract was subjected to distillation and concentrated under *vacuo* to yield a residue A of 6.3 gm. When monitored by TLC using (8:2) petroleum ether: ethyl acetate showed the presence of 2 major compounds with R_f values 0.62 and 0.54 respectively and 2 minor compounds with R_f values 0.84 and 0.18. The residue was subjected to column chromatography. The column was packed with 120 gm of silica gel. Initially the column was eluted with petroleum ether and with increasing amount of ethyl acetate and fractions of 20 ml were collected and monitored with TLC using petroleum ether and ethyl acetate (9:1) solvent system. Iodine vapour was used as the identification reagent. On eluting the column fraction 7 to 9, compound **CGA-I** (0.40 mg), 10 to 17, compound **CGA- II** (160 mg) were found to be homogeneous by TLC.

After defatting, the plant material was subjected to sequential extraction with chloroform (2X72 hrs) to yield residue B (11.6 g). Residue B on column chromatography and on elution with petroleum ether: ethyl acetate (8:2) yielded 46 gm of residue in the fractions 6-8 with on R_f value 0.49 compound **CGA-V**. Further three more compounds were isolated from the fractions 37-65 compound CGA-VI (53.2 mg), fractions 97-123 compound CGA-VII (81 mg) and fractions 124-144 compound **CGA-VIII** (76 mg) were obtained when the column was eluted with the solvent system petroleum ether and ethyl acetate (5:5) and were homogeneous by TLC. The structure of the compounds **CGA-I**, **CGA- II**, **CGA- V** and **CGA-VIII** were shown in "fig.1."

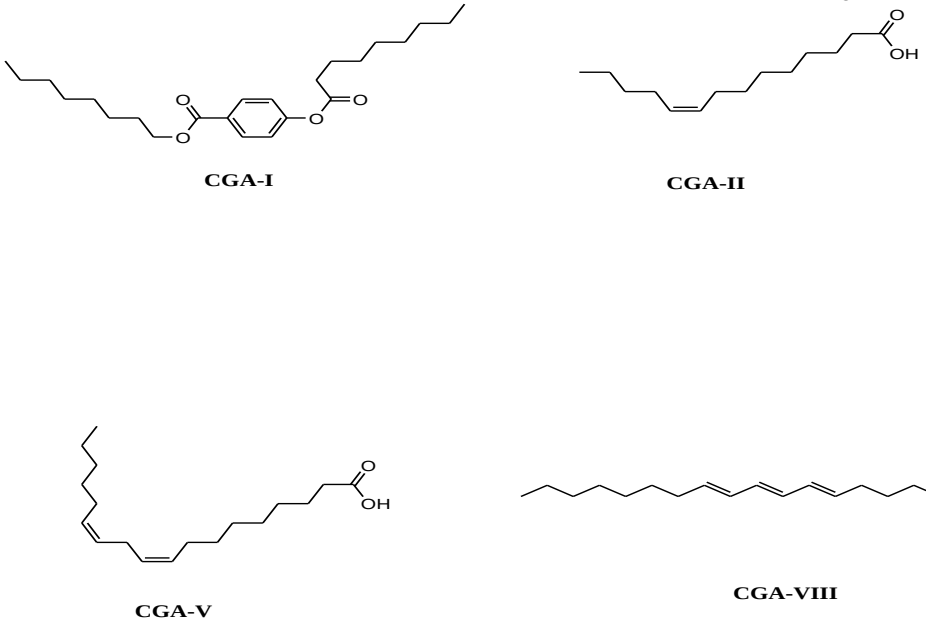

CGA-I **CGA-II**

CGA-V **CGA-VIII**

Figure 1: Structure of the compounds **CGA-I**, **CGA- II**, **CGA- V** and **CGA-VIII**

General

^{1}H-NMR and Spectra ^{13}C-NMR were recorded on a Bruker AM-400 (400 MHz) instrument; chemical shifts δ in ppm with TMS as internal standard, coupling constants J in Hz. Perkin –Elmer model 1650 IR instrument was used to carried the IR spectra.

CGA-I

IR ν_{max} (KBr): 1730, 1600, 2988, 1450 and 1375 cm^{-1}

^{1}H-NMR (400 MHz, $CDCl_3$, δ in ppm, J in Hz): 7.63, 7.45 (4H, dd, J= 6.2 Hz, 2.0 Hz, H-2, H-6, H-5), 4.00 (2H, t, H-2'), 2.29 (2H, t, H-2''), 2.00 (2H, m, H-3'), 1.56, 1.25 (2H, m), 0.832(12H).

^{13}C-NMR (100 MHz, $CDCl_3$, δ in ppm):74.93 (C=O), 163.56(C=O), 128.28 (C=C) 126.66(C-3, C-5), 127.07 (C-1, C-4), 124.46 (C-1), 126.66 (C-2, C-6), 34.57(C-2'').

CGA-II

IR ν_{max} (KBr): 1712, 1581, 2924, 1456 and 1375 cm^{-1}

Cite this article as: Velliangiri Prabhu, Subban Ravi, S. Elamaran, Murugan kamayan. "Isolation and characterisation of phytoconstituents using low polar solvents from the flowers of Couroupita guianensis." *International Conference on Systems, Science, Control, Communication, Engineering and Technology (2015)*: 225-228. Print.

^{1}H-NMR (400 MHz, $CDCl_3$, δ in ppm, J in Hz): 5.20 (2H, m), 2.10 (2H, d, H-2), 2.0 (2H, m), 1.29 (16 H, s).
^{13}C-NMR (100 MHz, $CDCl_3$, δ in ppm):174.72 (C=O), 130.02 (C=C), 128.04 (C=C), 22.21(C-C), 22.33(C-C), 24.77(C-C), 25.51(C-C), 26.90(C-C), 28.81(C-C), 28.97(C-C), 29.14(C-C), 29.25(C-C), 31.18(C-C), 31.54(C-C), 33.98(C-C), 41.67 (C-C), 14.16 (C-C).

CGA-V

IR ν_{max} (KBr): 1709, 1581, 2925, 2854 and 1465 cm^{-1}
^{1}H-NMR (400 MHz, $CDCl_3$, δ in ppm, J in Hz):5.29 (2H, m), 2.7, 2.8 (2H, d), 2.29 (2H, d, H-2), 2.0 (2H, m) 1.29 (16 H, s) 0.81 (6H, s).
^{13}C-NMR (100 MHz, $CDCl_3$, δ in ppm): 180.00 (COOH), 130.22, 130.02 (C=C) 128.07, 127.91 (C=C), 128.04 (C=C), 22.56 (C-C), 22.68(C-C), 24.71(C-C), 25.63(C-C), 27.18(C-C), 27.28(C-C), 27.20(C-C), 29.04(C-C), 29.14(C-C), 29.25(C-C), 29.35(C-C), 29.43(C-C), 29.58(C-C), 29.68(C-C), 31.52(C-C), 31.92(C-C), 33.94 (C-C).

CGA-VIII

IR ν_{max} (KBr): 1465, 2854, 2925, 1595 and 1375 cm^{-1}
^{1}H-NMR (400 MHz, $CDCl_3$, δ in ppm, J in Hz): 5.10 (2H, m), 2.01 and 1.93 (8H, m), 1.56 (3H, s), 1.18 (10H, m), 0.765 (12H, m).
^{13}C-NMR (100 MHz, $CDCl_3$, δ in ppm): 135.06, 134.85 (C=C), 131.18, 124.43 (C=C), 124.32, 124.29 (C=C), 22.68 (C-C), 25.66(C-C), 26.67(C-C), 26.78(C-C), 28.27(C-C), 29.35(C-C), 29.60(C-C), 29.69(C-C), 30.03(C-C), 31.92(C-C), 39.75(C-C), 39.73(C-C), 37.10(C-C), 37.02(C-C), 14.09(C-C), 15.98(C-C), 16.02(C-C), 17.65(C-C).

II. RESULT AND DISCUSSION

CGA-I

The IR spectra exhibited absorption bands at 1730 cm^{-1} showing the presence of a carbonyl group, 1600 cm^{-1} for a C=C group and at 2988 cm^{-1} and 1450 and 1375 cm^{-1} for the presence of C-H. The ^{1}H-NMR spectrum shows the presence of a multiplet of signals at δ 0.832 for 12 protons suggesting the presence of four methyl groups. This along with the complex multiplet signal at δ 1.56 (Fig 45) indicates the presence of two isopropyl groups. The broad singlet at δ 1.25 strongly suggests the presence of a long chain of methylene groups in the compound. The signal at δ 2.00 (H-3') is indicative of the presence of a methylene group in the β-position to an oxygen function. The triplet signal at δ 4.00 (H-2') is due a methylene group attached to an oxygen function. The triplet at δ 2.29 for two protons (H-2") may be assigned to a methylene group attached to a carbonyl group. Apart from this two signals were observed at δ 7.45 (H-2 and H-6) and 7.63 (H-3 & H-5) as doublet of doublets (J= 6.2 Hz, 2.0 Hz) suggests the presence of four aromatic protons. Complementing the above data the ^{13}C-NMR spectra showed two signals at δ 174.93 and 163.56 for two ester carbonyls in two different environments. In the aromatic region of the spectra it showed the presence of only signals at δ 128.28 (C-3, C-5), 126.66(C-2, C-6) (Fig 46) and a weak signal at δ 127.07 (for quaternary C-1, C-4) each for two carbons. There is only one signal is observed at δ 63.99 indicating the presence of only one carbon atom attached to the oxygen function. The signal at δ 34.57 is assigned to a carbon atom (C-2") attached to a carbonyl group. Eventhough the compound showed two carbonyl groups only one methylene group is observed under oxygen function and another methylene group is attached to the carbonyl group. This supports the assignments made in the ^{1}H-NMR spectral data for the signals at δ 2.29 and 4.00. It may be suggested that in the aromatic ring the C-1 position may be a phenolic position where it is esterified with a long chain fatty acid and the C-4 position may have a carboxylic acid group which is esterified with a long chain alcohol. Based on the above spectral data the assumption of structure of the compound may be assigned as (octyl 4-(nonanoyloxy) benzoate).

CGA-II

The IR spectra exhibited absorption bands at 1712 cm^{-1} showing the presence of a carbonyl group, 1581 cm^{-1} for a C=C group and at 2924 cm^{-1} and 1465 and 1375 cm^{-1} for the presence of C-H.

The ^{1}H-NMR spectrum shows the presence of a triplet signal at δ 0.83 for 3 protons suggesting the presence of a methyl group. The broad singlet at δ 1.29 for 16 protons strongly suggests the presence of a long chain of methylene groups in the compound. The triplet at δ 2.10 for two protons (H-2) is assigned to a methylene group attached to a carbonyl group The signal at δ 2.00 is indicative of the presence of a methylene group in the allylic position to the double bond. The multiplet signal at δ 5.20 (Fig 47) is due the protons of the double bond. This suggests the presence of a long chain unsaturated fatty acid.

The above assignment was supported by the ^{13}C-NMR spectral data by exhibiting a signal at δ 174.72 for a carbonyl group, δ 130.02 and 128.04 for the presence of a C=C double bond, 14.16 for a methyl group carbon, δ 41.67 for the α-carbon atom of the carbonyl group. A group of signals 22.21, 22.33, 24.77, 25.51, 26.90, 28.81, 28.97, 29.14, 29.25, 31.18, 31.54, 33.98 (Fig 48) are due to the long chain methylene groups carbon atom of the fatty acid. Presence of two carbon atoms in the unsaturated region of the spectrum suggests that only one double bond is present in the compound. Based on the above data the assumption of the compound is a unsaturated fatty acid (Myristoleic acid).

CGA-V

The IR spectra exhibited absorption bands at 1709 cm^{-1} showing the presence of a carbonyl group, 1581 cm^{-1} for a C=C group and at 2925, 2854 cm^{-1} and 1465 and 1375 cm^{-1} for the presence of C-H.

The ^{1}H-NMR spectrum shows the presence of a triplet signal at δ 0.81 for 6 protons suggesting the presence of two methyl group. This along with the complex multiplet signal at δ 1.56 indicates the presence of an isopropyl group. The broad singlet at δ 1.29 for 16

Cite this article as: Velliangiri Prabhu, Subban Ravi, S. Elamaran, Murugan kamayan. "Isolation and characterisation of phytoconstituents using low polar solvents from the flowers of Couroupita guianensis." *International Conference on Systems, Science, Control, Communication, Engineering and Technology (2015)*: 225-228. Print.

protons strongly suggests the presence of a long chain of methylene groups in the compound. The triplet at δ 2.29 for two protons (H-2) is assigned to a methylene group attached to a carbonyl group The signal at δ 2.00 is indicative of the presence of a methylene group in the allylic position to the double bond. The multiplet signal at δ 5.29 (Fig 49) is due the protons of the double bond. This suggests the presence of a long chain unsaturated fatty acid. Absence of bis-allylic protons between δ 2.7 and 2.8 indicates that the double bonds are conjugated.

The above assignment was supported by the ^{13}C-NMR spectral data by exhibiting a signal at δ 180.00 for a carbonyl group, δ 130.22,130.02 128.07 and 127.91 for the presence of two C=C double bond, 11.50 for a methyl group carbon, δ 33.94 for the α-carbon atom of the carbonyl group. A group of signals 22.56, 22.68, 24.71, 25.63, 27.18, 27.28, 27.20, 29.04, 29.14, 29.25, 29.35, 29.43, 29.58, 29.68, 31.52, 31.92 (Fig 50) are due to the long chain methylene groups carbon atom of the fatty acid. Based on the above data the assumption of the compound is Linoleic acid an unsaturated fatty acid with two double bonds conjugated to each other.

CGA-VIII

The IR spectra exhibited absorption bands at 1595 cm^{-1} for a C=C group and at 2925, 2854 cm^{-1} and 1465 and 1375 cm^{-1} for the presence of C-H.

The ^{1}H-NMR spectrum shows the presence of a multiplet signal at δ 0.765 for 12 protons suggesting the presence of four methyl group. The broad singlet at δ 1.18 for 10 protons strongly suggests the presence of a long chain of methylene groups in the compound. A group of signals at δ 1.56 indicates the presence of methyl groups attached to the unsaturated carbon atoms. The triplet at δ 2.01 and 1.93 for eight protons is assigned to a methylene group attached to allylic position position of the double bonds. The multiplet signal at δ 5.10 (Fig 51) is due the protons of the double bond. The above assignment was supported by the ^{13}C-NMR spectral data by exhibiting signals at δ 135.06, 134.85, 131.18, 124.43, 124.32 and 124.29 for the presence of three C=C double bond, 14.09, 15.98, 16.02 and 17.65 for four methyl group carbons, δ 39.75, 39.73, 37.10, and 37.02 belongs to the carbon adjacent to quaternary atoms, A group of signals 22.68, 25.66, 26.67, 26.78, 28.27, 29.35, 29.60, 29.69, 30.03 and 31.92 (Fig 52) are due to methylene groups of a long chain unsaturated hydrocarbon carbon atoms. Based on the above data the assumption of the compound is an unsaturated hydrocarbon with three double bonds conjugated to each other. It may be a sesquiterpenoid (8E, 10E, 12E)-icosa-8, 10, 12-triene).

II. CONCLUSION

A compound **CGA-(I)** octyl 4-(nonanoyloxy) benzoate along with myristoleic acid **(CGA-(II)**, linoleic acid **(CGA-(V)**, (8E, 10E, 12E)-icosa-8, 10, 12-triene) **(CGA-(VIII)** were isolated from *C. guianensis* and characterized by IR, ^{1}H-NMR and ^{13}C-NMR spectral data.

REFERENCES

[1] J.Bergman, J.O. Lindstrom and U. Tilstam, "The structure and properties of some indolic constituents in *Couroupita guianensis* Aubl," Tetrahedron, 41, pp. 2879-2881, 1985.

[2] Farrukh Aqil, Iqbal Ahmad, and Zafar Mehmood, "Antioxidant and Free Radical Scavenging properties of twelve traditionally usedIndian Medicinal Plants," Turk. Journal of Biol, 30, pp. 177-183, 2006.

[3] M.Geetha, M.B.Shankar, R. S. Mehta, and A.K. Saluja, "Antifertility activity of *Artabotrys odoratissimus* Roxb *Tissimus* Roxb and *Couroupit guianensis* Aubl," Journal of Nat. Remed, 5(2), pp. 121-125, 2005.

[4] B.Halliwell and J.M. Gutterisdge, *Free radicals in biology and medicine*," 2nd ed., Oxford: Clanrendon, 1999, pp. 148-166.

[5] M.M. Pinheiro, S.O. Bessa, C.E. Fingolo, R.M. Kuster, M.E. Matheus, F.S. Menezes, and P.D. Fernandes, "Antinociceptive activity of fractions from *Couroupita guianensis* Aubl. Leaves," J. of Ethnopharm, 127(2), pp. 407-413, 2010.

[6] D. Pradhan, P.K. Panda, and G. Tripathy, "Evaluation of the immunomodulatory activity of the methanolic extract of *Couroupita guianensis* Aubl flowers in rats," Nat. Prod. Rad, 8(1), pp. 37-42, 2008.

[7] V. Rajamanickam, A. Rajasekaran, S. Darlin quine, M. Jesupillai, and R. Sabitha, "Anthelmintic activity of the flower extract of *Couroupita guianensis*," Int. Journal of alt. Med, 8(1), 2009.

[8] J.B. Rane, S.J. Vahanwala, S.G. Golatkar, R.Y. Ambaye, and B.G. Khadse, "Chemical examination of the flowers of *Couroupita guianensis* Aubl," Ind. Journal of Pharmaceut. Sci, 63, pp. 72-73, 2001.

[9] A.K. Sen, S.B. Mahato, and N.L. Dutta, "Couroupitine A, a new alkaloid from Couroupita guianensis," Tetrahedron Letters, 7, pp. 609-610, 1974.

[10] G.E. Trease, and M.C. Evans, *Text book of pharmacognosy*, 12th ed., Bailer Tindall. London, pp. 343-382, 2002.

[11] S.P. Umachigi, K.N. Jayaveera, C.K. Ashok kumar, and G.S. Kumar, "Antimicrobial, wound healing, and antioxidant potential of *Couroupita guianensis* inrats," Pharmacol, 3, pp. 269-281, 2007.

[12] K.C. Wong, and D.Y. Tie, "Volatile constituents of *Couroupita guianensis* Aubl. Flowers," J. of Ess. Oil Res, 7, pp. 225-227, 1995.

Cite this article as: Velliangiri Prabhu, Subban Ravi, S. Elamaran, Murugan kamayan. "Isolation and characterisation of phytoconstituents using low polar solvents from the flowers of Couroupita guianensis." *International Conference on Systems, Science, Control, Communication, Engineering and Technology (2015)*: 225-228. Print.

International Conference on Systems, Science, Control, Communication, Engineering and Technology 2015 [ICSSCCET 2015]

ISBN	978-81-929866-1-6	**VOL**	01
Website	icssccet.org	**eMail**	icssccet@asdf.res.in
Received	10 - July - 2015	**Accepted**	31- July - 2015
Article ID	ICSSCCET050	**eAID**	ICSSCCET.2015.050

Optimization of Training phase of Elman Neural Networks by suitable adjustments on the Network parameters

N.Mohana Sundaram[1] , P.N Ramesh[2]
[1, 2] Faculty of Computer Science and Engineering
Karpagam Institute of Technology, Coimbatore

ABSTRACT : *The Elman Neural Network (ENN) is a type of recurrent network that has a context layer as an inside self-referenced layer .The ENN is trained in a supervised manner using the popular back propagation algorithm, based on the inputs and targets given to the network. Various parameters of the network like initialization of weights, types of inputs, number of hidden neurons, learning rate and momentum factor influence the training behaviour of the network. There exists no solid formula to guarantee that the network will converge to an optimum solution or to a faster convergence or convergence even occurs at all. If the parameters of the network are wrongly selected, then it may take a long time for the network to train or some times the network may not get converged at all. In this work the performance of the network is analyzed using extensive tests by adjusting the values of the above referred parameters to find the optimum condition of learning. A digital system, Binary to ASCII Converter is considered for carrying out the experiments. The optimum conditions are presented in this paper.*

Keyword: Elman neural network, weights, hidden neurons, network parameters, learning rate, momentum factor.

I. INTRODUCTION

A recurrent neural network called Elman Neural Network (ENN) was proposed by JEFFREY L.ELMAN which has two-layers back with an additional feedback connection from the output of the hidden layer to its input layer called context layer [1]. The additional units are called "Context Units". It is a recurrent network with context layer containing context units with a fixed weight of 1 such that the contents of hidden layer are copied to context layer on a one-to-one basis [1, 2,12] as shown in FIG 1.

Cite this article as: N.Mohana Sundaram, P.N Ramesh. "Optimization of Training phase of Elman Neural Networks by suitable adjustments on the Network parameters." *International Conference on Systems, Science, Control, Communication, Engineering and Technology (2015)*: 229-235 Print.

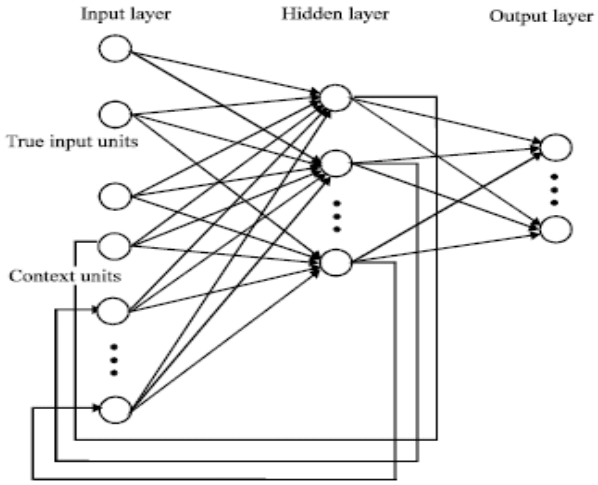

Fig 1. ELMAN network showing the additional Context layer

The context units save previous output values of hidden layer neurons and are fed back fully connected to hidden layer neurons and thus they serve as additional inputs to the network. During the operation of the net both the current input from the input layer and previous state of the hidden layer saved in the context layer are passed to the hidden layer. The hidden layer processes them and pass to the output layer.

II.TRAINING THE ENN

The famous Back Propagation Algorithm or the Error Back Propagation Algorithm is used to train the Elman Neural Network which updates the hidden–output, the input–hidden and the context–hidden weights in order to reduce the difference between the output of the output layer and its desired output. Since the network training algorithm is supervised, the desired outputs are necessary and serve as a reference to calculate errors. Basically, error back propagation algorithm consists of two passes through the different layers of the network: a forward pass and a back-ward pass. In the forward pass, input vector is applied to the input node of the network, and its effect propagates through the network layer by layer. Finally, a set of outputs is produced as the actual response of the network. The synaptic weights of the networks are all fixed during the forward pass. The backward pass starts at the output layer by passing error signals leftward through the network and recursively computing the local gradient for each neuron. This permits the synaptic weights of the net-work to be all adjusted in accordance with an error-correction rule.[2,8,12] The algorithm is stopped when the error has become small and within in the set tolerance error value. Finding the best set of weights and biases for the neural network is the objective of the training. Training with back-propagation is an iterative process. At each iteration, back-propagation algorithm computes a new set of neural network weight and bias values that in theory generate output values that are closer to the target values. So Back-propagation algorithm calculates the gradient of the error and then propagates error backward through the network to modify the weights and biases.[2,4,8,12].

II.MODELING AND SIMULATION

The Elman Network is modelled and simulated using MATLAB.The Problem considered for analysis is a digital system, "Binary to ASCII Encoder". The Seven Bit ASCII equivalent Binary code is the Input to the Network. The Output is the Normalized Decimal Equivalent of the ASCII.For Example the ASCII value of 'A' is 65. The equivalent Binary code is 1000001. So for 'A' the input is: 1000001 and the output is: 0.65 (65 normalized to 0.65) . In case of bipolar inputs the input is 1 -1 -1 -1 -1 -1 1.For 'B' the input is: 1000010 (in case of bipolar inputs it is 1 -1 -1 -1 -1 1 -1 and the output is 0.66 and so on.A set of 60 data a used for training and for testing/validation 30 data are used.The inputs are Binary values and the outputs are Analog values (Decimal values) which is more effective for the analysis.So the ENN has Seven (7) input neurons and One (1) output Neuron.The number of Hidden layer Neurons varied with different values to conduct the analysis. The number of neurons in Context layer is same as the number of neurons in hidden layer.Transfer function of the hidden neurons and output neurons are the Tan sigmoid function or the hyperbolic tangent function which is shown in Fig2.

Cite this article as: N.Mohana Sundaram, P.N Ramesh. "Optimization of Training phase of Elman Neural Networks by suitable adjustments on the Network parameters." *International Conference on Systems, Science, Control, Communication, Engineering and Technology (2015)*: 229-235 Print.

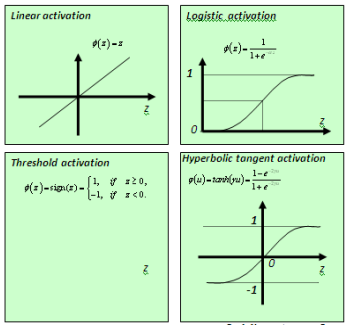

Fig 2. Various Activation Functions

The Sigmoid (logistic) function is chosen because the biological neurons are activated by similar function and it offers a fast response. Further as the outputs are positive analog values, the LOG Sigmoid is chosen rather than Tan Sigmoid. Error function is SSE (Sum Squared Error) which measures the performance of the network .The following Table shows the Architecture of the ENN and the parameters

Table 1
Table showing the ENN Architecture and parameters

Number of Input Neurons	7
Number of output Neurons	1
Number of Hidden Layers	1
Number of Hidden Neurons	Varied to find optimum
Activation Function for both layers	Tan Sigmoid
Performance function (error)	SSE(Sum Squared Error)
Training Algorithm	Back Propagation
Learning Rate	Varied to find optimum
Momentum factor	Varied to find optimum
Weight Initialization	Different methods

Also the training function for the network updates weight and bias values with Levenberg–Marquardt optimization. The self-adaptive learning function is the gradient descent with momentum weight and bias learning function.

III.DATA REPRESENTATION

For Binary inputs the data may be represented in Binary form (0, 1) or Bipolar Form (-1, 1).The output of a neuron depends on the factor 'input x weight'. If input is '0' then the output may be of a small value and the Gradient may be constant which results in long period of Convergence or No convergence at all.This suggests that learning may be improved if the input is represented in bipolar form and the bipolar sigmoid is used for the activation function In this work the Convergence take after more than 4700 epochs for binary inputs(fig 3a) and 2556 Epochs for Bipolar Inputs(Fig 3b) , the other conditions being same.

Fig 3a. The learning curve for Binary inputs

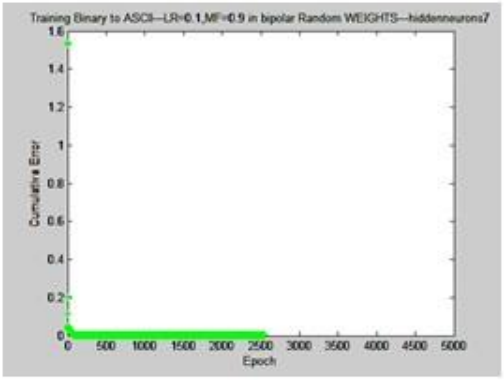

Fig 3b. The learning curve for bipolar inputs

Cite this article as: N.Mohana Sundaram, P.N Ramesh. "Optimization of Training phase of Elman Neural Networks by suitable adjustments on the Network parameters." *International Conference on Systems, Science, Control, Communication, Engineering and Technology (2015)*: 229-235 Print.

IV. WEIGHTS INITIALIZATION

Weight initialization is one of the most effective approaches in speeding up the training of all types of neural networks[2, 3, 5, 7, and 12]. In most of the cases all the initial weights of recurrent networks are set randomly instead of using any prior knowledge and thus the trained networks are vague to human and their convergence speed is slow.[2,3,5,7,12] The initial weights influence how rapidly the net converges during training phase.The initial assignment of value to weights brings a major impact towards the Learning Behavior of the Network.If the algorithm computes successfully the correct value of the weight (rather ∂w) it can converge to a faster solution.Otherwise the convergence may be slow or will not converge at all.Faster learning can be obtained by using

NGUYEN-WIDROW initialization. [7]

$$\beta=0.7(p)^{1/n}$$

where n=no of input units p=no of hidden units and β=scale factor.

The analysis is conducted with different weight initializations.In the beginning the random weights are set only with + weights and the convergence is not obtained even after 5000 epochs.The initial weights are set at random with both +ve and –ve initial weights and with 9 hidden neurons the the network converges at 2262 epochs.(fig 4a)

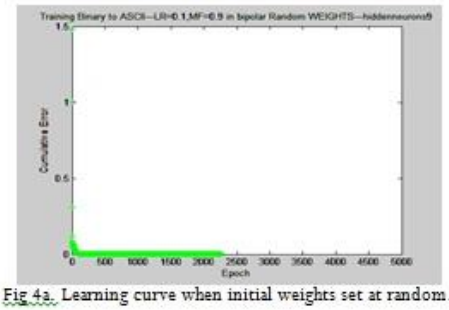

Fig 4a. Learning curve when initial weights set at random.

By setting initial weights using Nyguen-Widrow method (between -0.01 to +0.7), the network converges at 1351 epochs , other settings being the same.(fig 4b.)

Steps in NW initialization

Initialize weights with random numbers between -0.5 to +0.5

Compute the previous weights Vij(old).

Reinitialize weights as

$$Vij = \beta\ Vij(old).\ /\ I\ Vij(old)\ |$$

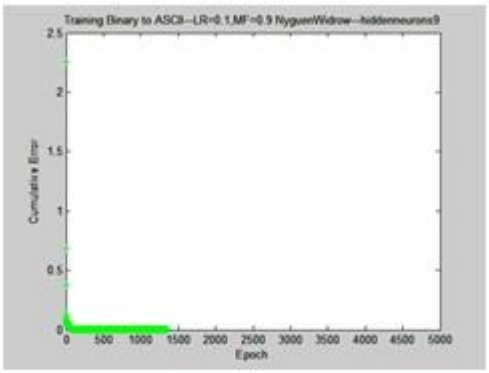

Fig 4b. Learning curve when initial weights set using Nyguen-widrow initialization.

Cite this article as: N.Mohana Sundaram, P.N Ramesh. "Optimization of Training phase of Elman Neural Networks by suitable adjustments on the Network parameters." *International Conference on Systems, Science, Control, Communication, Engineering and Technology (2015)*: 229-235 Print.

V.LEARNING RATE (Γ) AND MOMEMTUM FACTOR(A)

When using backpropagation in a network with n different weights w1, w2, …, wn, the i-th correction for weight wk is given by $\Delta wk(i) = -\gamma\, \partial E\, \partial wk + \alpha \Delta wk(i-1)$, where γ and α are the learning and momentum rate respectively.Normally, we are interested in accelerating convergence to a minimum of the error function which can be done by increasing the learning rate up to an optimal value. Introduction of the momentum rate allows the attenuation of oscillations in the iteration process.The adjustment of both learning parameters to obtain the best possible convergence is normally done by trial and error or by some kind of random search. Since the optimal parameters are highly dependent on the learning task, no general strategy has been developed to deal with this problem.When the learning rate is less, the learning is slow but the accuracy is high.But if it is higher more oscillations are produced and accuracy is very low even though the convergence is faster.In this work the analysis is conducted for learning rates of 0.1,0.2 and 0.3.Even for learning factor 0.2 there is no convergence and the error is high. The learning curves are shown in figures 5a,5b and 5c. When learning rate is high it can be observed more oscillations and more errors even though the learning is faster.

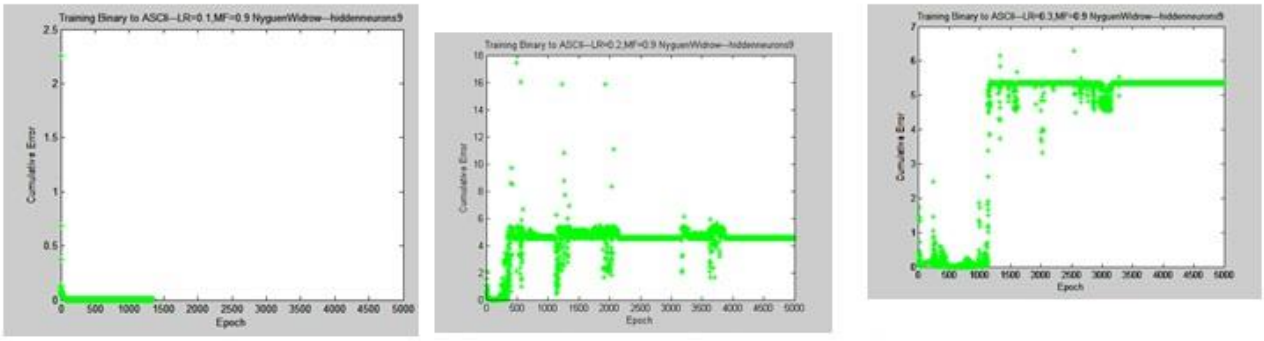

Fig 5a, 5b and 5c. Learning curves for learning rates 0.1, 0.2 and 0.3.

For higher learning rates more oscillations can be observed and more errors occur even though the convergence is faster.The Momentum factor is introduced to make the learning(convergence) faster by arresting the oscillations. In this work it is set at 0.9 and at 0.6 and lesser than 0.6 results in non-convergence. It can be observed from figures 6a and 6b that for mf=0.9 the learning curve converges at 1351 epochs while for mf=0.7 it converges at 3100 epochs , other conditions being the same.

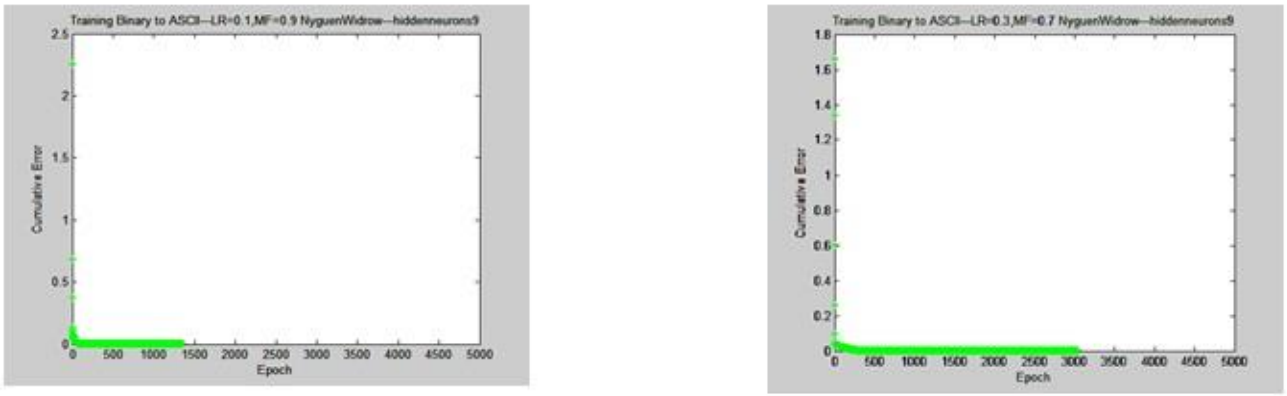

Fig 6a and 6b. Learning curves for mf=0.9 and mf=0.7

VI.NUMBER OF HIDDEN NEURONS:

Number of Hidden layer neurons play vital role in the performance. If more number of neurons is present then error calculations may consume more time and the convergence may be slower.If less number of neurons is present then the accuracy is lost.There is no Hard and fast rule or formula to fix the number of Hidden layer Neurons. In this work Number of Hidden Neurons are set as 5, ,9,12 and 14 and the performance is analyzed. The setting of different values to the network parameters and the effects are presented in Table 2.

Cite this article as: N.Mohana Sundaram, P.N Ramesh. "Optimization of Training phase of Elman Neural Networks by suitable adjustments on the Network parameters." *International Conference on Systems, Science, Control, Communication, Engineering and Technology (2015)*: 229-235 Print.

Table 2

Simulation Results --- Optimum condition is highlighted

NI=7, NO=7, NC=NH, Momentum factor = 0.9,
Input type= Bipolar inputs (-1,1) , SSE Tolerance= 0.0001

S.No.	LR	Weight initialization	NH	No of Epochs	% error * (calculated based on the number of wrong outputs out of 30 test data)
1	0.1	Random weights With both –ve and –ve values	5	2474	3.33
2			7	2350	3.33
3			9	1601	0
4			12	1693	0
5			15	2891	0
1	0.1	Nyguen- Widrow method Values between -0.01 to 0.70	5	1637	3.33
2			7	1712	0
3			9	1300	0
4			12	951	0
5			15	1255	0
1	0.2	Nyguen- Widrow method Values between -0.01 to 0.70	5	1432	66.66
2			7	2615	66.66
3			9	NO CONVERGANCE	
4			12		
5			14		

NI=7, NO=7, NC=NH, Momentum factor = 0.9,
Input type= Binary Inputs (0,1) , SSE Tolerance= 0.0001

S.No.	LR	Weight initialization	NH	No of Epochs	% error
1	0.1	Nyguen- Widrow method Values between -0.01 to 0.70	5	5085	6.66
2			7	4823	0
3			9	3745	0
4			12	3367	0
5			15	4756	0
1	0.1	Random weights With both –ve and –ve values	5	5800	0
2			7	4700	0
3			9	4050	0
4			12	NO Convergence	No output
5			15		

NI=7, NO=7, NC=NH, Momentum factor = 0.7,
Input type= Bipolar inputs , SSE Tolerance= 0.0001

S.No.	LR	Weight initialization	NH	No of Epochs	% error
1	0.1	Nyguen- Widrow method	5	5007	3.33
2			7	3702	0
3			9	3479	0
4			12	3063	0
5			14	4634	0

*The % error is calculated based on the number of incorrect outputs.Out of 30 input data if one output goes wrong then the % error is 1/30 (3.33%)

VII.DISCUSSIONS

A set of 60 data of containing 7 binary values (ASCII equivalent) and corresponding normalized decimal values are used for training.For testing 20 data are used.A set of 10 simulations are performed for each condition and the average values are tabulated. From the above shown results the weight initialization plays an important role in optimizing the learning with out affecting the accuracy. Using the Nyguen-Widrow weight initialization method the optimum condition is arrived with 951 epochs when the learning rate is 0.1, the momentum factor is 0.9 and the number of hidden neurons are 12.If the learning rate is increased even though quicker learning is achieved the errors are more implying that the network has not learned properly. If momentum factor is decreased the learning becomes slow.

VIII.CONCLUSION

In this work the effects the variations of the parameters like initialization of weights, number of hidden neurons, input data, learning rate and momentum factor on the training the Elman Neural Network are analyzed and the optimum condition of the parameters is arrived. Normally the bipolar data types are to be used rather than binary type , because for binary data the network will take a long time to get trained and sometimes no convergence is arrived. Like wise Weights are initialised using Nyguen-widrow method for faster and accurate learning. Further a small learning rate and a large momentum factor are to be set for faster and accurate learning.

REFERENCES

[1]. ELMAN, J. L. "Finding Structure in Time". Cognitive Science 14, 2 (apr 1990), 179–211.

[2]. ZhiQiang Zhang, Zheng Tang and Catherine Vairappan,"A Novel Learning Method for Elman Neural Network Using Local + Search", Neural Information Processing – Letters and Reviews, Vol. 11, No. 8, August 2007.

[3]. D.L. Wang, X.M. Liu and S.C. Ahalt, "On temporal generalization of simple recurrent networks,"Neural Networks 9 (1996) 1099-1118

[4]. Yu-Tzu Chang, Jinn Lin, Jiann-Shing Shieh and MaysamF. Abbod ," Optimization the Initial Weights of Artificial Neural Networks

Cite this article as: N.Mohana Sundaram, P.N Ramesh. "Optimization of Training phase of Elman Neural Networks by suitable adjustments on the Network parameters." *International Conference on Systems, Science, Control, Communication, Engineering and Technology (2015)*: 229-235 Print.

via Genetic Algorithm Applied to Hip Bone Fracture Prediction", Hindawi Publishing Corporation,Advances in Fuzzy Systems.Volume 2012, Article ID 951247, 9 pages doi:10.1155/2012/951247.

[5]. Jim Y.F. Yam, Tommy W.S. Chow, "A weight initialization method for improving training speed in feedforward neural network", Elsevier Neurocomputing 30 (2000), 219-232.

[6]. Herbert Jaeger, Fraunhofer Institute for Autonomous Intelligent Systems (AIS), "A tutorial on training recurrent neural networks, covering BPPT, RTRL, EKF and the"echo state network" approach", Fifth revision: Dec 2013

[7]. Derrick Ngyuyen and Bernard Widrow, "Improving the Learning Speed of 2 Layer Neural Nwtworks by choosing Initial Values of the Adaptive Weights", Information Systems Laboratory, Stanford University, CA 94305

[8]. Frauke Günther and Stefan Fritsch, "Neuralnet: Training of Neural Networks", The R Journal Vol. 2/1, June 2010, ISSN 2073-4859 [9]. A.Moghaddamnia , R.Remesan , M.HassanpourKashani , M.Mohammadi , D.Han e, J.Piri , "Comparison of LLR, MLP, Elman, NNARX and ANFIS Models—with a case study in solar radiation estimation" , Elsevier Journal of Atmospheric and Solar-Terrestrial Physics- 71 (2009) 975–982

[10]. Anqi Cui, Hua Xu , Peifa Jia, "An Elman neural network-based model for predicting anti-germ performances and ingredient levels with limited experimental data", Elsevier Expert Systems with Applications 38 (2011) 8186–8192.

[11]. Cheng-Yuan Liou , Jau-Chi Huang, Wen-Chie Yang, "Modeling word perception using the Elman network", Elsevier Neurocomputing 71 (2008) 3150– 3157

[12]. Zhihang Tang, Rongjun Li , "An Improved Neural Network Model and Its Applications" , Journal of Information & Computational Science 8: 10 (2011) 1881–1888.

Cite this article as: N.Mohana Sundaram, P.N Ramesh. "Optimization of Training phase of Elman Neural Networks by suitable adjustments on the Network parameters." *International Conference on Systems, Science, Control, Communication, Engineering and Technology (2015)*: 229-235 Print.

International Conference on Systems, Science, Control, Communication, Engineering and Technology 2015 [ICSSCCET 2015]

ISBN	978-81-929866-1-6	**VOL**	01
Website	icssccet.org	**eMail**	icssccet@asdf.res.in
Received	10 - July - 2015	**Accepted**	31- July - 2015
Article ID	ICSSCCET051	**eAID**	ICSSCCET.2015.051

Knowledge study of Anonymity Databases

P.Mayilvel kumarm[1], K.Kalaiselvi[2], R.Saranya[3], J.K.Kiruthika[4]
[1, 2, 4] Faculty CSE.
[3]Final year B.E CSE, Karpagam Institute of Technology, Coimbatore.

Abstract: *Knowledge Discovery in Databases (KDDs) is the process of identifying valid, novel, useful, and understandable patterns from large data sets. Data Mining (DM) is the core of the KDD process, involving algorithms that explore the data, develop models, and discover significant patterns. One way to enable effective data mining while preserving privacy is to anonymize the data set that includes private information about subjects before being released for data mining. Two common manipulation techniques used to achieve k-anonymity of a data set are generalization and suppression. Generalization refers to replacing a value with a less specific but semantically consistent value, while suppression refers to not releasing a value at all. Generalization is more commonly applied in this domain since suppression may dramatically reduce the quality of the data mining results if not properly used.In this project, we propose a new method for achieving k-anonymity named K-anonymity of Classification Trees Using Suppression (kACTUS). In kACTUS, efficient multidimensional suppression is performed.Thus, in kACTUS, we identify attributes that have less influence on the classification of the data records and suppress them if needed in order to comply with k-anonymity. Encouraging results suggest that kACTUS pedictive performance is better than that of existing k-anonymity algorithms. Attackers often have background knowledge, and we show that k-anonymity does not guarantee privacy against attackers using background knowledge. So we propose the novel and powerful privacy definition called L-diversity. L-Diversity provides privacy even when the data publisher does not know what kind of knowledge is possessed by the adversary. The main idea behind L-diversity is the requirement that the values of the sensitive attributes are well-represented in each group.*

Keywords- Anonymity ,privacy preservation, QI

I.INTRODUCTION

Anonymity typically refers [1,5,7,11]to the state of an individual's personal identity, or personally identifiable information, being publicly unknown. There are many reasons why a person might choose to obscure their identity and become anonymous. Several of these reasons are legal, legitimate and socially approved of many acts of charity are performed anonymously, as benefactors do not wish, for whatever reason, to be acknowledged for their action. Someone who feels threatened by someone else might attempt to hide from the threat behind various means of anonymity, a witness to a crime can seek to avoid retribution, for example, by anonymously calling a crime tip line. There are also many reasons to hide behind anonymity. Criminals typically try to keep themselves anonymous either to conceal the fact that a crime has been committed, or to avoid capture. Anonymity may also be created unintentionally, through the loss of identifying information due to the passage of time or a destructive event.

Cite this article as: P.Mayilvel kumarm, K.Kalaiselvi, R.Saranya, J.K.Kiruthika. "Knowledge study of Anonymity Databases." *International Conference on Systems, Science, Control, Communication, Engineering and Technology (2015)*: 236-240. Print.

II.PRIVACY PRESERVING DATA MINING

PRIVACY PRESERVING DATA MINING OR PPDM , IS A RESEARCH AREA CONCERNED WITH THE PRIVACY DRIVEN FROM PERSONALLY IDENTIFIABLE INFORMATION WHEN CONSIDERED FOR DATA MINING. PPDM PROVIDE SECURITY TO PROTECT DATA. PPDM HAVE DIFFERENT KIND OF ALGORITHMS. PPDM INCLUDES PRIVACY PRESERVING ASSOCIATION RULE MINING, PRIVACY PRESERVING CLUSTERING AND PRIVACY PRESERVING CLASSIFICATION.

III.QUASI-IDENTIFIERS

Combinations of attributes within the data that can be used to identify individuals. For example, the statistic given is that 87% of the population of the United States can be uniquely identified by gender, date of birth, and 5-digit zip code. Given that three-attribute "quasi-identifier", a dataset that has only one record with any given combination of those fields is clearly not anonymous – most likely it identifies someone. Datasets are "k-anonymous" when for any given quasi-identifier, a record is indistinguishable from k-1 others.

IV.MULTIDIMENSIONAL SUPPRESSION FOR PRIVACY PRESERVATION

SUPPRESSION REFERS TO REMOVING A CERTAIN ATTRIBUTE VALUE AND REPLACING OCCURRENCES OF THE VALUE WITH A SPECIAL VALUE "*" INDICATING THAT ANY VALUE CAN BE PLACED INSTEAD [6]. THE ORIGINAL ZIP CODES {06148, 06149} CAN BE GENERALIZED TO 0614*, THEREBY STRIPPING THE RIGHTMOST DIGIT AND SEMANTICALLY INDICATING A LARGER GEOGRAPHICAL AREA. THE DOMAINS IN DATABASES ARE USED TO DESCRIBE THE SET OF VALUES THAT ATTRIBUTES ASSUME. FOR EXAMPLE, THERE MIGHT BE A ZIP DOMAIN, A NUMBER DOMAIN AND A STRING DOMAIN. IN THE ORIGINAL DATABASE, WHERE EVERY VALUE IS AS SPECIFIC AS POSSIBLE, EVERY ATTRIBUTE IS CONSIDERED TO BE IN A GROUND DOMAIN. FOR EXAMPLE, 06148 AND 06149 ARE IN THE GROUND ZIP DOMAIN, Z0. IN ORDER TO ACHIEVE ANONYMITY THE ZIP CODES SHOULD BE LESS INFORMATIVE. THIS CAN BE DONE BY MAKING THE DOMAIN OF THEM AT HIGHER LEVEL Z1 IN WHICH THE LAST DIGIT HAS BEEN REPLACED BY '*'.

V.K-ANONYMITY

If the information for each person contained in the release cannot be distinguished from at least k-1 individuals whose information also appears in the release. If you try to identify a man from a release, but the only information you have is his birth date and gender. There are k people meet the requirement. This is k-Anonymity[1,4,9]. Each released record should be indistinguishable from at least(k-1) others on its QI attributes. Alternatively, cardinality of any query on released data should be atleast k. k-anonymity is(the first) one of many privacy definitions in this line of work.

VI. COMPLEMENTARY RELEASE ATTACK

Different releases can be linked together to compromise k- anonymity.

VI a. SOLUTION

Consider all of the released tables before release the new one, and try to avoid linking. Other data holders may release some data that can be used in this kind of attack. Generally, this kind of attack is hard to be prohibited completely.

VI b. L DIVERSITY

The l-Diversity principle advocates ensuring well represented values for sensitive attributes but does not define what well represented values mean. In a l-diverse q*-block an attacker would need l-1 pieces of background knowledge to eliminate l-1 sensitive values to infer positive disclosure. A q*-block is l-diverse if contains atleast l "well-represented" values for the sensitive attributes S.A table is l-diverse[11] if every q*-block is l-diverse. This implies that for a table to be entropy l-Diverse, the entropy of the entire table must be at least log(l). Therefore, entropy l-Diversity may be too restrictive to be practical. Less restrictive than entropy l-diversity .Let s1, …, sm be the possible values of sensitive attribute S in a q*-block. Assume we sort the counts n(q*,s1), …, n(q*,sm) in descending order with the resulting sequence r1, …, rm. We can say a q*-block is recursive (c,l)-diverse if r1 < c(r2+ …. +rm) for a specified constant c.

VI C. OVERVIEW OF THE PROJECT

To protect respondents' identity when releasing microdata, data holders often remove or encrypt explicit identifiers, such as names and social security numbers. De-identifying data, however, provide no guarantee of anonymity. Released information often contains other data, such as race, birth date, sex, and ZIP code, that can be linked to publicly available information to re-identify respondents and to infer information that was not intended for release. One of the emerging concept in microdata protection is k-anonymity,which has been recently proposed as a property that captures the protection of a microdata table with respect to possible re-identification of the re-spondents to which the data refer. k-anonymity demands that every tuple in the microdata table released be indistinguishably related to no fewer than k respondents. One of the interesting aspect of k-anonymity is its association with protection techniques that preserve the truthfulness of the data. In this chapter we discuss the concept of k-anonymity, from its original proposal illustrating its enforcement via generalization and suppression. We then survey and discuss research results on k-anonymity in particular with respect to algorithms for its enforcement. We also discuss different ways in which generalization and suppressions can be applied to satisfy k-anonymity and, based on them, introduce a taxonomy of k-anonymity solutions. k-anonymity requirement- Each release of data must

Cite this article as: P.Mayilvel kumarm, K.Kalaiselvi, R.Saranya, J.K.Kiruthika. "Knowledge study of Anonymity Databases." *International Conference on Systems, Science, Control, Communication, Engineering and Technology (2015)*: 236-240. Print.

be such that every combination of values of quasi-identifiers can be indistinctly matched to at least k respondents.Since it seems impossible, or highly impractical and limiting, to make assumptions on the datasets available for linking to external attackers or curious data recipients, essentially k-anonymity takes a safe approach requiring that,in the released table itself, the respondents be indistinguishable (within a given set) with respect to the set of attributes. To guarantee the k-anonymity requirement, k-anonymity

1. Read Dataset
2. Preprocessing the dataset

   If any missing values then

   Remove the column

   Elseif check validated data then

   Validate the dataset

   End
3. Built classification tree when threshold accuracy reached
4. Calculate quasi identifier for classification tree
5. Apply k anonymity process for training dataset

   Calculate accuracy
6. Apply k anonymity process for training dataset

   Calculate accuracy
7. Anonimize the datset based on higher accuracy
8. Apply L diversity based clustering
9. Anonimize the dataset based on clustered values.
10. Anonimized data.

VI d.DATABASE DESIGN

Table 1
DATASET

age	workclass	fnlwgt	edu	edu-num	marital-status	occupation	relationship	race	sex	capital-gain	capital-loss	hours-per-week	native-country	salary >50K
39	Private	77516	BA	13	Married	Executive	Not-in-family	White	M	2174	0	40	US	<=50K
39	Private	83311	BA	13	Married	Executive	Husband	White	M	0	0	13	US	<=50K
38	Private	215646	BA	9	Divorced	Executive	Not-in-family	White	M	0	0	40	US	<=50K
53	Private	234721	BA	7	Married	Executive	Husband	Black	M	0	0	40	US	<=50K
28	Private	338409	BA	13	Married	Executive	Wife	Black	M	0	0	40	Cuba	<=50K
37	Private	284582	BA	14	Married	Executive	Wife	White	M	0	0	40	Cuba	<=50K
49	Private	160187	BA	5	Married	Executive	Not-in-family	Black	M	0	0	16	Cuba	<=50K
52	State-gov	209642	BA	9	Married	Executive	Husband	White	M	0	0	45	Cuba	>50K
31	State-gov	45781	BA	14	Married	Executive	Not-in-family	White	M	14084	0	50	Cuba	>50K
42	State-gov	159449	MA	13	Married	Executive	Husband	White	M	5178	0	40	Cuba	>50K
37	State-gov	280464	MA	10	Married	Executive	Husband	Black	F	0	0	80	Cuba	>50K
30	State-gov	141297	MA	13	Married	Sales	Husband	Asian	F	0	0	40	Cuba	>50K
30	State-gov	141297	MA	13	Married	Sales	Husband	Asian	F	0	2	60	Cuba	>50K
30	State-gov	141297	MA	13	Married	Sales	Husband	Asian	F	0	1	80	Cuba	<=50K
34	State-gov	245487	7th-8th	4	Married	Sales	Husband	Indian	F	0	0	45	Mexico	<=50K

Table 2
DATASET

age	workclass	fnlwgt	edu	edu-num	marital-status	occupation	relationship	race	sex	native-country
39	Private	77516	BA	13	Married	Executive	Not-in-family	White	M	US
39	Private	83311	BA	13	Married	Executive	Husband	White	M	US
38	Private	215646	BA	9	Divorced	Executive	Not-in-family	White	M	US
53	Private	234721	BA	7	Married	Executive	Husband	Black	M	US
28	Private	338409	BA	13	Married	Executive	Wife	Black	M	Cuba
37	Private	284582	BA	14	Married	Executive	Wife	White	M	Cuba
49	Private	160187	BA	5	Married	Executive	Not-in-family	Black	M	Cuba
52	State-gov	209642	BA	9	Married	Executive	Husband	White	M	Cuba
31	State-gov	45781	BA	14	Married	Executive	Not-in-family	White	M	Cuba
42	State-gov	159449	MA	13	Married	Executive	Husband	White	M	Cuba
37	State-gov	280464	MA	10	Married	Executive	Husband	Black	F	Cuba
30	State-gov	141297	MA	13	Married	Sales	Husband	Asian	F	Cuba
30	State-gov	141297	MA	13	Married	Sales	Husband	Asian	F	Cuba
30	State-gov	141297	MA	13	Married	Sales	Husband	Asian	F	Cuba
34	State-gov	245487	7th-8th	4	Married	Sales	Husband	Indian	F	Mexico

Table 3
K-ANONYMITY TABLES BASED ON PRIVATE TABLE:

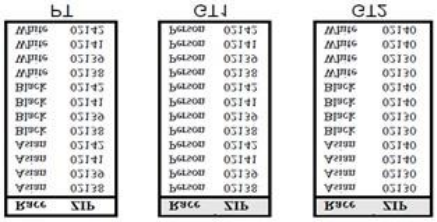

Cite this article as: P.Mayilvel kumarm, K.Kalaiselvi, R.Saranya, J.K.Kiruthika. "Knowledge study of Anonymity Databases." *International Conference on Systems, Science, Control, Communication, Engineering and Technology (2015)*: 236-240. Print.

TABLE 4
ANONYMIZED

age	workclass	fnlwgt	edu	Edun um	marital-status	Occupation	relationship	Race	sex	Native-country
<40	private	77516	BA	13	Married	Excecutie	*	Person	M	us
<40	private	83311	BA	13	Married	Excecutie	*	Person	M	us
<40	private	215646	BA	9	Divorced	Excecutie	*	Person	M	us
>50	private	234721	BA	7	Married	Excecutie	*	Person	M	us
<30	private	338409	BA	13	Married	Excecutie	*	Person	M	cuba
<40	private	284582	BA	14	Married	Excecutie	*	Person	M	Cuba
>40	private	160187	BA	5	Married	Excecutie	*	Person	M	Cuba
>50	State-gov	209642	BA	9	Married	Excecutie	*	Person	M	Cuba
>40	State-gov	45781	BA	14	Married	Excecutie	*	Person	M	Cuba
>40	State-gov	159449	MA	13	Married	Excecutie	*	Person	M	Cuba
<40	State-gov	280464	MA	10	Married	Excecutie	*	Person	F	Cuba
<40	State-gov	141297	MA	13	Married	Sales	*	Person	F	Cuba
<40	State-gov	141297	MA	13	Married	Sales	*	Person	F	Cuba
<40	State-gov	141297	MA	13	Married	Sales	*	Person	F	Cuba
<40	State-gov	245487	7th-8th	4	Married	Sales	*	Person	F	Mexico

VII.ALGORITHM

The algorithm is as follows:
Create a root node for the tree
If all examples are positive, Return the single-node tree Root, with label = +.
If all examples are negative, Return the single-node tree Root, with label = -.
If number of predicting attributes is empty, then Return the single node tree Root, with label = most common value of the target attribute in the examples.
Otherwise Begin
A = The Attribute that best classifies examples.
Decision Tree attribute for Root = A.
For each possible value, vi, of A,
Add a new tree branch below Root, corresponding to the test A = vi.
Let Examples(vi), be the subset of examples that have the value vi for A
If Examples(vi) is empty
Then below this new branch add a leaf node with label = most common target value in the examples
Else below this new branch add the subtree C4.5 (Examples(vi), Target_Attribute, Attributes – {A})
End
Return Root

VIII.CONCLUSION

WE PRESENTED A NEW METHOD FOR PRESERVING THE PRIVACY IN CLASSIFICATION TASKS USING K-ANONYMITY. THE PROPOSED METHOD REQUIRES NO PRIOR KNOWLEDGE REGARDING THE DOMAIN HIERARCHY TAXONOMY AND CAN BE USED BY ANY INDUCER. THE NEW METHOD ALSO SHOWS A HIGHER PREDICTIVE PERFORMANCE WHEN COMPARED TO EXISTING STATE-OF-THE-ART METHODS.
This work is motivated by the observation that although all previous k-anonymity techniques assume the existence of a PD, which can be used to breach privacy, none actually takes PD into account during the anonymization process. This omission leads to unnecessarily high information loss. In Fig. 1, if k ¼ 3, tuple G 2 MT does not require generalization, as PD already contains two other records (G1 and G2Þ with the same QI values. Based on this fact, we introduce the concept of k-join-anonymity (KJA) to reduce the information loss. Briefly, KJA anonymizes a superset of MT, which includes selected records from PD.In most practical anonymization scenarios, there exists public knowledge (e.g., voter registration data) that can be used by an attacker to breach privacy. On the other hand, this knowledge can also be exploited to reduce the information loss in the published data. Motivated by this observation, we introduce the concept of KJA and show how existing generalization algorithms can be adopted to take into account external databases. We demonstrate the effectiveness of KJA through an extensive experimental evaluation, using real and synthetic data sets. An interesting

Cite this article as: P.Mayilvel kumarm, K.Kalaiselvi, R.Saranya, J.K.Kiruthika. "Knowledge study of Anonymity Databases." *International Conference on Systems, Science, Control, Communication, Engineering and Technology (2015)*: 236-240. Print.

direction for future work is to apply the general concept of exploiting external knowledge to alternative forms of deidentification. For instance, since some k-anonymity algorithms (e.g., Mondrian) can be easily adapted to capture l-diversity, we expect that the availability of external information will also be beneficial in this case. Additionally, we plan to investigate the issue of updates in MT and PD. Assume that after the initial release of AT, the MT is modified and a new AT must be published. Meanwhile, the PD may have also been updated. A challenging issue is to incrementally update the AT, without compromising the privacy of MT or the utility of AT.

REFERENCES

[1] L. Sweeney, "k-Anonymity: A Model for Protecting Privacy," Int'l J. Uncertainty, Fuzziness and Knowledge-Based Systems, vol. 10, no. 5, pp. 557-570, 2002.
[2] P. Samarati, "Protecting Respondents' Identities in Microdata Release," IEEE Trans. Knowledge and Data Eng., vol. 13, no. 6, pp. 1010-1027, Nov./Dec. 2001.
[3] C. Bettini, X.S. Wang, and S. Jajodia, "The Role of Quasi-Identifiers in k-Anonymity Revisited," Technical Report abs/cs/0611035, Computing Research Repository (CoRR), 2006.
[4] R.J. Bayardo, Jr., and R. Agrawal, "Data Privacy through Optimal k-Anonymization," Proc. IEEE Int'l Conf. Data Eng. (ICDE), pp. 217-228, 2005.
[5] J. Xu, W. Wang, J. Pei, X. Wang, B. Shi, and A.W.-C. Fu, "Utility- Based Anonymization Using Local Recoding," Proc. ACM SIGKDD, pp. 785-790, 2006.
[6] K. LeFevre, D.J. DeWitt, and R. Ramakrishnan, "Incognito: Efficient Full-Domain k-Anonymity," Proc. ACM SIGMOD, pp. 49-60, 2005.
[7] K. LeFevre, D.J. DeWitt, and R. Ramakrishnan, "Mondrian Multidimensional k-Anonymity," Proc. IEEE Int'l Conf. Data Eng. (ICDE), p. 25, 2006.

Cite this article as: P.Mayilvel kumarm, K.Kalaiselvi, R.Saranya, J.K.Kiruthika. "Knowledge study of Anonymity Databases." *International Conference on Systems, Science, Control, Communication, Engineering and Technology (2015)*: 236-240. Print.